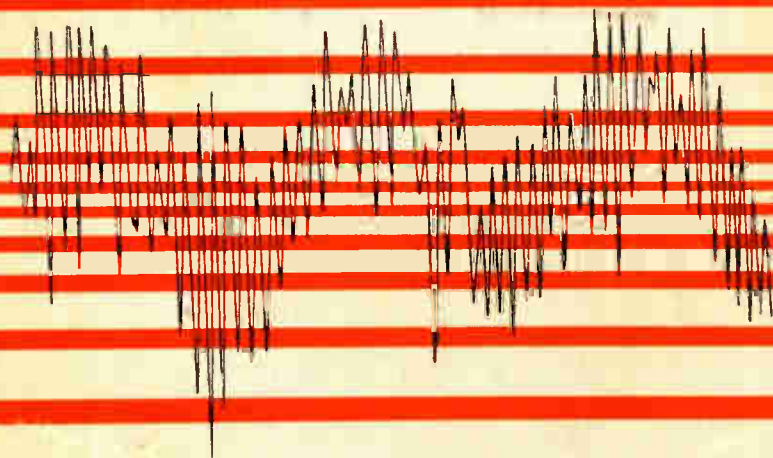


# LOUD SPEAKERS



THEORY  
PERFORMANCE  
TESTING AND DESIGN  
BY N. W. McLACHLAN

# LOUD SPEAKERS

THEORY, PERFORMANCE, TESTING AND DESIGN

BY N. W. McLACHLAN

Professor of Electrical Engineering, Emeritus, University of Illinois;  
Walker-Ames Professor of Electrical Engineering, University of Washington

There is probably no other work ever written which provides so comprehensive a coverage of the theory and practice of loud speaker design and testing. Utilizing both the author's original contributions and pertinent published work, this volume has become the classic reference and study manual in the field.

One feature which greatly increases the book's utility is its division into two almost equal parts. The first 12 chapters devote themselves to theory; chapters 13 to 20 deal with practical work. Because of this separation, readers whose work is mainly connected with testing and design will find in the latter part of the book material which may be immediately applied to the problem at hand. The mathematical reader, on the other hand, can study theory unhampered by the inclusion of practical details with which he may not be familiar. Throughout the volume, the development is in logical sequence. Treatment is as rigorous as possible, but with the consideration that it must appeal to engineers as well as theorists.

Chapter titles: Definitions, Principles of Sound Propagation; Fluid Pressure on Vibrators; Accession to Inertia; Vibrational Modes; Spatial Distribution of Sound from Vibrating Surfaces; Theory of Moving-Coil Principle; Hornless Speaker simulated by Coil-Driven Rigid Disk; Electrostatic Speakers; Theory of Horns; Sound Waves of Finite Amplitude; Transients; Driving Mechanisms; Magnets; Efficiency; Electrical Impedance Measurements; Response Curves; Measurement of Vibrational Frequencies of Conical Shells; Design of Horn Type Moving-Coil Speakers.

Unabridged and corrected version of the first edition. Appendix. Bibliography. Index. 165 illustrations and charts. xii + 399pp. \$588 Paperbound

## THIS DOVER EDITION IS DESIGNED FOR YEARS OF USE

**THE PAPER** is chemically the same quality as you would find in books priced \$5.00 or more. It does not discolor or become brittle with age. Not artificially bulked, either; this edition is an unabridged full-length book, but is still easy to handle.

**THE BINDING:** The pages in this book are SEWN in signatures, in the method traditionally used for the best books. These books open flat for easy reading and reference. Pages do not drop out, the binding does not crack and split (as is the case with many paperbacks held together with glue).

**THE TYPE IS LEGIBLE:** Margins are ample and allow for cloth rebinding.

# LOUD SPEAKERS

## THEORY PERFORMANCE, TESTING AND DESIGN

BY

**N. W. MCLACHLAN**

D.Sc. (ENGINEERING) LONDON

PROFESSOR OF ELECTRICAL ENGINEERING, EMERITUS,  
UNIVERSITY OF ILLINOIS

WALKER-AMES PROFESSOR OF ELECTRICAL ENGINEERING,  
UNIVERSITY OF WASHINGTON (1954)

CORRECTED EDITION

DOVER PUBLICATIONS, INC.  
NEW YORK      NEW YORK



TK  
6565  
oL6m3

Copyright © 1960 by Dover Publications, Inc.

All rights reserved under Pan American and International Copyright Conventions.

Published simultaneously in Canada by McClelland & Stewart, Ltd.

Published in the United Kingdom by Constable and Company Limited, 10 Orange Street, London W.C. 2.

This new Dover edition first published in 1960 is an unabridged and corrected version of the first edition published in 1934. It is published through special arrangement with Oxford University Press.

Manufactured in the United States of America

Dover Publications, Inc.  
180 Varick Street  
New York 14, N.Y.



## PREFACE

THE purpose of this book is to provide a fairly complete treatment of the theory and practice of loud speakers. The contents have been divided deliberately into two almost equal parts, Chapters I to XII being devoted to theory, whilst practical work is dealt with in Chapters XIII to XX. By separating theory and practice, those who have not had a mathematical training and whose work is mainly connected with testing and design, can turn to the chapters on practical work, whilst the mathematical reader will be able to read the theory, unhampered by the inclusion of practical details with which he may not be well acquainted. There are others who will desire to be familiar with both theory and practice, but to whom the theory, which on the whole is not elementary, may present difficulties. These readers will have to supplement their study by acquiring a knowledge of Bessel functions. To this end the author has written a book on Bessel functions and spherical harmonics for engineers, in which the theory and its applications to acoustical and electrical engineering are explained in a simple manner.

Throughout the present volume free use has been made of published work on the subject, and the author has endeavoured to evolve the theory in logical sequence, and to give its practical applications. New material has been added in places, whilst that which is of long standing has been recast to conform with the rest of the subject-matter. The treatment is as rigorous as possible, but of such a nature as will appeal to engineers. Owing to space limitations, it has been necessary to abbreviate both the analytical and descriptive work occasionally, but the reference list will aid those desiring to probe the subject more deeply.

The author has been very fortunate in securing the help of several friends. Dr. C. G. Lamb has read most of the manuscript and the proofs of Chapters I to XV. Mr. A. G. Warren has read the manuscript of published papers and the proofs of Chapters I to XV, whilst Dr. S. Goldstein has read the manuscript of Chapters II and XI. The author has great pleasure in acknowledging the valuable criticisms and suggestions made by these gentlemen. Mr. G. A. V. Sowter was associated with the author in a large amount of experimental work, when many hours were spent persuading conical shells to divulge their

vibrational secrets (Chapter XVIII). The author takes this opportunity of expressing his appreciation of Mr. Sowter's co-operation.

Best thanks are due to Messrs. L. B. Ault (B.T.-H. Co.), A. B. Howe (B.B.C.), H. L. Kirke (B.B.C.), H. Midgley (Midgley-Harmer), L. H. Paddle (Igranic Co.), and S. S. A. Watkins (Western Electric Co.) for information on certain topics mentioned in the reference list: also to various Editors for permission to use subject-matter and diagrams from the following publications: *Annalen der Physik* (Figs. 42, 43, 44), *Bell Technical Journal* (Figs. 82, 100, 104, 115, 117, 121), British Broadcasting Corporation (Fig. 120), *Journal Acoustical Society America* (Figs. 101, 122, 163, 164), *Journal American Institute Electrical Engineers*, *Journal Franklin Institute* (Figs. 62, 157), *Journal Society Motion Picture Engineers* (Figs. 161, 162), *Philosophical Magazine* (Figs. 13, 15, 16, 19-24, 53, 53 A, 54, 74, 96, 113, 124-6, 129-31, 139, 142, 148, 165), *Proceedings Institute Radio Engineers* (Figs. 84, 85, 116, 118, 119), *Proceedings Physical Society London* (Figs. 110, 132-7), *Proceedings Royal Society London* (Fig. 39), *Siemens-Zeitschrift* (Figs. 80, 81), *Wireless Engineer* (Figs. 36, 140, 141, 143), *Wireless World* (Figs. 77, 87, 88, 92, 114, 150, 162 A). The Editors of the *Philosophical Magazine*, *Siemens-Zeitschrift*, *Wireless Engineer*, *Wireless World*, and the Council of the Physical Society generously loaned blocks for the above mentioned diagrams.

Drs. H. Backhaus, W. L. Barrow, L. G. Bostwick, W. Hähnle, H. Neumann, H. Olson, E. Spenke, H. Stenzel, M. J. O. Strutt, Prof. R. D. Fay, Messrs. D. A. Oliver, L. J. Sivian, H. Vogt, and J. Weinberger very kindly supplied copies of their scientific papers and corresponded on various topics concerning them. These have all been of great service and it is hoped that, in treating the subject, full justice has been done not only to their work, but to that of others whose names are given in the references. The compilation thereof was greatly facilitated by a list of continental publications for which the author is much indebted to Messrs. Siemens of Berlin.

LONDON,  
February 1934.

N. W. M.

## CONTENTS

SYMBOLS . . . . .	viii
I. DEFINITIONS . . . . .	1
II. PRINCIPLES OF SOUND PROPAGATION . . . . .	9
III. FLUID PRESSURE ON VIBRATORS: ACCESSION TO INERTIA . . . . .	49
IV. VIBRATIONAL MODES . . . . .	63
V. SPATIAL DISTRIBUTION OF SOUND FROM VIBRATING DIAPHRAGMS . . . . .	94
VI. ACOUSTIC POWER RADIATED FROM VIBRATING SUR- FACES . . . . .	115
VII. THEORY OF MOVING-COIL PRINCIPLE. . . . .	131
VIII. HORNLESS SPEAKER SIMULATED BY COIL-DRIVEN RIGID DISK . . . . .	143
IX. ELECTROSTATIC SPEAKERS . . . . .	158
X. THEORY OF HORNS . . . . .	177
XI. SOUND WAVES OF FINITE AMPLITUDE . . . . .	198
XII. TRANSIENTS . . . . .	204
XIII. DRIVING MECHANISMS . . . . .	213
XIV. MAGNETS . . . . .	230
XV. EFFICIENCY . . . . .	253
XVI. ELECTRICAL IMPEDANCE MEASUREMENTS . . . . .	266
XVII. RESPONSE CURVES . . . . .	285
XVIII. MEASUREMENT OF VIBRATIONAL FREQUENCIES OF CONICAL SHELLS . . . . .	304
XIX. DESIGN CONSIDERATIONS IN HORNLESS MOVING- COIL SPEAKERS . . . . .	343
XX. DESIGN OF HORN TYPE MOVING-COIL SPEAKERS . . . . .	349
APPENDIX . . . . .	380
REFERENCES . . . . .	386
INDEX . . . . .	395

Figs. 77, 81, 82, 86, 88, 140, 141, 142, and 143 face respectively pages  
218, 224, 224, 229, 229, 334, 334, 335, 334

## SYMBOLS

THE list of symbols used herein is based upon the recommendations of the International Electrotechnical Commission. At first sight the list appears to be very formidable, but by systematic use no difficulty should be encountered. The great variety of symbols is due to the inclusion of three different sets of quantities in the analysis, namely, electrical, mechanical, and acoustical. To differentiate succinctly between electrical and mechanical quantities, the former are represented in general by capitals and the latter by small letters.\* The main exception is that of 'power', which is convertible from electrical to mechanical form and vice versa. Since  $p$  is used for sound pressure, the power is represented throughout by  $P$ . This does not lead to any confusion of thought, as will be evident on perusal of the text. Acoustical quantities being of a mechanical nature are represented also by small letters. They bear the subscript  $a$ , e.g.  $x_a$  the acoustical reactance. It has been necessary to supplement standard letters by others in heavy type. The purely mathematical symbols follow standard practice. It is a moot point whether  $i$  or  $j$  should be chosen to represent  $\sqrt{-1}$ . Electrical engineers use the latter, since  $i$  generally signifies the instantaneous value of a current. Since electrical quantities in general are shown by capital letters,  $i$  has been used to signify 'the imaginary' in conformity with works on pure and applied mathematics. There is a lack of standardization in the nomenclature of Bessel functions which is often quite confusing. This is especially the case if  $I_0$  is written for  $J_0$ ,  $Y_0$  for  $K_0$ , or when the order of the function is shown as an 'index'. The symbols adopted herein are those used by Gray, Mathews, and MacRobert [213] in their *Treatise on Bessel Functions*; also by Watson [221] in his *Theory of Bessel Functions*, as indicated by the reference numbers allotted to the symbols in question.

Throughout the text the root mean square values of all quantities varying cyclically are used, unless otherwise stated or implied. In differential or circuital equations, the implication of instantaneous values will be readily discerned. In other publications the strength of a sound source  $S$  is usually expressed in terms of the *maximum* displacement or velocity. In this book  $S$  refers to the r.m.s. strength of the source, which is more convenient for practical purposes. If the symbols are taken to signify maximum values, formulae for power must be divided by 2.

$a; a_r$	radius, mathematical constant; absorption coefficient.
$b$	radius $< a$ , mathematical constant or variable, breadth.
$c$	velocity of sound in free air, about $3.43 \times 10^4$ cm. sec. <sup>-1</sup> for room conditions. $c = \sqrt{(\gamma p_0 / \rho_0)} = \sqrt{(\kappa / \rho_0)}$ .
$d; db.$	distance between sound sources, or between electrodes in speaker; decibels.
$e; e$	base of Napierian logarithms; sound energy density.
$f; f_s; f$	total force, total pressure on area; space factor; force per unit area.
$g$	mathematical symbol.
$i$	$\sqrt{-1}$ .

\* There are several unimportant exceptions, e.g.  $S, T, V, \rho, \kappa, \mu$ , where it would be unwise to depart from well-established usage.



$k; k_1$	phase constant $\omega/c = 2\pi/\lambda$ ; constant as in $J_0(k_1 x)$ .
$l; l_g$	length, mathematical symbol; length of air gap in magnet.
$m; m_s; m_c$	total mass, mathematical symbol; effective mass; mass of coil and its former.
$m'_c; m_f$	mass of coil alone; mass of coil-former alone.
$m_i; m_n; m_g$	accession to inertia; natural mass; equivalent mass.
$n$	turns on a coil, mathematical symbol.
$p$	root mean square excess or sound pressure during wave transmission.
$p_0$	static fluid pressure.
$p$	total pressure during wave transmission ( $p + p_0$ ).
$p_i$	inertia or reactive component of sound pressure on a surface.
$p_a$	acoustic or resistive " " " " "
$q$	Young's modulus of elasticity.
$r; r$	radius, distance of spatial point from vibrator; mechanical resistance per unit area.
$r_s$	acoustical resistance of horn, conduit, tube, or the like.
$r_r$	mechanical resistance due to sound radiation.
$r_v$	" " " inherent loss <i>in vacuo</i> .
$r_e$	effective mechanical resistance due to radiation plus loss.
$r$	response = $20 \log_{10} p_{av}/(E/\sqrt{R})$ , where $p_{av}$ is the average pressure (see p. 289).
$s; s$	mechanical stiffness or constraint; condensation of medium.
$t$	time, thickness.
$u$	radial velocity of spherical vibrator, velocity of particles during passage of a sound wave.
$u_0, u_1, \text{etc.}$	harmonic components of radial <i>surface</i> velocity of spherical vibrator.
$v; v_r$	velocity of vibrator, air-particle velocity; radial velocity of propagation in diaphragm.
$w$	air-particle velocity parallel to $z$ -axis.
$x; x_s$	coordinate, radius of circle; effective mechanical reactance ( $\omega m_s$ ).
$x$	mechanical reactance per unit area.
$x_s$	acoustical reactance of horn, tube, or the like.
$y$	coordinate.
$z; z$	coordinate, $ka$ where $a$ is radius of vibrator; mechanical impedance per unit area.
$z_s$	acoustical impedance of horn, tube, or the like.
$z_e$	effective mechanical impedance in air ( $r_s + i\omega m_s$ ).
$z_v$	" " " <i>in vacuo</i> .
$\sim$	cycles per second.
$A; A_1$	area; constant.
$B; B_g$	magnetic flux density; flux density in air-gap of magnet.
$C^2; C_m; C$	electromechanical conversion factor; motional capacitance; capacitance.
$D; D_1$	mathematical operator $d/dt$ ; constant.
$E$	electromotive force, potential difference.

$F$ ; ${}_2F_1(\alpha, \beta, \gamma, x^2)$	magnetomotive force; the hypergeometric function, namely, $1 + \frac{\alpha\beta}{\gamma}x^2 + \frac{\alpha(\alpha+1)\beta(\beta+1)}{2!\gamma(\gamma+1)}x^4 + \dots$
$G$ ; $G_1$ ; $G_3$	$\frac{J_1(z)}{z}$ ; $\left[1 - \frac{J_1(2z)}{z}\right]$ ; $\frac{H_1(2z)}{z}$ , where $z = ka$ .
$G_3$	$\frac{\sin z}{z} = \sqrt{\left(\frac{\pi}{2z}\right)J_1(z)}$ .
$H$	magnetic field strength.
$H_0$ ; $H_1$	Struve's function of zero order [221]; of unit order.
$I$ ; $I$	alternating or direct current; moment of inertia.
$I_0$ ; $I_1$	modified Bessel function of the first kind of zero order [213]; of unit order.
$J_0$ ; $J_1$	Bessel's function of the first kind of zero order [213]; of unit order.
$K_0$ ; $K_1$	modified Bessel function of the second kind of zero order [213]; of unit order.
$L$ ; $L_0$	inductance; inductance of speaker with driving agent stationary.
$L_1$	inductance of speaker with driving agent moving freely.
$L_m$ ; $L_v$	motional inductance during vibration in air ( $L_1 - L_0$ ); same <i>in vacuo</i> ( $L_{1v} - L_0$ ).
$P$	power radiated as sound; propagation coefficient of cable.
$P$	power radiated from both sides of a rigid disk in an infinite rigid plane when $ka \leq 0.5$ .
$P_n(\mu)$	Legendre's function of order $n$ [217], $\mu = \cos \theta$ .
$Q$	quantity of electricity.
$R$	electrical resistance, distance from spatial point to vibrator.
$R_0$	electrical resistance of speaker with driving agent stationary.
$R_1$	electrical resistance of speaker with driving agent moving freely.
$R_m$	electrical motional resistance in air ( $R_1 - R_0$ ).
$R_r$	" " " due to sound radiation.
$R_t$	" " " " mechanical loss in air.
$R_v$	" " " " loss <i>in vacuo</i> .
$R_s$	Internal or anode resistance of thermionic valve.
$S$ ; $S$ , $S_0$	magnetic reluctance; strength of simple sound source = $U \times$ surface area.
$S_d$ ; $S_s(\mu)$	strength of double sound source; spherical harmonic.
$T$ ; $T_v$	kinetic energy of vibrating system in air; same <i>in vacuo</i> .
$U$	root mean square radial velocity of vibrating surface.
$V$ ; $V$	potential energy of deformation; volume.
$W$	energy.
$Y_0$ ; $Y_1$	Bessel's function of the second kind of zero order [221]; of unit order.
$Z$	electrical impedance ( $R + i\omega L$ ) = ( $R + iX$ ).
$Z_0$	" " of speaker when driving agent is stationary.
$Z_1$	electrical impedance of speaker when driving agent is moving freely.

$Z_m$	electrical motional impedance in air ( $Z_1 - Z_0$ ).	
$Z_0$	" " " in <i>vacuo</i> .	
$\alpha$ (Alpha)	decay factor in $e^{-\alpha t}$ ; $\sqrt{(k^2 - \beta^2/4)}$ in horn theory.	
$\beta$ (Beta)	flaring index of exponential horn; mathematical symbol.	
$\gamma$ (Gamma)	ratio of specific heats of air, mathematical symbol.	
$\delta$ ; $\partial$ (Delta)	mathematical symbol; partial differential.	
$\epsilon$ (Epsilon)	mathematical symbol.	
$\zeta_n$ (Zeta)	frequency correction factor [ $f_n(ika)/F_n(ika)$ ] in spherical harmonic analysis. For $f_n$ and $F_n$ see Chap. II.	
$\eta$ (Eta)	efficiency.	
$\theta$ (Theta)	angle in spherical harmonic analysis.	
$\kappa$ (Kappa)	dielectric coefficient; coefficient of cubical elasticity.	
$\lambda$ (Lambda)	wave-length of sound.	
$\mu$ ; $\mu_n$ (Mu)	magnetic permeability, $\cos \theta$ in spherical harmonic analysis, amplification factor of valve; effective magnetic permeability.	
$\nu$ (Nu)	mathematical symbol.	
$\xi$ ; $\xi_0$ (Xi)	displacement; central displacement, $\xi = \xi_0 e^{i\omega t}$ .	
$\dot{\xi}$ ; $\ddot{\xi}$	axial velocity and acceleration in harmonic motion.	
$\pi$ (Pi)	circle constant.	
$\omega$	mathematical symbol.	
$\rho_0$ (Rho)	normal density of air, about $1.22 \times 10^{-3}$ gm. cm. <sup>-3</sup> under room conditions.	
$\rho$	density of air during wave propagation (variable); density of material.	
$\rho_1$	specific resistance of conductor material; mass per unit area.	
$\rho_2$	density of material.	
$\sigma$ (Sigma)	Poisson's ratio $< 1$ .	
$\tau$ ; $\tau$ (Tau)	total radial tension of membrane; radial tension per unit length.	
$\phi$ (Phi)	{	velocity potential, $-\partial\phi/\partial x = u$ the particle velocity.
		angular distance from axis of symmetry in sound-distribution problems.
$\phi_0, \phi_1$ , etc.	harmonics of velocity potential in spherical harmonic analysis.	
$\varphi$	variable parameter, ratio of two quantities.	
$\chi$ (Chi)	angle of longitude in spherical coordinates.	
$\psi$ (Psi)	apical angle of cone.	
$\omega$ (Omega)	$2\pi \times$ frequency, pulsatace or circular frequency.	
$\Gamma$ (Gamma)	mathematical symbol representing the Gamma function.	
$\Delta$ (Delta)	" " ; dilatation of medium.	
$\Theta_n$ (Theta)	" "	
$\Lambda$ (Lambda)	" "	
$\Xi_n$ (Xi)	frequency correction factor $1/F_n(ika)$ in spherical harmonic analysis.	
$\Pi$ (Pi)	mathematical symbol.	
$\Sigma$ (Sigma)	" " signifying 'sum of'.	
$\Upsilon$ (Upsilon)	" "	

$\Phi$ (Phi)	total magnetic flux; total sound flux (not sound-energy flux).
$\Omega$ (Omega)	solid angle = (area of portion of spherical surface)/ $r^2$ , where $r$ is the radius.
$\nabla^2$	Laplace's operator 'Nabla squared' = $\frac{\partial^2}{\partial x^2} + \frac{\partial^2}{\partial y^2} + \frac{\partial^2}{\partial z^2}$ .

*Mathematical Signs*

$\doteq$ is approximately equal to.	$\neq$ is not equal to.
$\equiv$ is the analogue of.	$/$ divided by.
$>$ is greater than.	$\nexists$ is not greater than.
$<$ is less than.	$\nless$ is not less than.
$\gg$ is much greater than.	$\ll$ is much less than.
$\geq$ is equal to or greater than.	$\leq$ is equal to or less than.
$\propto$ varies as; is proportional to.	$\infty$ infinity, infinitely great.
$\rightarrow$ tends to, approaches.	

# LOUD SPEAKERS

# I

## DEFINITIONS

THE following list of definitions is given to avoid any ambiguity in the various terms used throughout the text. Those marked with an asterisk are based upon the standardization reports of the Acoustical Society of America.†

**1. Bar.** A pressure of one dyne per square centimetre. This is taken as the unit of pressure.

**2. Static pressure ( $p_0$ ).** The pressure in a fluid medium in the absence of sound waves (bar). Normal atmospheric pressure is nearly  $10^6$  bars, this being the force in dynes due to a mercury column 76 cm. high and  $1 \text{ cm.}^2$  in cross-section at  $0^\circ \text{C}$ .

**\*3. Sound pressure ( $p$ ).** The root mean square value of the excess pressure above or below  $p_0$  over a complete cycle of a steady wave (bar).

**\*4. Sound energy flux or power ( $P$ ).** The mean value over one cycle of the steady power or energy flow per second in a direction normal to any specified area (erg sec.<sup>-1</sup>;  $10^7$  erg sec.<sup>-1</sup> = 1 watt). In a progressive or expansive wave travelling with velocity  $c$ , the energy flux passing perpendicularly through an area  $A$  is

$$P = p^2 A / \rho_0 c \doteq p^2 A / 42.$$

where  $\rho_0 = 1.22 \times 10^{-3}$  gm. cm.<sup>-3</sup> and  $c = 3.43 \times 10^4$  cm. sec.<sup>-1</sup>, for room conditions at  $18^\circ \text{C}$ . and  $10^6$  bars.

**\*5. Sound energy density ( $e$ ).** The sound energy per unit volume  $p^2 / \rho_0 c^2$  (ergs cm.<sup>-3</sup>).

**6. Interference.** The partial or complete annulment or reinforcement of two or more sound waves of the same frequency having different or identical phases at any spatial point.

**7. Diffraction.** The change in the direction of propagation due to the bending of sound waves round an obstacle.

**\*8. Nodes.** Points, lines, or surfaces of a vibrating system which are at rest (zero amplitude). In a fluid there are pressure nodes and velocity nodes. At a pressure node the velocity is a maximum and vice versa.

† *J.A.S.A.* 2 (1931), 312; 5 (1933), 109.

- \*9. Antinodes.** Points, lines or surfaces having maximum amplitude. In a fluid pressure nodes are velocity antinodes, and vice versa.
- \*10. Partial nodes.** Points, lines or surfaces having a minimum amplitude. All practical nodal systems fall into this category owing to radiation and transmission losses which imply motion at the nodes to replenish the waste.
- 11. Coefficient of reflection.** The ratio of the power reflected from a surface to that impinging upon it.
- \*12. Coefficient of absorption ( $a_s$ ).** Unity minus the coefficient of reflection, this being the ratio of the power absorbed by a surface to that impinging upon it.
- \*13. Reverberation.** The persistence of sound in an enclosure due to repeated reflections after extinction of the source.
- \*14. Reverberation time.** The time required for the average energy density, initially in a steady state, to fall to  $10^{-6}$  its original value (60 decibels) after extinction of the source. The decay curve may take any form.
- \*15. Intensity level.** The number of decibels (definition 46) above an arbitrary reference-level of  $2 \times 10^{-4}$  bar, the latter corresponding to a power of  $10^{-16}$  watt  $\text{cm}^{-2}$  approximately. If  $p$  is the sound pressure, the intensity level is very nearly  $(74 + 20 \log_{10} p)$  decibels.
- 16. Threshold of audibility.** The minimum sound pressure in the ear canal due to a sine wave of prescribed frequency, which causes a sensation of tone in an absolutely silent place. Curves are usually given for the average ear. Sometimes the definition is applied to complex sounds. The sound pressure at the threshold is often expressed in decibels below some prescribed datum level.
- 17. Sensation level.** The difference between the intensity level and the threshold of audibility for the average ear (decibels).
- \*18. Loudness.** The subjective quality of a sound which governs the magnitude of the sensation felt by a normal ear. It is usually specified as the intensity level of a 1,000  $\sim$  note which causes the same sensation.

**19. Masking.** The increase in the threshold of audibility due to the presence of one or more auxiliary frequencies (decibels).

**20. Resistance of medium.** The ratio of the excess pressure to the in phase component of the particle velocity in a steady progressive wave. Under this condition  $p = \rho_0 cv$ , so the resistance of the medium is  $p/v = \rho_0 c$ . When the mechanical impedance per unit area of a vibrator is entirely resistive of value  $\rho_0 c$ , the resistance of the medium in which it vibrates is said to be matched.

**21. Sound flux.** The integral of elemental areas and the corresponding particle velocities in the direction of the normal taken over an imaginary surface in the path of a sound wave, i.e.  $\iint v dA$ . When the velocity is constant over the surface and normal to all parts thereof, the flux is the product velocity-area,  $vA$ . This must not be confused with sound energy flux (power).

**22. Baffle.** A structure or acoustic barrier which completely or partially prevents interference of sound waves from different parts of a vibrator which move in antiphase. In a rigorous sense this includes a horn. The commonest type of baffle is a flat board, the diaphragm or vibrator being in a hole at the centre. An infinite rigid plane is adopted in analytical work, this giving perfect screening, but cutting off one side of the vibrator (see Fig. 18 A).

**\*23. Acoustical impedance ( $z_a$ ).** The complex quotient of the pressure, assumed constant over an imaginary surface, and the sound flux through the surface. This gives  $z_a = p/Av$ . When either  $p$  or  $v$  or both vary over the surface,  $z_a$  is found by summing the acoustical admittances (see 26) over the surface, and then taking the reciprocal.

Thus 
$$z_a = 1 / \sum_{n=1}^{\infty} \frac{v_n A_n}{p_n} = 1 / \iint \left( \frac{v}{p} \right) dA \text{ (acoustical ohm).} \dagger$$

**\*24. Acoustical resistance ( $r_a$ ).** The real part of the acoustical impedance (acoustical ohm). It is associated with the dissipation of energy.

**\*25. Acoustical reactance ( $x_a$ ).** The imaginary part of the acoustical impedance (acoustical ohm). It is a wattless component and prevents the pressure and particle velocity being in phase.

†  $p$  and  $v$  must be in absolute units to obtain dyne sec. cm.<sup>-3</sup>.



- 26. Acoustical admittance** ( $1/z_a$ ). The reciprocal of the acoustical impedance (acoustical mho.)
- 27. Impedance per unit area** ( $z$ ). The complex quotient of the pressure and the particle velocity in a direction normal thereto ( $p/v$ ). When applied to a vibrator the radial velocity of the surface is intended.
- 28. Simulating impedance.** When the impedance per unit area of a sound source or the like cannot be found by rigorous methods, it is necessary to replace the source by a massless vibrator whose impedance per unit area can be evaluated. For example, the mouth of a horn might be replaced by a sphere one-half of which pulsates radially, whilst the other half is quiescent.
- 29. Accession to inertia** ( $m_i$ ). The additional mass or inertia of a vibrator due to the reciprocating flow of fluid in its neighbourhood.
- \*30. Mechanical impedance** ( $z_e$ ). The complex quotient of the driving force and the velocity it creates in the same direction at its point of application.† (Mechanical ohm or dyne cm.<sup>-1</sup> sec.)
- \*31. Mechanical resistance** ( $r_e$ ). The real part of the mechanical impedance. It is associated with dissipation of the energy supplied by the driver. (Mechanical ohm.)
- \*32. Mechanical reactance** ( $x_e$ ). The imaginary part of the mechanical impedance associated with a wattless component due to a mass or to fluid inertia. It causes the driving force to be out of phase with the velocity. (Mechanical ohm.)
- 33. Effective mass** ( $m_e$ ). The quotient of the mechanical reactance *at the driving point* and the pulsance  $\omega$ . It can be positive (mass), zero (resonance), or negative (stiffness). Curves showing the relationship between effective mass and frequency depend upon the position of the point of application of the driving force and its direction relative to some axis of the vibrator. For example, the effective mass of a centrally driven disk depends upon the direction of the drive relative to the axis. A different result is obtained if the drive is applied at some point between the centre and the edge. Accordingly, there is an infinite number of  $m_e$ -frequency curves for disks, cones, and

† The difference between acoustical and mechanical impedance must not be confused. In the one case waves travel in some form of conduit or channel which impedes their progress. The greater the area the smaller the impedance. In the mechanical form something is being driven, so the greater the area driving the medium the greater the impedance opposing motion.

the like. Unless otherwise stated a central axial drive is intended. (Gramme).

**34. Equivalent mass ( $m_q$ ).** The rigid mass which, when it moves with the same velocity as the point of maximum amplitude of a vibrator, has the same kinetic energy as the whole vibrator. (Gramme.)

**35. Stiffness ( $s$ ).** The static force required to cause a linear displacement of 1 unit (cm.), if the stressed structure were truly elastic over this range. In practice it is the slope of the force-displacement curve usually referred to the linear portion. (Dyne cm.<sup>-1</sup>.)

**36. Compliance ( $1/s$ ).** The reciprocal of the stiffness.

**37. Dynamic deformation curve.** The shape of a vibrator during vibration. In a rigorous sense the deformation refers to a 'surface'. When the vibrator is symmetrical about an axis, the dynamic deformation curve is the shape of a section by an axial plane.

**38. Electrical motional impedance ( $Z_m$ ).** The difference in electrical impedance of a sound reproducer or the like when the driving element is free and when it is fixed. It can be measured in a fluid or *in vacuo*. (Ohm.)  $Z_m = R_m + i\omega L_m$ .

**39. Motional inductance ( $L_m$ ).** The difference in inductance of a sound reproducer or the like when the driving agent is free and fixed. (Henry.)

**40. Motional capacitance ( $C_m$ ).** The capacitance concomitant with motion of the driving element of a sound reproducer due to its association with an electromagnetic or an electrostatic field. Its value can be found from the motional inductance since  $C_m = -1/\omega^2 L_m$ . (Farad.)

**41. Electrical motional resistance ( $R_m$ ).** The difference in electrical resistance of a sound reproducer or the like when the driving agent is free and when it is fixed. It includes the influence of mechanical loss and sound radiation. (Ohm.)

**42. Electrical radiation resistance ( $R_r$ ).** That portion of the electrical motional resistance due to the radiation of sound. (Ohm.)

**43. Electromechanical conversion factor ( $C^2$ ).** A factor used to convert an electrical quantity into its mechanical equivalent, and vice versa. In a moving-coil system  $z_e Z_m = C^2$  (Chap. VII), this being the square of the product of the length of wire and the mean magnetic flux density in the air-gap of the magnet  $(2\pi r n B_g)^2$  in absolute electro-

magnetic units.  $C$  is also the mechanical force on the coil per unit current (abs.): or the e.m.f. induced in the coil per unit axial velocity. (See Chap. VII.)

**44. Transient wave-form.** A species of wave-form which never attains the steady or continuous periodic state. A growth or 'start' transient occurs when an e.m.f. is applied to a reactive circuit, whilst a decay or 'stop' transient occurs when the current is interrupted by breaking the circuit. Effects of a similar nature occur with mechanical vibrators.

#### 45. Electrical and mechanical analogues

In the design of sound-reproducing apparatus and in the solution of various problems in the domain of acoustics it is often of material assistance to conduct the analysis in electrical terms and then transform to the mechanical ones. The necessary electrical quantities and their mechanical analogues are tabulated below:

<i>Electrical.</i>	<i>Mechanical.</i>
Voltage $E$	Force $f$ (dynes)
Current $I$	Velocity $u, v, \dot{\xi}$ (cm. sec. <sup>-1</sup> )
Quantity $Q$	Displacement $\xi$ (cm.)
Resistance $R$	Resistance $r$ (dyne sec. cm. <sup>-1</sup> )
Reactance $X$	Reactance $x$ (dyne sec. cm. <sup>-1</sup> )
Impedance $Z$	Impedance $z$ (dyne sec. cm. <sup>-1</sup> )
Inductance $L$	Mass $m$ (gm.)
Capacitance $C$	Compliance $1/s$ (cm. dyne <sup>-1</sup> )
1/Capacitance $1/C$	Stiffness $s$ (dyne cm. <sup>-1</sup> )
$Z = R + i\omega L$	$z = r + i\omega m$
$= R + iX$	$= r + ix$
$Z^2 = R^2 + (\omega L - 1/\omega C)^2$	$z^2 = r^2 + (\omega m - s/\omega)^2$
$E = IZ$	$f = vz = \omega\xi z = \dot{\xi}z$
$P = I^2R$	$P = v^2r = \omega^2\xi^2r = \dot{\xi}^2r$
$= (E^2/Z^2)R$	$= (f^2/z^2)r.$

The electrical quantities are preferably expressed in absolute electromagnetic units, but they can be, and often are, expressed in the practical or derived units volt, ampere, etc. Under the latter régime care must be exercised in transcribing from the electrical to the mechanical system, particularly when the two systems are interconnected. For example, in a hornless moving-coil speaker the

motional capacitance due to the coil vibrating in the magnetic field is  $C_m = m/C^2$ , where  $m$  is the total mass and  $C^2$  the electromechanical conversion factor (see definition 43). If  $m = 25$  gm. and  $C^2 = 10^{13}$ , the value of  $C_m$  is  $2.5 \times 10^{-12}$  absolute electromagnetic units. Since 1 farad is  $10^{-9}$  absolute e.m. units, the capacity is  $2.5 \times 10^3$  microfarads.

#### 46. The decibel

The unit of sound pressure is 1 dyne cm.<sup>-2</sup>, which is about  $10^{-6}$  the normal atmospheric pressure. Since the perceived intensity of sound is a relative thing, a unit is required which gives some conception of comparative loudness. Experimental measurements pertaining to the human ear indicate that variation in the perceived loudness of sound follows a logarithmic law approximately. If a pure note of  $500 \sim$  is sounded at a certain audible intensity (dynes cm.<sup>-2</sup>), it is heard by an observer at a definite loudness level. To increase the loudness level by a perceptible amount the acoustic power  $P$  must be augmented  $\varphi$  times, where  $\varphi$  can be determined by experiment. If the first loudness level is  $l$  and the second  $ml$ , the power densities in a room are  $P$  and  $\varphi P$ . Starting with  $ml$  and  $\varphi P$  as a new datum, let the loudness level again be augmented by  $ml$ . The two quantities are now  $2ml$  and  $\varphi(\varphi P) = \varphi^2 P$  respectively. The power corresponding to an  $n$ -fold increase in loudness level at  $m$  units a step is evidently  $P_n = P\varphi^n$ . Thus, taking logarithms, the number of degrees increase in loudness level corresponding to  $P_n$  is

$$n = \frac{\log_{10}(P_n/P)}{\log_{10} \varphi}.$$

For convenience  $\varphi$  is taken as 10, so  $n = \log_{10}(P_n/P)$ . The unit so obtained is termed the 'bel' after Graham Bell the inventor of the telephone. This being too large for most practical purposes it is customary to use the deci-bel. Thus  $n = 10 \log_{10}(P_n/P)$  decibels. The bel or the decibel is devoid of dimensions since it is the logarithm of a power ratio.

To put the preceding into more concrete form suppose we take an example. In loud speakers the power output for specified conditions varies with the frequency. If at  $1,500 \sim$ ,  $P = 15$  milliwatts, whilst at  $2,000 \sim$ ,  $P = 60$  milliwatts, the level at the latter frequency is then  $10 \log_{10}(60/15) = 6$  decibels above that at  $1,500 \sim$ . At any frequency a minimum variation in level is required before it can be detected by ear. The change in loudness level depends upon both intensity level and frequency. A common average figure is from 2 to 3 decibels, i.e.

a power ratio of 1.6 to 2. At frequencies below 200 ~ more than this is required, but it depends upon circumstances, e.g. the presence of other tones.

#### **47. Analytical substitute for conical shell**

The acoustical behaviour of a conical shell with or without a baffle (definition 22) has not yielded to analytical treatment yet. In problems associated with (a) sound pressure on vibrating surfaces, (b) power radiated at low frequencies, (c) spatial distribution and the like, it is convenient to replace the cone by a rigid circular disk vibrating in a rigid plane of infinite extent. The latter combination can be treated analytically. This is also a useful artifice in deriving the theory of coil-driven diaphragms. A cone with a finite baffle can be represented approximately at low frequencies by two spherical caps vibrating in the same direction at opposite ends of a diameter.

## II

### PRINCIPLES OF SOUND PROPAGATION

#### 1. Introduction

When a body of any shape whatsoever vibrates harmonically in a fluid of infinite extent, longitudinal waves are propagated outwards at the frequency of vibration. During wave transmission the fluid, in contiguous half wave-lengths, is condensed and rarefied cyclically. From an analytical viewpoint these states are identical except in regard to sign. From hydrostatical principles we know that if an excess (+ or -) pressure occurs at any point in a fluid, it is felt everywhere, i.e. it spreads out so to speak in every direction, just as a gas expands to fill a vessel into which it discharges. Consequently the excess pressure due to longitudinal waves caused by a vibrating body is transmitted in all directions. If we imagine a very small radially-pulsating sphere situated in the fluid, its pulsations spread out spherically and affect the whole space occupied by the fluid. The power transmitted through any concentric spherical surface is constant, and since the superficial area is  $4\pi r^2$  the power per unit surface varies as  $1/r^2$ . When  $r$  is large enough, the power is so small that the vibrations are undetectable. Expressed analytically the excess pressure at an infinite distance is evanescent.

During the passage of waves past any point in the fluid, the particles of which we conceive it to be constituted are in vibration. The greater the amplitude the larger the excess pressure. The particles are assumed to move to and fro along the direction of the wave.

We can commence with elementary physical facts pertaining to a fluid. If these are expressed in analytical form, it is possible to make calculations relating to the propagation of sound waves from vibrating bodies of different shapes. First of all we have to establish a form of stress-strain relationship. During wave transmission the density varies due to fluctuation in pressure. If  $\rho_0$  is the density in the undisturbed state and  $\rho$  the value at any epoch during transmission, the ratio

$$\frac{\rho - \rho_0}{\rho_0} = \frac{\delta\rho}{\rho_0} = s$$

is termed the *condensation*. From this we have

$$\rho = \rho_0(1 + s). \quad (1)$$

It should be observed that  $\delta\rho$  is not necessarily infinitesimal. In many propagation problems it is finite although only a small fraction of  $\rho_0$ . The change in density is accompanied by a corresponding alteration in volume, so we get

$$\frac{V-V_0}{V_0} = \frac{\delta V}{V_0} = \Delta,$$

the *dilatation* or change in volume per unit volume.

$$\text{Thus} \quad V = V_0(1+\Delta). \quad (2)$$

In any gas  $\rho V = \rho_0 V_0$ , which by aid of (1) and (2) gives

$$(1+s)(1+\Delta) = 1. \quad (3)$$

Provided  $s$  and  $\Delta \ll 1$ , (3) gives  $s = -\Delta$  which means that the characteristic of the medium for small variations in density and volume is sensibly linear.

In a fluid under pressure we can write

$$\frac{\text{stress}}{\kappa} = \text{volumetric strain} = -\frac{\delta V}{V_0}, \quad (4)$$

where  $\kappa$  is the bulk modulus or coefficient of cubical elasticity. Now stress is force per unit area =  $\delta p$ , so we have

$$\kappa = -\frac{V_0}{\delta V} \delta p = \frac{\delta p}{s}, \quad (5)$$

where  $\delta p$  is not necessarily infinitesimal. Since the gas law is of the form  $pV^n = \text{const.}$ , to secure constancy of  $\kappa$ ,  $\delta p$  must be a very small proportion of the steady pressure to which the fluid is subjected. But  $\delta p = p - p_0$ , so the total pressure is

$$p = p_0 + \kappa s. \quad (6)$$

Using the value of  $s$  from (1), we can write

$$p = p_0 + \kappa \left( \frac{\rho}{\rho_0} - 1 \right). \quad (7)$$

Formulae (6) and (7) are applicable, for a constant value of  $\kappa$ , when the variation in density and, therefore, the value of  $s$ , is small enough to preserve a linear characteristic, i.e. the working arc of the pressure-volume curve of the gas is small enough to be regarded as a straight line. In a rigorous sense an infinitesimal amplitude is implied.

## 2. Plane sound waves of infinitesimal amplitude

Since the bulk modulus of an incompressible fluid is infinitely large, so also is the velocity of propagation, provided the density is finite.

Consequently, the excess pressure due to vibration in the fluid is felt everywhere instantaneously. We know from experiments relating to Boyle's law or from various common devices, e.g. cycle or car tyre pumps, that air is readily compressed. This precludes the possibility of high velocities of propagation. If the velocity were thirty times its normal value, the well-known focusing of sound radiation from loud speakers would not occur in the audible frequency range.

A hypothetical train of plane waves is one which extends indefinitely in both directions, its front being plane, and its velocity

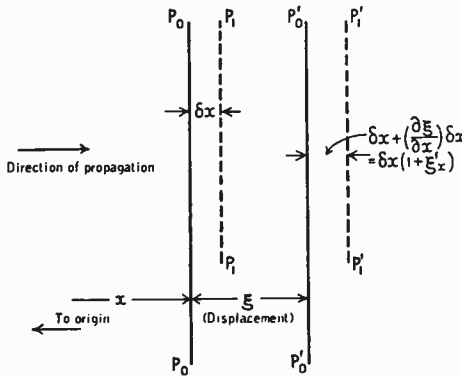


FIG. 1

constant. Expansion does not occur, and in the absence of dissipation its amplitude is maintained at a definite value. In practical acoustics, where sources are relatively small, plane waves in a rigorous sense do not exist. But over restricted distances there are cases where the propagation is approximately plane, although the pressure decreases with increasing distance, e.g.  $p \propto 1/r$

Referring to Fig. 1, consider a plane  $P_0P_0$  perpendicular to the paper situated at a distance  $x$  from a hypothetical source of plane waves. The air particles oscillate normal to  $P_0P_0$ , which is their mean position. At the instant depicted in the diagram the particles originally at  $P_0P_0$ , are shown at  $P'_0P'_0$ , which is distant  $\xi$  from  $P_0P_0$ . They are travelling towards the left. The particles initially at  $P_1P_1$  are now at  $P'_1P'_1$ .

The distance  $P_0P_1$ , originally  $\delta x$ , is now  $P'_0P'_1 = \delta x + \delta x(\partial \xi / \partial x)$ , where  $\partial \xi / \partial x$  is the rate at which  $\xi$  changes with distance  $x$ . Since there is no lateral expansion, the mass of fluid per unit area between



the planes  $P_0P_1$  is the same as that between  $P'_1P'_0$ , its density  $\rho$  must be less than its undisturbed value  $\rho_0$ .

$$\text{Thus } \rho \left( 1 + \frac{\partial \xi}{\partial x} \right) \delta x = \rho_0 \delta x, \text{ so } \rho = \rho_0 \left/ \left( 1 + \frac{\partial \xi}{\partial x} \right) \right. \quad (8)$$

this being known as the equation of continuity. Considering the forces acting on unit area of the plane, we have

force = mass  $\times$  acceleration

$$\delta p = -\rho_0 \delta x \frac{\partial^2 \xi}{\partial t^2},$$

$$\text{so } -\frac{1}{\rho_0} \frac{\partial p}{\partial x} = \frac{\partial^2 \xi}{\partial t^2}. \quad (9)^*$$

$$\text{If } \xi'_x = \frac{\partial \xi}{\partial x}, \quad \xi''_x = \frac{\partial^2 \xi}{\partial x^2},$$

then from (8)

$$\rho = \rho_0 / (1 + \xi'_x) \quad \text{or} \quad (1 + \xi'_x) = \rho_0 / \rho, \quad (10)$$

$$\text{so } \frac{\partial \rho}{\partial x} = -\rho_0 \frac{\xi''_x}{(1 + \xi'_x)^2}. \quad (11)$$

$$\text{From (10) and (11)} \quad -\frac{1}{\rho_0} \frac{\partial \rho}{\partial x} = \left( \frac{\rho}{\rho_0} \right)^2 \xi''_x. \quad (12)$$

Multiplying both sides of (12) by  $\partial p / \partial \rho$  we obtain

$$-\frac{1}{\rho_0} \frac{\partial p}{\partial x} = \left( \frac{\rho}{\rho_0} \right)^2 \frac{\partial p}{\partial \rho} \xi''_x. \quad (13)$$

Equating (9) and (13) we get

$$\frac{\partial^2 \xi}{\partial t^2} = \left( \frac{\rho}{\rho_0} \right)^2 \frac{\partial p}{\partial \rho} \frac{\partial^2 \xi}{\partial x^2}. \quad (14)$$

This equation is valid for any amplitude whatever be the relationship between pressure and volume, e.g.  $pV = \text{const.}$ ,  $pV^\gamma = \text{const.}$

From (7) by partial differentiation,  $\partial p / \partial \rho = \kappa / \rho_0$ , whilst in (14)  $\rho = \rho_0$  when the pressure variation is infinitesimal. Thus from (14) we obtain, under the latter condition [216],†

$$\frac{\partial^2 \xi}{\partial t^2} = c^2 \frac{\partial^2 \xi}{\partial x^2}, \quad (15)$$

where  $c^2 = \kappa / \rho_0$ .

\* Since  $p = p + p_0$ ,  $\partial p = \partial p$  and the latter has been used frequently in what follows.

† All numbers in square brackets denote the reference list at the end of the book.

The complete solution of (15) is

$$\begin{aligned}\xi &= f_1(w) + f_2(z) \\ &= f_1(x-ct) + f_2(x+ct),\end{aligned}\quad (16)$$

where  $f_1$  and  $f_2$  are arbitrary functions of  $x$  and  $t$ .

Formula (16) gives the displacement of a particle, at any time  $t$ , whose undisturbed distance from the origin is  $x$ . Obviously the dimensions of  $ct$  are the same as those of  $x$ , which implies that  $c$  is a velocity. Taking the term  $f_1(x-ct)$ , if  $t$  increases by  $t_1$  and  $x$  by  $ct_1$  we get  $f_1[x+ct_1-c(t+t_1)] = f_1(x-ct)$  so that  $\xi$  is unaltered. Hence  $f_1(x-ct)$  represents a wave travelling in the positive direction of  $x$  with velocity  $c$ . Similarly  $f_2(x+ct)$  represents a wave travelling in the reverse direction. With the latter we are not immediately concerned, so that for our particular purpose the solution of (15) is  $\xi = f_1(x-ct)$ . This represents the form of the disturbance at the source. If the latter is harmonic, we can write the particle displacement from its central position at  $x$  as

$$\xi = \xi_0 \cos(kx - \omega t) = \xi_0 \cos(\omega t - kx). \quad (17)$$

At any time  $t$  the wave form is given by  $\xi = \xi_0 \cos(kx - \alpha)$ , where  $\alpha = \omega t$ , so the wave-length  $\lambda = 2\pi/k$ . Since the velocity  $c = \lambda f$ , it follows that  $k = \omega/c = 2\pi/\lambda$ .

Differentiating (17) twice we get

$$\frac{\partial^2 \xi}{\partial x^2} = -k^2 \xi_0 \cos(kx - \omega t) \quad (18)$$

and 
$$\frac{\partial^2 \xi}{\partial t^2} = -\omega^2 \xi_0 \cos(kx - \omega t). \quad (19)$$

It follows from (18) and (19) that

$$\frac{\partial^2 \xi}{\partial t^2} = c^2 \frac{\partial^2 \xi}{\partial x^2}. \quad (20)$$

Thus (15) is reproduced, as it always will be, whatever function is employed to represent the wave form.\*

### 3. Three-dimensional sound waves of infinitesimal amplitude

Consider a very small parallelepiped or box of volume  $\delta x \delta y \delta z$  at some point in a fluid (Fig. 2), through which longitudinal waves are travelling. The fluid in the parallelepiped is in motion. Sometimes it is rarefied, at others condensed. Consequently the density varies, and

\* This explains in a concrete way, the meaning of 'arbitrary function'.

since the volume is unaltered, its mass changes cyclically. There are two variables, (1) the density, (2) the particle velocity. The coordinates of the point  $A$  on the parallelepiped being  $x, y, z$  with reference to some suitable origin  $O$ , let the particle velocities parallel to the three axes be  $u, v, w$ , respectively. The foundation of an analytical relationship between the quantities involved is the constancy of volume  $\delta x \delta y \delta z$ . The mass of fluid lost per unit time at any epoch is the product of volume and change in density per unit time. Thus the rate of mass change of the volume  $\delta x \delta y \delta z$  is

$$-\frac{\partial \rho}{\partial t} (\delta x \delta y \delta z), \quad (21)$$

where the negative sign indicates decrease of density with time.

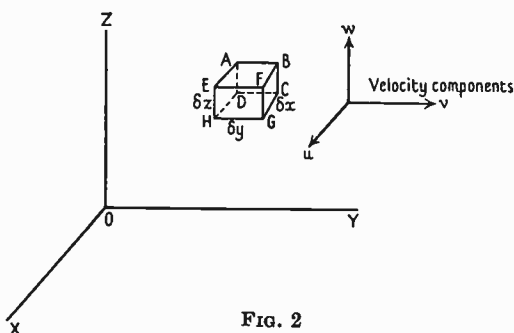


FIG. 2

Now consider the fluid flow into and out of the faces of the parallelepiped. Owing to change in density and velocity over the length  $\delta x$ , the amount entering  $ABCD$  differs from that leaving  $EFGH$ . The mass flow per second at  $ABCD$  into the parallelepiped is the product of area, particle velocity, and density, namely,

$$\delta y \delta z (\rho u). \quad (22)$$

If the rate of change of velocity-density with distance is  $\partial(\rho u)/\partial x$ , the change in mass per second per unit area in the length  $\delta x$  is  $\frac{\partial(\rho u)}{\partial x} \delta x$ .

Thus the mass flow per second through  $EFGH$  out of the parallelepiped becomes

$$\delta y \delta z (\rho u) + \frac{\partial(\rho u)}{\partial x} (\delta x \delta y \delta z). \quad (23)$$

The difference between (22) and (23), namely,  $\frac{\partial(\rho u)}{\partial x} (\delta x \delta y \delta z)$  is the

difference in the mass of fluid entering and leaving the parallelepiped in the direction of the  $x$ -axis. Similarly the variations along the  $y$ - and  $z$ -axes are  $\frac{\partial(\rho v)}{\partial y}(\delta x \delta y \delta z)$  and  $\frac{\partial(\rho w)}{\partial z}(\delta x \delta y \delta z)$ , respectively. Thus by addition the total mass flowing out of the parallelepiped per second is

$$\left[ \frac{\partial(\rho u)}{\partial x} + \frac{\partial(\rho v)}{\partial y} + \frac{\partial(\rho w)}{\partial z} \right] (\delta x \delta y \delta z).$$

Since this is equal to the rate of decrease of mass within the parallelepiped, using (21), we have

$$\left[ \frac{\partial(\rho u)}{\partial x} + \frac{\partial(\rho v)}{\partial y} + \frac{\partial(\rho w)}{\partial z} \right] (\delta x \delta y \delta z) = -\frac{\partial \rho}{\partial t} (\delta x \delta y \delta z). \quad (24)$$

Hence

$$\frac{\partial(\rho u)}{\partial x} + \frac{\partial(\rho v)}{\partial y} + \frac{\partial(\rho w)}{\partial z} = -\frac{\partial \rho}{\partial t}. \quad (25)$$

The relationship in (25) is known as the equation of *continuity* [219]. In this equation there are no restrictions regarding the amplitude of the sound waves. When the latter is infinitesimal, we have from (1) by differentiation,  $\frac{\partial \rho}{\partial t} = \rho_0 \frac{\partial s}{\partial t}$ , and in (25)  $\rho = \rho_0$ , so

$\frac{\partial(\rho u)}{\partial x} = \rho_0 \frac{\partial u}{\partial x}$ . Thus for infinitesimal amplitudes (25) can be written

$$-\Phi' = \frac{\partial u}{\partial x} + \frac{\partial v}{\partial y} + \frac{\partial w}{\partial z} = -\frac{\partial s}{\partial t}, \quad (26)$$

this being another form of the equation of continuity which we shall require later on. ( $-\Phi'$  is the flux change per unit vol., see def. 21.)

#### 4. Equations of motion

The variation in pressure along the  $x$ -axis of the parallelepiped in

Fig. 2 is  $\frac{\partial p}{\partial x} \delta x$ , so the resultant force on the parallelepiped in the

direction of  $x$  is  $-\frac{\partial p}{\partial x}(\delta x \delta y \delta z)$ . The mass of fluid subjected to this pressure is  $\rho(\delta x \delta y \delta z)$ , the acceleration parallel to the  $x$ -axis being  $\partial u / \partial t$  provided the particle velocity is small.\*

Since force = mass  $\times$  acceleration, we have

$$-\frac{\partial p}{\partial x} = \rho \frac{\partial u}{\partial t} \quad (27)$$

with similar expressions for the  $y$ - and  $z$ -axes.

\* When  $u$  is not small, i.e. for finite amplitudes, the acceleration is  $\frac{\partial u}{\partial t} + u \frac{\partial u}{\partial x}$ .

From (6) by differentiation  $\frac{\partial p}{\partial x} = \kappa \frac{\partial s}{\partial x}$  provided  $s$  is small enough for  $\kappa$  to be constant. Substituting this value in (27) and putting  $\rho = \rho_0$ , we get

$$\frac{\partial u}{\partial t} = -\frac{\kappa}{\rho_0} \frac{\partial s}{\partial x} = -c^2 \frac{\partial s}{\partial x} = -\frac{1}{\rho_0} \frac{\partial p}{\partial x}, \quad (28)$$

since  $\kappa/\rho_0 = c^2$  for infinitesimal amplitudes. The expressions involving  $y$  and  $z$  are similar to (28).

### 5. Velocity potential ( $\phi$ )

Before going further it is necessary to introduce a new function termed the velocity potential. It was first introduced into hydrodynamical problems over a century ago by Lagrange. By definition we have

$$u = -\frac{\partial \phi}{\partial x}, \quad (29)$$

where  $\phi$  is the velocity potential and  $u$  is the particle velocity parallel to the  $x$ -axis. The expressions for the velocity components  $v$  and  $w$  are similar. An electrical illustration may clarify the situation. Consider the flow of current in a purely resistive conductor. If the resistance per unit length is  $R$ , the resistance of a length  $\partial x$  is  $R \partial x$ , the voltage drop due to a current  $I$  being

$$\partial E = -RI \partial x.$$

Thus if  $R$  is unity

$$I = -\frac{\partial E}{\partial x},$$

so that on comparison with (29),  $I$  is equivalent to the particle velocity and  $E$  to the velocity potential. A formula of type (29) is valid, i.e. a velocity potential  $\phi$  exists, when viscosity and heat conduction are neglected, and the motion is assumed to be started by mechanical forces having a potential energy function [216].

### 6. Pressure at any point in fluid

From (28)  $-\frac{\partial p}{\partial x} = \rho_0 \frac{\partial u}{\partial t}$ , and from (29)  $u = -\frac{\partial \phi}{\partial x}$ ,

$$\text{so} \quad \frac{\partial p}{\partial x} = \rho_0 \frac{\partial^2 \phi}{\partial x \partial t} = \rho_0 \frac{\partial}{\partial x} \left( \frac{\partial \phi}{\partial t} \right). \quad (30)$$

Integrating (30) we get  $p = \rho_0 \frac{\partial \phi}{\partial t} + \text{const.}^*$  When the fluid is in a quiescent state we can put  $\phi = 0$ , so that  $\partial \phi / \partial t = 0$  and  $p = p_0$  the normal atmospheric pressure. Hence  $p = \rho_0 \frac{\partial \phi}{\partial t} + p_0$  and the excess pressure

$$p = \rho_0 \frac{\partial \phi}{\partial t}. \quad (31)$$

This is an important relationship which is valid for infinitesimal amplitudes.

### 7. The equation for $\phi$

From (28) and (30)  $c^2 \frac{\partial \mathbf{s}}{\partial x} = \frac{\partial}{\partial x} \left( \frac{\partial \phi}{\partial t} \right)$ , and by integration,

$$c^2 \mathbf{s} = \frac{\partial \phi}{\partial t} + \text{const.}, \dagger$$

whence 
$$\frac{\partial \mathbf{s}}{\partial t} = \frac{1}{c^2} \frac{\partial^2 \phi}{\partial t^2}. \quad (32)$$

Since  $u = -\partial \phi / \partial x$ ,  $v = -\partial \phi / \partial y$  and  $w = -\partial \phi / \partial z$ , we have from (26) and (32)

$$-\left[ \frac{\partial^2 \phi}{\partial x^2} + \frac{\partial^2 \phi}{\partial y^2} + \frac{\partial^2 \phi}{\partial z^2} \right] = -\frac{1}{c^2} \frac{\partial^2 \phi}{\partial t^2} = -\Phi' \quad (32a)$$

or 
$$\nabla^2 \phi - \frac{1}{c^2} \frac{\partial^2 \phi}{\partial t^2} = 0, \quad (33)$$

where 
$$\nabla^2 = \frac{\partial^2}{\partial x^2} + \frac{\partial^2}{\partial y^2} + \frac{\partial^2}{\partial z^2}.$$

The condition expressed in (33) must be satisfied at every point in a fluid through which sound waves are transmitted [219]. If the differentials in  $y$  and  $z$  are omitted from the left-hand side of equation (32 a), we obtain

$$\frac{\partial^2 \phi}{\partial t^2} = c^2 \frac{\partial^2 \phi}{\partial x^2}, \quad (34)$$

which is identical with (15) excepting that  $\xi$  is replaced by  $\phi$ . Thus (34) represents the condition to be satisfied in plane wave propagation.

For sinusoidal motion  $\phi = \phi_1 \cos \omega t$  and  $\partial^2 \phi / \partial t^2 = -\omega^2 \phi$ .

\* Strictly this should be  $p = \rho_0 \frac{\partial \phi}{\partial t} + f(t) + \text{const.}$ , but in the present instance a function independent of  $x$  is not required.

† See footnote to § 6.

Substituting this in (33) we get

$$\frac{\partial^2 \phi}{\partial x^2} + \frac{\partial^2 \phi}{\partial y^2} + \frac{\partial^2 \phi}{\partial z^2} + k^2 \phi = 0. \quad (35)$$

Written in Laplacian notation (35) becomes

$$(\nabla^2 + k^2)\phi = 0, \quad (36)$$

and this is the condition to be satisfied everywhere in the fluid when the pressure variations are infinitesimal and harmonic.

### 8. Solution of $(\nabla^2 + k^2)\phi = 0$ for spherical vibrations

The simplest vibrations with which we can deal pertain to a sphere. By varying its radius or making it vibrate in different ways, a considerable amount of information can be obtained which is of service in the design and operation of loud speakers. Since we are concerned with surface vibrations only, it is now necessary to deduce an expression for the velocity potential at any point in the fluid, due to vibration of the sphere. Consider Fig. 3 where the source is a sphere of radius  $a$  whose centre is  $O$ . Let  $P_1$  be an arbitrary point, on an outer concentric spherical surface of radius  $r$ , whose rectangular coordinates with respect to the centre as origin are  $x, y, z$ . Then we have to determine  $\phi$  to satisfy (36). The first step is to transform to spherical coordinates, namely  $r, \theta, \chi$ , where  $x = r \sin \theta \cos \chi$ ,  $y = r \sin \theta \sin \chi$ ,  $z = r \cos \theta$  (see Fig. 3). If we proceed on analytical lines to effect the transformation from rectangular to polar coordinates, the work will be tedious and protracted. It is simpler to establish the required condition regarding  $\phi$ , *ab initio*, from purely physical considerations. In Fig. 4  $ABCD$  is an elemental area  $\delta A$  on a spherical surface, the particle velocity normal thereto being  $v_n$ . The 'flux', or volume of fluid flowing per unit time through  $\delta A$  is  $v_n \delta A = -\delta A (\partial \phi / \partial n)$  from (29), where  $n$  is written to signify that the direction is along the normal to the surface. Since we established (36) on the basis that  $\rho = \rho_0$ , we now regard the variation in density across an elemental volume to be negligible. The variables are, therefore, the particle velocity  $-\partial \phi / \partial n$  and the area  $\delta A$ , both of which alter progressively as the fluid passes from one area  $\delta A$  ( $ABCD$ ) to another  $\delta A_1$  ( $EFGH$ , Fig. 4). The difference in flux entering  $\delta A$  and that leaving  $\delta A_1$ , in the direction of the normal, is the product of length and flux change per unit length,  $\delta \Phi = -\frac{\partial}{\partial n} \left( \frac{\partial \phi}{\partial n} \delta A \right) \delta n$ . We have now to apply this formula to the

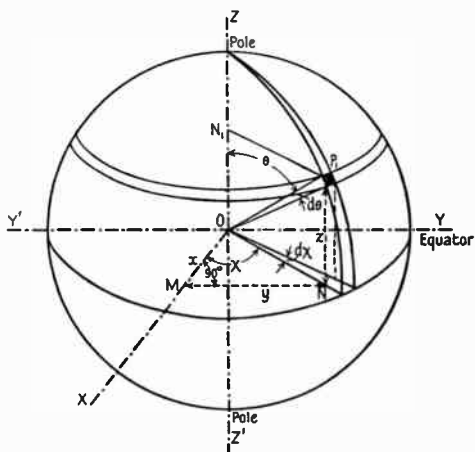


FIG. 3. Diagram illustrating spherical polar coordinates.

$ON = P_1 N_1 = r \sin \theta$ ;  $OM = x = r \sin \theta \cos \chi$ ;  $MN = y = r \sin \theta \sin \chi$ ;  
 $ON_1 = P_1 N = z = r \cos \theta$ ;  $OP_1 = r =$  radius of sphere;  $\theta =$  angle  $ZOP_1$ ;  
 $\chi =$  longitude. The area shown black is  $r \sin \theta d\chi \cdot r d\theta = r^2 \sin \theta d\theta d\chi$ .  
 Elementary zonal area =  $2\pi r^2 \sin \theta \cdot r d\theta = -2\pi r^2 d\mu$ ;  
 $\mu = \cos \theta$ .

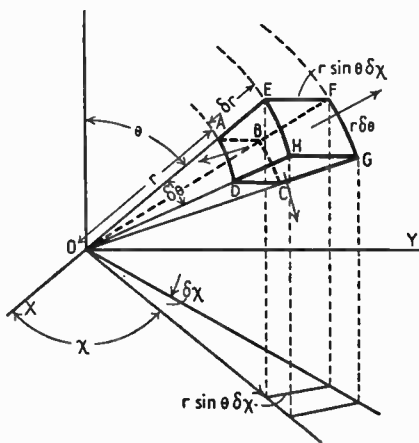


FIG. 4

elemental volume  $ABCDEFGH$  of Fig. 4. Taking the flux change across this volume in three mutually perpendicular directions we have for  $ABCD$ ,  $EF GH$ :

$$\delta A = r^2 \sin \theta \delta \theta \delta \chi,$$



$$\text{so } \delta\Phi_1 = -\frac{\partial}{\partial r} \left( \frac{\partial\phi}{\partial r} r^2 \sin\theta \delta\theta \delta\chi \right) \delta r, \quad (37)$$

where  $\delta r$  is now written for  $\delta n$ .

For *DCGH, ABFE*:

$$\delta A = r \sin\theta \delta r \delta\chi, \quad \partial n = r \partial\theta,$$

$$\text{so } \delta\Phi_2 = -\frac{\partial}{\partial\theta} \left( \frac{\partial\phi}{r\partial\theta} r \sin\theta \delta r \delta\chi \right) \delta\theta; \quad (38)$$

and for *BCGF, ADHE*:

$$\delta A = r \delta r \delta\theta, \quad \partial n = r \sin\theta \partial\chi,$$

$$\text{so } \delta\Phi_3 = -\frac{\partial}{\partial\chi} \left( \frac{\partial\phi}{r \sin\theta \partial\chi} r \delta r \delta\theta \right) \delta\chi. \quad (39)$$

Adding (37), (38), (39) and dividing by the elemental volume

$$r^2 \sin\theta \delta\theta \delta\chi \delta r,$$

we get

$$-\frac{1}{r^2} \left[ \frac{\partial}{\partial r} \left( r^2 \frac{\partial\phi}{\partial r} \right) + \frac{1}{\sin\theta} \frac{\partial}{\partial\theta} \left( \frac{\partial\phi}{\partial\theta} \sin\theta \right) + \frac{1}{\sin^2\theta} \left( \frac{\partial^2\phi}{\partial\chi^2} \right) \right] = -\Phi', \quad (40)$$

this being the flux change per unit volume. From (32 a) and (35)

$$\Phi' = \frac{1}{c^2} \frac{\partial^2\phi}{\partial t^2} = -k^2\phi$$

for harmonic motion, so that on expansion of the first term in (40) we obtain

$$r^2 \frac{\partial^2\phi}{\partial r^2} + 2r \frac{\partial\phi}{\partial r} + \frac{1}{\sin\theta} \frac{\partial}{\partial\theta} \left( \sin\theta \frac{\partial\phi}{\partial\theta} \right) + \frac{1}{\sin^2\theta} \left( \frac{\partial^2\phi}{\partial\chi^2} \right) + k^2 r^2 \phi = 0, \quad (41)$$

which is a well-known differential equation [217] of spherical harmonics.\* This equation is merely (33) expressed in spherical coordinates, and any sinusoidal value of  $\phi$  at a point in the fluid must satisfy it. To simplify (41) we can consider the case where  $\phi$  is symmetrical about the polar axis *ZOZ'* and does not vary with  $\chi$ . Then  $\partial^2\phi/\partial\chi^2 = 0$  and (41) degenerates to

$$r^2 \frac{\partial^2\phi}{\partial r^2} + 2r \frac{\partial\phi}{\partial r} + \frac{1}{\sin\theta} \frac{\partial}{\partial\theta} \left( \sin\theta \frac{\partial\phi}{\partial\theta} \right) + k^2 r^2 \phi = 0. \quad (42)$$

This equation is applicable when the vibration of a sphere is radial or axial. Its solution [217] involves zonal surface harmonics, or as they are usually designated, after their discoverer, Legendre functions. These functions are denoted by  $P_n(\mu)$ , where  $n$  signifies the order

\* From a physical viewpoint a spherical harmonic represents a sphere deformed in a certain way. It has nothing to do with frequency.

and  $\mu = \cos \theta$  (Fig. 3). In the solution,  $P_n(\mu)$  is associated with a complex constant, so that instead of using  $P_n(\mu)$  alone, we have  $S_n(\mu) = c_1 P_n(\mu)$ , where  $S_n(\mu)$  stands for a spherical harmonic of order  $n$  and  $c_1$  is of the form  $x + iy$ .\*

The value of  $\phi$  which satisfies (42) can be expressed as a series, or harmonic expansion, each term of which is separately a solution. Thus if  $\phi_n$  is proportional to the zonal harmonic of order  $n$ , the solution of (42) can be written [217]

$$\phi = \phi_0 + \phi_1 + \dots + \phi_n. \quad (43)$$

The orders of the harmonics which appear in any particular expansion are solely dependent upon the radial velocity of the spherical surface, i.e. its dynamic deformation curve (see definition 37). The solution of (42) [219] for order  $n$  is

$$\phi_n = \frac{1}{r} S_n(\mu) e^{-z} f_n(z) + \frac{1}{r} S_n^1(\mu) e^{z} f_n(-z), \quad (44)$$

where  $z^* = ikr$ ,  $r$  = distance of point from centre of sphere, and

$$f_n(z) = 1 + \frac{n(n+1)}{2} z^{-1} + \frac{(n-1)\dots(n+2)}{2.4} z^{-2} + \dots + \frac{1.2.3\dots 2n}{2.4.6\dots 2n} z^{-n}. \quad (45)$$

The first term in (44) refers to sound propagated outwards from the vibrating sphere, whilst the second represents radiation inwards. With the latter we are not concerned, so this radiation will be regarded as completely absorbed. Thus for our particular purpose

the solution of (42) is  $\sum_{n=0}^{\infty} \phi_n$ , where

$$\phi_n = \frac{S_n(\mu)}{r} e^{-z} f_n(z). \quad (46)$$

In this formula the spherical harmonic  $S_n(\mu)$  determines the influence of the angle  $\theta$  in Fig. 3 upon the value of  $\phi_n$ .

The solution of (42) can also be given in terms of Bessel functions whose order is half an odd integer, i.e.  $\pm(n + \frac{1}{2})$ , but the above form is more suitable for our purpose.

### 9. Relationship between $\phi$ and radial velocity of surface

The particle velocity due to the  $n$ th harmonic at a point distant  $r$  from the centre of the sphere is from (29) and (46)

$$v_n = -\frac{\partial \phi_n}{\partial r} = -\frac{\partial}{\partial r} \left( \frac{1}{r} S_n(\mu) e^{-z} f_n(z) \right). \quad (47)$$

\* These symbols must not be confused with the cartesian coordinates,  $x, y, z$ .

Remembering that  $S_n(\mu)$  is independent of  $r$  and that  $z = ikr$ , we get, on differentiating the bracketed quantity,

$$-\frac{\partial \phi_n}{\partial r} = + \frac{S_n(\mu)e^{-z}}{r^2} \{(1+z)f_n(z) - zf'_n(z)\}, \quad (48)$$

where 
$$f'_n(z) = \frac{\partial f_n(z)}{\partial z}. \quad (49)$$

Denoting the bracketed quantity in (48) by  $F_n(z)$

$$v_n = -\frac{\partial \phi_n}{\partial r} = \frac{S_n(\mu)e^{-z}}{r^2} F_n(z). \quad (50)$$

By virtue of the imaginary in  $e^{-z}$  and  $F_n(z)$ , the particle velocity is complex and appears in the form  $x+iy$ . At the surface  $-\partial\phi/\partial r$  is equal to the radial velocity of the sphere, and it can be represented by an harmonic expansion. Thus if  $u$  is the radial velocity at any point on the sphere, we have

$$u = u_0 + u_1 + \dots + u_n + \dots \quad (51)$$

which is akin to (43). In (51)  $u_n$  is proportional to the zonal harmonic of order  $n$ . Since  $u_n = v_n$  at the surface of the sphere where  $r = a$ , we have from (50)

$$u_n = \frac{S_n(\mu)}{a^2} e^{-ika} F_n(ika), \quad (52)$$

and, therefore, 
$$S_n(\mu) = + \frac{a^2 u_n e^{ika}}{F_n(ika)}, \quad (53)$$

where  $a$  is the radius of the sphere.

Substituting the value of  $S_n(\mu)$  from (53) in (46) we get \*

$$\phi_n = \frac{a^2}{r} e^{ik(a-r)} u_n \frac{f_n(ikr)}{F_n(ika)}, \quad (54)$$

this being the velocity potential due to the  $n$ th harmonic at a distance  $r$  from the centre of the sphere. At the surface,  $r = a$  and (54) reduces to

$$\phi_n = a u_n \zeta_n, \quad (55)$$

where  $\zeta_n = \frac{f_n(ika)}{F_n(ika)}$ , which is a factor depending upon the frequency of vibration and the order of the harmonic. Several of the functions  $f_n$  and  $F_n$  are given in Tables [219] 1 and 2.

\* When  $r$  is very great  $f_n(ikr) = 1$ .

TABLE 1

$$F_n(ikr) = x + iy; \quad \frac{1}{|F_n(ikr)|^2} = \frac{1}{x^2 + y^2}$$

$n$	$x$	$y$
0	1	$kr$
1	2	$kr - 2/kr$
2	$4 - 9/k^2r^2$	$kr - 9/kr$
3	$7 - 60/k^2r^2$	$kr - 27/kr + 60/k^2r^2$

TABLE 2

$$f_n(ikr) = x' + iy'. \quad \text{When } kr \text{ is very great } f_n(ikr) = 1.$$

$n$	$x'$	$y'$
0	1.0	0
1	1.0	$-1/kr$
2	$1 - 3/k^2r^2$	$-3/kr$
3	$1 - 15/k^2r^2$	$-6/kr + 15/k^2r^2$

From the preceding analysis it is clear that if  $u$  is the radial velocity of the sphere, it must be expressed as an harmonic expansion, so that on multiplication of each component by the appropriate factor [see (55)] and subsequent substitution in (42) the result is zero; that is to say, the condition  $(\nabla^2 + k^2)\phi = 0$  is satisfied for each individual harmonic.

Since the radial amplitude at any point of the spherical surface is proportional to the radial velocity  $u$ , it follows that if the zonal harmonics are plotted with respect to  $\mu$  or  $\theta$  and added, the result represents the dynamic deformation curve to some scale.

## 10. Formulae for zonal spherical harmonics (Legendre functions or polynomials)

TABLE 3

Formula	Order
$P_0 = 1$	Zeroth
$P_1 = \mu$	Unit
$P_2 = \frac{1}{2}(3\mu^2 - 1)$	Second
$P_3 = \frac{1}{2}(5\mu^3 - 3\mu)$	Third
$P_4 = \frac{1}{8}(35\mu^4 - 30\mu^2 + 3)$	Fourth
$P_5 = \frac{1}{8}(63\mu^5 - 70\mu^3 + 15\mu)$	Fifth
and so on.	
$\mu = \cos \theta$	

Polynomials of higher orders can be found by aid of the recurrence formula

$$P_{n+1}(\mu) = \left(\frac{2n+1}{n+1}\right)\mu P_n(\mu) - \left(\frac{n}{n+1}\right)P_{n-1}(\mu).$$

Harmonics of two orders are plotted in Fig. 5 A. The zeroth order corresponds to radial action of the sphere as a whole, since the deformation is identical every-

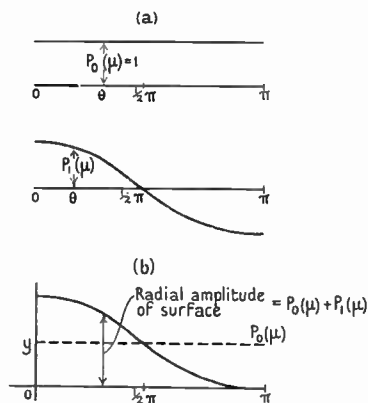


FIG. 5 A and B

where. Unit order yields a cosine curve and signifies that the axial velocity is constant, whilst the radial velocity varies as  $\mu = \cos \theta$ . Odd harmonics contain odd powers of  $\mu$ , and even harmonics even powers of  $\mu$ . Thus vibration of the sphere which is symmetrical about the equatorial plane (Fig. 3) entails even harmonics only. On the other hand, vibration of the sphere which is identical directionally in the two hemispheres, e.g. axial motions as a

whole, is associated exclusively with odd harmonics. Deformation of the surface corresponding to the sum of the zeroth and unit harmonics is portrayed in Fig. 5 B, this being  $P_0(\mu) + P_1(\mu)$ .

## 11. Expansion of radial velocity in zonal spherical harmonics

From (51) we have the radial velocity at any point on the sphere

$$u = u_0 + u_1 + \dots + u_n,$$

where  $u_n = A_n P_n(\mu)$ ,  $A_n$  being a constant to be determined. Thus we get

$$u = A_0 P_0(\mu) + A_1 P_1(\mu) + \dots + A_n P_n(\mu) + \dots \quad (56)$$

To find the  $n$ th coefficient  $A_n$  we proceed as with Fourier's series, i.e. multiply both sides of (56) by  $P_n(\mu) d\mu$  and integrate. Since  $\theta$  varies from 0 to  $\pi$  over the spherical surface,  $\cos \theta = \mu$  has limits  $\pm 1$ . Now

$$\int_{-1}^{+1} P_m(\mu) P_n(\mu) d\mu = 0$$

when  $m \neq n$  (compare the Fourier case). If  $m = n$  the above integral is  $1/(n + \frac{1}{2})$ , so

$$\int_{-1}^{+1} u P_n(\mu) d\mu = A_n \int_{-1}^{+1} [P_n(\mu)]^2 d\mu = \frac{A_n}{n + \frac{1}{2}}$$

or 
$$A_n = (n + \frac{1}{2}) \int_{-1}^{+1} u P_n(\mu) d\mu. \quad (57)$$

Thus the  $n$ th harmonic in the expansion of the radial velocity is

$$u_n = (n + \frac{1}{2}) P_n(\mu) \int_{-1}^{+1} u P_n(\mu) d\mu. \quad (58)$$

When the sphere is deformed over a portion of its surface only, the integral in (58) must be split up. If one hemisphere is quiescent,

$$u_n = (n + \frac{1}{2}) P_n(\mu) \int_0^1 u P_n(\mu) d\mu + 0. \quad (59)$$

We are now in a position to solve any problem relating to the vibration of a sphere which involves zonal surface harmonics.

## 12. Small spherical source. (Point source)

From (54) the velocity potential due to the harmonic of order zero which pertains to a radially pulsating sphere is

$$\phi = \frac{a^2}{r} e^{-ik(r-a)} U \frac{f_0(ikr)}{F_0(ika)}, \quad (60)$$

since  $u = u_0 = U$ . The value of  $\phi$  in (60) is the solution to (41) when the motion of the spherical surface is independent of  $\theta$  and  $\chi$ . We then have

$$\frac{\partial^2 \phi}{\partial r^2} + \frac{2}{r} \frac{\partial \phi}{\partial r} + k^2 \phi = 0. \quad (60a)*$$

From Table 2  $f_0(ikr) = 1$ , and since  $a$  is very small  $F_0(ika) = 1$ . Thus (60) can be written

$$\phi = \frac{a^2 U}{r} e^{-ik(r-a)}, \quad (61)$$

where  $U$  is the root mean square radial velocity of the surface pulsating harmonically. Now the area of the vibrating surface is  $4\pi a^2$ , whilst the flux or amount of fluid passing outwards per second is  $4\pi a^2 U = S$ , this velocity-area being known as the strength of the source.

\* The solution of (60a) is  $\phi = \frac{A_1 e^{-ikr}}{r} + \frac{B_1 e^{ikr}}{r}$ . The first term represents a diverging wave and the second a converging wave. For our purpose, therefore,  $\phi = \frac{A_1 e^{-ikr}}{r}$ ,  $A_1$  being found from the condition that the surface velocity  $U = \left(-\frac{\partial \phi}{\partial r}\right)_{r=a}$ . By taking  $ka \ll 1$ , (61) is reproduced.

From this relationship  $a^2 = S/4\pi U$ , which on substitution in (61) yields

$$\phi = \frac{S}{4\pi r} e^{-ik(r-a)}. \quad (62)$$

When  $a$  is evanescent, a so-called 'point source' is obtained and then

$$\phi = \frac{Se^{-ikr}}{4\pi r}. \quad (63)$$

The particle velocity at a point distant  $r$  is, from (29) and (63),

$$v = -\frac{\partial\phi}{\partial t} = \frac{S}{4\pi} e^{-ikr} \left[ \frac{ik}{r} + \frac{1}{r^2} \right], \quad (64)$$

or taking the modulus  $|v| = \frac{S}{4\pi} \sqrt{\left(\frac{k^2}{r^2} + \frac{1}{r^4}\right)}, \quad (65)$

this being the root mean square value.

From (31)  $p = \rho_0 \partial\phi/\partial t$ . To determine  $\partial\phi/\partial t$  the time factor  $e^{i\omega t}$  must be introduced, so we write (63) in the form

$$\phi = \frac{Se^{-i(kr-\omega t)}}{4\pi r}, \quad (66)$$

which is tacitly understood to hold in all our work.

Differentiating (66) with respect to  $t$  and then omitting the time factor, we obtain

$$p = i\rho_0 \omega \phi, \quad (67)$$

i.e.

$$p = \frac{i\rho_0 \omega S}{4\pi r} e^{-ikr}. \quad (67a)$$

### 13. Power radiated by simple source

The power passing radially through unit area on the surface of a sphere of radius  $r$ , whose centre is that of the source, is the product of pressure (67 a) and the component of the velocity *in phase* therewith (force  $\times$  distance per sec.). The required velocity is the term  $\frac{S}{4\pi} \frac{ik}{r}$  from (64), the distance phase factor  $e^{-ikr}$  being omitted.

Thus the power per unit area is  $\rho_0 \omega^2 S^2 / 16\pi^2 r^2 c$ , since  $k = \omega/c$ . The area of the spherical surface through which the radiation passes being  $4\pi r^2$ , the total power radiated is

$$P = \frac{\rho_0 \omega^2 S^2}{4\pi c}. \quad (68)$$

Writing  $S = UA = 4\pi a^2 \omega \xi_0$ , where  $\xi_0$  is the r.m.s. amplitude, by aid of (68) we obtain

$$P = \frac{4\pi\rho_0 a^4 \omega^4 \xi_0^2}{c}, \tag{69}$$

and this is the power radiated by a radially pulsating sphere of radius  $a$  provided  $ka \leq 0.25$ .

### 14. Deductions from foregoing analysis

From (64) it is seen that the particle velocity consists of two parts in time quadrature. Neglecting the factor  $e^{-ikr}$ , the part  $\frac{S ik}{4\pi r}$  is in phase with the pressure, whilst  $S/4\pi r^2$  is in quadrature. Near the source

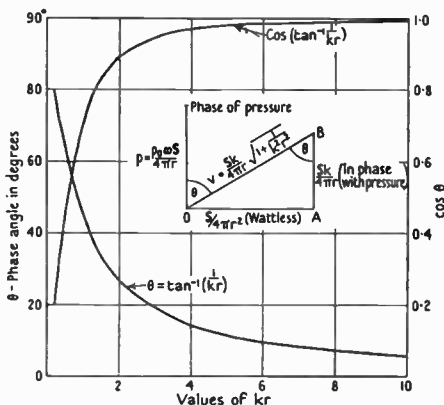


FIG. 6. Diagram illustrating relationship between the pressure and particle velocity in a spherical wave near the source.

the wattless component  $S/4\pi r^2$  preponderates since  $r^2 \ll r/k$ , the pressure and velocity being well out of phase. The angle between  $p$  and  $v$  is clearly  $\theta = \tan^{-1}(1/kr)$ , and the power factor is

$$\cos \theta = \cos \left( \tan^{-1} \frac{1}{kr} \right) = \frac{1}{\sqrt{\{1 + (1/k^2 r^2)\}}}$$

Curves illustrating this are given in Fig. 6. When  $\theta$  is small,

$$\theta = \frac{1}{kr} = \frac{\lambda}{2\pi r},$$

or  $r = \lambda/2\pi\theta$ . Now  $\cos \theta = 0.984$  when  $\theta = 10^\circ$ , so that  $r = 9\lambda/\pi^2$ , which means that for all practical purposes the pressure and particle



velocity are in phase one wave-length from the source. In evaluating the sound radiated by vibrators of various kinds, use is made of the fact that the pressure and particle velocity are *in phase* at a great distance from the source. In (64) by choosing  $r$  large enough, the first term can be made to swamp the second. Then omitting  $i$ ,  $v = kS/4\pi r$ ,  $p = \rho_0 \omega S/4\pi r$ , and since  $k = \omega/c$  it follows that  $p = \rho_0 cv$  when  $p$  and  $v$  are *in phase*. If  $v$  is the in-phase part of the velocity, the relationship is valid up to the source. Although the pressure and particle velocity fall out of phase as the source is approached, the power remains constant. From (67 a) and (68) we find that  $P = 4\pi r^2 p^2 / \rho_0 c$ , so that by placing a pressure-measuring device (a microphone) within a wave-length of the source,  $p$ , and therefore the power, can be found. For accurate results the microphone must be sufficiently small to leave the sound-field undisturbed. Also the distribution of radiation must be uniform, i.e. the source must be small compared with the wave-length (see Chap. V, § 1). The velocity component  $S/4\pi r^2$  from (64) is associated with a flow of fluid chiefly in the neighbourhood of the source. It is entirely wattless and merely adds to the inertia of the source, thereby reducing the driving force available for doing useful work.

In a rigorous sense the results in this section apply to a pulsating sphere when the wave-length is large compared with its radius  $a$ . The distance  $r$  is measured from the centre of the sphere and cannot be less than  $a$ . The analysis, however, can be used for a disk or a conical diaphragm provided  $\lambda \gg a$  and  $r \gg 10a$ .

### 15. Extension of 'tiny source' concept

So long as the dimensions of a vibrator are small compared with the wave-length, it can be regarded as a point source\* except in its immediate neighbourhood. This follows from the fact that the radiation due to any elemental area on the surface, assumed to act alone, is propagated uniformly into infinite space. Since the difference in distances from a remote point  $P_1$  to any two elemental areas on the vibrator is small compared with the wave-length, all pressures arrive

\* It is well to realize that this is merely a mathematical artifice. If the strength of the source  $S = UA$  is to remain finite, though very small, then since  $A \rightarrow 0$ ,  $U \rightarrow \infty$ , which would have disastrous consequences in practice! The point source is, therefore, applicable to infinitesimal amplitudes only. In considering a flat diaphragm or a conical diaphragm of radius  $a$  as a point source, formulae (63), (64), (67 a), and Fig. 6 are only applicable when  $r \gg 10a$ .

at  $P_1$  in substantially the same phase. Thus interference does not occur, and the point source concept is permissible. Formula (68) is valid provided  $\mathbf{S}$  represents the product of superficial area and radial velocity, the latter being constant in the cases considered hitherto. When  $u$  is variable, we have  $d\mathbf{S} = u dA$  as an elemental source, so the strength of the whole source is  $\mathbf{S} = \iint u dA$ . For example, in the case of a sphere one-half of which is quiescent, the other vibrating axially,  $u = U \cos \theta$  from 0 to  $\frac{1}{2}\pi$  and zero from  $\frac{1}{2}\pi$  to  $\pi$  (Fig. 20), so we get

$$\begin{aligned} \mathbf{S} &= 2\pi a^2 U \int_0^{\frac{1}{2}\pi} \cos \theta \sin \theta d\theta \\ &= \pi a^2 U = \frac{1}{2}UA = \pi a^2 \omega \xi_0, \end{aligned} \quad (70)$$

where  $\xi_0$  is the r.m.s. amplitude,  $\omega \xi_0 = U$ , and  $A$  is the superficial area of the hemisphere. From (68) and (70) the power radiated by the hemisphere is

$$P = \frac{\rho_0 \pi a^4 \omega^4 \xi_0^2}{4c}. \quad (71)$$

If the radiation from one side of a rigid disk or a conical shell of radius  $a$  is suppressed,  $\mathbf{S} = \pi a^2 U = \pi a^2 \omega \xi_0$  provided of course  $\lambda \gg a$ . The power radiated is therefore identical with that from an axially vibrating hemisphere as in (71). For *radial* vibration of the hemisphere the effective area is  $2\pi a^2$ , so  $\mathbf{S} = 2\pi a^2 \omega \xi_0$  and

$$P = \frac{\rho_0 \pi a^4 \omega^4 \xi_0^2}{c}, \quad (72)$$

this being one-quarter the power radiated if the whole sphere were in action radially. [Compare with (69) where  $\mathbf{S}$  has double the value given by (72).]

As a final example, take the case of two hemispheres vibrating in opposition at each end of a spherical diameter. The strength of the source is obviously double that of one hemisphere in (71), and the power four times as much, since from (68)  $P$  varies as  $\mathbf{S}^2$ . The result is therefore identical with (72) as might be anticipated, since the effective areas are equal. The preceding formulae for  $P$  are valid at low frequencies where the propagation is spherical. At higher frequencies the propagation departs from the spherical type and the formulae are no longer valid. It is then necessary to use spherical harmonic analysis as shown in Chapter VI.

### 16. Influence of solid angle

Hitherto we have confined our attention to radiation into spherical space, i.e. in all directions. Choosing the source as origin the solid angle into which it discharges is  $4\pi$ . Imagine a small rigid circular disk vibrating axially in an equal aperture in an infinite rigid plane.\* The solid angle into which each side of the disk radiates sound is  $2\pi$ . If  $S$  is now identical with that for one side of the disk without the plane, the particle velocity is doubled since diffusion from the side in question takes place into one-half of infinite space. Hence the pressure is doubled also, which is evident from (64) and (67 a) when  $4\pi$  is replaced by  $2\pi$ . At a great distance from the disk, where  $p$  and  $v$  are in phase, the power per unit area is quadrupled. But since the integration now extends over a hemisphere, the total power radiated by one side of the disk is not quadrupled but doubled. The influence of the plane, therefore, is to double both the rate of working and the total pressure on the source due to radiation. It is shown in the preceding section that the power from *one* side of a rigid disk radiating into infinite space is  $\frac{\rho_0 \pi a^4 \omega^4 \xi_0^2}{4c}$ . From above it follows that the power radiated from *one* side when the disk vibrates in an infinite plane, where  $\Omega = 2\pi$ , is

$$P = \frac{\rho_0 \pi a^4 \omega^4 \xi_0^2}{2c} \quad (72 a)$$

The power from both sides is, therefore,

$$P = \frac{\rho_0 \pi a^4 \omega^4 \xi_0^2}{c}, \quad (73)$$

provided  $\lambda \gg a$ . These results are of prime importance in the design of hornless speakers with large baffles.

From (63) the velocity potential at a distance  $r$  from a simple source radiating into infinite space is  $\phi = Se^{-ikr}/4\pi r$ . Introducing the infinite plane close to the source halves the solid angle, so

$$\phi = \frac{Se^{-ikr}}{2\pi r}. \quad (74)$$

Applying this to a vibrating area  $A$  forming part of the plane, we have from the previous section,  $S = \iint u dA$ , and from (74)

$$\phi = \frac{1}{2\pi} \iint \frac{ue^{-ikr}}{r} dA. \quad (75)$$

\* This is to be regarded as an infinite baffle (see definition 22).

In (75)  $u$  is the radial velocity of the element which varies in general according to the location of  $dA$  on the vibrating surface. In this case it is normal to the plane. From (29)  $u = -\partial\phi/\partial n$ , where  $n$  is written for  $x$ . Substituting this value of  $u$  in (75), we obtain the very important formula

$$\phi = -\frac{1}{2\pi} \iint \frac{\partial\phi}{\partial n} \frac{e^{-ikr}}{r} dA. \tag{76}$$

The preceding integral gives the velocity potential at a distance  $r$  due to the combined effect of elemental areas  $dA$ , vibrating with normal velocity  $u = -\partial\phi/\partial n$  on one side of an infinite plane. The motion being harmonic, then  $u = -\partial\phi/\partial n = \omega\xi$ . Formula (76) is the basis of all analyses pertaining to the distribution of sound radiation from flat surfaces vibrating in an infinite rigid plane.

In general when the solid angle is reduced below  $4\pi$  to a value  $\Omega$ , we have for a simple source

$$\phi = \frac{Se^{-ikr}}{\Omega r}, \tag{77}$$

from which it follows that the particle velocity and the pressure are both increased in the ratio  $4\pi/\Omega$ . The power per unit area on a distant surface of radius  $r$  is  $16\pi^2/\Omega^2$  of its value for diffusion into the whole of infinite space. Since the area intercepted by the solid angle is  $\Omega r^2$  the power is increased in the ratio  $\frac{16\pi^2}{\Omega^2} \frac{\Omega r^2}{4\pi r^2} = \frac{4\pi}{\Omega}$ . Thus from (71)

the power radiated by a small disk vibrating axially with velocity  $\omega\xi_0$  near the apex of a conical horn of *infinite length* and solid angle  $\Omega$  is

$$\frac{4\pi}{\Omega} \frac{\rho_0 \pi a^4 \omega^4 \xi_0^2}{4c} = \frac{\rho_0 \pi^2 a^4 \omega^4 \xi_0^2}{\Omega c} = \frac{\rho_0 \omega^2 S^2}{\Omega c}. \tag{78}$$

Formula (78) is valid when  $\lambda \gg 10 a/\Omega^{\frac{1}{2}}$ , where  $a$  is the radius of the disk which fits the small end of the cone perfectly. As  $\Omega$  diminishes the pressure on the disk increases, the phase angle between the pressure and surface velocity decreases so the power factor rises.\* In fact the arrangement becomes increasingly efficient. A greater amount of useful work is done and the fluid flow associated with inertia pressure decreases with reduction in the solid angle  $\Omega$ . Finally, when  $\Omega \rightarrow 0$  the formula fails and other means have to be adopted to find the power from a rigid disk at one end of an infinite cylindrical tube. It is clear, however, that since the pressure and velocity are in phase, the inertia

\* Since the size of disk is fixed, its distance from the apex of the cone increases with decrease in  $\Omega$ . Thus  $\cos \theta = \cos[\tan^{-1}(1/kr)]$  steadily approaches unity. For practical purposes we can imagine the small end of the cone to be removed.

component is evanescent. Thus the impedance of an infinite cylindrical tube is a pure resistance, whether or not its diameter is small compared with the wave-length ( $\Omega = A/r^2$ , so in (12) Chap. X put  $r = \infty$ ).

The preceding formulae embodying  $\Omega$  are only applicable when the cone extends to infinity. For example they could not be used for a conical diaphragm 5 cm. radius at the small end of a conical horn 180 cm. long. Here the power transmitted by the diaphragm at low frequencies is reflected at the mouth of the horn. The strength of the reflected wave increases with fall in frequency. It is in antiphase with the transmitted wave, so the low-frequency output steadily decays due to neutralization. Above a certain frequency the influence of reflection is unimportant as shown in Chapter X on Horns.

### 17. Double source

When a small circular disk vibrates axially in free fluid, the pressure at any point therein consists of two components, one from the front, the other from the rear. These components are in opposite phase at the disk or at any two points symmetrically situated respecting its plane, and the vibrator is known as a double source. Moreover, any diaphragm vibrating in free fluid without a baffle (see definition 22), or with a finite baffle at low frequencies, is regarded as a double source. The shape of the diaphragm is immaterial. If in the baffleless state the size of the diaphragm is evanescent, a double point source is obtained. This is another delightful mathematical fiction. Since every point in the fluid is equidistant from both sides of the source, the net pressure is zero unless the amplitude of the disk is infinite!

Consider two equal simple sources  $+S, -S$  of opposite phase distant  $2d$  from each other (Fig. 7A). From (63) the velocity potential at  $P_1$  due to the first is

$$\phi_2 = \frac{S e^{-ikr_2}}{4\pi r_2},$$

and to the second

$$\phi_1 = -\frac{S e^{-ikr_1}}{4\pi r_1}.$$

The net velocity potential due to the two sources is thus ( $r \gg d$ )<sup>1</sup>

$$\begin{aligned} \phi &= \phi_2 + \phi_1 = \frac{S}{4\pi} \left\{ \frac{e^{-ik(r-d\cos\theta)}}{r-d\cos\theta} - \frac{e^{-ik(r+d\cos\theta)}}{r+d\cos\theta} \right\} \\ &= \frac{S e^{-ikr}}{2\pi(r^2 - d^2 \cos^2\theta)} \{d \cos\theta \cos(kd \cos\theta) + ir \sin(kd \cos\theta)\}. \quad (79) \end{aligned}$$

When  $d \ll r$ , 
$$\phi = \frac{iS \sin(kd \cos \theta) e^{-ikr}}{2\pi r} \tag{80}$$

Since  $\sin \alpha \doteq \alpha$  when  $\alpha = kd \cos \theta$  is small, (80) reduces to

$$\phi = \frac{i(2Sd)k \cos \theta e^{-ikr}}{4\pi r}, \tag{81}$$

provided  $kd \leq 0.5$  and  $r \gg d$ .

Neglecting the imaginary  $i$ , and apart from the factor  $\cos \theta$ , we see on comparison of (81) and (63) that  $(2Sdk) = S_d$  can be regarded as

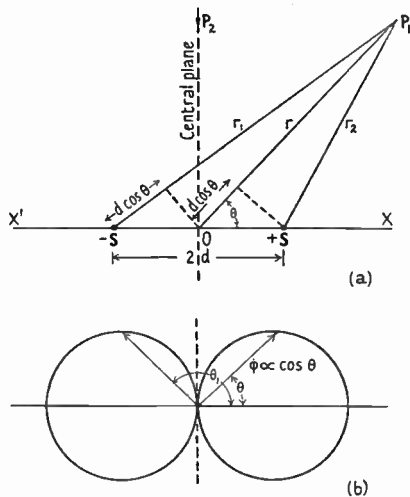


FIG. 7 A and B

the strength of the source.  $\cos \theta$  designates the spatial distribution of the sound radiated as shown in Fig. 7 B. Care must be exercised to interpret the strength of a double source correctly.  $S_d$  increases with increase in  $d$  because larger separation entails reduced interference from the oppositely vibrating simple sources. In practice the strength of a double source does not increase indefinitely with increase in  $d$ , since (81) is only applicable when  $kd \leq 0.5$  and  $d \ll r$ . This aspect of the subject is discussed in detail in sections 20 and 21. In formula (79) when  $kd$  is sufficiently small,  $\cos(kd \cos \theta) \doteq 1$ , and

$$\sin(kd \cos \theta) \doteq kd \cos \theta.$$

If  $d$  is small also,  $r^2 \gg d^2 \cos^2 \theta$  quite near the source, and (79) reduces to

$$\phi = \frac{S_d \cos \theta e^{-ikr}}{4\pi r k} \left( \frac{1}{r} + ik \right). \tag{82}$$

The component  $S_a \cos \theta / 4\pi r^2 k$  is associated with flow of the fluid in the neighbourhood of the source (see definition 29), whilst

$$\frac{iS_a \cos \theta}{4\pi r} \quad (82a)$$

is associated with the radiation of sound. The inertia component being dependent upon  $1/r^2$  falls away rapidly with increase in distance from the source.

### 18. Power from double source

At a great distance from a double source, if  $kd \leq 0.5$  we have from (81)

$$\phi = \frac{iS_a k \cos \theta e^{-ikr}}{4\pi r}$$

From (29) the particle velocity at a distance  $r$  is

$$v = -\frac{\partial \phi}{\partial t} = \frac{S_a k \cos \theta e^{-ikr}}{4\pi} \left( \frac{i}{r^2} - \frac{k}{r} \right), \quad (83)$$

and from (31) the pressure

$$\begin{aligned} p &= \rho_0 \frac{\partial \phi}{\partial t} \\ &= -\frac{\rho_0 \omega S_a k \cos \theta e^{-ikr}}{4\pi r}, \end{aligned} \quad (84)$$

the time factor  $e^{i\omega t}$  being inserted before differentiation and removed afterwards. The power passing through unit area on the surface of a sphere of radius  $r$  whose centre is the source, is the product of pressure and the velocity in phase therewith. From (83) the velocity is

$$\frac{-S_a k^2 \cos \theta}{4\pi r},$$

whilst the pressure is given by (84). Thus the power per unit area  $\Delta P = \rho_0 \omega^4 S_a^2 \cos^2 \theta / 16\pi^2 r^2 c^3$ . To find the total power radiated by the double source, this expression must be integrated over the whole spherical surface of radius  $r$ . Referring to Fig. 3, the power passing through a zonal surface of radius  $P_1 N_1 = r \sin \theta$  is  $dP = \Delta P 2\pi r^2 \sin \theta d\theta$ , so the total power

$$\begin{aligned} P &= -\frac{\rho_0 \omega^4 S_a^2}{4\pi c^3} \int_0^{\pi} \cos^2 \theta d(\cos \theta) \\ &= \frac{\rho_0 \omega^4 S_a^2}{12\pi c^3}, \end{aligned} \quad (85)$$

provided  $kd \leq 0.5$ .

Formula (85) is applicable to a disk or a conical diaphragm vibrating in a finite baffle at low frequencies where the propagation (not the distribution) is spherical. If the baffle is circular of radius  $d$ , this being several times the diameter of the diaphragm,

$$S_d = 2Sdk = 2\pi a^2 d \omega^2 \xi_0 / c^*$$

Owing, however, to the conditions differing from those of two separate sources in free fluid,  $d$  must be replaced by an effective value. As shown in § 21 this is found by experiment to be about  $0.7d$  which gives strength of the double source  $S_d$  as  $1.4\pi da^2 \omega^2 \xi_0 / c$ . Inserting this value of  $S_d$  in (85) we find that the power from a baffled diaphragm is given approximately by

$$P = \frac{\pi \rho_0 d^2 a^4 \omega^8 \xi_0^2}{6c^3} \quad (kd \leq 0.5). \tag{86}$$

This shows that at any low frequency the power increases as the square of the size of the baffle, provided the amplitude of vibration is constant. In practice if the driving force is invariable in magnitude, increase in  $d$  is accompanied by a decrease in amplitude due to enhanced radiation and inertia pressure on the diaphragm, i.e. the mechanical impedance increases (see definition 30).

Apart from the reduction in amplitude cited above, (86) must be interpreted with caution, since the power tends to infinity as  $d \rightarrow \infty$  which is impossible. It has been stipulated that  $kd \leq 0.5$ , but (86) can be extended up to  $kd = \frac{1}{2}\pi$  without serious practical error. If  $d = 90$  cm. its effective value is  $0.7 \times 90 = 63$  cm. and the upper frequency limit of (86) is  $100 \sim$ . At this frequency halving the radius of the baffle to 45 cm. results in a reduction in power to  $\frac{1}{4}$ , i.e. 6 decibels, which could easily be detected by ear. When  $kd > \frac{1}{2}\pi$  the analysis in § 21 must be used.

### 19. Vibrator without baffle

When the radius of the baffle is comparable with that of the diaphragm the above analysis is invalid. We have defined the strength of a double source as  $S_d = 2Sdk$ , where  $S$  represents the strength of a single source and  $2d$  is the distance between the two sources of opposite phase. This can also be expressed by the integral  $\iint v^2 dk dA = S_d$  where  $dA$  represents two elemental areas (each  $dA$ ) at the extremities of a line of length  $2d$ . For example,  $dA$  might be like portions at each end of a chord parallel to the polar axis of an axially vibrating sphere.

\*  $\xi$  is the r.m.s. value; also in section 19.



It follows that  $S_d$  is in the nature of a velocity-area. At frequencies where the wave propagation is spherical, it can be shown [215] that

$$\phi = i \left[ \left( V + \frac{m_i}{\rho_0} \right) \omega \xi_0 \right] \frac{k \cos \theta e^{-ikr}}{4\pi r}, \quad (87)$$

where  $V$  is the volume of the solid and  $m_i$  is the accession to inertia, i.e. the added mass due to the fluid (see definition 29, and Chap. III).

Comparison with the formula (82 a) shows that the strength of the source is now  $S_d = \left( V + \frac{m_i}{\rho_0} \right) k \omega \xi_0$ . Using (85) the power radiated by a vibrator acting as a double source is

$$P = \frac{\rho_0 \omega^6 \xi_0^2}{12\pi c^3} \left( V + \frac{m_i}{\rho_0} \right)^2. \quad (88)$$

For an axially vibrating sphere of radius  $a$ ,  $m_i/\rho_0 = \frac{2}{3}\pi a^3$  (Chap. III, Table 4, when  $ka < 0.5$ ), whilst  $V = \frac{4}{3}\pi a^3$ . Substituting these values in (88) the power is

$$P_s = \frac{\rho_0 \pi a^6 \omega^6 \xi_0^2}{3c^3}. \quad (89)$$

Formula (89) is identical with no. 3 in Chapter VI, Table 9 ( $ka \leq 0.5$ ) found by another method. For a circular disk of radius  $a$ ,  $m_i/\rho_0 = \frac{8}{3}a^3$  (Chap. III, § 4, method 2), whilst  $V = 0$ . Thus from (88) the power radiated is

$$P_d = \frac{16}{27\pi} \frac{\rho_0 a^6 \omega^6 \xi_0^2}{c^3}. \quad (90)$$

The influence of shape is seen by taking the ratio of the power from a sphere to that from a disk of equal radius executing the same axial amplitude. Thus from (89) and (90)

$$\frac{P_s}{P_d} = \frac{9\pi^2}{16} \doteq \frac{5.6}{1}.$$

The superiority of the sphere is due to reduced interference of the radiation from the two hemispheres vibrating in opposite phase, since the distance from pole to pole of the sphere is  $\pi a$  whereas that for the disk from centre to centre is only  $2a$ . Also the radial velocity of the sphere falls off towards the equator, whilst that of a disk is constant, so the interference is greater in the latter case.

## 20. Flat baffle\*

When a rigid circular disk vibrates axially, the air on each side of it is alternately compressed and rarefied. If the air at the front is com-

\* See definition 22.

pressed, that at the rear is rarefied, so there is a pressure difference between the two. Consider any point  $P_2$  in Fig. 7A, in the plane of a baffless disk at  $O$ , vibrating along the axis  $X'OX$ . Radiation reaching  $P_2$  from both sides of the disk consists of two components of equal magnitude, one being positive, the other negative, so the pressure on the plane is zero everywhere. At  $P_1$  the radiation is partly positive and partly negative, but  $P_1$  is nearer one side of the disk than the other, so complete neutralization does not occur (see Fig. 7B at an angle  $\theta$  where  $\phi \neq 0$ ).

If the disk is associated with a concentric coplanar rigid plane several times its own diameter, the length of the air-path between the two sides is increased. The greater the diameter of the plane, the smaller the interference between the radiation from the two sides of the disk. In practice the plane is simulated by a flat baffle board. As we shall show later, there is a limit beyond which increase in diameter of the baffle is ineffective in augmenting the power.

To assess the magnitude of the interference at  $P_1$  it is essential to consider the wave-length of the vibrations. If the waves are long compared with the diameter of the disk, radiation from the back and front of the disk reaches points like  $P_1$  almost in anti-phase unless a baffle is used. If the distance from the rear to  $P_1$  is augmented by a baffle, the phase angle decreases and the output increases. Rise in frequency entails reduction in  $\lambda$ , so with a baffle of fixed dimensions the consequent diminution in phase angle is accompanied by enhanced output. At high frequencies, where  $\lambda$  is comparable with the diameter of the disk, the radiation is projected from each face of the disk in the form of a beam (Chap. V) and the influence of a baffle in increasing the output is negligible.

It is hardly feasible to treat either a flat disk or a conical shell in a flat baffle by rigorous analytical methods. The interference between front and rear is serious at low frequencies only, and with a *flat* baffle the air distance between the two faces is the chief item. On this understanding the problem can be readily treated by a simple artifice. At low frequencies the sound distribution from one side of the disk acting alone is spherical, and at a great distance the disk can be regarded as a small source. Thus the double source concept of § 17 can be applied.

From (80) the velocity potential at a distant point  $P_1$  due to the

double source is  $\phi = \frac{iS \sin(kd \cos \theta)}{2\pi r}$ , where  $e^{-ikr}$  has been dropped.

But from (67) the pressure  $p = i\rho_0 \omega \phi$  which on substitution of  $\phi$  from above gives

$$p = \frac{\rho_0 \omega S}{2\pi r} \sin(kd \cos \theta), \quad (r \gg d) \quad (91)$$

the negative sign being omitted.

When  $kd \cos \theta = \frac{1}{2}(2n-1)\pi$ ,  $n$  being a positive integer, the pressure is a maximum, whilst for  $kd \cos \theta = n\pi$  it is zero. Corresponding to any angle  $\theta$  (except  $\frac{1}{2}\pi$ ) there are series of zero and maximum values of pressure as either the frequency or the distance between the sources, or both, is increased. This is of paramount importance in testing loud speakers with finite baffles, either in 'dead' rooms or in the open air. If the microphone is stationed at any angle  $\theta$  with the axis of the speaker, there are one or more frequencies throughout the acoustical register where the above effect is experienced. On the axis  $\cos \theta = 1$ , so the conditions for maxima and zeros are  $kd = \frac{1}{2}(2n-1)\pi$  and  $kd = n\pi$ , respectively. In practice with a flat baffle conditions are not absolutely those postulated above, and the zero is replaced by a minimum. These points are exemplified in Fig. 118 which represents an actual outdoor test. The minimum occurs at 460 ~ and the maximum at 230 ~. The influence of baffle size is also shown in the same diagram. Below 200 ~ there is an almost constant difference of 7 decibels between the curves for baffles 4 ft. and 2 ft. 6 in. square, respectively. At 460 ~ the smaller baffle gives the greater output. Thus if one listens on the axis to a 460 ~ note whilst the size of the baffle is gradually increased, a point is reached when the loudness is a minimum.

The distribution of radiation for various values of  $kd$  is shown in Fig. 8, where it is seen that a baffled double source has definite directional characteristics. At very low frequencies the polar curve is two circles. As the frequency rises, interference occurs on the axis and for  $kd = \pi$  the pressure is evanescent. It is instructive to compare these curves with those for an axially vibrating sphere [156 a]. The latter is a double source without a baffle, and the distribution is represented by two circles. The influence of a baffle, therefore, is to modify the interference between the two sides of the diaphragm in such a manner that the spatial distribution is altered profoundly, a series of maxima and zeros occurring on the axis.

## 21. Power radiated

From Chap. VI, § 1, formula (2), we have

$$P = \frac{4\pi r^2}{\rho c} \int_0^{\frac{1}{2}\pi} p^2 \sin \theta \, d\theta.$$

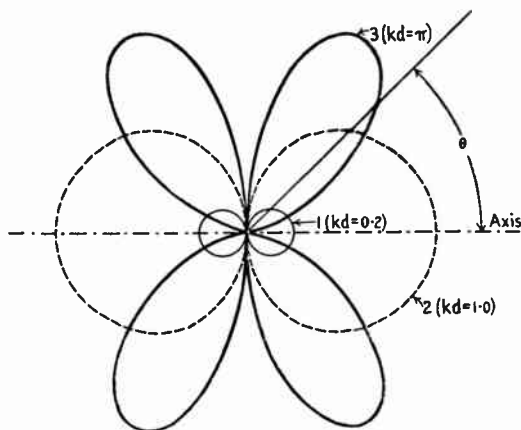


FIG. 8

Using formula (91) for  $p$  we obtain

$$\begin{aligned} P &= -\frac{\rho_0 \omega^2 S^2}{\pi c kd} \int_0^{\frac{1}{2}\pi} \sin^2(kd \cos \theta) \, d(kd \cos \theta) \\ &= \frac{\rho_0 \omega^2 S^2}{2\pi c kd} \int_0^{\frac{1}{2}\pi} [1 - \cos(2kd \cos \theta)] \, d(kd \cos \theta) \\ &= \frac{\rho_0 \omega^2 S^2}{2\pi c} \left( 1 - \frac{\sin 2kd}{2kd} \right), \end{aligned} \quad (92)$$

provided  $r \gg d$ . The expression in brackets is plotted in Fig. 9, the curve being somewhat similar in appearance to that of

$$G_1 = \left[ 1 - \frac{J_1(2ka)}{ka} \right]$$

shown in Fig. 17. Apart from the first maximum, which exceeds unity, the power radiated does not increase with increase in the separation of the sources beyond  $2d = \frac{1}{2}\lambda$ . The power oscillates about a value equal to that radiated by one side of a rigid disk in an infinite baffle at low frequencies when the propagation is spherical,  $S$  being

identical in both cases (disk and simple source). The ultimate result of using a large baffle is in effect to shut off one-half of the loud speaker. This approximates to the case of an infinite flat baffle. But we must not fall into the error of assuming that the two cases are identical in all respects, for the distribution of radiation with the finite baffle is focused, whereas with an infinite baffle it is uniform in all directions, provided  $ka \leq 0.5$ ,  $a$  being the diaphragm radius.

These results are applicable to radiation into free space when the distance  $r$  from the centre of the diaphragm is large compared with

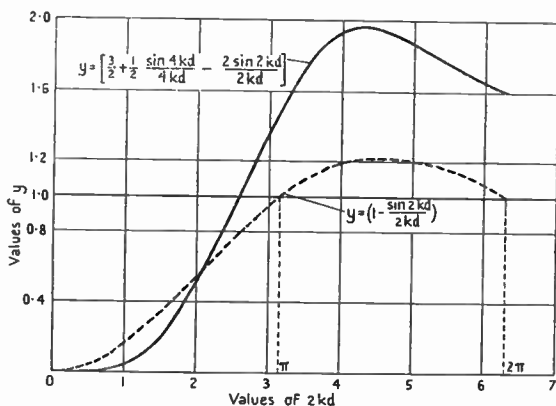


FIG. 9

the length of the side of the baffle (if square). In an ordinary room conditions are modified due to reflection and to standing waves. Consequently the power radiated and the sound distribution will differ from that obtained above.

If we assume  $2d$  to represent the distance round the baffle from centre to centre of the diaphragm, we have to find  $2d$  in terms of the length of the side of the baffle. From Fig. 118 with a baffle 4 ft. square the output decays below 200  $\sim$ , whilst with a baffle 2 ft. 6 in. square the turning-point is 300  $\sim$ .

The corresponding values of  $\frac{1}{2}\lambda$  are 2.8 ft. and 1.86 ft., respectively. Neglecting the baffle being square instead of circular, the 4 ft. baffle corresponds to  $2d = 2.8$  ft. and the 2 ft. 6 in. baffle to  $2d = 1.86$  ft. On the average, therefore, it appears that between 200  $\sim$  and 300  $\sim$  the equivalent separation of two simple sources is about 0.7 times the side of the baffle. From a practical viewpoint the difference in

loudness-level, when  $2d$  or  $2.8d$  is taken as the side of the baffle, is not very serious at low frequencies. Thus, where economy is desirable, a satisfactory working rule is to make the side of a square baffle not less than one-half of the lowest wave-length to be adequately reproduced. When it is desired to reach  $50 \sim$  adequately, a hole in the wall is the best solution. The speaker then does double duty and serves two rooms at once, although this may not always be desirable. If the radiation from the rear of the diaphragm is discharged into an enclosure of small volume, care must be exercised to avoid resonances.

Reverting to (92), when  $2kd \leq 1$ , as it will be at very low frequencies,

$$1 - \frac{\sin 2kd}{2kd} \div \frac{2}{3}k^2d^2$$

and the power radiated is

$$P = \frac{\rho_0 \omega^4 S^2 d^2}{3\pi c^3}, \quad (93)$$

which is identical with (85), since  $S_d = 2Sd$ . Assuming  $d$  is much greater than the radius of the diaphragm, the power at a given frequency increases as the square of the side of the baffle, provided the diaphragm amplitude is constant. In practice, owing to the finite size of the diaphragm it may increase more rapidly than this for small baffles, which seems to be borne out by Fig. 118. The ratio of the squares of the baffle-sides in Fig. 118 is 2.56, whereas the power ratio is 5.

Although (93) is inapplicable when  $d = a$ , it then reduces to the formula for the power radiated by an axially vibrating sphere of radius  $a$  provided  $S = \pi a^2 \omega \xi_0$ , and  $ka \ll 1$ .

## 22. Influence of infinite baffle on power radiated [121 b] when driving force is constant

Hitherto we have considered the effect of increasing the size of baffle when the diaphragm amplitude is maintained constant. We now proceed to examine the increase in power when the force is constant and the baffle is made infinite.

At low frequencies the power radiated from a rigid disk without a baffle is, from (90),

$$P' = \frac{16}{27\pi} \frac{\rho_0 a^6 \omega^2 \xi_0'^2}{c^3}, \quad (94)$$

and from both sides with an infinite baffle it is [from (72)]

$$P = \frac{\pi \rho_0 a^4 \dot{\xi}_0^2}{c} \quad (95)$$

We have now to express  $P'$  and  $P$  in terms of a constant driving force  $f$ . Assuming the acoustic load to be negligible, we can write  $f = m_e \ddot{\xi}_0 = m_e \omega \dot{\xi}_0$  so that

$$\dot{\xi}_0 = \frac{f}{\omega m_e} = \frac{f}{\omega m_i'(1+\beta')}, \quad (96)$$

where  $m_e = m_n + m_i'$  and  $\beta' = m_n/m_i'$ .

Thus  $\dot{\xi}_0'^2 = \frac{f^2}{\omega^2 m_i'^2 (1+\beta')^2}$  without the baffle,

and  $\dot{\xi}_0^2 = \frac{f^2}{\omega^2 m_i^2 (1+\beta)^2}$  with the baffle. (97)

Inserting the values of  $\dot{\xi}_0'^2$  and  $\dot{\xi}_0^2$  in (94), (95), and remembering that  $m_i$  for an infinite baffle at low frequencies\* [3a] is  $2m_i'$ , we obtain the ratio

$$\frac{P}{P'} = \frac{27\pi^2}{64} \left(\frac{1}{ka}\right)^2 \left(\frac{1+\beta'}{1+\beta}\right)^2, \quad (98)$$

provided  $ka \leq 0.5$ . Taking  $a = 10$  cm. radius,  $f = 50 \sim$ ,  $\beta = 3.4$ ,  $\beta' = 1.7$  the ratio in (98) is 130/1. Thus the use of an infinite baffle at  $50 \sim$  would raise the level 21 decibels. From a practical viewpoint this must be interpreted in the proper manner. Since the radiation from one side of the disk is excluded by the baffle, the power diffused in, say, a 'dead' room would only be one-half that given by the formula. The above ratio would be 65/1 and the intensity-level 18 decibels above that for the baffless disk in the centre of the dead room. Here again it must be recognized that although the general power-level is raised 18 decibels, the distribution from the baffless disk is focused and concentrated on the axis. Moreover, at an axial point, say 8 to 10 radii distant from the disk, the influence of the baffle would be less than that computed above.

When the driving force is fixed [121 b], we can also compare an unbaffled axially vibrating sphere with the baffled rigid disk. Thus,

$$\frac{P}{P_s} = \frac{3\pi}{8} \left(\frac{1}{ka}\right)^2 \left(\frac{1+\beta_s}{1+\beta}\right)^2, \quad (99)$$

\* See p. 57 just prior to Method 2.



where 
$$\beta_s = \frac{\text{mass of sphere}}{m_i \text{ of sphere}} = \frac{m_s}{m_{is}}$$

and  $P_s$  is the power radiated by the sphere.

Assuming the natural masses of the disk and sphere to be equal, the result in (99) is several times less than that in (98). At high frequencies, when  $ka$  is large ( $> 3$ ), considerable focusing occurs, the wave propagation is sensibly plane, and the influence of a baffle is comparatively slight. Taking the above ratio under this condition we find

$$\frac{P}{P_s} = \frac{3}{2} \left( \frac{m_{is}}{m_i} \right)^2 \left( \frac{1+\beta_s}{1+\beta} \right)^2 = \frac{3}{2} \left( \frac{m_{is}+m_s}{m_i+m_n} \right)^2 \doteq \frac{3}{2}, \quad (100)$$

provided  $m_s = m_n$  and  $ka > 3.0$ , since  $m_{is}$  and  $m_i$  then tend to zero. The ratio in (100) is about 1 per cent. of the value deduced from (99) at  $50 \sim$ .

### 23. Acoustical images

The use of optical and electrical images is so familiar that extension of the principle to acoustics is almost self-evident. Suppose we have a simple source situated in front of and close to a very extensive flat wall whose absorption coefficient is zero, as shown in Fig. 10. The effect of reflection can be simulated by an image source of identical phase and strength situated on the perpendicular and distant  $d$  from the wall. The analytical procedure is very simple. The velocity potential

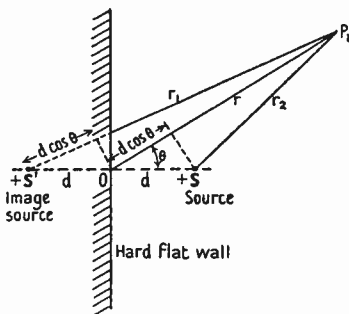


FIG. 10

at any point distant  $r$  from a simple source is, by (63),  $\phi = S e^{-ikr} / 4\pi r$ . Thus the velocity potential at  $P_1$  due to the source and its image is (Fig. 10)

$$\phi = \frac{S}{4\pi} \left( \frac{e^{-ikr_2}}{r_2} + \frac{e^{-ikr_1}}{r_1} \right). \quad (101)$$

When both  $r_1$  and  $r_2 \gg d$ , (101) can be written

$$\begin{aligned} \phi &= \frac{S e^{-ikr}}{4\pi r} (e^{ikd \cos \theta} + e^{-ikd \cos \theta}) \\ &= \frac{S}{2\pi r} \cos(kd \cos \theta), \end{aligned} \quad (102)$$



the distance phase factor  $e^{-ikr}$  having been dropped. Since  $\phi$  varies with  $\theta$ , it is clear that the wall, so to speak, endows the source with directional properties. When  $kd \cos \theta = \frac{1}{2}(2n+1)\pi$  the pressure vanishes, whilst for  $kd \cos \theta = n\pi$  it is a maximum,  $n$  being any positive integer. As the source approaches the wall the directional characteristic fades away until when  $d = 0$ ,  $\phi = S/2\pi r$ , which is double the velocity potential due to a simple source in the open. This follows from the fact that the source discharges into a solid angle of  $2\pi$  instead of  $4\pi$ , the open-space value.

In modern acoustical problems associated with reflection in damped enclosures, there is appreciable absorption at the boundaries. The strength of v.p. due to the image source then becomes  $(1-a_s)^{\frac{1}{2}} S e^{-ikr}/4\pi r$  for a single flat wall, where  $a_s$  is the absorption coefficient of the wall (see definition 12). Then we have.

$$\phi = \frac{S e^{-ikr}}{4\pi r} \{e^{ikd \cos \theta} + b e^{-ikd \cos \theta}\}, \quad (103)$$

where  $b = (1-a_s)^{\frac{1}{2}}$ .

$$\text{Thus} \quad |\phi| = \frac{S}{4\pi r} \{(1+b^2) + 2b \cos(2kd \cos \theta)\}^{\frac{1}{2}}. \quad (104)$$

If  $a_s = 0$ , (104) reduces to (102), whilst if  $a_s = 1$ , complete absorption occurs and  $\phi$  has its free-space value  $S/4\pi r$ .

## 24. Power radiated by simple source near flat wall

From formula (2), Chap. VI, this is

$$P = \frac{2\pi r^2}{\rho_0 c} \int_0^{\frac{1}{2}\pi} p^2 \sin \theta \, d\theta,$$

the radiation being into one-half of infinite space, i.e. one side of the wall. Since  $p = i\rho_0 \omega \phi$ , we obtain, on substitution from (102) in the above formula,

$$\begin{aligned} P &= -\frac{\rho_0 \omega^2 S^2}{2\pi c (kd)} \int_0^{\frac{1}{2}\pi} \cos^2(kd \cos \theta) \, d(kd \cos \theta) \\ &= -\frac{\rho_0 \omega^2 S^2}{4\pi c} \left[ \cos \theta + \frac{\sin(2kd \cos \theta)}{2kd} \right]_0^{\frac{1}{2}\pi} \\ &= \frac{\rho_0 \omega^2 S^2}{4\pi c} \left[ 1 + \frac{\sin 2kd}{2kd} \right]. \end{aligned} \quad (105)$$

When the wall is absent  $d = \infty$  and  $P = \rho_0 \omega^2 S^2 / 4\pi c$ , which is identical with the radiation from a simple source in free space. If the source is very near the wall,\*  $P = \rho_0 \omega^2 S^2 / 2\pi c$ , hence the output is doubled. This latter value is identical with the output from one side of a rigid disk in an infinite plane when the propagation is spherical. See (72a) § 16 with  $S = \pi a^2 \omega \xi_0$ .

### 25. Reflection from wall when baffle is used

The use of one wall of a room, having a hole for the speaker, thereby constituting in effect an infinite baffle, is generally frowned upon in domestic circles. Consequently, when a baffle is employed, the speaker is placed near a wall indiscriminately. The wall reflects the waves (of opposite sign) from the rear of the diaphragm to the front, so the power output and the spatial distribution are modified accordingly. If the speaker is set across a corner, with the baffle near the two walls, a resonant cavity is formed, and the output over a certain frequency range may be augmented, whereas over another range it may be reduced owing to reflection. As the speaker is withdrawn from the corner, its lower register appears to decay due to reduction in resonance. Provided attention is confined to a large flat wall in free space, and the baffle is of moderate size, the problem is amenable to analytical treatment by aid of the principle of acoustical images (§ 23). The equivalent arrangement of simple sources is shown schematically in Fig. 11.

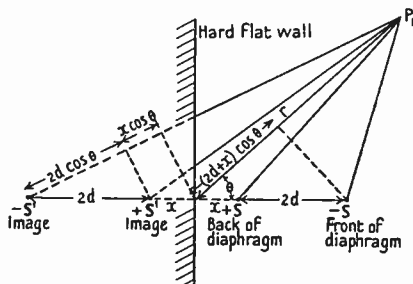


FIG. 11

When  $r \gg 4d + 2x$  the velocity potential at  $P_1$  is

$$\phi = \frac{S}{4\pi r} \{ e^{-ik(r-x \cos \theta)} + e^{-ik(r+x \cos \theta)} - e^{-ik[r-(2d+x) \cos \theta]} - e^{-ik[r+(2d+x) \cos \theta]} \} \tag{106}$$

$$= \frac{S e^{-ikr}}{2\pi r} (\cos z - \cos mz), \tag{107}$$

where  $z = kx \cos \theta$  and  $m = \{1 + (2d/x)\}$ ,  $\theta$  being the angular distance

\*  $d \rightarrow 0$ , so  $\frac{\sin 2kd}{2kd} = 1$ .

from  $P_1$  to the intersection of the wall and the line of sources. The radiation characteristic can be plotted from (107), and a representative example is given in Fig. 12, curve 2. For comparison the characteristic without the wall is shown in curve 1.

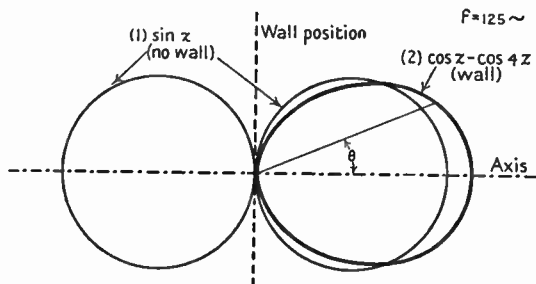


FIG. 12. Curves showing effect of wall in modifying the low-frequency sound distribution from a loud speaker with a flat baffle.

$$\sin z = \sin(kd \cos \theta) \doteq kd \cos \theta; \text{ for } \cos z - \cos 4z, \text{ see (107).}$$

## 26. Power radiated using baffle near flat wall

Proceeding on the same lines as in § 21, the power radiated is

$$P = \frac{\rho_0 \omega^2 S^2}{2\pi c(kx)} \int_0^{kx} (\cos^2 z - 2 \cos z \cos mz + \cos^2 mz) dz, \quad (108)$$

since 
$$-\sin \theta d\theta = \frac{d(kx \cos \theta)}{kx} = \frac{dz}{kx},$$

and the limits of  $\theta$  are 0 to  $\frac{1}{2}\pi$ , the wall reducing the solid angle to  $2\pi$ .

Integrating (108) and inserting the limits, we find

$$P = \frac{\rho \omega^2 S^2}{4\pi c} \left\{ 2 + \frac{\sin 2kx}{2kx} + \frac{\sin 2k(x+2d)}{2k(x+2d)} - 2 \left[ \frac{\sin 2kd}{2kd} + \frac{\sin 2k(d+x)}{2k(d+x)} \right] \right\}. \quad (109)$$

When the baffle is removed and  $d = 0$  as a consequence, the power is zero, owing to complete interference, since we postulate small sources. If  $x = \infty$ , the speaker is well removed from the wall, and

$$P = \frac{\rho \omega^2 S^2}{2\pi c} \left\{ 1 - \frac{\sin 2kd}{2kd} \right\}, \quad (110)$$

which is identical with (92), § 21, as we should expect. If  $x$  is small

compared with  $d$ ,

$$P = \frac{\rho\omega^2 S^2}{2\pi c} \left\{ \frac{3}{2} + \frac{1}{2} \frac{\sin 4kd}{4kd} - \frac{2 \sin 2kd}{2kd} \right\}. \quad (111)$$

The influence of the wall in the proximity of the speaker is found on comparison of (110) and (111), which is exhibited in Fig. 9. The maximum effect of the wall occurs when  $2kd = 4.18$ , the power then being 1.63 times its free-space value. At lower frequencies a point is reached when wall reflection becomes injurious due to enhanced interference between the two sides of the diaphragm. The analysis shows that the influence of a wall is to augment the lower register for wave-lengths less than  $2\pi d$ , provided the speaker is near enough, but not sufficiently close to introduce effects beyond the scope of the hypothesis on which the formula is based.

Since  $\{1 - (\sin 2kd/2kd)\}$  is substantially unity when  $2kd > \pi$ , it follows that the influence of the wall is then represented by

$$\left[ \frac{3}{2} + \frac{1}{2} \left( \frac{\sin 4kd}{4kd} \right) - 2 \left( \frac{\sin 2kd}{2kd} \right) \right].$$

In an ordinary room, owing to reflection, the above results will be modified.

### 27. Mechanical impedance of spherical vibrators

On the assumption that the vibrator is devoid of mass, we can establish a formula for the mechanical impedance per unit area of vibrating surface [121 b]. By definition 27,

$$z = \frac{\text{pressure}}{\text{radial velocity}} = \frac{p}{u}.$$

Thus 
$$z = \frac{(p_0 + p_1 + \dots + p_n)}{u}, \quad (112)$$

where  $p_0, \dots, p_n$  are the pressures due to the various harmonics. From (55) and the relationship  $p_n = i\rho_0 \omega \phi_n$  we obtain

$$p_n = i\rho_0 \omega a u_n \zeta_n = i\rho_0 c z u_n \zeta_n.$$

Thus the mechanical impedance per unit area is

$$z = \frac{i\rho_0 c z}{u} (u_0 \zeta_0 + u_1 \zeta_1 + \dots + u_n \zeta_n + \dots), \quad (113)$$

only those harmonics which occur in the expansion of the radial velocity  $u$  being chosen.

(a) *Radially pulsating sphere.* Here  $u = u_0 = U = a$  constant, and  $\zeta_0 = \left(\frac{1-iz}{1+z^2}\right)$ , so the impedance per unit area is

$$\begin{aligned} z &= r + ix \\ &= \rho_0 c \left( \frac{z^2}{1+z^2} + \frac{iz}{1+z^2} \right) \end{aligned} \quad (114)$$

where  $z = ka$ . The real component of  $z$  is the acoustic radiation resistance per unit area, whilst the imaginary part is associated with the accession to inertia (see definition 29). At high frequencies, when  $ka$  is sufficiently large, the inertia component is negligible and the impedance is

$$z = \rho_0 c. \quad (115)$$

The physical interpretation of (115) is that the impedance of the sphere is equal to that of the medium (see definition 20).

(b) *Radially pulsating hemisphere.* Here  $u_0 = \frac{1}{2}U$ ;  $u_1 = \frac{3}{4}U\mu$ ;  $\zeta_0 = \left(\frac{1-iz}{1+z^2}\right)$ ;  $\zeta_1 = \frac{2+z^2-iz^3}{4+z^4}$ , as found from Tables 1, 2. Substituting these values in (113) we obtain, for the spherical harmonics of zero and unit orders,

$$z = \frac{\rho_0 c}{2} \left\{ \left( \frac{z^2}{1+z^2} \right) + \frac{3}{2}\mu \left( \frac{z^4}{4+z^4} \right) + i \left[ \left( \frac{z}{1+z^2} \right) + \frac{3}{2}\mu \left( \frac{2z+z^3}{4+z^4} \right) \right] \right\}. \quad (116)$$

To attain a more accurate result when  $z$  is large, additional harmonics are required. It is seen from (116) that  $z$  varies with  $\mu$ , and at the pole (Fig. 3), where  $\mu = 1$ ,  $z$  exceeds  $\rho_0 c$  the resistance of the medium (definition 20) when  $z$  is large. The value of  $z$  from (116) is then approximately  $\frac{5}{4}\rho_0 c$ . At the equator  $\mu = 0$  and  $z = \frac{1}{2}\rho_0 c$ . Inclusion of higher harmonics would reduce  $z$  at the pole but not at the equator, since  $\mu$  is then zero. On the average the value of  $z$  over the surface approximates to the value  $\rho_0 c$  when  $z$  is large and higher harmonics are incorporated. Formulae (114) and (116) will be required to provide the values of simulating terminal impedances for horns of finite length in Chapter X (see definition 28).

### III

## FLUID PRESSURE ON VIBRATORS: ACCESSION TO INERTIA

### 1. Pressure at any point on rigid disk\* vibrating in an infinite rigid plane [3 b]

The velocity potential at a point  $P$  (Fig. 13) due to an elemental area  $dA$  vibrating axially with harmonic motion is, from (76), Chap. II,

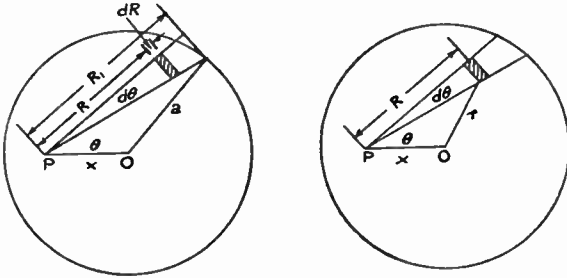


FIG. 13

$$d\phi = \frac{1}{2\pi} \frac{e^{-ikR}}{R} \dot{\xi}_0 dA; \quad (1)$$

where  $R$  is the distance from  $P$  to  $dA$ , and  $\dot{\xi}_0 = -\partial\phi/\partial n$  is the velocity of  $dA$  normal to the plane. From (31) Chap. II,

$$p = \rho_0 \frac{\partial\phi}{\partial t} = i\rho_0 \omega\phi,$$

the time factor  $e^{i\omega t}$  being inserted before and removed after differentiation. Thus from (1)

$$dp = \frac{i\rho_0 \omega \dot{\xi}_0}{2\pi} \frac{e^{-ikR}}{R} dA. \quad (2)$$

To determine the pressure at *any* point on a vibrating rigid disk forming part of the plane, we have to apply formula (2) over the entire surface of the disk. Referring to Fig. 13, the pressure at  $P$  due to the elemental area  $R dR d\theta$  is

$$dp = \frac{i\rho_0 \omega \dot{\xi}_0}{2\pi} \frac{e^{-ikR}}{R} R dR d\theta. \quad (3)$$

\* See definition 47.

The total pressure at  $P$  due to the whole disk is, therefore

$$p = \frac{i\rho_0 c \dot{\xi}_0}{\pi} \int_0^\pi d\theta \int_0^{R_1} k e^{-ikR} dR, \quad (4)$$

since  $k = \omega/c$ .

The evaluation [3 b] of this integral is too extensive to be included here, so the result alone is given.

The pressure at any point distant  $x$  from the centre ( $b = x/a$ ) of the disk is

$$\begin{aligned} p &= p_a + ip_i \quad (\text{acoustic} + \text{inertia component in quadrature}) \\ &= \rho_0 c \dot{\xi}_0 \left\{ \left[ \frac{z^2}{2!} g_2 - \frac{z^4}{4!} g_4 + \frac{z^6}{6!} g_6 - \dots \right] + i \left[ z g_1 - \frac{z^3}{3!} g_3 + \frac{z^5}{5!} g_5 - \dots \right] \right\}, \quad (5) \end{aligned}$$

where [3 b]

$$g_2 = 1$$

$$g_4 = 1 + 2b^2$$

$$g_6 = 1 + 6b^2 + 3b^4$$

$$g_8 = 1 + 12b^2 + 18b^4 + 4b^6$$

$$g_{2r} = {}_2F_1[-(r-1), -r; 1; b^2]$$

$$g_1 = F\left(-\frac{1}{2}, \frac{1}{2}, 1, b^2\right)$$

$$g_3 = F\left(-\frac{3}{2}, \frac{1}{2}, 1, b^2\right) + \frac{3}{2}b^2 F\left(-\frac{1}{2}, \frac{1}{2}, 2, b^2\right)$$

$$g_5 = F\left(-\frac{5}{2}, \frac{1}{2}, 1, b^2\right) + 5b^2 F\left(-\frac{3}{2}, \frac{1}{2}, 2, b^2\right) + \frac{15}{8}b^4 F\left(-\frac{1}{2}, \frac{1}{2}, 3, b^2\right)$$

$$g_7 = F\left(-\frac{7}{2}, \frac{1}{2}, 1, b^2\right) + \frac{21}{2}b^2 F\left(-\frac{5}{2}, \frac{1}{2}, 2, b^2\right) + \frac{105}{8}b^4 F\left(-\frac{3}{2}, \frac{1}{2}, 3, b^2\right) +$$

$$+ \frac{35}{16}b^6 F\left(-\frac{1}{2}, \frac{1}{2}, 4, b^2\right)$$

$$g_9 = F\left(-\frac{9}{2}, \frac{1}{2}, 1, b^2\right) + 18b^2 F\left(-\frac{7}{2}, \frac{1}{2}, 2, b^2\right) + \frac{189}{4}b^4 F\left(-\frac{5}{2}, \frac{1}{2}, 3, b^2\right) +$$

$$+ \frac{105}{4}b^6 F\left(-\frac{3}{2}, \frac{1}{2}, 4, b^2\right) + \frac{315}{128}b^8 F\left(-\frac{1}{2}, \frac{1}{2}, 5, b^2\right)$$

The total pressure at any point on the disk consists of two components in quadrature: (a) the load component, associated with sound radiation, in phase with the velocity of the disk, (b) the inertia component, associated with the flow of fluid in the neighbourhood of the disk, in phase quadrature with the velocity. The vector diagram illustrating these relationships is shown in Fig. 14.

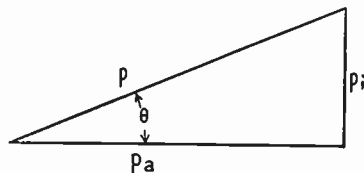


FIG. 14

If the disk were

massless its impedance per unit area at any point of radius  $x = ba$  would be

$$z = \frac{p}{\dot{\xi}_0} = \rho_0 c \left\{ \left[ \frac{z^2}{2!} g_2 - \frac{z^4}{4!} g_4 + \frac{z^6}{6!} g_6 \dots \right] + i \left[ z g_1 - \frac{z^3}{3!} g_3 + \frac{z^5}{5!} g_5 \dots \right] \right\} \quad (6)$$

$$= r_e + i x_e.$$

### 2. Variation in pressure over the surface of rigid disk

From (5) the acoustic pressure at any radius  $x$  is

$$p_a \doteq \rho_0 c \dot{\xi}_0 \left\{ \frac{z^2}{2!} - \frac{z^4}{4!} (1 + 2b^2) + \frac{z^6}{6!} (1 + 6b^2 + 3b^4) - \right.$$

$$\left. - \frac{z^8}{8!} (1 + 12b^2 + 18b^4 + 4b^6) + \right.$$

$$\left. + \frac{z^{10}}{10!} (1 + 20b^2 + 60b^4 + 40b^6 + 5b^8) \right\}, \quad (7)$$

where  $b = x/a$ .

The portion of the series given in (7) can be used to evaluate  $p_a$  for values of  $z (= ka) \leq 2.0$ .<sup>\*</sup> For greater values of  $ka$  additional terms must be incorporated to secure accuracy [see 3 b].

The acoustic pressure variation over the surface for several values of  $z$  is portrayed graphically in Fig. 15. At low frequencies the pressure is constant, but the edge pressure diminishes relatively as  $ka$  increases. Beyond a certain point the central pressure decays and ultimately vanishes when  $ka = 2\pi$  or  $\omega/2\pi = 3,400 \sim$  for a disk 10 cm. radius. Above this frequency it oscillates between zero and a constant maximum.

The inertia component of the pressure calculated from the imaginary part of (5) is also plotted in Fig. 15. At the centre it is about three times the acoustic pressure when  $ka = 0.5$ , but falls away towards the edge. As  $ka$  increases, the acoustic pressure rises more rapidly than the inertia pressure, whilst at  $ka = 2.0$  it is appreciably the greater of the two.

The total pressure  $\sqrt{(p_a^2 + p_i^2)} = p$  and its phase angle  $\theta_1$  with the axial velocity are also shown in Fig. 16. Even at low frequencies the total pressure is not constant and falls towards the edge. To preserve constant pressure at small values of  $ka$ , the velocity of the disk when

<sup>\*</sup> When  $ka = 2.0$  the error using only 5 terms is about 1 per cent. In acoustical work this is negligible.



flexible would have to increase with the radius ultimately becoming infinite at the edge. In fact for  $ka < 0.5$  the velocity must vary as  $1/(a^2 - x^2)^{1/2}$  to preserve uniform pressure over the surface.

### 3. Total acoustic pressure on one side of rigid disk

This is found by integrating the acoustic pressure given by (5) over the surface of the disk. Thus the total acoustic pressure or force

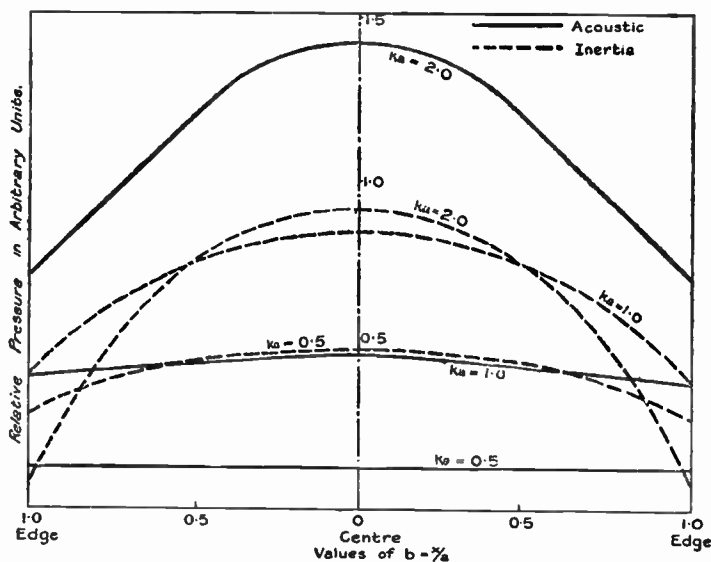


FIG. 15. Curves showing acoustic and inertia pressure on the surface of a rigid disk vibrating in an infinite baffle, for various values of  $ka$ .

associated with sound radiation is [3 b]

$$f_a = 2\pi \int_0^a p_a x dx = 2\pi a^2 \int_0^1 p_a b db,$$

where  $p_a$  is given by (5). Substituting for  $p_a$  in the integrand above we obtain

$$f_a = 2\pi a^2 \rho_0 c \xi_0 \int_0^1 \left[ \frac{z^2}{2!} b - \frac{z^4}{4!} (b + 2b^3) + \frac{z^6}{6!} (b + 6b^3 + 3b^5) - \frac{z^8}{8!} (b + 12b^3 + 18b^5 + 4b^7) + \dots \right] db$$

$$\begin{aligned}
 &= 2\pi a^2 \rho_0 c \xi_0 \left[ \frac{z^2}{2.2!} - \frac{z^4}{4!} + \frac{5z^6}{2.6!} - \frac{21z^8}{2.8!} + \dots \right] \\
 &= \rho_0 c \xi_0 A \left[ \frac{(2z)^2}{2.4} - \frac{(2z)^4}{2.4^2.6} + \frac{(2z)^6}{2.4^2.6^2.8} - \frac{(2z)^8}{2.4^2.6^2.8^2.10} \dots \right] \\
 &= \rho_0 c \xi_0 A \left[ 1 - \frac{J_1(2z)}{z} \right] = \rho_0 c \xi_0 A G_1, \quad (8)
 \end{aligned}$$

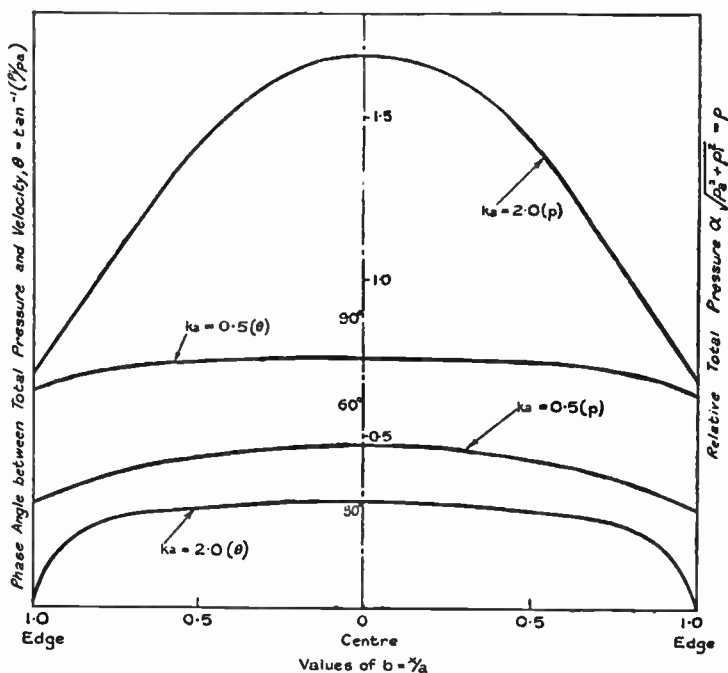


FIG. 16. Curves showing the total pressure and the phase angle between it and the axial velocity of the rigid disk of Fig. 15.

where

$$G_1 = \left[ 1 - \frac{J_1(2z)}{z} \right].$$

The function  $G_1$  is plotted in Fig. 17 [219].

This is identical with the value obtained by the late Lord Rayleigh [219] using an entirely different but less direct method. The inertia component of the pressure is found in like manner as shown in § 4 below.

#### 4. Accession to inertia ( $m_i$ )

The vibration of a body in a fluid is accompanied by two salient effects, (a) sound waves are propagated outwards, (b) a cyclically varying flow of fluid occurs in the neighbourhood of the body. To maintain this flow the driving force must include an inertia or wattless component. If  $u$  is the normal velocity of an elemental surface area, the kinetic energy of the fluid associated therewith [216] is  $dT = \frac{1}{2}u^2 dm_i$ , where  $m_i$  is termed the 'accession to inertia' [219]. The

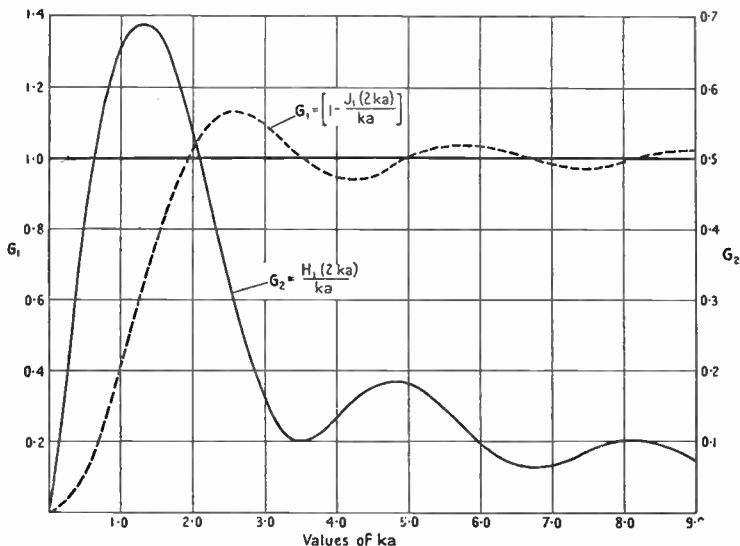


FIG. 17

influence of this reactive component in the driving force is to increase the phase angle between the total pressure and the surface velocity, and, therefore, to reduce the power factor.

If the body is a flexible circular disk centrally driven, the mass of fluid disturbed reduces the frequencies of the vibrational modes. The fundamental symmetrical centre-moving mode (one nodal circle) of a free edge aluminium disk, 10 cm. radius, 0.055 cm. thick occurs at  $120 \sim$  in air, but at  $21.8 \sim$  in water. In the latter case the accession to inertia is *ten* times the natural mass of the disk, whereas in air it is only  $1/800$  of this value.

Consider the vibration of a rigid circular disk along the axis  $X'OX$  as shown in Fig. 18 A. At an adequately high frequency the wave-length

is less than the radius of the disk. Owing to interference in the space beyond the disk, the radiation is propagated in beam formation (Chap. V, § 1). For simplicity imagine the beam to be a coaxial right cylinder of equal radius to the disk. There can then be no local flow of fluid in the vicinity of the disk. The air in contact with the disk is set in vibration, but it moves axially and *does not spread out*, i.e. there is no divergence from the source. Thus the inertia pressure on the disk is zero. The other pressure component being in phase with the

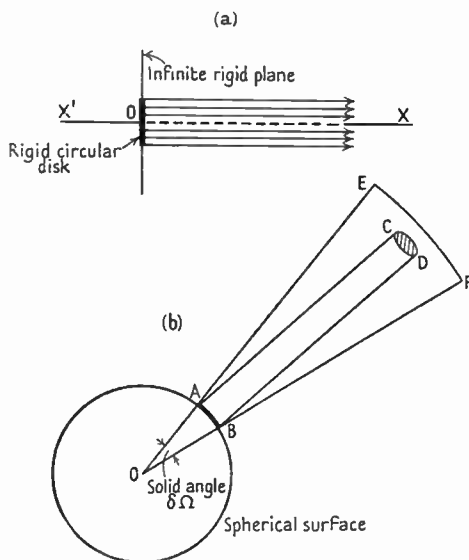


FIG. 18 A and B

velocity is associated entirely with sound radiation. Similar reasoning applies to a disk vibrating at one end of a very long cylindrical tube of the same radius, provided reflection from the open end is negligible.

One case which invariably presents a little difficulty is that of a radially vibrating sphere. Owing to spherical symmetry, there appears to be no divergence of radiation from any particular part of the surface. Moreover, it seems to follow that local flow is absent and the accession to inertia is zero. It is easy to show the fallacy of this argument. Imagine  $AB$  (Fig. 18 B) to be a tiny portion of a radially pulsating sphere. This area controls the radiation within that part of

the solid angle  $\delta\Omega$  situated beyond the precincts of the sphere. In the absence of divergence, the radiation would be confined to the cylinder  $ABCD$ . In practice, however, the radiation diverges to fill the solid angle  $ABEF$ , so there must be local flow, and it follows that a radially pulsating sphere is not devoid of accession to inertia.

There are two analytical methods of deriving  $m_i$  for both of which a knowledge of the inertia component of the pressure (or the velocity potential) at any point on the surface is essential. If the normal velocity is identical everywhere, the total pressure, and hence  $m_i$ , is found by integrating over the surface. When the velocity is variable, the kinetic energy associated with each element must be integrated over the surface, and the result divided by half the square of the velocity of some selected point. This gives  $m_i$  in terms of the velocity of the point chosen.

It is usual to select the driving point, so that the reactance due to  $m_i$  can be treated in the usual way. When, however, the edge velocity exceeds that at the centre, the former should be chosen.

*Method 1.* To illustrate the first method we shall find  $m_i$  for a rigid circular disk vibrating in an infinite rigid plane. From (5) the inertia pressure at any point on the disk is, omitting the imaginary  $i$ ,

$$p_i = \rho_0 c \xi_0 \left\{ z g_1 - \frac{z^3}{3!} g_3 + \frac{z^5}{5!} g_5 \dots \right\}. \quad (9)$$

The inertia pressure on an annulus of radius  $x$  and radial width  $dx$  is  $2\pi p_i x dx$ , so that the total inertia pressure on one face of the disk is

$$2\pi \int_0^a p_i x dx = 2\pi a^2 \int_0^1 p_i b db, \quad (10)$$

since  $b = x/a$ .

To integrate the hypergeometric functions  $g_1, g_3$ , etc., the following integrals are required:

$$\left. \begin{aligned} \int_0^1 {}_2F_1(\alpha, \beta, \gamma, b^2) b^{2\gamma-1} db &= \frac{1}{2\gamma} {}_2F_1(\alpha, \beta, \gamma+1, 1), \\ \text{where } \gamma &= 1, 2, 3, \text{ etc.} \\ \int_0^1 {}_2F_1(\alpha, \beta, 1, b^2) b^3 db &= \frac{1}{2} \{ {}_2F_1(\alpha, \beta, 2, 1) - \frac{1}{2} {}_2F_1(\alpha, \beta, 3, 1) \}, \\ \int_0^1 {}_2F_1(\alpha, \beta, 2, b^2) b^5 db &= \frac{1}{4} \{ {}_2F_1(\alpha, \beta, 3, 1) - \frac{1}{2} {}_2F_1(\alpha, \beta, 4, 1) \}. \end{aligned} \right\} \quad (11)$$

Having integrated (10) in terms of the hypergeometric functions on the right-hand side of (11), it is necessary to evaluate these by aid of Gauss's formula

$${}_2F_1(\alpha, \beta, \gamma, 1) = \frac{\Gamma(\gamma)\Gamma(\gamma-\alpha-\beta)}{\Gamma(\gamma-\alpha)\Gamma(\gamma-\beta)}. \quad (12)$$

The total inertia pressure on one side of the disk is then found to be [3 b]

$$\begin{aligned} f_i &= \frac{\rho_0 c \xi_0}{k^2} \left\{ \frac{(2z)^3}{1^2 \cdot 3} - \frac{(2z)^5}{1^2 \cdot 3^2 \cdot 5} + \frac{(2z)^7}{1^2 \cdot 3^2 \cdot 5^2 \cdot 7} - \dots \right\} \\ &= 4\rho_0 c a^2 \xi_0 \left\{ \frac{2z}{1^2 \cdot 3} - \frac{(2z)^3}{1^2 \cdot 3^2 \cdot 5} + \frac{(2z)^5}{1^2 \cdot 3^2 \cdot 5^2 \cdot 7} - \dots \right\}. \end{aligned} \quad (13)$$

The series within the brackets is  $\pi H_1(2z)/4z$ , where  $H_1$  is Struve's function of unit order. Since mass = force/acceleration =  $f_i/\omega \xi_0$ , the accession to inertia

$$m_i = \frac{\rho_0 c A}{\omega} \frac{H_1(2z)}{z} = \frac{\rho_0 c A}{\omega} G_2, \quad (14)$$

where\*  $G_2 = H_1(2z)/z$  and (14) applies to *one* side of the disk only. At low frequencies when the infinite plane is removed, formula (14) gives  $m_i$  for *both* sides of the disk, i.e. the infinite plane doubles  $m_i$ . The function  $G_2$  [3 b, 219] is plotted in Fig. 17.

*Method 2.* To illustrate the second method [1, 4] involving the kinetic energy of the fluid, we choose a flexible circular disk vibrating in an infinite rigid plane. For a disk whose dynamic deformation curve (definition 37) is†  $\xi = \xi_{\max}(1 - \phi b^2)$ , the inertia pressure at any point thereon can be shown to be [4]

$$p_i = i\rho_0 \omega \xi_{\max} a \left\{ (1 - \phi) {}_2F_1\left(-\frac{1}{2}, \frac{1}{2}, 1, b^2\right) + \frac{2}{3}\phi {}_2F_1\left(-\frac{3}{2}, \frac{1}{2}, 1, b^2\right) \right\}, \quad (15)$$

provided the propagation is substantially spherical, i.e.  $ka \leq 0.5$ . The maximum kinetic energy of the fluid associated with an elemental area  $dA$  moving with normal velocity  $\dot{\xi}_{\max}$  is [216]

$$dT = \frac{1}{2} \rho_0 \phi i \dot{\xi}_{\max}^2 dA, \quad (16)$$

where  $\phi_i$  is the inertia component of the velocity potential at the surface of the disk. Now from (31), Chap. II,  $p = \rho_0 \partial\phi/\partial t$ , so introducing the time factor  $e^{i\omega t}$  and removing it after differentiation,

$$p_i = i\rho_0 \omega \phi_i \quad \text{or} \quad \phi_i = -\frac{i p_i}{\rho_0 \omega}. \quad (17)$$

\* Alternatively  $m_i = \pi\rho_0 a^3 \{H_1(2z)/z^2\}$  = mass of a cylinder of air of radius  $a$  and height  $a\{H_1(2z)/z^2\}$ .

† In this section *maximum* values of the cyclically varying quantities  $\xi$  and  $p_i$  are implied.

Inserting the value of  $\phi_i$  from (17) in (16) we obtain

$$dT = -\frac{ip_i \xi dA}{2\omega}.$$

The kinetic energy associated with an annulus of radius  $x$  and width  $dx$  is  $-ip_i \xi x dx = -i\pi a^2 p_i \xi b db$ , since  $b = x/a$ . Thus using the value of  $p_i$  from (15) the kinetic energy of the fluid associated with

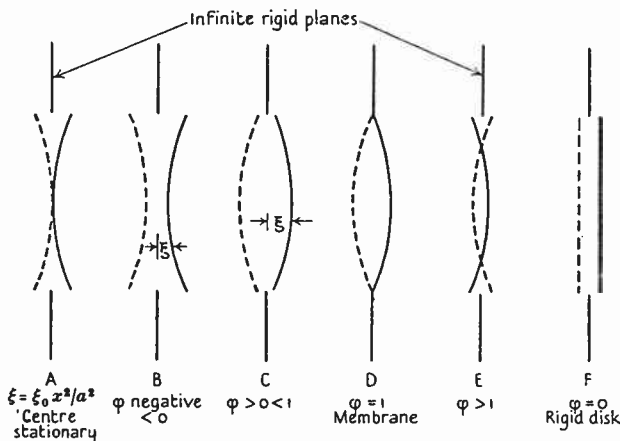


FIG. 19. Diagram showing various forms of dynamic deformation curve of the type  $\xi = \xi_0(1 - \varphi x^2/a^2)$ .

one side of the disk is

$$T = \pi \rho_0 a^3 \xi_{\max}^2 \int_0^1 [(1-\varphi)F_1 + \frac{2}{3}\varphi F_2](1-\varphi b^2)b db. \quad (18)$$

The upper limit of integration in (18) is 1, since this is the value of  $b$  when  $x = a$ ; also  $F_1 = F(-\frac{1}{2}, \frac{1}{2}, 1, b^2)$ , and  $F_2 = F(-\frac{3}{2}, \frac{1}{2}, 1, b^2)$ .

Performing the integration in (18) by aid of the integrals in (11) and using Gauss's formula (12) to reduce the hypergeometric functions, we finally obtain [4]

$$T = \frac{4}{3}\rho_0 a^3 \xi_{\max}^2 (1 - \frac{14}{15}\varphi + \frac{5}{21}\varphi^2). \quad (19)$$

In terms of the central velocity  $T = \frac{1}{2}m_i \xi_{\max}^2$ , so the accession to inertia is

$$m_i = \frac{8}{3}\rho_0 a^3 (1 - \frac{14}{15}\varphi + \frac{5}{21}\varphi^2) \quad (20)$$

for one side of the disk only.

By allotting certain values to  $\varphi$ , the value of  $m_i$  for various dynamic deformation curves shown in Fig. 19 can be found. For a rigid

disk  $\varphi = 0$ , so  $m_i = \frac{8}{3}\rho_0 a^3$ , which is identical with the value found from (14) when  $z \leq 0.5$  (spherical propagation). When  $\varphi = 2$ , the disk vibrates with a nodal circle whose radius is  $x = a/\sqrt{2}$ . The value of  $m_i$  is then  $\frac{8}{35}\rho_0 a^3$  which is approximately 8.6 per cent. that of a rigid disk. The very large reduction in  $m_i$  is due to the two equal areas on either side of the nodal circle vibrating in antiphase. By differentiating (19) with respect to  $\varphi$  the kinetic energy is found to be a minimum when  $\varphi = 1.96$ . This is substantially the case of the nodal circle at  $x = a/\sqrt{2}$ . When  $\varphi = 1$  we obtain a first approximation to a membrane in its gravest mode. Here  $m_i$  for one side is  $0.813\rho_0 a^3$  or about 0.305 that for a rigid disk. If  $\varphi > 2$  the edge amplitude exceeds that at the centre. The edge velocity is  $\xi_{\max}(\varphi - 1)$ , so that in terms of this velocity

$$m_i = \frac{8}{3} \frac{\rho_0 a^3}{(\varphi - 1)^2} \left(1 - \frac{14}{15}\varphi + \frac{5}{21}\varphi^2\right). \quad (21)$$

If in the expression  $\xi = \xi_{\max}(1 - \varphi b^2)$  we make  $\varphi \rightarrow -\infty$  but keep  $\xi_{\max}\varphi$  finite, the case of a centre-stationary mode of vibration is obtained and (21) reduces to

$$m_i = \frac{40}{63}\rho_0 a^3 \quad (22)$$

expressed in terms of the edge velocity.

A slight modification of the preceding method can be applied to the case of a free-edge disk with a nodal diameter. In terms of the maximum edge velocity,  $m_i$  for one side is  $\frac{4}{15}\rho_0 a^3$  which is precisely  $\frac{1}{10}$  that for a rigid disk.

### 5. Vibrators without a baffle [3 c]

In practical speaker problems we are usually concerned with conical diaphragms. So far the conical shell has not yielded its secrets to the analyst, and it is, therefore, necessary to compromise. When a very large baffle is employed, formula (14) can be used. In the absence of a baffle and in cases where the loud speaker operates in a small cabinet, the problem must be attacked from a different standpoint. The only geometrical solid which lends itself readily to analytical treatment, and at the same time can be used as an approximation, is the sphere. By aid of spherical harmonic analysis the accession to inertia for various types of vibration (see Fig. 20) can be found [3 c] and some typical results are given in Table 4. The total accession to inertia is the sum of that due to the various harmonics in the expansion of the radial velocity. In general, two or three harmonics



give an adequately accurate result at low frequencies. Each harmonic component is associated with a frequency correction factor. That for

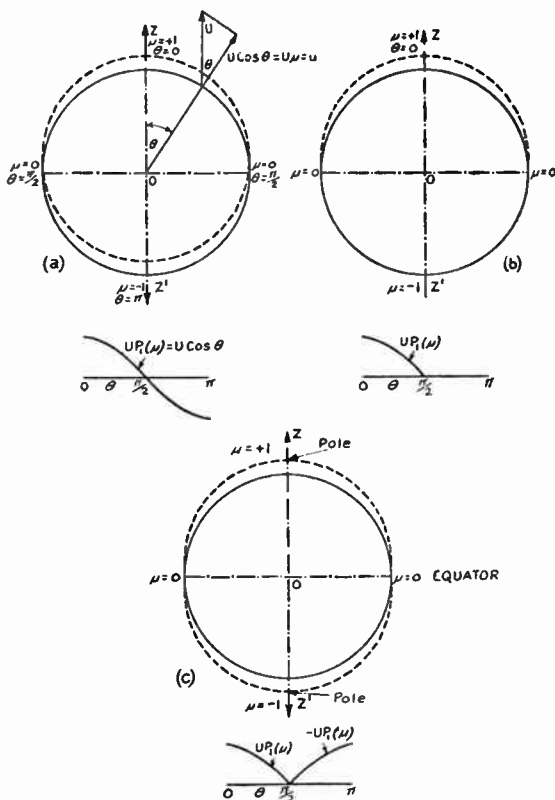


FIG. 20

(a) Sphere vibrating axially.

Radial velocity  $u = U\mu$ .

(b) One hemisphere vibrating axially, the other quiescent.

$u = U\mu$  from  $0$  to  $\frac{1}{2}\pi$ , and  $u = 0$  from  $\frac{1}{2}\pi$  to  $\pi$ .

(c) Two hemispheres vibrating axially in opposition.

$u = U\mu$  from  $0$  to  $\frac{1}{2}\pi$ , and  $u = -U\mu$  from  $\frac{1}{2}\pi$  to  $\pi$ .

a sphere vibrating axially [3 c, 219] is  $\zeta_{1r} = \frac{2+k^2a^2}{4+k^4a^4}$ , which has been plotted in Fig. 21. It has a maximum value of 0.6 when  $ka$  is 0.91.

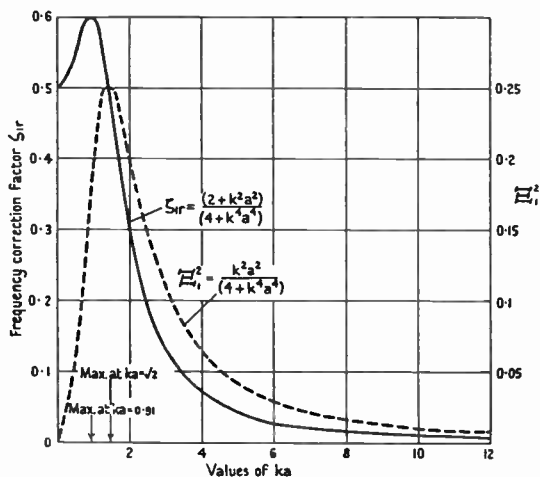


FIG. 21

TABLE 4

Accession to inertia of various vibrators [3 c, 4]

Type of vibrator	Dynamic deformation curve	Accession to inertia $m_i$
1. Free-edge disk, with nodal diameter, in infinite rigid plane.	$\xi = \xi_0 \frac{x}{a} \cos \theta$ $a = \text{radius}$	$\frac{1}{15} \rho_0 a^3$ when $ka < 0.5, n > 0$ .
2. Sphere vibrating radially.	$u = U$	$\frac{4\pi\rho_0 a^3}{1+k^2a^2} = 4\pi\rho_0 a^3 \zeta_{or}$
3. Sphere vibrating axially.	$u = U\mu = U \cos \theta$	$\frac{8}{3}\pi\rho_0 a^3 \left( \frac{2+k^2a^2}{4+k^2a^2} \right) = \frac{8}{3}\pi\rho_0 a^3 \zeta_{or}$
4. Two hemispheres vibrating in opposition along their common axis.	$u = U \cos \theta$ from $\theta = 0$ to $\frac{1}{2}\pi$ $u = -U \cos \theta$ from $\theta = \frac{1}{2}\pi$ to $\pi$	$1.1\pi\rho_0 a^3$ when $ka \leq 0.5$
5. One hemisphere quiescent, the other vibrating radially.	$u = U$ from $\theta = 0$ to $\frac{1}{2}\pi$ $u = 0$ from $\theta = \frac{1}{2}\pi$ to $\pi$	$1.41\pi\rho_0 a^3$ when $ka \leq 0.5$
6. One hemisphere quiescent, the other vibrating axially.	$u = U \cos \theta$ from $\theta = 0$ to $\frac{1}{2}\pi$ $u = 0$ from $\theta = \frac{1}{2}\pi$ to $\pi$	$0.44\pi\rho_0 a^3$ when $ka \leq 0.5$
7. Sphere with $n$ nodal circles passing through the poles.	$u = U \sin^n \theta \sin n\chi$	$\frac{2^{n+1}}{1.3 \dots (2n+1)} \left( \frac{n!}{n+1} \right) \pi\rho_0 a^3$ when $ka \leq 0.5, n > 0$ .

For a sphere 10 cm. radius, 0.91 corresponds to a frequency of 490  $\sim$ . As a first approximation this factor can be applied to rigid disks and conical shells for the same values of  $ka$ , when there is no baffle or when the latter is quite small compared with the wave-length. The value of  $m_i$  is found by multiplying the value for an infinite flat baffle by  $\zeta_{1r}$ , i.e.  $m_i = 2\rho_0 c A G_2 \zeta_{1r} / \omega$ .

To simulate the effect of a large baffle two spherical caps at each end of a diameter can be taken, both vibrating in the same direction. More than three harmonics will be required for accuracy.

## IV

### VIBRATIONAL MODES\*

#### 1. Circular disks

Imagine a free-edge homogeneous loss-free circular disk *in vacuo* driven centrally by an harmonic force. Since there is neither radiation nor transmission loss, the impedance at the driving point is wholly reactive. If the radial velocity of propagation is very high, so that the ratio  $2\pi v_r/\omega$  is always very large, the time taken for energy to be transmitted from the centre to the edge will be small compared with the duration of a quarter cycle. Thus the disk behaves substantially as a rigid structure and in a practical sense it moves as a whole. For these conditions to be manifested at 3,000  $\sim$ , a disk 10 cm. radius would have to be very thick and, therefore, unduly heavy. The amplitude and the sound radiation in air would be minute.

In practical acoustics this condition does not occur, the radial velocity is relatively low and the disk does not move as a whole. Thus there is a progressive phase shift along any radius. The inherent forces are due to inertia and elasticity. The waves propagated radially outwards are of an elastic nature and suffer reflection at the edge, there being no energy loss in the ideal case. Starting at zero frequency the effective mass (see definition 33) of the disk as presented to the driving mechanism is obviously its natural mass. As  $\omega/2\pi$  increases, a point is reached when the reflected wave arrives at the centre in antiphase with the transmitted wave. Since no loss occurs, these waves are equal but opposite, and the disk vibrates with its centre stationary. The driving force

$$f = m_e \omega^2 \xi_0 \quad \text{or} \quad m_e = f/\omega^2 \xi_0,$$

and since  $\xi_0 = 0$  at the centre, the effective mass is infinite. The effective mass of a centrally-driven free-edge homogeneous circular disk at any frequency is given by [38]

$$m_e = \frac{4\pi\rho t}{k_1^2} \left\{ \frac{B}{A + 0.116B + C} \right\}, \quad (1)$$

where  $\rho$  = density of material;  $k_1^4 = \frac{12\omega^2\rho(1-\sigma^2)}{qt^2}$

$a$  = radius;

\* Only the *symmetrical* modes of disks, cones, etc., are considered here.

$$t = \text{thickness (uniform); } \frac{B}{A} = \frac{a_2 c_1 - a_1 c_2}{c_2(b_1 + d_1) - c_1(b_2 + d_2)}$$

$$\frac{C}{A} = -\frac{a_2(b_1 + d_1) - a_1(b_2 + d_2)}{c_2(b_1 + d_1) - c_1(b_2 + d_2)}; \quad a_1 = J_1(k_1 a)$$

$$a_2 = \frac{2(1-\sigma)}{k_1 a} J_1(k_1 a) - J_0(k_1 a); \quad b_1 = Y_1(k_1 a)$$

$$b_2 = \frac{2(1-\sigma)}{k_1 a} Y_1(k_1 a) - Y_0(k_1 a); \quad c_1 = I_1(k_1 a); \quad d_1 = -K_1(k_1 a)$$

$$c_2 = I_0(k_1 a); \quad d_2 = K_0(k_1 a).$$

Using formula (1) the curves of Fig. 22 for a centrally driven

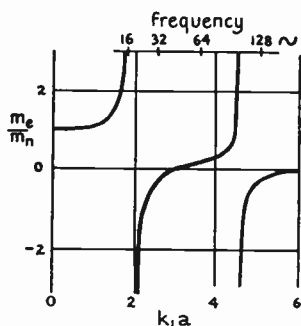


FIG. 22. Effective mass curves of centrally driven free-edge aluminium disk, 10 cm. radius, 0.0185 cm. thick.

aluminium disk 10 cm. radius, 0.0185 cm. thick were computed [38]. Starting at zero frequency where  $m_e$  and  $m_n$  are identical, the former is almost constant up to  $k_1 a = 1.2$ . Thereafter it rises rapidly until at  $k_1 a = 1.9$  it becomes infinite when the first centre-stationary mode occurs. An approximate analogy to this mode can be drawn from the impedance of a resistanceless parallel  $LC$  circuit [35 b]. The effective inductance is  $L_e = L/(1 - \omega^2 LC)$ . It increases from  $L$  at zero frequency to infinity at  $\omega^2 LC = 1$ , where the 'centre-stationary'

condition is simulated. In passing through the point

$$\omega^2 LC = 1 \quad \text{or} \quad \omega = \sqrt{1/LC},$$

the phase changes abruptly by  $180^\circ$ , i.e. it reverses. This also occurs in the disk case of Fig. 22 where  $m_e = +\infty$ . The reactance at the driving point is then of an elastic nature, but infinite in magnitude, i.e. the effective dynamical stiffness is infinite and the compliance zero. Beyond this frequency  $m_e$  (now negative) increases until at approximately  $k_1 a = 3.0$  it is zero. The direct and reflected waves annul each other on a circle whose radius is  $0.68a$ . This circle is therefore nodal and the portions of the disk on either side move in antiphase. Under these circumstances the elastic and inertia forces over the disk annihilate each other. Moreover, the effective mass is evanescent, and with a finite driving force the amplitude would tend

to be infinite! In practice, where vibration occurs in air, the impedance is purely resistive. The amplitude is finite owing to radiation and transmission loss, whilst the frequencies of the vibrational modes are reduced due to fluid inertia.

It is of interest to consider a simple way of ascertaining the radius of the first nodal circle on a free edge centrally driven disk of constant or variable thickness. Assume the dynamic deformation curve to be of the type  $\xi = \xi_0(1 - \varphi x^2/a^2)$ , where  $\varphi$  is a variable parameter. The condition to be fulfilled is that the integral of the momentum over the disk shall vanish, i.e. there must be as much negative as positive momentum. Thus

$$\sum mv = 2\pi\xi_0 \int_0^a \rho_1 \left(1 - \varphi \frac{x^2}{a^2}\right) x dx = 0, \quad (2)$$

where  $\rho_1$  is the mass per unit area and  $\xi_0(1 - \varphi x^2/a^2)$  is the axial velocity at a radius  $x$ . For a uniform disk  $\rho_1$  is constant and we find the value  $\varphi = 2$ . At the nodal radius  $\xi = 0$ , so  $1 - (2x^2/a^2) = 0$  or  $x = a/\sqrt{2}$ , which is a fair approximation to the exact value  $0.68a$ .

Reverting to Fig. 22, as  $\omega/2\pi$  rises beyond the point where  $m_e = 0$ , the latter increases and the former cycle of events is repeated *ad infinitum*. The second frequency for which  $m_e = \infty$  corresponds to one nodal circle and stationary centre (point circle), whilst the second frequency where  $m_e = 0$  gives two nodal circles of radii  $0.39a$  and  $0.84a$ . So long as the disk is homogeneous, the values of  $k_1 a$  corresponding to the centre-stationary and centre-moving modes of vibration are independent of size and material. The shape of the aluminium disk at various frequencies is illustrated in Fig. 23. These configurations hold for any disk provided the values of  $k_1 a$  are identical.

Curves of like nature are obtained when the centre of the disk is removed and the resulting annulus is driven at its inner edge. When the outer edge of a centrally driven disk or an annulus is clamped, the driving mechanism is immobile at zero frequency, so the effective

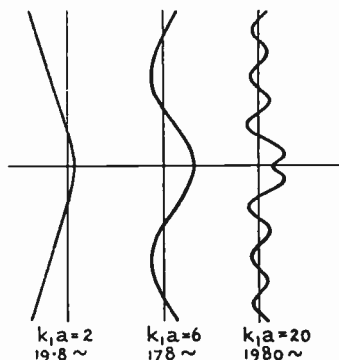


FIG. 23. Dynamic deformation curves of disk in Fig. 22 at various frequencies.

mass is negatively infinite. The curves take the form [38] illustrated in Fig. 22 from  $k_1 a = 1.9$  upwards.

## 2. Flexible reeds

The same arguments are applicable to flexible reeds [38] under various terminal or boundary conditions. For a simple cantilever reed clamped at one end and driven harmonically at the other [114c]

$$m_e = \frac{\rho_1}{k_2} \left( \frac{1 + \cosh k_2 l \cos k_2 l}{\sinh k_2 l \cos k_2 l - \cosh k_2 l \sin k_2 l} \right), \quad (3)$$

where  $k_2^4 = \rho_1 \omega^2 / qI$ ;  $\rho_1$  = mass per unit length;  $I$  the moment of inertia of a rectangular section =  $\frac{bd^3}{12}$ ;  $l$  = free length.

The effective mass curves are identical in form with those for a clamped-edge disk.

When the reed is free at one end but clamped and driven at the other [38],

$$m_e = \frac{\rho_1}{k_2} \left( \frac{\cosh k_2 l \sin k_2 l + \sinh k_2 l \cos k_2 l}{1 + \cosh k_2 l \cos k_2 l} \right). \quad (4)$$

The curves for this case correspond to those of Fig. 22 for a free edge disk.

## 3. Conical shells

The results in the preceding section indicate in a broad sense what is to be expected when conical and other shells, symmetrical about a polar axis, are driven. At the same time it must be recognized that these 'driven' frequencies, where modes occur, correspond to the natural frequencies when the vibrator is impulsed *in vacuo*. Whereas disks lend themselves so readily to mathematical analysis, conical shells have so far been recalcitrant to the inquisition of the mathematician. It is impossible, therefore, to present hypothetical curves exhibiting the effective mass of a conical shell driven *in vacuo*. In a subsequent chapter, however, it will be shown that curves of a somewhat similar nature to those for disks have been obtained empirically, using conical shells. The vibrational frequencies are not separated by wide frequency intervals as in the case of the equivalent flat disk. Fortunately for purposes of sound reproduction they occur in cluster formation (see Chap. XVIII).

## 4. Reed-driven circular disks

When a cantilever or other class of reed is used to drive a circular disk the system is complex and its vibrational frequencies differ from

those of either constituent [114 a, c]. If  $m_d$  and  $m_r$  represent, respectively, the effective mass of the disk and reed referred to their junction point, the centre-moving vibrational frequencies of the combination occur when the effective mass at the driving point vanishes, i.e.  $m_d + m_r = 0$ . The frequencies in question are, therefore, found by adding the expressions for  $m_d$  and  $m_r$ , as given above, and solving for  $\omega$ . Preferably they are found graphically by plotting the disk and reed curves using the same axes and inverting the ordinates of

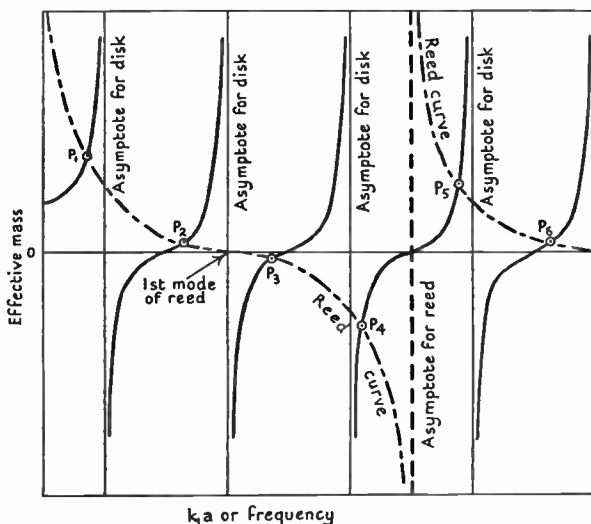


FIG. 24. Effective mass-frequency curves for finding vibrational frequencies of a reed-driven disk.

one, e.g. the reed curve. The points of intersection  $P_1, P_2$ , etc. are the roots of

$$m_d + m_r = 0.$$

The condition for stationary centre modes is  $m_d + m_r = \infty$ . This is satisfied at any asymptote of  $m_d$  or  $m_r$ . These statements are illustrated graphically in Fig. 24. The second asymptote for the reed occurs at the same frequency as  $m_e = 0$  for the disk and a stationary-centre mode ensues.

Provided the first frequency of the combination is well below the first mode of the reed for which  $m_r = 0$ , the system can be treated as a disk driven by a simple helical spring. If  $s$  is the stiffness of the reed at its point of attachment to the disk, under the above



condition  $s = \omega^2(m_e + m_0)$ , where  $m_e$  is the effective mass of the disk to which is added a small portion  $m_0$  for the reed.\* By plotting  $m_e = \{(s/\omega^2) - m_0\}$ , the point of intersection with the disk curve gives the fundamental vibrational frequency of the combination.

### 5. Reed-driven conical shells

If the effective mass curves of the shell could be computed, the treatment would be similar to that for reed-driven disks. As this cannot be

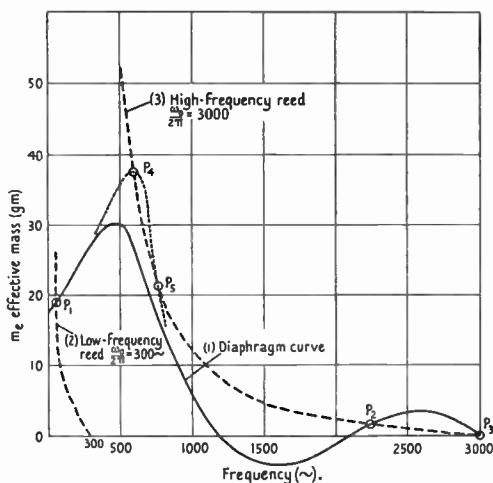


FIG. 25. Effective mass-frequency curves for finding vibrational frequencies of reed-driven cone.

done, the procedure is to determine  $m_e$  for the shell experimentally, as shown in Chapter XVI. The cone should have its usual complement of nuts and connecting rod for attachment to the reed. There are two principal cases to be considered, (a) reed frequency low, (b) reed frequency high. In Fig. 25 curve 1 is for a conical shell, whilst 2 and 3 relate respectively to reeds having fundamental frequencies of 300 ~ and 3,000 ~. Owing to diaphragm transmission loss, the  $m_e$  curve is akin to a damped sine wave oscillation. Even at low frequencies the effective mass is not outstandingly high. Consequently the 3,000 ~ reed curve does not intersect the diaphragm curve at low frequencies but passes above it. This entails a reduced

\* If  $\omega_0/2\pi$  is the fundamental reed frequency when unloaded,  $m_0 = s/\omega_0^2$ .

amplitude at the frequency where, but for the absence of loss, intersection would occur. The effective mass on the reed is the difference in the ordinates of curves (1) and (3). At  $100 \sim$  it is very large indeed, so the amplitude and, therefore, the sound output are insignificant. As  $\omega/2\pi$  rises the effective mass falls until from  $650$  to  $1,000 \sim$  it is relatively small. A minimum value occurs between these frequencies. The mechanical impedance is also a minimum somewhere within this range. Thus  $r_e/z_e$  has a maximum value; so also has the output. Considered on a decibel basis the output will be fairly constant over the above range. The two curves intersect at  $P_2$  and  $P_3$  and these points correspond to vibrational modes where the output will be greatest. The  $3,000 \sim$  reed curve intersects the curve for another diaphragm, a portion of which is shown dotted. In this case there will be vibrational modes at  $P_4$  and  $P_5$ .

The low-frequency reed curve (2) intersects the diaphragm curve (1) at about  $50 \sim$  where a prominent mode occurs. If the remainder of the reed curves are plotted as in Fig. 24, there may be intersections at higher frequencies. In all cases the combined impedance is solely resistive where the curves intersect, i.e. it is  $r_e = z_e$ .

## 6. Centring devices

In hornless moving-coil speakers it is customary to provide a centring device to preserve axial motion of the coil, thereby eliminating wobble and ultimate damage due to the coil rubbing on the magnet. This device takes various forms, some of which are shown in Fig. 26. Although the theoretical  $m_e$  curves might be difficult to determine rigorously by analytical methods, it is easy to see that the principles enunciated above and illustrated graphically are applicable here. The lowest frequency of a conical diaphragm on a centring device depends upon the stiffness of the latter. For good reproduction it should be less than  $30 \sim$ . Up to  $200 \sim$  a hornless speaker diaphragm can be taken to move as a whole, so  $m_e = m_n + m_i$ . Suppose the curves of Fig. 22 represent  $m_e$  of the centring device driven at its point of attachment to the coil, there being no loss. If the effective mass of the diaphragm is set off below the horizontal axis, the vibrational frequencies correspond to the points of intersection of the two sets of curves. In practice loss occurs and the fundamental vibration is the most powerful. It must not be assumed, however, without experimental evidence that because the fundamental is inaudible,

the higher modes of the combination in the lower register are not of importance.

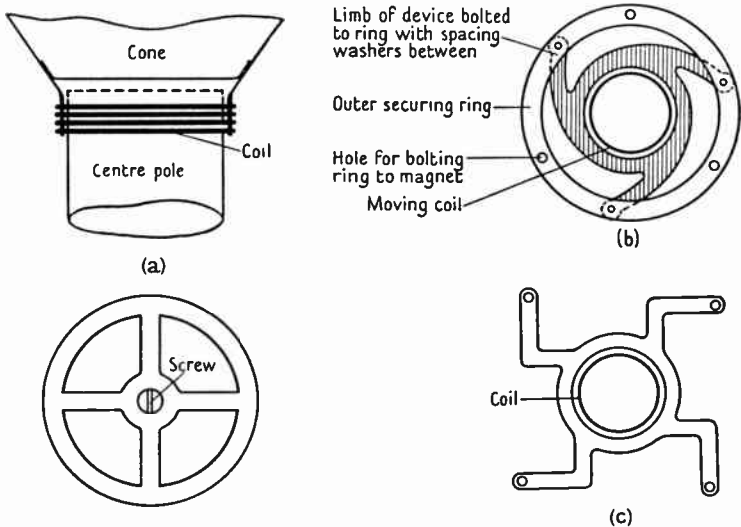


FIG. 26. Diagram illustrating three centring devices for moving-coil loud speakers.

### 7. Flexible annular surround

Consider the system shown diagrammatically in Fig. 27 A. The conical shell is supported on an annular surround and the driving coil has no centring device. There are three principal low frequencies of vibration [114 a]: (a) the diaphragm vibrates axially as a whole on the surround, the system being akin to a mass and helical spring, (b) the diaphragm vibrates transversely (side to side) under the surround constraint, this being a form of wobble, (c) the surround itself vibrates as an annular membrane. The problem before us is to determine each frequency. The only case which presents difficulty is (b). To bring the whole problem within the scope of simple analysis the following artifice is adopted.

In Fig. 27 B  $m_n$  is a rigid rectangular block representing the diaphragm, whilst the annular surround is simulated by rectangular membranes above and below the block. Provided  $m_n$  is much greater than the mass of the two membranes

$$\omega_1 = \sqrt{\frac{s}{m_e}}, \quad (5)$$

where  $m_e = m_n + m_i$ ;  $s$  = axial stiffness. By considering torsional oscillation about the axis  $XX'$

$$\omega_2 = \sqrt{\frac{3s}{m_n}}, \quad (6)$$

the accession to inertia being negligible for this mode of vibration.

Thus 
$$\frac{\omega_2}{\omega_1} = \sqrt{\frac{3(m_n + m_i)}{m_n}} = \sqrt{3(1 + \varpi)}, \quad (7)$$

where  $\varpi = m_i/m_n$ .

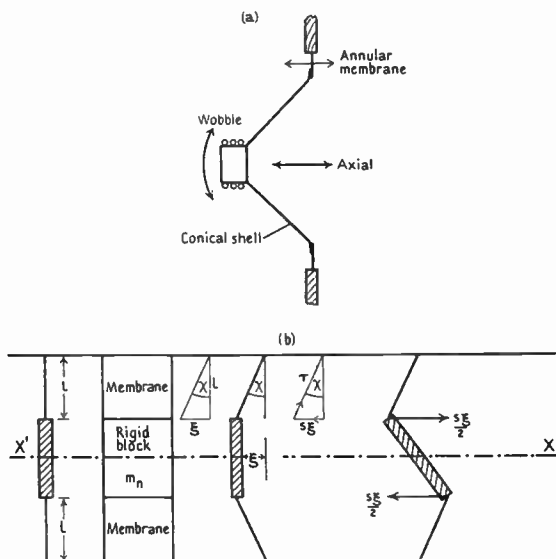


FIG. 27. Diagrams illustrating three forms of oscillation in a moving-coil system.

Knowing  $\omega_1$  for the conical diaphragm on its surround, also the values of  $m_n$  and  $m_i$  (7) is used to calculate the frequency of the wobble. In general it is about twice the frequency obtained from (5).

The fundamental frequency of the surround vibrating as an annular membrane can be estimated approximately by supposing it to act in the same manner as a stretched string [114 a]. Then

$$\omega_3 = \pi \sqrt{\frac{\tau}{m_{es} l}}, \quad (8)$$

where  $m_{es}$  = effective mass of surround including  $m_s$ ;  
 $\tau$  = total radial tension at inner circumference =  $2\pi b\tau$ ;  
 $l$  = radial width of surround.

From Fig. 27 B we have, for small displacements,

$$\text{Axial force} = \tau\chi = s\xi,$$

$$\text{or} \quad \tau = \frac{s\xi}{\chi} = sl,$$

which on substitution in (8) yields

$$\omega_3 = \pi \sqrt{\frac{s}{m_{es}}}. \quad (9)$$

Although this result is adequate for most practical requirements below 200  $\sim$ , the method is not rigorous. The complete solution is given in a later section, where it is shown that in hornless speakers the higher modes follow the sequence 2, 3, 4, etc. Thus if the fundamental is found from (9) the overtones are obtained by multiplication. In practice, the radial tension is not always constant round the periphery of the membrane. This broadens the fundamental resonance band and mitigates its severity.

The ratio of the surround frequency to that of the diaphragm moving axially on the surround is from (5) and (9)

$$\frac{\omega_3}{\omega_1} = \pi \sqrt{\frac{m_e}{m_{es}}}, \quad (10)$$

where  $m_e$  is the effective mass of the diaphragm and a portion of the surround including the appropriate accession to inertia.

The addition of a centring device eliminates the wobble or renders it innocuous. The main axial frequency is now increased due to the additional constraint. If the centring device imposes a constraint  $s_1$  the new frequency of the diaphragm is

$$\omega'_1 = \frac{1}{2\pi} \sqrt{\frac{s+s_1}{m_e}}; \quad (11)$$

$$\text{also} \quad \frac{\omega_3}{\omega'_1} = \pi \sqrt{\frac{m_e s}{m_{es}(s+s_1)}}, \quad (12)$$

provided the diaphragm vibrates as a rigid structure,  $s$  and  $s_1$  being of the same order of magnitude. When this is not so, the procedure is that given in § 13.

## 8. Air chamber due to re-entrant cone

When a conical diaphragm has a re-entrant cone at the vertex, as shown in Fig. 28 A, and there is little clearance between the coil and centre pin of the magnet, the air-chamber so formed may cause resonance. The electrical analogue of the mechanical system is shown in Fig. 28 B. The inductance simulates the effective mass of the diaphragm with respect to the chamber, the condenser represents

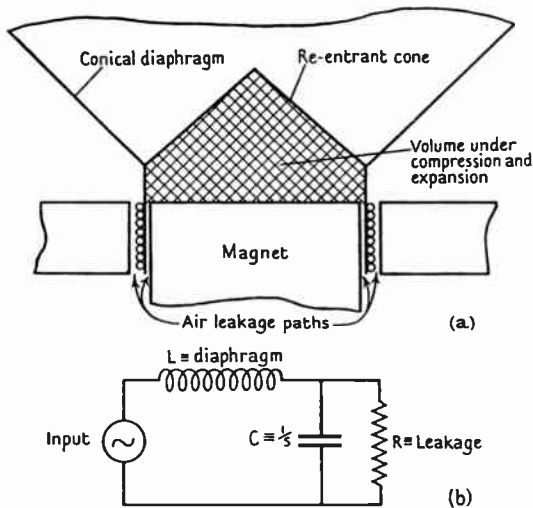


FIG. 28 A and B

the compliance or reciprocal of the chamber stiffness, whilst the resistance is equivalent to the effect of air leakage between coil and magnet.

Neglecting the influence of leakage, the vibrational frequency is

$$\omega = \sqrt{\frac{1}{LC}} \equiv \sqrt{\frac{s}{m_e}} \quad (13)$$

We have now to find  $s$  the chamber stiffness in the absence of air leakage.

Using the adiabatic gas law  $pV^\gamma = \text{const.}$  we have on differentiating both sides with respect to the displacement  $\xi$ ,

$$\frac{\partial}{\partial \xi} [pV^\gamma] = \gamma p V^{\gamma-1} \frac{\partial V}{\partial \xi} + V^\gamma \frac{\partial p}{\partial \xi} = 0 \quad (14)$$

Multiplying by  $A/V'$ , where  $A$  is the circular area within the coil-former, we get

$$\frac{\gamma p A}{V} \frac{\partial V}{\partial \xi} = - \frac{A}{\partial \xi} \frac{\partial p}{\partial \xi}. \quad (15)$$

The quantity on the right in (15) represents the force per unit displacement, i.e.  $s$ . The negative sign signifies that the pressure in the chamber increases as  $\xi$  decreases, i.e. the slope of the dynamical characteristic is negative. Now the change in volume is  $\partial V = A \partial \xi$ , which on substitution in the left side of (15) gives

$$s = \frac{\gamma A^2 p_0}{V}, \quad (16)$$

since  $p_0$  is the normal atmospheric pressure.

$$\text{From (13) and (16)} \quad \omega = \sqrt{\left( \frac{\gamma A^2 p_0}{V m_e} \right)}. \quad (17)$$

This formula is unsuitable for finding the frequency due to the re-entrant cone, since  $m_e$  varies with frequency as shown in Chapter XVI, so we have to resort to a graphical procedure. The effective mass-frequency curve of the diaphragm is obtained experimentally with the re-entrant cone decapitated to render it innocuous, i.e.  $s = 0$ :  $m_e = s/\omega^2$  is plotted using the same coordinate axes. The points where the curves intersect give the vibrational frequencies. Taking a numerical example with practical values, let  $A = 20 \text{ cm.}^2$ ,  $V = 40 \text{ cm.}^3$ ,  $p_0 = 10^6 \text{ dynes cm.}^{-2}$ , we obtain  $s = 1.41 \times 10^7 \text{ dynes cm.}^{-1}$ . Thus  $m_e = \frac{1.4 \times 10^7}{\omega^2}$  from which the data in Table 5 were compiled.

TABLE 5

<i>Effective mass</i> $m_e$ (gm.)	<i>Resonant frequency</i> (~)
140	50
35	100
0.35	1,000
0.085	2,000

Consider the effective mass curve (2) of Fig. 111. If the data in Table 5 were plotted on the same coordinate axes, the curves would intersect just above 100 ~ and again above 1,500 ~. The magnitude of the acoustical effect in both cases depends upon the air leakage. At 100 ~ the leak is much greater than that above 1,500 ~.

Consequently unless the clearance is small the low resonance will be insignificant. At the higher frequencies it is sometimes quite prominent as shown in curve 1, Fig. 136. This graphical procedure is approximate since the stiffness of the chamber may, in turn, influence the effective mass of the diaphragm.

### 9. Composite vibration of coil, coil former,\* and diaphragm

This trio constitutes a complex vibrational system whose properties it is now proposed to examine analytically. In a rigorous sense the mechanical system is represented by the analogous electrical circuit of Fig. 29 A. The driving coil is replaced by a fixed inductance at the

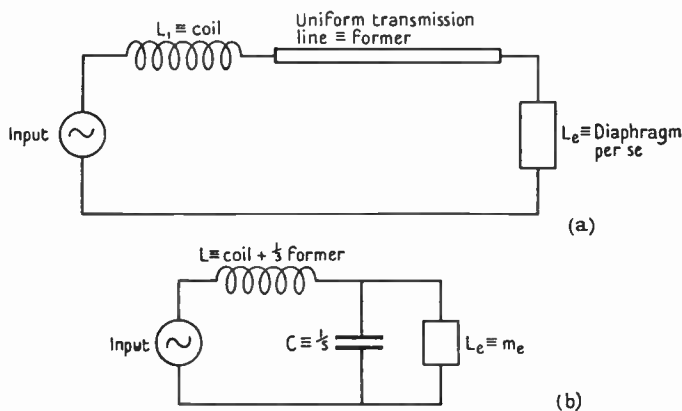


FIG. 29 A and B

sending end of a short uniform transmission line representing the cylindrical former, the termination being an effective inductance which can be positive, negative, or zero, thereby simulating the effective mass of the diaphragm as presented to the coil former. This circuit can easily be analysed by aid of well-known electrical transmission line formulae. The coil former in practice is very short, the transmission time  $l/\sqrt{(q/\rho)}$  being of the order  $10^{-6}$  to  $10^{-5}$  sec., so the application of transmission formulae to such a simple problem would be like using a steam-hammer to crack a nut. An approximately analogous circuit is sketched in Fig. 29 B in which  $\frac{1}{3}$  the mass of the free length of the former is added to that of the coil. If we imagine

\* This is the neck or unwound portion of the cylindrical former between coil and diaphragm.



the alternator to be short-circuited, the natural frequency of the remainder is

$$\omega = \sqrt{\left(\frac{L+L_e}{LL_e}\right) \frac{1}{C}}, \quad (18)$$

since the inductance of  $L$  and  $L_e$  in parallel is  $LL_e/(L+L_e)$ . Transforming (18) to its mechanical analogue, we get

$$\omega = \sqrt{\left(\frac{m_c+m'_e}{m_c m'_e}\right) s}, \quad (19)$$

where  $s$  = stiffness of coil former =  $qA/l$ ,  $A$  = section,  $l$  = length,

$m_c$  = mass of coil +  $\frac{1}{3}$  mass of free length of former,

$m'_e$  = effective mass due solely to diaphragm.

When the effective mass is infinite we have from (19), dividing above and below by  $\sqrt{(m'_e)}$ ,

$$\omega = \sqrt{(s/m_c)}. \quad (19a)$$

This gives the fundamental frequency of the coil on the unwound length of the coil former when the diaphragm end is immobile, and will be recognized as a simple mass and helical spring formula.

Reverting to (19), since  $m'_e$  varies with frequency, an indeterminate condition obtains, and as it stands the formula is useless for finding the natural modes of the system. By transposition (19) can be written

$$m'_e = \frac{m_c}{\{(\omega^2 m_c/s) - 1\}}. \quad (20)$$

For a specified coil and former (20) gives the effective mass of the diaphragm required for resonance at any selected value of  $\omega$ . Consequently if  $m'_e$  from (20) and  $m_c$  for the diaphragm (usually found by experiment) are plotted using the same coordinate axes, the points of intersection satisfy (20). Thus the abscissae of these points give the vibrational frequencies of the system. For an average case  $s$  is of the order  $10^9$  to  $10^{10}$  dynes  $\text{cm.}^{-1}$ , whilst  $m_c$  varies from 2.5 to 6.5 gm. which means that up to at least 2,000  $\sim, m'_e \doteq m_c$ . Thus for resonance to occur between 0 and 2,000  $\sim$ , the effective diaphragm mass must be negative and numerically equal to that of the coil plus one-third of the free former length.

The graph of (20) is shown by the full line curve in Fig. 30. The effective mass is infinite when  $\omega^2 m_c/s - 1 = 0$  or  $\omega = \sqrt{(s/m_c)}$ , which is identical with (19a) if the diaphragm end of the former is fixed. The dotted line curve in Fig. 30 represents the effective mass of a diaphragm, apart from that of the coil and former, which was sub-

tracted. The intersections with the full line curve give the vibrational modes of the system. The effective mass of the diaphragm is quite small beyond 3,500  $\sim$ , and there are no vibrational modes at higher audible frequencies, since the curves do not intersect. It follows, therefore, that if the vibrational frequency of the coil on the former, when the diaphragm end is clamped, is adequately high, there is no combined longitudinal oscillation of the system during sound reproduction.

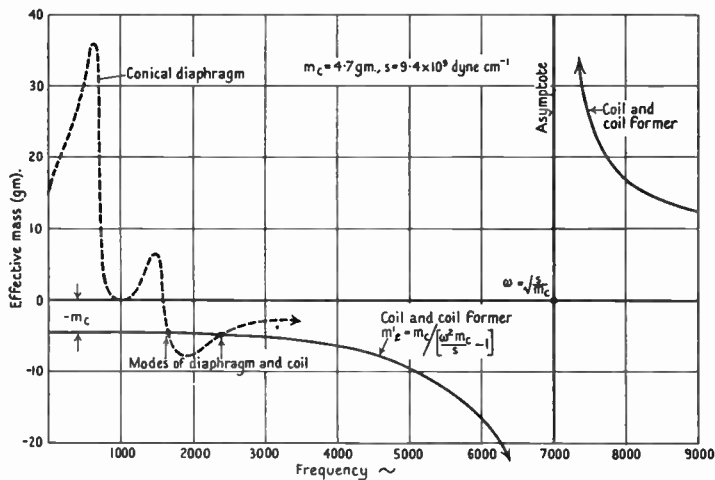


FIG. 30

Before leaving this subject it is of interest to note that if the connexion between the former and diaphragm be of a flexible nature, the asymptote in Fig. 30 will occur at say 1,500  $\sim$ . Thus up to 1,400  $\sim$  the reproduction will be fairly normal resonance probably occurring in the neighbourhood of 1,500  $\sim$  (according to the effective mass curve of the diaphragm). Above 1,500  $\sim$  the full line curve lies well above the diaphragm curve, so the combined effective mass is large. Consequently the amplitude is appreciably reduced and the upper register lost. It is easy to corroborate this by experiment.

In the solution of vibrational problems under review two salient methods are employed, (a) electrical analogue, (b) effective mass. Where the structure can be analysed into simple mass and stiffness components, or into an equivalent transmission line *where the waves are longitudinal*, the electrical analogue is probably the simpler

process. But where the vibrations are flexural, as in a disk or reed, or transverse as in a membrane, the procedure is inapplicable and it is necessary to rely upon the effective mass method. Examples illustrating the procedure in loud speaker design are given hereafter.

### 10. Annular membrane loaded statically at inner radius

Before treating the vibrational aspect of the subject it is well to deal with the mechanical and geometrical properties of a statically loaded membrane. A practical arrangement encountered in certain hornless speakers is illustrated in Fig. 31. A membrane or a cloth cone

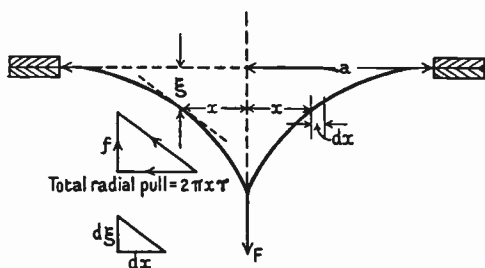


FIG. 31. Diagram illustrating forces on circular membrane.  $F$  is applied to a small metal attachment.

formed from a circular sector is held securely between two outer clamping rings and centrally loaded on a small central circle. A disk immediately assumes the shape of Fig. 31, whilst a cone of  $90^\circ$  apical angle preserves a straight slant side. On treatment with a solution of celluloid in acetone or other suitable solvent, the astringent influence of the dope causes the cone to assume the form of Fig. 31. When dry the shape is maintained on removal of the load.

To treat the problem analytically we shall deal with a perfectly elastic homogeneous circular membrane loaded as above.

From Fig. 31

$$\frac{f}{2\pi x\tau} = -\frac{d\xi}{dx}, \quad (21)$$

where  $2\pi x\tau$  is the total horizontal radial tension on the ring of radius  $x$ .

From (21)

$$\int d\xi = -\frac{f}{2\pi\tau} \int \frac{dx}{x} + A_1,$$

so

$$\xi = \frac{f}{2\pi\tau} \log_e \frac{1}{x} + A_1. \quad (22)$$

At the clamped edge  $x = a$  and  $\xi = 0$ , so the shape of the membrane is given by

$$\xi = \frac{f}{2\pi\tau} \log_e \frac{a}{x}. \tag{23}$$

If the centre is clamped to a metal disk, radius  $b$ , its displacement is

$$\xi_0 = \frac{f}{2\pi\tau} \log_e \frac{a}{b}. \tag{24}$$

### 11. Symmetrical modes of circular membrane *in vacuo* [215]

Referring to Fig. 31, consider an annulus of radius  $x$  and radial width  $dx$ . The force acting vertically is

$$-\frac{\partial}{\partial x} \left[ 2\pi x \tau \frac{\partial \xi}{\partial x} \right] dx,$$

and for stability this must be equal to the accelerational force  $-2\pi x dx \rho_1 \ddot{\xi}$ , where  $\rho_1$  is the mass of the membrane per unit area.

Thus equating these two forces we obtain

$$\frac{\tau}{\rho_1 x} \frac{\partial}{\partial x} \left( x \frac{\partial \xi}{\partial x} \right) = \ddot{\xi},$$

or

$$\frac{\tau}{\rho_1 x} \left( x \frac{\partial^2 \xi}{\partial x^2} + \frac{\partial \xi}{\partial x} \right) = \ddot{\xi} = -\omega^2 \xi, \tag{25}$$

for harmonic motion.

The differential equation of the dynamical system, in the absence of radial modes of vibration, is, therefore,

$$\frac{d^2 \xi}{dx^2} + \frac{1}{x} \frac{d\xi}{dx} + \frac{\omega^2 \rho_1 \xi}{\tau} = 0. \tag{26}$$

Writing  $k_1^2 = \omega^2 \rho_1 / \tau$ , and inserting this value in (26), we obtain

$$\frac{d^2 \xi}{dx^2} + \frac{1}{x} \frac{d\xi}{dx} + k_1^2 \xi = 0. \tag{27}$$

The solution to this equation involves two kinds of Bessel functions both of zero order. Thus

$$\xi = A_1 J_0(k_1 x) + B_1 Y_0(k_1 x). \tag{27 a}$$

When  $x = 0$ ,  $Y_0 = -\infty$ , which does not fit our requirements, since  $\xi$  must be finite, so  $B_1 = 0$ .

Thus 
$$\xi = A_1 J_0(k_1 x) \tag{28}$$

is the desired solution. To find  $A_1$  suppose the central amplitude of a steady oscillation in the absence of resistive loss to be  $\xi_0$ . Then

$\xi = \xi_0$  when  $x = 0$ , and since  $J_0(0) = 1, A_1 = \xi_0$ . Thus the dynamic deformation curve for the ideal loss-free state is given by the equation

$$\xi = \xi_0 J_0(k_1 x). \quad (29)$$

This curve is plotted in Fig. 32, the origin representing the centre of the diaphragm. At the clamped edge  $x = a$  and  $\xi = 0$ , so  $J_0(k_1 a) = 0$  is a condition which must always be fulfilled. In the absence of a driving force, the diaphragm can vibrate only in one or more of its natural modes. These correspond to the values of  $k_1 a$  for which  $J_0(k_1 a) = 0$ , i.e. to the roots of the latter. We assume that the mem-

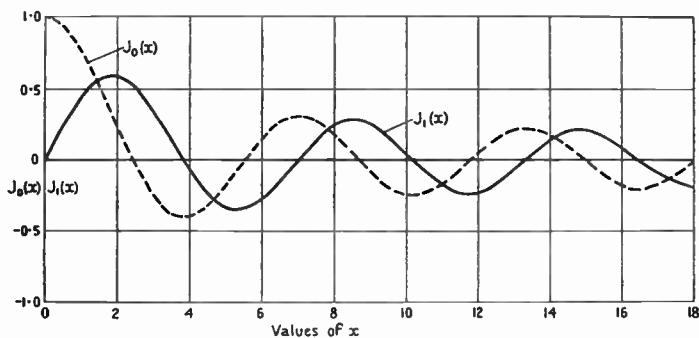


FIG. 32. Bessel functions of the first kind of zero and unit orders.  
In reading diagram replace  $x$  by  $k_1 x$ .

brane is caused to vibrate in one of its natural modes by an external agency. It is then left to continue the harmonic vibration with constant amplitude. At the first vibrational mode  $J_0(k_1 a) = 0$  and (see Fig. 32)

$$k_1 a \doteq 0.766\pi \doteq 2.4,$$

so the dynamic deformation is given, to a scale where the central amplitude is  $\xi_0$ , by the curve from  $k_1 x = 0$  to  $k_1 a = 0.766\pi$ . For the second mode  $k_1 a \doteq 1.757\pi$  so the shape includes the portion between this value and the origin. Thus the value  $k_1 x = 0.766\pi$  now corresponds to the first nodal circle, since at the corresponding radius  $\xi = 0$ . The radius is therefore  $\frac{0.766}{1.757}a = 0.436a$ . The higher modes can be treated in like manner. Beyond the first, there is an almost constant difference of  $\pi$  between consecutive roots. As a first approximation the  $n$ th root is obtained from  $(k_1 a)_n = \pi(n - 0.244)$ . To test this let  $n = 5$ ; then  $ka = 4.756\pi$ , whereas the more accurate [213]

value is  $4.7527\pi$ . The approximate formula is sufficiently accurate for practical purposes.

## 12. Annular membrane in vacuo

For the free vibrations the membrane is clamped at its outer and inner radii  $a$ ,  $b$ . The boundary conditions being  $\xi = 0$  at  $x = a$ , and at  $x = b$ , we have on substitution in (27 a)

$$A_1 J_0(k_1 a) + B_1 Y_0(k_1 a) = 0 \quad (30)$$

$$A_1 J_0(k_1 b) + B_1 Y_0(k_1 b) = 0. \quad (31)$$

For these equations to form a consistent system, the condition written determinantly is

$$\begin{vmatrix} J_0(k_1 a) & Y_0(k_1 a) \\ J_0(k_1 b) & Y_0(k_1 b) \end{vmatrix} = 0, \quad (32)$$

from which, on expansion, we get

$$J_0(k_1 a)Y_0(k_1 b) - J_0(k_1 b)Y_0(k_1 a) = 0. \quad (33)$$

The vibrational frequencies are found on solution of this equation for  $k_1$  as follows [213, 213 b].

The  $s$ th root of  $J_0(\varphi y)Y_0(y) - J_0(y)Y_0(\varphi y) = 0$ ,  $\varphi > 1$ , is given by

$$y = \omega + \frac{p}{\omega} + \frac{q - p^2}{\omega^3} + \frac{r - 4pq + 2p^3}{\omega^5} + \dots, \quad (34)$$

where

$$\omega = \frac{s\pi}{\varphi - 1}, \quad p = \frac{-1}{8\varphi}, \quad q = \frac{100(\varphi^3 - 1)}{3(8\varphi)^3(\varphi - 1)}, \quad r = \frac{-34336(\varphi^5 - 1)}{5(8\varphi)^5(\varphi - 1)},$$

$\varphi = a/b$ ,  $\varphi y = k_1 a$ ,  $y = k_1 b$ ,  $s$  = number of root (1, 2, 3, etc.). By way of example let  $a/b = 15/12 = 1.25$ , a value suitable for the surround of a hornless speaker. To find the first root of (33) we have  $\omega = 4\pi$ ,  $p = -0.1$ ,  $q = 0.127$ ,  $r = -0.84$ . From (34) it is clear that the first root is substantially  $k_1 b = 4\pi$ , the higher roots being  $8\pi$ ,  $12\pi$ , and so on. If the frequency of the fundamental mode is  $120 \sim$  (see Fig. 126), the higher values are  $240 \sim$ ,  $360 \sim$ , etc. Consequently in speakers where the width of the annular surround ( $a - b$ ) is a small fraction of the minor radius  $b$ , the vibrational modes follow the sequence of the first  $n$  natural numbers.

We have now to determine the dynamic deformation curve of the annulus. Since it is clamped at both boundaries ( $a$ ,  $b$ ) an arbitrary radius  $x_0$  must be selected and given an amplitude, say  $\xi_0$ . The necessary boundary conditions are  $\xi = 0$  at  $x = a$  and  $x = b$ ; also

$\xi = \xi_0$  at  $x = x_0$ . Substituting these quantities in (27 a) we obtain

$$\xi = \xi_0 \left[ \frac{J_0(k_1 x)Y_0(k_1 a) - J_0(k_1 a)Y_0(k_1 x)}{J_0(k_1 x_0)Y_0(k_1 a) - J_0(k_1 a)Y_0(k_1 x_0)} \right], \quad (35)$$

where  $x \geq b$ ,  $x_0 > b < a$ .

### 13. Effective mass of annulus driven axially at inner radius

When the annulus is driven harmonically at its inner radius by a diaphragm, as in the hornless moving-coil speaker, in the absence of loss the impedance at the driving ring is  $\omega m_e$ , where  $m_e$  is the effective mass. This can be positive, negative, or zero, according as the reaction is due to inertia, compliance (elasticity), or is evanescent. The latter condition corresponds to a vibrational mode of the *driven* annulus and the central amplitude increases without limit,\* since the inertia and elastic forces over the membrane balance out. From (21) the axial force at any radius is  $f = -2\pi x \tau (d\xi/dx)$ . To ascertain  $\xi$ , the conditions are  $\xi = 0$  when  $x = a$ , and  $\xi = \xi_0$  when  $x = b$ . Inserting these in (27 a) the expression for the amplitude is

$$\xi = \xi_0 \left[ \frac{J_0(k_1 x)Y_0(k_1 a) - J_0(k_1 a)Y_0(k_1 x)}{J_0(k_1 b)Y_0(k_1 a) - J_0(k_1 a)Y_0(k_1 b)} \right]. \quad (36)$$

Performing the differentiation  $d\xi/dx$  and inserting the result in the above formula, we obtain

$$f = 2\pi \xi_0 \tau k_1 x \left[ \frac{J_1(k_1 x)Y_0(k_1 a) - J_0(k_1 a)Y_1(k_1 x)}{J_0(k_1 b)Y_0(k_1 a) - J_0(k_1 a)Y_0(k_1 b)} \right]. \quad (37)$$

This force at a radius  $x$  is opposed by the accelerational component  $-\omega^2 \xi m_e$ . Equating this to (37) the effective mass at the inner radius  $b$  is

$$m_e = -\frac{2\pi b \rho_1}{k_1} \left[ \frac{J_1(k_1 b)Y_0(k_1 a) - J_0(k_1 a)Y_1(k_1 b)}{J_0(k_1 b)Y_0(k_1 a) - J_0(k_1 a)Y_0(k_1 b)} \right], \quad (38)$$

since  $\xi = \xi_0$  when  $x = b$ , and  $\tau/\omega^2 = \rho_1/k_1^2$ .

The natural vibrations occur when the denominator of (38) is zero† which makes  $m_e$  infinite, since the inner radius is then immobile. This corresponds to the centre-stationary modes of a disk. At the centre-moving modes  $m_e$  vanishes, and when the driving mechanism is massless,

$$J_1(k_1 b)Y_0(k_1 a) - J_0(k_1 a)Y_1(k_1 b) = 0. \quad (39)$$

The values of  $k_1$  are found on solution of (39). Thus the effective mass curves of a membrane are somewhat similar to those of a disk. (See curve 1, Fig. 33 for illustration.)

\* Provided the driving mechanism is massless.

† See also (33).

When the radius of the driving-ring vanishes, the effective mass can be found as a limiting case of (38). Thus when  $b$  is small,  $J_1(k_1b) \doteq 0$ ,  $J_0(k_1b) \doteq 1$ ,  $Y_1(k_1b) \doteq -2/\pi k_1b$ , and  $Y_0(k_1b) \doteq (2/\pi) \log_e(k_1b)$ . Substituting these values in (38) we find that when  $b \rightarrow 0$ ,

$$m_e = 0.$$

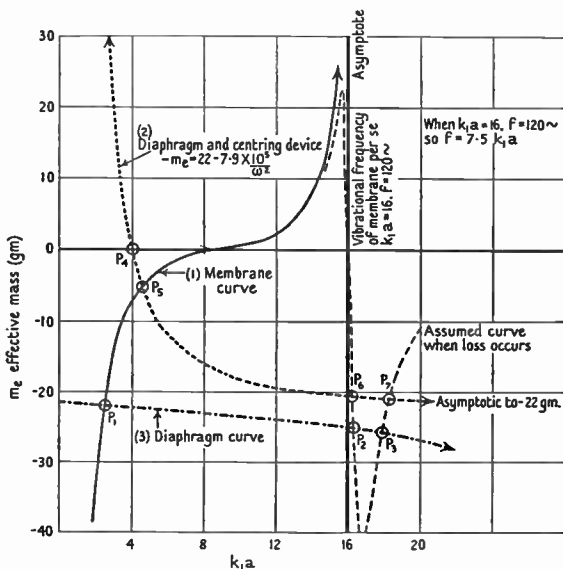


FIG. 33. Effective mass curves of annular membrane and conical diaphragm. The points of intersection give the vibrational frequencies of the combination.

From a physical aspect this is seen readily from Fig. 31 and expression (23) where  $\xi = \infty$  when  $x = 0$ . The total horizontal tension at any section is  $2\pi x\tau$ . When  $x$  vanishes, so also does the tension, so there is no restraint and theoretically the driving force causes the extension to approach an infinite value.

Annular membranes are used in hornless speakers to support the diaphragm at its periphery. Experimental evidence indicates that the effective mass of a rubber\* annulus undergoes profound variation at the first vibrational mode (diaphragm all but stationary). Before

\* Leather is used in practice since rubber perishes. It cannot be regarded as 'elastic'.



resonance it becomes highly positive and thereafter negative as shown in Fig. 33 and in Fig. 111, curve 2. This is in accordance with the theory given above. An approximate method of solving the problem of the diaphragm and its surround is given in § 7. We shall now deal with the matter more rigorously on the assumption that the membrane is not influenced by accession to inertia. Actually this is impossible unless the annulus is extremely heavy. Curve 1, Fig. 33 shows the effective mass of an annular surround driven at its inner radius. When  $k_1 a = 8.5$ ,  $m_e = 0$ , so that the driven mass is that of the diaphragm only. At  $k_1 a = 16$ , where in the present case  $\omega/2\pi = 120 \sim$ , the annulus executes its first vibrational mode with its inner radius stationary (see also Fig. 126). In practice two cases arise, (a) a centring device is used to prevent wobble as explained in § 6; (b) the air-gap in the magnet of a speaker is large enough for the centring device to be omitted, or the axial constraint it imposes is negligible compared with that due to the surround. Taking (a) first, if  $s$  is the stiffness of the centring device of negligible mass, the effective mass of the system, assuming the diaphragm to move as a whole, is  $m_e = m_d - s/\omega^2$ . The structure being rigid means that this is the value of  $m_e$  when the diaphragm is driven by the coil or from the inner ring of the surround. Consequently, if the effective mass  $m_e = m_d - s/\omega^2$  is plotted using the same coordinate axes as those for the membrane (inverted), the intersections represent the vibrational modes of the trio. This has been done in Fig. 33.  $P_4$  is the vibrational frequency with the centring device in the absence of the surround ( $30 \sim$ ), whilst  $P_5$  is the actual value ( $35 \sim$ ) with the surround. In practice there is transmission loss in and radiation from the membrane. To illustrate this, the probable shape of the membrane curve is shown dotted. The diaphragm curve 2 cuts the latter in two points  $P_6, P_7$  close together, and these are associated with vibrational modes of the annulus *per se*, as shown in Figs. 125, 126. If  $s$ , the dynamical coefficient of the centring device, is replaced by that of a reed, the solution applies to a reed-driven cone with an annular surround (see Figs. 75 B and 76).

In the absence of a centring device the diaphragm curve is indicated by (3).  $P_1$  corresponds to vibration of the diaphragm as a whole on the surround, whilst  $P_2, P_3$  are associated with vibrational frequencies of the latter as an annular membrane. They correspond to the points in Fig. 126 where curve 2 intersects the static inductance curve

between 100 and 150  $\sim$ . \* The ratio of the mean frequency of  $P_2P_3$  to that of  $P_1$  is about 7/1, which agrees quite well with the value found experimentally. The diaphragm mass of 22 gm. includes its own accession to inertia, but not that of the surround. If curve 3 is lowered bodily about 7 gm. the accession to inertia due to the surround is taken into account. It is then assumed that  $m_i$  is the accession to inertia for a diaphragm whose radius is the mean value for the surround. Obviously the vibrational frequencies alter but little. A similar procedure can be used for curve 2.

The difference between the present method and the simple procedure where the surround is treated as a pure constraint is due to inclusion of inertia effect which was ignored in the latter method. As the frequency rises, inertia becomes important owing to its interaction with the elastic property of the surround. For example when  $k_1 a = 8.5$  the effective mass of the surround is zero. When  $k_1 a$  just exceeds 8.5,  $m_e$  is positive. This means that the mechanical impedance of the surround at its inner radius is not given by the simple formula  $m_e = s/\omega$ .

If the surround were devoid of mass, but retained its elasticity, the axial stiffness when driven from the inner radius would be from (24)

$$s = f/\xi_0 = 2\pi\tau \left| \log_e \frac{a}{b} \right|. \quad (40)$$

Although the analysis has been used to illustrate the behaviour of large conical diaphragms having annular surrounds, it can also be applied to the moving-coil horn speaker of Chapter XX. In this case the damping is high and the vibrational modes are not marked. The effective mass can be measured as described in Chapter XVI.

#### 14. Membrane driven by constant force per unit area

This case approximates to the electrostatic speaker shown in Fig. 59. Assuming loss-free conditions *in vacuo* the equation of motion is obtained by aid of § 11. The force relationship is

inertia + elastic = driving

$$\text{or} \quad \rho_1 \frac{\partial^2 \xi}{\partial t^2} - \tau \left( \frac{\partial^2 \xi}{\partial x^2} + \frac{1}{x} \frac{\partial \xi}{\partial x} \right) = \mathbf{f}, \quad (41)$$

where  $\mathbf{f} = \mathbf{f}_0 e^{i\omega t}$  per unit area.

\* The radial tension of the surround is not uniform, so there are two maxima instead of one as indicated in Fig. 33.

The motion being harmonic  $\partial^2\xi/\partial t^2 = -\omega^2\xi$ , hence (41) becomes

$$\frac{\partial^2\xi}{\partial x^2} + \frac{1}{x} \frac{\partial\xi}{\partial x} + k_1^2 \xi = -\frac{\mathbf{f}}{\tau}, \quad (42)$$

where  $k_1^2 = \omega^2\rho_1/\tau$ .

From § 11 the complementary function of (42) is  $\xi = A_1 J_0(k_1 x)$ . To find a particular integral assume  $\xi = \zeta(t)$ , this being a function of  $t$  but not of  $x$ . Then  $\partial^2\xi/\partial x^2$  and  $\partial\xi/\partial x$  are both zero. On substitution in (42) we obtain

$$k_1^2 \zeta(t) = -\frac{\mathbf{f}}{\tau} \quad \text{or} \quad \zeta(t) = -\frac{\mathbf{f}}{k_1^2 \tau}. \quad (43)$$

The complete solution of (42) for our immediate purpose is therefore

$$\xi = A_1 J_0(k_1 x) - \frac{\mathbf{f}}{k_1^2 \tau}. \quad (44)$$

At the clamped edge  $x = a$ ,  $\xi = 0$  which on substitution in (44) gives the constant

$$A_1 = \frac{\mathbf{f}}{k_1^2 \tau J_0(k_1 a)}. \quad (44a)$$

Using this value of  $A_1$  in (44), the amplitude at any radius  $x$  is

$$\xi = \frac{\mathbf{f}}{\rho_1 \omega^2} \left[ \frac{J_0(k_1 x)}{J_0(k_1 a)} - 1 \right]. \quad (45)$$

By plotting  $x$  and  $\xi$  the shape of the diaphragm can be obtained. At all vibrational modes the driving force causes the amplitude to be infinite—in theory—excepting at nodal circles and the clamped edge. If we imagine the driving force to be removed when the central amplitude is  $\xi_0$ , the shape of the diaphragm at a vibrational mode is given by  $\xi = \xi_0 J_0(k_1 x)$  and it remains unaltered as time progresses, provided no loss occurs. The frequencies of the modes and the radii of the nodal circles are identical with those in § 11. When  $J_0(k_1 x) = J_0(k_1 a)$  in (45) the amplitude is zero and a nodal circle occurs although the frequency may not correspond to a vibrational mode. Inspection of the curve for  $J_0$  shows that the necessary condition is that  $k_1 a$  shall exceed the value corresponding to the first minimum of  $J_0$ . Now  $J'_0 = -J_1$  so the condition is that  $k_1 a$  exceeds the first zero of  $J_1$ , i.e. 3.83.

Since  $\mathbf{f} = \mathbf{f}_0 e^{i\omega t}$  the velocity at any point is

$$v = \frac{\partial\xi}{\partial t} = \frac{i\mathbf{f}}{\rho_1 \omega} \left[ \frac{J_0(k_1 x)}{J_0(k_1 a)} - 1 \right]. \quad (46)$$

The impedance per unit area at any radius is

$$z = \frac{f}{v} = -i\rho_1\omega \left[ \frac{J_0(k_1 a)}{J_0(k_1 x) - J_0(k_1 a)} \right]. \quad (47)$$

The effective mass per unit area

$$m_e = \frac{z}{i\omega} = \frac{-\rho_1 J_0(k_1 a)}{J_0(k_1 x) - J_0(k_1 a)}. \quad (48)$$

At a vibrational mode  $J_0(k_1 a) = 0$ , so  $m_e$  is evanescent provided

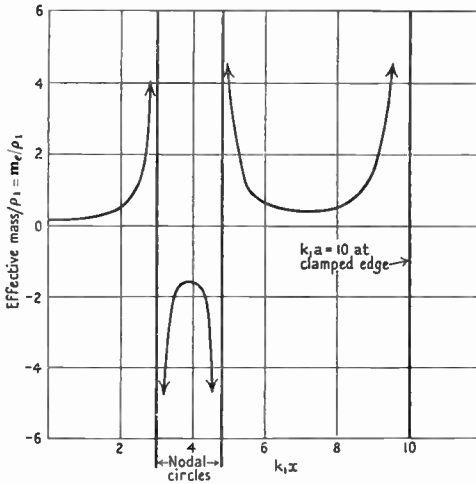


FIG. 34. Effective mass curves of circular membrane driven by a force uniformly distributed over its surface.  $m_e/\rho_1$  is calculated from (48).

the system is free from loss. The effective mass is infinite when  $J_0(k_1 x) = J_0(k_1 a)$ . At frequencies below the first root of  $J_1(k_1 a)$  this can only happen at the clamped edge, but as shown above, there is more than one value for which  $J_0(k_1 x) = J_0(k_1 a)$  provided  $k_1 a > 3.83$ . Effective mass curves are plotted in Fig. 34,  $k_1 a$  having the value 10 at the clamped edge.

### 15. Narrow rectangular strip membrane

This type of membrane is used in the electrostatic speaker described in Chapter IX, § 8 and Chapter XIII, § 11. Referring to Fig. 35, the membrane is supported at its sides, but not at its ends, so that there is no tension perpendicular to the paper. If  $\tau$  is the tension per unit

breadth, then from Fig. 35,  $\frac{\tau_v}{\tau} = -\frac{\partial \xi}{\partial x}$  or  $\tau_v = -\tau \frac{\partial \xi}{\partial x}$ , where  $\tau_v$  is the vertical component of the tension. The rate of change of  $\tau_v$  is  $\frac{\partial \tau_v}{\partial x} = -\tau \frac{\partial^2 \xi}{\partial x^2}$ , and the change in this component is

$$\partial \tau_v = -\tau \frac{\partial^2 \xi}{\partial x^2} \partial x. \quad (49)$$

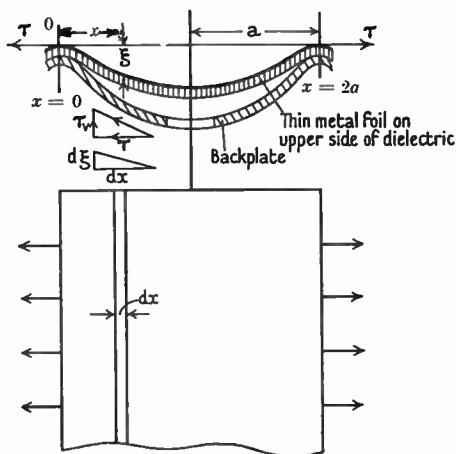


FIG. 35. Diagram illustrating construction of electrostatic speaker.

The accelerational force on a rectangle of width  $\partial x$  and unit breadth is

$$-\rho_1 \partial x \frac{\partial^2 \xi}{\partial t^2}. \quad (50)$$

For equilibrium we have from (49) and (50)

$$\frac{\partial^2 \xi}{\partial x^2} = \frac{\rho_1}{\tau} \frac{\partial^2 \xi}{\partial t^2}. \quad (51)$$

For harmonic motion the solution\* of (51) complying with the condition  $\xi = 0$  when  $x = 0$  and  $2a$ , is

$$\xi = \sin \frac{n\pi x}{2a} (A_1 \cos \omega t + B_1 \sin \omega t), \quad (52)$$

where  $(n\pi/2a)^2 = \omega^2 \rho_1 / \tau$ .

\* This means that the membrane executes one mode at a time.

From (52) the natural frequencies of the membrane are given by

$$\omega = \frac{\pi n}{2a} \sqrt{\frac{\tau}{\rho_1}}, \quad (53)$$

where  $n = 1, 2, 3$ , etc.

### 16. Influence of accession to inertia in lowering frequency

Hitherto the analysis has been based on vibration *in vacuo*. With heavy membranes, the accession to inertia in air is not very serious, but in certain cases with which we shall have to deal later, the fundamental frequency may be lowered about 50 per cent. or so [1, 4 b]. Cases of this nature cannot, in general, be solved by rigorous methods, and we are driven to approximations or to experimental determinations. Assuming the dynamic deformation surface to be identical in air and *in vacuo*, the potential energy of the diaphragm is unaltered. Moreover, the kinetic energy alone is affected, and with it the frequency of vibration. The latter being inversely proportional to the square root of the total equivalent mass (see definition 34) it follows that

$$\frac{\omega}{\omega_v} = \sqrt{\frac{m_q}{m_q + m_i}} = \sqrt{\frac{1}{1 + m_i/m_q}}, \quad (55)$$

where

$m_q$  is the equivalent mass during vibration *in vacuo*,

$\omega/2\pi$  is the frequency in air,

$\omega_v/2\pi$  is the frequency *in vacuo*.

The accession to inertia is determined as shown in § 4, Chap. III, but the analysis is very protracted unless the distribution of radiation is spherical. To evaluate  $m_q$  we proceed as follows: taking a dynamic deformation curve of the type  $\xi = \xi_{\max}(1 - \varphi x^2/a^2)$ , the kinetic energy of an annulus of radius  $x$  and width  $dx$  is  $\frac{1}{2}\rho_1 \dot{\xi}^2 2\pi x dx$ , so the kinetic energy of the whole membrane is

$$\pi \rho_1 \dot{\xi}_{\max}^2 \int_0^a \left[ 1 - \varphi \left( \frac{x}{a} \right)^2 \right] x dx = m_n (1 - \varphi + \frac{1}{3}\varphi^2) \frac{1}{2} \dot{\xi}_{\max}^2. \quad (56)$$

Thus  $m_q = m_n(1 - \varphi + \frac{1}{3}\varphi^2)$ . When  $\varphi = 1$  we obtain an approximation to a membrane vibrating in its gravest mode. The equivalent mass is then  $m_q = \frac{1}{3}m_n$ . If the membrane vibrates in an infinite flat baffle and the sound propagation is spherical,  $m_i = 1.6\rho_0 a^3$  (Chap. III). Thus  $m_i/m_q = 1.5\rho_0 a/\rho_1$ . For a membrane of thin aluminium foil  $\rho_1 = 4 \times 10^{-3}$  gm. cm.<sup>-2</sup>,  $a = 20$  cm. Taking  $\rho_0$  for air at 20° C. as

$1.2 \times 10^{-3}$  gm. cm.<sup>-3</sup> at normal pressure,  $m_i/m_q = 9$ . Thus the ratio  $\omega/\omega_v = \sqrt{1/10} \doteq 0.32$ , which means that the accession to inertia causes a 68 per cent. reduction in the frequency of the gravest mode of the aluminium diaphragm. It is to be remarked that, so long as the sound distribution is uniform, this percentage is independent of the radial tension of the diaphragm, and, therefore, of the fundamental frequency. Taking  $m_i$  with a small baffle at low frequencies to be one-half the above value, we find  $\omega/\omega_v = \sqrt{1/5} = 0.43$ . If the fundamental frequency in air were 130  $\sim$ , that *in vacuo* would be about 300  $\sim$ . The calculations for higher vibrational modes are very complicated and need not be dealt with here.

TABLE 5A

*Equivalent mass of various vibrators*

Type of vibrator	Dynamic deformation curve of section	Equivalent mass $m_e$
1. Circular membrane, radius $a$ , in infinite baffle.	$\xi = \xi_{\max} J_0(k_1 x)$	$m_n [J_0^2(k_1 a) + J_1^2(k_1 a)]$
2. Circular membrane, radius $a$ , at vibrational mode in infinite baffle.	$\xi = \xi_{\max} J_0(k_1 x)$	$m_n J_1^2(k_1 a)$
3. Free-edge disk with nodal circle at $r = a/\phi^{\frac{1}{2}}$ , in infinite baffle.	$\xi = \xi_{\max} \{1 - \phi(x/a)^2\}$ $\phi \leq 2$	$m_n \{1 - \phi + \frac{1}{3}\phi^2\}$
4. Free-edge disk with stationary centre, in infinite baffle.	$\xi = \xi_{\max} (x/a)^2$	$\frac{1}{3}m_n$
5. Free-edge disk with $p$ nodal diameters, in infinite baffle.	$\xi = \xi_{\max} (x/a)^p \cos p\theta$	$m_n/2(p+1)$

### 17. Influence of radiation and transmission loss on dynamic deformation surface

Hitherto our remarks have been based on ideal conditions where radiation and transmission loss are negligible. The influence of these is particularly noticeable in tracing nodal figures with sand on centrally-driven thin disks. When the central amplitude is small, but sufficient to cause a slow motion of the sand over the surface, the sand collects on a circle which appears to be at rest. If the amplitude is increased beyond a certain degree, the sand dances quite vigorously. During vibration without loss, the energy transmitted radially outwards from the centre is equal to that reflected inwards from the periphery. At a nodal position complete annulment occurs, provided the disk is homogeneous and adequately thin.

When loss occurs, the transmitted energy exceeds that reflected, there is a relative phase shift of the direct and reflected waves, and complete neutralization cannot occur. Hence in practice, in fluid or *in vacuo*, nodal lines in a rigorous sense are non-existent [107 a]. So-called nodes are actually positions of minimum amplitude. In the ideal case parts of the disk on opposite sides of a nodal line move in antiphase. By measuring the maximum amplitude of the disk at different radii, the dynamic deformation surface can be found. This shape is preserved at all parts of a cycle of the driving force although the amplitude at any radius varies harmonically. Radiation and loss cause a phase difference between the maximum amplitude at various radii. Hence if measurements of the maximum amplitude are made, the shape of the disk cannot be obtained, since it changes progressively throughout a cycle of the driving force. The shape at any epoch could be plotted if the phase were known at various radii. The nodal circles sweep from the centre to the periphery and back cyclically and are only nodal in a momentary sense.

These remarks can be illustrated by reference to propagation of electric waves in a loaded cable earthed at the far end to simulate a free edge disk. The cable case is not strictly analogous to the disk. In the former the waves are longitudinal, whilst in the latter they are flexural and involve bending which has no electrical analogue. The current at a point in the cable corresponds to the amplitude of the disk at some radius. For unit input voltage and unit characteristic impedance the current is

$$I = \frac{\cosh Pl(l-x)}{\sinh Pl}, \quad (57)$$

where  $P$  = propagation coefficient,  $l$  = length of cable, and  $x$  = distance from the sending end.

Using well-known identities (57) can be written

$$I = \left[ \frac{\cosh^2 \alpha(l-x) - \sin^2 \beta(l-x)}{\sinh^2 \alpha l + \sin^2 \alpha l} \right]^{\frac{1}{2}}, \quad (58)$$

where  $\alpha$  = attenuation coefficient,  $\beta = 2\pi/\lambda$  the wave-length coefficient, whilst the phase angle between voltage and current is

$$\tan^{-1}[\tanh \alpha(l-x)\tan \beta(l-x)] - \tan^{-1}[\cosh \alpha l \tan \beta l].$$

Since the denominator of (58) is constant for any value of  $x$ , it can



be omitted, so we consider the expression

$$y = [\cosh^2\alpha(l-x) - \sin^2\beta(l-x)]^{\frac{1}{2}} \quad (59)$$

In Fig. 36A the horizontal broken line represents  $\cosh^2\alpha(l-x)$  when there is neither resistance nor leakance ( $\alpha = 0$ ). Curve 2 corresponds to  $\alpha > 0$  when loss occurs, whilst curve 3 represents  $\sin^2\beta(l-x)$ ,  $\beta$  having an arbitrary value. The current distribution in the absence of loss in the cable is found by subtracting curves 1 and 3, the result being shown by the broken line in Fig. 36B. This corresponds to the amplitude of the disk at various radii. The diagram represents the maximum displacement, not the shape during vibration, since all displacements are shown positive. The phase from  $\pi/2\beta$  to  $3\pi/2\beta$  is

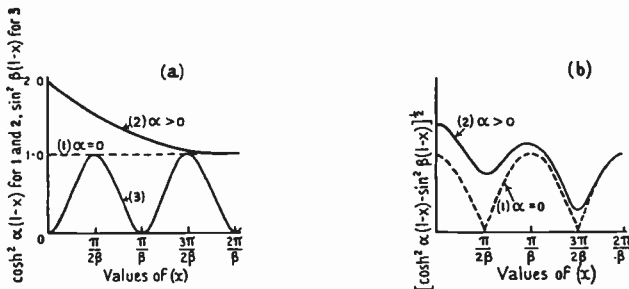


FIG. 36. Diagrams illustrating the influence of transmission loss in transforming nodes into positions of minimum amplitude.  $l \equiv 2\pi/\beta$ .

opposite to that from 0 to  $\pi/2\beta$  and from  $3\pi/2\beta$  to  $2\pi/\beta$ . Thus the current flows in opposite directions in these sections of the cable. The positions  $\pi/2\beta$  and  $3\pi/2\beta$  represent true nodes since there is no loss. The value of  $y$  (irrespective of phase which varies with  $x$ ) when  $\alpha > 0$  is found by taking the difference between curves 2 and 3. This is shown by the full line curve of Fig. 36 B which, owing to phase shift of the current with  $x$ , is not an instantaneous picture of the cable current. Since loss occurs nodes are absent, so  $\pi/2\beta$  and  $3\pi/2\beta$  are positions of minimum amplitude.

Assuming the point corresponding to  $3\pi/2\beta$  to be the centre of a vibrating disk and  $2\pi/\beta$  its edge, the curve between the two illustrates a centre-stationary vibrational mode. The curvature is of the wrong sign, but this is immaterial for our present purpose. In the loss-free case the central amplitude of the disk is zero, whilst the whole disk vibrates in phase, the amplitude increasing with the radius.

Loss necessitates central motion to replenish the energy dissipated. Thus the centre is a position of minimum amplitude. If the centre of the disk is represented by the point  $\pi/\beta$  and the edge by  $2\pi/\beta$ ,  $3\pi/2\beta$  represents a nodal circle when  $\alpha = 0$ , but a position of minimum amplitude when  $\alpha > 0$ . This corresponds to the first centre-moving mode of vibration. With the point  $\pi/2\beta$  for centre, the second centre-stationary mode is simulated, and so on.

It is well to realize, therefore, that if the vibrational amplitude of a diaphragm under the action of a powerful driving force is measured at different radii, the plotted curve shows the maximum displacement, but owing to phase changes along the radius it does not represent the dynamic deformation surface at any epoch.

## SPATIAL DISTRIBUTION OF SOUND FROM VIBRATING DIAPHRAGMS

### 1. Rigid disk in infinite baffle\*

In Fig. 37A let  $D$  be a rigid circular disk vibrating axially in an infinite rigid plane. The radiation at  $P_1$  is the sum of that from all the elemental areas into which the disk can be divided.

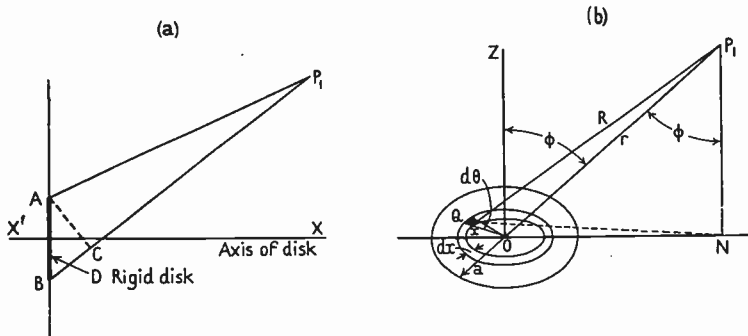


FIG. 37 A and B. Diagram illustrating analysis of sound distribution from a rigid disk in an infinite plane.  $\theta = \angle QON$ ,  $x = OQ$ .

Since  $P_1$  is nearer to  $A$  than to  $B$ , the radiation from  $B$  will be out of phase with that from  $A$  by an amount  $2\pi(BC)/\lambda$ , where  $BC$  is the difference in the two distances. At low frequencies, when  $BC$  is small compared with  $\lambda$ , the phase difference is negligible and the radiation from all parts of the disk arrives at  $P_1$  almost simultaneously. Thus the distribution at a considerable distance from the disk is spherical in type, i.e. it is uniform, and the pressure everywhere on a hemispherical surface of radius  $r$  is identical. At high frequencies when  $BC$  is comparable with or even greater than  $\lambda$ , there is at  $P_1$  a definite phase displacement of the radiation which arrives from various parts of the disk. In particular, if  $BC = \frac{1}{2}\lambda$ , the radiation from  $A$  and  $B$  is in opposite phase, and almost complete annulment occurs. Under this condition interference of the radiation from the surface of the disk occurs in the surrounding space, and the sound is propagated in the form of a beam whose angular width decreases with increase

\* See definition 47.

in the frequency of vibration [154a]. The problem which confronts us, therefore, is to determine analytically the pressure in space at any frequency. The succeeding analysis is based upon the following hypotheses:

1. The disk radiates into free fluid.
2. The displacement is small and varies.
3. The distance from the centre of the disk to spatial points, where the pressure is required, is large compared with the radius, e.g. ten or more times as large. Consequently the sound pencil from the disk to a distant point can be regarded as a series of parallel lines of different lengths. This condition prevails in practice, since for comfortable audition the listener is stationed at an appreciable distance from a loud speaker.

From (2), Chap. III, the pressure at any point distant  $R$  from an elemental area  $dA$  vibrating with normal velocity  $\dot{\xi}_0$  is

$$\begin{aligned} dp &= \frac{i\rho_0\omega\dot{\xi}_0}{2\pi} \frac{e^{-ikR}}{R} dA \\ &= \frac{\rho_0\ddot{\xi}_0}{2\pi} \frac{e^{-ikR}}{R} dA, \end{aligned} \quad (1)$$

$i$  being omitted since it is not required. To determine the pressure at  $P_1$  due to the whole disk, it is necessary to integrate (1) over its surface. From the geometry of Fig. 37 B we have

$$\begin{aligned} R^2 &= ON^2 + P_1N^2 + x^2 - 2ONx \cos \theta \\ &= r^2 + x^2 - 2ONx \cos \theta. \end{aligned}$$

Since  $ON = r \sin \phi$ ,

$$\begin{aligned} \text{we get } R^2 &= r^2 + x^2 - 2rx \sin \phi \cos \theta \\ &= r^2 \left( 1 + \frac{x^2}{r^2} - \frac{2x}{r} \sin \phi \cos \theta \right). \end{aligned}$$

Since by hypothesis  $x^2/r^2 \ll 1$ , we obtain

$$R = r \left( 1 - \frac{x}{r} \sin \phi \cos \theta \right) = r - x \sin \phi \cos \theta. \quad (2)$$

Inserting this value of  $R$  in (1), the pressure at  $P_1$  due to the whole disk is

$$p = \frac{\rho_0\ddot{\xi}_0}{2\pi r} \int_0^a x dx \int_0^{2\pi} e^{-ik(r-x\sin\phi\cos\theta)} d\theta \quad (3)$$

since  $dA = x dx d\theta$  and, so far as the influence of distance on the pressure amplitude is concerned,  $R \doteq r$ . In the exponential index,

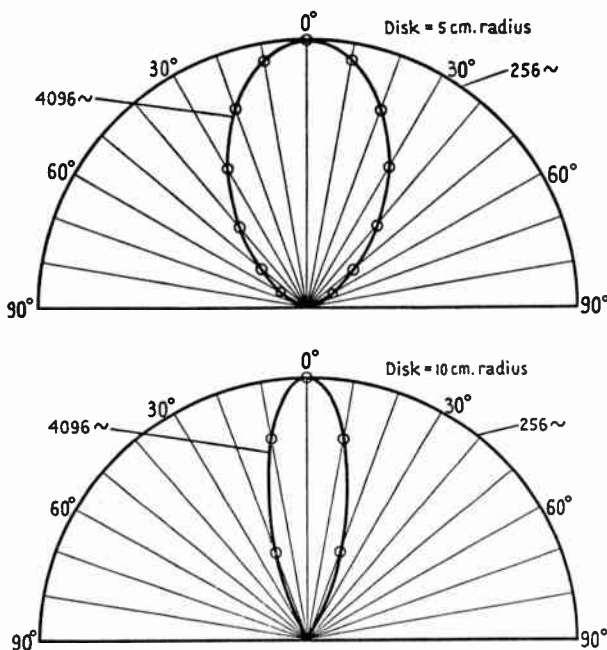


FIG. 39. Curves showing distribution of sound pressure from vibrating rigid disks of radii 5 cm. and 10 cm. at frequencies of 256 ~ and 4,096 ~. The curves are applicable at distances from the disks equal to or greater than ten radii, i.e.  $r \geq 10a$ . The disks vibrate in an infinite plane.

## 2. Axial pressure near rigid disk

In deriving a formula for the pressure near the disk we must dispense with the assumption of parallel rays of sound used in § 1 and treat the problem rigorously. From (1) the pressure at a point  $P_1$  on the axis, due to an annulus of radius  $x$  and width  $dx$ , is (Fig. 40)

$$dp = \rho_0 \ddot{\xi}_0 \frac{e^{-ikR}}{R} x dx.$$

$$\text{Since } r^2 + x^2 = R^2, \quad 2x dx = 2R dR,$$

and so

$$\begin{aligned} p &= \rho_0 \ddot{\xi}_0 \int_r^{R_1} e^{-ikR} dR, \\ &= (\rho_0 \ddot{\xi}_0 / ik) (e^{-ikr} - e^{-ikR_1}), \\ &= (2\rho_0 \ddot{\xi}_0 / k) e^{-\frac{1}{2}ik(R_1+r)} \sin \frac{1}{2}k(R_1-r). \end{aligned} \quad (8)$$

Apart from phase, the scalar pressure is [150, 155a]

$$|p| = \left| \frac{2\rho_0 \xi_0}{k} \sin \frac{1}{2}k(R_1 - r) \right|. \quad (9)$$

Formula (9) indicates that when  $\sin \frac{1}{2}k(R_1 - r) = 0$ , i.e.

$$R_1 - r = 2\pi n/k,$$

the pressure vanishes, and there is an isolated nodal point. Since  $k = 2\pi/\lambda$  the condition for a nodal point can be written  $R_1 - r = n\lambda$ ,

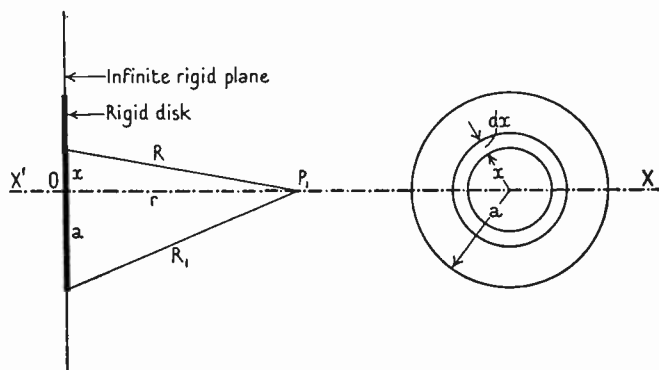


FIG. 40.

where  $n$  is a positive integer. Taking  $a = 10$  cm. radius,  $\omega/2\pi = 4,096 \sim$ , at normal temperature and pressure  $\lambda = 8.25$  cm. and there is only one node which occurs 1.93 cm. from the disk. When the frequency is  $8,192 \sim$  there are two nodes which occur at distances of 1.93 and 10 cm., respectively, from the disk. In general the node most remote from the disk occurs when  $n = 1$ . These results are of great importance when axial air pressure measurements are made with a condenser microphone. If the microphone is too near the disk—or more usually a conical diaphragm or the mouth of a horn—variations in the readings will occur at high frequencies due to interference. Such measurements near the source do not indicate truly the performance of the device at large distances where listeners are usually stationed.

The minimum distance for the microphone can be calculated from the preceding analysis. The node farthest from the disk occurs when  $R_1 - r = \lambda$  and, therefore the condition to be satisfied is that

$R_1 - r < \lambda$ . By aid of Fig. 40 this can be expressed as follows:

$$\begin{aligned}\sqrt{(r^2 + a^2)} - r &< \lambda, \\ r^2 + a^2 &< \lambda^2 + 2\lambda r + r^2,\end{aligned}$$

or 
$$r > \frac{a^2}{2\lambda} - \frac{1}{2}\lambda,$$

or 
$$r > \frac{a^2\omega}{4\pi c} - \frac{\pi c}{\omega}, \quad (10)$$

where  $r$  is always positive.

For practical purposes the second term in (10) can be ignored, so the condition is  $r > a^2\omega/4\pi c$ . It will be realized that when  $r$  satisfies this condition the microphone may be just past the node, where a certain degree of interference exists. To ensure complete freedom from interference, it is safe to use  $r > a^2\omega/2\pi c$  as a working condition.

### 3. Rigid rectangular plate in infinite baffle

This case is of importance, since it is represented approximately in practice by the Blatthaller loud speaker described in Chapter XIII, § 7. Referring to Fig. 41, the line  $OP_1$  has direction cosines  $\cos \alpha$ ,  $\cos \gamma$  with the  $x$ - and  $z$ -axes, respectively. The projection of a point in the rectangle (lying in the  $xz$ -plane where  $y = 0$ ) on the line  $OP_1$ , is then  $x \cos \alpha + z \cos \gamma$ , where  $\alpha$  and  $\gamma$  are the angles made by  $OP_1$  with the  $x$ - and  $z$ -axes, respectively. Thus since  $OP_1$  and  $QP_1$  are substantially parallel, we have

$$R = r - (x \cos \alpha + z \cos \gamma). \quad (11)$$

From (1) the pressure at  $P_1$  due to an elemental area  $dxdz$  is

$$dp = \frac{\rho_0 \ddot{\xi}_0}{2\pi r} e^{-ik(r - (x \cos \alpha + z \cos \gamma))} dxdz, \quad (12)$$

since  $r \doteq R$  so far as distance is concerned. Removing the distance phase factor  $e^{-ikr}$ , the pressure at  $P_1$  due to the whole rectangle whose sides are  $2a$  and  $2b$  is [159 a]

$$p = \frac{\rho_0 \ddot{\xi}_0}{2\pi r} \int_{-a}^{+a} e^{ikx \cos \alpha} dx \int_{-b}^{+b} e^{ikz \cos \gamma} dz \quad (13)$$

$$= \frac{2\rho_0 \ddot{\xi}_0 ab}{\pi r} \left[ \frac{\sin z_1}{z_1} \right] \left[ \frac{\sin z_2}{z_2} \right], \quad (14)$$

where  $z_1 = ka \cos \alpha$  and  $z_2 = kb \cos \gamma$ .

It is convenient to express  $z_1$  and  $z_2$  in terms of co-latitude  $\theta$  and longitude  $\chi$ . From Fig. 41 we have

$$\cos \alpha = \sin \theta \cos \chi \quad \text{and} \quad \cos \gamma = \cos \theta.$$

Thus (14) becomes

$$p = \frac{2\rho_0 \ddot{\xi}_0 ab}{\pi r} \left[ \frac{\sin(ka \sin \theta \cos \chi)}{ka \sin \theta \cos \chi} \right] \left[ \frac{\sin(kb \cos \theta)}{kb \cos \theta} \right]. \quad (15)$$

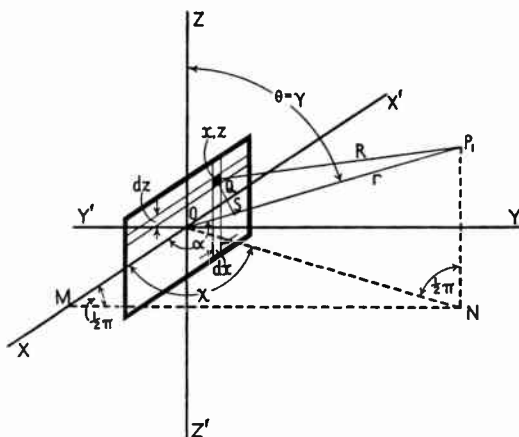


FIG. 41. Diagram illustrating analysis of sound distribution from a rigid rectangular plate vibrating in an infinite plane. The projection of  $Q$  on  $OP_1$  is  $OS = x \cos \alpha + z \cos \gamma$ .  $r \gg$  longer side of plate.

In the  $yz$ -plane  $x = 0$ ,  $\chi = \frac{1}{2}\pi$ ,

so 
$$p = \frac{2\rho_0 \ddot{\xi}_0 ab}{\pi r} \frac{\sin(kb \sin \varphi)}{kb \sin \varphi}, \quad (16)$$

where  $\varphi = \frac{1}{2}\pi - \theta$ .

Likewise in the  $xy$ -plane  $\theta = \frac{1}{2}\pi$  and

$$p = \frac{2\rho_0 \ddot{\xi}_0 ab}{\pi r} \frac{\sin(ka \sin \phi)}{ka \sin \phi}, \quad (17)$$

where  $\phi = (\frac{1}{2}\pi - \chi)$ .

The function  $G_3 = \frac{\sin(ka \sin \phi)}{ka \sin \phi}$  is identical with

$$\left( \frac{\pi}{2ka \sin \phi} \right)^{\frac{1}{2}} J_{\frac{1}{2}}(ka \sin \phi), \quad (18)$$



where  $J_{\frac{1}{2}}$  is Bessel's function of order  $\frac{1}{2}$ . It is plotted in Fig. 38 alongside that of the curve for  $\frac{J_1(ka \sin \phi)}{ka \sin \phi}$  which represents the distribution for a rigid disk. The focusing of the radiation from the rectangle in the  $xy$ -plane, for equal values of  $ka$ , is greater than that of the rigid disk. It is specially interesting to note that the distribution from the rectangle in the  $xy$ -plane, or from a square in the  $yz$ - and  $xy$ -planes, is identical with that from a flexible circular disk of radius  $a$ , whose dynamic deformation curve takes the form  $\xi = \frac{\xi_0 a}{\sqrt{(a^2 - x^2)}}$  (see Table 7). The maximum radius vector of the subsidiary loop for the rectangle or the flexible disk is 18 per cent. of the axial pressure. This exceeds that for the rigid disk, as will be seen from Fig. 38. Referring to the rectangle, it will be evident that the greater  $a$  the smaller is the angular width of the sound beam. Thus at high frequencies where focusing occurs, the angle of the beam will be smaller for the long than for the short side of the rectangle. If we imagine a plane containing the  $y$ -axis to be rotated from the  $zy$  position, the angle of the beam in the plane will gradually decrease until a minimum is attained in the  $xy$  position. From a physical viewpoint this variation in focusing is easily understood, since the narrower the vibrator the smaller is the phase difference in the radiation from its elements at any point in the axial plane parallel to the narrow edge.

#### 4. Circular membrane at symmetrical vibrational modes

In previous problems the velocity has been constant over the vibrator, whereas for a vibrating membrane it varies from the centre to the clamped edge. Consequently the distribution of radiation will differ from that for a rigid disk of equal radius. The following assumptions are required in addition to those in § 1:

1. Neither the acoustic loading (resistance+reactance) nor the transmission loss in the material of the diaphragm causes an alteration in its shape.
2. Portions of the membrane moving in the same direction at any instant are in phase, whilst on either side of a nodal line they are antiphase.

The dynamic deformation curve of a circular membrane at a vibrational mode is, from Chapter IV, § 11,  $\xi = \xi_0 J_0(k_1 x)$ . From (4),

neglecting  $e^{-ikr}$ ,

$$p = \frac{\rho_0 \ddot{\xi}_0}{2\pi r} \int_0^a x J_0(k_1 x) dx \int_0^{2\pi} e^{ikx \sin \phi \cos \theta} d\theta. \quad (19)$$

The first integral is  $2\pi J_0(kx \sin \phi)$ , so (19) becomes

$$\begin{aligned} p &= \frac{\rho_0 \ddot{\xi}_0}{r} \int_0^a J_0(k_1 x) J_0(kx \sin \phi) x dx \\ &= \frac{\rho_0 \ddot{\xi}_0}{r} \left( \frac{a}{k_1^2 - k^2 \sin^2 \phi} \right) \{ k_1 J_0(ka \sin \phi) J_1(k_1 a) - \\ &\quad - k \sin \phi J_0(k_1 a) J_1(ka \sin \phi) \} \quad [213]. \end{aligned} \quad (20)$$

At a vibrational mode  $J_0(k_1 a) = 0$ , so (20) reduces to

$$p = \frac{\rho_0 \ddot{\xi}_0}{r} \left( \frac{k_1 a}{k_1^2 - k^2 \sin^2 \phi} \right) J_0(ka \sin \phi) J_1(k_1 a). \quad (21)$$

When  $k_1^2 \gg k^2 \sin^2 \phi$  (21) becomes

$$p = \frac{\rho_0 \ddot{\xi}_0 a^2}{r} \left( \frac{J_1(k_1 a)}{k_1 a} \right) J_0(ka \sin \phi), \quad (22)$$

$$= \frac{\Upsilon}{r} J_0(ka \sin \phi), \quad (23)$$

where  $\Upsilon = \rho_0 \ddot{\xi}_0 a^2 \frac{J_1(k_1 a)}{k_1 a}$ .

An annular membrane can be treated in a similar manner (see Table 7).

## 5. Axial pressure at vibrational modes

On the axis  $\sin \phi = 0$  and (22) becomes

$$p = \frac{\rho_0 \omega \ddot{\xi}_0 a^2}{r} \left[ \frac{J_1(k_1 a)}{k_1 a} \right]. \quad (23a)$$

The axial pressure obviously has zeros corresponding to those of  $J_1(k_1 a)$ . In practice, however, the shape of the diaphragm differs from that assumed in obtaining (22), since the nodal lines are actually positions of minimum amplitude (see Chap. IV, § 17). The zeros may be obliterated in consequence of this. In the hypothetical case they occur when  $k_1 a \doteq 3.83, 7.01, 10.17, 13.3, 16.47, 19.6$ , etc. [213]

### 6. Free-edge disk with $n$ nodal diameters [156 c]

From the geometry of Fig. 42 using spherical coordinates we have

$$\begin{aligned} r_1^2 &= QN^2 + P_1N^2 \\ &= x^2 + r^2 \cos^2 \phi - 2rx \sin \phi \cos(\theta - \chi) + r^2 \sin^2 \phi \\ &\doteq r^2 - 2rx \sin \phi \cos(\theta - \chi), \quad \text{since } x^2 \ll r^2; \end{aligned}$$

so  $r_1 = r - x \sin \phi \cos(\theta - \chi).$

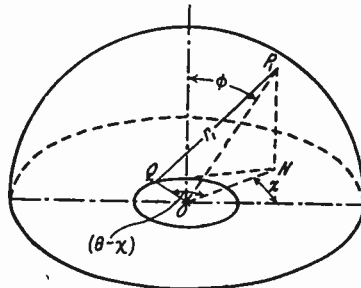


FIG. 42.  $OP_1 = r$ ;  $OQ = x$  (radius of annulus as in Fig. 37 B).

Let the dynamic deformation curve be of the type  $\xi = \xi_0(x/a)^n \sin n\theta$ . From (4) the pressure at a distant point is

$$p = \frac{\rho_0 \ddot{\xi}_0}{2\pi r} \int_0^a \left(\frac{x}{a}\right)^n x dx \int_0^{2\pi} \sin n\theta e^{ikx \sin \phi \cos(\theta - \chi)} d\theta, \quad (24)$$

where the factor  $e^{-ikr}$  has been omitted.

Expressing the first integral as a series of products of Bessel and circular functions, we have [213]

$$p = \frac{\rho_0 \ddot{\xi}_0}{2\pi r a^n} \int_0^a x^{n+1} dx \int_0^{2\pi} \sin n\theta \left[ J_0(z) + 2 \sum_{m=1}^{\infty} i^m J_m(z) \cos m(\theta - \chi) \right] d\theta, \quad (25)$$

where  $z = kx \sin \phi$ .

Integrating the products of the circular functions in (25) we obtain

$$p = \frac{\rho_0 \ddot{\xi}_0 \sin n\chi}{r a^n} \int_0^a x^{n+1} J_n(kx \sin \phi) dx, \quad (26)$$

the other terms vanishing, since  $\int_0^{2\pi} \sin n\theta \cos m(\theta - \chi) = 0$  unless  $m = n$ .

The sign and occurrence of the imaginary depends upon  $n$ , but it does not affect the scalar value of  $p$ .

Integrating (26) by parts we find that the pressure [156 c] is

$$p = \frac{\rho_0 \ddot{\xi}_0 a^2}{r} \sin n\chi \frac{J_{n+1}(ka \sin \phi)}{ka \sin \phi}. \quad (27)$$

Here we no longer have the simple condition of symmetry about the polar axis which characterizes preceding examples. To visualize the spatial distribution we consider the pressure at a point situated in a plane containing the axis of symmetry. When the plane con-

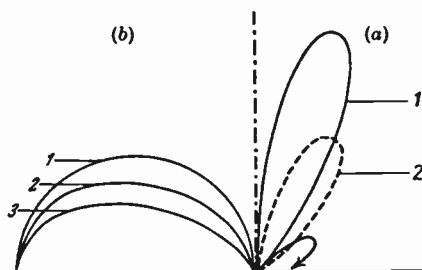


FIG. 43. (a) Sound distribution from free edge disk  $a = 10$  cm. radius vibrating with one (curve 1) and with two (curve 2) nodal diameters at  $4,096 \sim$  or  $ka = 7.56$ .

(b) Distribution from 10 cm. disk with 1, 2, and 4 (curve 3) nodal diameters at low frequencies when  $ka \leq 0.5$ .

The distribution is that on a plane midway between two contiguous diameters, when  $r \geq 10a$ , and the disks vibrate in an infinite plane.

tains a nodal diameter, any point in it is symmetrically situated with reference to equal and oppositely vibrating areas. Consequently the pressure at any point on the plane is zero. Since this plane contains the axis, it follows that the pressure vanishes there also. If we choose any non-axial point in the plane and imagine the latter to rotate about the axis, the pressure thereat gradually increases in accordance with a sine law, attaining a maximum value midway between consecutive nodal diameters. As rotation of the plane is continued the pressure dies away according to the same law. Thus with  $n$  nodal diameters there would be  $2n$  maxima and an equal number of zeros during one complete revolution of the plane. The distribution of radiation with one and two diameters on a median plane is exhibited in curves 1 and 2, Fig. 43 A, where  $ka = 7.56$  and  $\omega/2\pi = 4,096 \sim$ . At low frequencies when  $ka \leq 0.5$  the curves for one, two, and four diameters are shown in Fig. 43 B.

Formulae for the spatial distribution in various additional cases

are given in Table 7. Dynamic deformation curves have been assumed which are in close accord with the shape corresponding to different vibrational modes *in vacuo*. The general case of a flexible disk is given without approximation, but the arithmetical labour involved in plotting the polar curve is quite formidable.

The distribution of radiation from a circular disk having nodal circles at various radii is illustrated in Fig. 44, comparison being

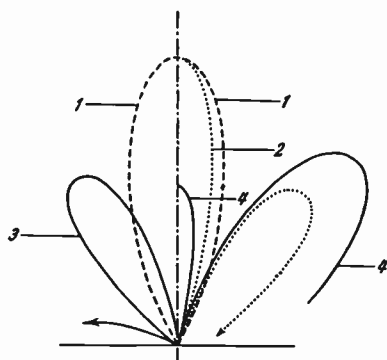


FIG. 44. Diagram showing sound pressure distribution at 4,096  $\sim$ .

(1) Rigid disk of radius  $a = 10$  cm. in infinite plane (scale full size).

(2) Flexible disk with nodal circle at  $x = a/2$  (twice full size).

(3) " " " "  $x = a/\sqrt{2}$  (twice full size).

(4) " " " "  $x = a/1.25$  (full size).

The disks vibrate in an infinite plane and the distribution is that when  $r \geq 10a$ .

made with that from a rigid disk of the same outer radius. When the radius of the nodal circle is  $r = a/\sqrt{2}$  the axial pressure vanishes owing to interference of the two equal areas on either side of the circle vibrating in antiphase.

## 7. Vibrators without a baffle or with a finite baffle

To gain an approximate idea of the sound distribution from diaphragms without a baffle [156a], it is necessary to substitute a sphere vibrating in various ways. This involves spherical harmonic analysis an account of which is given in Chapter II. From (54) Chap. II, the velocity potential at a distance  $r$  from the centre of a sphere due to the  $n$ th harmonic, is

$$\phi_n = \frac{a^2}{r} e^{ik(a-r)} u_n \frac{f_n(ikr)}{F_n(ika)}. \quad (28)$$

TABLE 7

## Spatial sound distribution for various radiators in infinite rigid plane

$z = ka \sin \phi$ ;  $z_1 = kb \sin \phi$ ;  $p = \rho_0 \ddot{\xi}_0 \Re/r$ , excepting (20);  $a =$  radius of vibrator.

Type of vibrator	Dynamic deformation curve	$\Re =$ Radiation characteristic
1. Rigid disk.	$\xi = \xi_0$ .	In neighbourhood of disk, see [151].
2. Free-edge disk [156c].	$\xi = \xi_0 \{1 - (\varphi x^2/a^2)\}$ .	$a^3 \left[ (1 - \varphi) \frac{J_1(z)}{z} + 2\varphi \frac{J_2(z)}{z^2} \right]$ .
3. Rigid annular ring, radii $a, b$ ; central hole fitted with rigid disk [156c].	$\xi = \xi_0$ .	$a^3 \frac{J_1(z)}{z} - b^3 \frac{J_1(z_1)}{z_1}$ .
4. Rigid elliptical disk, axes $2a, 2b$ [161].	$\xi = \xi_0$ .	$ab \frac{J_1(z_0)}{z_0}$ , where $z_0 = k\sqrt{a^2 \cos^2 \alpha + b^2 \cos^2 \beta}$ , $\alpha, \beta$ being angles between radius vector and axes in plane of disk.
5. Clamped-edge disk in gravest mode [156c].	$\xi = \xi_0 \{1 - (x^2/a^2)\}^2$ .	$8a^3 \frac{J_2(z)}{z^3}$ .
6. Clamped-edge disk [156c] with one nodal circle at $r = a/\varphi^{\frac{1}{2}}$ .	$\xi = \xi_0 \{1 - (x^2/a^2)\}^2 \{1 - (\varphi x^2/a^2)\}$ .	$a^3 \left[ 8(1 - \varphi) \frac{J_2(z)}{z^3} + 48\varphi \frac{J_4(z)}{z^4} \right]$ .
7. Clamped-edge disk with stationary centre [156c].	$\xi = \xi_0 \{1 - (x^2/a^2)\} x^2/a^2$ .	$8a^3 \left[ \frac{J_2(z)}{z^3} - 6 \frac{J_4(z)}{z^4} \right]$ .
8. Free-edge disk with two nodal circles [156c].	$\xi = \xi_0 \{1 - (\varphi_1 x^2/a^2)\} \{1 - (\varphi_2 x^2/a^2)\}$ . For a homogeneous disk without nodal diameters $\varphi_1 = 6.58$ , $\varphi_2 = 1.353$ , giving nodal radii $0.39a$ and $0.86a$ .	$a^3 \left\{ [1 - (\varphi_1 + \varphi_2) + \varphi_1 \varphi_2] \frac{J_1(z)}{z} + 2[(\varphi_1 + \varphi_2) - 2\varphi_1 \varphi_2] \frac{J_2(z)}{z^2} + 8\varphi_1 \varphi_2 \frac{J_3(z)}{z^3} \right\}$ .
9. Free-edge disk [156c] with $n$ nodal diameters and one nodal circle at $r = a \sqrt{\frac{n+2}{n+4}}$ .	$\xi = \xi_0 \{1 - (\varphi x^2/a^2)\} (x/a)^n \sin n\theta$ $\varphi = \frac{(n+4)}{(n+2)}$ $\theta$ is the angle between radius $x$ and $0^\circ$ .	$2a^3 \frac{\sin n\chi}{(n+2)} \left\{ -\frac{J_{n+1}(z)}{z} + (n+4) \frac{J_{n+2}(z)}{z^2} \right\}$ , $\chi$ is the angle between axial plane containing point, and a nodal diameter.

TABLE 7 (continued)

Type of vibrator	Dynamic deformation curve	$\mathfrak{R}$ = Radiation characteristic
10. Free-edge disk with stationary centre [156c].	$\xi = \xi_0(x/a)^2$ .	$a^2 \left[ \frac{J_1(z)}{z} - \frac{2J_2(z)}{z^2} \right]$ .
11. Free-edge disk with [156c] stationary centre and nodal circle at $r = a\sqrt{\frac{2}{3}}$ .	$\xi = \xi_0 \{1 - (\varphi x^2/a^2)\}(x/a)^2$ , $\varphi = \frac{2}{3}$	$a^2 \left[ -\frac{1}{2} \frac{J_1(z)}{z} + 4 \frac{J_2(z)}{z^2} - 12 \frac{J_3(z)}{z^3} \right]$ .
12. Flexible disk.	$\xi = \xi_0 \{a/\sqrt{a^2 - x^2}\}$ .	$a^2 \frac{\sin z}{z} = a^2 \left( \frac{\pi}{2z} \right)^{\frac{1}{2}} J_{\frac{1}{2}}(z)$ .
13. Circular membrane at gravest mode [156c].	$\xi = \xi_0 \{1 - (x^2/a^2)\}$ .	$a^2 \left[ 2 \frac{J_2(z)}{z^2} \right]$ .
14. General case of circular membrane at a vibrational mode, where $J_n(k_1 a) = 0$ , $n$ = number of nodal diameters.	$\xi = \xi_0 J_n(k_1 x) \sin n\theta$ $\xi = \xi_0 J_n(k_1 x) \cos n\theta$ See (9) for definitions of $\theta$ and $\chi$ .	$\frac{\pi a}{k_1^2 - k^2 \sin^2 \phi} \left\{ \frac{\sin n\chi}{\cos n\chi} \right\} k_1 J_n(z) J_{n+1}(k_1 a)$ where $k_1 \neq k \sin \phi$ .

15. Annular membrane clamped at outer radius and driven by rigid disk at the inner radius.

$$\xi = \xi_0 \left[ \frac{J_0(k_1 x) Y_0(k_1 a) - J_0(k_1 a) Y_0(k_1 x)}{J_0(k_1 b) Y_0(k_1 a) - J_0(k_1 a) Y_0(k_1 b)} \right]$$

Radiation from disk is suppressed.

16. Rectangular membrane.

$\xi = \xi_0 \{1 - (x/b)\}$  on one side of centre.

$\xi = \xi_0 \{1 + (x/b)\}$  on other ,, ,,

17. Annular membrane clamped at inner and outer edges. No centre hole.

$$\xi = \xi_1 \left[ \frac{J_0(k_1 x) Y_0(k_1 a) - J_0(k_1 a) Y_0(k_1 x)}{J_0(k_1 x_1) Y_0(k_1 a) - J_0(k_1 a) Y_0(k_1 x_1)} \right]$$

where  $\xi_1$  is the displacement at an arbitrary radius  $x_1$ .

18. Spherical shell with  $n$  nodal circles passing through the poles (no infinite plane) [156 a].

$u = U \sin^{\theta} \sin n\chi$   
 = radial velocity.  
 $\chi$  = longitude.

$$b_1 \frac{J_1(z)}{z} + \frac{k_1}{k_1^2 - k^2 \sin^2 \phi} \left\{ \frac{a J_0(z) [J_0(k_1 a) Y_1(k_1 a) - Y_0(k_1 a) J_1(k_1 a)] - b J_0(z_1) [J_0(k_1 b) Y_1(k_1 b) - Y_0(k_1 b) J_1(k_1 b)]}{J_0(k_1 a) Y_0(k_1 b) - J_0(k_1 b) Y_0(k_1 a)} \right\}$$

$k_1 \neq k \sin \phi$ .

For this and additional cases see [161].

$$\frac{k_1}{k_1^2 - k^2 \sin^2 \phi} \left\{ \frac{a J_0(z) [J_0(k_1 a) Y_1(k_1 a) - Y_0(k_1 a) J_1(k_1 a)] - b J_0(z_1) [J_0(k_1 b) Y_1(k_1 b) - Y_0(k_1 b) J_1(k_1 b)]}{J_0(k_1 a) Y_0(k_1 x_1) - J_0(k_1 x_1) Y_0(k_1 a)} \right\}$$

where  $k_1 \neq k \sin \phi$ .

$\sin^{\theta} \sin n\chi$ .



At a great distance  $f_n(ikr) = 1$ , so (28) can be written

$$\phi_n = \frac{a^2}{r} e^{ik(a-r)} \frac{u_n}{F_n(ika)} = \frac{a^2}{r} u_n \Xi_n e^{ik(a-r)}, \quad (29)$$

where  $\Xi_n = 1/F_n(ika)$ .

The pressure due to this harmonic is

$$\begin{aligned} p &= i\rho_0 \omega \phi_n \\ &= \frac{\rho_0 \omega a^2}{r} u_n \Xi_n, \end{aligned} \quad (30)$$

where  $e^{ik(a-r)}$  has been omitted since it is constant at a given value of  $r$ .

Although  $\Xi_n$  can be written in the form  $x_n + iy_n$  it must not be inferred that the pressure and the particle velocity at a great distance from the source are out of phase. The physical meaning of (30) is that the sound pressure at a great distance is out of phase with the radial velocity of the surface of the sphere.

To find the total pressure at the spatial point under consideration, we have to determine the harmonic components  $u_0, u_1, \dots$ , in the expansion of the radial velocity  $u = u_0 + u_1 + \dots + u_n$ . Then the pressure is given by

$$\begin{aligned} p &= p_0 + p_1 + \dots + p_n + \dots \\ &= \frac{\rho_0 \omega a^2}{r} \{(u_0 x_0 + u_1 x_1 + u_2 x_2 + \dots) + i(u_0 y_0 + u_1 y_1 + \dots)\} \end{aligned} \quad (31)$$

$$= \frac{\rho_0 \omega a^2}{r} (A + iB). \quad (32)$$

The scalar value of the pressure is, therefore,

$$|p| = \frac{\rho_0 \omega a^2}{r} \sqrt{(A^2 + B^2)}, \quad (33)$$

where

$$A = (u_0 x_0 + u_1 x_1 + \dots)$$

and

$$B = (u_0 y_0 + u_1 y_1 + \dots).$$

To facilitate evaluation of  $|p|$ , a series of values of  $x_n$  and  $y_n$ , corresponding to the range  $ka = 0$  to 10, is given in Table 8.

When the vibration of the sphere is symmetrical about the polar axis  $ZOZ'$  (Fig. 3), the  $n$ th component of the radial velocity is

$$u_n = (n + \frac{1}{2}) P_n(\mu) \int_{\mu}^{\mu} u P_n(\mu) d\mu, \quad (34)$$

the limits of integration depending upon the distribution of the radial velocity over the surface [156 a].

TABLE 8

$ka$	$x_0$	$x_1$	$x_2$	$x_3$	$x_4$	$x_5$	$y_0$	$y_1$	$y_2$	$y_3$	$y_4$	$y_5$
0	1.0	0	0	0	0		0	0	0	0	0	
0.5	0.8	+0.125	-0.024	-0.001			-0.4	+0.22	+0.0135	-0.0018		
1.0	0.5	+0.2	-0.056	-0.0133	+0.001		-0.5	+0.2	+0.09	-0.0085	-0.0015	
2.0	0.2	-0.1	+0.188	-0.1			-0.4	-0.2	+0.268	-0.05		
3.0	0.1	-0.082	+0.33	+0.0234			-0.3	-0.246	0	-0.265		
4.0	0.059	-0.054	+0.2				-0.235	-0.216	-0.1			
5.0	0.038	-0.366	+0.16	+0.217			-0.192	-0.183	-0.128	-0.0038		
10.0	0.01	-0.01	+0.04	+0.0677	+0.1	+0.108	-0.1	-0.1	-0.1		-0.041	+0.0103

**8. One hemisphere vibrating radially, the other quiescent**

In this case the radial velocity  $u = U$  from  $\mu = +1$  to 0, and it is zero from  $\mu = 0$  to  $-1$  (see Fig. 20). Proceeding on the above lines we ultimately find

$$A \doteq U\left\{\frac{1}{2}x_0 + \frac{3}{4}\mu x_1 - \frac{7}{32}(5\mu^3 - 3\mu)x_3 + \frac{11}{256}(63\mu^5 - 70\mu^3 + 15\mu)x_5\right\}, \quad (35)$$

$$B \doteq U\left\{\frac{1}{2}y_0 + \frac{3}{4}\mu y_1 - \frac{7}{32}(5\mu^3 - 3\mu)y_3 + \frac{11}{256}(63\mu^5 - 70\mu^3 + 15\mu)y_5\right\}. \quad (36)$$

Using Table 8 the distribution of radiation can be calculated for various values of  $ka$  [156 a].

Polar curves for  $ka = 2.0$  and  $10.0$  are plotted in Fig. 45. This case is of interest in connexion with an exponential horn, where a radially pulsating hemisphere is used as a simulating impedance.

**9. Sphere with latitudinal nodal circles**

The preceding principles are applicable to any dynamic deformation curve of the spherical surface. It may be desired to approximate to the distribution from a radiator, itself analytically intractable, by using a sphere with one or more nodal circles coaxial with the polar axis. Let the radial velocity be

$$u = U\{1 - (\varphi x^2/a^2)\} = U(1 - \varphi \sin^2\theta) = U\{1 - \varphi(1 - \mu^2)\}. \quad (37)$$

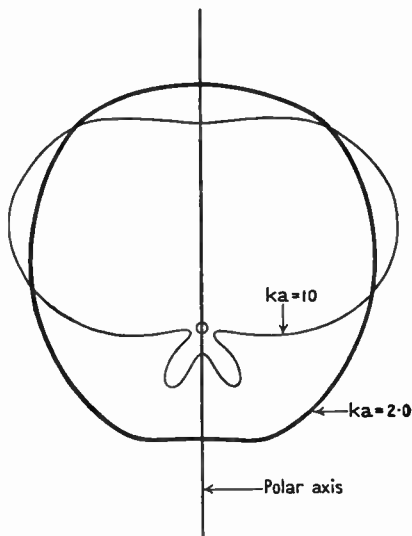


Fig. 45. Sound pressure distribution from radially vibrating hemisphere, the other hemisphere being quiescent. The hemisphere vibrates in free fluid and  $r \geq 10a$ .

If  $\varphi = 2$  there are two nodal circles, one in each hemisphere, at  $\theta = \frac{1}{2}\pi$  and  $\frac{3}{2}\pi$ , i.e.  $\mu = \pm 1/\sqrt{2}$  since  $u = (2\mu^2 - 1)$ .

### 10. Cone with finite baffle

An approximation to this case at low frequencies, when the cone moves rigidly, can be obtained by using two spherical caps at the extremities of a spherical diameter, the direction of vibration being the same in both cases. The distance from pole to pole on the sphere is made equal to the distance from centre to centre round the flat baffle, assumed to be circular. The radius of the spherical cap is equal that at the base of the cone.

### 11. Distribution from a group of radiators

In public address systems, whether for open air or cinema work, it is always necessary to use more than one loud speaker. The problem which confronts us is to find the resulting sound field when the distribution from each radiator and its position relative to the remainder is known. We have already seen that when the surface dimensions of a radiator are small compared with the wave-length, spherical propagation ensues. When several rigid disks are placed in juxtaposition, so that their surfaces are coplanar or nearly so, the area is increased and focusing starts at a lower frequency than it does from an individual radiator. Although the angle of the sound beam is less for  $n$  radiators than it is for one, the ultimate area covered is larger. The angle and the area are augmented by arranging the polar axes of the radiators as normals of a convex surface. For example, they might be arranged on the surface of a portion of a cylinder or a spherical cap.

Neglecting the alteration in output from any radiator due to the presence of the remainder, suppose we take the simple case of  $n$  identical radiators on a straight line, the separation between contiguous units being constant. If the radiators are rigid disks set in an infinite baffle, all moving simultaneously in the same direction, the radiation from each is given by formula (6). To determine the resultant pressure at any point the contributions from all the radiators must be summed, due regard being paid to phase. At a great distance from the group the maximum pressure due to each unit is almost the same. From Fig. 46, assuming the sound rays from  $P_1$  to each unit to be parallel, the distances are, respectively,

0,  $d \cos \theta$ ,  $2d \cos \theta, \dots, (n-1)d \cos \theta$ , corresponding to the phase angles  
 $0, kd \cos \theta, 2kd \cos \theta, \dots, (n-1)kd \cos \theta$ .

The pressure due to  $S_0$  is proportional to  $G \cos \omega t$ ,  $S_1$  to  $G \cos(\omega t + \alpha)$  and  $S_{n-1}$  to  $G \cos[\omega t + (n-1)\alpha]$ , where

$$G = \frac{J_1(ka \sin \phi)}{ka \sin \phi} \text{ and } \alpha = kd \cos \theta.$$

The total pressure at  $P_1$  is therefore dependent upon  $G \sum_0^{n-1} \cos(\omega t + n\alpha)$ .

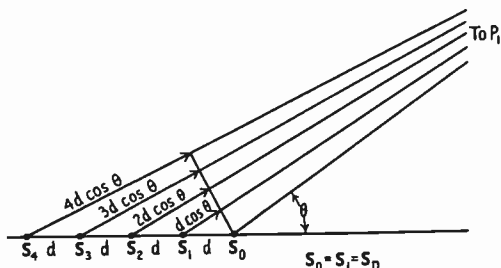


FIG. 46. Illustrating linear arrangement of five rigid disks vibrating in the same phase in an infinite plane.

By the well-known addition formula for cosines in arithmetica progression, we obtain [161]

$$p = \frac{\rho \ddot{x}_0 a^2}{r} G \left[ \frac{\sin \frac{1}{2} n \alpha}{\sin \frac{1}{2} \alpha} \right] \cos[\omega t + \frac{1}{2}(n-1)\alpha]. \tag{38}$$

At any particular frequency the group is equivalent to a single rigid disk whose amplitude of vibration is  $\sin \frac{1}{2} n \alpha / \sin \frac{1}{2} \alpha$  that of any individual member. This quantity of course varies with frequency, so that a single radiator cannot be used to simulate a group in ordinary practice.

The characteristic of a group of five disks at low frequencies where  $G$  is constant is illustrated in Fig. 47. As foreshadowed in the argument given above, the additional vibrating area causes focusing to commence at a frequency lower than that for a single radiator. At higher frequencies, if the radiators are well spaced, it is obvious that they will not interfere seriously with one another since each has a narrow beam of its own. The radiation characteristic [161] is from (38),

$$\mathfrak{R} = G \sin \frac{1}{2} n \alpha / \sin \frac{1}{2} \alpha. \tag{39}$$

When the radiators touch externally and the radius  $a_1$  is made to

vanish whilst their number increases so that  $2na_1$  is the length of the group, the system degenerates into a line. The radiation can then be regarded as that from a cylinder of very small radius vibrating normal to its axis. Now  $G = \frac{J_1(ka_1 \sin \phi)}{ka_1 \sin \phi}$  and when  $a_1 \rightarrow 0$ ,  $G = \frac{1}{2}$ .

Also  $\alpha = kd \cos \theta = 2ka_1 \cos \theta$ , which in the limit gives

$$\sin \frac{1}{2}n\alpha = \sin(kna_1 \cos \theta) = \sin(ka \cos \theta),$$

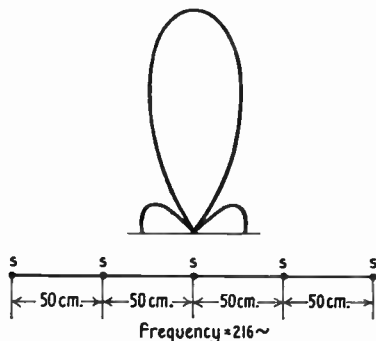


FIG. 47. Distribution of sound pressure at a relatively great distance from the five disks in Fig. 46.

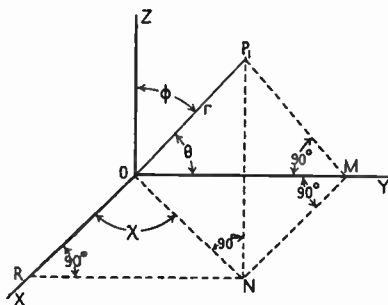


FIG. 48.  $OM$  is in the line of sources.

where  $a = na_1$ , this being half the length of the line. Since  $\frac{1}{2}\alpha \rightarrow 0$ ,  $\sin \frac{1}{2}\alpha \rightarrow \frac{1}{2}\alpha$  and (39) becomes  $\mathfrak{R} = \frac{\sin(ka \cos \theta)}{ka_1 \cos \theta}$ . If each radiator is chosen to give  $1/n$  the total radiation, the characteristic becomes

$$\mathfrak{R} = \frac{\sin(ka \cos \theta)}{kna_1 \cos \theta} = \frac{\sin(ka \cos \theta)}{ka \cos \theta}. \quad (40)$$

Putting  $\phi = \frac{1}{2}\pi - \theta$ ,  $\mathfrak{R} = \frac{\sin(ka \sin \phi)}{(ka \sin \phi)} = \frac{\sin z}{z} = G_3$ . It should be observed, however, that the latter formula applies solely to radiation in a plane containing the line. In any other plane it is different; for example in one perpendicular to the paper and bisecting the line, the characteristic is obviously a circle. In Fig. 48,  $\theta$  is the angle between  $OP_1$  and  $OM$ , so  $\cos \theta = \sin \phi \cos \chi$  and the radiation characteristic becomes  $\mathfrak{R} = \frac{\sin(ka \sin \phi \cos \chi)}{(ka \sin \phi \cos \chi)}$ . The preceding case corresponds to  $\chi = \frac{1}{2}\pi$  giving  $\mathfrak{R} = \sin z/z = 1$ , since  $z = 0$ . The distribution is, therefore, uniform as stated.

## VI

### ACOUSTIC POWER RADIATED FROM VIBRATING SURFACES

#### 1. Methods of evaluating power

There are two principal methods of evaluating the power radiated from a vibrating surface: (1) by integrating the product of the acoustic or resistive component of the pressure and the normal velocity over the surface; (2) by integrating the product of the pressure and velocity in space at a great distance from the radiator. The choice of method depends upon circumstances. Determination of the pressure distribution over a vibrating surface is usually a protracted process (see Chap. III), and the analytical expressions are very lengthy. At a vibrational mode, the driving force is in phase with the surface velocity. In certain cases an approximate estimate of the power can then be obtained on the assumption that the driving force is proportional to the velocity, provided the dynamic deformation curve and  $r_r$ , the resistance per unit area, are known (§ 3). In general, however, the second method is easier to apply than the first. At a great distance from a vibrating surface, the pressure and the particle velocity are in phase. If the spatial pressure distribution is known, the power radiated from the vibrator can usually be determined by analysis. A knowledge of the pressure distribution over the surface is then immaterial.

#### 2. Plane surfaces vibrating in an infinite flat baffle

At a great distance  $r$  from a vibrator imagine a concentric hemispherical surface, on one side of the plane, across which the power is transmitted. If  $p$  is the sound pressure and  $v$  the particle velocity, the power passing through unit area is  $pv$ , since at a great distance  $p$  and  $v$  are in phase. Now from Chap. II, § 14,  $p = \rho_0 cv$ , so  $v = p/\rho_0 c$  and the power per unit area is  $p^2/\rho_0 c$ . For an elementary area  $dA$  we have  $dP = (p^2/\rho_0 c) dA$ . Accordingly, the power transmitted through the hemispherical surface is

$$\frac{1}{\rho_0 c} \iint p^2 dA. \quad (1)$$

From Fig. 3 the elementary zonal area on the sphere is seen to be  $dA = 2\pi r^2 \sin \phi d\phi$ , where  $\phi$  is written for  $\theta$ . Thus the power radiated

from *both* sides of the vibrating surface is

$$P = \frac{4\pi r^2}{\rho_0 c} \int_0^{\frac{1}{2}\pi} p^2 \sin \phi \, d\phi. \quad (2)$$

To determine  $P$  it is merely necessary to insert the value of  $p^2$  in (2) and integrate. In general our problems relate to flexible surfaces where variations in velocity and phase occur. To obtain analytical expressions for  $P$ , the dynamic deformation curve of the surface in a fluid is assumed to be identical with that of a loss-free structure *in vacuo*. As we showed in Chap. IV, § 17, this cannot be true in practice, since loss converts the nodal lines into positions of minimum amplitude. Consequently formulæ obtained on the above hypothesis must be regarded as approximate. Nevertheless they are decidedly better than nothing at all, and serve as a useful guide in the design of modern loud-speaking apparatus.

The premier example which springs to mind is that of a rigid disk. It so happens that this particular vibrator has been studied in detail and the surface pressure is known (Chap. III), so the power is found quite simply, as shown in Chap. VIII, § 2. We shall, therefore, choose another case.

### 3. Membrane at symmetrical modes of vibration

From (23) Chap. V the pressure at any point far distant from the centre is

$$p = \frac{\Upsilon}{r} J_0(ka \sin \phi), \quad (3)$$

provided  $k_1^2 \gg k^2 \sin^2 \phi$ , which entails a low fundamental frequency.

Incorporating the pressure from (3) in (2) we obtain

$$P = \frac{4\pi \Upsilon^2}{\rho_0 c (ka)} \int_0^{\frac{1}{2}\pi} (ka \sin \phi) J_0^2(ka \sin \phi) \, d\phi. \quad (4)$$

To evaluate this integral the following formula [221] is required:

$$J_n^2(x) = \sum_{m=0}^{\infty} (-1)^m \frac{(2n+2m)!}{m!(2n+m)!(n+m)!^2} (\frac{1}{2}x)^{2(n+m)}, \quad (5)$$

where  $n$  is a positive integer. Applying this formula to the integrand of (4) we get

$$P = \frac{4\pi \Upsilon^2}{\rho_0 c} \sum_{m=0}^{\infty} (-1)^m \frac{(2m-1)(2m-3)\dots 1}{2^m(m!)^3} (ka)^{2m} \int_0^{\frac{1}{2}\pi} \sin^{2m+1} \phi \, d\phi. \quad (6)$$

$$\text{Since } \int_0^{2\pi} \sin^{2m+1}\phi \, d\phi = \frac{2^m m!}{(2m+1)(2m-1)\dots 1}, \quad (7)$$

we ultimately find that the power radiated from both sides of the membrane at a vibrational mode is,

$$P = \frac{4\pi\Upsilon^2}{\rho_0 c} \sum_{m=0}^{\infty} (-1)^m \frac{1}{(m!)^2(2m+1)} (ka)^{2m} \quad (8)$$

$$= 4P \left[ \frac{J_1(k_1 a)}{k_1 a} \right]^2 \left\{ 1 - \frac{(ka)^2}{1!^2 3} + \frac{(ka)^4}{2!^2 5} - \frac{(ka)^6}{3!^2 7} + \dots \right\} \quad (9)$$

$$= \frac{4P}{ka} \left[ \frac{J_1(k_1 a)}{k_1 a} \right]^2 \left[ \sum_{r=0}^{\infty} J_{2r+1}(2ka) \right], \quad (9a)$$

where  $P = \frac{\rho_0 \pi a^4 \omega^4 \xi_0^2}{c} = \rho_0 c A (ka)^2 \xi_0^2$ , this being the power radiated from both sides of a rigid disk vibrating in an infinite baffle when  $ka \leq 0.5$ .

In the membrane type of electrostatic speaker, described in Chapters IX and XIII, the driving force, which is distributed over the surface, causes a central amplitude  $\xi_0$ . Before the power can be calculated from (9) the value of  $\xi_0$  must be found. At a vibrational mode the effective mass vanishes (Chap. IV), the driving force being then in phase with the velocity of the membrane. The velocity is  $v = \dot{\xi}_0 J_0(k_1 x)$  and the driving force per unit area for both sides is  $f$ , its surface distribution being assumed uniform throughout, i.e. the perforations in the fixed electrodes are ignored. The power radiated from both sides of an elementary ring of radius  $x$  and width  $dx$  is, therefore,  $2\pi f \dot{\xi}_0 J_0(k_1 x) x \, dx$ . Accordingly the power radiated by the whole membrane is,

$$\begin{aligned} P &= 2\pi f \dot{\xi}_0 \int_0^a J_0(k_1 x) x \, dx \\ &= 2f \dot{\xi}_0 A \left[ \frac{J_1(k_1 a)}{k_1 a} \right], \end{aligned} \quad (10)$$

where  $A = \pi a^2$ , the area of one side.

Thus the central velocity

$$\dot{\xi}_0 = \frac{P}{2fA} \left[ \frac{k_1 a}{J_1(k_1 a)} \right]. \quad (11)$$

Substituting the value of  $\dot{\xi}_0$  from (11) in (9) the power, expressed



in terms of the driving force, is

$$P = \frac{f^2 A}{\rho_0 c} \left\{ \frac{1}{(ka)^2 - \frac{(ka)^4}{1!^2 3} + \frac{(ka)^6}{2!^2 5} - \frac{(ka)^8}{3!^2 7} + \dots} \right\}. \quad (12)$$

When  $ka > 1.4$  the series in the denominator of (12) is substantially unity, so the formula degenerates to

$$P = \frac{f^2 A}{\rho_0 c}. \quad (13)$$

This surprisingly simple expression shows that, under the specified conditions, the power is the same at all vibrational modes, provided  $ka > 1.4$ .

At modes above the fundamental, the membrane exhibits nodal lines on each side of which it moves in phase opposition. If, therefore, the driving force is in phase with the velocity on one side of a nodal line, it is in antiphase with that on the other. Consequently, for the power to be invariable, the central velocity must increase with rise in frequency. That this is true can be seen from (11), since  $\left[ \frac{k_1 a}{J_1(k_1 a)} \right]$  increases with rise in frequency.

#### 4. Free-edge disk with $n$ nodal diameters [121a]

From (27), Chap. V, the sound pressure is given by

$$p = \frac{\rho_0 a^2 \ddot{\xi}_0}{r} \left\{ \sin n\chi \left[ \frac{J_{n+1}(x)}{x} \right] \right\}.$$

Here  $dA$  is  $r^2 \sin \phi \, d\phi \, d\chi$  (Fig. 3, substituting  $\phi$  for  $\theta$ ), so using (1) we get the power radiated from both sides as

$$\begin{aligned} P &= \frac{2\rho_0 a^4 \ddot{\xi}_0^2}{c} \int_0^{1\pi} \frac{J_{n+1}^2(x)}{x^2} \sin \phi \, d\phi \int_0^{2\pi} \sin^2 n\chi \, d\chi \\ &= 2P \int_0^{1\pi} \frac{J_{n+1}^2(x)}{x^2} \sin \phi \, d\phi, \end{aligned} \quad (14)$$

since the first integral is  $\pi$ .

\* This can also be written  $P = \frac{(fA)^2}{\rho_0 c A} = \frac{\text{mean square of total force}}{\text{mechanical resistance}}$ . In an electrical circuit at resonance we have the analogous formula  $P = E^2/R$ .

By aid of formula (5) and the substitution  $x = ka \sin \phi$  in (14), we obtain

$$P = 2P \sum_{m=0}^{\infty} (-1)^m \frac{(2n+2m+2)!}{m!(2n+m+2)!((n+m+1)!)^2 2^{2(n+m+1)}} (ka)^{2(n+m)} \times \int_0^{\frac{1}{2}\pi} \sin^{2(n+m)+1} \phi \, d\phi.$$

Using (7) this ultimately becomes

$$P = P \left\{ \sum_{m=0}^{\infty} (-1)^m \frac{1}{m!(2n+m+2)!(n+m+1)} (ka)^{2(n+m)} \right\} \quad (15)$$

$$= \frac{P}{(n+1)(ka)^2} \left[ J_{2n+2}(2ka) + 2 \sum_{r=0}^{\infty} J_{2n+2r+3}(2ka) \right]. \quad (15 a)$$

When  $ka \leq 0.5$ ,  $P$  is given to an adequate degree of accuracy by the first term of the series, i.e. when  $m = 0$ . For one nodal diameter  $n = 1$  and the power [121 a]

$$P = P \frac{(ka)^2}{48} = \frac{P}{192}, \quad (16)$$

when  $ka = 0.5$ .

Expressed alternatively, for equal output the amplitude at the edge of the disk is  $\sqrt{192} \doteq 14$  times that of a rigid disk. For two nodal diameters when  $ka = 0.5$ , which corresponds to a frequency of 270  $\sim$  for a disk 10 cm. radius,

$$P = \frac{P}{34,560}. \quad (17)$$

This happens to be identical with the output from a disk of equal radius vibrating with a nodal circle at  $r = a/\sqrt{2}$ , provided the edge amplitude with a nodal diameter is the same as the central amplitude with a nodal circle. The ratio of the power in (16) to that in (17) is 180/1, which demonstrates the rapid decay in output with increase in the number of nodal diameters *at low frequencies, the edge amplitude being constant*. It is of practical interest to compare this result with experimental observations on a conical paper shell (Chap. XVIII, curve 1, Fig. 125). As the number of nodal diameters increases the output decays, slowly at first, but as the frequency rises beyond a certain point, the output fades rapidly. The large output is due to the seam of the cone which introduces asymmetry therefore reducing the interference in space.

### 5. Free-edge disk with one nodal circle

For a dynamic deformation curve  $\xi = \xi_0(1 - 2x^2/a^2)$  the radius of the nodal circle is  $x = a/\sqrt{2}$ . Using the preceding analytical methods and formula 2, Table 7, it is easy to show that [121 a] the power radiated is

$$P = P \left\{ \frac{1 \cdot 2}{3!6!} (ka)^4 - \frac{2 \cdot 3}{4!7!} (ka)^6 + \frac{3 \cdot 4}{5!8!} (ka)^8 \dots \right\} \quad (18)$$

$$= P \left\{ \frac{1}{3(ka)^2} + \frac{J_3(2ka)}{(ka)^3} \left[ 1 - \frac{2}{(ka)^2} \right] - \frac{6J_4(2ka)}{(ka)^4} \right\}. \quad (18 a)$$

When  $ka \leq 0.5$ ,

$$P = \frac{P(ka)^4}{2,160}. \quad (19)$$

If  $ka = 0.5$ , we obtain

$$P = \frac{P}{34,560}, \quad (20)$$

which illustrates the enormous acoustic short-circuit effect due to the oppositely vibrating inner and outer portions of the disk. If the radius of the nodal circle is  $0.68a$ , which is the correct value for free symmetrical vibrations,  $P = P/770$ . Thus a 45-fold increase in  $P$  is obtained by reducing the nodal radius 3.8 per cent., *provided the amplitude is equal in both cases*. In the absence of inherent mechanical loss, the power for constant driving force when  $x = a/\sqrt{2}$ , exceeds that when  $x = 0.68a$ , since at resonance  $P = f^2/r_r$  and  $r_r$  is smaller in the former case.

In practice owing to inherent mechanical loss this conclusion may be invalid. When  $ka > 2$  the interference is much reduced, and with  $x = a/\sqrt{2}$  and  $ka = 4$ , the power radiated for constant amplitude is  $P = P/4.4$ .

### 6. Power from flexible and rigid disks driven by equal forces [121 a]

Hitherto our comparisons have been confined mainly to equal amplitudes. In practice, since the effective mass vanishes at a symmetrical vibrational mode, the mechanical impedance is much reduced and the amplitude under a given driving force correspondingly increased. It is proposed to compare the power radiated by baffeless rigid and flexible disks, having the same natural mass, being driven by equal forces. The driving agent is a moving coil as used in hornless speakers.

For a certain aluminium disk,  $a = 10$  cm., and the frequency corresponding to one nodal circle is  $120 \sim (ka = 0.23)$  [114c]. When alternating current in the moving coil is provided by a thermionic valve in the usual way, the driving force is equal in both cases provided the currents are the same. It follows that the power ratio is that of the electrical motional resistances  $R_m/R'_m$ . For the rigid disk from Chap. II, § 19, formula (90),  $P' = \frac{16}{27\pi} \frac{\rho_0 a^6 \omega^4}{c^3} (\xi_0^2)$ , so the

mechanical radiation resistance is  $r'_r = \frac{16}{27\pi} \frac{\rho_0 a^6 \omega^4}{c^3}$ . From Chapter VII

the electrical motional resistance is  $R'_m = \frac{r'_r C^2}{(r'_r{}^2 + \omega^2 m_e'^2)} = \frac{r'_r C^2}{\omega^2 m_e'^2}$  since

$r'_r \ll \omega m_e'$ . Now for a rigid baffleless disk as above\*  $m_e' = 58.5$  gm. and from Chap. XVI, Table 21,  $C^2 = 2 + 10^4$ ]. Using these data we find that  $R'_m$  is  $2.1 \times 10^{-5}$  ohms which is extraordinarily small, being in fact 1/300 of the value with an infinite baffle. By experiment  $R_m$  was found to be 39.5 ohms [114c] so the power ratio flexible disk / rigid disk =  $\frac{R_m}{R'_m} = \frac{39.5}{2.1 \times 10^{-5}} = 1.88 \times 10^6$  which is colossal.

In practice where a step-down transformer is used between the coil and valve circuits, the alternating current falls to a very low value due to increased resistance at the resonance frequency of the flexible disk. Taking the valve resistance as 1,600 ohms, transformer ratio 40/1, the resistance in the valve circuit at resonance is equivalent to about  $40 \times (40)^2 = 6.4 \times 10^4$  ohms. The current is therefore reduced in the ratio †  $\frac{3,200}{6.4 \times 10^4} = \frac{1}{20}$ , so the power ratio at resonance is only 1/400 the value computed above. Thus  $R_m/R'_m = 4.7 \times 10^3$  so that the output from the flexible disk is 37 decibels above that for the rigid disk when both are driven off the same power valve using equal signal voltages. At 1,850  $\sim$  the corresponding values are 2,600/1 for constant current, and 370/1 with the valve circuit. In assessing these ratios at 1,850  $\sim$  the power from a baffleless disk is assumed equal to that from both sides of a rigid disk in an infinite baffle when the radiation is highly focused from both sides (see Chap. II, § 22, and Chap. V, § 1).

\*  $m_a = 55$  gm. including disk and coil;  $m_i = 3.5$  gm. without the baffle this being half the value in an infinite baffle (see § 4, method 1, Chap. III).

† The static resistance of the coil  $R_0 \doteq 1$  ohm, so that in the valve circuit it becomes 1,600 ohms, making a total of 3,200 ohms.

### 7. Spherical radiators without a baffle\*

As yet the baffless conical shell has defied the methods of modern analysis. In certain instances approximate results can be obtained by substituting the case of a sphere vibrating in various ways. The present section is included with this in view. The radiated power will be determined by integrating the pressure and particle velocity over a concentric spherical surface at a great distance, where the pressure and particle velocity are in phase. If the sound pressure due to the  $n$ th spherical harmonic is  $p_n$ , and the particle velocity  $v_n$ , the power transmitted through unit area of a spherical surface of radius  $R$  is  $p_n v_n = p_n^2 / \rho_0 c$ , since  $p_n = \rho_0 c v_n$ . The total power is the integral over the spherical surface. Thus  $P = \frac{1}{\rho_0 c} \iint p_n^2 dA$  where  $p_n$  is the root mean square pressure. Since  $dA = -2\pi r^2 d\mu$  (see Fig. 3) it follows that the power associated with the  $n$ th harmonic is [121 b]

$$P_n = -\frac{2\pi r^2}{\rho_0 c} \int_{-1}^{+1} p_n^2 d\mu. \quad (21)$$

If the pressure at any point on the distant spherical surface is expressed as a series of harmonic terms, the integral of the square of this series, taken over the surface, is equal to that of the sum of the squares of separate terms. This follows from the fact that

$$\int_{-1}^{+1} P_n(\mu) P_m(\mu) d\mu$$

is zero excepting when  $m = n$ , which is similar to the case of Fourier's series applied to an electrical circuit. Thus in finding the power radiated by a vibrating sphere, it is merely necessary to add the contributions from each spherical harmonic.

From (54), Chap. II, the velocity potential due to the  $n$ th harmonic, at a great distance  $r$  from the centre of the sphere, is

$$\phi_n = \left(\frac{a^2}{r}\right) u_n \Xi_n e^{i\omega t}.$$

The pressure due to this harmonic

$$p_n = \rho_0 \left(\frac{\partial \phi_n}{\partial t}\right) = i\rho_0 a^2 \omega u_n \Xi_n / r \quad (22)$$

\* For a cone with a finite baffle the suggestion in Chap. V, § 10, applies.

where the time factor  $e^{i\omega t}$  has been dropped. The radial velocity of the surface due to the  $n$ th harmonic can be written

$$u_n = U\Theta_n \quad \text{where } u = Uf(\mu), \quad U = \dot{\xi}_0$$

$$\text{and (a)} \quad \Theta_n = (n + \frac{1}{2})P_n(\mu) \int_{-1}^{+1} f(\mu)P_n(\mu) d\mu, \quad (23)$$

$$\text{(b)} \quad \Theta_n = (2n + 1)P_n(\mu) \int_0^1 f(\mu)P_n(\mu) d\mu, \quad (24)$$

the respective fields of application being defined below.

Formula (23) is applicable when the two hemispheres have identical motions in the same direction, whilst (24) applies when the motions are equal but opposite. If one hemisphere alone is operative, (24) must be halved. From expressions (21), (22) and the above value of  $u_n$ , we find that the power associated with the  $n$ th spherical harmonic is given [121 b] by

$$P_n = 2P\Xi_n^2 \int_{-1}^{+1} \Theta_n^2 d\mu, \quad (25)$$

where  $\Xi_n^2 = \frac{1}{|F_n(ika)|^2} = \frac{1}{x^2 + y^2}$  (Table 1) is a correction factor dependent upon the distribution of radiation in space. The integration in (25) extends over the *entire* surface of the sphere, since each harmonic is concerned with the complete sphere.

### 8. Sphere vibrating radially

Since the dynamic deformation curve is identical in all directions, we are concerned solely with the zonal harmonic of order zero. The value of  $\Theta_0$  in (23) is, therefore, unity and

$$P_0 = 4P\Xi_0^2.$$

But from Table 1,  $\Xi_0 = \frac{1}{1 + ika}$ , so  $\Xi_0^2 = \frac{1}{1 + k^2a^2}$  and

$$P_0 = \frac{4P}{1 + k^2a^2}. \quad (26)$$

This result is usually derived in connexion with a spherical source whose size is small compared with the wave-length under consideration. Moreover, the correction term  $1/(1 + k^2a^2)$  does not then appear except in the form unity, i.e. when  $ka = 0$  or is quite small.

### 9. Sphere vibrating radially, driven by constant radial force per unit area

In treating this problem we shall assume  $m_e$  (definition 33), apart from  $m_i$  (definition 29), to be constant at all frequencies, i.e. there are no resonances. The mechanical resistance (definition 31)  $r_r$  is found from the relationship  $P_0 = r_r \xi_0^2$ . Thus from (26)

$$r_r = \frac{4P}{(1+k^2a^2)\xi_0^2} = 4\pi a^2 \rho_0 c \left( \frac{k^2 a^2}{1+k^2 a^2} \right). \quad (27)$$

The effective mass  $m_e = m_i + m_n$

$$= m_i(1+\beta), \quad \text{where } \beta = \frac{m_n}{m_i}.$$

From (2), Table 4, Chap. III,  $m_i = \frac{4\pi a^3 \rho_0}{1+k^2 a^2} = \frac{r_r}{\omega k a}$ .

Thus 
$$m_e = \frac{r_r}{\omega k a} (1+\beta). \quad (28)$$

The power radiated is

$$P = r_r \xi_0^2 = r_r \left( \frac{f}{z_e} \right)^2, \quad (29)$$

$f$  being the total driving force on the surface.

Since  $z_e = \sqrt{(r_r^2 + \omega^2 m_e^2)}$  and  $f$  is constant, it follows from (29) that  $P \propto \frac{r_r}{r_r^2 + \omega^2 m_e^2}$ . Substituting the value of  $m_e$  from (28) and of  $r_r$  from (27), when the driving force is constant, we obtain

$$P \propto \frac{1}{4\pi a^2 \rho_0 c} \left[ \frac{1+k^2 a^2}{(1+\beta)^2 + k^2 a^2} \right]. \quad (30)$$

Provided  $\beta = m_n/m_i$  is small compared with unity, i.e. the accession to inertia is much greater than the natural mass of the shell, the power is constant at all frequencies. Thus we have the ideal hypothetical acoustic reproducer. In general this condition will be much more easily obtained in water than in air, owing to the low density of the latter. When  $\beta$  is not negligible compared with unity, it follows from the preceding formulae that, for constant power output, the driving force must vary as  $\left\{ \frac{(1+\beta)^2 + k^2 a^2}{1+k^2 a^2} \right\}^{\frac{1}{2}}$ . At low frequencies when  $k^2 a^2 \ll 1$ ,  $\beta$  is constant, so also is the output for a given driving force. This conclusion applies equally to any rigid body vibrating in an infinite baffle when the sound distribution is spherical.

In our spherical vibrator if  $f$  is constant, we see from (29) that the amplitude  $\xi_0$  varies as  $\frac{1}{\omega z_e} = \frac{1}{\omega \sqrt{(r_r^2 + \omega^2 m_e^2)}}$ . Inserting the values of  $r_r$  and  $m_e$  in this formula we find that  $\xi_0 \propto \frac{1+k^2 a^2}{\omega^2 \sqrt{\{(1+\beta)^2 + k^2 a^2\}}}$ , and since by hypothesis  $\beta \ll 1$ ,

$$\xi_0 \propto \frac{\sqrt{(1+k^2 a^2)}}{\omega^2}. \quad (31)$$

At low frequencies, when  $ka$  is small,  $\xi_0 \propto 1/\omega^2$ , whilst at high frequencies, where  $ka$  is large,  $\xi_0 \propto 1/\omega$ , which indicates the greater influence of the in-phase acoustic force at higher frequencies.

Proceeding on similar lines it can be shown that, when an axially vibrating sphere is driven by a constant force, the power

$$P \propto \frac{k^2(4+k^4 a^4)}{\{(1+\beta)^2(2+k^2 a^2)^2+k^6 a^6\}}. \quad (32)$$

When  $ka$  is small the power

$$P \propto \frac{k^2}{(1+\beta)^2} \propto \frac{\omega^2}{c^2(1+\beta)^2}. \quad (33)$$

Thus as zero frequency is approached the power is evanescent due to interference of radiation from the two hemispheres which constitute a double source. It is important to observe that this acoustic short-circuit effect increases with decrease in frequency, whilst the accession to inertia remains unaltered. Whereas the power is governed by spatial interference due to phase relationships, the accession to inertia depends upon the flow of fluid associated with the motion, and obviously this can never vanish. At high frequencies when  $ka$  is large, (30) reduces to  $1/4\pi a^2 \rho_0 c$  and the power is constant provided  $ka \gg (1+\beta)$ .

## 10. Two hemispheres vibrating oppositely along the common axis

The axial velocities of the two hemispheres being  $U$  and  $-U$  it follows that the radial velocities are given by  $u = Uf(\mu)$ , where  $f(\mu) = \mu$  from 1 to 0 and  $-\mu$  from 0 to  $-1$ , Fig. 20c. Owing to symmetry of the motion about an equatorial plane, the expansion of  $u$  contains even harmonics only. Hence we use formula (24), for the integrand of (25). Thus

$$\Theta_0 = \int_0^1 \mu d\mu = \frac{1}{2},$$



$$\begin{aligned} \text{and} \quad \Theta_2 &= \frac{5}{2}(3\mu^2-1) \int_0^1 \frac{1}{2}\mu(3\mu^2-1) d\mu \\ &= \frac{5}{16}(3\mu^2-1), \end{aligned}$$

higher harmonics not being of material importance. Then we have

$$P_0 = 2P\Xi_0^2 \int_{-1}^{+1} \frac{1}{2} d\mu = \frac{P}{(1+k^2a^2)}, \quad (34)$$

this being one-quarter the power radiated by a sphere pulsating radially throughout.

$$\begin{aligned} P_2 &= 2P\Xi_2^2 \int_{-1}^{+1} \frac{25}{256}(9\mu^4-6\mu^2+1) d\mu \\ &= \frac{5}{16}P \left( \frac{k^4a^4}{81+9k^2a^2-2k^4a^4+k^6a^6} \right). \end{aligned} \quad (35)$$

When  $ka \leq 0.5$  the power radiated is due almost entirely to  $P_0$ . If the driving force is constant and the acoustic (resistive) component is negligible compared with that due to inertia, the power radiated at low frequencies is

$$P_0 = \frac{f^2}{\pi a^2 \rho_0 c (1+\beta)^2}. \quad (36)$$

provided  $ka \leq 0.5$ .

The power is constant and independent of frequency. This is in striking contrast with the result in the previous section when the two hemispheres moved in the *same* direction. The difference is due to the absence of interference, since the hemispheres in the present case cause pressure changes of like sign.

A fact of unusual interest is the equality in low frequency radiation ( $ka \leq 0.5$ ) from (a) two oppositely vibrating hemispheres, (b) both sides of a rigid disk in an infinite baffle, (c) a radially pulsating hemisphere, provided the velocities and radii are equal in all cases. From this we deduce that if a loud speaker is situated in the centre of a room, a baffle is unnecessary if two diaphragms are actuated axially in opposition. Since an infinite baffle excludes one-half of the total radiation, the output from the differential scheme is twice that from one side of the disk. It is also double that from a single diaphragm in a finite baffle. The above rests on the assumption that the radiation from the inner faces of the diaphragms is suitably dealt with, i.e. that it can be absorbed, although this is a difficult matter at low frequencies. A design embodying these features is shown schematically

in Fig. 49. The diaphragms are attached to opposite sides of the axis of the coil, which is rotatable as in a moving-coil ammeter. The principle can be extended to a polyhedron so that the axes of the diaphragms lie in intersecting planes, thereby approximating to a spherical source emitting sound equally along all its radii [89].

When comparison of output is based on constant driving force, the advantage of a multi-diaphragm system is offset by the additional inertia. The only gain, therefore, is the elimination of the baffle.

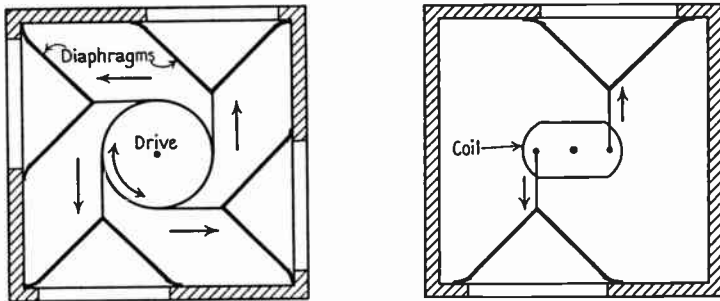


FIG. 49. Diagram illustrating multi-diaphragm moving-coil loud speaker.

Additional formulae for the power radiated from vibrators of various types are given in Table 9.

### 11. Comparison of power radiated by various vibrators at low frequencies

When  $ka \leq 0.5$ ,  $r \geq 10a$  and the entire surface vibrates in the same phase, the radiator, whatever be its shape, can be regarded as a simple source.\* Under this condition the power radiated from a sphere is comparable with that from a rigid disk of the same radius (which can be simulated by a conical shell moving as a whole). The power varies as  $(uA)_e^2 \omega^2 / \Omega$ , where  $u$  is the radial velocity normal to the surface, and  $(uA)_e$  is the effective velocity-area. Data for various vibrators are given in Table 10. The comparison is based upon  $(uA)_e^2 / \Omega$ , since  $\omega$  is the same for all. For a hemisphere vibrating axially, the other hemisphere being quiescent, the radial velocity is  $u = U \mu = U \cos \theta$  (Fig. 20). To find the effective velocity-area, it is necessary to integrate over the surface of the hemisphere. Thus

\* A sphere vibrating axially is therefore excluded, since the radial velocities in the two hemispheres are in opposite phase, i.e. it is a double source.

TABLE 9

Power radiated by various vibrators

Since  $P = r_e \omega^2 \xi_0^2$ , the effective mechanical resistance is  $r_e = P/\omega^2 \xi_0^2$ , in terms of a driving force whose velocity is  $\omega \xi_0$ , and can be found from the table.

Type of vibrator	Dynamic deformation curve	Power radiated as sound
1. Rigid annular ring radii $a$ and $b$ in infinite rigid plane. Hole fitted with stationary rigid disk.	$\xi = \xi_0$ .	$2\rho_0 c \xi_0^2 \left\{ A_a G_{1a} + A_b \left[ G_{1b} - 2 \sum_{m=0}^{\infty} (-1)^m \frac{F[-m, -(m+1), 2, b^2/a^2]}{(2m+2)!} (ka)^{2(m+1)} \right] \right\},$ <p>where <math>G_{1a} = \left[ 1 - \frac{J_1(2ka)}{ka} \right]</math>; <math>G_{1b} = \left[ 1 - \frac{J_1(2kb)}{kb} \right]</math>.</p> <p><math>A_a, A_b</math> = area of outer and inner circles respectively. Both sides of ring are included.</p>
2. Clamped-edge disk in gravest mode, with infinite plane [121 a].	$\xi = \xi_0(1 - (x^2/a^2))^2$ .	$32P \left\{ \frac{3.5}{3!6!} - \frac{5.7}{4!7!} (ka)^2 + \frac{7.9}{5!8!} (ka)^4 - \dots \right\},$ <p>where <math>P = \rho_0 \pi a^4 \omega^4 \xi_0^2 / c</math>.</p>
3. Spherical shell vibrating axially [121 b].	$u = U \cos \theta$ (radial velocity).	$P \cdot \frac{4}{3} \left( \frac{k^2 a^2}{4 + k^4 a^4} \right) = P \cdot \frac{4}{3} \Xi_1^2.$
4. Spherical shell vibrating axially and driven by constant force [121 b].	$u = U \cos \theta$ (radial velocity).	$\frac{3k^2 a^2 (4 + k^4 a^4)}{4\pi a^2 \rho_0 c \{ (1 + \beta)^2 (2 + k^2 a^2)^2 + k^6 a^6 \}} f^2,$ <p>where <math>f</math> = constant force, <math>\beta = m_n/m_i</math>.</p>
5. One hemisphere vibrating radially, the other quiescent [121 b].	$u = U$ from $\theta = 0$ to $\frac{1}{2}\pi$ . $u = 0$ from $\theta = \frac{1}{2}\pi$ to $\pi$ (radial velocity).	$P \left\{ \frac{1}{1 + k^2 a^2} + \frac{3}{4} \left( \frac{k^2 a^2}{4 + k^4 a^4} \right) \right\} \text{ (approximately).}$

6. One hemisphere vibrating axially, the other quiescent [121 b].

$$u = U \cos \theta \text{ from } \theta = 0 \text{ to } \frac{1}{2}\pi$$

$$u = 0 \text{ from } \theta = \frac{1}{2}\pi \text{ to } \pi$$

(radial velocity).

7. Spherical shell with  $n$  nodal circles passing through poles [121 b].

$$u = U \sin^a \theta \sin n\chi$$

(radial velocity).

8. Group of rigid disks.

$$\xi = \xi_0.$$

9. Rigid elliptical disk in infinite rigid plane.

$$\xi = \xi_0.$$

10. Rigid rectangular plate in infinite rigid plane.

$$\xi = \xi_0.$$

$$P \left\{ \frac{1}{4(1+k^2a^2)} + \frac{1}{3} \left( \frac{k^2a^2}{4+k^4a^4} \right) + \dots \right\}.$$

$$\frac{2^{n+1}n!}{1 \cdot 3 \dots (2n+1)} \Xi_n^a P.$$

For  $\Xi_n^a$  see Table 1, Chapter II, when  $r = a$ .

See [122].

See [122].

See [122].

the velocity-area for a zonal ring in co-latitude  $\theta$  is  $2\pi Ua^2 \cos \theta \sin \theta d\theta$ , and the total for the hemisphere is found on integration of this between the limits 0 and  $\frac{1}{2}\pi$  which gives  $U\pi a^2 = UA$ , where  $A$  is half the superficial area. The effective velocity-area is obviously half that of a radially pulsating hemisphere, but equal to that of one side of a rigid disk or a conical shell vibrating axially in an infinite plane.

The comparison in Table 10 is made on the basis of radiation from one side of a rigid disk in an infinite plane, since in practice this is all that would be available in an enclosed space.

TABLE 10

*Comparison of low-frequency power from various vibrators having equal radial velocities ( $U$ )*

$ka \leq 0.5$ ;  $A = \pi a^2$ ; diffusion into free space or 'dead' room. For the infinite baffle condition, the wall in which the vibrator oscillates must be non-absorbent.

<i>Vibrational system</i>	<i>Effective velocity area (<math>uA</math>)<sub>e</sub></i>	<i>Solid angle <math>\Omega</math></i>	$(uA)_e^2/\Omega$	<i>Power ratio to rigid disk</i>	<i>Actual power</i>
Sphere radially.	$4UA$	$4\pi$	$4(UA)^2/\pi$	8	$4P$
Hemisphere radially in infinite plane (baffle).	$2UA$	$2\pi$	$2(UA)^2/\pi$	4	$2P$
One hemisphere radially without infinite plane; the other quiescent.	$2UA$	$4\pi$	$(UA)^2/\pi$	2	$P$
One hemisphere axially without infinite plane; the other quiescent.	$UA$	$4\pi$	$(UA)^2/4\pi$	$\frac{1}{2}$	$\frac{1}{2}P$
Two hemispheres in opposition.	$2UA$	$4\pi$	$(UA)^2/\pi$	2	$P$
One side of rigid disk or other flat surface of equal area in infinite plane (baffle).	$UA$	$2\pi$	$(UA)^2/2\pi$	1	$\frac{1}{2}P$
One side of rigid disk without plane, the other side screened.	$UA$	$4\pi$	$(UA)^2/4\pi$	$\frac{1}{2}$	$\frac{1}{2}P$
Rigid disk or conical diaphragm in finite baffle.				1 (approx.)	$\frac{1}{2}P$ (approx.)

## VII

### THEORY OF MOVING-COIL PRINCIPLE

#### 1. Analysis

Initially the treatment is based upon the following hypotheses [79 b]:

(a) The diaphragm and driving coil behave dynamically as a rigid structure.

(b) For generality a linear axial elastic constraint  $s$  is included. This might be a centring device for the coil, an annular surround for the diaphragm or both of these.

(c) The resistive force due to sound radiation and mechanical losses is proportional to the axial velocity  $\dot{\xi}$ .

(d) There is neither mutual inductance nor mutual capacity between the coil and the magnet, i.e. only the static magnetic field is taken into account.

(e) The radial magnetic field is uniform throughout the travel of the coil and is undistorted by the current.

(f) The alternating current driving the coil is supplied by a valve and a perfect transformer having neither loss, leakage, nor capacity, with unity ratio, Fig. 51 A. The transformer prevents the valve feed current from passing through the coil, thereby avoiding a permanent deflexion. The signal voltage applied to the valve grid is  $E_g$ , and the magnification factor  $\mu$ , so the equivalent voltage in the anode circuit is  $\mu E_g = E$ , as shown in the equivalent circuits in Fig. 51 B, C, D, E, which are discussed later.

Consider the mechanical forces acting on the coil. We have reactive + resistive + constraint = driving force, or symbolically,

$$mD^2\xi + r_e D\xi + s\xi = CI, \quad (1)$$

where  $m$  = natural mass of diaphragm, coil, etc. + accession to inertia,

$C$  = force per unit current = e.m.f. per unit velocity (see definition 43).

Consider the electrical forces in the circuit:

reactive + resistive + motional (induced) = driving, or symbolically,

$$LDI + RI + CD\xi = E, \quad (2)$$

where  $L = \text{total inductance in the coil circuit, coil at rest,}$

$R = \text{total resistance in the coil circuit, coil at rest.}$

$$E = E_{\max} \sin \omega t.$$

In solving (1) and (2) for the steady state we can write  $D = i\omega$ . Thus (1) becomes

$$-m\omega^2\xi + ir_e\omega\xi + s\xi = CI, \quad (3)$$

and (2) becomes

$$i\omega LI + RI + iC\omega\xi = E. \quad (4)$$

From (3)

$$\xi = \frac{CI}{(s - m\omega^2) + i\omega r_e}. \quad (5)$$

Substituting the value of  $\xi$  from (5) in (4) we obtain

$$E = I \left[ R + i\omega L + \frac{C^2}{r_e + i(\omega m - s/\omega)} \right]. \quad (6)$$

From (6) the electrical impedance of the complete circuit is

$$Z = \frac{E}{I} = R + i\omega L + C^2 \frac{[r_e - i(\omega m - s/\omega)]}{r_e^2 + (\omega m - s/\omega)^2} \quad (7)$$

or

$$Z = (R + R_m) + i\omega(L + L_m). \quad (8)$$

$R, L$  are the respective resistance and inductance in circuit when the coil is stationary and include all additional apparatus.

The quantities  $R_m$  and  $L_m$  are called the motional electrical resistance and the motional electrical inductance respectively. They can be combined into the motional electrical impedance, thus  $Z_m = R_m + i\omega L_m$ .

From (7) we obtain

$$R_m = \frac{r_e C^2}{r_e^2 + (\omega m - s/\omega)^2} \quad (9)$$

$$= \frac{r_e C^2}{z_e^2} \quad (10)$$

$$= \frac{C^2 \cos^2 \theta}{r_e}, \quad (11)$$

where  $z_e = \sqrt{\{r_e^2 + (\omega m - s/\omega)^2\}}$  is the mechanical impedance,

and the mechanical power factor  $\cos \theta = r_e/z_e$  (see Fig. 50).

Also

$$L_m = \frac{(s/\omega^2 - m)C^2}{z_e^2} \quad (12)$$

$$= \frac{C^2 \sin^2 \theta}{s - \omega^2 m} = \frac{(1 - \cos^2 \theta)C^2}{s - \omega^2 m}. \quad (13)$$

The motional inductance can be positive, negative, or zero according to the relative interaction of mass and constraint. Below the mechanical resonance frequency  $L_m$  is positive, at resonance, where  $s = m\omega^2$ , it is zero, whilst above resonance it is negative. If desired the negative condition can be regarded as a condenser effect and treated accordingly. Thus  $C_m = -\frac{1}{\omega^2 L_m}$ , and since  $L_m$  is negative,  $C_m$  has a positive sign numerically. Both  $R_m$  and  $L_m$  are attributable to the back e.m.f. induced in the coil due to motion in the magnetic field. The phase of the coil velocity, and therefore of the induced e.m.f., relative to the driving force (current) obviously depends upon the mechanical impedance. It follows that  $R_m$  and  $L_m$ , being dependent upon the back e.m.f., are related to the mechanical impedance.

The motional electrical capacity is

$$C_m = -\frac{1}{\omega^2 L_m} = \frac{(m - s/\omega^2)}{C^2(1 - \cos^2\theta)}. \quad (14)$$

The circuitual current is

$$I = \frac{E}{Z} = \frac{E}{[(R + R_m)^2 + \omega^2(L + L_m)^2]^{\frac{1}{2}}} \\ = \frac{E}{[(R + R_m)^2 + \{\omega L - (1/\omega C_m)\}^2]^{\frac{1}{2}}}. \quad (15)$$

The relationship between the mechanical quantities is shown vectorially in Fig. 50.

From (11) and (13)  $\frac{\omega L_m}{R_m} = \left(\frac{r_e}{s/\omega - \omega m}\right) \tan^2\theta$ . But from Fig. 50  $\frac{r_e}{(s/\omega - \omega m)} = \cot\theta$ , so  $\omega L_m/R_m = \tan\theta$ . It follows that if the vector diagram of the motional electrical impedance is drawn, the mechanical power factor  $\cos\theta$  corresponds to the motional electrical power factor  $\cos\theta = R_m/Z_m$ . On physical grounds this is obvious, since the mechanical and electrical resistances and reactances must correspond, respectively.

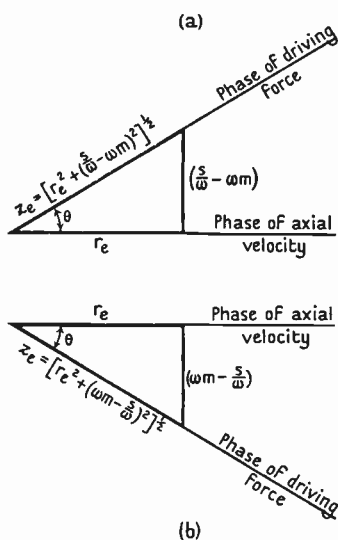


FIG. 50. Diagrams illustrating mechanical impedance of moving-coil system. Read clockwise.



Now from above  $\cos \theta = \frac{r_e}{z_e} = \frac{R_m}{Z_m}$ , so  $\cos^2 \theta = \frac{r_e R_m}{z_e Z_m}$ . Inserting this value in (11) we obtain

$$z_e Z_m = C^2 \quad (16)$$

giving a concise relationship between the electrical and mechanical systems. Electromechanical coupling exists in virtue of the magnetic field, and  $C^2$  can be regarded as the *electromechanical conversion factor* (see definition 43).

From (10) and (16) the mechanical resistance is

$$r_e = \frac{C^2 R_m}{Z_m^2}, \quad (17)$$

and from (12) and (16) the *effective mass* (see definition 33)

$$m_e = m - s/\omega^2 = -\frac{C^2 L_m}{Z_m^2}. \quad (18)$$

When  $s = 0$  the system is devoid of mechanical resonance. This condition is approached in practice when the frequency on the annular surround and centring device is well below audibility, e.g.  $< 20 \sim$ . The stiffness  $s$  is then the sum of the individual axial stiffnesses of the surround and the centring device. Thus (9) becomes

$$R_m = \frac{r_e C^2}{r_e^2 + \omega^2 m^2} = \frac{r_e C^2}{z_e^2}, \quad (19)$$

and (14) reduces to

$$C_m = \frac{m}{C^2}, \quad (20)$$

since, in general, for a large diaphragm without a horn  $\cos^2 \theta \ll 1$ . The series and parallel equivalent circuits are now as shown in Fig. 51 D, E. The above formulae can be used to determine the total impedance of a loud speaker *per se*, the value being  $[(R_0 + R_m)^2 + \{\omega L_0 - (1/\omega C_m)\}^2]^{\frac{1}{2}}$ . From Fig. 51 D it is seen that the static inductance  $L_0$  and motional capacitance  $C_m$  constitute a resonant system. If the total circuitual resistance is sufficiently low, damped oscillations will occur in the *absence of mechanical constraint*. In practice the resistance is much too high for this to happen, and with a steady applied e.m.f. the resonant frequency is inconspicuous.

Hitherto we have considered the various motional impedances to be in *series*, as shown in Fig. 51 B. Using a well-known transformation the motional impedance can be represented by a parallel circuit as shown in Fig. 51 C. The analytical expressions for the three com-

ponents are now very simple: thus

$$R'_m = \frac{C^2}{r_e}, \quad L'_m = \frac{C^2}{s}, \quad \text{and} \quad C'_m = \frac{m}{C^2}. \quad (21)$$

The circuit of Fig. 51 c is the parallel *electrical equivalent* of the moving-coil system. Moreover, if the coil system were replaced by

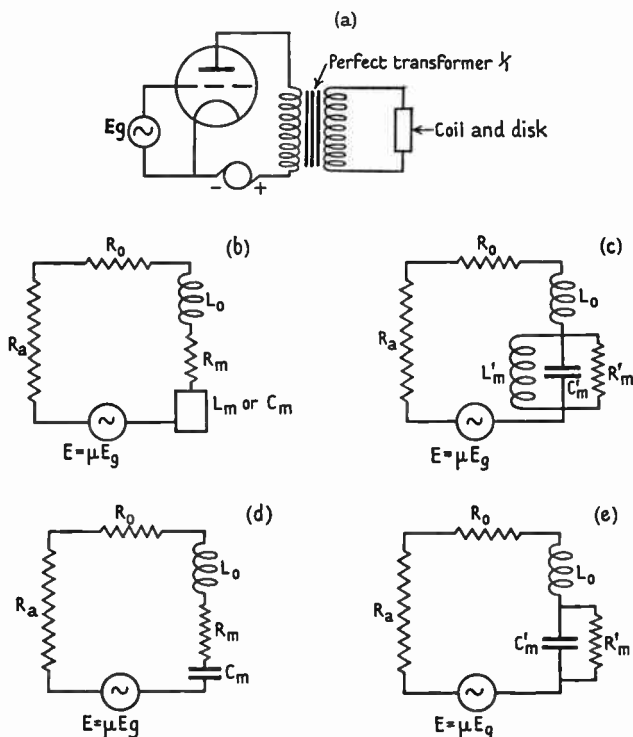


FIG. 51.

- (a) Valve circuit for coil driven disk.  
 (b) Circuit equivalent to (a), series arrangement.  
 (c) Circuit equivalent to (a), parallel arrangement.  
 (d) Circuit equivalent to (a), series arrangement,  $s = 0$ .  
 (e) Circuit equivalent to (a), parallel arrangement,  $s = 0$ .

this circuit, the voltage, current, phase, and power would be identical in both cases. When  $m$  and  $r_e$  are constant, the three quantities in (21) are independent of frequency and the equivalent circuit is applicable to transients.

If an harmonic e.m.f. of constant maximum  $\mu E_g$  is applied to the circuit of Fig. 51 c the current is reduced to a fraction of its normal value when its frequency is equal to the resonant frequency of the system. Under this condition the impedance of the equivalent circuit is very high, and the current-frequency curve has a deep crevasse. This is shown distinctly in the experimental curve of Fig. 149.

## 2. Extension of the analysis to flexible diaphragms

By considering only the forces operating at the driving point, the foregoing analysis can be extended to include any form of mechanical impedance. Just as any electrical circuit, however complex, can be resolved into an effective resistance and an effective inductance in series, so also can a mechanism at the driving point be regarded as an effective mechanical resistance in series with an *effective* mass. The latter can be positive, negative, or zero according to circumstances. (See definition 33.)

The concept of effective mass at the driving point is of inestimable value in the investigation and physical interpretation of vibrational problems. If we are presented with a mysterious box having two external terminals, said to harbour inert electrical circuits, its performance under steady conditions can be predicted by aid of an A.C. bridge. Measurement reveals that it has an effective resistance and an effective inductance at all frequencies. These are the only quantities required to calculate the steady current in any known circuit to which the box may be connected. The contents of the box may be simple or complicated, but they are of no importance except in the case of transients. The same can be said of any mechanical system whose driving point is under dynamical examination. Symbolically the mechanical impedance  $z_e = r_e + i\omega m_e$ , where  $m_e$  is now the effective mass. It is of paramount importance that  $m_e$  be not confused with  $m_q$  the equivalent mass. (See definition 34.) It so happens that in the special case of a rigid structure vibrating *in vacuo*, the natural, effective, and equivalent masses are identical.

From what precedes there should be no difficulty in realizing that the foregoing analysis is valid for any mechanical system whatsoever, provided attention is paid to the driving point alone. This happens in practice, since the mechanical reactions are measured at the driving coil.

It is evident from (9) and (18) that  $(m - s/\omega^2)$  is the effective

mass of a rigid diaphragm with constraint. Knowing  $L_m$  and  $Z_m$  from A.C. measurements,  $m_e = (m - s/\omega^2)$  can be calculated using (18), so the value of  $s$  can be found. This case occurs in loud speakers where  $s$  is due to the combined effect of centring device and surround.\* The resonance frequency is, of course,  $\omega = \sqrt{s/m}$ . Below this point  $m_e$  is negative, and above it is positive.

In general we have from (17) the effective mechanical resistance

$$r_e = \frac{C^2 R_m}{Z_m^2}, \quad (22)$$

and from (18) the effective mass

$$m_e = -\frac{C^2 L_m}{Z_m^2}, \quad (23)$$

where  $Z_m = [R_m^2 + \omega^2 L_m^2]^{\frac{1}{2}}$ . Thus both quantities can be found by electrical measurements of motional resistance and motional inductance.

These results are valid for the steady state only. If a diaphragm is subjected to an impulse, all its natural frequencies are excited. The higher the individual frequency the greater the damping. As time progresses after the shock, the higher modes are quickly extinguished, finally leaving only the fundamental (see Fig. 140). Consequently the shape, the resistance, the accession to inertia, and, therefore, the effective mass of the diaphragm, referred to the coil, change progressively from the beginning of the motion. Thus, if  $m_e$  were used in equation (1) in place of  $m$ , the analysis would be invalid. In practice, provided the principal vibrations are separated by wide frequency intervals, they can be studied independently within certain limits.

### 3. Predetermination of coil current

Having tentatively settled the general design of the vibrational system of a loud speaker, it is a wise policy to calculate the coil current over the frequency range to be covered. To do so it is necessary to know the static and motional components of the coil impedance, i.e.  $(R_0 + R_m)$  and  $(L_0 + L_m)$ , together with the valve resistance  $R_a$ . The static values can only be found accurately by experiments on similar models, since calculation *ab initio* is rather hazardous owing to the influence of the iron of the magnet. With the aid of Table 36 an

\* In a horn speaker having a small diaphragm the surround and centring device is usually one unit.

approximation can be obtained in certain cases. The motional values can be calculated only on the assumption that the system moves as a rigid structure, unless the effective resistance and effective mass are available from previous experimental data. Since  $z_e Z_m = C^2$  we have from (22) and (23)

$$L_m = -\frac{C^2 m_e}{z_e^2}, \quad (24)$$

$$R_m = \frac{C^2 r_e}{z_e^2}, \quad (25)$$

where  $z_e = \sqrt{r_e^2 + \omega^2 m_e^2}$ ; and as we assumed  $r_e$  and  $m_e$  to be known, the electrical motional impedance can be computed.

To determine  $r_e$  and  $m_e$  in certain cases, for example the horn type speaker of Fig. 82 A, it is essential to proceed as shown in Chapter XX. The analogous electrical circuit is drawn and then resolved into the form  $R'_e + i\omega L'_e$ , after which  $R'_e$  and  $L'_e$  are transformed to their mechanical analogues  $r_e$  and  $m_e$ . The latter are then used in formulae (24) and (25).

In all the preceding work for simplicity the various electrical quantities have been referred directly to the anode circuit of the power valve. There ought, however, to be no difficulty in applying the analysis to the secondary circuit of a step-down transformer. If  $n_1/n_2$  is the ratio of the turns, we have the new values for the anode circuit of the valve as  $\left(\frac{n_1}{n_2}\right)^2 R_m$ ,  $\left(\frac{n_1}{n_2}\right)^2 L_m$  and  $\left(\frac{n_2}{n_1}\right)^2 C_m$ .\*

#### 4. Transients †

A study of the equivalent diagrams provides interesting information [79 b]. We have already indicated the possibility of oscillation in the absence of constraint in Fig. 51 D, so we pass on to discuss Fig. 51 E. If we imagine a battery to be switched in circuit to replace the alternator, a voltage is applied to the circuit rising instantly from zero to  $E$ . We can assume this to last a very short time before being switched off. The impulse so obtained can be resolved into a spectrum of frequencies, infinite in number, from zero upwards. The low frequencies are impeded by  $C'_m$ , although part are by-passed by  $R'_m$ . The high frequencies are by-passed by  $C'_m$  but impeded by  $L_0$ . Thus there is a definite relative phase shift of the high and low frequency components of the impulse. The attenuation of the former by  $L_0$  reduces the rate of rise of the coil current, and the impulse is rounded, i.e. the steepness

\*  $R_m$ ,  $L_m$ ,  $C_m$  refer to secondary circuit.

† Definition 44.

of the wave front is curbed. From a physical viewpoint the charging current to  $C'_m$  is represented by acceleration of the mechanical system.\* The by-passing influence of  $R'_m$  represents the damping due to sound radiation and mechanical loss. As the velocity increases so also does the back e.m.f., due to the coil moving in the magnetic field. Thus the charging current taken by  $C'_m$  and, therefore, the coil current and velocity increase exponentially to their final values.

When the battery voltage  $E$  is suddenly removed and replaced by a short circuit, the electromagnetic energy  $\frac{1}{2}L_0 I^2$  and the electrostatic energy  $\frac{1}{2}C'_m V^2$  have both to be dissipated. The system is consequently not dead-beat and the tail of the transient is drawn out instead of being vertical. Interpreted physically the kinetic energy of the mechanical system is expended in keeping it in motion against the opposing influence of air resistance and electromagnetic damping. This is represented by discharge of  $C'_m$  through  $R'_m$  and the remainder of the circuit. The case where  $s \neq 0$  can be considered in like manner by aid of Fig. 51c. There is only one possible oscillation frequency, and this depends upon the various circuit coefficients. In general the  $L'_m C'_m$  combination predominates, and the frequency is given by  $\omega = \sqrt{(1/L'_m C'_m)} = \sqrt{(s/m)}$ , this being the value for the mechanical system. Unless the influence of radiation, frictional loss, and electromagnetic damping is large enough, damped oscillations will accompany each transient, as shown in Fig. 140. In a hornless speaker it is usual to rely upon electromagnetic damping at low frequencies. For this purpose the magnetic field should be strong, and the natural frequency on open circuit below audibility. In a horn moving-coil speaker the radiation resistance is large, so the natural oscillations are highly damped as shown in Fig. 144 B.

### 5. Measurement of inherent mechanical loss

In every vibrating structure there is a certain amount of loss in addition to that associated with the radiation of sound. Apart from air friction between the coil and magnet, also eddies and skin friction at the diaphragm, this can be found by auxiliary measurements *in vacuo* [41].

Let  $R_l$  = electrical motional resistance due to inherent loss in air,

$r_v$  = mechanical resistance due to inherent loss *in vacuo*.

\* This is not an electrical analogue where current is equivalent to velocity.

When the diaphragm vibrates in air, neglecting additional loss we have

$$r_v \doteq \frac{C^2 R_l}{Z_m^2}, \quad (26)$$

whilst *in vacuo*

$$r_v = \frac{C^2 R_v}{Z_v^2}. \quad (27)$$

From (26) and (27) we obtain

$$R_l = \left(\frac{Z_m}{Z_v}\right)^2 R_v. \quad (28)$$

It is important to realize that  $R_r$  is not  $(R_m - R_v)$  and that  $R_l \neq R_v$ . This is due to the fact that the power loss in air differs from that *in vacuo* owing to the increased axial velocity of the coil in the latter case, arising from reduction in mechanical impedance due to removal of the load. By virtue of the relationship between  $z_e$  and  $Z_m$  ( $z_e Z_m = C^2$ ), and since  $v \propto 1/z_e$  for a given force, it follows that  $Z_m/Z_v$  is the ratio of the velocity *in vacuo* to that in air. Whence the electrical motional resistance due to loss is  $R_v(Z_m/Z_v)^2$ .

From these measurements the accession to inertia can also be determined. Let  $L_m, L_v$  be the motional inductance in air and *in vacuo*, respectively, and  $m_{ea}, m_{ev}$  the effective mass in air and *in vacuo*, respectively.

Then from (23)

$$m_{ea} = -\frac{C^2 L_m}{Z_m^2} \quad (29)$$

and

$$m_{ev} = -\frac{C^2 L_v}{Z_v^2}. \quad (30)$$

The accession to inertia is, therefore,

$$m_i = m_{ea} - m_{ev} = C^2 \left( \frac{L_v}{Z_v^2} - \frac{L_m}{Z_m^2} \right), \quad (31)$$

or alternatively

$$m_i = \frac{C^2 L_m}{Z_m^2} \left( \frac{L_v}{L_m} \left( \frac{Z_m}{Z_v} \right)^2 - 1 \right). \quad (32)$$

In the above procedure it is tacitly assumed that the shape of the dynamic deformation curve of the diaphragm is identical in air and *in vacuo*. Where hornless speakers are concerned, the motional resistance and inductance at higher frequencies are each the difference of two relatively large and nearly equal quantities. An error of 1 per cent. in either entails a large error in the difference between them, so great care and judgement must be exercised in using this method and in interpreting the results. This is discussed in detail in Chap. XVI, § 3.

For horn speakers, where the resistive component is an appreciable proportion of the mechanical impedance, the method should be of real value. Owing to removal of the resistive component *in vacuo*, the testing current must be kept within bounds to prevent excessive diaphragm amplitude. The effective mass-frequency curves, which can be plotted from the above type of measurement, are of great utility in studying the vibrational characteristics of the system, provided the mechanical loss is insufficient to mask the influence of elasticity and inertia.

## 6. Influence of magnetic field strength

This can be examined by aid of the formulae deduced in the previous sections. The square of the flux density in the gap,  $B_g^2$ , appears in the electromechanical conversion factor  $C^2$  (see definition 43). From (10) and (11) we see that the motional resistance increases directly as  $C^2$  and therefore as  $B_g^2$ . Thus when the coil current is constant at all frequencies the power increases as  $B_g^2$ .

In hornless speakers the current at low frequencies is reduced by increase in  $B_g$ , since from (14) and (20) the motional capacitance varies inversely as  $B_g^2$ . This is not usually serious in practice, since it helps to offset the resonance due to the surround and centring device. If a high resistance valve is used, the current is not materially influenced.

The magnetic field introduces damping owing to the back e.m.f. induced in the coil due to its motion. This is useful in hastening the decay of the motion or in rendering the natural oscillations of the system aperiodic, but to do so the field must be intense.

## 7. Output circuits

The circuit between the power valve and the speaker may take various forms, which are illustrated in Figs. 52 and 147, the equivalent diagrams being appended in each case. The choke-condenser output of Fig. 147 A is used with so-called high-resistance coils. When  $L$  and  $C$  are sufficiently large so that the frequency  $\frac{\omega}{2\pi} = \frac{1}{2\pi\sqrt{LC}}$  is below audibility, the equivalent circuit takes the form in 147 B. Otherwise the circuit is that of 147 D. Fig. 52 A illustrates a simple transformer circuit, the primary winding having  $n_1$  turns and the secondary  $n_2$ . Owing to leakage of the magnetic flux between the windings, an inductance must be added in series with the coil. To obtain the



equivalent resistance and inductance (the leakage inductance is  $L'_1$ ) in the anode circuit, the secondary values are multiplied by  $(n_1/n_2)^2$ . The equivalent capacity is found by dividing the secondary capacity

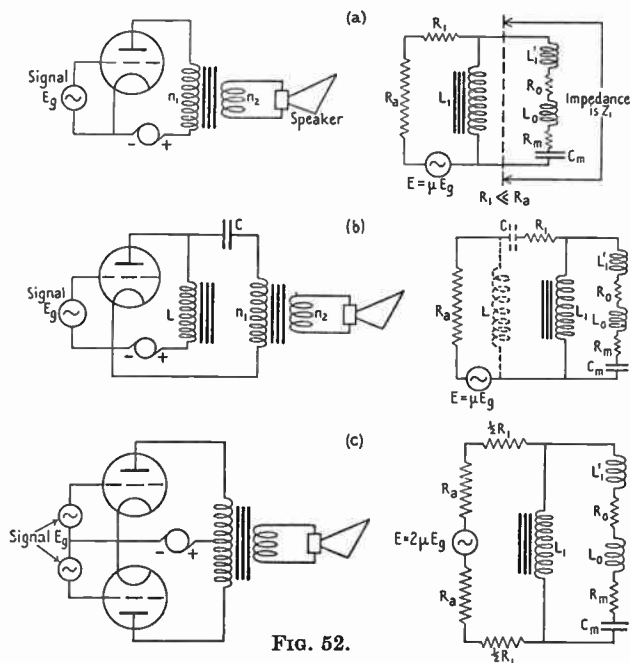


FIG. 52.

- (a) Transformer coupled speaker with equivalent circuit.  
 (b) Choke-condenser-transformer coupled speaker with equivalent circuit.  
 (c) Push-pull arrangement of transformer coupled speaker with equivalent circuit.

by  $(n_1/n_2)^2$ . In the equivalent circuit of Fig. 52 A,  $L_1$  represents the primary inductance of the transformer, and  $R_1$  its resistance. To prevent the anode feed current polarizing the transformer core, thereby lowering its inductance, the choke-condenser feed of Fig. 52 B, or the push-pull arrangement of Fig. 52 C can be used.

## VIII

### HORNLESS SPEAKER SIMULATED BY COIL-DRIVEN RIGID DISK

1. HAVING found the analytical relationships between the electrical and mechanical systems, if we know the mechanical impedance  $r_e + i\omega m_e$ , the power radiated by the vibrating system can then be calculated [77, 78, 79, 81]. To bring the problem within the scope of analysis we assume the diaphragm to be represented by a rigid circular disk vibrating in an equal aperture in an infinite rigid plane. The reaction on the disk consists of two components, (a) a load component in phase with the velocity, (b) an inertia component in quadrature with the velocity. The latter is due to the disk causing vibration of a mass of fluid in its neighbourhood. The kinetic energy of this fluid is  $T = \frac{1}{2}m_i v^2$ , where  $v$  is the axial velocity of the disk, and  $m_i$  the additional mass due to the fluid. The vector diagram for the *acoustical* portion of the system is shown in Fig. 14. The total force on the disk is the vector sum of the acoustic, or resistive, and inertia components, as shown in Chapter III.

Thus for *both* sides of the disk

$$f = 2\rho_0 cA \{G_1 + iG_2\} \dot{\xi}_0 \quad (1)$$

$$= (r_r + ix) \dot{\xi}_0 = (r_r + i\omega m_i) \dot{\xi}_0, \quad (1a)$$

where

$$G_1 = 1 - \frac{J_1(2ka)}{ka},$$

$$G_2 = \frac{H_1(2ka)}{ka},$$

$$r_r = \text{radiation resistance}^* = 2\rho_0 cA G_1,$$

$$m_i = \text{accession to inertia} = \frac{2\rho_0 cA}{\omega} G_2 = 2\pi\rho_0 a^3 \left[ \frac{H_1(2z)}{z^2} \right],$$

$$A = \pi a^2, \text{ where } a \text{ is the radius of the disk.}$$

Curves of the functions  $G_1, G_2$  are plotted in Fig. 17. Using the expansion of  $J_1(2ka)$  the function  $G_1$  can be written

$$G_1 = \frac{z^2}{1.2} - \frac{z^4}{1.2^2 \cdot 3} + \frac{z^6}{1.2^2 \cdot 3^2 \cdot 4} - \dots, \quad (2)$$

where  $ka = z$ .

\* Since there is no inherent mechanical loss  $r_r$  replaces  $r_e$ . The acoustic resistance per unit area varies with the radius (see Chap. III), so  $r_r/A = 2\rho_0 cG_1$  is a mean value.

At low frequencies when  $z$  is small, i.e.  $\leq 0.5$ ,

$$G_1 \doteq \frac{1}{2}z^2. \quad (3)$$

As  $z$  increases so also does  $G_1$ , due to decrease in the term  $J_1(2z)/z$ . When  $z = 1.9$ ,  $G_1 = 1$ , and as  $z$  increases  $G_1$  ultimately oscillates about this value, as shown in Fig. 17. Interpreted physically, when the frequency or the radius of the disk is large enough to violate the relationship  $G_1 = z^2/2$  appreciably, interference of the radiation from various parts of the disk occurs in space, i.e. there is a departure from spherical wave propagation. As the frequency or the radius is increased still more, focusing of the sound due to interference gradually becomes more pronounced until  $G_1 = 1$  ( $ka = 1.9$ ), after which the acoustic pressure on the disk oscillates about a constant value. Under this condition wave propagation at a great distance from the disk is sensibly plane. An important fact is that under this condition the *mean* resistance over the disk due to sound radiation is  $\rho_0 c$  per unit area. This being identical with the resistance of the medium per unit area, it follows that for values of  $ka \geq 1.9$  the medium is matched.\*

For a disk 10 cm. radius, focusing in air at normal temperature and pressure commences approximately at 250  $\sim$ , whereas for a 5 cm. disk the corresponding frequency is 500  $\sim$ . As shown in Fig. 55, the power radiated is not affected until a much higher frequency is reached. In water, where the velocity of sound is some four times greater than in air, these values would be increased to 1,000  $\sim$  and 2,000  $\sim$ , respectively.

By expanding  $H_1(2ka)$  we obtain

$$G_2 = \frac{H_1(2z)}{z} = \frac{4}{\pi} \left\{ \frac{(2z)}{1^2 \cdot 3} - \frac{(2z)^3}{1^2 \cdot 3^2 \cdot 5} + \frac{(2z)^5}{1^2 \cdot 3^2 \cdot 5^2 \cdot 7} - \dots \right\} \quad (4)$$

At low frequencies when  $z < 0.43$  the value of  $G_2$  for most purposes is given with adequate approximation by the first term of the series. Thus we can write

$$G_2 \doteq \frac{8z}{3\pi}. \quad (5)$$

The accession to inertia is  $m_i = 2\rho_0 c A G_2 / \omega$ , and it gradually decreases as  $z$  increases beyond the value 0.43. This is due to interference which entails a reduction in the mass of fluid in motion. For a disk 10 cm. radius,  $m_i \dagger = 7.0$  gm. at 50  $\sim$  but only 2.4 gm. at

\* See definition 20.

† When  $z \leq 0.43$ ,  $m_i = (16/3)\rho_0 a^3$ .

1,000  $\sim$ . For a disk 2 cm. radius,  $m_i$  is almost constant up to 1,000  $\sim$ . At frequencies where the sound radiation is highly focused and the angle of the principal sound beam is small, the wave propagation is nearly plane, so  $m_i$  is negligible compared with the mass of the disk.

## 2. Power radiated as sound

The power radiated as sound from both sides of the disk is

$$\begin{aligned} P &= v^2 r_r \quad (\text{see (45), Chap. I}) \\ &= \omega^2 \xi_0^2 [2\rho_0 c A G_1] \\ &= 2\rho_0 c A \omega^2 \xi_0^2 G_1. \end{aligned} \quad (6)$$

When  $ka \leq 0.5$ ,  $G_1 = k^2 a^2 / 2$ , so (6) becomes

$$P = \frac{\rho_0 \pi a^4 \omega^4 \xi_0^2}{c}. \quad (7)$$

This is a formula we shall use frequently in power problems. At high frequencies when  $ka \geq 1.9$ ,  $G_1 = 1$ , so (6) becomes

$$P = 2\rho_0 c A \omega^2 \xi_0^2. \quad (8)$$

We have now to find  $\xi_0$  in terms of the driving force  $f$ . Since  $r_r$  is usually small compared with the effective mass of the disk (which includes the mass of the driving coil and  $m_i$ ), the mechanical impedance is substantially

$$z_e = \omega m_e = \omega(m_d + m_c + m_i). \quad (9)$$

Now the driving force  $f = vz_e = \omega \xi_0 z_e$ , so

$$\xi_0 = \frac{f}{\omega^2 m_e}. \quad (10)$$

Substituting the value of  $\xi_0$  from (10) in (6) the power radiated is

$$P = \frac{2\rho_0 c A}{\omega^2} \left(\frac{f}{m_e}\right)^2 G_1. \quad (11)$$

When  $ka \leq 0.5$  (11) becomes

$$P = \frac{\rho_0 \pi a^4}{c} \left(\frac{f}{m_e}\right)^2, \quad (12)$$

and when  $ka \geq 1.9$

$$P = \frac{2\rho_0 c A}{\omega^2} \left(\frac{f}{m_1}\right)^2, \quad (13)$$

where  $m_1 = m_d + m_c$  since  $m_i \rightarrow 0$ .

From (12) it is evident that, so long as  $f$  is constant at low frequencies, the power radiated remains unaltered even at sub-audible

values. This is explained by the increase in amplitude, since the latter varies inversely as the square of the frequency.

At high frequencies, when  $ka \geq 1.9$ , the power decreases inversely as the square of the frequency, although the radiation resistance  $r_r$  is constant. This is due to the amplitude varying inversely as the frequency. Thus if the driving force, and therefore the coil current, were constant at all audible frequencies, the output from the lower would far exceed that from the upper register. It follows that a rigid disk 10 cm. radius would be useless as an agent for obtaining satisfactory sound reproduction from 40 to 10,000  $\sim$ . As we shall see later (Chap. XII, § 1), however, the reproduction is substantially perfect on the axis at a distance of 10 or more radii, provided the dimensions of the detecting device are small compared with the shortest sound wave to be reproduced. The above analysis gives some idea of the results to be obtained from a hornless system with 'inertia' control.

### 3. Numerical illustration of analytical expressions

The ultimate performance of the device under consideration depends, amongst other things, upon the current in the moving coil. To determine this, it is necessary to know  $m_e \cos \theta$ ,  $C_m$ , and  $R_r$ . These quantities

TABLE 11

*Radius of disk = 5 cm. Mass of disk = 2.5 gm. Mass of coil = 5 gm.*

<i>f.</i> <i>Frequency</i> <i>(cycles per</i> <i>second)</i>	<i>m<sub>e</sub>.</i> <i>Effective</i> <i>mass (gm.)</i>	<i>cos θ.</i> <i>Acoustic</i> <i>power</i> <i>factor</i>	<i>C<sub>m</sub>.</i> <i>Motional</i> <i>capacity</i> <i>(microfarad)</i>	<i>R<sub>r</sub>.</i> <i>Electrical</i> <i>radiation</i> <i>resistance</i> <i>(ohms)</i>
50	8.36	$2.8 \times 10^{-3}$	0.33	26
100	8.36	5.7	0.33	26
200	8.36	11.4	0.33	26
500	8.3	28.5	0.33	26
1,000	8.16	52	0.33	25
2,000	7.82	69	0.31	17.5
4,000	7.53	36	0.3	4.8
8,000	7.5	18	0.3	1.2

have been calculated for three disks of different sizes, namely, 5 cm., 10 cm., and 15 cm. radius, respectively. Moreover, the influence of the size of the disk can be seen. The results have been tabulated and are given in Tables 11, 12, and 13.

The variation in effective mass is more pronounced the greater the diameter of the disk. In each case the mass decreases with rise in frequency, as explained previously. The acoustic power factor, and therefore the total sound pressure on the disk, increases with the diameter. In each of the three cases the power factor attains a

TABLE 12

*Radius of disk = 10 cm. Mass of disk = 10 gm.*

<i>f.</i> Frequency (cycles per second)	<i>m<sub>e</sub>.</i> Effective mass (gm.)	cos $\theta$ . Acoustic power factor	<i>C<sub>m</sub>.</i> Motional capacity (microfarad)	<i>R<sub>r</sub>.</i> Electrical radiation resistance (ohms)
50	22	$1.8 \times 10^{-2}$	0.88	66
100	22	3.6	0.88	66
200	22	7.2	0.88	66
500	20.2	17	0.81	69
1,000	17.4	25	0.7	58
2,000	15.2	14	0.61	18
4,000	15	7	0.6	4.5
8,000	15	3.5	0.6	1.1

TABLE 13

*Radius of disk = 15 cm. Mass of disk = 22.5 gm.*

<i>f.</i> Frequency (cycles per second)	<i>m<sub>e</sub>.</i> Effective mass (gm.)	cos $\theta$ . Acoustic power factor	<i>C<sub>m</sub>.</i> Motional capacity (microfarad)	<i>R<sub>r</sub>.</i> Electrical radiation resistance (ohms)
50	50.7	$3.77 \times 10^{-2}$	2.0	59
100	50.7	7.2	2.0	57
200	49.5	14.5	2.0	58
500	40.4	32	1.66	59
1,000	29.3	35	1.14	46
2,000	27.5	17.1	1.1	12
4,000	27.5	8.7	1.1	1.3
8,000	27.5	4.4	1.1	0.3

maximum value. This is explained by a consideration of the velocity of the disk and the interference at various frequencies.

Assuming the axial driving force and the effective mass to be constant, the power is constant if  $ka \leq 0.5$ . The acoustic pressure is power/velocity; and since velocity  $\propto 1/\omega$ , the pressure increases with frequency, provided the wave propagation is spherical. But a point is reached when the propagation deviates from the spherical

type and gradually assumes that of plane waves. Moreover, as the frequency increases from 50 cycles upwards, a turning-point is reached, due to interference, where the total acoustic pressure on the disk decreases, whilst the mass reactance increases with rise in frequency. The motional capacitance, which exists by virtue of the back e.m.f. induced in the coil due to its motion in the magnetic field, increases with the mass (and radius) of the disk. This is explained by the reduced axial motion and therefore lower velocity of the larger disk, which generates a smaller back e.m.f. In each case the motional capacity decreases with rise in frequency, owing to the reduction in the accession to inertia of the disk.

So long as the wave propagation is spherical, the electrical radiation resistance  $R_r$  is substantially constant. When, however, interference commences,  $R_r$  decreases, until at 8,000  $\sim$  it is a small fraction of its value at 50  $\sim$ . From the tabular values it is seen that over the range 50 to 2,000 cycles the greatest output is obtained from a disk 10 cm. radius. Above 2,000 cycles the output is greatest from the smallest disk, viz., 5 cm. radius. If the mass of a disk driven by a constant axial force varies as the square of the radius, the radiation over a given band of frequencies increases with decrease in the size of the disk. At the higher frequencies this must be so, since the interference effect is less prominent with small disks than with large ones, whilst at low frequencies the accession to inertia is less. Now this is not in keeping with the results just quoted. The apparent paradox can readily be explained if we consider the effect of the coil. Its mass is a much greater proportion of the total mass with a small than with a large diaphragm. Hence the acoustic power factor and the output of the small diaphragm are reduced accordingly. Moreover, in the present system there is a certain radius of disk for which the acoustic output over a definite frequency band is a maximum.

#### 4. Current in the moving coil

The coil current at any frequency is controlled by the impedance of the coil in motion, together with  $R_a$ , the internal alternating current resistance of the valve. The latter has been allotted a value of 4,000 ohms.\* The impedance of the coil in motion depends upon four factors, namely: (1) the effective resistance at rest, (2) the electrical radiation resistance, (3) the effective inductance at rest, (4) the

\* This is decidedly high for a triode, but it serves to illustrate the analytical work.

motional capacity. Items (1) and (3) have been ascertained by bridge measurements (Table 36), whilst (2) and (4) have been calculated from the formulae developed herein.

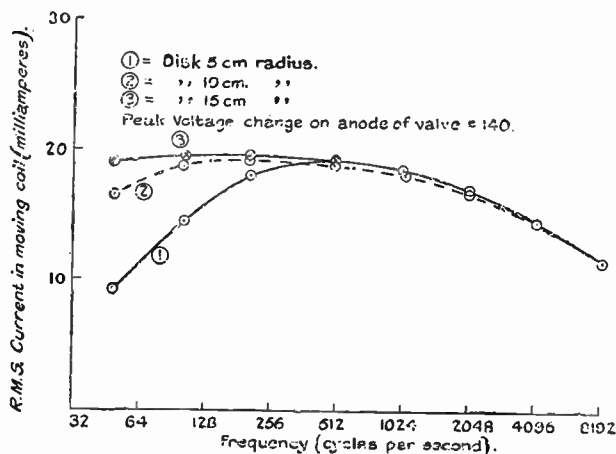


FIG. 53. Curves showing current in moving coil at various frequencies.

#### Details of Coil and Magnetic Field

Mean radius of coil . . . . .	$r = 2.5$ cm.
Number of turns . . . . .	$n = 10^3$ .
Mass of coil . . . . .	$= 5$ gm.
Mean strength of radial magnetic field . . . . .	$B_g = 10^4$ c.g.s. units.
	$C = \begin{cases} 2\pi r n B_g \\ 1.58 \times 10^8. \end{cases}$
Internal resistance of valve . . . . .	$R_a = 4 \times 10^3$ ohms.

Using the formula  $I = \frac{E}{\{(R_0 + R_r + R_a)^2 + (\omega L_0 - 1/\omega C_m)^2\}^{1/2}}$  and postulating a peak sine-wave voltage change of 140 volts on the anode of the valve, the coil current has been calculated for three disks at frequencies varying from 50 to 8,000 cycles per second. The results are shown graphically in Fig. 53. At low frequencies the larger the diaphragm the larger the current. This is due to the lesser amplitude and velocity of the larger disk by virtue of its greater inertia. Thus the back e.m.f. induced by the motion of the coil in the magnetic field decreases as the radius of the disk increases. At the higher



frequencies, although the induced e.m.f. is negligible, the coil current is curbed due to increase in the effective resistance (iron loss) and reactance of the coil. Moreover, the coil current at these frequencies is approximately the same for all three disks.

### 5. Reactance of moving coil

The reactance of the coil, namely  $\left(\omega L_0 - \frac{1}{\omega C_m}\right)$ , varies from a negative

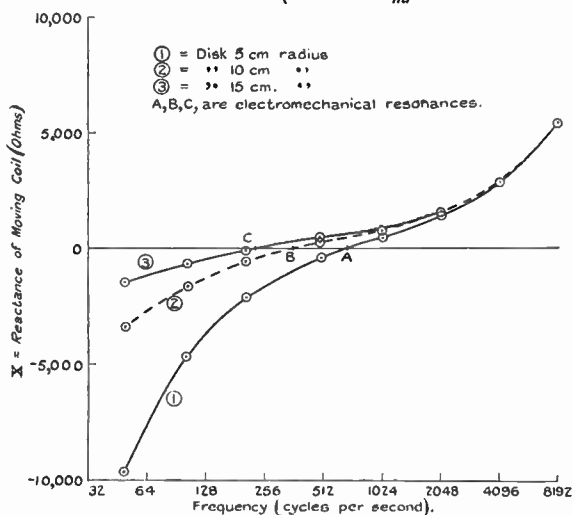


FIG. 53 A. Curves showing reactance of moving coil at various frequencies.

value through zero to a positive value, the latter being due to its inductance. The negative reactance at low frequencies exists by virtue of the large back e.m.f. induced in the moving coil. Since the smaller the disk the larger the amplitude, and therefore the axial velocity, the low-frequency reactance of the 5 cm. disk is greater than that of the other two. When the reactance is zero,  $\omega L_0 = 1/\omega C_m$ , and this occurs at the electromechanical resonance frequency. The greater the effective mass of the disk and coil the lower the electromechanical resonance frequency. These points are shown by the reactance curves of Fig. 53A. At frequencies above or below the resonance point, the current 'lags' or 'leads' on the impressed e.m.f.  $E = \mu E_0$  of Fig. 51 D. The further the frequency from resonance the greater the 'wattless' component of the current.

## 6. Axial pressure

It is shown in Chapter V that the axial pressure at distances exceeding a certain number of diameters from the disk is independent of the frequency, so long as the acceleration of the disk is constant and  $\omega/2\pi$  is not too high. This necessitates constant driving force and constant effective mass throughout the frequency range under consideration. In our particular case both of these factors are variable. The deviation

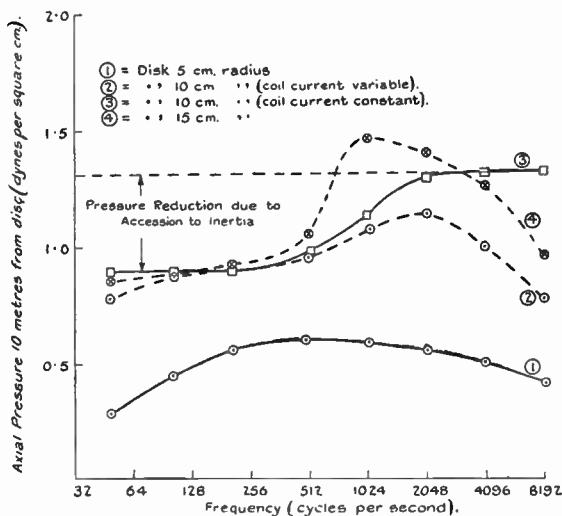


FIG. 54. Curves showing axial pressure 10 metres from disks at various frequencies.

from constant pressure is seen from the curves, Fig. 54. Curves 1, 2, and 4 indicate the pressure variation for the three disks when the current and effective mass vary with the frequency. The pressure caused by the 5 cm. disk is relatively small, due to the influence of the mass of the coil, as explained previously. At the lower frequencies, there is little difference between the pressures caused by the 10 cm. and 15 cm. disks, but the pressure is greater for the 15 cm. disk at the higher frequencies, although the total energy output is less due to increased mass reactance.

Curve 3 indicates the pressure variation for the 10 cm. disk when the driving force is constant. The smaller pressure at frequencies below 2,000 cycles is due to the greater effective mass caused by 'accession to inertia'. In each case the oscillations in the curves at the

higher frequencies due to oscillation in the function  $G_1$  have been disregarded.

### 7. Power radiated as sound

The power radiated as sound from the three disks is shown in Fig. 55. The vertical scale is a logarithmic one, since the sensitivity of the ear progresses in a logarithmic manner. The output

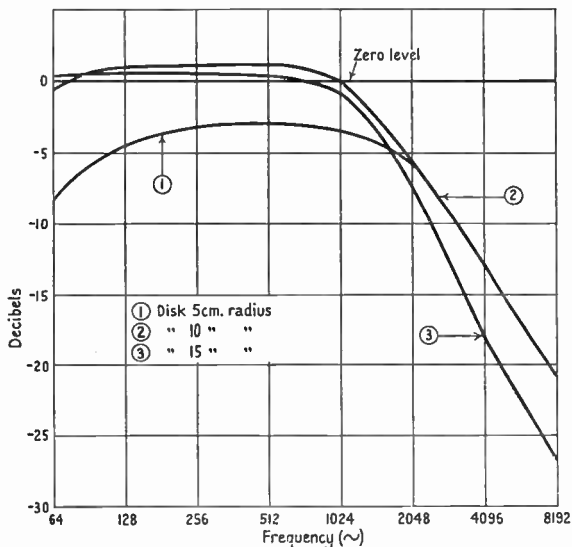


FIG. 55. Curves showing power level at various frequencies.

from the two larger disks is appreciably greater than that from the 5 cm. disk over the frequency range 50 to 1,000 cycles. Thereafter the output from the larger disks falls off rapidly, until at the higher frequencies it is very small for all three disks. This is due to the mass reactance  $\omega m_e$  which reduces the amplitude of vibration, thereby causing the axial velocity to decrease inversely as the frequency and the sound output inversely as the square of the frequency, when  $f$  is constant. Consequently the smaller the mass of the system, for a disk of given radius, the greater the upper frequency output. This can be seen from (13). In a massless system the power would increase with rise in frequency owing to a gradual reduction in  $m_i$ , and a corresponding increase in the radiation resistance. For a disk 10 cm. radius, it is seen from Table 12 that  $m_i$  is negligible above

2,000  $\sim$ , so the mechanical impedance at higher frequencies is substantially  $z_e = r_e = 2\rho_0 c A G_1$ . Apart from the oscillation in  $G_1$ , as shown in Fig. 17,  $r_e = 2\rho_0 c A$ , the medium is matched (definition 20), and the sound power  $f^2/2\rho_0 c A$  is then independent of frequency.

Owing to vibrational modes in the upper register, the effective mass of a conical diaphragm is quite small, so the massless condition is approached. Above a certain frequency, however, the output decays rapidly due to transmission loss and mass reactance of the coil.

## 8. Performance of reed-driven rigid disk

By aid of the analysis in Chapter VII the performance of a reed-driven rigid circular disk vibrating in an infinite flat baffle can be computed. It is assumed that the reed is elastically controlled and operates like a simple helical spring. The analysis is applicable to a cantilever reed so long as the frequency is well below the fundamental resonance of *the reed alone* [96 a].

Owing to the neutralization of inertia by the reed stiffness, the acoustic power factor, radiation resistance, power output, and axial pressure at the resonance frequency of the combination far exceed the values for a coil-driven rigid disk at any frequency. The bulk of the energy is concentrated over a comparatively narrow frequency band. It follows that a rigid disk driven by an elastic reed is useless for loud-speaker work. In practice, however, reed-driven speakers give tolerably good results over a limited frequency range. The reason is that the 'break-up' of the diaphragm acts in such a way that a fairly uniform output is obtained over a definite frequency range [96 a].

## 9. Optimum mass of moving coil

(a) *Hornless speaker.* It is natural to anticipate that under given conditions there is a certain coil mass for which the output is a maximum. When  $X_1$ , the total electrical reactance of the coil in motion, is small compared with  $R_a$  the valve resistance, the condition for maximum distortionless output is  $(R_0 + R_m) = \varphi R_a$ , where  $\varphi$  is a constant determined from the valve characteristics. For a triode it usually lies between 2 and 3. We have, therefore, to choose a coil which gives the maximum output when this condition is satisfied. The power radiated as sound is

$$P = R_r I^2 = R_r \frac{E^2}{Z^2} \quad (14)$$

From (19), Chap. VII,

$$R_m = \frac{r_e}{z_e^2} C^2 = \frac{r_e B_g^2 l^2}{z_e^2}, \quad (15)$$

and of this (which includes inherent mechanical loss) the portion due to sound radiation is

$$R_r = \frac{r_r B_g^2 l^2}{z_e^2}, \quad (15 a)$$

where  $z_e^2 = r_e^2 + \omega^2(m'_e + m_c)^2$ ;  $m'_e = m'_1 + m_i$  and  $m'_1$  is the effective mass of the diaphragm alone *in vacuo*. The electrical impedance when the coil vibrates is  $Z = \sqrt{\{(R_0 + R_m + R_a)^2 + X_1^2\}}$ . Since  $R_m \ll (R_0 + R_a)$  in a hornless speaker, and by hypothesis  $X_1$  can be disregarded, we have  $Z \doteq (R_0 + R_a)$ . Thus the optimum condition is  $R_0 \doteq \varphi R_a$  and we obtain

$$Z = (\varphi + 1)R_a. \quad (16)$$

Substituting the values of  $Z$  and  $R_r$  from (16) and (15 a) in (14) the power radiated is

$$\begin{aligned} P &= \frac{E^2 B_g^2 r_r l^2}{(\varphi + 1)^2 R_a^2 z_e^2} \\ &= \frac{K l^2}{r_e^2 + \omega^2(m'_e + m_c)^2}, \end{aligned} \quad (17)$$

where  $K = E^2 B_g^2 r_r / (\varphi + 1)^2 R_a^2$ .

But  $R_0 = \frac{\rho_1 l}{A}$ ,  $m_c = \rho_2 l A$ ; so

$$l^2 = \frac{R_0 m_c}{\rho_1 \rho_2}, \quad (18)$$

where  $\rho_1$  = specific resistance of wire of coil,

$\rho_2$  = density of wire of coil.

Since  $R_0 = \varphi R_a$  we have from (18)

$$l^2 = \frac{\varphi R_a m_c}{\rho_1 \rho_2}. \quad (19)$$

Substituting the value of  $l^2$  from (19) in (17) with  $K_1 = K l^2 / m_c$

$$P = \frac{K_1 m_c}{r_e^2 + \omega^2(m'_e + m_c)^2}, \quad (20)$$

where  $m'_e$  includes coil former, coil insulation, diaphragm and accession to inertia, i.e. everything but the wire on the coil.

The maximum value of  $P$  for varying coil mass is found by

differentiating (20) and equating to zero. Thus the required condition is

$$\omega m_c = \sqrt{(r_e^2 + \omega^2 m_e'^2)} = z_d$$

or

$$m_c = \frac{1}{\omega} \sqrt{(r_e^2 + \omega^2 m_e'^2)} = \frac{z_d}{\omega}, \quad (21)$$

which being interpreted means that the coil reactance is equal to the diaphragm impedance. It should be noticed that the analysis is valid whether the diaphragm moves as a rigid structure or not, provided there are no violent fluctuations in mechanical impedance which introduce appreciable electrical reactance. For ordinary hornless speakers the analysis is valid from about 120 ~ up to 2,000 ~ after which frequency the inductive reactance becomes important. If the latter is incorporated in the equations by substituting  $L_0 = k_1 m_c$  the analysis becomes unduly complicated and loses practical interest. Owing to variation in  $r_e$  and  $m_e'$  throughout the audible register, the optimum mass varies with frequency. Some data pertaining to this aspect of the problem are presented in Table 14.

TABLE 14

*Showing optimum coil mass at various frequencies*

Frequency. ~	Effective mass of diaphragm, coil-former, etc. $m_e'$ (gm.)	Mechanical resistance. $r_e$ (mech. ohms)	Optimum coil mass. $m_c$ (gm.)
150	22	negligible	22
1,800	-7	$9.8 \times 10^4$	11

At low frequencies, where the diaphragm moves as a whole, the optimum coil mass is equal to that of the diaphragm. As the frequency rises the impedance of the latter falls, so also does the optimum coil mass. For a rigid disk the optimum coil mass would be the natural mass of the disk plus  $m_i$  the accession to inertia. Beyond the frequency where  $ka = 0.43$  it would decrease with fall in  $m_i$ .

In any hornless speaker the coil mass must lie between definite limits for good tonal balance over the frequency range to be covered. A heavy coil reduces the amplitude at high frequencies and the upper register is curbed. On the other hand, a very light coil means that the optimum condition probably occurs in the neighbourhood of the cone resonances, which are then unduly enhanced. The result is

aurally distressing, being reminiscent of juvenile paper-and-comb orchestras.

(b) *Horn speaker.* In a hornless speaker the radiation resistance is a much smaller proportion of the static coil resistance than in a horn speaker. It was, therefore, neglected in (a) above, but will now be taken into consideration. Formula (17) stands unaltered but we have to find a new value for  $l^2$ . The optimum condition is that  $R_0 + R_m = \varphi R_a$ . Inserting the value of  $R_0$  from (18) and that of  $R_m$  from (15 a) we have

$$l^2 \left( \frac{r_r B_g^2}{z_e^2} + \frac{\rho_1 \rho_2}{m_c} \right) = \varphi R_a. \quad (22)$$

Substituting the value of  $l^2$  from (22) in (17) we get

$$P = \frac{K_2 m_c}{k_1 m_c + k_2 [r_e^2 + \omega^2 (m_e' + m_c)^2]}, \quad (23)$$

where  $k_1 = r_r B_g^2$  and  $k_2 = \rho_1 \rho_2$ . By differentiation the optimum condition is found to be

$$\omega m_c = \sqrt{(r_e^2 + \omega^2 m_e'^2)} \quad (24)$$

which is identical with the previous case.

There are several practical points worthy of mention in connexion with this analysis. No restriction has been placed on the number of turns, the radius, or the length of the coil. A tacit assumption is made that the iron loss increases or decreases proportionately to coil resistance, i.e. it is equivalent to the specific resistance  $\rho_1$ , being greater than its normal value, but constant. This, however, is not of much importance. In a horn speaker the effective mass of the system, apart from the coil, depends upon the surround and the throat-chamber stiffness. The effective resistance is also affected by the latter. To find  $r_e$  and  $m_e'$  the procedure is that outlined in Chapter XX.  $m_e' = m_e - m_c$ , where  $m_e$  is given by (5) in Chapter XX.

Since the mechanical impedance  $\sqrt{(r_e^2 + \omega^2 m_e'^2)}$ , apart from the coil, varies with frequency, the optimum coil mass varies also. If the optimum coil could be used throughout the frequency range, we should have  $m_c = \sqrt{\{(r_e/\omega)^2 + m_e'^2\}}$ . Data bearing on this topic are set forth in Table 15, these being computed from Chap. XX, § 2.

The coil mass increases rapidly with fall in frequency. The large negative effective mass  $m_e'$  at 100  $\sim$  is due mainly to the surround constraint. At zero frequency it is infinitely negative (see Chap. IV). Above about 1,000  $\sim$  the negative value of  $m_e'$  is associated with the

chamber stiffness (see Chap. XX or Chap. IV, § 8). For uniformity of output from 100  $\sim$  to 4,000  $\sim$  the actual coil mass is less than a gramme, i.e. about the optimum value at 2,000  $\sim$ . If the optimum were chosen as say 3.23 gm., as it would be at 500  $\sim$ , the upper register would be appreciably attenuated. Hence, as in the case of the hornless speaker, the coil mass must be chosen carefully for good tonal balance.

TABLE 15

*Showing optimum coil mass for horn speaker*

<i>Frequency.</i> $\sim$	<i>Mechanical resistance.</i> $r_e$ (mech. ohms)	<i>Effective mass of diaphragm alone.</i> $m'_e$ (gm.)	<i>Optimum coil mass.</i> (gm.)
100	$10^4$	-16.7	23.1
200	$10^4$	-3.8	8.8
500	$10^4$	-0.44	3.2
1,000	$10^4$	-0.12	1.6
2,000	$9.6 \times 10^3$	0	0.8

In Chap. XX, § 3, it is of interest to observe that the coil mass is chosen from the relationship  $m_c = 2r_e/\omega_c$ , where  $\omega_c/2\pi$  is the upper cut-off frequency. On the basis that the coil reactance is equal to the diaphragm impedance, we should have  $\omega m_c = r_e$  or  $m_c = r_e/\omega$ . Thus the coil mass would steadily increase with fall in frequency. The formula  $m_c = 2r_e/\omega_c$  gives a coil where the optimum condition occurs at  $\omega_c/\pi$ , but this is outside the range covered.



# IX

## ELECTROSTATIC SPEAKERS

### 1. General principles

The essential components of a simple electrostatic speaker are shown diagrammatically in Fig. 56 A. One plate  $P_1$  is fixed, the other plate

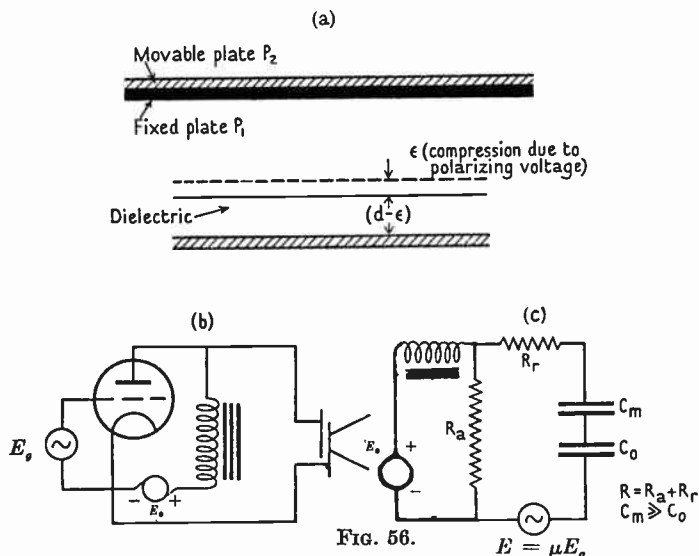


FIG. 56.

- (a) Schematic arrangement of electrostatic speaker.  
 (b) Valve circuit diagram of electrostatic speaker, the grid voltage being  $E_g$ .  
 (c) Equivalent diagram of electrostatic speaker. The impressed voltage is  $E = \mu E_g$ .  $C_m$  is the motional capacity and  $C_0$  the static capacity when the dielectric thickness is  $(d - \epsilon)$ . In §§ 3, 5, speaker signal voltage  $\doteq E/\sqrt{1 + \omega^2 C_0^2 R^2}$ .

$P_2$  being movable and therefore responsible for sound radiation. If a steady D.C. voltage was applied between the plates, the attractive force would cause  $P_2$  to approach  $P_1$  and ultimately stay there unless prevented from doing so. This action follows from the law of inverse squares, namely  $f \propto E/d^2$ . It is imperative, therefore, to introduce some form of elastic constraint between  $P_1$  and  $P_2$ . For analytical purposes it is immaterial how this is effected, so long as the force-displacement law is known. To make the analysis tractable we must perforce deal with *linear* differential equations. Thus the force-displacement law should be linear. Accordingly we postulate a thin

dielectric substance in which the law of compression is  $f = sx$ , where  $x$  is the displacement in the direction of  $f$ .

If an alternating voltage be applied across  $P_1P_2$ , then since the attraction is independent of polarity, the diaphragm moves towards the plate during each half cycle. The relationships are indicated in Fig. 57 A, where curve 2 corresponds to the acoustic output. It can

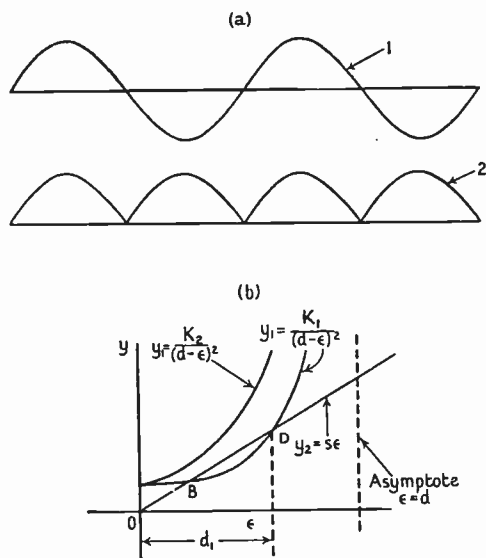


FIG. 57.

- (a) Diagram illustrating electromechanical rectification in electrostatic speaker, when used without a polarizing voltage.  
 (b) Illustrating condition for stability in electrostatic speaker.

be resolved by Fourier's theorem into an infinite series of frequencies. The sine wave input is, therefore, reproduced with an infinite retinue of harmonics, and electromechanical rectification ensues. If a polarizing voltage, large in comparison with the signal voltage, is superposed thereon, the action of the device undergoes a remarkable transformation. The steady voltage causes the dielectric to be compressed by an amount  $\epsilon$ . The signal voltage causes a fractional variation in the compression according to an harmonic law. When the signal voltage is additive, the dielectric is compressed  $\epsilon + \Delta\epsilon$ , whilst at the middle of the next half cycle it is compressed  $\epsilon - \Delta\epsilon$ . The force varies

as  $1/d^2$ , but if  $\Delta\epsilon$  is a small fraction of the dielectric thickness, the variation with distance can be disregarded and the action is linear. Thus, if the dielectric is massless, the device reduces mechanically to an harmonically driven mass on a simple coil spring. The diaphragm is the mass, the dielectric provides the spring effect, whilst the alternating electric force does the driving. Under such conditions the acoustic output will be a replica of the voltage input, provided the amplitude of vibration is minute.

The effect of the polarizing voltage is twofold, (1) it minimizes rectification, (2) it enhances the sensitivity enormously. The latter effect is readily shown by analysis as follows:

$$\text{The force per unit area } f \propto (E_0 + E)^2 \quad (1)$$

where  $E_0 =$  polarizing voltage

and  $E =$  signal voltage on speaker.

$$\text{Expanding (1)} \quad f \propto E_0^2 + 2E_0 E + E^2. \quad (2)$$

In the absence of  $E_0$  the force due to the signal  $\propto E^2$ . With polarization

$$\text{the force due to the signal } \propto 2E_0 E, \quad (3)$$

where  $E^2$  is neglected, since  $E$  is assumed small in comparison with  $E_0$ . Thus the polarizing voltage increases the driving force in the ratio  $2E_0 E/E^2 = 2E_0/E$ , so the power is augmented  $(4E_0^2/E^2)$ fold. If  $E = E_0/10$  the output is increased 400 times. A like effect obtains in telephone receivers with magnetic reeds or diaphragms, due to polarization by the permanent magnet. The fact that a telephone characteristic is non-linear accounts for sound reproduction from radio broadcasting when 'phones are used direct in the aerial circuit.

We can now examine the problem in greater detail [23]. Suppose the signal voltage consists of two sine waves of different frequencies, so that  $E = E_1 \cos \omega_1 t + E_2 \cos \omega_2 t$ . The total voltage impressed on the speaker is  $E_0 + E_1 \cos \omega_1 t + E_2 \cos \omega_2 t$ , and the force

$$f \propto [E_0 + E_1 \cos \omega_1 t + E_2 \cos \omega_2 t]^2. \quad (4)$$

Expanding (4) and using the identities  $\cos^2 \theta = (1 + \cos 2\theta)/2$ ;  $2 \cos \theta \cos \phi = \cos(\theta + \phi) + \cos(\theta - \phi)$ , we obtain

$$\begin{aligned} f \propto & E_0^2 + \frac{1}{2} E_1^2 + \frac{1}{2} E_2^2 + && \text{steady inaudible} \\ & + 2E_0(E_1 \cos \omega_1 t + E_2 \cos \omega_2 t) + && \text{signal} \\ & + \frac{1}{2}(E_1^2 \cos 2\omega_1 t + E_2^2 \cos 2\omega_2 t) + && \text{double frequencies} \\ & + E_1 E_2 [\cos(\omega_1 + \omega_2)t + \cos(\omega_1 - \omega_2)t] && \text{sum and difference} \\ & && \text{frequencies.} \quad (5) \end{aligned}$$

The output contains four alien frequencies whose individual powers depend upon the square of the ratio of signal to polarizing voltage. Let  $E_1 = E_2 = E_0/4$ , then the power ratio of each double frequency to the signal is  $(E_1/4E_0)^2 = \frac{1}{256}$ , and for the sum and difference frequencies it is  $\frac{1}{64}$ . Expressed in decibels the signal is 24 db. above each double frequency and 18 db. above each difference frequency. On the whole, therefore, we see that the law of attraction  $f \propto (\text{voltage/distance})^2$  inhibits large amplitude and sensitivity. In practice, to avoid creation of alien frequencies of appreciable magnitude, it is imperative to operate over a limited portion of the characteristic where the arc of the curve is substantially linear.

The compression of the dielectric due to the polarizing voltage  $E_0$  is  $\epsilon$ . If the unstrained thickness is  $d$ , the distance between the plates is  $d - \epsilon$  (Fig. 56 A). The total attractive force is

$$f_0 = \frac{\kappa A E_0^2}{8\pi(d - \epsilon)^2} = \frac{\kappa A}{8\pi} C_1^2, \quad (6)$$

where

$$C_1 = E_0 b$$

and

$$b = 1/(d - \epsilon).$$

The capacity of the condenser is

$$C_0 = \frac{\kappa A b}{4\pi}, \quad (7)$$

so (6) can be written

$$f_0 = \frac{2\pi E_0^2 C_0^2}{\kappa A} = \frac{2\pi Q_0^2}{\kappa A}, \quad (8)$$

where  $Q_0 = E_0 C_0$  the total charge on the plates. During operation the charge varies, so

$$f_i = \frac{2\pi Q_i^2}{\kappa A}, \quad (9)$$

where  $Q_i = (Q_0 + Q)$ , and  $Q =$  charge due to signal voltage.

Using (6) and replacing  $E_0$  by  $E_0 + E$ , when  $E_0^2 \gg E^2$  and  $d_1^2 \gg \xi^2$  ( $d_1 = d - \epsilon$ ), it can be shown that the driving force  $f \propto \frac{E_0^2}{d_1^2} \left( \frac{E}{E_0} + \frac{\xi}{d_1} \right)$  approximately. To avoid distortion  $f$  must be proportional to  $E$  the signal voltage, so  $E/E_0 \gg \xi/d_1$ . If the largest permissible value of  $E/E_0$  is  $\frac{1}{4}$ , that of  $\xi/d_1$  probably lies between  $\frac{1}{12}$  and  $\frac{1}{20}$ . This reveals a serious amplitude ( $\xi$ ) limitation in a system operating according to the law  $f \propto E^2/d_1^2$ . A large vibrating area is required therefore to obtain appreciable low-frequency sound output.

## 2. Limitation of voltage

When a constant unidirectional voltage  $E_0$  is applied to the plates, the condition of equilibrium is, force due to  $E_0 =$  constraint due to dielectric, or

$$\frac{\kappa A E_0^2}{8\pi(d-\epsilon)^2} = s\epsilon. \quad (10)$$

To investigate the condition of stability it is convenient to plot  $y_1 = \frac{\kappa A E_0^2}{8\pi} \frac{1}{(d-\epsilon)^2}$  and  $y_2 = s\epsilon$  as shown in Fig. 57 B. Curve 1 is wholly above the straight line  $y_2 = s\epsilon$ , so (10) is not satisfied and the system is unstable. Curve 2 cuts the line in two points  $B$  and  $D$ , the former representing the desired condition of stability. The point  $D$  would be reached if sufficient external force were applied to the movable plate to reach  $d_1$ . If the voltage were now increased slightly, instability would ensue. Obviously  $d_1$  represents the ultimate amplitude limit due to the signal. From the above it follows that the condition for stability is that the rate of change of force with distance must be less than the coefficient of stiffness, i.e.  $\partial y_2/\partial \epsilon > \partial y_1/\partial \epsilon$  or  $s > \kappa A E_0^2 / \{4\pi(d-\epsilon)^3\}$ . This argument is applicable where the relationship between elastic force and distance holds, for values of  $(d-\epsilon)$ , right down to zero when the plates touch. With a thin sheet-rubber dielectric a point is reached after which compression substantially ceases and instability is prevented. Since the force-displacement relationship is then non-linear, the output contains alien frequencies.

## 3. Equations of motion

Considering the forces acting on the diaphragm we have

reactive + resistive + constraint = driving force,

or, symbolically,

$$m_e D^2 \xi + r_e D \xi + s(\xi + \epsilon) = \frac{2\pi}{\kappa A} (Q_0 + Q)^2. \quad (11)$$

Equation (11) is not linear in  $Q$ , since it contains a term in  $Q^2$ . Consequently its solution involves a Fourier expansion. Now

$$(Q_0 + Q)^2 = Q_0^2 + 2Q_0 Q + Q^2$$

and when  $Q \ll Q_0$  the last term can be dropped, and the equation becomes

$$m_e D^2 \xi + r_e D \xi + s(\xi + \epsilon) = \frac{2\pi}{\kappa A} (Q_0^2 + 2Q_0 Q). \quad (12)$$

From (8) and (10) the steady force due to  $E_0$  is  $s\epsilon = (2\pi/\kappa A)Q_0^2$ , so (12) becomes

$$m_e D^2\xi + r_e D\xi + s\xi = C_1 Q, \quad (13)$$

where  $C_1 = 4\pi Q_0/\kappa A = E_0 b$ , from (6) and (8).\* It is important to notice that  $C_1$  is the alternating force per unit quantity of electricity. This compares with  $C$ , the force per unit current in Chapter VII. Since  $Q = I/D = I/i\omega$ , it follows that the equivalence of electromagnetic and electrostatic systems under steady conditions is expressed by the formula  $C_1^2/\omega^2 \equiv C^2$ .

Considering the circual e.m.f.s, we have

motional + reactive + resistive = driving.

$$\text{Thus} \quad \frac{Q_t}{C} + RDQ_t = E_0 + E, \quad (14)$$

$$\text{or} \quad \left(\frac{Q_0}{C} - E_0\right) + \frac{Q}{C} + RDQ = E, \dagger \quad (14a)$$

$$\text{where} \quad C = C_0 \left(1 + \frac{\xi}{(d-\epsilon)}\right) = C_0(1 + b\xi), \quad (15)$$

$$Q_t = Q_0 + Q \doteq E_0 C_0 + EC_0/\sqrt{(1 + \omega^2 C_0^2 R^2)}, \quad (15a)$$

$E_0 - Q_0/C_0(1 + b\xi)$  is the e.m.f. due to capacity change arising from motion of the armature and  $Q/C_0(1 + b\xi)$  is the e.m.f. to send the current through the condenser, i.e. the reactive component. From (14a) and (15a)

$$RDQ + \frac{Q_0 + Q}{C_0(1 + b\xi)} = E_0 + E. \quad (16)$$

Since  $\xi$  occurs in the denominator of the second term in (16) the equation is unsuitable. If, however,  $\xi$  is small compared with  $1/b$ , i.e.  $b\xi \ll 1$ , (16) can be written

$$RDQ + \frac{(Q_0 + Q)}{C_0}(1 - b\xi) = \frac{Q_0}{C_0} + E$$

$$\text{or} \quad E = RDQ + \frac{Q}{C_0} - C_1 \xi, \quad (17)$$

where  $(Q_0/C_0)b\xi = C_1\xi$  is the back e.m.f. due to motion of the diaphragm which causes a variation in capacity. The term  $Qb\xi/C_0$  is neglected since  $Q$  is small compared with  $Q_0$ .

We have now to solve (13) and (17). From the former we obtain

$$\xi = \frac{C_1 Q}{m_e D^2 + r_e D + s}. \quad (18)$$

\*  $C_1 C$  = force per unit signal voltage on speaker. † Impressed voltage (Fig. 56c).

Substituting the value of  $\xi$  from (18) in (17), writing  $Q = I/D$  and  $D = i\omega$  for the steady state, we get

$$E = \left[ R - \frac{i}{\omega C_0} + \frac{C_1^2/\omega^2}{r_e + i(\omega m_e - s/\omega)} \right] I. \quad (19)$$

From (19) the electrical impedance of the complete circuit is

$$Z = \frac{E}{I} = R - \frac{i}{\omega C_0} + \frac{(C_1^2/\omega^2)[r_e - i(\omega m_e - s/\omega)]}{r_e^2 + (\omega m_e - s/\omega)^2} \quad (20)$$

or 
$$Z = (R + R_m) + i \left( \omega L_m - \frac{1}{\omega C_0} \right). \quad (21)$$

In this formula  $R$  and  $C_0$  are the total circuital resistance and capacity, respectively, in the absence of vibration. The motional electrical resistance

$$R_m = \left( \frac{C_1^2}{\omega^2} \right) \frac{r_e}{r_e^2 + (\omega m_e - s/\omega)^2} = \left( \frac{C_1^2}{\omega^2} \right) \frac{r_e}{z_e^2}, \quad (22)$$

and the motional electrical inductance

$$L_m = \left( \frac{C_1^2}{\omega^2} \right) \frac{(s/\omega^2) - m_e}{z_e^2}, \quad (23)$$

where the mechanical impedance  $z_e = \sqrt{\{r_e^2 + (\omega m_e - s/\omega)^2\}}$ . The above can also be expressed as a motional capacity, thus

$$C_m = -\frac{1}{\omega^2 L_m} = \left( \frac{\omega^2}{C_1^2} \right) \frac{m_e - (s/\omega^2)}{(1 - \cos^2 \theta)}, \quad (24)$$

where the mechanical power factor  $\cos \theta = r_e/z_e$ . The circuital current is

$$I = \frac{E}{Z} = \frac{E}{\{(R + R_m)^2 + (\omega L_m - 1/\omega C_0)^2\}^{1/2}}. \quad (25)$$

These formulae are identical with those given in Chapter VII for the moving-coil loud speaker excepting that  $(C_1^2/\omega^2)$  is written in place of  $C^2$ .

From (16), Chap. VII, the relationship between the electrical and mechanical systems in the present instance is obviously

$$z_e Z_m = \frac{C_1^2}{\omega^2}. \quad (26)$$

Thus

$$r_e = \left( \frac{C_1^2}{\omega^2} \right) \frac{R_m}{Z_m^2}, \quad (27)$$

and

$$m_e - s/\omega^2 = - \left( \frac{C_1^2}{\omega^2} \right) \frac{L_m}{Z_m^2}. \quad (28)$$

The preceding electrical quantities pertain to a *series* arrangement

of the circuit. For the parallel arrangement of Fig. 51 c we have from (19), Chap. VII, substituting  $C_1^2/\omega^2$  for  $C^2$

$$R'_m = \left(\frac{C_1^2}{\omega^2}\right) \frac{1}{r_e}, \quad L'_m = \left(\frac{C_1^2}{\omega^2}\right) \frac{1}{s}, \quad \text{and} \quad C'_m = \left(\frac{\omega^2}{C_1^2}\right) m_e, \quad (29)$$

for steady conditions.

#### 4. Magnitude of motional capacity

To obtain an approximate estimate of  $C_m$  take the following data:

Circular diaphragm in infinite baffle . . .  $a = 20$  cm.,  $A = 1,257$  cm.<sup>2</sup>

Thickness of rubber dielectric . . .  $d = 5 \times 10^{-2}$  cm.

Mass per unit area of diaphragm and dielectric . . . . . =  $5 \times 10^{-2}$  gm. cm.<sup>-2</sup>

Young's modulus of dielectric . . .  $q = 5 \times 10^9$  dynes cm.<sup>-2</sup>

Then since  $\frac{\text{stress}}{\text{strain}} = q = \frac{f}{\xi} \frac{l}{A}$ , the force per unit compression is

$$s = \frac{f}{\xi} = \frac{Aq}{d}, \quad (30)$$

where  $d$  replaces  $l$ .

From these data  $s = 1.26 \times 10^{14}$  dynes cm.<sup>-1</sup> for the whole area. Turning to (24), the formula for  $C_m$ , we have to find the effective mass of the diaphragm *per se*. This is a complex problem, since the amplitude at any point in the dielectric increases from the fixed plate to the armature. For the moment it will be taken as one-half the natural mass. This gives a value 31.4 gm. to which must be added the accession to inertia  $m_i$ . Below 125  $\sim$  it is  $\frac{3}{8}\rho a^3$  for one side, this being 28 gm. The total mass is therefore 31.4 + 28 = 59.4 gm. At 100  $\sim$   $s/\omega^2$  is  $3.13 \times 10^8$ , so that  $m_e$  is completely swamped. This occurs throughout the audible register. It is easy to show that  $r_e^2$  is also insignificant, so that  $\cos^2\theta \ll 1$  and we can write

$$C_m = \frac{s}{C_1^2}. \quad (31)$$

Now  $C_1 = E_0 b$ , so with  $E_0 = 500$  volts and  $b = 1/(d - \epsilon) = 25$  we obtain

$$C_m = \frac{1.26 \times 10^{14}}{(1.25 \times 10^{12})^2} 10^{15} = 8 \times 10^4 \text{ microfarads,*}$$

which shows that the back e.m.f. due to motion of the armature can

\* Note conversion of volts to absolute electromagnetic units.



be neglected. This follows since  $C_m \gg C_0$  the latter being much less than a microfarad. Consequently the speaker can be treated as a rigid disk 20 cm. radius with axial constraint  $s$ . The driving force at any frequency depends upon the relative impedance of the power valve and speaker, also upon the type of output circuit.

### 5. Performance

From (22) since both  $r_e$  and  $\omega m_e \ll s/\omega$  the mechanical impedance  $\doteq s/\omega$ , and

$$R_r = C_1^2 \frac{r_e}{s^2}. \quad (32)$$

Referring to Fig. 56 c the power radiated is  $I^2 R_r$ , where

$$I = \frac{E}{Z} = \frac{E}{\sqrt{(R^2 + 1/\omega^2 C_0^2)}} = \frac{\omega C_0 E}{\sqrt{(1 + \omega^2 C_0^2 R_a^2)}}, \quad (33)$$

since both  $R_r$  and  $1/\omega C_m \ll R_a$

$$\text{Thus} \quad P = I^2 R_r = \frac{E^2 C_0^2 C_1^2 \omega^2 r_e}{s^2 (1 + \omega^2 C_0^2 R_a^2)}. \quad (34)$$

From (13) the driving force is  $f = C_1 Q = EC_0 C_1 / (1 + \omega^2 C_0^2 R_a^2)^{\frac{1}{2}}$ , so

$$P = f^2 \left( \frac{\omega}{s} \right)^2 r_e = \frac{f^2 r_e}{z_e^2}. \quad (35)$$

If  $\omega^2 C_0^2 R_a^2 \gg 1$ ,  $E = \text{const.}$ ,

$$P = \left( \frac{E^2 C_1^2}{R_a^2 s^2} \right) r_e. \quad (36)$$

Accordingly the output is constant provided  $r_e$  is independent of frequency. For a rigid disk 20 cm. radius in an infinite baffle,  $r_e$  rises gradually up to 500  $\sim$  after which it is substantially constant. Thus the power is invariable down to 500  $\sim$  after which it decays. Below 125  $\sim$  it varies inversely as the square of the frequency. If, however, the radius of the plate is increased to such a value that the wave propagation remains sensibly plane down to 100  $\sim$ , the output will be constant. To secure this condition the radius  $a \doteq 100$  cm., so the diaphragm will be about 7 feet diameter.

Reverting to our 20 cm. diaphragm, if we assume  $\omega^2 C_0^2 R_a^2 \gg 1$  at 500  $\sim$ ,  $R_a$  is of the order  $10^5$  ohms which suggests the use of a pentode. The radiation resistance  $R_r = r_e C_1^2 / s^2 \times 10^{-9} = 5 \times 10^{-9}$  ohms and so the output is totally inadequate to be of any practical value. As we shall see later this is due to the enormous magnitude of  $s$ , the stiffness,

which prevents an adequate amplitude being obtained. If  $R_a$  were a triode of 1,600 ohms resistance, then  $\omega^2 C_0^2 R_a^2 \ll 1$ , and above 500  $\sim$   $f$  is constant, so

$$\frac{P}{f^2} = \frac{\omega^2 r_e}{s^2}. \quad (37)$$

$P/f^2$  increases as the square of the frequency above 500  $\sim$  and decreases as the fourth power below 125  $\sim$ . Here again the output is too small for practical requirements. The power can be levelled up to some extent by aid of an auxiliary choke or an autotransformer as shown in

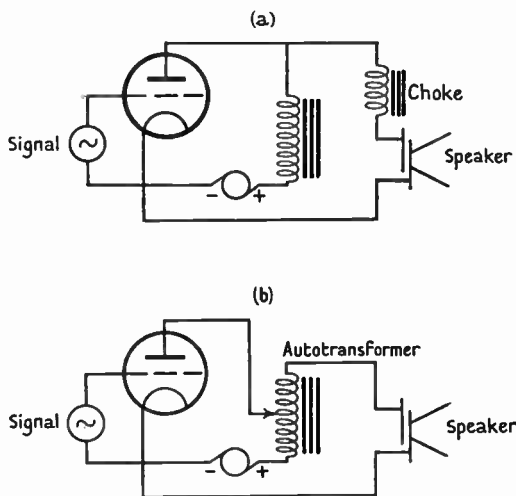


FIG. 58. Valve circuit diagrams of electrostatic speaker.

Fig. 58A, B. In both cases resonance is obtained at a certain frequency, and thereafter the inductance in circuit reduces the voltage on the speaker as the frequency rises (see § 11, Chap. XIII).

## 6. Effective mass of dielectric

As a point of interest, before passing on to the next section, we pause to consider the mechanical action of the dielectric by a more rigorous method than that adopted previously. Neglecting lateral expansion and contraction, the dielectric within its elastic limit can be likened to an extremely stumpy bar fixed at one end and acted upon at the free end by an harmonic force. This again can be simulated by a short electric cable with one end free, a driving e.m.f. being applied

to the other. The sending end impedance is

$$Z = Z_0 \coth Pl, \quad (38)$$

where  $Z_0$  = surge impedance of infinite cable

$$\doteq \sqrt{L/C};$$

$P$  = propagation coefficient =  $i\omega\sqrt{LC}$ , both of these values implying zero loss;

$L, C$  = inductance and capacity per unit length respectively

and  $l$  = length of cable.

$$\text{Thus } Z = \sqrt{\left(\frac{L}{C}\right)} \coth[i\omega l\sqrt{LC}] = -i\sqrt{\left(\frac{L}{C}\right)} \cot[\omega l\sqrt{LC}]. \quad (39)$$

Translating (39) into its mechanical analogue, we have

$$z_e = -i\sqrt{(m_n s)} \cot\left(\omega\sqrt{\frac{m_n}{s}}\right), \quad (40)$$

since  $L \equiv m_n/d$ ;  $C \equiv 1/sd$ ;  $d = l$ ;  $m_n$  = natural mass of whole dielectric;  $s$  = total stiffness.

At low frequencies  $\omega\sqrt{(m_n/s)} \ll 1$  and (40) can be written

$$z_e = -i\frac{\sqrt{(m_n s)}}{\omega\sqrt{(m_n/s)}} = -is/\omega. \quad (41)$$

In the absence of loss  $z_e = i\omega m'_e$  so the effective mass of the system at the driving surface is

$$m'_e = -\frac{s}{\omega^2}, \quad (42)$$

which is identical with the value we used above. Obviously the effective mass is negatively infinite at zero frequency. From (40) it is seen that  $z_e$  vanishes when  $\omega\sqrt{(m_n/s)} = \frac{1}{2}\pi(2n+1)$ , since resonance occurs due to the wave reflected from the fixed plate. For the case treated previously where

$$s = 1.26 \times 10^{14} \quad \text{and} \quad m_n \doteq 63 \text{ gm.}$$

the first vibrational mode ( $n = 0$ ) occurs at  $\omega = \frac{1}{2}\pi\sqrt{(s/m_n)}$ , namely,  $3.5 \times 10^5 \sim$  which is much too high to obtain a reasonable output from an electrostatic speaker. The rising characteristic is explained, therefore, by the fact that up to  $3.5 \times 10^5 \sim$  the system operates on the lower side of the resonance curve. Thus the arrangement is akin to working a short-wave radio circuit at medium wave-lengths—the signal strength is conspicuous by its absence.

From formula (40) it is seen that a family of effective mass curves similar to those of a vibrating reed are obtained (Chap. IV). The

essential difference is that in the present case (which holds equally for a short bar driven at its free end), the motion is longitudinal, whereas in the reed it is flexural.

The preceding analysis of effective mass is valid only in the ideal loss-free case *in vacuo*. In air it would be essential to introduce resistance and accession to inertia. This, however, would upset the simplicity of our present argument and will not be studied here.

### 7. Effect of reducing the stiffness ( $s$ )

We have already seen that working below the fundamental resonance frequency of the system entails a rising characteristic. Also that a very high resonance frequency means correspondingly low sensitivity. To reduce  $s$  and retain the present mechanical system, the dielectric thickness must be increased. Since this also lessens the sensitivity such procedure is impracticable. Instead of squeezing a laminar dielectric, suppose the mechanical construction to be such that a reasonable length is in *direct tension*. The stiffness will then be reduced enormously. An arrangement of this nature is described and illustrated in Chap. XIII, § 11. It is clear that the sagging portion in each channel or depression is a vibrator of the stretched membrane type investigated analytically in Chap. IV, § 15. The fundamental frequency can be much lower than that in the previous type of speaker. It can be varied by altering the size of the depressions or by increasing the tension. If the fundamental were 100  $\sim$ , then owing to close intervals between the modes of the membrane, a large number of modes would occur up to 5,000  $\sim$ . Assuming adequate damping, there is no apparent reason why the resonances should be distressing. There is a secondary source of stiffness and loss due to the presence of the hollows and perforations in the back plate. During vibration the air between the membrane and the plate is alternately compressed and rarefied. At low frequencies it escapes readily by the perforations thereby introducing a mechanical impedance which subdues the resonances. As the frequency rises the pneumatic stiffness of the air-pocket becomes of importance, since the air does not escape so easily. This will modify the behaviour of the system.

### 8. Circular membrane type [30 b, 31, 32]

This is shown diagrammatically in Fig. 59 and described in Chap. XIII, § 12, to which reference should be made. For analytical purposes the

diaphragm is equivalent to a membrane devoid of inherent stiffness. Assuming for simplicity that the distances between the membrane and either fixed electrode (grid) is constant at all radii, the forces per unit area on the two sides during operation are, respectively, proportional [26] to  $\left(\frac{E_0 + E/2}{d - \xi}\right)^2$  and  $\left(\frac{E_0 - E/2}{d + \xi}\right)^2$ , where  $E_0$  is the polarizing voltage and  $E$  the signal voltage across the grids. The

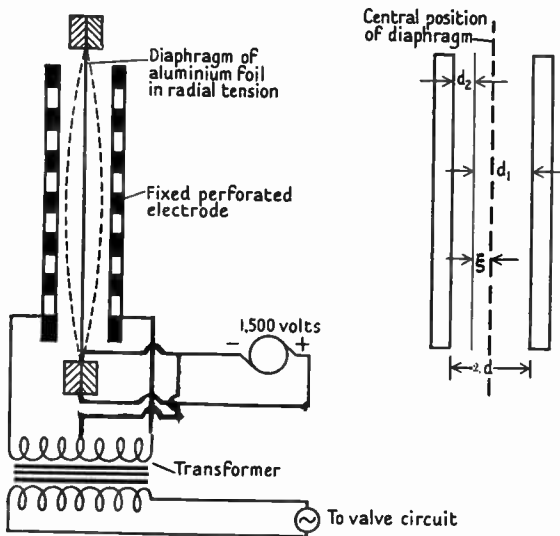


FIG. 59. Diagrammatic views of stretched membrane electrostatic speaker.

resultant force on the membrane varies as the difference between these quantities, so

$$f \propto \frac{4E_0^2}{(d^2 - \xi^2)^2} \left[ \xi d + (d^2 + \xi^2) \frac{E}{2E_0} \right], \quad (43)$$

the term in  $E^2$  being neglected since  $E_0 \gg E$ . Let  $h = \xi/d$  and (43) becomes [30 b]

$$f \propto \frac{4E_0^2}{d^2(1-h^2)^2} \left[ h + (1+h^2) \frac{E}{2E_0} \right]. \quad (44)$$

To obtain a linear relationship between  $f$  and  $E$ , the conditions are (a),  $E(1+h^2)/2E_0 \gg h$ , or approximately  $E/2E_0 \gg \xi/d$ , since  $h^2 \ll 1$ ; (b)  $1 \gg h^2$ , as implied in (a), so  $d \gg \xi$ . Condition (a) means that the signal voltage must be an appreciably greater proportion of the

polarizing voltage than the amplitude is of the distance between the membrane and either grid. If the maximum value of  $E/2E_0$  is taken as  $\frac{1}{3}$ ,  $\xi$  should not exceed  $d/20$  say. The ratio  $E/2E_0$  must itself be limited to avoid the introduction of serious alien frequencies due to mechanical rectification as shown in § 1. Using the above restrictions in (44) we obtain the linear relationship

$$f \propto \frac{2E_0 E}{d^2}. \quad (45)$$

The foregoing rests on the assumption that the membrane moves with equal amplitude throughout, the force being uniformly distributed over its surface. Practical conditions differ in several respects: (a) the membrane is curved during vibration; (b) the distance between it and the grids increases from the edge inwards to allow adequate clearance at the centre; (c) the driving force is not uniformly distributed over the surface, since the grids have slots or perforations through which the sound can escape. Since the apparatus is too complex for rigorous treatment, it will be replaced by a suitable model. Accordingly we take two uniformly spaced flat grids having circular perforations of small radius, the membrane being symmetrically situated between them. The perforations are to be ignored and the force per unit area assumed constant on both sides of the membrane. The sound radiation will be regarded as that from a diaphragm open at both sides operating in an infinite baffle in free air. Owing to focusing of the radiation the baffle is unnecessary above a frequency of  $500 \sim$  for a membrane of radius  $a = 20$  cm. The shape of the diaphragm during vibration depends upon the distribution of pressure over its surface and vice versa so that neither can be readily evaluated. As a first approximation the shape of the diaphragm *in vacuo* will be used at resonant frequencies, as shown in Chap. VI, § 3 where the power radiated from the membrane is determined.

### 9. Power at non-resonant frequencies

Although the shape might be taken as at (45) Chap. IV,  $f$  is not in phase with the velocity, since the mechanical impedance per unit area is now of the form  $z_e = r_e + i\omega m_e$ . Difficulty is encountered with the pressure distribution over the surface, so the problem will be treated in a simpler manner. The experimental work on disks and conical shells described in Chapter XVI indicates that above the first mode, variations in  $m_e$  are curbed considerably due to losses. With

a very light membrane there is no reason to doubt the validity of this statement. Accordingly above  $500 \sim (ka > 1.9)$  the membrane will be simulated by a rigid circular disk of equal mass and radius in an infinite flat baffle. The power radiated from both sides is

$$P = \xi_0^2 r_r = \left(\frac{fA}{z_e}\right)^2 r_r$$

or

$$\frac{P}{f^2} = \left(\frac{A}{z_e}\right)^2 r_r, \quad (46)$$

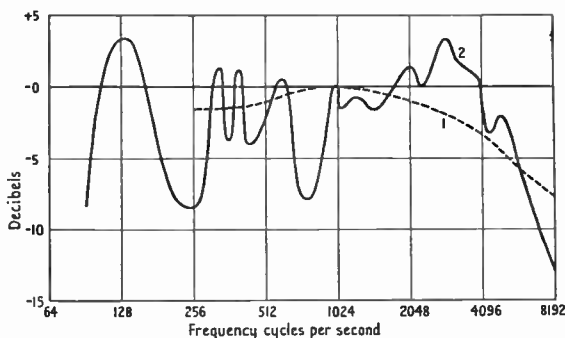


FIG. 60. Comparison of measured (curve 2) and calculated (curve 1) output curves of stretched membrane electrostatic speaker.

where  $z_e^2 = r_r^2 + \omega^2(5 + m_i)^2$ , 5 gm. being the diaphragm mass. Since  $ka > 1.9$ , the mechanical resistance  $r_r = 2\rho_0 cA$ , whilst

$$m_i = \frac{2\rho_0 cAG_2}{\omega},$$

as shown in Chapter III. Performing the requisite calculations for a diaphragm 20 cm. radius, the ratio  $P/f^2$  is plotted in Fig. 60, curve 1.\* Apart from the maximum at  $1,000 \sim$  it is fairly constant up to  $2,000 \sim$  after which it decays with rise in frequency. The lack of pronounced variation in  $P/f^2$  from  $500$  to  $2,000 \sim$  is due to  $r_r$  being large in comparison with the mass reactance. At higher frequencies the latter becomes of greater importance, so the amplitude, and therefore the output, is reduced. Curve 2 of Fig. 60, arranged to be at zero level with curve 1, at  $1,000 \sim$ , illustrates the output from an actual

\* If  $\frac{P}{f^2} = \frac{P}{(fA)^2}$  is used, the curve is the same shape;  $f$  and  $E$  assumed constant.

speaker. Naturally owing to vibrational modes it shows greater fluctuations than curve 1, but the general trend is of the same character. Above 3,000  $\sim$  curve 2 decays more rapidly than curve 1, since in the latter case no allowance was made for (a) mechanical loss which increases with frequency; (b) reduction in voltage across the speaker due to fall in reactance relative to the remainder of the output circuit, as shown in Fig. 85.

### 10. Comparison of power at resonant and non-resonant frequencies

When  $ka > 1.9$  the power ratio for constant driving force is that of formulae (13), Chap. VI, and (46) above. Thus

$$\varphi = \frac{z_e^2}{\rho_0 c A r_r} = \frac{2z_e^2}{r_r^2}, \quad (47)$$

since  $2\rho c A = r_r$ .

Substituting the value of  $z_e^2$  from the previous section in (47) we obtain

$$\varphi = 2 \left[ 1 + \frac{\omega^2}{r_r^2} (5 + m_i)^2 \right]. \quad (48)$$

From 500 to 1,000  $\sim$   $\varphi$  is nearly 2, and increases with rise in frequency, owing to the influence of mass reactance. At the gravest mode (130  $\sim$ )  $ka \doteq 0.5$  and  $P$  is 4.3 times its value when  $ka > 1.4$ . Thus  $\varphi$  is 8.6, but in practice the electrodes are specially shaped to cause large damping at the centre of the diaphragm, so the output at 130  $\sim$  is of the same order as that at higher modes, as shown in curve 2, Fig. 60. It is, of course, to be expected that the output at resonant frequencies exceeds that at intervening points.

### 11. Axial pressure

On the axis  $\phi = 0$ , so from (23 a) Chap. V the pressure in free air or in a 'dead' room is

$$p = \frac{\rho \omega \xi_0 a^2}{r} \left[ \frac{J_1(k_1 a)}{k_1 a} \right] \quad (49)$$

and has zeros corresponding to the roots of  $J_1(k_1 a)$ , i.e.  $k_1 a = 3.83, 7.01, 10.17$ , etc. the frequencies *in vacuo* being approximately 490, 900, 1,300  $\sim$ . In an ordinary room, apart from standing wave effects, the axial zeros would be obliterated by reflection. From Chap. VI,



§ 3 the axial velocity at a resonant frequency is

$$\dot{\xi}_0 = \frac{P}{2fA\Lambda}, \quad (50)$$

where  $\Lambda = \left[ \frac{J_1(k_1 a)}{k_1 a} \right]$ .

Substituting this value of  $\dot{\xi}_0$  in (49) the axial pressure is

$$p = \frac{\rho\omega P}{2\pi r f} \quad (51)$$

since  $A = \pi a^2$ .

The result in (51) shows that when  $P$  and  $f$  are invariable, the axial pressure at a definite distance increases directly with the frequency of the vibrational mode. Owing to losses, the diaphragm shape is modified and the axial pressure will not increase so rapidly as (51) indicates. Above a certain point it will decrease due to increase in frictional losses.

## 12. Influence of accession to inertia

As shown in Chapter IV, the diaphragm mass is so small that the fundamental mode is reduced from 310  $\sim$  (its value *in vacuo*) to 130  $\sim$  in air, due to accession to inertia which is about 1.5 times the mass of the diaphragm. The frequencies of the higher modes *in vacuo* can be determined from the roots of  $J_0(k_1 a)$ . From Chapter IV the first root  $k_1 a = 2.4$  corresponds to 310  $\sim$ , so the remainder found by simple proportion are 710, 1,110, 1,520, 1,930  $\sim$ , and so on at intervals of approximately 400  $\sim$ . Accordingly at higher frequencies there are several modes per octave.

## 13. Numerical example [30 b]

If  $E$  is the signal voltage applied to the outer grids, as shown in Fig. 59, the force on the diaphragm, neglecting perforations, is

$$f = \frac{EE_0 A}{4\pi d^2},$$

$d$  being the (uniform) distance between the membrane and either grid. Taking  $a = 20$  cm.,  $d = 1.2$  mm.,  $E = 300$  volts,  $E_0 = 1,500$  volts, the total force driving the membrane is  $2.25 \times 10^4$  dynes. In a good hornless moving-coil speaker the force for  $\frac{1}{2}$  this voltage variation on the power valve would be about nine times as great. For

the electrostatic speaker at 130  $\sim$  formula (13), Chap. VI, gives

$$P = \frac{4.3f^2}{\rho_0 cA} = 0.01 \text{ watt.}$$

Also from (50) the central amplitude is 0.11 mm. This amplitude at 130  $\sim$  corresponds to the use of an infinite baffle, but without grid damping of the membrane. In practice the power is about  $\frac{1}{4^3}$  of the above value and the corresponding amplitude is 0.05 mm. It is important to notice that if the separation  $d$  were reduced from 1.2 to 0.5 mm. the increased driving force would cause an amplitude of 0.3 mm. It might be thought that the criterion  $Ed/2E_0\xi \gg 1$  of § 8 is violated, thereby introducing alien frequencies in the output. It must be remembered, however, that in practice the membrane is curved, whereas the above criterion refers to equal amplitude throughout. For equal power in the latter case, the amplitudes corresponding to  $d = 1.2$  mm. and 0.5 mm. are, respectively, 0.024 mm. and 0.14 mm., so  $Ed/2E_0\xi = 5$  and 0.36. The first figure is satisfactory, but the second involves serious distortion. Owing to increase in driving force with decrease in  $d$ , the amplitude is increased. Thus  $Ed/2E_0\xi$  decreases, and there is a minimum permissible value of  $d$ , however small the signal voltage may be, if distortion is to be avoided. Hence the greater the sensitivity or force per unit signal voltage, the smaller the permissible amplitude and power output before serious distortion occurs. In practice the radiation, inherent losses and grid damping are adequate to make the nodal circles positions of minimum amplitude. Consequently the shape of the diaphragm alters progressively throughout a cycle, so the minimum  $d$  and maximum  $\xi$  are best found experimentally. Obviously owing to inequality of  $\xi$  over the membrane, the central value can exceed that found from the distortion criterion.

The above argument and numerical data reveal the limitation of the electrostatic speaker dependent upon the square law  $f \propto (E/d)^2$ . It is not generally realized that the restriction of signal voltage is of less importance than that of amplitude. For large power output the obvious escape from this dilemma is to augment the area in vibration by using a plurality of units.

According to (50) since  $P/f$  is constant for uniform output at vibrational modes

$$\xi_0 \propto \frac{1}{\omega} \left[ \frac{k_1 a}{J_1(k_1 a)} \right] = \frac{1}{\omega \Lambda}. \quad (52)$$

At the first mode  $k_1 a = 2.4$ ,  $\Lambda = 0.217$ , whilst at the fifth mode with four nodal circles  $k_1 a = 14.93$ ,  $\Lambda = 0.0138$ . Assuming  $m_i$  at the latter mode to be negligible, the frequency is  $1,930 \sim$  and  $\xi_0$  is 6 per cent. greater than its value at  $130 \sim$ , which is taken to be  $0.05 \text{ mm}$ . This is associated with enhanced spatial interference due to oppositely vibrating annuli on either side of a nodal circle, so the central amplitude must be adjusted accordingly to give compensation, thereby preserving constant output. If the membrane moved as a whole,  $\xi_0 \propto 1/\omega$  at higher frequencies where  $ka \geq 1.9$ .

# X

## THEORY OF HORNS

### 1. Fundamental equation

On the assumptions given below, the theory of sound propagation in a horn can be established. The consequences of the assumptions will

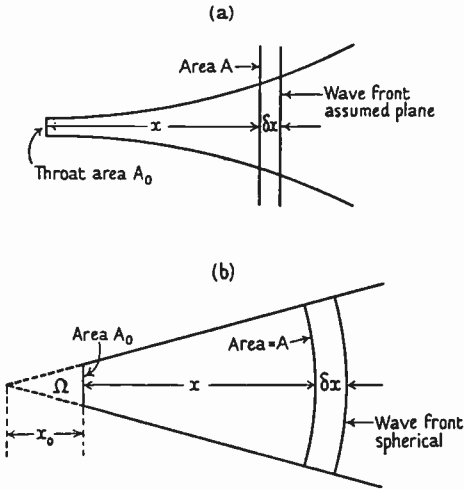


FIG. 61.

be discussed later. The analysis is admittedly approximate because rigorous methods have not been developed yet. In any case they would introduce real analytical difficulties. In the long run one might be compelled to present the solution as a series of special cases all requiring considerable arithmetical labour before a satisfactory result is obtained. Meanwhile a good deal of useful information for design purposes can be derived from an analysis, which, although approximate, has been of signal service in the design of modern loud-speaking apparatus.

Consider the arrangement shown in Fig. 61 A where  $\delta x$  is a short axial length included between two parallel planes normal thereto. The volume of this element is  $A\delta x$ , where  $A$ , the cross-sectional area, is given as an arbitrary function of  $x$ . Using the method of Chapter II for infinitesimal amplitudes, we see that the change in the mass of

fluid per unit time, in this constant volume, due to condensations and rarefactions concomitant with the passage of sound waves is

$$-\frac{\partial(\rho A)}{\partial t} \delta x,$$

$\delta x$  being invariable with time. The difference in the mass of fluid entering one plane and leaving the other in unit time is  $\rho \frac{\partial(uA)}{\partial x} \delta x$ , this being  $\rho$  times the change in 'velocity-area'.

By virtue of the continuity of the fluid these two quantities must be equal, so

$$\rho \frac{\partial(uA)}{\partial x} = -\frac{\partial(\rho A)}{\partial t}. \quad (1)$$

Expanding both sides of (1) we get

$$\rho \left( u \frac{\partial A}{\partial x} + A \frac{\partial u}{\partial x} \right) = - \left( \rho \frac{\partial A}{\partial t} + A \frac{\partial \rho}{\partial t} \right). \quad (2)$$

From (29), Chap. II,  $u = -\frac{\partial \phi}{\partial x}$ ; from (1) and (32)  $\frac{\partial \rho}{\partial t} = \rho_0 \frac{\partial s}{\partial t} = \frac{\rho_0}{c^2} \frac{\partial^2 \phi}{\partial t^2}$ ; and for infinitesimal amplitudes  $\rho = \rho_0$ , whilst  $\partial A / \partial t = 0$ , since the area at any value of  $x$  is independent of time. Using these substitutions in (2) we obtain

$$\frac{\partial^2 \phi}{\partial x^2} + \left[ \frac{1}{A} \frac{\partial A}{\partial x} \right] \frac{\partial \phi}{\partial x} - \frac{1}{c^2} \frac{\partial^2 \phi}{\partial t^2} = 0. \quad (3)$$

Since

$$\frac{\partial \log A}{\partial x} = \frac{1}{A} \frac{\partial A}{\partial x}$$

(3) can be written [67]

$$\frac{\partial^2 \phi}{\partial x^2} + \frac{\partial(\log A)}{\partial x} \frac{\partial \phi}{\partial x} - \frac{1}{c^2} \frac{\partial^2 \phi}{\partial t^2} = 0, \quad (4)$$

this being the fundamental horn equation for infinitesimal amplitudes.

If the motion is simple harmonic, we can write  $\phi = \phi_1 \cos \omega t$ , which gives  $\partial^2 \phi / \partial t^2 = -\omega^2 \phi$ . Substituting this value in (4) and remembering that  $k = \omega/c$ , we find that

$$\frac{d^2 \phi}{dx^2} + \frac{d(\log A)}{dx} \frac{d\phi}{dx} + k^2 \phi = 0, \quad (5)$$

which is the most convenient form of the horn equation. To determine the propagation of sound waves in any horn, we take the algebraic function  $A$  which represents its cross-section at various distances from the throat, differentiate its logarithm, insert the result in (5), and solve as a differential equation of the second order.

Before considering particular cases it is well to examine the hypotheses upon which (5) is based. These are as follows:

1. The shell of the horn is rigid and its inner surface smooth.
2. As in other problems herein the motion of the fluid is irrotational.
3. To avoid reflection and interference the axis of the horn is linear (no bends); also the length of the horn is infinite.
4. The fluid is inviscid and there is an absence of friction between it and the inner surface of the horn.
5. The pressure variations are infinitesimal.
6. The pressure is uniform over the wave front (assumed to be plane)\* as it travels along the expanding section of the horn.

The assumption of irrotational motion of the fluid particles has been taken for granted so often that it seems idle to specify it now. But those who have extinguished matches by draughts in the neighbourhood of horns or free-edge conical diaphragms, where the amplitude is large at low frequencies, will realize that appreciable rotatory motion can occur. Along the inner surface of a horn, where rapid change of curvature exists, there is a likelihood of eddies and rotatory motion. At the junction with the throat chamber careful design is required to reduce eddies. No experimental evidence exists regarding either eddies or the influence of viscosity and skin friction on the inner surface. It seems logical to argue that the smoother the surface, the smaller the curvature and its rate of change, the less will be the rotatory motion and frictional loss within the horn. At the mouth it is difficult to avoid vortices when the output is large.

The assumption of infinitesimal pressure amplitude is seriously violated in the neighbourhood of the *diaphragm* at the throat, where it may approach  $10^4$  dynes  $\dagger$  cm.<sup>-2</sup>. This condition obtains in public address systems for picture theatres or the like. It is treated in Chap. XI, § 9.

The equality of pressure over a plane wave front perpendicular to the axis is hardly in keeping with one's notions of physical processes. If the area  $A$  is that of the *curved* wave front, over which the sound pressure is assumed to be constant, this difficulty is surmounted. Since the plane and curved wave fronts are almost equal in area, it is unlikely that the assumption of a plane front introduces

\* See last paragraph in this section.

† Normal atmospheric pressure is approximately  $10^6$  dynes cm.<sup>-2</sup>

discrepancies of appreciable magnitude in the theory of infinite horns. In a conical horn the ratio of the plane and curved wave front areas is constant, so the analysis is valid in either case.

## 2. Conical horn

The cross-sectional area at any axial distance  $x$  from the throat is  $A = \Omega(x+x_0)^2$ , where  $x_0$  is the distance of the throat from the vertex (fictitious), and  $\Omega$  is the solid angle of the cone Fig. 61 B.

We have

$$\begin{aligned} \frac{d(\log A)}{dx} &= \frac{d}{dx} \{ \log \Omega + 2 \log(x+x_0) \} \\ &= \frac{2}{x+x_0}. \end{aligned}$$

Substituting this in (5) the horn equation to be solved is

$$\frac{d^2\phi}{dx^2} + \frac{2}{(x+x_0)} \frac{d\phi}{dx} + k^2\phi = 0, \quad (6)$$

which is identical in form with (60 a) of Chapter II, where the vibrations of a radially pulsating sphere were in question. This is to be expected, since we are now treating spherical propagation in a solid angle  $\Omega$  of infinite extent. The complete solution of (6) is

$$\phi = \frac{A_1 e^{-ik(x+x_0)}}{x+x_0} + \frac{B_1 e^{ik(x+x_0)}}{x+x_0}, \quad (7)$$

$A_1$  and  $B_1$  being arbitrary constants. The first term in (7) represents a divergent wave emanating from the throat of the horn (due to a vibrating diaphragm) and travelling in the positive direction of  $x$ . The second term represents a convergent wave travelling towards the throat in the negative direction of  $x$ . We shall confine our attention to the condition where the divergent wave alone exists, which implies that the constant  $B_1 = 0$ . The velocity potential at any cross-section distant  $x$  from the throat of the horn is, therefore,

$$\phi = A_1 \frac{e^{-ikr}}{r}, \quad (8)$$

where  $r = x+x_0$ .

From (29), Chap. II, the particle velocity is

$$\begin{aligned} v &= -\frac{\partial\phi}{\partial r} \\ &= A_1 \left( \frac{1}{r} + ik \right) \frac{e^{-ikr}}{r}, \end{aligned} \quad (9)$$

and from (31), Chap. II, the pressure

$$p = \rho_0 \frac{\partial \phi}{\partial t} = iA_1 \rho_0 \omega \frac{e^{-ikr}}{r}, \quad (10)$$

where the time factor  $e^{i\omega t}$  is introduced before differentiation and removed afterwards. The acoustical impedance at any point  $x$  along the horn is (see definition 23)

$$z_a = \frac{p}{Av} = \frac{i\rho_0 \omega}{A\{(1/r) + ik\}} = \frac{i\rho_0 c}{A} \left( \frac{kr}{1 + ikr} \right), \quad (11)$$

which on rationalization of the denominator yields

$$z_a = \frac{\rho_0 c}{A} \left( \frac{k^2 r^2 + ikr}{1 + k^2 r^2} \right). \quad (12)$$

Thus the acoustical resistance is

$$r_a = \frac{\rho_0 c}{A} \left( \frac{k^2 r^2}{1 + k^2 r^2} \right) \quad (13)$$

and the acoustical reactance is

$$x_a = \frac{\rho_0 c}{A} \left( \frac{kr}{1 + k^2 r^2} \right). \quad (14)$$

Formulae (13) and (14) are identical with the values obtainable from (114), Chap. II, for a radially pulsating sphere of radius  $r$ .

The phase angle between the total pressure and the particle velocity is evidently

$$\begin{aligned} \theta &= \tan^{-1} \frac{x_a}{r_a} \\ &= \tan^{-1} \frac{1}{kr}, \end{aligned} \quad (15)$$

which implies that  $p$  and  $v$  fall into phase with (a) increase in distance from the source, (b) increase in frequency, or with both of these. This agrees with our results in connexion with simple sources in Chapter II.

When the source is one side of a diaphragm of area  $A_0$  fitting closely to the small end of the horn, the accession to inertia is

$$m_i = \frac{\rho_0 A_0 x_0}{1 + k^2 x_0^2}, \text{ and the radiation resistance is } r_r = \frac{\rho_0 c A_0 k^2 x_0^2}{1 + k^2 x_0^2}. \text{ When}$$

$k^2 x_0^2 \gg 1$ ,  $m_i$  is negligible, whilst  $r_r = \rho_0 c A_0$ , which is identical with the value for plane waves or for a radially pulsating sphere under identical conditions, as we should expect. The radiation resistance per unit area is  $\rho_0 c$ , which is identical with that of the medium (see definition



20). The velocity of propagation in the horn is obviously identical with that of waves in free fluid, that is,  $c$ .

### 3. Exponential horn [58]

Here the area at a cross-section distant  $x$  from the throat is  $A = A_0 e^{\beta x}$ , where  $\beta$  governs the rate of expansion of internal area or flaring of the horn.  $d(\log A)/dx = \beta$ , so equation (5) becomes

$$\frac{d^2\phi}{dx^2} + \frac{\beta d\phi}{dx} + k^2\phi = 0. \quad (16)$$

This is a linear equation of the second order with constant coefficients and its solution depends upon the relative values of  $\beta$  and  $k^2$ . The normal case for our purpose is when  $k^2 > \frac{1}{4}\beta^2$ , and then

$$\phi = A_1 e^{\lambda_1 x} + B_1 e^{\lambda_2 x}, \quad (17)$$

where  $\lambda_1$  and  $\lambda_2$  are roots of the auxiliary equation

$$\lambda^2 + \beta\lambda + k^2 = 0.$$

$$\text{Thus } \left. \begin{matrix} \lambda_2 \\ \lambda_1 \end{matrix} \right\} = -\frac{1}{2}\beta \pm i\sqrt{(k^2 - \frac{1}{4}\beta^2)}. \quad (18)$$

Since we are concerned with the transmitted wave only, then, as in (7),  $B_1 = 0$ , and the solution we require is

$$\phi = A_1 e^{-(\frac{1}{2}\beta + i\alpha)x}, \quad (19)$$

where  $\alpha = \sqrt{(k^2 - \frac{1}{4}\beta^2)}$ .

Proceeding on the same lines as in § 2,

$$v = -\frac{\partial\phi}{\partial x} = A_1(\frac{1}{2}\beta + i\alpha)e^{-(\frac{1}{2}\beta + i\alpha)x} \quad (20)$$

$$p = \rho_0 \frac{\partial\phi}{\partial t} = iA_1 \rho_0 \omega e^{-(\frac{1}{2}\beta + i\alpha)x} \quad (21)$$

$$z_a = \frac{p}{Av} = \frac{i\rho_0 \omega}{A(\frac{1}{2}\beta + i\alpha)} = \frac{\rho_0 \omega (\alpha + i\frac{1}{2}\beta)}{A(\alpha^2 + \frac{1}{4}\beta^2)}.$$

Since  $\alpha^2 + \frac{1}{4}\beta^2 = k^2$ , the acoustical impedance is

$$z_a = \frac{\rho_0 c}{A} \left\{ \sqrt{\left(1 - \frac{\beta^2}{4k^2}\right)} + i \frac{\beta}{2k} \right\}, \quad (22)$$

and is inversely proportional to  $A$ . The acoustical resistance is

$$r_a = \frac{\rho_0 c}{A} \sqrt{\left(1 - \frac{\beta^2}{4k^2}\right)}, \quad (23)$$

and the acoustical reactance

$$x_a = \frac{\rho_0 c}{A} \frac{\beta}{2k}. \quad (24)$$

If the source is one side of a diaphragm of area  $A_0$  fitting closely at the throat of the horn, the mechanical resistance is

$$r_r = \rho_0 c A_0 \sqrt{\left(1 - \frac{\beta^2}{4k^2}\right)},$$

and the accession to inertia  $m_i = \rho_0 c A_0 (\beta/2k\omega)$ . The phase angle between pressure and particle velocity, namely,

$$\theta = \tan^{-1} \frac{\beta/2k}{\sqrt{\{1 - (\beta^2/4k^2)\}}},$$

is constant throughout the length of the horn, as also is the power factor  $\cos \theta = \sqrt{\{1 - (\beta^2/4k^2)\}}$ . This expression for  $\cos \theta$  follows from the fact that the vector triangle has sides 1,  $\beta/2k$ , and  $\sqrt{\{1 - (\beta^2/4k^2)\}}$ . Moreover, when  $k^2 \gg \frac{1}{4}\beta^2$ , as it will be at high frequencies,  $\cos \theta = 1$ . The impedance per unit area is then purely resistive and equal to that of the medium, namely,  $\rho_0 c$  (see definition 20). If  $k^2 = \frac{1}{4}\beta^2$ , the resistance is zero and the reactance per unit area becomes  $\rho_0 c$ . The power is then zero and the horn is said to 'cut-off'. The critical or cut-off frequency is given by the relationship  $\omega_c = \frac{1}{2}\beta c$ , so the frequency is  $\beta c/4\pi$ .

When  $k^2 < \frac{1}{4}\beta^2$  the solution to (16) is  $\phi = A_1 e^{-i(\beta + \alpha_1)x}$ , where  $\alpha_1 = \sqrt{(\frac{1}{4}\beta^2 - k^2)}$ . Then the acoustical impedance

$$z_a = \frac{p}{Av} = \frac{i\rho\omega}{A(\frac{1}{2}\beta + \alpha_1)} = \frac{i\rho_0 c}{A} \left\{ \frac{\beta}{2k} - \sqrt{\left(\frac{\beta^2}{4k^2} - 1\right)} \right\} \quad (25)$$

and is wholly reactive, since only the inertia component exists. In the limit, when  $\omega \rightarrow 0$ ,  $z_a$  is evanescent.

Introducing the time factor into (19), we have  $\phi = A_1 e^{-i(\beta + i\alpha)x + i\omega t}$ , the real part of which is

$$\begin{aligned} \phi &= A_1 e^{-i\beta x} \cos(\omega t - \alpha x) \\ &= A_1 e^{-i\beta x} \cos(\alpha x - \omega t). \end{aligned} \quad (26)$$

With a vibrating sphere or in a conical horn reduction in  $\phi$  with increase in  $x$ , due to expansion of the wave front, is determined by the factor  $1/x$ , whereas in the present case we have the exponential decay factor  $e^{-i\beta x}$ . Comparing (26) with (17) in Chapter II, we see that  $\alpha \equiv k$ , so the velocity of propagation along the horn is

$$c' = \frac{\omega}{\sqrt{(k^2 - \frac{1}{4}\beta^2)}} = \frac{c}{\sqrt{\{1 - (\beta^2/4k^2)\}}}. \quad (27)$$

As the cut-off frequency is approached,  $\beta^2/4k^2 \rightarrow 1$ , the velocity increases rapidly and ultimately [according to (27)] becomes infinite!

\* Phase velocity when  $\omega > \omega_c$ .

It is hardly necessary to comment upon this theoretical deduction. In partial extenuation it may be stated that, in finite horns, the phase velocity in the neighbourhood of the critical frequency (calculated from the combined influence of the transmitted and reflected waves) is found to be much greater than  $c$  (see § 8).

#### 4. Bessel horns [56]

When the expansion curve of the horn takes the form  $A = A_0(x+x_0)^m$

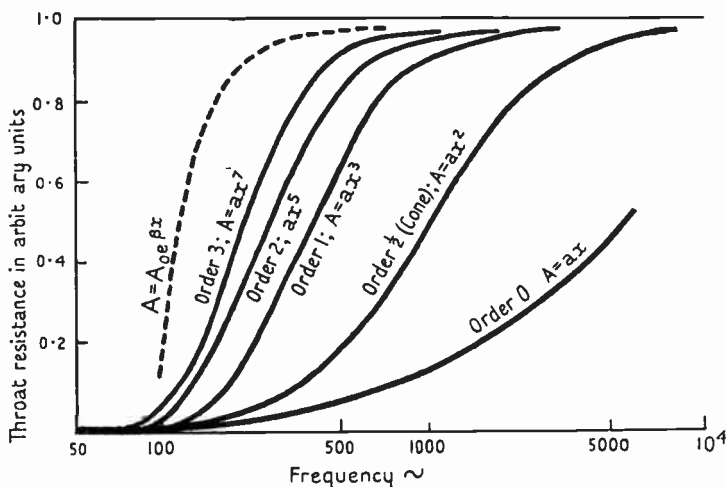


FIG. 62. Curves showing relationship between throat resistance and frequency for Bessel horns of various orders.  $x$  signifies  $x+x_0$ .

the solution of (5) involves Bessel functions. This type of horn is, therefore, associated with Bessel's name. The conical horn, where  $m = 2$ , is a particular case in which Bessel functions of fractional order can be represented by circular functions. This holds for all even values of  $m$ . The response at low frequencies increases with increase in the flaring index  $m$ , as shown in Fig. 62. The physical reason is that as  $m$  increases, the phase angle between the pressure and particle velocity at the throat gradually decreases, due to the expansion of the wave front taking place more slowly. For horns of the same length it can be shown that, when the respective throat and mouth areas are equal, an exponential horn is geometrically identical with a horn of the type  $A = A(x+x_0)^m$ , where  $m$  tends to infinity. Apart from frictional and viscous loss, the exponential

horn is better than any type of Bessel horn where  $m$  is finite [164 b, 177 b].

### 5. Power in horns of infinite length

(a) *Conical horn.* The particle velocity at any point distant  $r$  from the fictitious vertex is, by (9),

$$v = A_1 \left( \frac{1}{r} + ik \right) \frac{e^{-ikr}}{r}, \quad (28)$$

where  $r = x + x_0$ . At the throat  $x = 0$ ,  $r = x_0$ , and  $v = v_0$ . Substituting these values in (28) we find that

$$A_1 = v_0 x_0^2 \frac{1 - ikx_0}{1 + k^2 x_0^2} e^{ikx_0}. \quad (29)$$

Using this value of  $A_1$  in (10) and omitting the exponential factor, the pressure per unit area is

$$p = \rho_0 \omega v_0 x_0 \left( \frac{i + kx_0}{1 + k^2 x_0^2} \right). \quad (30)$$

The power at the throat area being the product of velocity and total in-phase force is

$$P = \frac{\rho_0 c A_0 v_0^2 k^2 x_0^2}{1 + k^2 x_0^2}. \quad (31)$$

Taking the strength of the source as  $A_0 v_0 = S_0$  (Chap. II, § 12) we have

$$P = \frac{\rho_0 c S_0^2}{A_0} \left( \frac{k^2 x_0^2}{1 + k^2 x_0^2} \right). \quad (32)$$

If  $\Omega$  is the solid angle of the horn, the cross-sectional area at a distance  $x_0$  from the fictitious vertex is  $\Omega x_0^2$  approximately. When  $\Omega$  is small the error is negligible. Thus (32) can be written

$$P = \frac{\rho_0 c S_0^2}{\Omega} \left( \frac{k^2}{1 + k^2 x_0^2} \right). \quad (33)$$

If  $\Omega = 2\pi$  and  $x_0 \rightarrow 0$  we have the case of an infinite baffle, and the power is then

$$P = \frac{\rho_0 \omega^2 S_0^2}{2\pi c} = \frac{\rho_0 \pi a^4 \omega^4 \xi_0^2}{2c}, \quad (34)$$

which is identical with formula (72 a) in Chapter II for the radiation from one side of a rigid disk of radius  $a$  when the sound distribution is spherical, i.e.  $ka \leq 0.5$ . Formula (31) can also be written

$$P = \rho_0 c A_0 \omega^2 \xi_0^2 \left( \frac{k^2 x_0^2}{1 + k^2 x_0^2} \right). \quad (35)$$

When  $x_0 \rightarrow \infty$ ,  $A_0 \rightarrow \infty$ , the vibrating surface becomes an infinite rigid plane and the power radiated from one side is

$$P = \rho_0 c A_0 \omega^2 \xi_0^2, \quad (36)$$

which is identical in form with (8) in Chapter VIII for plane wave propagation from a rigid disk.

From (33) it is clear that when the strength of the source  $S_0$  is fixed, e.g. a diaphragm of given radius executing a definite amplitude, the power increases as the diaphragm loading is augmented by reduction of the solid angle of the conical horn.

(b) *Exponential horn.* The particle velocity at the throat of the horn, where  $x = 0$ , is  $v = v_0$ . Inserting these values in (20), rationalizing and using  $\alpha^2 = (k^2 - \frac{1}{4}\beta^2)$ , we get

$$A_1 = \frac{v_0}{k^2} (\frac{1}{2}\beta - i\alpha). \quad (37)$$

Inserting this value of  $A_1$  in (21), the pressure per unit area is

$$p = \frac{\rho_0 c v_0}{k} (\alpha + i\frac{1}{2}\beta). \quad (38)$$

The power is

$$p v_0 A_0 = \rho_0 c A_0 v_0^2 \sqrt{\left(1 - \frac{\beta^2}{4k^2}\right)}, \quad (39)$$

the real part of (38) being used. Since  $S_0 = A_0 v_0$ , we obtain

$$P = \frac{\rho_0 c S_0^2}{A_0} \sqrt{\left(1 - \frac{\beta^2}{4k^2}\right)}. \quad (40)$$

For equal diaphragm amplitudes and throat areas at any given frequency (identical source strengths), the relative power from conical and exponential horns depends upon the quantities  $\left(\frac{k^2 x_0^2}{1 + k^2 x_0^2}\right)$  and  $\sqrt{\{1 - (\beta^2/4k^2)\}}$  [see (32) and (40)]. These are plotted in Fig. 63 (for a certain value of  $x_0$ ), from which the superiority of the exponential horn is immediately apparent. This can be explained by the fact that in the latter the particle velocity and pressure are in much closer phase relationship at low frequencies than in a conical horn. The slow exponential flaring near the throat is, therefore, of great advantage compared with the relatively rapid expansion of the conical type which permits, or rather invokes, considerable circulation of fluid near the source. This motion, being associated with an inertia or wattless component, curbs the diaphragm amplitude and prevents

matching of the horn impedance with that of the medium (see definition 20). In the above comparison, if the value of  $x_0$  in the conical horn is made sufficiently large, the diaphragm diameter being constant, the solid angle is reduced correspondingly. At low frequencies the factor  $k^2 x_0^2 / (1 + k^2 x_0^2)$  is sensibly unity and the two infinite horns (conical and exponential) are equally efficient above the cut-off frequency. In practice, however, this does not hold for horns of finite length. If the cut-off frequency is  $50 \sim$  the conical horn is some 30 times longer than the exponential horn, the initial and final

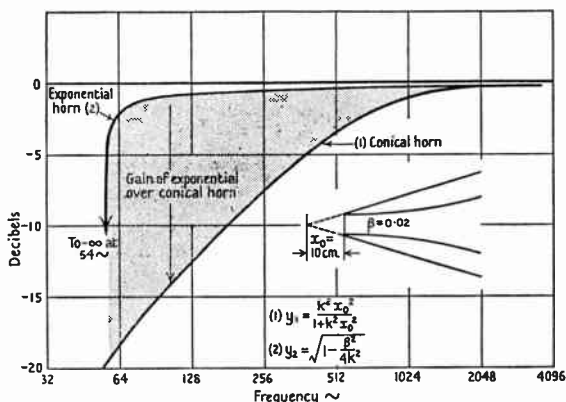


FIG. 63. Curves showing gain of exponential over conical horn under certain conditions.

openings being equal in both cases. Consequently the cost of the conical horn would be prohibitive.

If a diaphragm is considered to radiate into one-half of infinite space through a close-fitting hole in an infinite flat baffle, the impedance of the medium is matched when  $ka \geq 1.9$  (definition 20, Chap. VIII, § 1). With a diaphragm 1 cm. radius matching does not occur until the frequency is  $10^4 \sim$ . A horn enables this condition to occur below  $100 \sim$ . Its function is, therefore, to make the impedance at its mouth equal to that of the external medium at as low a frequency as possible. Since the propagation above  $10^4 \sim$  is substantially a plane-wave type, the horn can be removed without serious change in output, provided the diaphragm is the same size as the horn throat.\* In general this is not so, and for a definite

\* In the above theory we have assumed that the diaphragm is the same size as the horn throat.

diaphragm amplitude the horn increases the power output in the ratio  $(A_d/A_0)^2$ , provided the particle velocity is in phase with the pressure.

If the mass of the diaphragm and the surround stiffness were both extremely small, the diaphragm area  $A_d$  could be equal to that of the horn throat  $A_0$ . Since this condition cannot be realized in practice, a throat chamber is required to obtain an acoustical transformer effect. The diaphragm impedance is then matched to that of the horn over a wide frequency band (see Chap. XX).

## 6. Exponential horn of finite length

Hitherto we have dealt with horns of infinite length where the transmitted wave alone exists. When the axial length of the horn is finite, as it must be in practice, propagation from the mouth calls for consideration. At low frequencies the outgoing wave encounters a region of lower pressure at the mouth. The velocity of the particles in the wave front suddenly increases, thereby causing a local fall in pressure. By virtue of the continuity of the medium the layer immediately behind the wave front is also affected, so its velocity increases with accompanying pressure drop. This process is maintained right back to the source (throat). Thus a backwards travelling or reflected wave is created and interferes with the transmitted wave. The interference depends upon the impedance at the mouth. If the final opening is small, at low frequencies the reflected wave is of such magnitude and phase as to reduce seriously the transmitted wave and, therefore, the power radiated as sound. In fact the sudden release of pressure at the mouth, where it can diffuse in all directions, introduces a marked discontinuity, unless the impedance of the horn termination is comparable with that of the medium.

To ascertain the influence of the mouth diameter and reflection thereat is a problem which—at the moment—has not been solved by rigorous methods. The impedance at any point in the opening is the complex quotient of the pressure and the particle velocity normal to the wave front at the point in question. The resistance and reactance components per unit area, into which this complex quotient can be resolved, will, for simplicity, be taken as those at the corresponding section of an infinite horn. Their values from (23), (24) are  $r = \rho_0 c \sqrt{1 - (\beta^2/4k^2)}$  and  $x = \rho_0 c \beta/2k$ . The ratio reactance to resistance is  $y/\sqrt{1 - y^2}$ , where  $y = \beta/2k$ , and it is plotted in Fig. 64,

curve 1. For one side of a massless rigid disk in an infinite rigid plane we have, from Chap. VIII, § 1,  $r = \rho_0 c A G_1$  and

$$x = \rho_0 c A H_1(2z)/z = \rho_0 c A G_2,$$

these being the total values over the disk. As shown in Fig. 15, they are not constant but vary from the centre to the edge. Taking

$\frac{x}{r} = \frac{H_1(2z)}{z G_1(2z)} = \frac{G_2}{G_1}$  we obtain the mean value over the surface. This

is portrayed in Fig. 64, curve 2, the abscissa being chosen to give an intersection with curve 1 in the neighbourhood of  $ka = 2$  or

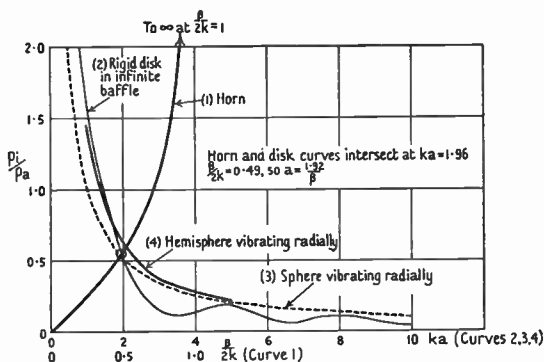


FIG. 64. Curves showing  $p_i/p_a = x/r$  (the ratio of reactance to resistance per unit area) in an exponential horn (1), and also at the surfaces of massless vibrators (2), (3), (4).

$\beta/2k = 0.5$ , where the ordinates of the two curves are almost equal. From Fig. 64 the product  $(\beta/2k)ka$  at the intersection gives  $a = 1.92/\beta$ . For values of  $k$  corresponding to the range  $ka = 1.25$  to  $2.0$ , it will then be found that the mean impedance per unit area of the disk is equal to the impedance (assumed constant) at a cross-section of the horn of equal radius. Within these limits the disk will simulate the horn if the latter discharges into semi-infinite space, and the reflected wave does not upset the hypothetical conditions for the terminal impedance in respect to the transmitted wave. Outside these limits the resistance and reactance components for the disk differ from those for the horn, the inertia component of the latter exceeding that of the former.

When  $ka = 2.0$  the mean resistive component over the rigid disk is equal to the resistance of the medium  $\rho_0 c$ , although at the centre of the disk it is greater and at the edge less than  $\rho_0 c$ . Assuming the



efficiency of transfer at the horn mouth to be adequate under this condition, we find that  $a = 2/k = \lambda/\pi$ . This gives a rough estimate of the radius of the horn opening when  $\omega/2\pi = c/\lambda$  is the lowest frequency to be adequately reproduced. The cut-off frequency is given by  $\beta = 2k$  and from above  $a = 1.92/\beta \doteq \lambda/2\pi$ . It appears, therefore, that the radius of the opening should lie between  $\lambda/\pi$  and  $\lambda/2\pi$ , i.e. from  $\frac{1}{2}$  to  $\frac{1}{4}$  the wave-length of the lowest note, to be satisfactorily reproduced. When  $ka = 2.0$  the pressure on the infinite rigid plane is 0.6 that on the axis of the horn, provided the distance  $r \gg a$ . This means that the plane increases the output from the horn when  $ka = 2$ , and modifies the sound distribution compared with that which occurs in its absence. In general, horns do not flare into walls, so we must seek other means of investigating the problem.

As a first approximation to the conditions to be satisfied at the mouth of the horn: (a) the ratio of the mean values per unit area of the resistive and reactive components of the *simulating impedance* (see definition 28) should tally with that for an infinite horn; (b) the medium should be matched resistively at the same frequency by both horn and simulating impedance. The ratio in (a) can be calculated for the two cases, but the matching frequency of a finite horn can only be accurately determined by empirical methods.

The simulating impedances it is intended to discuss are, (a) a radially vibrating sphere [58], (b) a radially vibrating hemisphere [121 b], the other hemisphere being quiescent. It is important to notice that the sphere is not to be used as a substitute for the horn opening. The idea is that the mean impedance per unit area of massless vibrators of the above type is used to replace that of the horn which is unknown. To simulate the horn termination identically, not only the impedance but the spatial distribution of radiation would have to be reproduced. In the latter respect a pulsating sphere is ruled out, since the distribution therefrom is uniform; a hemisphere is better, and, in fact, tolerably good up to a certain value of  $ka$ , beyond which the focusing of the horn is the greater.

The impedance per unit area of a radially vibrating sphere is, from (114), Chap. II,

$$z = \rho_0 c \left[ \frac{z^2}{1+z^2} + \frac{iz}{1+z^2} \right] = r + ix. \quad (41)$$

The components  $r$  and  $x$  are plotted for various values of  $ka$  in Fig. 65, curves 1 and 2, whilst  $x/r$  is shown in curve 3, Fig. 64. From curve 1,

Fig. 65, it is seen that when  $ka = 2$  the resistive component is 0.8 that of the medium, whilst from  $ka = 0.8$  to 2 the ratio  $x/r$  is in close agreement with the values for the horn over the range  $\beta/2k = 0.8$  to 0.5.\* Thus we have a fairly good basis of comparison.

The impedance per unit area of a radially pulsating hemisphere is, from (116), Chap. II,

$$z = \frac{1}{2}\rho_0 c \left[ \left( \frac{z^2}{1+z^2} \right) + \frac{3}{2}\mu \left( \frac{z^4}{4+z^4} \right) + i \left[ \left( \frac{z}{1+z^2} \right) + \frac{3}{2}\mu \left( \frac{2z+z^3}{4+z^4} \right) \right] \right], \quad (42)$$

where  $\mu = \cos \theta$ , as in Fig. 3. The first and third terms correspond

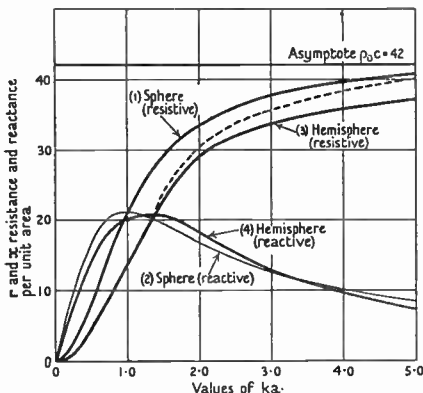


FIG. 65. Curves showing resistance and reactance of (a) a pulsating sphere, (b) a pulsating hemisphere (the other hemisphere being quiescent) for various values of  $ka$ .

to a radially pulsating sphere [see (41)], whilst the second and fourth terms pertain to an axially vibrating sphere. The combination of these vibrations involving spherical zonal harmonics of zeroth and unit orders gives a first approximation to a pulsating hemisphere. To attain greater accuracy additional harmonics (3, 5, etc.) are required, but these would make the analysis unduly protracted. Owing to the presence of  $\mu$  in (42),  $z$  varies with  $\theta$ . By integrating the impedance over the area of the active hemisphere and dividing by that area, a mean value of  $z$  is obtained. From Fig. 3 the area of an annular zone is  $2\pi a^2 \sin \theta d\theta$ , and the integral required is  $2\pi a^2 \int_0^{\frac{1}{2}\pi} \sin \theta \cos \theta d\theta$ , since  $\mu = \cos \theta$ . The value of this is  $\pi a^2$ , and

\* Observe the reversal of order. The comparison is over corresponding ranges of  $ka$  and  $\beta/2k$ .

since the area of the hemisphere is  $2\pi a^2$ , the mean is  $\frac{1}{2}$ . The mean value of the impedance per unit area over the hemisphere is, therefore,

$$z = \frac{1}{2}\rho_0 c \left\{ \left( \frac{z^2}{1+z^2} \right) + \frac{3}{4} \left( \frac{z^4}{4+z^4} \right) + i \left[ \left( \frac{z}{1+z^2} \right) + \frac{3}{4} \left( \frac{2z+z^3}{4+z^4} \right) \right] \right\} \quad (43)$$

$$= r + ix.$$

The quantities  $r$  and  $x$  are plotted in Fig. 65, curves 3 and 4, whilst  $x/r$  is shown in Fig. 64, curve 4. At low values of  $z = ka$  the resistive component is less than that for a complete sphere, since the vibrating area in the latter case is twice that in (43). As  $ka$  increases, the resistance  $r$  in both cases approaches that of the medium asymptotically (see definition 20). The slower growth in  $r$  for the hemisphere is due, in part, to the reduced area, but also to the absence of harmonics of higher order in (43). The ratio  $x/r$  is greater than that for the sphere or the horn, i.e. the power factor of either of the two latter exceeds that of the hemisphere.

### 7. Formula incorporating simulating impedance

To determine the result of using any form of simulating impedance (see definition 28) at the opening of the horn, it is essential to deduce a formula in which impedances can be combined. Since  $p = z_a A v$ , the pressure (assumed uniform over the orifice) in the transmitted wave is, from (22),

$$p_1 = \rho_0 c v_1 \Pi_1,$$

where  $\Pi_1 = \sqrt{\{1 - (\beta^2/4k^2)\}} + i\beta/2k$ ;

$$\text{so} \quad v_1 = \frac{p_1}{\rho_0 c \Pi_1}. \quad (44)$$

For the reflected wave

$$p_2 = -\rho_0 c v_2 \Pi_2;$$

$$\text{so} \quad v_2 = -\frac{p_2}{\rho_0 c \Pi_2}, \quad (45)$$

where  $\Pi_2 = \sqrt{\{1 - (\beta^2/4k^2)\}} - i\beta/2k$ , the minus sign signifying that  $c$  is negative, owing to reversal of the direction of wave motion. If  $p$  and  $v$  are, respectively, the pressure and particle velocity in the radiated wave [58],

$$p = p_1 + p_2 \quad (46)$$

$$\text{and} \quad v = v_1 + v_2. \quad (47)$$

The terminal impedance per unit area (assumed uniform over the horn mouth) is

$$z = \frac{p}{v} = \frac{p_1 + p_2}{v_1 + v_2}. \quad (48)$$

From expressions (44) to (48) and the identity  $\Pi_1 \Pi_2 = 1$  the ratio of the pressure in the radiated wave to the original pressure (in an infinite horn) is found to be

$$\frac{p}{p_1} = \frac{p_1 + p_2}{p_1} = \frac{z(\Pi_1 + \Pi_2)}{z\Pi_1 + \rho_0 c} \quad (49)$$

$$= \frac{2z\sqrt{\{1 - (\beta^2/4k^2)\}}}{z[\sqrt{\{1 - (\beta^2/4k^2)\}} + (i\beta/2k)] + \rho_0 c} \quad (50)$$

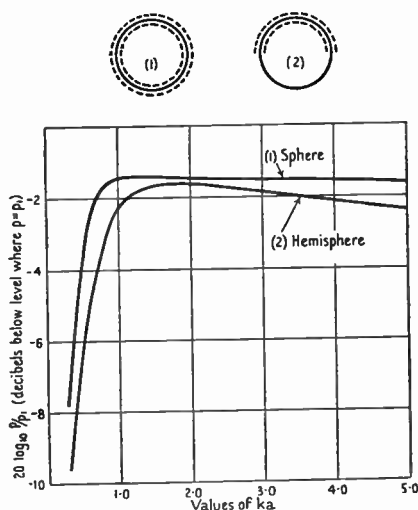


FIG. 66.

By inserting the value of  $z$  from the formula for the simulating impedance in (50) the ratio of the pressure in the radiated wave to that transmitted in the absence of reflection is determined. This ratio can be converted to decibels if desired. By choosing values of  $\beta$  and  $k$ , the influence of the radius of the horn opening can be ascertained by aid of (50).

In Fig. 66 two curves are given corresponding to  $\beta = 0.02$ ,  $f = 75 \sim (\beta/2k = 1/\sqrt{2})$ , the terminal impedances being a radially vibrating sphere (curve 1), and a radially vibrating hemisphere (curve 2). For the former the ratio  $p/p_1$  attains a steady value sooner than for the latter. This is to be expected, since  $z$  in one case exceeds that in the other, and the impedance change at the mouth is lessened. It seems reasonable to believe that the hemisphere is the more representative of the two owing to its shape and smaller surface. The

area is twice the plane area of the orifice. A reduction in the radius of the hemisphere would be equivalent to increasing  $ka$  in Fig. 66. For example, if it were  $a/\sqrt{2}$ , the abscissae require multiplication by  $\sqrt{2}$ , so the new value for  $ka = 2.0$  is 2.828. The proper choice of radius can only be determined by means of experimental methods.

Both curves in Fig. 66 attain maximum values which are relatively inconspicuous. There is little difference between the curves when  $ka = 1$ , so this can be regarded as a turning-point. Thus, if the lowest frequency is reproduced at a level not more than 2.5 decibels below normal,  $ka$  must not be less than unity. Putting  $ka = 1$  we get  $a = \lambda/2\pi$ , or the radius of the opening should not be less than one-sixth of the length of the longest wave to be reproduced. At 75 ~ this means that  $a = 75$  cm., i.e. the diameter is 5 feet and the axial length 15 feet, provided the throat radius is 1 cm. If the radially pulsating hemisphere were to be replaced by one of radius  $a/\sqrt{2}$  as mentioned above, the radius of the final opening of the horn would be  $5\sqrt{2} \doteq 7$  feet.

A different set of curves will be obtained for each value of  $k$ , but the maxima always occur at the same value of  $ka$ . As  $k$  increases  $\sqrt{\{1 - (\beta^2/4k^2)\}} \rightarrow 1$ ,  $\beta/2k \rightarrow 0$ , and expression (50) approaches asymptotically the value

$$\frac{p}{p_1} = \frac{2z}{z + \rho_0 c} \quad (51)$$

For large values of  $ka$ , i.e. at high frequencies,  $z$  tends to the value  $\rho_0 c$  for both sphere and hemisphere, provided harmonics of higher orders are used in (43). Thus the ratio  $p/p_1$  approaches unity and the system is devoid of reflection.

### 8. Influence of terminal reflection on throat impedance

The influence of reflection at the *mouth* of a horn is embodied in (50). The reflected wave travels up the horn and ultimately reaches the throat. The pressure at any point within the horn is the vector sum of those due to the transmitted and the reflected waves. It differs, therefore, from that in a horn of infinite length. Modification in the throat impedance due to the reflected wave can be determined as shown below [49].

The complete solution to the exponential horn equation is given in (17), and contains two arbitrary constants. When  $k^2 > \frac{1}{4}\beta^2$ , we have

$$\phi = e^{-i\beta x}(C_1 \cos \alpha x + D_1 \sin \alpha x), \quad (52)$$

where  $\alpha = \sqrt{(k^2 - \frac{1}{4}\beta^2)}$ .

The particle velocity

$$\begin{aligned} v &= -\frac{\partial\phi}{\partial x} \\ &= e^{-i\beta x}\{C_1(\alpha \sin \alpha x + \frac{1}{2}\beta \cos \alpha x) - D_1(\alpha \cos \alpha x - \frac{1}{2}\beta \sin \alpha x)\} \\ &= ke^{-i\beta x}\{C_1 \sin(\alpha x + \theta) - D_1 \cos(\alpha x + \theta)\}, \end{aligned} \quad (53)$$

where  $\theta = \tan^{-1}\beta/2\alpha$ . The pressure at the mouth from (52) is

$$p_2 = i\rho_0 \omega \phi_2 = i\rho_0 \omega e^{-i\beta x_2}\{C_1 \cos \alpha x_2 + D_1 \sin \alpha x_2\}, \quad (54)$$

where  $x_2$  is the distance of the mouth from the throat. The impedance per unit area at the mouth is, from (53) and (54),

$$z_2 = \frac{p_2}{v_2} = i\rho_0 c \frac{(C_1 \cos \alpha x_2 + D_1 \sin \alpha x_2)}{\{C_1 \sin(\alpha x_2 + \theta) - D_1 \cos(\alpha x_2 + \theta)\}}. \quad (55)$$

Transposing (55) we obtain

$$\frac{D_1}{C_1} = \frac{z_2 \sin(\alpha x_2 + \theta) - i\rho_0 c \cos \alpha x_2}{z_2 \cos(\alpha x_2 + \theta) + i\rho_0 c \sin \alpha x_2}. \quad (56)$$

At the throat  $x_2 = 0$ ,  $\sin \theta = \beta/2k$ ,  $\cos \theta = \alpha/k$ , so, from (55),

$$z_0 = \frac{i\rho_0 \omega C_1}{\frac{1}{2}\beta C_1 - \alpha D_1} = \frac{i\rho_0 \omega}{[\frac{1}{2}\beta - \alpha(D_1/C_1)]}. \quad (57)$$

Substituting in (57) for  $D_1/C_1$  from (56), the throat impedance per unit area is

$$\begin{aligned} z_0 &= -\frac{i\rho_0 \omega \{z_2 \cos(\alpha x_2 + \theta) + i\rho_0 c \sin \alpha x_2\}}{z_2 \{\alpha \sin(\alpha x_2 + \theta) - \frac{1}{2}\beta \cos(\alpha x_2 + \theta)\} - i\rho_0 c \{\alpha \cos \alpha x_2 + \frac{1}{2}\beta \sin \alpha x_2\}} \\ &= \frac{\rho_0 c \{z_2 \cos(\alpha x_2 + \theta) + i\rho_0 c \sin \alpha x_2\}}{\{\rho_0 c \cos(\alpha x_2 - \theta) + iz_2 \sin \alpha x_2\}} \end{aligned} \quad (58)$$

$$= (r_0 + ix_0). \quad (59)$$

When  $\theta$  is small enough to be neglected

$$r_0 = \rho_0 c \left[ \frac{\rho_0 c z_2}{z_2^2 + (\rho_0^2 c^2 - z_2^2) \cos^2 \alpha x_2} \right] \quad (60)$$

and

$$x_0 = \rho_0 c \left[ \frac{(\rho_0^2 c^2 - z_2^2) \sin 2\alpha x_2}{2\{z_2^2 + (\rho_0^2 c^2 - z_2^2) \cos^2 \alpha x_2\}} \right]. \quad (61)$$

The above condition respecting  $\theta$  is ensured when  $k \gg \frac{1}{2}\beta$ , i.e. well beyond the cut-off point where the pressure and particle velocity are almost in phase. The value of  $z_2$  at the horn mouth is taken to be that of a pulsating hemisphere (§ 6). When the reactive component of  $z_2$  is small  $z_2 \doteq \rho_0 c$ , and the throat impedance is  $\rho_0 c A_0$  which is wholly resistive. This is to be expected since the condition  $z_2 = \rho_0 c$

at the mouth means that the horn impedance matches that of the medium and there is no reflected wave.

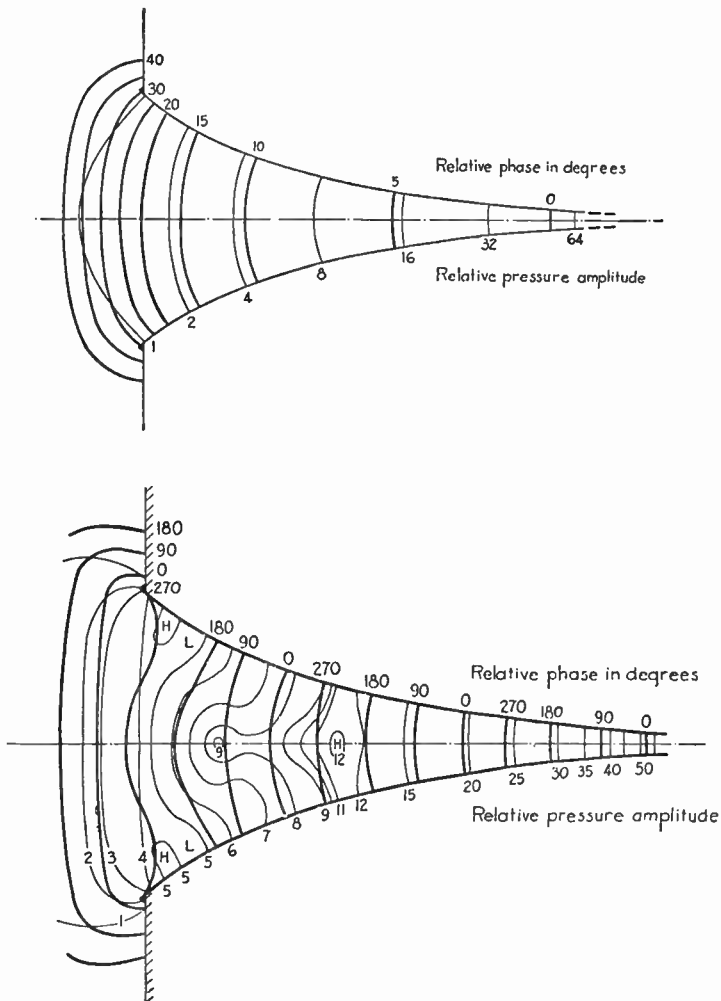


FIG. 67. Relative pressure and its phase in exponential horn 173 cm. long; mouth diameter 72 cm.,  $\beta = 0.046$ .  $\omega/2\pi = 120 \sim$  (top) and  $800 \sim$  (bottom).

### 9. Velocity of propagation in finite exponential horn

In a plane progressive wave (Chap. II, § 2) the particle displacement  $\xi = \xi_0 \cos(\omega t - kx)$ , where  $kx = \theta$  is the phase angle at a distance  $x$

from the source. If the propagation velocity varies with  $x$ , so also does  $k$ . Then we have  $\theta = \int_0^x k dx$ . When  $\theta$  is plotted against  $x$ , the slope  $d\theta/dx = k$ . In a finite horn, near its cut-off point especially, the issue is complicated by the reflected wave. If, however, the propagation is regarded as unidirectional, an effective or composite velocity can be found. It is to be clearly understood that this is not necessarily the velocity in the absence of reflection. From the data [57] of Fig. 67 curves can be plotted showing  $\theta$  at various distances from the horn throat. Since the pressure variations are small, the possibility of change of wave form is negligible\* and the phase velocity at any abscissa is  $c' = \omega/k$ . The value of  $\beta$ , the flaring index, is 0.046, so from the formula  $\omega/2\pi = \beta c/4\pi$ , the cut-off frequency for an infinite horn is  $120 \sim$ . This is also the frequency used during the experiments. At the throat  $c'$  is 25 times  $c$ , whilst just within the mouth it is  $6c$ , and 40 cm. beyond  $c' = 2c$ . The high throat velocity is to be expected from the theory of infinite horns given above.

At  $800 \sim$ , where the influence of reflection is relatively small,  $c'$  is fairly uniform down the horn, being  $5 \times 10^4$  cm. sec.<sup>-1</sup> compared with †  $3.8 \times 10^4$  cm. sec.<sup>-1</sup> for an infinite horn. Just beyond the mouth it is  $3.9 \times 10^4$  cm. sec.<sup>-1</sup>.

\* See Chapter XI.

† Using formula (27).



## XI

### SOUND WAVES OF FINITE AMPLITUDE

#### 1. Introduction

It is stated in Chapter II that the theory of sound is based upon infinitesimal pressure amplitudes. In modern sound-reproducing apparatus, and in all musical instruments capable of generating large sound pressure (orchestra and pedal organ), the amplitudes at the source are anything but infinitesimal. The pressure used in fog-horns

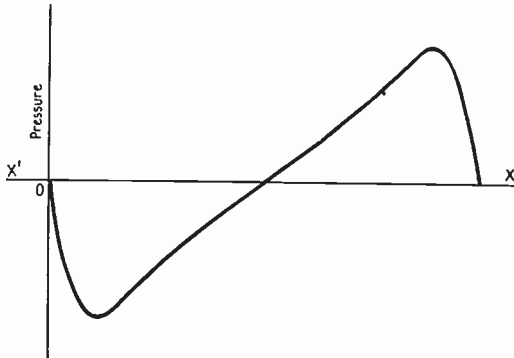


FIG. 68. Curve showing wave form distortion due to large sound pressure amplitude.

and sirens is colossal from the viewpoint of simple theory, whilst that at the throat of a powerful public address horn-type speaker may reach a value of  $2 \times 10^4$  dynes  $\text{cm.}^{-2}$ , i.e.  $\frac{1}{50}$  the normal atmospheric pressure (see § 9). Since a sound pressure of 5 dynes  $\text{cm.}^{-2}$  on the ear-drum is quite loud, the great strength of the above source will be realized.

At any instant during the propagation of a *plane* sound wave of finite amplitude, the density of the medium varies from a maximum at a crest to a minimum at a trough. The velocity of propagation gradually decreases from the crests to the troughs, so the former steadily gain on the latter. The result of this is shown in Fig. 68, which indicates a profound alteration in wave form. The process continues until the wave-slope becomes vertical and a discontinuity or abrupt change in the smooth passage of the wave is presumed to occur. Beyond this point the previous mathematical analysis ceases

to have any physical significance. No experimental evidence exists relating to discontinuities associated with steady wave motion. There is, however, much information regarding sound impulses due to projectiles [223]. Measurements on pulses due to explosions, the pressure being released from a tube open at one end, disclose velocities varying from  $1.2 \times 10^5$  cm. sec.<sup>-1</sup> near the tube to the normal value of  $3.43 \times 10^4$  cm. sec.<sup>-1</sup> at some distance therefrom [53].

Mathematical analyses, relating to finite amplitudes, have so far been restricted to the case of plane waves [52, 54, 55, 216, 219]. Since there is no expansion during the progress of a plane wave, the change in type is much more marked than it is in an expansive wave emitted by a large conical diaphragm or from a horn. Provided the pressure at the throat of a horn does not exceed a certain value, expansion of the wave will prevent discontinuity, but not change in type. The fact that no serious change in type with public address systems has been reported indicates that, with the throat pressures used at present, the output does not contain harmonics of any relative importance.

The complete mathematical analysis associated with sound waves of finite amplitude is much too detailed for inclusion here. We shall show (see [229]) how the differential equation for a horn of any cross-section is obtained, using the assumptions in Chapter X, excepting that relating to infinitesimal amplitudes.

## 2. Sound waves of finite amplitude in a horn

In Fig. 69 consider a stratum lying between two parallel\* planes perpendicular to the axis of the horn. Its undisturbed thickness at  $x$  is  $dx$ , and its cross-sectional area  $A = A_0 \phi(x)$ , where  $\phi(x)$  is a function of  $x$ , the distance from the throat. At any instant during the passage of a sound wave, particles originally at  $x$  are at  $x + \xi$ . The thickness of the stratum is now  $dx + (\partial \xi / \partial x) dx = dx(1 + \xi')$ . If we write  $z = x + \xi$ , then  $z' = \partial z / \partial x = (1 + \xi')$ , so the new thickness is  $z' dx$  and the corresponding area  $A_0 \phi(x + \xi) = A_0 \phi(z)$ . Since the mass of the lamina remains constant, by equating masses we get

$$\rho_0 dx A_0 \phi(x) = \rho dx z' A_0 \phi(z)$$

$$\text{or} \quad \frac{\rho}{\rho_0} = \frac{1}{\chi z'}, \quad (1)$$

where  $\chi = \phi(z) / \phi(x)$ .

\* See the last paragraph of § 1, Chap. X, regarding a *plane wave front*.

By differentiating (1) we obtain

$$-\frac{1}{\rho_0} \frac{\partial \rho}{\partial x} = \frac{z''}{\chi(z')^2} + \frac{\chi'}{\chi^2 z'}, \quad (2)$$

where  $z'' = \partial^2 z / \partial x^2 = \partial^2 \xi / \partial x^2 = \xi''$ , and  $\chi' = \partial \chi / \partial x$ .

For adiabatic working  $\mathbf{p} = p_0(\rho/\rho_0)^\gamma$ ,

$$\begin{aligned} \text{so} \quad \frac{\partial \mathbf{p}}{\partial \rho} &= \frac{\gamma p_0}{\rho_0} \left( \frac{\rho}{\rho_0} \right)^{\gamma-1} = c^2 \left( \frac{\rho}{\rho_0} \right)^{\gamma-1}, \\ &= \frac{c^2}{(\chi z')^{\gamma-1}}. \end{aligned} \quad (3)$$

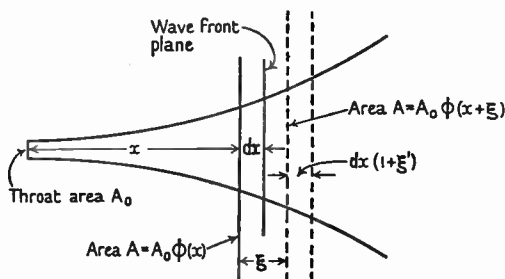


FIG. 69.  $\xi$  is the particle displacement.

Multiplying both sides of (2) by  $\partial \mathbf{p} / \partial \rho$  from (3), we obtain

$$-\frac{1}{\rho_0} \frac{\partial \mathbf{p}}{\partial x} = c^2 \left\{ \frac{z''}{(z')^{\gamma+1} \chi^\gamma} + \frac{\chi'}{(z')^\gamma \chi^{\gamma+1}} \right\}. \quad (4)$$

The difference in total pressure on the two sides of the lamina is  $-(\partial \mathbf{p} / \partial x) dx A_0 \phi(z)$ . This is equal to the product of the laminar mass and the axial acceleration, so

$$-\frac{\partial \mathbf{p}}{\partial x} dx A_0 \phi(z) = \rho_0 \ddot{\xi} A_0 \phi(x) dx$$

or

$$-\frac{1}{\rho_0} \frac{\partial \mathbf{p}}{\partial x} = \frac{\ddot{\xi}}{\chi}, \quad (5)$$

where  $\ddot{\xi} = \partial^2 \xi / \partial t^2$ .

Equating (4) and (5), we get

$$z'' + \frac{z' \chi'}{\chi} = \frac{(z')^{\gamma+1} \chi^{\gamma-1}}{c^2} \ddot{\xi}. \quad (6)$$

This is the horn equation for finite amplitudes.

\* Since the abscissa is  $(x + \xi)$  the pressure difference is  $-\frac{\partial \mathbf{p}}{\partial(x + \xi)} dx(1 + \xi') A_0 \phi(z)$ .

Now  $\partial(x + \xi) = \partial x + \partial \xi / \partial x = \partial x(1 + \xi')$ , so the pressure difference is  $-\frac{\partial \mathbf{p}}{\partial x} dx A_0 \phi(z)$ .

### 3. Plane waves of finite amplitude

Since the wave-front is assumed to be plane, the analysis is rigorous for plane waves. In this case  $\phi(x)$  is constant, so  $\chi = 1$  and  $\chi' = 0$ . Thus (6) becomes

$$z'' = \frac{(z')^{\gamma+1} \ddot{\xi}}{c^2} \quad (7)$$

Since  $z'' = \xi''$  and  $z' = 1 + \xi'$ , (7) can be written

$$\xi'' = \frac{(1 + \xi')^{\gamma+1} \ddot{\xi}}{c^2}, \quad (8)$$

which is a well-known equation for plane waves of finite amplitude [216, 219]. For infinitesimal amplitude  $\xi' \ll 1$ , so

$$\xi'' = \frac{\ddot{\xi}}{c^2}, \quad (9)$$

which is identical with expression (15), Chap. II.

### 4. Spherical waves of finite amplitude

The analysis in § 2 is exact for spherical wave propagation from a radially pulsating sphere or in a conical horn. In either case the area of the spherical wave-front is given by  $A = \Omega x^2$ , where  $\Omega$  is the solid angle. The area of the plane wave-front in a conical horn is  $A = A_1 x^2$ , where  $A_1$  is a constant and  $x$  is the distance from the vertex. Thus the formulae for plane and spherical wave-fronts differ only in the coefficients  $\Omega$  and  $A_1$ , so the analysis is valid in both cases.

The value of  $\chi$  is

$$\left(\frac{x + \xi}{x}\right)^2 = \left(1 + \frac{2\xi}{x} + \frac{\xi^2}{x^2}\right),$$

$$\text{so} \quad \chi' = 2\left(\frac{\xi'}{x} - \frac{\xi}{x^2}\right) + 2\xi\left(\frac{\xi'}{x^2} - \frac{\xi}{x^3}\right). \quad (10)$$

For finite amplitudes (6) is to be solved, using these values of  $\chi$  and  $\chi'$ . In the case of infinitesimal amplitudes the problem is best solved by the method of Chapter X, using the velocity potential.

### 5. Exponential horn

In this case  $A = A_0 e^{\beta x}$ , so  $\phi(x) = e^{\beta x}$  and  $\phi(z) = e^{\beta(x+\xi)}$ . Thus  $\chi = \phi(z)/\phi(x) = e^{\beta\xi}$  and  $\chi' = \beta\xi' e^{\beta\xi}$ . Accordingly for finite amplitudes (6) becomes

$$\xi'' + \beta\xi'(1 + \xi') = \frac{e^{(\gamma-1)\beta\xi}}{c^2} (1 + \xi')^{\gamma+1} \ddot{\xi}. \quad (11)$$

For infinitesimal amplitudes  $\xi$  tends to zero,  $\xi' \ll 1$ , and (11) degenerates to

$$\xi'' + \beta\xi' - \frac{\ddot{\xi}}{c^2} = 0. \quad (12)$$

For harmonic motion  $\ddot{\xi} = -\omega^2\xi$ , so (12) becomes

$$\xi'' + \beta\xi' + k^2\xi = 0, \quad (13)$$

which is identical in form with (16) of Chapter X.

## 6. Particle velocity

In deriving equation (1) attention is concentrated on a particle whose displacement from its undisturbed abscissa  $x$  at any instant is  $\xi$ . This is the method adopted by Lagrange [216] and equation (6) is *exact*. Care must be exercised in interpreting  $\partial\xi/\partial t$ . It represents the velocity of a particle of varying abscissa  $x+\xi$ . It is not the velocity at the point  $x$ , but that at a *variable* abscissa  $x+\xi$ . The particle velocity at  $x$ , i.e. the velocity with which the particle passes through this point, is  $u = \frac{\partial\xi}{\partial t} - \xi \frac{\partial u}{\partial x}$ . If in the second-order term  $u$  is taken as  $\partial\xi/\partial t$ , to the second degree of approximation

$$u = \frac{\partial\xi}{\partial t} - \xi \frac{\partial^2\xi}{\partial x\partial t}. \quad (14)$$

## 7. Sound pressure

The solution of equation (11) is obtained for  $\xi$ , whereas in practice the sound pressure  $p_1$  is required. Now from Chapter II  $c^2 = \gamma p_0/\rho_0$ , so  $p_0 = \rho_0 c^2/\gamma$ .

Also

$$\begin{aligned} p_1 &= (\mathbf{p} - p_0) = p_0 \left( \frac{\mathbf{p}}{p_0} - 1 \right) \\ &= \frac{\rho_0 c^2}{\gamma} \left( \frac{\mathbf{p}}{p_0} - 1 \right) \end{aligned} \quad (15)$$

by substitution from above. But for adiabatic changes

$$\frac{\mathbf{p}}{p_0} = \left( \frac{\rho}{\rho_0} \right)^\gamma = \left( \frac{1}{\chi z'} \right)^\gamma \quad (16)$$

from (1). Substituting for  $\mathbf{p}/p_0$  from (16) in (15), we obtain the excess pressure

$$p_1 = \frac{\rho_0 c^2}{\gamma} \left\{ \frac{1}{(\chi z')^\gamma} - 1 \right\}. \quad (17)$$

Now  $\chi$  and  $z'$  can be expressed in terms of  $\xi$  and its derivatives. Thus, if the value of  $\xi$  from (11) is used, the sound pressure at any

point on the axis of the horn can be found. The value of  $p_1$  from (17) is the excess pressure at the point  $x + \xi$ . Following the procedure in § 6, the excess pressure at abscissa  $x$  is  $p = p_1 - \xi(\partial p / \partial x)$ .

### 8. Boundary condition

In solving (11) we imagine the action at the horn throat to be due to a rigid diaphragm of area  $A_0^*$  whose motion is defined by  $\xi = \xi_{\max} \cos \omega t$ . The velocity of the diaphragm is  $u = -\omega \xi_{\max} \sin \omega t$ . The sound pressure on the diaphragm, due to the fundamental, is  $p = -\rho_0 c \omega \xi_{\max} \sin(\omega t - \alpha)$ , where  $\alpha$  is the phase angle between pressure and velocity. The power delivered to the horn is the mean value of the product  $p A_0 u$  over a complete cycle of the diaphragm motion. This is  $\frac{1}{2} \rho_0 c \omega^2 \xi_{\max}^2 A_0 \cos \alpha$ , where  $\cos \alpha$  is the power factor. As the wave travels along the horn it changes in type, and harmonics are created. Since there is no dissipation the power must be constant, the amount due to the fundamental frequency being reduced by that associated with the harmonics.

### 9. Magnitude of sound pressure at throat of horn

The simplest procedure is to consider the power delivered to the throat above the cut-off frequency of the horn, where the pressure and particle velocity are in phase for sinusoidal motion. The radiation resistance at the throat is  $r_r = \rho_0 c A_0$  (Chap. X), and the power radiated is  $P = \frac{1}{2} r_r \xi_{\max}^2$ . Thus the particle velocity  $\dot{\xi}_{\max} = \sqrt{(2P/r_r)}$ . Since  $p_{\max} A_0 = r_r \dot{\xi}_{\max}$ , we obtain

$$p_{\max} = \sqrt{(2Pr_r)/A_0} = \sqrt{(2\rho_0 c P/A_0)} \tag{18}$$

by substitution from above. Now  $\rho_0 c \doteq 42$ ,  $A_0 = \pi a_0^2$ , and if we make  $P = 1$  watt ( $10^7$  ergs sec.<sup>-1</sup>), the throat pressure per watt radiated is

$$p_{\max} = 1.64 \times 10^4 / a_0 \text{ dyne cm.}^{-2}. \tag{19}$$

Taking  $a_0 = 4$  cm. (see Chap. XX), the maximum throat pressure is  $4.1 \times 10^3$  dyne cm.<sup>-2</sup>, or about  $\frac{1}{250}$  part of an atmosphere. The particle amplitude is, from above,

$$\begin{aligned} \xi_{\max} &= \frac{1}{\omega \sqrt{\left(\frac{2P}{r_r}\right)}} = \frac{390}{\omega a_0} \\ &= 0.3 \text{ cm. at } 50 \sim, \end{aligned} \tag{20}$$

which corresponds to a maximum velocity of 94 cm. sec.<sup>-1</sup>.

\* In a rigorous sense, to fit the horn, the area of the diaphragm would have to follow the law  $A = A_0 e^{\pm x}$  from  $x = -\xi_{\max}$  to  $\xi_{\max}$ .

## XII

### TRANSIENTS [79 b]

1. OUR theory hitherto has been concerned solely with the steady state. A loud speaker with a good steady-state response curve can usually be guaranteed to reproduce transients well. We have now to inquire into the theory of the process and make comparison between hypothetical and actual cases. First of all assume we have a coil-driven rigid disk as in Chapter VII, the disk being set in an infinite flat baffle, the coupling between valve and coil to be a perfect transformer. Suppose the coil current is a replica in magnitude and time-displacement of the e.m.f. representing the transient as applied to the grid of the valve. Also let the disk be so small that the accession to inertia is either constant or negligible over the important frequency range occupied by the transient. The force on the disk, and therefore its acceleration, is a replica of the e.m.f. applied to the grid, provided the acoustic resistance is small compared with the mass reactance, *i.e. the control is largely due to inertia*. But in Chapter V [§ 1, formula (7)] it was proved that the axial pressure, at a point far enough away from the disk, varies directly as the acceleration of the disk. Hence, under these conditions, the acoustic reproduction of the transient will be perfect, provided the pressure variations at the said point are in phase with the acceleration of the disk. This is substantially correct when the frequency is small compared with the product of sound velocity and axial distance. If this condition is violated, there will be a phase shift of the higher frequency components of the impulse, thereby altering its shape and introducing distortion. Moreover, the higher the component frequencies of the transient, the greater must be the distance from the disk to obtain distortionless reproduction.

The conditions postulated above can be treated by reference to equations (1) and (2), Chapter VII. If the transient is represented by  $E = \chi(t)$ , the current will be proportional thereto, provided  $LDI$  and  $CD\xi$  are small compared with  $R$ . This means that  $L$  and  $C$  must be insignificant in comparison with  $R$ . The coil current then takes the form  $I = A_1 \chi(t)$ . Inserting this value in (1) we obtain

$$mD^2\xi + r_e D\xi + s\xi = CA_1 \chi(t).$$

Since the sound pressure at a distant point depends upon the accelera-

tion  $D^2\xi$ , it follows that for faithful reproduction  $r_e$  and  $s$  should be evanescent. In other words, the influence of the electrical inductance and the factor  $C$ , together with the mechanical stiffness  $s$  and radiation resistance, must be subservient to  $m$ . Thus inertia is destined to be the controlling factor. Under this condition transients will be reproduced on the axis with little distortion.

Let us consider the three coil-driven rigid disks 5 cm., 10 cm., and 15 cm. radius treated in Chapter VIII: the effective mass varies with frequency. Under circumstances where applied grid voltage and coil current are linearly related, there will be a relatively reduced acceleration corresponding to the low-frequency components of the transient. Thus the axial pressure of these components will be reduced relative to those at high frequencies, thereby introducing distortion. In practice the coil current for a given grid voltage depends upon the impedance of the complete anode circuit. The current, as in Fig. 53, varies appreciably with frequency, a maximum occurring at electro-mechanical resonance. On either side of this point, the component sine wave oscillations, into which the transient can be analysed, are reduced in magnitude and altered in phase. Moreover, distortion occurs throughout the frequency range. By keeping the time-constant of the circuit as low as possible, the distortion of the components at the upper end of the frequency range can be reduced.

By combining the influence of variation in effective mass with that due to electrical impedance, the resulting distortion of the transient can be obtained. The effective mass and the driving force, for a given signal e.m.f., both vary with frequency, so that the acceleration and, therefore, the axial pressure do likewise. The precise degree of distortion depends, of course, upon the shape of the transient, i.e. upon the relative magnitudes and phases of the components in its spectrum.

So far we have dealt solely with transients occurring on the *axis* of the disk. If we choose a remote point well away from the axis we are faced with evanescence of the higher frequencies due to interference (Chap. V, § 1). Moreover, this must be added to the preceding sources of distortion. In this discussion we tacitly assume that the instrument used for detection does not disturb the sound field, i.e. the pressure distribution in the medium. At frequencies of the order  $10^4$  ~ the wave-length is 3.4 cm. and the human body alters the distribution materially, the sound being intensified at the head due to reflection; with a microphone the pressure is doubled.



## 2. Initial part of transient of the form $e^{-\alpha t} \sin \omega t$

Whatever its shape, a transient can be expressed mathematically by a Fourier integral. It consists of an infinite spectrum of frequencies ranging from zero upwards. Not only are the amplitudes of the component frequencies important but also their phases. In an acoustic impulse which rises very rapidly to its maximum value, the higher frequency components of its spectrum are of paramount importance. If the higher frequencies are curbed, due to inductance in the electrical portion of the reproducing circuit, the initial sharpness of the impulse is reduced. A Fourier integral is somewhat cumbersome for our present purpose, so we shall take a type of transient where this procedure is not needed. For general purposes a transient of the type  $e^{-\alpha t} \sin \omega t$  is suitable for analytical treatment. First of all we shall take an approximation, and treat the matter rigorously afterwards. The first term of the series for  $\sin \omega t$  is  $\omega t$ , so we can take the form  $t e^{-\alpha t}$  as a first approximation and apply it to the case of a coil-driven rigid disk (Chap. VII). In incorporating this transient in the analysis of Chapter VII, the driving e.m.f.  $E$  is to be replaced by  $E_0 t e^{-\alpha t}$ . If the natural frequency of the system is well below audibility, the term involving the constraint  $s$  can be neglected. The third-order differential equation ultimately obtained embodies not only the mechanical forces, but also the influence of electrical circuit damping.

Considering the mechanical and electrical forces associated with the system, as in Chapter VII, we have

$$mD^2\xi + r_e D\xi = CI, \quad (1)$$

$$LDI + RI + CD\xi = E_0 t e^{-\alpha t}. \quad (2)$$

From (1)  $I = (mD^2\xi + r_e D\xi)/C$ , which on substitution in (2) gives

$$(D^3 + \beta D^2 + \gamma D)\xi = \theta t e^{-\alpha t}, \quad (3)$$

where  $\beta = \left(\frac{R}{L} + \frac{r_e}{m}\right)$ ;  $\gamma = \frac{(r_e R + C^2)}{mL}$ ;  $\theta = \frac{E_0 C}{mL}$ .

To find the complementary function of (3) we put

$$[D(D^2 + \beta D + \gamma)]\xi = 0,$$

so  $D\xi = 0$  or  $\xi = \xi_1$ ; also

$$(D^2 + \beta D + \gamma)\xi = 0,$$

to which there are three forms of solution, according as the motion of the system when left to itself is aperiodic, critical, or oscillatory. In general the circuital resistance is too high to permit oscillation due

to the influence of the magnetic field (see Chap. VII), so the solution is given for the aperiodic state. Consequently, when  $\theta = 0$ , (3) is satisfied by

$$\xi = A_1 e^{\lambda_1 t} + B_1 e^{\lambda_2 t} + \xi_1, \quad (4)$$

this being the complementary function.  $A_1$  and  $B_1$  are arbitrary constants to be determined later on. The indices  $\lambda_1, \lambda_2$  are given by

$$\left. \begin{aligned} \lambda_1 \\ \lambda_2 \end{aligned} \right\} = \frac{-\beta \pm \sqrt{(\beta^2 - 4\gamma)}}{2}. \quad (5)$$

To obtain a particular solution of (3) we obviously assume  $\xi = (C_1 + D_1 t)e^{-\alpha t}$ . Substituting this in (3) and conducting the requisite analytical operations we ultimately get

$$D_1 = -\frac{\theta}{\alpha(\alpha^2 - \alpha\beta + \gamma)} \quad (6)$$

and

$$\varphi D_1 = \alpha C_1, \quad (7)$$

where

$$\varphi = \frac{3\alpha^2 - 2\alpha\beta + \gamma}{\alpha^2 - \alpha\beta + \gamma}. \quad (7a)$$

The complete solution of equation (3) is, therefore,

$$\xi = A_1 e^{\lambda_1 t} + B_1 e^{\lambda_2 t} + (C_1 + D_1 t)e^{-\alpha t} + \xi_1. \quad (8)$$

The applied e.m.f. being  $E_0 t e^{-\alpha t}$ , it follows that when  $t = 0$  the system is quiescent. Hence the velocity  $D\xi = 0$ , and the acceleration  $D^2\xi = 0$ , these being conditions with which the solution must comply. From (8), by differentiation and the substitution  $\varphi D_1 = \alpha C_1$ , we obtain

$$D\xi = A_1 \lambda_1 e^{\lambda_1 t} + B_1 \lambda_2 e^{\lambda_2 t} + D_1 e^{-\alpha t} [(1-\varphi) - \alpha t] \quad (9)$$

and

$$D^2\xi = A_1 \lambda_1^2 e^{\lambda_1 t} + B_1 \lambda_2^2 e^{\lambda_2 t} + D_1 \alpha e^{-\alpha t} [(\varphi - 2) + \alpha t]. \quad (10)$$

Inserting the conditions  $D\xi = 0$ ,  $D^2\xi = 0$ ,  $t = 0$  in (9) and (10), we get

$$A_1 \lambda_1 + B_1 \lambda_2 = D_1 (\varphi - 1), \quad (11)$$

$$A_1 \lambda_1^2 + B_1 \lambda_2^2 = D_1 \alpha (2 - \varphi). \quad (12)$$

Solving these simultaneous equations, we find that

$$A_1 \lambda_1^2 = \frac{D_1 \lambda_1}{\lambda_1 - \lambda_2} \{ \alpha (2 - \varphi) + \lambda_2 (1 - \varphi) \} \quad (13)$$

$$= D_1 \phi, \quad (14)$$

and

$$B_1 \lambda_2^2 = -\frac{D_1 \lambda_2}{\lambda_1 - \lambda_2} \{ \alpha (2 - \varphi) + \lambda_1 (1 - \varphi) \} \quad (15)$$

$$= D_1 \chi. \quad (16)$$

Substituting (14) and (16) in (10), we get

$$\frac{D^2\xi}{D_1} = \phi e^{\lambda_1 t} + \chi e^{\lambda_2 t} + \alpha e^{-\alpha t}[(\varphi - 2) + \alpha t]. \quad (17)$$

Since the axial pressure depends upon the acceleration and  $D_1$  is constant, (17) represents the complete solution of the problem. In (17) the original transient is proportional to  $\alpha^2 t e^{-\alpha t}$ , whilst the re-

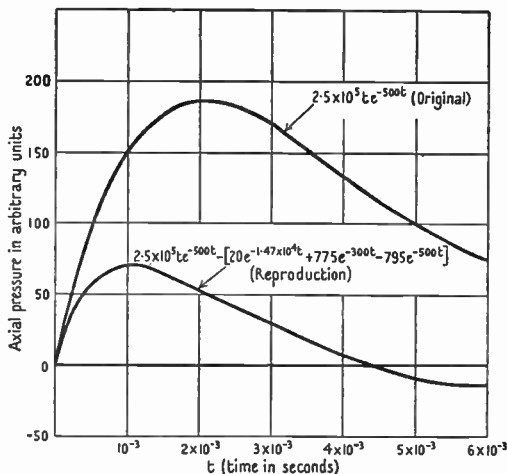


FIG. 70. Diagram showing reproduction of the transient  $E = 2.5 \times 10^5 t e^{-500t}$  on the axis of a coil-driven rigid disk, freely suspended in an infinite flat baffle.

mainder  $\phi e^{\lambda_1 t} + \chi e^{\lambda_2 t} + \alpha(\varphi - 2)e^{-\alpha t}$  is proportional to the difference between the reproduced and the original wave forms.

We will now give some typical examples. To determine the influence of the first quarter-cycle and part of the second quarter-cycle of a sine wave, the exponent  $\alpha$  is made four times the frequency, since the maximum value of  $t e^{-\alpha t}$  occurs when  $t = 1/\alpha$ . For example, to investigate a frequency of  $125 \sim$  we put  $\alpha = 500$ . To avoid complication, the power valve has a choke-condenser output (Fig. 105) with  $L$  and  $C$  very large, so that the natural frequency is well below audibility. Transients reproduced by a coil-driven rigid disk 10 cm. radius freely suspended in an infinite baffle, as perceived at a great axial distance therefrom, are plotted in Figs. 70, 71. The basic frequencies are  $125 \sim$  and  $5,000 \sim$  corresponding to  $\alpha = 500$  and

$2 \times 10^4$ . Variation in the electrical and mechanical quantities with frequency has been taken into account.

At  $125 \sim$  the reproduced pressure rises less rapidly than the original, attains a maximum more quickly, and then decays after the manner of an oscillatory circuit with large damping. This apparent 'elastic' effect is due to the magnetic field which, as shown in Chapter VII,

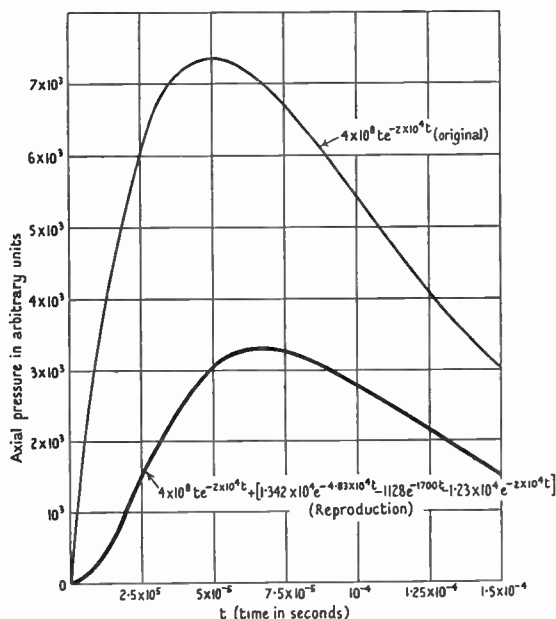


FIG. 71. Showing reproduction of the transient  $4 \times 10^8 t e^{-2 \times 10^4 t}$  by a coil-driven rigid disk in an infinite flat baffle.

is capable, when strong enough, of creating an oscillatory condition. The negative value beyond the abscissa  $4.4 \times 10^{-3}$  must not be misinterpreted. It does not necessarily signify that the coil is then on the negative side of its equilibrium position, because Fig. 70 refers solely to acceleration, not to amplitude. The zero means that the coil has attained the maximum distance from its origin and then commences to return. Between  $t = 6 \times 10^{-3}$  and  $9 \times 10^{-3}$  the motion changes direction, and the coil drifts outwards again. In fact, the circumstances are closely allied to those in a fluxmeter, where the maximum deflexion is a measure of the total flux interlinkage. If

the control were evanescent, the meter coil would arrive at a certain position and stay there. The transient  $E_0 te^{-\alpha t}$  signifies that a definite quantity of electricity is discharged through the system. In a fluxmeter  $R$  and  $r_e$  are negligible, whereas in the coil-disk combination they are not. The accurate measurement of flux depends upon inertia control and electromagnetic damping, whereas when the natural frequency of the system is well below audibility faithful sound reproduction involves inertia control alone. On the other hand, if the natural frequency is high, the conditions are akin to those in an oscillograph. Transients are accurately reproduced when the damping is critical and the frequencies of the main sine-wave components are well below that of the undamped oscillograph. These conditions are not suitable in a speaker, since the sensitivity would be much too low.

The ultimate position of the coil and disk is easily found from the preceding analysis. If  $\xi = 0$  when  $t = 0$ , then from (8)

$$\xi_1 = -[A_1 + B_1 + C_1]. \quad (18)$$

Using (7), (13), and (15) we get

$$\xi_1 = \frac{[\alpha^2(2-\varphi) + \alpha(1-\varphi)(\lambda_1 + \lambda_2) + \varphi\lambda_1\lambda_2]}{\alpha\lambda_1\lambda_2}. \quad (19)$$

Again from (8) when  $t = \infty$ , since all the exponents are negative,  $\xi = \xi_1$ , so the final resting-place of the coil is determined by (19). In general  $\xi$  will not be zero, so that for loud-speaker reproduction, in the absence of elastic constraint, a radial field of great axial length is required! To curb the spatial flights of the coil, it is imperative to apply elastic control in the form of a centring device, an annular surround, or both of these. Then the reproduced wave form is modified. The equations for this case are

$$mD^2\xi + r_e D\xi + s\xi = CI, \quad (20)$$

$$LDI + RI + CD\xi = E_0 te^{-\alpha t}, \quad (21)$$

giving ultimately

$$(D^3 + \beta_1 D^2 + \gamma_1 D + \delta_1)\xi = \theta_1 te^{-\alpha t}. \quad (22)$$

The complementary function of (22) is of the form

$$\xi = A_1 e^{\lambda_1 t} + B_1 e^{\lambda_2 t} + C_1 e^{\lambda_3 t},$$

whilst the particular integral is  $\xi = (D_1 + E_1 t)e^{-\alpha t}$ . The former can only be found in suitable form if numerical values are introduced. The three arbitrary constants are obtained from the conditions:

(1)  $t = 0, \xi = 0$ ; (2)  $t = 0, D\xi = 0$ ;  $t = 0, D^2\xi = 0$ . The complementary function in the solution may involve (a) a damped sine wave superposed on a decay curve, (b) only a decay curve. In case (a)  $\lambda_1, \lambda_2$  are imaginary, whilst  $\lambda_3$  is negative. For (b)  $\lambda_1, \lambda_2, \lambda_3$  are all real. Obviously the resulting reproduction of the transient depends upon the relationships between the circuital coefficients. If the complementary function is of an oscillatory nature, the natural period of the system, plus an additional aperiodic curve, is superposed on the wave form  $te^{-\alpha t}$ . The arithmetical work associated with this case is quite straightforward and is left to the reader. The results obtained in practice from systems having more than one degree of freedom are portrayed in Figs. 140, 142, 143, 144. Even if the damping, due to the magnetic field, is adequate to ensure the aperiodic state, it appears, from above, that in general the magnetic field and acoustic damping cause distortion in an ideal system where inertia control alone is the desideratum. In a practical system there is no doubt that suppression of the periodic state results in improved reproduction.

From Figs. 70, 71 it is seen that in the reproduced version the steepness of the wave fronts of both high and low frequency transients are reduced, that of the former more than that of the latter. From a practical viewpoint too much attention must not be paid to the initial kick, since it takes the ear about 0.1 sec. to appreciate the pitch of a sound. The chief point concerning the majority of transients is the higher frequency components following the kick. If the system reproduces these adequately, the ear will doubtless be satisfied, provided the original wave form following the kick is not travestied too seriously.

### 3. Complete transient of the type $e^{-\alpha t} \sin \omega t$

When the axial constraint is feeble and the transient takes the form  $E_0 e^{-\alpha t} \sin \omega t$ , equation (3) can be written

$$(D^3 + \beta D^2 + \gamma D)\xi = \theta e^{-\alpha t} \sin \omega t. \quad (23)$$

As before, the complementary function is  $A_1 e^{\lambda_1 t} + B_1 e^{\lambda_2 t} + \xi_1$ . To find a particular integral, assume  $\xi = e^{-\alpha t}(C_1 \sin \omega t + D_1 \cos \omega t)$ . Then  $C_1$  and  $D_1$  are obtained on solution of the simultaneous equations:

$$\left. \begin{aligned} C_1 y_1 + D_1 z_1 &= \theta \\ C_1 y_2 + D_1 z_2 &= 0 \end{aligned} \right\}, \quad (24)$$

where

$$y_1 = -2\alpha\omega^2(\alpha-1) + \beta(\alpha^2 - \omega^2) - \gamma\alpha,$$

$$y_2 = -\omega(\alpha^2 - \omega^2) - 2\alpha\beta\omega + \gamma\omega,$$

$$z_1 = \omega(\alpha^2 + \omega^2)(\alpha-1) + 2\alpha\beta\omega - \gamma\omega,$$

$$z_2 = -2\alpha\omega^2(\alpha-1) + \beta(\alpha^2 + \omega^2) - \gamma\alpha.$$

Accordingly the complete solution of (23) is

$$\xi = A_1 e^{\lambda_1 t} + B_1 e^{\lambda_2 t} + e^{-\alpha t}(C_1 \sin \omega t + D_1 \cos \omega t) + \xi_1. \quad (25)$$

Differentiating (25), the velocity is

$$D\xi = A_1 \lambda_1 e^{\lambda_1 t} + B_1 \lambda_2 e^{\lambda_2 t} + e^{-\alpha t}[(C_1 \omega - D_1 \alpha) \cos \omega t - (C_1 \alpha + D_1 \omega) \sin \omega t], \quad (26)$$

and the acceleration

$$D^2\xi = A_1 \lambda_1^2 e^{\lambda_1 t} + B_1 \lambda_2^2 e^{\lambda_2 t} + e^{-\alpha t}[\{C_1(\alpha^2 - \omega^2) + 2D_1 \alpha \omega\} \sin \omega t + \{D_1(\alpha^2 - \omega^2) - 2C_1 \alpha \omega\} \cos \omega t]. \quad (27)$$

The values of  $C_1$  and  $D_1$  having been found from (24) they are inserted in (26) and (27). These two equations are then solved, subject to the conditions  $\xi = 0$ ,  $D\xi = 0$ ,  $D^2\xi = 0$  at  $t = 0$ , as before. The solution yields  $\xi_1$ ,  $A_1$ ,  $B_1$  and is therefore complete. To determine the reproduced version of the original transient  $E_0 e^{-\alpha t} \sin \omega t$  is then merely a matter of arithmetic, which is left to the reader. Care must be exercised to avoid confusion between  $\alpha$  and  $\omega$ . The former can now be made independent of  $\omega$ , whereas in the previous transient,  $te^{-\alpha t}$ , it was written  $\alpha = 4\omega/2\pi$  for convenience.

This analysis would be applicable to the moving-coil horn type speaker of Chapter XX (method 1) if the chamber stiffness were absent. A rigorous solution for this case entails undue complication and will not be given. An oscillogram illustrating the effect of a severe electrical impulse in a horn speaker is reproduced in Fig. 144. The natural vibrations of the system are delineated clearly, so that they will accompany the acoustic output of transients.

### XIII

#### DRIVING MECHANISMS

1. THERE are three principal types of driving mechanisms for loud speakers, (a) a flexible reed of magnetic material or its equivalent situated in a magnetic field which is varied by the signal current; (b) a coil or a zigzag strip, carrying the signal current, situated in a strong magnetic field; (c) a diaphragm forming the movable plate of a condenser, the other plate being fixed. A steady or polarizing voltage is

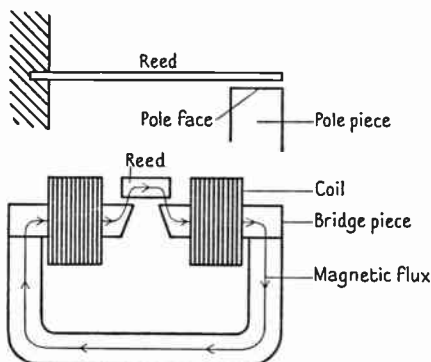


FIG. 72. Schematic diagram of cantilever reed movement.

applied to the two plates and the signal voltage superposed thereon. There are other methods of actuating diaphragms, using crystals of Rochelle salts, which have been developed recently (Chap. XIX, § 1, Chap. XX, § 16). Of all methods the moving-coil is the best [183 a].

#### 2. Cantilever reed type

This class of drive includes various designs, the simplest of which is shown diagrammatically in Fig. 72. The U-shaped permanent magnet sends flux through a bridge-piece of laminated stampings, on each side of which is wound a fine wire coil usually of 600 to 1,500 ohms resistance. The centre of the bridge is arched and has an air-gap above which the reed is poised. By means of a screw the distance between the reed and the pole-piece can be varied. The cone diaphragm is attached to a point on the reed, usually near the centre of the air-gap. When alternating current flows in the coils the



magnetic field through the reed fluctuates in strength accordingly, and the reed vibrates in response thereto.

By virtue of the inverse square law, as the reed approaches the pole-piece the magnetic force increases rapidly. The reverse occurs when the reed moves away. To obtain sensitivity the adjustment screw is operated until the reed is very close to the pole-piece. When it gets within a certain distance, the magnetic pull overcomes the mechanical stiffness of the reed and a click is heard as the reed flops on to the pole face. There is consequently a minimum working distance which increases with the amplitude of vibration. Owing to the inverse square law, the relationship between deflexion and

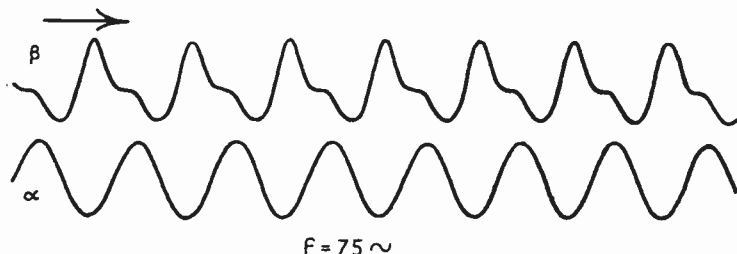


FIG. 73. Record of acoustic output from reed-driven conical diaphragm when the amplitude of the reed exceeds the limit of linearity. Curve ( $\alpha$ ) = input to windings; curve ( $\beta$ ) = acoustic output from diaphragm.

current is not linear. Thus with a sine wave input of moderate amount, the radiated sound contains alien frequencies. These increase with the amplitude of the reed and are, therefore, most noticeable when reproducing low frequencies. The oscillogram [96 a] of Fig. 73 illustrates this point. Within definite amplitude limits this defect can be overcome by suitably adjusting the position of the reed with reference to the pole-pieces as illustrated in Fig. 74.

The force between the reed and pole-piece, though not quite uniformly distributed over the lower face of the former, can be considered to act at the *centre of magnetic force* [96 a]. Taken as a single force it causes the same deflexion when acting at the centre of magnetic force as when distributed over the reed. When a direct current flows in the coils the reed is bent towards the pole face and  $x_2$  is nearer thereto than  $x_1$ . The attractive force on the reed is therefore greater at  $x_2$  than at  $x_1$  and the centre of magnetic force shifts outwards along the reed causing an increase in the moment  $l_1 f$ . If this increases more

rapidly than  $ls$ , where  $s$  is the stiffness, instability results and the mechanism is rendered inoperative by the reed flopping on the pole-piece.

In Fig. 74 c the point  $A$  is slightly lower than the plane of the pole face whereas in Fig. 74 b it is higher. Also the reed is inclined at an angle *above* this plane instead of below it as in Fig. 74 b. The reed approaches the poles due to increase in coil current and the attraction is greatest at  $x_1$ , this point being nearer to the poles than  $x_2$ . Thus the centre of magnetic force moves *towards* the support and its leverage is reduced as the reed deflexion and the current increase. By finding the correct setting for the reed, linear proportionality between current and deflexion can be secured over a limited range. It is also possible by a suitable mechanism to swing the reed about a definite axis such that its distance from the pole face can be properly adjusted for various amplitudes. In this case instability is substantially abolished. To obtain the best results, it is imperative that the apparatus should be made to a high degree of accuracy so that there is no backlash.

The magnetic pull on the reed is proportional to  $B^2$  where  $B$  is the flux density. If  $B$  is not uniform the force depends upon the sum of all the elemental forces acting on the reed over its working face, i.e.  $f \propto \int B^2 dA$ . For simplicity we shall assume that  $B$  is uniform. When a.c. flows,  $B$  fluctuates between  $B + \delta B$  and  $B - \delta B$ , where  $\delta B$  is the small change in density. The *increase* in force due to the current during a positive half-cycle is proportional to

$$(B + \delta B)^2 - B^2 = B^2 + 2B \delta B + \delta B^2 - B^2 \\ \doteq 2B \delta B,$$

where  $\delta B^2$  is neglected since it is usually small compared with

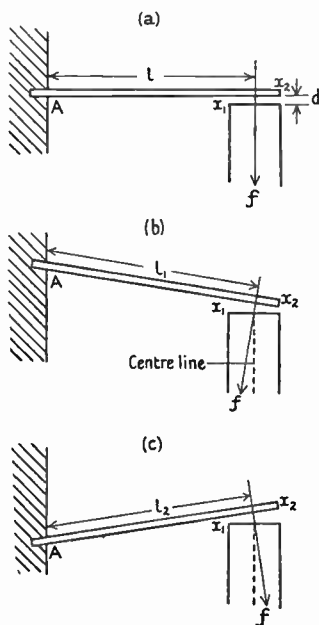


FIG. 74. Diagrams illustrating method of obtaining a linear characteristic in cantilever reed drive.

$2B \delta B$ . Obviously the force decreases by the same amount during the negative half-cycle. Alien frequencies are created when  $\delta B$  (coil current sinusoidal) is comparable with  $B$ , since the term  $\delta B^2$  entails a double frequency. When the input is large and contains a plurality of tones, the non-linear characteristic causes sum and difference and other alien tones to be created. The low-frequency vibrations of relatively large amplitude cause the high-frequency vibrations to be modulated. A simple illustration of this is given in Chap. IX, § 1, formulae (4) and (5).

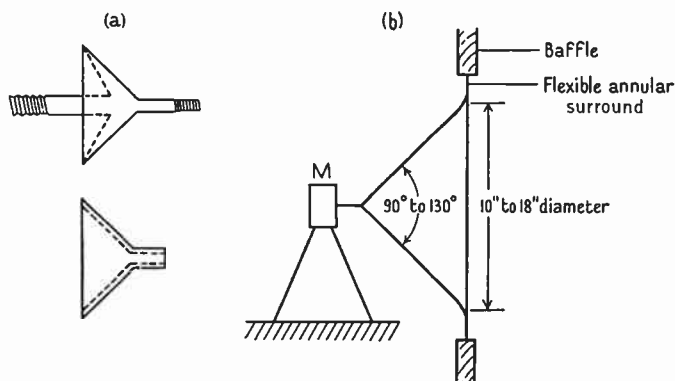


FIG. 75.

The working force on the reed, for a given coil current, depends upon  $B$  and, therefore, on the strength of the permanent magnet. This cannot be increased indefinitely owing to rise in reluctance and ultimate saturation of the pole-piece. Under this condition, although  $B$  increases,  $\delta B$  decreases and  $B \delta B$  is less than its value with a weaker magnet. This is due to the bridge-piece and reed being operated above the knee of the magnetization curve. The change  $\delta B$  depends upon the incremental permeability, and this decreases with increase in  $B$ . The greater static force also necessitates a larger minimum gap to prevent instability. Thus the value of  $\delta B$  is again decreased due to the greater reluctance of the longer gap.

The reed is usually associated with a fairly large conical paper diaphragm supported in a suitable manner at its periphery. The method of connecting the two is important. To avoid loss of high notes, a short rigid bar with conical nuts or the like, as shown in Fig. 75 A, is recommended [218]. This should be as light as possible

consistent with the requisite rigidity, since large mass curbs the amplitude at high frequencies where the effective mass of the cone itself is quite small.

At any instant during vibration, pressure waves on each side of the cone are of opposite sign. The pressure at any spatial point is due to radiation from both sides of the diaphragm. Moreover, interference occurs and it is necessary to minimize this by using a baffle to shield the two sides of the diaphragm from each other's influence. In Fig. 75 B a flat baffle is indicated since this gives good quality for domestic purposes. Cabinets are generally used for convenience, however, since the radio apparatus can be housed therein. These contribute their quota of resonance especially if the sides are fairly flexible. Coloration is quite marked when the speaker is situated near a wall, especially at a corner, or in association with other furniture forming a partial enclosure. This effect, however, is not very noticeable unless the speaker itself has a good lower register.

A so-called directional baffle [12, 13] (Chap. XX) can be used. This increases the loading on the diaphragm, thereby permitting a reduction in its size. The scheme is hardly suitable for domestic speakers owing to the large dimensions of the baffle.

### 3. Inductor dynamic mechanism

The driving mechanism known by this name is shown schematically [190] in Fig. 76. Two square rods of soft iron are connected and held in position between the pole-pieces of two U-shaped magnets by flexible reeds *RR*. The system is symmetrical about the centre line. The magnets are arranged so that the polarity of the pole-pieces is that shown in the diagram. By itself each iron bar would normally move inwards, but in conjunction with the reeds and connecting rod a balanced system is formed. Coils of wire are wound round alternate limbs of the pole-pieces. During operation the magnetic field in the air-gap at one side is strengthened, whilst at the other it is weakened. This is obtained by suitable coil connexions. Thus during one half-cycle one bar moves into a stronger field and the other into a weaker field, the position being reversed in the next half-cycle. The mechanism oscillates, therefore, at the same frequency as the current. The paper cone, complete to the vertex, is secured to the connecting rod by the usual conical nuts. It is supported at its periphery by a leather surround. The lowest natural frequency of the system depends upon

three things, (a) the effective mass of the whole diaphragm plus the driving mechanism; (b) the combined stiffness of the reeds and the surround; (c) the strength of the magnetic field. In the absence of coil current, a definite force is required to overcome the stiffness of the reeds and surround together with the magnetic attraction. If the relationship between magnetic pull and displacement is linear of the form  $f_1 = s_1 x$ , and if that for the mechanical part of the system is also linear, say  $f_2 = s_2 x$ , we have  $f_1 + f_2 = f = x(s_1 + s_2) = sx$ , where  $s$  is the combined stiffness of the system. Treating the arrangement

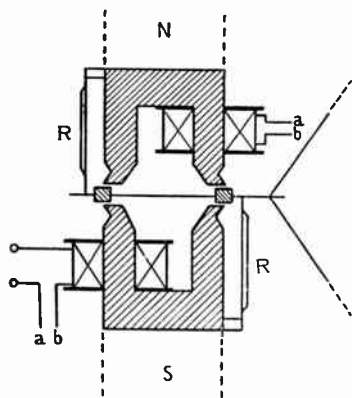


FIG. 76.

To avoid reduction of output in this region the mass of the driving mechanism should be small. The remarks concerning baffles and the like apply equally to this case. There is a definite tendency for the lower register to be accentuated unless the mechanism is adequately damped. A representative inductor speaker is illustrated photographically in Fig. 77 [190].

#### 4. Balanced armature mechanism

This form of reed movement is shown diagrammatically [218] in Fig. 78. The flat stiff reed is kept in its equilibrium position between two pole-pieces  $NS$  associated with a powerful permanent magnet. The operating coils encompass the reed and reside within the U-shaped pole-pieces. During idle periods the magnetic flux passes directly from  $N$  to  $S$  at each side as indicated. When current flows in the coils

$\omega = \sqrt{(s/m_e)}$ , where  $m_e$  is the effective mass of the diaphragm including the accession to inertia  $m_i$  (Chap. III). As a first approximation, below  $100 \sim m_e$  is the sum of the natural mass and  $m_i$ . The stiffness is adjusted to make the natural frequency about  $70 \sim$ . To determine the frequencies of the higher vibrational modes of the system, it is necessary to have recourse to experimental methods.

As in certain other speakers, the upper register is due mainly to vibrational modes of the cone.

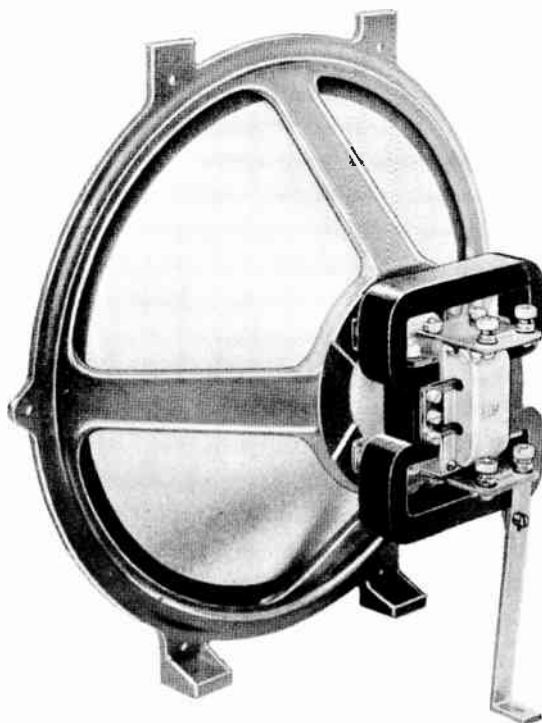


FIG. 77. Inductor dynamic loud speaker.



the reed is magnetized and attracted alternately to each side. In the absence of constraint, if the reed were given a slight motion towards one side, it would move on to the pole-piece, since in the central position it is in unstable equilibrium. It is necessary, therefore, to introduce some form of elastic control. Either the reed is mounted on a torsional member or it is associated with some form of cantilever or other spring. The natural frequency, in the absence of the cone, etc., may be about 2,000  $\sim$ . The movement is attached to a paper cone as shown schematically in Fig. 75 B. Owing to increase in magnetic force as the reed approaches the pole-pieces, the relation-

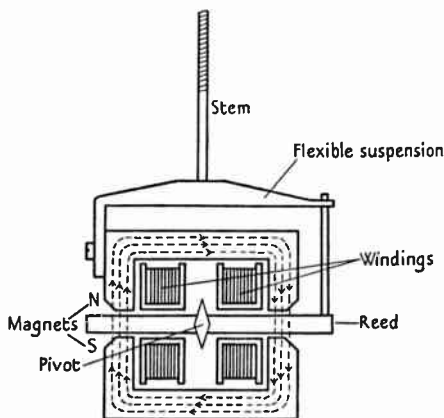


FIG. 78. Diagram illustrating balanced armature reed movement.

ship between current and deflexion is not linear for amplitudes of the order required to radiate middle or low frequencies at the proper strength. The output when large tends to be tinged with alien frequencies, since the current-displacement curve is linear over a small region only. It has an advantage over the simple 'uncorrected' cantilever type, since the characteristic is symmetrical and the linear amplitude range greater.

### 5. Moving-coil hornless speaker

The principle involved in this type of driving mechanism is illustrated [87] in Fig. 79. A permanent magnet or an electromagnet is used to create a radial flux in a circular gap of short radial length. The circular coil of wire is held concentrically in the gap by aid of a centring



device. When a current passes through the coil, it is impelled axially either one way or the other, according to the direction of the current. It will be noticed that the radial field is everywhere at right angles to the coil, and therefore to the current sheet therein. Consequently the motive force due to the interaction of the two magnetic fields is at right angles to both the radial field and the plane of the wire, i.e. in an axial direction.

If the coil current is constant at all frequencies, it might be inferred that the driving force is invariable. Owing to losses in the iron core

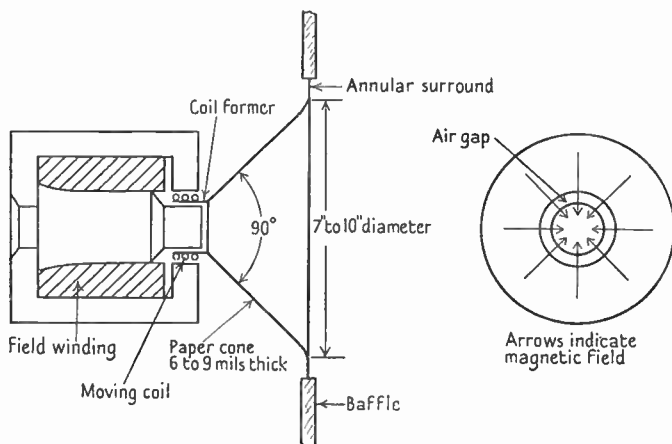


FIG. 79. General arrangement of moving-coil hornless speaker.

of the magnet there is a phase difference between the alternating current in the moving coil and the flux it produces. In fact the current can be resolved into a magnetizing component and a loss component in quadrature. The magnetizing component is from 0.9 to 0.95 of the total current, but its value depends upon the type and material of the magnet and the frequency of the current in the moving coil. Except for this, which from an acoustical viewpoint is not very serious, the force is proportional to the current—within limits—and independent of frequency. This seems to put the hall-mark of perfection on the coil drive, apart from any idiosyncrasies introduced by the diaphragm. Owing, however, to variation in the radial field along the axis of the coil (Chap. XIV) and to the large amplitudes necessitated at low frequencies, care must be exercised in design and operation to avoid the creation of alien frequencies.

The coil is usually associated with a conical paper diaphragm supported annularly at its edge. In commercial speakers the annulus is frequently some type of leather. It should be elastic over a reasonable diaphragm amplitude, i.e. the relationship between force and axial constraint should be linear over the working range. In many cases this does not hold, and the low-frequency amplitude is restricted, with consequent flattening of the wave form, thereby introducing alien frequencies. These may occur in a part of the audible spectrum where the ear is highly sensitive [211]. To ensure absence of wobble, centring of the coil in relation to the magnet pin is imperative. Various forms of centring device are illustrated in Fig. 26. This component must also have a linear force-displacement characteristic over the normal working amplitude. The annular surround and the centring device, together with the diaphragm, form a low-frequency resonating system. In many moving-coil speakers low-frequency resonance is used to obtain an adequate bass output in order to balance that in the upper register due to the cone resonances. As in other species of hornless speaker, a baffle is required to reduce the interference or short-circuit effect due to sound waves of opposite sign from the two sides of the diaphragm. For household purposes flat baffles give better quality than a cabinet full of radio gear. A properly designed box baffle with absorbent material arranged as shown in Fig. 120 is a very good solution of the problem [180], but there must be no radio gear to impede the sound waves. Since the lower register in this type of speaker is much more powerful than in reed types, cabinet resonances must be carefully avoided.

By using a directional baffle (which is really another name for a horn), the resistive load on the diaphragm and, therefore, the efficiency can be increased to several times the value with a flat baffle. A speaker of this type is described in Chapter XX.

## 6. Moving-coil membrane speaker

In another type of speaker the moving coil is attached eccentrically (1.6 cm. out of centre) to a stretched circular membrane of aluminium foil 26 cm. in diameter\* and 0.002 cm. thick. The foil is kept taut by two clamping rings, these being held between two felt rings in an outer metal framework. The system is one having a large number of

\* The diameter and thickness can be varied according to the frequency range to be covered by an individual speaker.

resonances or vibrational modes in the audible frequency range, the lowest being in the neighbourhood of 100  $\sim$ . There are several modes per octave in the upper register, but none is unduly prominent. The focusing or beam effect at the upper frequencies (see Chap. V) is much less marked than that obtained with a conical diaphragm. In fact up to 4,000  $\sim$  the distribution is fairly uniform. From the viewpoint of rigid disk theory this is equivalent to a reduction in the radius with increase in frequency [90 a].

By making simple assumptions, e.g. that the drive is concentric instead of eccentric, an approximate theory of the speaker can be deduced by aid of Chap. IV, § 13, Chap. V, § 4, item 16, Table 7, and Chap. VI. The theory of the membrane type electrostatic speaker, driven uniformly over the whole surface, will serve as a useful guide (Chap. IX, § 8). The sound distribution can be calculated from formula 16, Table 7. This formula is based upon the shape of the membrane *in vacuo*. An alteration occurs during vibration in air, so it is advisable, before coming to any definite conclusion, that the sound distribution found experimentally should be compared with that obtained by calculation.

## 7. Blatthaller speaker

In the moving-coil speaker with a conical diaphragm the force is applied to a narrow annulus near the vertex of the cone. At high frequencies the system does not behave as a rigid structure, and there is a phase difference between the velocity at the coil and that further down the cone. When it is desired to radiate appreciable acoustic power, a diaphragm of large superficial area is required. If a circular moving coil and a very large cone were used, the above phase effect would be injurious to good reproduction. By distributing the driving force over the surface of the diaphragm, the frequency at which the phase difference becomes serious can be elevated considerably. This principle is illustrated in Fig. 80 [12, 13, 203, 204]. A large corrugated duralumin plate, or several smaller plates side by side, is covered with low resistance copper conductor in zigzag fashion. The conductor is situated in a strong magnetic field ( $2 \times 10^4$  lines  $\text{cm.}^{-2}$ ) normal to its length and parallel to the plane of the diaphragm. To reduce leakage, which tends to be large in a magnetic system of this configuration, the field coils are situated directly round the air-gap, i.e. the latter is at the centre of the coil as illustrated in

Fig. 80. This blots out a portion of the sound radiation, but is not so serious as might be imagined, because the air gets squeezed out transversely. Such magnet design is much more effective than that where the coils are free of the diaphragm altogether. The air-gap and flux density between adjacent pole faces is such that the force per unit area amounts to as much as 20 Kg. With an input power of 800 [13 b] watts to the diaphragm conductor, the sound output is said to be 200 watts, giving an efficiency of 25 per cent. This high value can

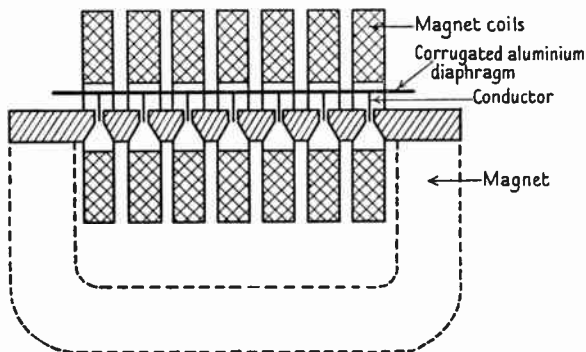


FIG. 80. Arrangement of magnet and diaphragm in Blatthaller speaker.

only be realized in a flat baffle system by aid of an intense magnetic field, a conductor of low resistance and a large radiating surface of small mass (Fig. 81). Assuming the diaphragm to be equivalent to a rigid circular disk 50 cm. radius, the external medium is matched resistively from 200  $\sim$  upwards (definition 20 and Chap. VIII). As we have already shown in Chap. V, § 3, owing to focusing there is a dearth of higher frequencies *outside* a relatively narrow central sound beam. Moreover, unless resonance occurs at higher frequencies, the radiated power for constant input will fall with rising frequency. By appropriate orientation, several units can be used to cover a wide angle.

### 8. Riffel speaker

This instrument is somewhat similar to the Blatthaller, but differs constructionally. It consists of a long straight conductor in the air-gap of a powerful electromagnet dissipating about 200 watts. The conductor is fixed to the bottom of a V-groove at the centre of

a corrugated rectangular aluminium diaphragm and lies along its length. The transverse rectangular corrugations extend almost to the long edges which are clamped and act as hinges. During operation the conductor moves parallel to itself, and the V-groove permits the diaphragm to bend so that there is but little mechanical constraint, i.e. the fundamental frequency is very low. Although this type of speaker gives good quality it is too inefficient to be used for commercial purposes. The diaphragm is usually set in a large flat baffle.

### 9. Horn loud speaker

In general this type of speaker is actuated by a moving coil driving a small diaphragm within the coil [9, 18], as shown in Fig. 82 A.\* The coil and diaphragm is attached to a flexible annulus whose outer edge is securely clamped to an electromagnet. The natural frequency of the combination on the annulus depends upon the frequency range of the loud speaker. For the range 60 to 4,500  $\sim$  it is usually about 400  $\sim$  *in vacuo* with the coil circuit open [18]. The diaphragm is shaped to spherical curvature to give rigidity,† so that it moves as a whole over a wide frequency band. It breaks up at higher frequencies and assists in keeping the output fairly constant above 2,000  $\sim$ . The obstruction *H*, apart from reducing the throat area and thereby increasing the air particle velocity, acts as a phase equalizer. The clearance between the diaphragm and *H* gradually increases with the radius. Thus during vibration the velocity of the air particles most remote from the throat of the horn is increased. This ensures that up to quite high frequencies the pressure from all parts of the diaphragm arrives at the horn throat in substantially the same phase. Another device for accomplishing the same purpose is shown in Fig. 163.

In the unit illustrated in Fig. 82 B the coil is a single layer of aluminium ribbon [18]  $1.5 \times 10^{-2}$  in. wide  $2 \times 10^{-3}$  in. thick wound on edge. The 50 turns are held together by a film of insulating lacquer  $2 \times 10^{-4}$  in. thick, the coil being baked after winding. This type of coil is self supporting and 90 per cent. of it is metal. It can be made accurately to specified dimensions, thus permitting small clearances between it and the pole-pieces. This is of material assist-

\* Special high-frequency horn speakers are described in Chap. XX, § 16.

† Some idea of the enormous increase in rigidity when diaphragms are *conical* will be gleaned from Chap. XVIII, § 21.

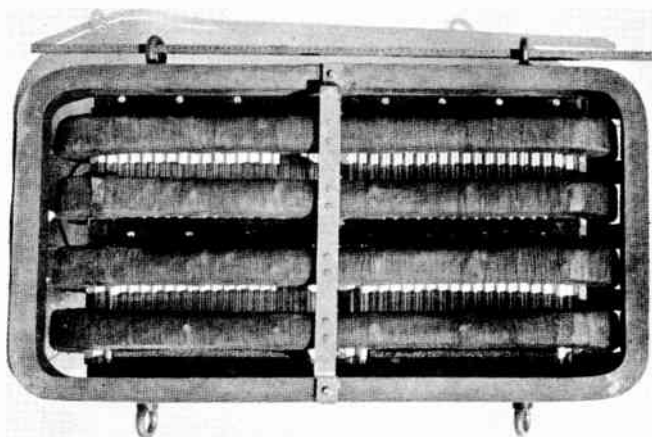


FIG. 81. Photograph of large Blatthaller speaker showing field coils and corrugated duralumin diaphragm [13 b].

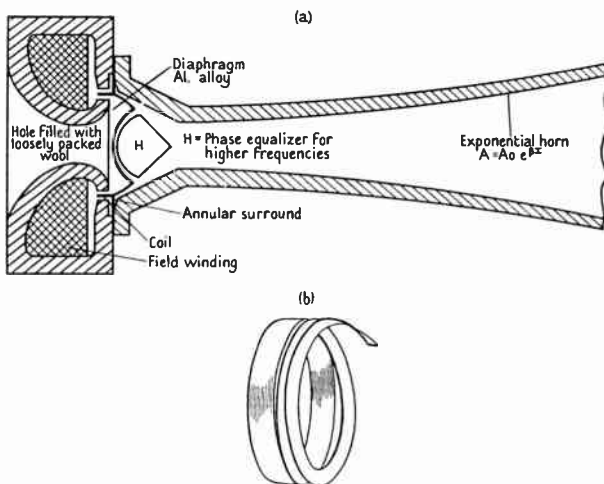


FIG. 82. (a) General arrangement of small diaphragm type moving-coil horn speaker; (b) coil of aluminium tape (on edge), 2 in. diam., 0.015 in. wide, 0.002 in. thick, insulating lacquer 0.0002 in. thick [18].



ance in obtaining the high flux density of 20,000 in the air-gap, and in the dissipation of heat via the electromagnet. The influence of radiation from the black outer surface of the latter is very marked. For an input of 10 watts the temperature rise of the coil is  $64^{\circ}\text{C}$ . in the magnet and  $116^{\circ}\text{C}$ . out of it. As shown in Fig. 82 A, the back of the magnet is flared to avoid tube resonance. This cavity is usually loosely packed with absorbent material. The efficiency of a receiver of this type with a suitably designed exponential horn is 30 per cent. over a wide frequency range. This aspect of the subject is discussed in Chapter XV.

### 10. Use of lever mechanism for altering amplitude

In all types of drive discussed hitherto there is a definite amplitude limitation beyond which alien frequencies become serious. The maximum permissible amplitude depends upon the driving mechanism. It is much greater for a moving coil than for a stiff cantilever reed whose natural frequency exceeds 2,000  $\sim$ . The greatest amplitudes are required at low frequencies, and it is now proposed to see what happens when a simple mechanical transformer, i.e. a lever, is used. At first sight it may appear that a definite advantage will be gained by using a small movement for the driving mechanism and a large one for the diaphragm. The scheme is illustrated diagrammatically in Fig. 83 the lever ratio being  $l_2/l_1 = n$ . To simplify the analysis the lever will be regarded as a massless ratio-arm. The resistance at *A* is  $r_2$  and the reactance  $\omega m_e$ , where  $r_2$  is due to mechanical loss in the cone and sound radiation, whilst  $m_e$  is the effective mass of the cone together with its attachments. At *B* the resistance is  $n^2 r_2$  and the reactance  $\omega(n^2 m_e + m_c)$ , where  $m_c$  is the mass of the driving coil and its attachments. If the driving force is  $f$ , the coil velocity is

$$v_1 = \frac{f}{z_1} = \frac{f}{\sqrt{\{n^4 r_2^2 + \omega^2(n^2 m_e + m_c)^2\}}}$$

The power radiated as sound is  $v_1^2 n^2 r_r$ , where  $r_r$  is the resistance at *A* due to sound radiation. Thus the sound power is

$$P = \frac{n^2 f^2 r_r}{n^4 r_2^2 + \omega^2(n^2 m_e + m_c)^2}$$

At any particular frequency the power is a maximum when

$$n^2 = \frac{\omega m_c}{\sqrt{(r_2^2 + \omega^2 m_e^2)}} = \frac{\text{coil reactance}}{\text{diaphragm impedance}}$$



this being analogous to the case of an electrical transformer. Measurements of  $r_2$  and  $m_e$  (Chap. XVI) reveal variation in both quantities throughout the frequency range. The diaphragm impedance attains a maximum at low frequencies, after which it fluctuates and becomes small in the neighbourhood of the vibrational modes. Thus no optimum lever ratio exists for a wide band of frequencies. At low frequencies  $r_2 \ll \omega m_e$ , so  $n = \sqrt{(m_c/m_e)}$ . Now  $m_e \gg m_c$ , so that  $n$  should be less than unity. This entirely defeats our proposal to reduce the coil amplitude and, in fact, actually increases it. At high frequencies where  $m_e$  is small the lever ratio exceeds unity. It follows,

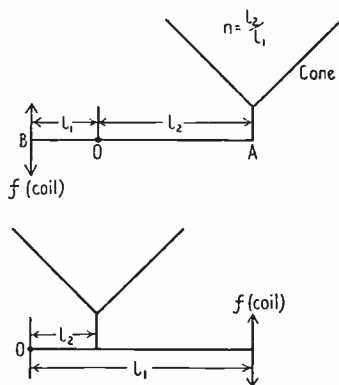


FIG. 83. Diagram illustrating lever principle applied to hornless loud-speaker mechanism.

therefore, that the use of a lever ratio exceeding unity will reduce the lower frequencies at the expense of the upper, and this is corroborated by experiment. In fact, variation in lever ratio constitutes a form of tone control. With any type of driving unit there is a certain lever ratio which gives the best result over a specified frequency range. Its value can be found experimentally. In a cantilever reed drive the ratio is less than unity. This gives the middle frequencies a better chance to reveal themselves.

### 11. Rectangular membrane condenser speaker

A cross-section of a portion of the instrument is given in Fig. 84 A.  $a$  is a rigid corrugated plate [23, 28, 29] with perforations whilst  $b$  is a special rubber type dielectric about  $1.2 \times 10^{-2}$  cm. thick, the outer surface of which is coated with beaten metal leaf about  $2 \times 10^{-4}$  cm.

thick. The speaker is made up in  $8" \times 12"$  units of this type. The longitudinal corrugations are  $3 \times 10^{-3}$  cm. deep and 1.9 cm. between adjacent crests. The working polarizing voltage varies between 500 and 600, this high value being essential to produce pure tones with a moderate signal voltage and reasonable efficiency. If the voltage is too high, the dielectric is drawn tightly against the fixed plate, thereby restricting the amplitude and the output. During operation the rubber, so to speak, rolls down the depressions in the fixed plate.

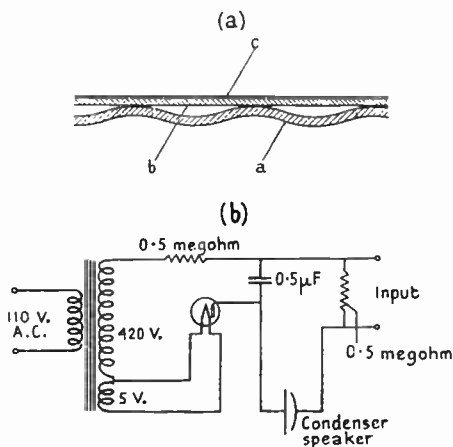


FIG. 84.

(a) Cross-section of electrostatic speaker [28, 29].

(b) Biasing unit for electrostatic speaker.

It is thereby in direct tension, which is very different from compression between two flat surfaces as in Fig. 56 A. This action occurs to an extent when the polarizing voltage is high and the rubber is drawn to fit the curvature of the fixed plate. The direct tensile action enables a greater amplitude to be obtained for a given signal strength.

Response curves taken with constant input voltage indicate general flatness from  $100 \sim$  to  $1,000 \sim$ , after which there is a strong rising characteristic to a maximum at about  $5,000 \sim$ . Thereafter the curve drops slowly, but the output is considerable at  $10^4 \sim$  [23]. The curve is said to be singularly free from irregularities. Two types of output circuit are shown diagrammatically in Figs. 56, 84 B. The voltage across the speaker gradually decreases with rise in frequency owing to fall in its impedance. Typical curves for various values of  $R_a C_0$

combinations are given in Fig. 85.\* By automatically reducing the signal voltage in this manner—due to increased  $R_a I$  drop in the valve—the rising characteristic of the speaker can be offset as described in Chapter IX. A suitable value of  $R_a C_0$  for a unit  $8 \times 12$  in. is  $6.5 \times 10^{-5}$ , where  $R_a$  is in ohms and  $C_0$  in farads. For a 24-section speaker  $R_a C_0 = 1.8 \times 10^{-4}$ , this larger value being required, since the focusing of the radiation is greater than with a single section. The

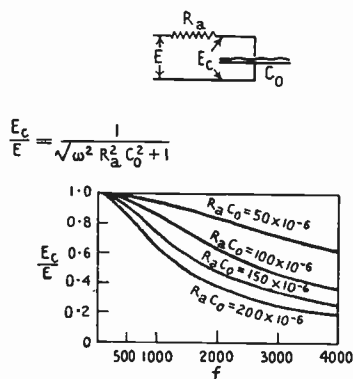


FIG. 85. Voltage division between valve and condenser.  $E_c/E$  is the fraction of the applied voltage across the condenser.

angle of the high-frequency† beam is about  $15^\circ$  on each side of the normal to the armature [23]. As in other classes of speaker a baffle is used.

## 12. Circular membrane condenser speaker

The arrangement is shown diagrammatically in Fig. 59, where the very thin diaphragm of aluminium alloy [31, 32, 33] under radial tension is symmetrically situated between two grid-like electrodes (see Fig. 86). The perforations in the electrodes permit sound radiation. A polarizing or steady direct voltage of 1,500 is applied between each fixed electrode and the diaphragm, so that it is pulled equally in both axial directions being therefore in static equilibrium. Signal voltages up to a maximum of about 400 are applied across the fixed electrodes. This causes the potential difference on one side to fall and on the other to rise by the same amount. Thus the attraction on one side is

\*  $R_a$  is the power-valve resistance and  $C_0$  the capacity of the speaker.

† Precise frequency unknown.

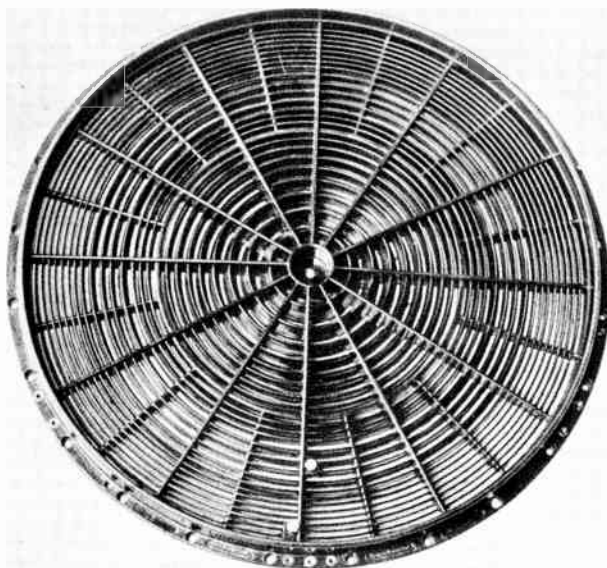


FIG. 86. Photograph of electrode of stretched membrane electrostatic speaker [31, 32].

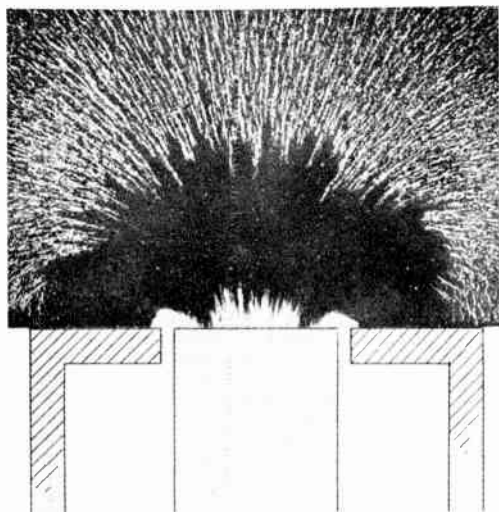


FIG. 88. External leakage flux distribution in electromagnet with full excitation.



reduced whilst on the other it is increased, so the diaphragm oscillates with the alternating current. The arrangement although dependent solely upon attraction can be regarded from an analytical viewpoint as 'push-pull'. Actually of course it is a differential action. As with other speakers a baffle is necessary to reduce interference between the front and rear of the diaphragm.

The diaphragm is in reality a radially tensioned membrane 38 cm. diameter, its mass per unit area being  $4 \times 10^{-3}$  gm. This corresponds to a thickness of  $1.5 \times 10^{-3}$  cm. (0.6 mil) and a density of about 2.7 gm. cm.<sup>-3</sup>. The distance between the diaphragm and the electrodes gradually increases from the edge to the centre since the amplitude of vibration is greatest there.

The electrodes are made of bakelite and coated with an electrically conducting colloidal carbon mixture. This layer is then covered with an insulating material having a nitro-cellulose base and containing mineral products. It is thickest at the edges of the electrodes, the disruptive strength being 2,000 volts A.C. As would be expected from theoretical considerations (Chap. IV, § 14) the diaphragm exhibits vibrational modes which can be demonstrated in the usual way by aid of fine sand. The disposition of the sand indicates that there is an appreciable amount of damping of the diaphragm. If the damping were small the sand would form a thin line at the edge and at a nodal circle. The influence of loss on the shape of the diaphragm\* is discussed in Chap. IV, § 17. From Fig. 86 it is seen that the ribs of the electrodes are broadened at certain places to increase the damping and subdue the lower vibrational modes, since they are the most powerful. The first vibrational mode occurs about 130 ~. It is much lower than the value *in vacuo* owing to accession to inertia as described in Chap. IV, § 16. In a moving-coil speaker the large back e.m.f., induced in the coil when the diaphragm resonates on the surround, is accompanied by a large decrease in operating current (Fig. 149). A similar but less pronounced effect occurs when a diaphragm resonates in an electrostatic field.

The output circuit from the power valve can either be a resistance-capacity, choke-capacity, or a transformer type, as shown in Fig. 59. It appears that the voltage across the speaker should fall with frequency, as in Fig. 85, to avoid accentuation of the higher frequencies [32]. The theory of this speaker is given in Chap. IX, § 8.

\* During vibration, i.e. the dynamic deformation surface (see definition 37).

## XIV MAGNETS

1. A conventional design of electromagnet for hornless moving-coil loud speakers is illustrated diagrammatically in Fig. 87. The magnetic flux passes from the central pole to the outer pole ring, or vice versa,

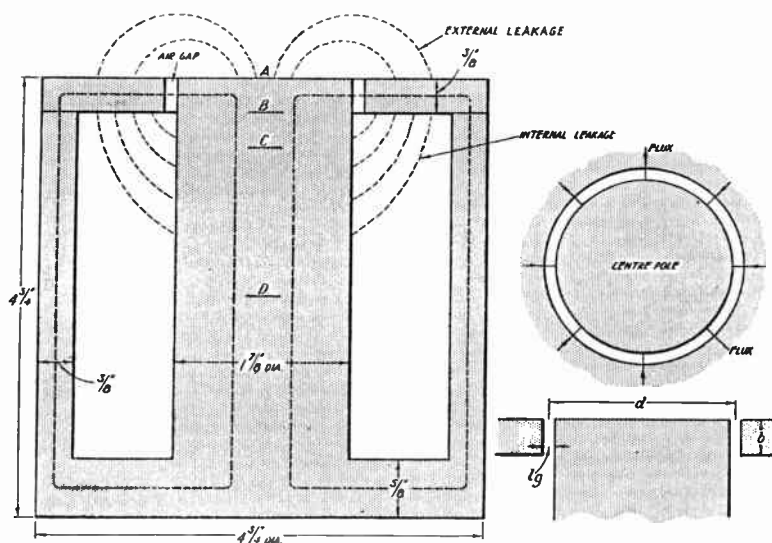


FIG. 87. Dimensional drawing of a typical electromagnet as used for the measurement of flux density.

according to the so-called polarity, i.e. North or South. Part of the flux traverses the air-gap and is disposed radially. This is the useful or working flux. The remainder 'leaks' out of the gap and follows the dotted paths within and without the magnet. Fig. 88 is a photograph of leakage flux taken by placing a piece of sensitive paper in front of the magnet, sprinkling iron filings on it and exposing to sunlight. Full field strength was employed and the flux paths near the magnet have not been reproduced in the figure, since the attractive force was strong enough to overcome the friction between the filings and the sensitive paper. Moreover, all the filings within a certain area were drawn to the magnet and can be seen adhering to the pole-pieces.

There are two principal methods of measuring flux in the air-gap of a magnet: (1) by weighing, (2) by fluxmeter or ballistic galvanometer using a search coil. Before embarking upon a description of these methods, it is well to examine the nature of the system upon which it desired to make measurements. If the central and outer pole-pieces are truly concentric and the constructional materials magnetically homogeneous, the radial field will be symmetrical about the polar axis of the magnet. Consider a plane passing through the longitudinal centre of the gap. In the event of symmetry on each side of this plane the magnetic field will be symmetrical, but not necessarily

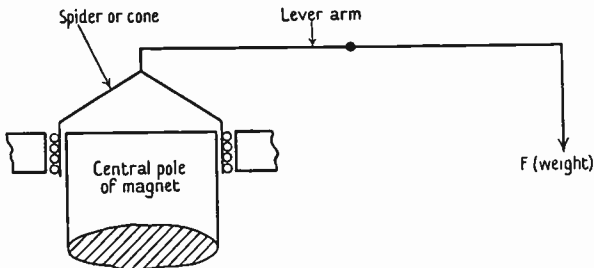


FIG. 89. Lever arrangement for flux measurements.

the same at various distances from the plane, owing to leakage from the inner and outer pole cheeks. The design of Fig. 87 is asymmetrical since the magnet is wholly on one side. It follows that the leakage will be different at each end of the gap. This, however, does not have a serious effect on the flux distribution in the gap. Since the air-gap is in parallel with the leakage paths, the reluctance is modified, and the radial field strength is substantially uniform over only a fraction of the axial length.

Coming now to methods of measuring the gap flux, No. 1 is quite simple but not conducive to high accuracy unless precautions are taken. It does, however, have the merit of measuring the field under conditions more closely allied to practice than No. 2. The schematic diagram in Fig. 89 illustrates the basic principle. The coil is attached to a lever mechanism and the force upon it, due to a given current, is balanced by a weight. The force in dynes is  $2\pi rn B_g I$ ,  $I$  being in absolute units. Thus  $B_g$  can be calculated. The essential difference between the above condition and that in practice is twofold; (a) the coil is in vibration, (b) the current is alternating which may influence



the distribution. However, the field can be measured with a speaker coil carrying a steady current of the order of magnitude used in practice. This current will undoubtedly modify the field distribution, but the modification is not likely to be serious with a powerful electromagnet.

In the second method the undisturbed distribution of field is obtained by aid of a search coil [100 a, b]. The flux measured is that interlinked with the coil and passing through the area encompassed

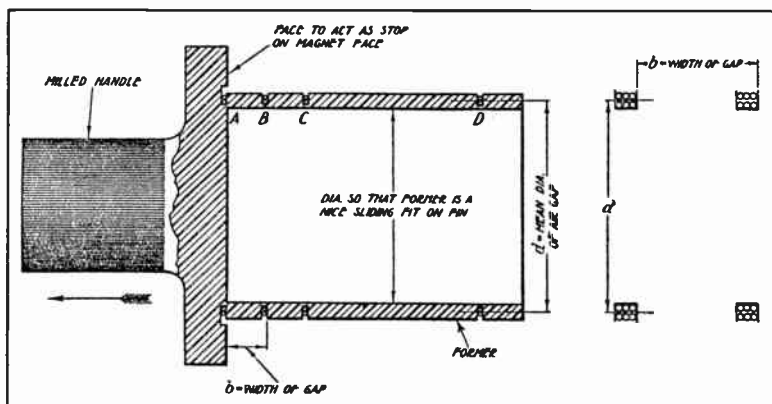


FIG. 90. Diagrammatic sketch of differential search coil. The leads from the coils are flexed and brought out through the handle. They may be taken to terminals or to a switch which enables coils to be used separately or any pair connected in opposition. Great accuracy accrues when the axial length of the coils is as small as possible. This is due to the flux density not being uniform.

by it. The magnetic field in Fig. 87 passes radially through the surface of the coil, but to complete the magnetic circuit it must go down the central pole in an axial direction. Consequently the flux passes through the area encompassed by the coil. This flux is the sum of the active gap flux plus the external leakage. In measuring the former it is essential to eliminate the latter from the meter reading.

Two narrow low-resistance coils *A*, *B*, identical in all respects, and separated by the axial length of the gap, are shown diagrammatically in Fig. 90. The external leakage and the working flux pass through *B*, but only the leakage flux through *A*. If these coils are connected in opposition and joined to a fluxmeter or to a ballistic galvanometer, double the flux interlinkage (line-turns) is obtained on reversing the field current of an electromagnet. In this way the total useful gap

flux can be found for various degrees of magnetization. By winding *A* and *B* on a former and either inserting it in or withdrawing it from the magnet, the gap flux is obtained. The scheme just described is known as the differential coil method [100 a].

If coil *B* is used alone and drawn from one end of the gap to the other, the whole gap flux is cut. Consequently the fluxmeter or ballistic galvanometer measures the flux-interlinkage. Both methods permit the rapid testing of either permanent magnets or electromagnets in a factory. The axial distribution of flux is of importance in considering the production of alien tones caused by large low-frequency

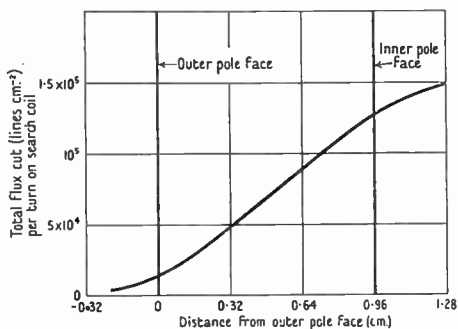


FIG. 91. Diagram illustrating method of measuring flux at any point along the axis of a speaker magnet.

amplitudes. To determine this the foregoing methods can be modified slightly. By constructing a former with a number of closely spaced coils, each pair can be used in turn to determine the flux in the intervening space. This also applies to measurement of leakage flux within and without the magnet. The field current can be reversed or the former withdrawn from the magnet. As an alternative a single coil can be used. By means of a micrometer screw [100 b, 104], it can be inserted at various distances inside or outside the magnet. When the coil is withdrawn or inserted, it cuts all the flux between its initial and final positions. The flux-displacement curve so obtained takes the form illustrated in Fig. 91. The ordinate anywhere represents the total flux cut up to that point (abscissa). The flux density can be determined either directly from the reading or by aid of the curve. If  $\delta x$  represents a small axial displacement, the area through which the flux passes radially is  $2\pi r\delta x$ , where  $r$  is the mean coil radius.

The total flux passing through this area is  $\delta\Phi$ . Thus the flux density at the midpoint of  $\delta x$  is  $\delta\Phi/2\pi r \delta x = B_g$ . In the limit when  $\delta x$ ,  $\delta\Phi$  are infinitesimal, the flux density is

$$B_g = \frac{1}{2\pi r} \frac{d\Phi}{dx} = \frac{\text{slope of curve}}{\text{mean circumference of coil}}$$

The two curves illustrated in Fig. 92 were obtained in this way. The flux obtained by withdrawing a single coil from the position C, Fig. 87,

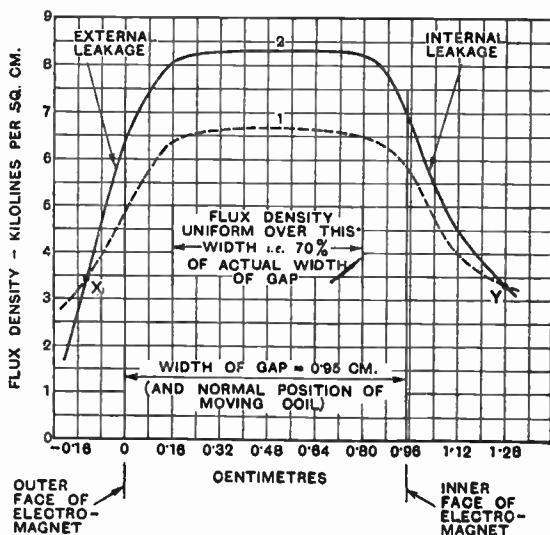


FIG. 92. Diagram showing distribution of flux in air gap of electromagnet of Fig. 87. Curve 1 is for a gap of  $\frac{1}{8}$  in. (0.32 cm.) and curve 2 for a gap of  $\frac{3}{32}$  in. (0.24 cm.). It should be observed that the leakage with the smaller gap falls below that for the larger gap at the points X, Y.

exceeds appreciably that on withdrawal of a differential coil whose axial length is that of the gap. This shows that a considerable proportion of flux 'leaks' and does not enter the annular air-gap. The percentage leakage, however, is not an absolute criterion of the efficacy of the magnet. The proportion of the total m.m.f. acting at the gap is the important item. In the ideal case, i.e. with a magnet of infinite permeability, all the m.m.f. would be expended at the gap. Under this condition the m.m.f. is  $B_g l_g = 1.257nI$ , where  $nI$  is the total ampere turns and  $l_g$  the radial length of the gap. Data are given in Table 16

showing, (a) the gap flux density  $B_g$  calculated from this formula, (b) that obtained by experiment. The ratio of the two (b/a) represents the proportion of the total ampere-turns spent on the gap. The remainder is wasted on the reluctance of the magnet and in creating leakage. The leakage and main magnet paths are in parallel, and for this reason the large relative value of the leakage flux must not be regarded too seriously. Owing to decrease in permeability of the magnet with increase in flux density, the m.m.f. expended thereon increases also. This is illustrated by the data [100 a] in Table 16.

TABLE 16

Dimensions of gap:  $l_g = 0.238$  cm., axial length 0.95 cm., mean diameter 5 cm.

Total ampere turns on magnet	Gap flux lines cm. <sup>-2</sup>		Percentage Ratio (b/a)
	Theoretical (a)	Actual (b)	
1,000	5,280	4,600	87
2,000	10,560	8,600	82
3,000	15,840	10,600	67

It should be noted that the leakage flux is not the difference between columns (2) and (3).

With 3,000 ampere-turns the proportion of total magnetomotive force at the gap is less the shorter the latter. This is due to the greater flux density which is associated with lower permeability of the magnetic material.

The influence of reduction in the radial length of the gap is exhibited in Fig. 93. The gap density is increased some 25 per cent. by a corresponding air-gap reduction from 0.32 to 0.238 cm. A further decrease to 0.16 cm. would give a density of about 12,000 compared with 8,000 for 0.32 cm. The number of ampere-turns is 2,650, entailing a watt loss of 33. The futility of cast iron for loud speaker magnet construction is clearly indicated by curve 3, Fig. 93, and column 4, Table 17. This is due to the low permeability of the material.

TABLE 17

Total ampere turns on magnet	Percentage of total ampere-turns used on air-gap		
	Steel magnet 0.32 cm. gap	Steel magnet 0.238 cm. gap	Cast iron magnet 0.278 cm. gap
1,000	86	87	40
2,000	84	82	35
3,000	73	67	29

## 2. Permanent magnets

The methods of flux measurement are identical with those for electro-magnets except that there is no field winding through which the

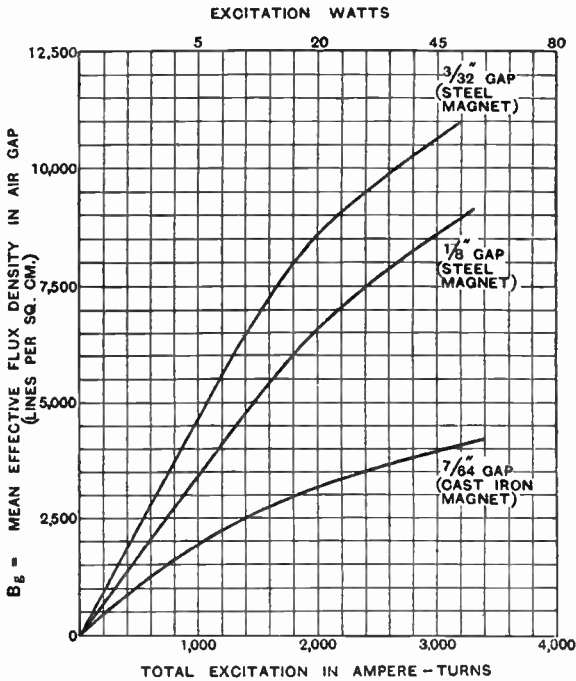


FIG. 93. Mean air-gap flux-density plotted against ampere-turns. Remanence has been neglected.

current can be reversed. In general, however, this method would not be used for an electromagnet. There are two main classes of magnet steel, (a) with a percentage of tungsten, (b) with a percentage of cobalt. The cobalt content varies up to 35 per cent. Since cobalt is an expensive metal, a 35 per cent. steel must be used in moderation where economy is concerned. The object to be attained is to produce a magnet of suitable strength and dimensions at a reasonable price. With this end in view it is customary to employ magnet steel containing from 9 to 15 per cent of cobalt, although 35 per cent. is used in certain cases. The leakage in a permanent magnet is usually higher than that in an electromagnet working under similar conditions, i.e. gap density, area, and length. To obtain densities of the same order

as those cited in connexion with electromagnets would necessitate a large, heavy, and relatively costly permanent magnet. An approximate outline of the factors governing the design of permanent magnets is given below.

The  $(B, H)$  quadrant of a typical 9 per cent. cobalt magnet steel is shown in Fig. 94, curve 1. This represents the relationship between the flux density and the demagnetizing or negative value of  $H$  in a uniform ring of magnet steel having no air-gap. As soon as an air-gap is introduced, conditions are changed. Point  $B_{rem}$  on the curve is obtained by highly magnetizing an endless test piece and then removing the magnetization. To obtain the quadrantal curve the magnetization is reversed until the value  $H_c$ , known as the coercive force, is reached. In practical magnets demagnetization is caused by surface polarity incident to the presence of an air-gap, but it never reaches so far as the point  $H_c$ .

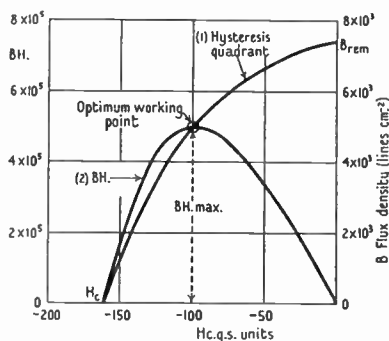


FIG. 94. Hysteresis quadrant and  $BH$  curve for 15 per cent. cobalt magnet steel.

There is a certain point on the quadrant where the product of the ordinate and abscissa  $BH$  is a maximum, and this gives the optimum working condition. The energy obtainable with a magnet used for loud speakers, moving-coil ammeters, voltmeters, and the like is then a maximum for a given volume of metal. As shown in § 5 the power obtainable from a loud speaker is

$$P = KB_g^2 V_g f_s, \tag{1}$$

$K$  = constant. Assuming ideal conditions, where leakage is absent, the flux density in the magnet is identical with that in the gap, provided the cross-sectional areas are equal and the magnet uniform. When the area of the magnet exceeds that of the gap the density in the magnet is

$$B_m = \frac{B_g A_g}{A_m} \text{ or } B_m A_m = B_g A_g. \tag{2}$$

In practice leakage occurs along the magnet, so  $H$  varies throughout the length. Since there is no applied m.m.f.,  $B_g l_g - \int_0^{l_m} H_m dl_m$  must

be zero, i.e. the gap flux is maintained in virtue of the retentiveness of the steel. As a first approximation the variation in  $H$  along the magnet may be neglected, so we can replace  $\int_0^{l_m} H_m dl_m$  by  $H_m l_m$ . Thus in the hypothetical case of zero leakage,  $B_g l_g = H_m l_m$ . Alternatively, suppose a toroidal magnet of length  $l_m$  is uniformly wound with  $n$  turns of wire. The demagnetizing m.m.f. due to a current  $I$  is  $1.257 nI = H_m l_m$ . If the magnet is now at the same point as it is with an air-gap, the magnetic potential for the gap is equal to the demagnetizing m.m.f. or

$$B_g l_g = H_m l_m. \quad (3)$$

From (2) and (3)  $B_g^2 l_g A_g = B_m H_m l_m A_m$

or  $B_g^2 V_g = B_m H_m V_m$ ,

which with the aid of (1) gives

$$P = (B_m H_m) \frac{V_m f_s K}{8\pi}. \quad (4)$$

Thus for given power the volume of the magnet

$$V_m \propto \frac{1}{B_m H_m} \quad (5)$$

since  $f_s$  and  $K$  are fixed for any specific design. Thus the volume of the magnet is a minimum when  $B_m H_m$  is a maximum. A curve of  $BH$  against  $H$  is shown in Fig. 94, and the optimum working point is where  $BH$  has its maximum value. Using the subscript 'op' to signify optimum values for the magnet, we have, from (3),

$$l_{op} = \frac{B_g l_g}{H_{op}}. \quad (6)$$

$B_g$  and  $l_g$  are settled initially, whilst  $H_{op}$  is the value obtained from the curve where  $B_m H_m$  is a maximum. In this way the length of the magnet can be determined for the ideal case of zero leakage.

From (2)

$$A_{op} = \frac{B_g A_g}{B_{op}}, \quad (7)$$

where  $B_{op}$  is obtained from Fig. 94. This completes the design of the magnet so far as calculation is concerned.

We saw in § 1 that considerable leakage occurs in electromagnets and this applies even more acutely to permanent magnets. The percentage leakage varies with the shape and design of the magnet, but is usually from 50 to 60 per cent., i.e. the total flux is from 2 to

2.5 times the gap flux. Consequently in practical design this must be taken into account.

### 3. Effect of non-uniform axial distribution of gap flux

The force on the moving coil carrying a current  $I$  is  $CI$ . At low frequencies, if the amplitude is large, the coil moves out of the gap an appreciable distance. In so doing the mean flux density associated with it decreases, and the driving force is no longer proportional to the current. Consequently the acoustic output contains alien frequencies. If these are of sufficient amplitude and occur in the range 500 to 3,000  $\sim$  where the ear is most sensitive [211], the reproduction will be unpleasant. To radiate 0.125 watt in free air at 50  $\sim$  from a diaphragm 10 cm. radius necessitates an amplitude of 0.65 cm.\* Thus a coil used in the magnet of Fig. 87 moves well into the leakage field and distortion occurs. Another effect of the leakage field is described in § 6. Owing to reduction in radial field outside the gap the coil tends to move progressively into the weaker portion and a form of rectification occurs. Distortion is absent provided the product of mean flux density and turns is constant throughout the travel of the coil. This happens if the field is uniform and remains so despite the coil current. For large low-frequency output an axial gap length appreciably in excess of the coil length, or vice versa, is implied. The former necessitates a larger and more costly magnet. To ensure uniformity the pole-pieces can be shaped as shown [192] in Fig. 95. The inner and outer pole-pieces are chamfered at each end of the air-gap whilst the coil length exceeds the width of the parallel portion and preferably the whole gap. The flux is concentrated chiefly in the narrow parallel portion. Even though distortion of the weaker field in the chamfered part ensues, due to coil current, the flux interlinkage will be substantially constant. Whilst such a scheme is satisfactory for moderate acoustic output, it is preferable to use a special loud speaker for large low-frequency output or to adopt the horn or directional baffle type (Chap. XX).

### 4. Flux density considerations in electromagnet

In designing a loud speaker magnet it is customary to commence by specifying the dimensions of the gap and the mean flux-density required therein. Allowing for leakage, by aid of experimental

\* This applies to one side of the diaphragm in a very large baffle.



data, and knowing approximately the total flux at various parts of the circuit (from tests on similar designs), the cross-section of metal required can be allocated. When, however, we are confronted with a magnet and have no knowledge of the flux density therein, it is rather difficult to make accurate calculations. This is due to variation in permeability with flux density, and to the unknown value of the leakage. We are aware by measurement that the total flux in Fig. 87 near the base of the centre pin is about  $3.1 \times 10^5$  lines, whilst that in the gap

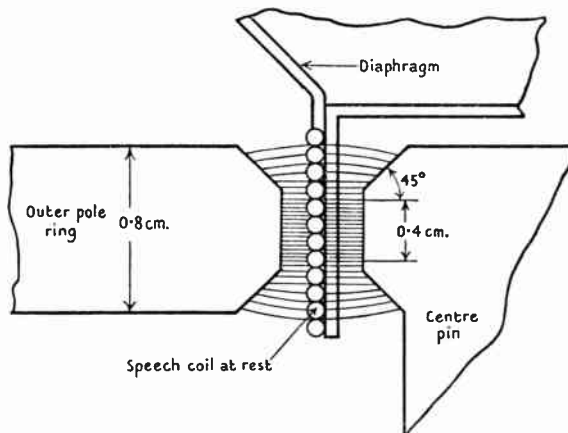


FIG. 95. Diagram showing speaker magnet with chamfered poles and coil longer than the air gap. The flux distribution is for zero coil current.

is  $1.86 \times 10^5$  lines for a certain magnetization. Unless the leakage is measured by search coils placed in various positions within and without the magnet, it cannot be known to any degree of accuracy. It can be calculated approximately, but this is a protracted process which we will not attempt here.

In the absence of leakage the total flux is constant throughout the magnetic circuit. On this basis, with the aid of well-known formulae and a permeability curve of the steel, the reluctances of the various portions of the circuit in Fig. 87, for a total flux  $\Phi = 3.1 \times 10^5$  lines, were calculated to be as follows:

Air-gap  $S_1 = 1.07 \times 10^{-2}$ ; centre pin  $S_2 = 4 \times 10^{-3}$ ; annular base  $S_3 = 4 \times 10^{-5}$ ; outer shell  $S_4 = 1.76 \times 10^{-4}$ ; outer pole ring  $S_5 = 3.3 \times 10^{-4}$ . The total reluctance is  $1.5 \times 10^{-2}$ , necessitating 3,750

ampere turns, which, in the absence of leakage, yields a gap density of  $2 \times 10^4$  lines cm.<sup>-2</sup> Comparing this with the actual case we find that 3,000 ampere turns gives a gap density of only 12,500, which emphasizes the importance of leakage and magnetic reluctance. The centre pin accounts for nearly 30 per cent. of the whole reluctance and the leakage therefrom is appreciable. Owing to crowding of the flux at the junction of the pin and the base this portion works at low permeability. It is reasonable to suppose that the design of Fig. 87 could be improved (*a*) by using a pin of material of higher permeability at large flux densities or one of ordinary material of greater cross-section, this being reduced to the diameter in the gap by a 30° chamfer;\* (*b*) increasing the thickness of the base and using a generous fillet between the pin and the base; (*c*) increasing the thickness of the outer pole ring and tapering it down slowly to the air-gap. The reluctance associated with the base and the pole ring is not conspicuous in the preceding calculations, since the assumed permeability curve was for good steel. In practice the reluctance may be important according to the magnetic quality of the metal. In case (*a*) it is feasible to use cobalt iron (not steel) for the outer end of the pin, where the diameter is reduced. Provided the price was not prohibitive this metal could also be used for the inner portion of the outer pole ring. To minimize the influence of axial non-uniformity of the magnetic field in the air-gap, the centre pin may be extended outside the outer pole ring, whilst the latter can be chamfered as shown in Fig. 95.

### 5. The output criterion of the magnet [101]

To obtain the quantity upon which the output from any given electromagnet or permanent magnet depends, it is necessary to deduce the acoustic power in terms of the flux density and the dimensions of the air-gap.

The acoustical power is

$$P = I_2^2 R_r, \quad (8)$$

where  $I_2$  is the coil current. For any given type of diaphragm, by (25), Chap. VII,

$$R_r = \varpi C^2, \quad (9)$$

where  $\varpi$  is a parameter dependent upon the diaphragm and the frequency. The current is governed by the coil impedance and the power valve resistance  $R_a$ . The former varies throughout the audible

\* See Fig. 79.

register. At electromechanical resonance, where the coil reactance vanishes, the impedance is purely resistive. For maximum distortionless output the condition is  $R_1 = \varphi R_d$ , where  $\varphi$  depends upon the valve characteristics, but usually lies between 2 and 3. The ratio of the transformer  $n_1/n_2 = \sqrt{(R_1/R_2)}$ . For maximum output  $R_1$ , and therefore the anode current (A.C.), is constant for a given grid voltage.

$$\text{Thus } I_2 = \frac{I_1 n_1}{n_2} = I_1 \sqrt{\left(\frac{R_1}{R_2}\right)},$$

$$\text{or } I_2^2 = \frac{I_1^2 R_1}{R_2} = \frac{K_1}{R_2} \quad (10)$$

since both  $I_1$  and  $R_1$  are constant.

$$\text{Now } R_2 = R_c + R_i + R_d + R_r,$$

where  $R_c$  = copper resistance of coil,

$R_i$  = electrical resistance due to iron loss,

$R_d$  = electrical resistance due to diaphragm loss,

$R_r$  = electrical radiation resistance due to sound.

The iron and diaphragm losses introduce unknown quantities, so they will be omitted, and we shall write

$$R_2 = R_c + R_r. \quad (11)$$

From (8), (10), (11) the acoustic output

$$P = \frac{K_1 R_r}{R_c + R_r}$$

$$\text{or } \frac{P}{K_1} = \frac{1}{1 + (1/x)}, \quad (12)$$

where  $x = R_r/R_c$ .

Formula (12) gives a curve of the type illustrated in Fig. 96. When  $x = 0$ ,  $R_r = 0$ ,  $P = 0$  and there is no radiation (*in vacuo*). The output depends upon\*  $x$ , and it will be regarded as the criterion of the system. The D.C. resistance of the coil is  $R_c = \rho_1 l/A$ , where  $l = 2\pi r n$ ,  $A$  = cross-section =  $bl_g f_s/n$

$$f_s = \frac{\text{total copper section}}{\text{section of gap}} = \text{space factor.}$$

Substituting above for  $l$  and  $A$  we obtain

$$R_c = \frac{2\pi r n^2 \rho_1}{bl_g f_s}. \quad (13)$$

\* This is not to be interpreted as 'directly proportional to'  $x$ .

Thus from (9) and (13)

$$x = \frac{R_r}{R_c} = \frac{\omega C^2 b l_g f_s}{2\pi r n^2 \rho_1} \quad (14)$$

Substituting  $C = 2\pi r n B_g$  in (14) we obtain

$$x = \frac{\omega}{\rho_1} [2\pi r b l_g] f_s B_g^2 = \frac{\omega}{\rho_1} B_g^2 V_g f_s, \quad (15)$$

where  $V_g$  is the volume of the annular air-gap. So far as the magnet is

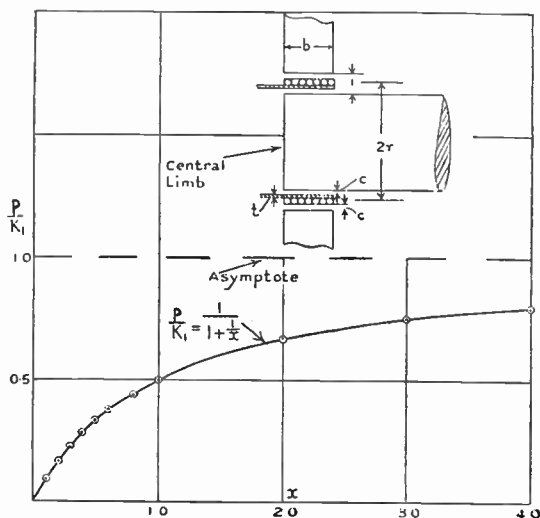


FIG. 96.

Curve illustrating the expression  $P = \frac{K_1}{1+(1/x)}$  or  $\frac{P}{K_1} = \frac{1}{1+(1/x)}$ ,  
and diagram showing dimensions of air-gap of magnet.

concerned the criterion is  $B_g^2 V_g f_s$ , this being  $8\pi$  times the magnetic energy in the volume occupied by the metal of the coil. Thus the criterion can be expressed as  $B_g^2 \times \text{volume of copper} = B_g^2 V_c$ .

In specifying a magnet, it is obvious that a statement of the flux density by itself has no value, since the gap dimensions are left out of account. Also a statement of  $B_g^2 V_g$  is meaningless, for of two magnets with equal values of  $B_g^2 V_g$  the air-gap of one might be inadequate to accommodate a suitable coil. This is where the space factor becomes important. With a gap of 0.16 cm.,  $f_s$  has a value of from 0.4 to 0.5, whereas for a 0.08 cm. gap  $f_s$  varies from 0.2 to 0.3. Consequently

the energy output from the smaller air-gap is less than that from the larger.

The problem can be viewed from another angle. With an air-gap of 0.16 cm., we could accommodate 50 turns of wire having a resistance  $R_c$ , whereas in the more restricted space available with a 0.08 cm. gap, the diameter of the wire would be much smaller and its resistance appreciably in excess of  $R_c$ . Thus the dead loss in the latter case would exceed that in the former, with a corresponding reduction in current and, therefore, in sound output.

It follows that the specification of a magnet should be accompanied by the quantity  $B_g^2 V_g f_s$  and the gap dimensions, so that  $f_s$  can be computed.

By hypothesis the  $B_g^2 V_g f_s$  criterion applies when the coil reactance is zero. If the best magnet is selected on the  $B_g^2 V_g f_s$  basis, it will fulfil the optimum condition in the lower register of an actual reproducer where iron and diaphragm loss occur. The output in the upper register is influenced by the mass, diameter, etc. of the coil, but no definite relationship has been established analytically. Moreover, it is out of the question to incorporate this in the preceding analysis.

A point of interest arises when economical considerations are waived. Assume we have a magnet with  $l_g = 0.96$  cm., the remaining quantities being equal to that of another magnet with  $l_g = 0.16$  cm. From the above criterion the output with the former magnet would appreciably exceed that from the latter. The ratio of the outputs is not  $\frac{0.96 f_s}{0.16 f_s}$  since  $P \propto \frac{1}{1 + (1/x)}$ , and it is not proportional to  $B_g^2 V_g f_s$  since the latter varies as  $x$ . With a 0.96 cm. gap a coil of 50 turns can have a very low resistance indeed, but the reactance will be unaltered. Thus the increased output will only be felt over a limited band of frequencies where the copper loss is an important fraction of the impedance. At the same time the large mass of the coil\*—unless aluminium were used—would restrict the amplitude causing a reduction in the output, particularly at the higher frequencies. Moreover, a gap of this length is of no practical value. If  $B_g^2 V_g f_s$  remains constant, an increase in radius of the coil is accompanied by a larger output. The inductive and motional capacitive reactances both

\* This statement is made on general grounds where hornless or horn speakers are concerned. If only a limited low-frequency register is to be covered, a heavy coil can be used.

increase proportionately to the square of the radius, so that the increase in output is again limited to a definite frequency band, *unless the current is constant at all frequencies*. Under the latter condition the internal resistance of the valve is so high that there is little damping of the natural oscillations, which assume undue prominence. The preceding argument shows that the quantity  $B_g^2 V_g f_s = B_g^2 V_c$  must be used with discretion.

We are now in a position to deal with the factor  $B_g^2 V_g / 8\pi$  which is sometimes cited by manufacturers as a criterion. As we have seen above, the output from a loud speaker is only proportional to  $B_g^2 V_g$  when the radiation resistance is small compared with the copper resistance. This is approximately true for a number of reproducers where the resonances are relatively weak. But it is inapplicable to a moving-coil reproducer of the horn variety where the radiation resistance is 0.3 that of the total resistance. Also we have shown by preceding examples that  $B_g^2 V_g$  has to be used in conjunction with other information connected with the reproducer. Moreover, it should be clear that  $B_g^2 V_g / 8\pi$  does not tell the whole story by any means, and that details of the air-gap are a necessary adjunct.

## 6. Rectification due to leakage field of magnet: Mathieu's equation [229]

In any circular type of magnet used for loud speakers it is obvious that the radial field must diminish rapidly, as a leakage field, outside the air-gap. At low frequencies the amplitude of the diaphragm may be so large that the coil moves well into the leakage field. The force exerted upon it, arising from the mutual influence of the current and magnetic field, is then a function of the distance of the coil from its central position.\* With a moving-coil speaker having very weak axial constraint, the diaphragm moves out of the magnet at low frequencies when the amplitude is large [100a, 101, 185]. A considerable axial force is required to restore the diaphragm to its normal position, and on removal of this force the diaphragm darts outwards again. Clearly there is a unidirectional displacement, and the action simulates rectification. In fact it has been designated electromechanical rectification.

To explain the effect it is preferable to consider a simple hypothetical case. Fig. 97A represents a circular coil situated in a radial

\* Unless the axial length of the coil exceeds that of the gap as in Fig. 95, so that the total flux embraced is the same for all working positions of the coil.

magnetic field whose strength varies linearly from the point  $O$  (compare this with the leakage field on the left in Fig. 92). The coil is fed with alternating current of constant r.m.s. value from a high resistance source. If  $A$  is the extreme position of the coil at any specified epoch, assume the current to have its maximum value  $I_{\max}$ . The coil is then momentarily at rest with maximum force urging it in the direction  $x_1$ . It moves with increasing velocity until  $B$  is reached, when the current and the driving force are zero. At  $B$  the kinetic energy  $\frac{1}{2}mv^2$  is a maximum. The coil passes  $B$  and ultimately

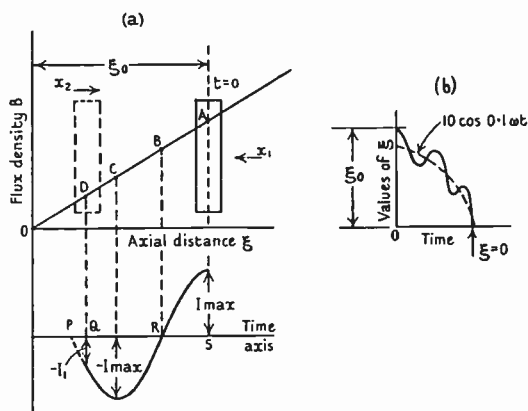


FIG. 97. Diagram illustrating electromechanical rectification effect due to a coil moving in a non-uniform radial magnetic field (Mathieu equation).

stops when the work done upon it is  $\frac{1}{2}mv^2$ . Since the field gradually decreases to the left of  $B$ , the velocity at  $C$  is not zero when the current is  $-I_{\max}$ . Consequently the coil moves beyond  $C$  and stops at  $D$  where the current is  $-I$ , this being less (arithmetically) than  $-I_{\max}$ . The coil now returns in the direction  $x_2$ , the current and magnetic field being less than at  $A$ . The accelerational period is reduced to  $PQ$  which is a fraction of  $RS$ . Clearly the coil cannot reach  $A$ , and in the long run it experiences an axial displacement in the direction  $x_1$ . In the case of a loud speaker the action is due to the leakage field. Since the value of the radial field is greater within than without the magnet, the coil moves outwards. If, however, the equilibrium position, in the absence of driving current, is brought further within the magnet, the coil will move inwards when supplied

with A.C. Owing to the small travel due to proximity of the magnet spool, it usually bounces off and wends its way outwards, unless the system is specially designed to avoid this.

The mathematical analysis of the above phenomenon is illuminating and involves a form of Mathieu equation [80 b]. Being of considerable practical importance the analysis is given in full.

Let  $k' = B/\xi =$  slope of line in Fig. 97 A,

then  $C = 2\pi r n B = 2\pi r n k' \xi.$

Neglecting mechanical loss and radiation and assuming absence of axial constraint, the differential equation of the system moving in a linear radial field is

$$m_e \frac{d^2\xi}{dt^2} + CI \cos \omega t = 0. \quad (16)$$

Writing  $\omega t = z$  and substituting in (16) we obtain

$$\frac{d^2\xi}{dz^2} + q\xi \cos z = 0, \quad (17)$$

where  $q = 2\pi r n k' I / \omega^2 m_e.$

This differential equation is a particular case of a Mathieu type whose canonical form can be written as

$$\frac{d^2\xi}{dz^2} + (a + q \cos z)\xi = 0. \quad (18)$$

In our case the parameter  $a$  is zero. To solve (17) assume [222]

$$\xi = \sum_{n=-\infty}^{+\infty} a_n e^{(n+\mu)iz}. \quad (19)$$

Substituting (19) in (17) and equating like powers of  $e^{iz}$  to zero, we obtain the recurrence relationship

$$-2a_n(\mu+n)^2 + q(a_{n-1} + a_{n+1}) = 0, \quad (20)$$

or 
$$a_n - \frac{q}{2(\mu+n)^2}(a_{n-1} + a_{n+1}) = 0, \quad (20 a)$$

from which the coefficients  $a_n$  can be determined in terms of  $a_0$ ,  $\mu$ , and  $q$ . Eliminating coefficients from the system of equations represented by (20 a), we get the infinite determinant;



$$\begin{vmatrix}
 \cdot & \cdot & \cdot & \cdot & \cdot & \cdot & \cdot & \cdot & = 0. \\
 \cdot & \frac{-q}{2(\mu-2)^2} & 1 & \frac{-q}{2(\mu-2)^2} & 0 & 0 & 0 & \cdot & \\
 \cdot & 0 & \frac{-q}{2(\mu-1)^2} & 1 & \frac{-q}{2(\mu-1)^2} & 0 & 0 & \cdot & \\
 \cdot & 0 & 0 & \frac{-q}{2\mu^2} & \boxed{1} & \frac{-q}{2\mu^2} & 0 & \cdot & \\
 \cdot & 0 & 0 & 0 & \frac{-q}{(2\mu+1)^2} & 1 & \frac{-q}{2(\mu+1)^2} & \cdot & \\
 \cdot & 0 & 0 & 0 & 0 & \frac{-q}{2(\mu+2)^2} & 1 & \cdot & \\
 \cdot & \cdot & \cdot & \cdot & \cdot & \cdot & \cdot & \cdot & 
 \end{vmatrix}$$

Taking the first three columns and rows about the origin as an approximation, we get the sextic equation

$$2\mu^6 - 4\mu^4 + \mu^2(2 - q^2) - q^2 = 0. \quad (21)$$

Putting  $q = \frac{1}{5}$ , this being a reasonable practical value when the frequency of the coil current is 50  $\sim$ , (21) becomes

$$50\mu^6 - 100\mu^4 + 49\mu^2 - 1 = 0. \quad (22)$$

The roots of (22) are  $\mu = \pm 1.1$ ,  $\pm 0.89$ , and  $\pm 0.16$ . From the recurrence relationship in (20) we obtain the three equations

$$\left. \begin{aligned}
 -2(\mu-1)^2 a_{-1} + q a_0 + 0 &= 0 \\
 q a_{-1} - 2\mu^2 a_0 + q a_1 &= 0 \\
 0 + q a_0 - 2(\mu+1)^2 a_1 &= 0
 \end{aligned} \right\}, \quad (23)$$

the two zero terms being present since only a third order determinant is involved.

Solving (23) for  $a_{-1}$  and  $a_1$  in terms of  $a_0$  and using the six values of  $\mu$  from (22), we obtain the results in Table 18.

TABLE 18

$\mu$	$a_{-1}$	$a_{+1}$
1.1	$10a_0$	$0.023a_0$
-1.1	$0.023a_0$	$10a_0$
0.89	$0.83a_0$	$0.028a_0$
-0.89	$0.028a_0$	$0.83a_0$
0.16	$0.142a_0$	$0.074a_0$
-0.16	$0.074a_0$	$0.142a_0$
Total	$11.097a_0$	$11.097a_0$

The approximate solution of equation (17) is, therefore,

$$\begin{aligned} \xi = a_0(10e^{0.1iz} + e^{1.1iz} + 0.023e^{2.1iz} + \\ + 0.023e^{-2.1iz} + e^{-1.1iz} + 10e^{-0.1iz} + \\ + 0.83e^{-0.11iz} + e^{0.89iz} + 0.028e^{1.89iz} + \\ + 0.028e^{-1.89iz} + e^{-0.89iz} + 0.83e^{0.11iz} + \\ + 0.142e^{-0.84iz} + e^{0.16iz} + 0.074e^{1.16iz} + \\ + 0.074e^{-1.16iz} + e^{-0.16iz} + 0.142e^{0.84iz}). \end{aligned} \quad (24)$$

When  $t = 0$ ,  $z = 0$  and  $\xi = \xi_0$ . Inserting these values of  $\xi$  and  $z$  in (24) we find that

$$a_0 = \frac{\xi_0}{28.2}. \quad (25)$$

Thus

$$\begin{aligned} \xi = \frac{\xi_0}{28.2} (20 \cos 0.1z + 1.66 \cos 0.11z + 2 \cos 0.16z + 0.282 \cos 0.84z + \\ + 2 \cos 0.89z + 2 \cos 1.1z + 0.148 \cos 1.16z + 0.056 \cos 1.89z + \\ + 0.046 \cos 2.1z). \end{aligned} \quad (26)$$

From (26) it is evident there are 9 components whose frequencies differ from that of the driving current. The actual values are found on multiplying 0.1, 0.11, etc. by the frequency, i.e. 50 in this particular case. The relative importance of any component depends upon the magnitude of its coefficient. Neglecting those with small coefficients we find that the coil displacement is given approximately by

$$\xi = \frac{\xi_0}{14.1} (10 \cos 0.1\omega t + \cos 0.16\omega t + \cos 0.89\omega t + \cos 1.1\omega t). \quad (27)$$

The chief feature of (27) is the reduction in frequency of the main component to one-tenth that of the driving current.\* The amplitude is, however, ten times that of the other three components. A rough idea of the curve represented by (27) is shown in Fig. 97 B. The coil reaches the position  $\xi = 0$  just before the quarter-cycle of the  $(0.1\omega/2\pi)$ th component. Since the magnetic field is absent to the left of the origin ( $\xi = 0$ ), the coil then experiences no force due to the alternating current in it. Once this position is reached the coil cannot return and in absence of mechanical resistance it moves on with constant horizontal velocity. In this way the electromechanical rectification effect can be explained. If the field were negative, to the

\* The smaller the driving current the lower are the component frequencies and the longer the time taken by the coil to come out of the magnet.

left of the origin, the motion of the coil would be periodic and it would return. The main frequency, however, would be one-tenth that of the driving current.

The complete solution of equation (17) contains an infinite number of alien frequencies which may mar the reproduced sound if the low-frequency amplitude is too large.

In equation (18) suppose  $q = 0$ , then the alternating current in the coil is zero. The parameter  $a$  can be either positive or negative. In the former case, provided the magnetic field is negative behind the

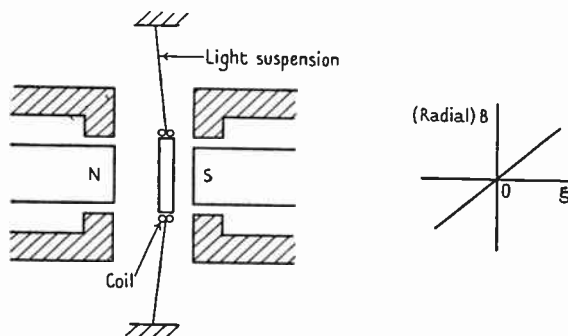


FIG. 98. Illustrating arrangement for demonstrating the stability and instability conditions in a Mathieu equation.

origin, we have ( $z = \omega t$ ),

$$\frac{d^2\xi}{dz^2} + a\xi = 0, \quad \text{so} \quad \xi = A_1 \cos(\sqrt{a}z + \epsilon), \quad (28)$$

the motion being periodic and stable. When  $a$  is negative

$$\frac{d^2\xi}{dz^2} - a\xi = 0, \quad \text{so} \quad \xi = A_1 \cosh \sqrt{a}z + B_1 \sinh \sqrt{a}z, \quad (29)$$

and the amplitude increases in one direction without limit as time progresses, there being no oscillation. These conditions correspond to a steady direct current in the coil. According to its direction it promotes oscillation ( $a$  positive) or causes the coil to move into the denser part of the field ( $a$  negative). A practical arrangement to demonstrate these effects is shown schematically in Fig. 98. It is interesting to note that oscillation is caused by a steady unidirectional current in the absence of mechanical constraint.

The physical condition corresponding to a positive value of  $a$  can

also be obtained if the coil is suspended, as shown in Fig. 98, there being an axial elastic constraint acting towards the origin. Using the mechanical constraint or the direct current, or both, to make  $a$  positive, the passage of sinusoidal alternating current through the coil gives physical conditions represented by the canonical form of Mathieu's equation (18). The solution is periodic, according to the relative values of  $a$  and  $q$ .

### 7. Influence of flux variation within the air-gap [185 b]

When the outer pole ring of the magnet is quite narrow the axial variation in flux density within the gap may be appreciable. Assuming the distribution to follow some definite law, it is possible to show that the output, even at small amplitudes, contains alien frequencies. The force on the coil per unit current is

$$C = \int_{-(1b-\xi)}^{1b+\xi} \frac{B_g l d\xi}{b},$$

where  $l$  is the total length of wire uniformly spaced on the coil,  $b$  the axial gap width, and  $\xi$  the distance of the coil from its central position. Assuming the axial distribution of flux to be  $B_g = B - \varphi\xi^2$ , where  $\varphi$  is a constant, the above integral gives  $C = C_1 - \varphi l\xi^2$ , where  $C_1 = Bl - \varphi lb^2/12$ . In practice, where the surround and centring device impose an axial stiffness or constraint, the differential equation of motion, neglecting radiation and loss, is

$$m_e \frac{d^2\xi}{dt^2} + s\xi = (C_1 - \varphi l\xi^2)I \cos \omega t. \tag{30}$$

Putting  $\omega t = z$ , (30) becomes

$$\frac{d^2\xi}{dz^2} + (a\xi^2 - b)\cos z + c\xi = 0, \tag{31}$$

where

$$a = \frac{\varphi Il}{\omega^2 m_e}; \quad b = \frac{IC_1}{\omega^2 m_e}; \quad \text{and } c = \frac{s}{\omega^2 m_e} = \left(\frac{\omega_0}{\omega}\right)^2,$$

$\omega_0$  corresponding to the fundamental frequency of the diaphragm on the axial constraint. (31) is a non-linear equation whose solution comprises an infinite number of terms having different frequencies. To reduce distortion, the construction shown in Fig. 95 may be adopted. Then  $C$  will be almost constant throughout the travel of the coil.

## 8. Effect of complex driving force

Hitherto our analyses have been based upon sinusoidal driving forces. In practice the wave form of the driving force is complex. The influence of electro-mechanical rectification is to introduce not only alien frequencies due to each separate frequency, but sum and difference frequencies in addition. If the rectification effect is eliminated by the artifice described in § 3, the influence of non-linearity of the axial constraint will, in general, be responsible for the creation of additional frequencies together with sum and difference frequencies. In both cases this can be regarded as a modulation effect where the large low-frequency amplitude causes the higher frequencies to be rectified on a non-linear characteristic. A simple analysis, relating to a condenser speaker working on a parabolic characteristic ( $f \propto E^2$ ) is given in Chap. IX, § 1, (4) and (5). The coefficients of the alien frequencies are called *modulation products*. Under either of the above conditions it is possible to create frequencies lower than any of those supplied to the grid of the power valve, i.e. sub-frequencies.

It is found in certain speakers that the motions of the coil and diaphragm, for a given forward and reverse direct current, are different [163 a]. This is due to, (a) the coil not being centrally placed in the air-gap; (b) the magnetic field being asymmetrical about the axial centre of the gap; (c) asymmetrical restoring force due to the centring device and surround. The reproduction under these conditions will be tinged with alien frequencies.

## EFFICIENCY

1. THERE are a variety of ways in which the efficiency of a loud speaker can be defined, and care must be exercised to avoid confusion. The most important definitions relate to, (a) acoustic efficiency, (b) absolute efficiency; but there are others which we shall not discuss. We are not here concerned with the efficiency based on the power supplied to the valve from the high-tension source. The efficiency obtained using (a) is that mainly required in practical design (see Chap. XX). In (b) and (c) the valve is regarded as an A.C. supply source of resistance  $R_a$ , and the efficiencies obtained must be interpreted with this in mind. See [48] for a critique on efficiency.

(a) *The acoustic efficiency*

$$\begin{aligned}\eta_a &= \frac{\text{power radiated as sound}}{\text{power input to driving agent}} \\ &= \frac{I^2 R_r}{I^2 R_1} = \frac{R_r}{R_1} = \frac{R_r}{R_0 + R_m},\end{aligned}\quad (1)$$

where  $R_m$  is the motional resistance including mechanical losses.\* In the ideal case the entire resistance is due to radiation and  $\eta_a = 1$ . Since  $\eta_a$  is a power ratio, it can be expressed in decibels below zero-level, so

$$10 \log_{10} \eta_a = 10 \log_{10} \frac{R_r}{R_1} \text{ decibels.} \quad (2)$$

The acoustic efficiency varies with frequency according to the type of loud speaker. For instance, in a moving-coil horn speaker designed to cut off at 60  $\sim$ , the efficiency rises sharply to a definite value which is well maintained up to 3,000–4,000  $\sim$ , after which it falls away.

(b) *Absolute efficiency for optimum output with a given power valve.* Since a loud speaker is associated with a thermionic power valve, the latter must be taken into account in an estimate of efficiency [125, 130]. If  $R_a$  is the A.C. valve resistance and  $R$  the radiation resistance of the ideal loud speaker in series therewith, the power radiated for a given grid swing is a maximum when  $R_a = R$ . The efficiency is then 50 per cent. This is easily proved as follows: Let  $E$  = impressed

\* As a first approximation  $\eta_a = R_r / (R_0 + R_m)$  provided the mechanical loss  $\ll R_r$ .

e.m.f.,  $I =$  circuit current: then  $I = E/(R+R_a)$  and the power radiated as sound is

$$P = I^2 R = \frac{E^2 R}{(R+R_a)^2}. \quad (3)$$

If we take  $dP/dR$  and equate to zero,  $(R_a+R)^2 - 2R(R_a+R) = 0$ , from which it is found that  $R_a = R$ . Inserting this value in (3) the power radiated is

$$P = \frac{E^2}{4R}, \quad (4)$$

and this is the maximum obtainable from the valve for a definite grid swing.

When an actual speaker is connected in the valve circuit, the radiation resistance is only a fraction of  $R$ , whilst the reactance causes a reduction in current, particularly at high frequencies. The acoustic power is

$$I^2 R_r = \left[ \frac{E}{Z_t} \right]^2 R_r, \quad (5)$$

where  $Z_t^2 = (R_a + R_1)^2 + \omega^2 L_1^2$ . All quantities are referred to the anode circuit of the valve. If a transformer is used its losses may or may not be included in those of the speaker. As it is an integral part of the apparatus the losses should be included. To do so it is essential to measure  $R_1$  and  $L_1$  on the valve side of the transformer. When the latter is excluded, the requisite values of  $R_1$ ,  $L_1$  are found by direct measurement on the speaker, the results then being multiplied by the square of the turns-ratio of the transformer.

The absolute efficiency for a given power valve is defined as

$$\eta_{ab} = \frac{\text{acoustic output with actual speaker in circuit}}{\text{acoustic output with ideal speaker in circuit}}.$$

From (4) and (5) we obtain

$$\eta_{ab} = \frac{4RR_r}{Z_t^2} = \frac{4R_a R_r}{Z_t^2} \quad (6)$$

since  $R = R_a$ .

Converting (6) to decibels,

$$10 \log_{10} \eta_{ab} = 10 \log_{10} \frac{4R_r R_a}{Z_t^2}. \quad (7)$$

In the ideal case  $Z_t = 2R_a$ ,  $R_r = R_a$  and the decibel-level is zero. From (6) and (7) it is seen that  $\eta_{ab}$  varies with change in  $R_a$ . To ensure a definite basis of comparison it is essential that  $R_a$  be fixed, since it determines the circuit condition.

(c) *Absolute efficiency based on distortionless output.* The maximum distortionless output is obtained when the load resistance is  $\varphi$  times that of the valve;  $\varphi$  is a parameter found from the valve characteristics. Its value is from 2 to 3 for a triode and from  $\frac{1}{2}$  to  $\frac{1}{3}$  for a pentode. The absolute efficiency for a given grid voltage swing exceeds that in § 2. The maximum possible output, before the curved portions of the valve characteristics are encroached upon, is now greater, since the permissible grid swing exceeds that when  $R = R_a$  and  $\varphi = 1$ .

In the case of the ideal speaker the total circuital resistance for maximum output is  $R + R_a = R_a(\varphi + 1)$ , and the power radiated

$$P = I^2 \varphi R_a = \frac{E^2 R_a \varphi}{R_a^2 (\varphi + 1)^2} = \frac{\varphi}{(\varphi + 1)^2} \frac{E^2}{R_a}. \quad (8)$$

For the actual speaker the acoustic power is

$$I^2 R_r = \frac{E^2 R_r}{Z_t^2}. \quad (9)$$

From (8) and (9)

$$\eta'_{ab} = \frac{(\varphi + 1)^2}{\varphi} \frac{R_r R_a}{Z_t^2}. \quad (10)$$

When  $\varphi = 1$  formula (10) reduces to (6). Expressed in decibels, we have

$$10 \log \eta'_{ab} = 10 \log_{10} \frac{(\varphi + 1)^2}{\varphi} \frac{R_r R_a}{Z_t^2}. \quad (11)$$

The absolute efficiency as defined above complies with conditions frequently observed in practice. As in the preceding section, the valve resistance must be specified to put the results on a comparative basis.

(d) *Mechanical efficiency.* This aspect of the subject has received scant attention.

$$\begin{aligned} \eta_{me} &= \frac{\text{acoustic output}}{\text{mechanical input at driving agent}} \\ &= \frac{R_r}{R_m}. \end{aligned} \quad (12)$$

## 2. Measurement of efficiency

To obtain the acoustic efficiency  $\eta_a = R_r/R_1$  the measured values of  $R_r$  and  $R_1$  are required. These can be found as described in Chap. XVI, §§ 2, 3. Now from Chap. VII, § 5,

$$R_r = R_m - R_l = R_m - \left( \frac{Z_m}{Z_v} \right)^2 R_v,$$



so that the efficiency is

$$\eta_a = \frac{[R_m - (Z_m/Z_v)^2 R_v]}{R_1} \quad (13)$$

The results set forth in Table 19 for a hornless speaker with baffle 4 ft. square were obtained by aid of a vacuum chamber and an A.C. bridge [41]. The transformer was not included in the measurements. Up to 1,500  $\sim$  the mechanical loss was not serious, but thereafter it became of importance and increased with rise in frequency. It follows that useful information regarding efficiency can be obtained below 1,500  $\sim$  without a vacuum chamber. The efficiency must then be regarded as a gross or apparent value where  $\eta_{ap} = R_m/R_1$ , the mechanical loss being included in  $R_m$ . Data pertaining to such tests are given in [44] Table 20. The speaker in question has a strong magnetic field and a diaphragm whose dimensions are as stated. It is considerably more efficient than either of the cases cited in Table 19. This is largely due to the intense field. For comparison the efficiency of a rigid disk of equal radius in an infinite baffle, driven by the same system, is given. At low frequencies it is about  $\frac{1}{4}$  that of the speaker, whilst above 1,000  $\sim$  it decays rapidly due to mass reactance (Chap VIII). The comparison must be clearly understood. Since an infinite baffle shuts off half the sound, from a practical viewpoint the efficiency of the rigid disk is only one-half the values given in Table 20.

TABLE 19

*Efficiency of commercial speaker using 90° paper cones 7.5 and 15 cm. radius. Other conditions unknown*

Frequency $\sim$	Acoustic efficiency $\eta_a$ per cent.	
	7.5 cm.	15 cm.
400	4.5	7.5
600	6.8	7.3
800	4.2	9.0
1,000	4.0	6.0
1,200	4.6	2.6
1,600	2.8	7.0
2,800	6.0	6.0
3,200	2.8	2.0

Region of cone  
resonances.

The acoustic efficiency and radiation resistance are only criteria of output when the current is constant at all frequencies. To obtain the actual output it is necessary to multiply  $R_m$  by the square of the

TABLE 20

Showing apparent efficiency of coil-driven conical diaphragm with rubber surround at various frequencies

$B_s = 1.1 \times 10^4$  lines cm.<sup>-2</sup>, radius of diaphragm 12.2 cm., width of surround 1.8 cm., thickness of paper  $2.1 \times 10^{-2}$  cm.,  $n = 1,200$  turns,  $\psi = 90^\circ$ ,  $m_s = 4.7$  gm.

Frequency ~	Apparent radiation resistance ( $R_m$ ) ohms		Apparent efficiency $\eta_{ap}$ per cent.	
	Cone in baffle 6 ft. square	Rigid disk in infinite baffle	Cone	Rigid disk (both sides)
300	336	79	16.1	4.3
500	346	83	15.9	4.3
1,000	396	59	18.3	not calculated
2,000	192	15.6	7.9	0.69
3,000	394	7.1	12.6	0.26

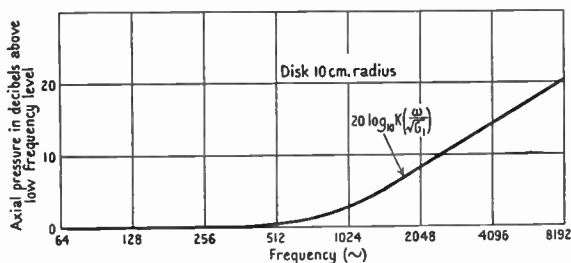


FIG. 99. Curve showing variation in axial sound pressure with frequency, due to a rigid disk 10 cm. radius vibrating in an infinite flat baffle, when the sound power is constant.

current, i.e.  $E^2/Z_i^2$ . If the power radiated by a rigid disk were constant at all frequencies, the axial pressure would increase considerably with rise in frequency above 1,000 ~. This follows immediately from the beam or focusing effect (Chap. V). Assuming the axial power-level to be zero at 300 ~, where the distribution is uniform in all directions, its value at other frequencies for constant output is plotted in Fig. 99. Up to 3,000 ~ there is no serious discrepancy between the axial output of the cone and that of Fig. 99. Above 4,000 ~ the cone output decays rapidly. Below 4,000 ~ the radiation from the conical diaphragm reckoned on a decibel basis is fairly uniform when the listener is suitably situated in an ordinary room. On the axis the upper register is rather powerful.

### 3. Horn speaker

Bridge measurements of a similar character to those in § 2 can be made with horn type moving-coil speakers. The efficiency of these instruments is higher than that of the hornless type, and the mechanical loss is a smaller proportion of the total power. Consequently the apparent efficiency gives a fairly accurate idea of the performance to be expected in practice. Curve 1 of Fig. 100 shows the efficiency of a unit of the type [50] illustrated in Fig. 82 A. To test the unit it was connected to a uniform tube 50 feet long, whose cross-section was

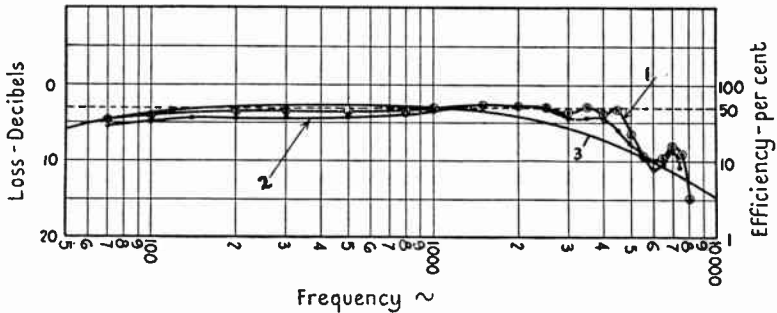


FIG. 100. Curves showing efficiency of moving-coil horn speaker of Fig. 82 A at various frequencies, measured with a long tube of uniform bore, in place of horn.

identical with that of the throat. The *acoustical* impedance at the throat is a resistance of value  $\rho_0 c/A$  (not  $\rho_0 cA$  which is the mechanical impedance\*), being in the case under review about 17 c.g.s. units. To avoid reflection at the far end of the tube the acoustic termination should have this value. It was simulated by using a number of short narrow slits having an impedance of about  $z_a = 17 + i.16 \times 10^{-4} \omega$  c.g.s. units. At low frequencies, where  $\omega$  is small,  $z_a = 17$  since the inertia component is negligible. At the higher frequencies, although the latter is relatively important, there is considerable attenuation in the tube, so that the energy reflected back to the throat due to improper matching at the far end is small. By using a vacuum chamber the mechanical loss could be obtained, but the input would have to be restricted owing to removal of the load.

The method used to compare the actual and apparent efficiencies was an acoustical one. The power delivered by the diaphragm to the

\* See definitions 23, 30.

tube, when the pressure and particle velocity are in phase, is

$$\frac{p^2}{r_a} = \frac{p^2 A}{\rho_0 c} = \frac{p^2}{17}$$

for the present case. To measure the pressure in the neighbourhood of the throat it is necessary to use a condenser microphone in such a manner that the operating conditions are unchanged by its presence. Accordingly an annular slit was provided on the side of the tube a short way from the diaphragm of the speaker. The acoustical impedance of this was fifteen times greater than that of the tube, so that propagation along the latter was undisturbed. This is analogous to using a high series resistance with a voltmeter, so that little power is drawn from the test circuit. The slit communicated with a condenser microphone via a conical-shaped chamber. The combination was calibrated, and the tube pressure read directly on an ammeter connected in the output circuit of the microphone amplifier.

The efficiency obtained in this way [50] is given in curve 2, Fig. 100. Comparison with curve 1 shows that the mechanical loss in the system is a small proportion of the electrical input. Above 1,500  $\sim$  the efficiency exceeds that to be expected from theoretical conditions, on the assumption that the diaphragm acts as a rigid structure (curve 3). It appears, therefore, that the upper register is dependent upon resonances, as in other types of speaker. These are doubtless due to vibrational modes of the diaphragm. Information on this matter could be obtained from effective mass curves taken *in vacuo* (Chap. XVI, §§ 5, 6). Over a wide frequency band the efficiency is 50 per cent., which is of unquestionable advantage for public address or entertainment purposes. In commercial production and use, where an exponential horn is employed, the efficiency over the same frequency band is about 30 per cent. It is of importance to indicate that with efficiencies of this order, even in the absence of mechanical loss, the output at a resonant frequency cannot exceed three times the normal output. This statement is made on the assumption that the normal output applies to the frequency range where diaphragm resonances are not responsible for the high efficiency of 30 per cent.

#### 4. Measurement of absolute efficiency

In decibels this is  $10 \log_{10} \frac{4R_a R_r}{Z_t^2}$ , as shown in § 1 (b), so that measurements have to be made to find  $R_r$ ,  $R_1$ , and  $L_1$ . For a horn speaker,

where the mechanical loss is relatively small,  $R_r = R_m$ , so that the essential data are obtained from measurements with the driving agent free and stationary. The result of tests on a horn type moving-coil speaker, covering a range from 3,000 to 12,000  $\sim$ , is illustrated [39] in Fig. 101. If it is desired to express these results in the form given in § 1 (c), it is merely necessary to raise the level throughout by 1 decibel, i.e.  $10(\log_{10} 5 - \log_{10} 4)$ . This is based on the value  $\varphi = 2.5$ . Then  $(\varphi + 1)^2/\varphi = 5$ , whereas in § 1 (b) it is only 4. The difference is of no practical importance.

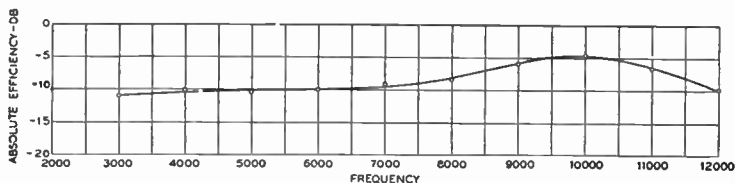


FIG. 101. Efficiency of high-frequency horn speaker relative to the ideal as determined from motional impedance measurements.

## 5. Direct measurement of radiated power

Instead of finding the radiation resistance  $R_r$  by bridge measurements, it can be determined from acoustical measurements. If a 'dead' room of fairly large dimensions is used, two conditions can be obtained: (a) the speaker (if of the hornless type) can be tested with its baffle in position, this being equivalent to a free air condition where the instrument is a double source; (b) the speaker may be flush with one of the highly absorbent walls where the free air condition is simulated, one side of the speaker being screened. If it is desired to approximate to an infinite baffle, the wall in which the speaker is set should be large, flat, non-absorbent, and non-resonant. The baffle condition can only be obtained when the pressure is doubled in the plane of the diaphragm.

Owing to local variation in curvature of the diaphragm surface and to the seam,\* the radiation has not circular symmetry about the polar axis. Nevertheless for practical purposes it will be assumed that the degree of asymmetry is small. If a series of pressure measurements is taken by aid of a calibrated microphone, at a distance not less than 12 radii from the speaker [140], for various angles in a horizontal plane containing the axis, the polar curve is obtained. From Chap. VI, § 1, the power radiated as sound is  $P = (1/\rho_0 c) \iint p^2 dA$ , where  $p^2$  is

\* This does not apply to moulded seamless cones.

the mean square pressure. When the speaker is set in one wall, the integration is to be extended over a hemisphere whose radius is that of the microphone from the speaker. To do this it is customary to adopt a graphical method as shown in Fig. 102, where the polar curve *OMM* is given for constant input current, although it can be given for constant voltage to the grid of the power valve. The latter procedure, however, limits the curve to a particular valve resistance. The polar radii of this curve represent pressure, but since  $p^2$  is required it is necessary to square each radius vector. This gives the

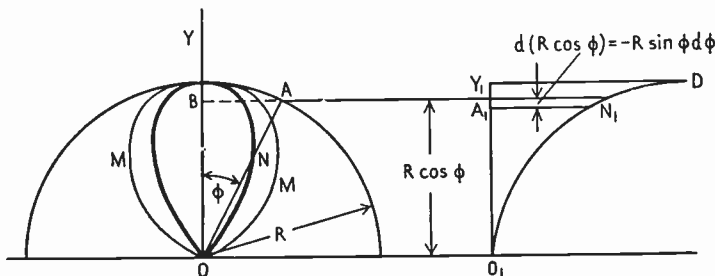


FIG. 102. This diagram is used to represent (1)  $p$ , the sound pressure at various angles with the axis of a loud speaker (curve *OMM*); (2)  $p^2$  (curve *ONY*); (3) the cross-section of a hemisphere of radius  $R$ . If the area  $A = O_1N_1DY_1$  is measured by a planimeter in  $\text{cm.}^2$ ,

$$P = 2\pi R^2 p_{ax}^2 A / \rho_0 c (O_1Y_1)^2 \text{ ergs sec.}^{-1},$$

where  $p_{ax}$  is the r.m.s. axial pressure and  $O_1Y_1$  is in cm. The formula in the text is  $P = \frac{2\pi RA}{\rho_0 c}$ , which agrees with the foregoing when the appropriate scale factors are used.

curve *ONB* which corresponds to  $p^2$  on a hemisphere of radius  $R$ , when the pressure and particle velocity are in phase. Taking the elemental annulus at  $A$ , its area is  $2\pi(AB)R d\phi = 2\pi R^2 \sin \phi d\phi$ . The power passing through it is  $(2\pi R^2 / \rho_0 c) p^2 \sin \phi d\phi$ , where  $p^2$  is the mean square pressure. The total output is the summation of this over the hemisphere, namely,  $(2\pi R^2 / \rho_0 c) \int_0^{\frac{1}{2}\pi} p^2 \sin \phi d\phi$ . Draw a vertical line  $O_1Y_1$  and project the point  $A$  horizontally across; set off  $A_1N_1 = ON = p^2$ . The curve  $O_1N_1D$  is obtained in this way. Now the vertical ordinate at  $A_1$  is evidently  $R \cos \phi$ , and therefore the elemental strip is  $d(R \cos \phi) = -R \sin \phi d\phi$ . Thus, neglecting the negative sign, the area  $O_1N_1DY_1$  is  $R \int_0^{\frac{1}{2}\pi} p^2 \sin \phi d\phi$  and the power

is therefore  $2\pi R/\rho_0 c$  times this area. The latter can readily be found by aid of a planimeter. To convert the power to watts it is merely necessary to multiply by  $10^{-7}$ .

Difficulties are often encountered at low frequencies due to inadequate absorption, thus permitting standing waves to arise. Under such conditions it is preferable to make measurements out-of-doors [11, 135]. If the speaker is buried in the ground with the diaphragm flush to the surface, the infinite baffle condition is simulated. Care must be taken to ensure that the reaction on the lower side does not influence the results. Unless adequate precautions are observed, an added stiffness will accrue due to the subterranean chamber, thereby influencing the lower register.

## 6. Linearity tests

Throughout a sound-reproducing system it is imperative that the action of each component should be linear [96 a]. Thus when a sine wave is applied at the transmitter it should be radiated—excluding any distortion due to the medium—as a sine wave at the reproducer. In this respect it is of the utmost importance to know whether the deformation and general behaviour of diaphragms and their associated components under the action of vibrational forces is linear. There are several ways in which tests can be conducted:

(a) The reproducer is arranged in a 'dead' room and a record taken of the axial sound pressure with steadily increasing input, at a series of frequencies. By aid of an oscillograph the output wave form can be seen. The graph of input versus output at any particular frequency should be a straight line. If it curls over with increase in input, non-linear action is present. This is not an infallible test unless the wave form is always sinusoidal.

(b) The output can be taken to an electrical harmonic analyser and the power in the various components of the wave form ascertained. The output limit for a definite degree of distortion can then be found.

(c) The input and output wave forms can be magnified and applied, respectively, to two pairs of control plates of a cathode ray [86] oscillograph. The resulting figure can either be photographed or a note made when distortion reaches the permissible limit. In the absence of distortion the figure is either a straight line or an ellipse.

A record from a hornless moving-coil speaker showing flattening of the wave form due to a surround of inadequate elastic properties

and to the external leakage field (Chap. XIV) is given in Fig. 103. With a pseudo-elastic surround acting symmetrically about the equilibrium position of the coil, the positive and negative half-waves would be identical. Since they are not, the influence of variation in the magnetic field beyond the air-gap is in evidence. This, of course, only asserts itself when the amplitude is large at low frequencies. So far as reed-driven speakers are concerned, it is impossible to avoid harmonics at low frequencies with a diaphragm of reasonable diameter unless the natural frequency of the reed is fairly low. Under this condition the upper register is usually weak, except on the axis of the diaphragm (Chap. VIII). Since in all classes of speaker the

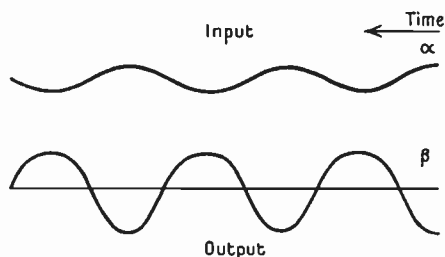


FIG. 103. Oscillograph records illustrating non-linear characteristic of hornless moving-coil speaker.

amplitude decreases with rise in frequency, the tests for harmonic-creating propensities should be conducted with large amplitudes at low frequencies. Nevertheless it is necessary to conduct tests throughout the audible range as rattling may occur at certain frequencies.

The second method of test, using an harmonic analyser, is illustrated by the curves of Fig. 104 for a horn type moving-coil speaker at [18] 60  $\sim$ . With an input of 2.5 watts the harmonic content in the output is 1 per cent. The output of the fundamental is 0.5 watt and the harmonic content is 20 decibels below that of the fundamental. Although this is a wide margin, it must be interpreted with care. The ear is much more sensitive to higher harmonics than to the fundamental, but the latter tends to mask the former by raising the threshold of audibility. Consequently, if the harmonic content were only 10 decibels below the fundamental, a definite degree of impurity would probably ensue, but this depends upon the intensity-level. It may seem strange that the sound-



output in Fig. 104 rises more slowly than the input power, since for absence of distortion the relationship should be linear. The explanation is that the coil temperature rises with increase in

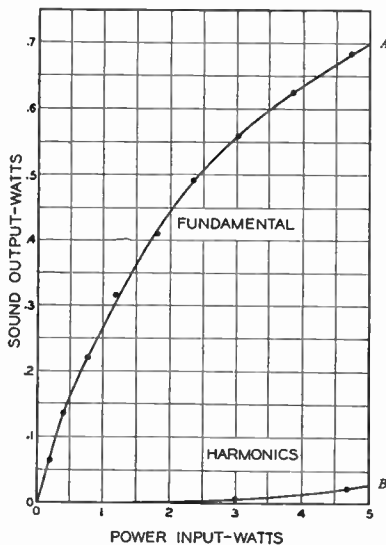


Fig. 104. Power output at 60 ~.

fall in frequency. Moreover, it is preferable to choose a mean value of 500 ~ in order to make the test really stringent. This will be an appropriate test for the low-frequency load capacity. Since in practice the current is greatest at low frequencies, the range above 500 ~ does not call for serious consideration. Thus a test to the limit at 500 ~ ought to give an adequate idea of the power-handling capabilities of the instrument. If any doubts exist it is a simple matter to conduct the test at lower frequencies.

The coil temperature can be found approximately by bridge measurements of D.C. resistance. If the normal value is known, the rise can be calculated by taking the per cent. increase in resistance per 1° C. By aid of a change-over switch the endurance test can be momentarily interrupted to ascertain the temperature. A more accurate way is to remove the coil from the magnet and obtain a resistance/temperature curve, so that by measuring the former *in situ*, the latter can be read from the chart.

input, so for a given watt loss the current is lower. This difficulty is surmounted by plotting the input current against the output.

## 7. Endurance tests

Although a loud speaker may be capable of handling large input, it is necessary to know what power can be supplied indefinitely for a given temperature rise of the operating coils. In a test of this nature the cooling effect of the air must be taken into account. Owing to the greater velocity at low frequencies, the input for a given temperature rise may alter with

## 8. Strength test

For a given input the coil excursions at 50 ~ cause stresses in the centring device and surround of a moving-coil speaker much in excess of those at 500 ~, owing to the greater amplitude in the former case. It is advisable, therefore, to conduct a strength test at the lowest frequency to be adequately reproduced, the input being sufficient to give the desired information. Many hornless speakers capable of large output at 500 ~ will fail at 50 ~, owing to weakness of the centring device. Long before rupture occurs there will probably be non-linear action of the centring device and surround, thereby introducing alien frequencies.

## ELECTRICAL IMPEDANCE MEASUREMENTS

1. WHEN the impedance alone is required, apart from its resistive and reactive components, the simplest procedure is to apply a voltage of variable frequency to the grid of the power valve and make direct measurements of current through the speaker and the voltage across its terminals. The arrangement is shown diagrammatically in Fig. 105. A Moullin or other high-impedance type voltmeter  $E$  must be

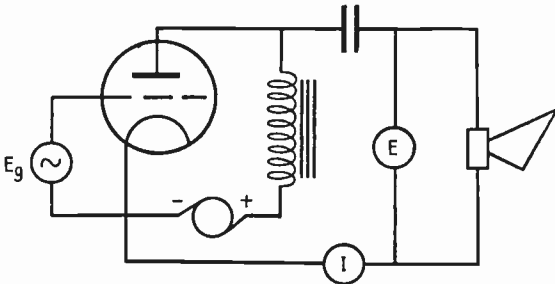


FIG. 105. Simple circuit for approximate impedance measurements of speaker.

used. Measurements on a hornless moving-coil speaker are illustrated [113 a] in Fig. 106. The sudden rise in impedance at 50  $\sim$  is due to resonance of the diaphragm as a whole on the surround, whilst the upward trend above 300  $\sim$  is caused by inductive reactance. Peculiarities due to diaphragm performance above 300  $\sim$  have been omitted. The current through the speaker and power valve varies with frequency in a manner akin to that shown in Fig. 149.

2. The most accurate method of measurement is by aid of some type of alternating current bridge. Experience seems to indicate that a bridge of the mutual inductance type illustrated in Fig. 107 A, B will give the greatest accuracy [91, 96 b]. This method, of course, enables the resistive and reactive components to be found separately, the latter being in the guise of an effective inductance which may be positive, zero, or negative. The two latter conditions represent resonance and capacity effects, respectively.

The average variable mutual standard inductance is usually de-

signed for currents of a milliampere or so. Consequently, if tests are to be conducted at current values corresponding to those which obtain in practice, the apparatus must be specially designed to avoid overheating. Under these circumstances a preliminary test must be made to discover the current through the speaker at various frequencies to give a certain loudness-level at a specified frequency, when constant voltage is applied to the grid of the power valve. During bridge tests this value of current is used in the speaker. Such procedure necessitates a powerful source, since a good deal of current is drained off by the bridge, whilst the auxiliary resistances cause a drop in voltage. The only reason for using currents identical with those in practice is to allow for the variation in resistance and inductance due to the magnetic material in the driving unit. A rough test is adequate to show whether variation in resistance and inductance with current is serious. If it is not, there is no reason to be fastidious, so the measurements can be made with standard apparatus. Naturally the tests are conducted with the speaker in a 'dead' room, so that no sound reaches the observer, whilst room reaction and microphone effect is eliminated. The latter is very disturbing at low frequencies when a visual detector is used. When the measurements are not conducted to determine the vibrational characteristics of the speaker, but are required for general purposes, the output power transformer should be included.

The necessity for constructing and wiring up the bridge to reduce all stray inductive and capacity effects to a minimum cannot be too strongly emphasized. Everything must be suitably screened, but not in such a way that the value of the standard mutual inductance alters due to eddy currents induced in the screen. In fact, it would be preferable to use an astatic type of mutual inductance if this was available. The input to and output from the bridge must be associated with transformers whose windings are electrostatically screened

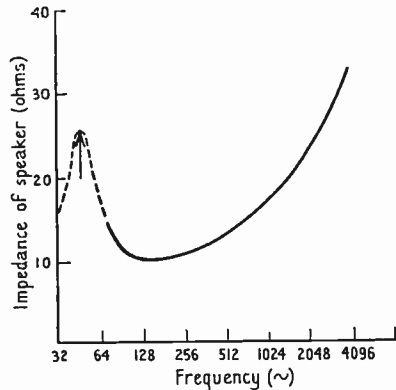


FIG. 106. Impedance-frequency curve of hornless moving-coil speaker measured with apparatus of Fig. 105.

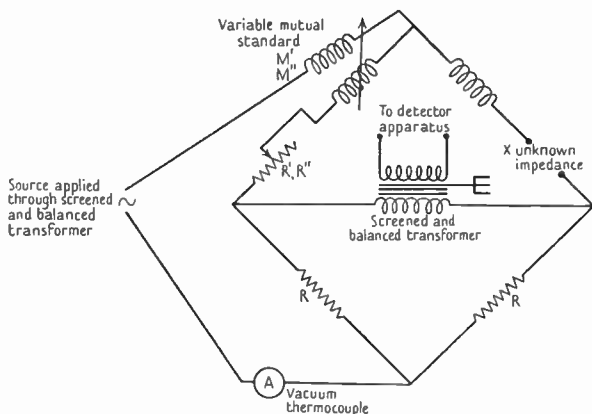


FIG. 107 A. Heaviside equal ratio bridge for use up to  $L = 0.22$  henry.

$$L = 2(M' - M'') \quad M'' = \text{leads reading with } X \text{ short-circuited.}$$

$$M' = \text{reading with } X. \quad R'' = \text{ " " " "}$$

$$R = R' - R''. \quad R' = \text{reading with } X. \quad \text{ " "}$$

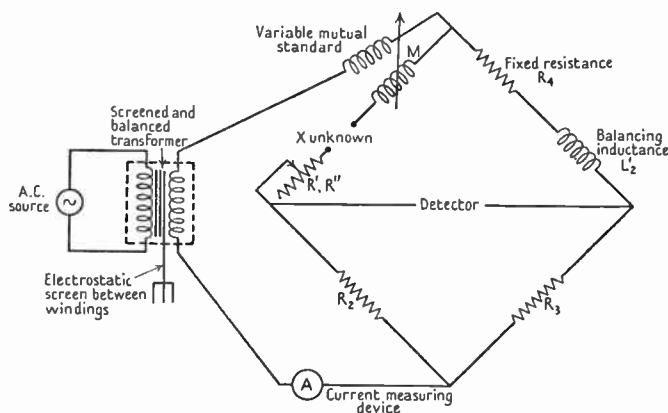


FIG. 107 B. Heaviside unequal ratio bridge for  $L > 0.22$  henry.

$R_2 = 9R_3$  or  $99R_3$  according to balancing inductance;  $R_4$  is approximately  $1/9$  or  $1/99$  that of  $R$ .

$$L = \left( \frac{R_2 + R_3}{R_3} \right) (M'' - M') \quad R = \left( \frac{R_2 + R_3}{R_3} \right) (R'' - R')$$

See Fig. 107 A.

and balanced. Also an external transformer screen of some high permeability magnetic alloy is required. The out-of-balance currents should be amplified by a suitable valve amplifier, and then filtered to

sift out any harmonics generated in the speaker, before being passed on to the detector. All leads must be screened, including those to the telephone, and the screens efficiently earthed. Success in measurements of this type at frequencies above 1,000  $\sim$  depends almost entirely upon the efficacy of the screening and earthing arrangements, although care must be exercised regarding impurities in the mutual inductance due to stray inductance and self-capacity.

The methods of detection can be visual or aural according to the frequency. Below 300  $\sim$  a good vibration galvanometer serves the purpose, and being highly selective there is no necessity to incorporate a filter. When, however, the frequency falls below 100  $\sim$  the measurements require considerable patience and skill, especially if there are any sharp resonances of the type illustrated in Fig. 125, curve 1. As an alternative to the vibration galvanometer the out-of-balance voltage can be rectified in the usual way, but it ought to be filtered first. The zero reading of an instrument in the anode circuit of a valve detector indicates balance. For frequencies exceeding 300  $\sim$ , two pairs of telephones having resonances at 800 and 2,500  $\sim$  can be employed, the latter doing service up to 4,000  $\sim$ . Beyond this frequency either a heterodyne or some form of visual detector should be used.

For investigating certain scientific aspects of the loud-speaker problem, the above method has proved valuable. Other bridges, whilst being adequate for certain purposes, have failed to reveal the idiosyncrasies of the speaker. They are, however, of value for ordinary test purposes. A simple direct bridge can be used where inductance (or capacity) and resistance in one arm are varied until each equals its counterpart in the speaker. The balance is checked by a screened and balanced differential transformer and a visual detector is used.

Whatever method is employed errors will arise above 1,000  $\sim$  unless all auxiliary resistances are free from self-inductive and self-capacity effects, whilst inductances must be free from the latter.

### 3. Speaker measurements. General considerations

When the driving mechanism is free to operate in the usual way, the effective resistance  $R_1$  and the effective inductance  $L_1$  can be determined to a high degree of accuracy. If the mechanism is restrained and cannot move, the static values  $R_0$  and  $L_0$  are found. Then the

respective differences are due to the motion of the coil or reed, whichever is used. Thus the motional resistance  $R_m = R_1 - R_0$  and the motional inductance  $L_m = L_1 - L_0$ .  $R_m$  includes sound radiation, mechanical losses, and a variable part due to the iron of the magnet whether permanent or energized. When the radiation resistance is a small fraction of  $R_1$ , the quantities  $R_1$ ,  $R_0$  are nearly equal. Under this condition great care is required in obtaining and interpreting the results. This applies particularly when measurements are made *in vacuo* to find the actual radiation resistance due to sound. Important features associated with these measurements are discussed below.

In hornless speakers  $R_m$  is usually a small fraction of  $R_0$ , and it is not easy to determine its value accurately from readings with the coil free and stationary, for the following reasons [96 b]:

1. It is almost impossible to have the coil in the same mean position for free and for fixed measurements unless the latter are obtained by fixing the coil rigidly by aid of paraffin wax. This is particularly the case at the higher frequencies, as shown by the lead-block experiment in Chap. XVIII, § 20. An amplitude of a few microns corresponds to a loud sound at 3,000  $\sim$ . By aid of paraffin wax the sound can be eliminated entirely.

2. If the free and fixed measurements are made separately, it is necessary that the temperature of the coil should be identical in each case. The temperature of the electromagnet gradually rises with time owing to heating of the magnet coil,\* unless the current is maintained till the temperature is steady.

The temperature coefficient of copper is 0.4 per cent. per degree Centigrade. A variation in temperature of 15°C. can easily occur, with a consequent rise of 6 per cent. in the resistance of the coil. Thus, if  $R_1$  were measured at 20°C., at the beginning of a day and  $R_0$  at 35°C. at the end of the day, the value of  $R_0$  would be 6 per cent. high. Under this condition low-frequency tests on a diaphragm with reinforced edge (where  $R_1 - R_0$  is small) would reveal a negative sound output, since  $R_1 - R_0$  is less than 6 per cent. The stationary and free measurements must be taken at close time intervals after the magnet has attained a steady temperature. Temperature constancy can be checked by means of a D.C. bridge.

3. The iron loss varies according as the coil is free or stationary,

\* This difficulty disappears when a permanent magnet is used.

and when the output is small this usually results in  $R_m$  being negative at frequencies of the order 4,000  $\sim$  upwards.

If possible no attempt should be made to fix the coil by mechanical means. With an electromagnet of low remanence, the fixed condition is simulated by short-circuiting the winding of the magnet on itself. The error incurred in  $R_0$  due to variation in iron loss, with and without the field, is about 1 per cent. For any particular type of magnet tests should be made to discover whether  $L_0$  is the same when the coil is fixed with the field on, and when free, the field winding being closed on itself. Obviously this procedure is inapplicable to reed-type speakers. In this case the only safe way is to take measurements of  $R_1$ , meanwhile keeping a check on the coil temperature and the testing current. Without altering the adjustment, molten paraffin wax is used to fix the reed, the measurements then being repeated. In this class of speaker, however, the variation in iron loss is often sufficient to vitiate the results, so the experimenter must be discreet in making deductions as to performance. The method is clearly satisfactory for making impedance measurements of  $R_1$  and  $L_1$  alone, so that the operating current in a valve circuit can be computed.

Assuming actual fixation of the coil, we can consider a case where  $(R_1 - R_0) = R_m$  is only 2 per cent. of  $R_0$ . To obtain  $R_m$  to an accuracy of 1 per cent. it is necessary to measure  $R_1$  and  $R_0$  to  $\pm 1/200$  of 2 per cent.—i.e. 1 part in 10,000. Apart from the first two sources of error enumerated above, the variation in iron loss entirely precludes any hope of attaining this degree of accuracy. When the diaphragm loss is added as a further complication, the difficulty of measuring the actual *sound* output from a reproducer of low efficiency by electrical means is evident.

These remarks apply mainly to hornless speakers whose efficiency is, in general, below 10 per cent. With horn or directional baffle moving-coil units, the efficiency ranges from 20 to 40 per cent., so that  $R_m$  is a goodly proportion of  $R_0$ . One of the chief points in testing these speakers is to avoid temperature variation of the moving coil.

#### 4. Effective mass

This is defined in Chap. I, p. 4, and has been discussed in Chapter IV. As an introduction to the practical aspect of the situation, the ideal case of a rigid mass vibrating on a massless helical spring will be



treated. The simplest procedure is to use the electrical analogue in Fig. 108. The mass is driven by an alternating force  $f$  causing a velocity  $v$ , the corresponding electrical quantities being  $E$  and  $I$ . The electrical impedance is  $E/I = Z = \{\omega L - (1/\omega C)\}$ , which can be written  $\omega L_e$ , where  $L_e$  is the effective inductance. Analogously we have the mechanical impedance  $z_e = \omega m_e = \{\omega m - (s/\omega)\}$ , so the effective mass is  $m_e = \{m - (s/\omega^2)\}$ . Taking  $m = 20$  gm. and  $s$  the stiffness of the spring as  $2 \times 10^6$  dynes cm.<sup>-1</sup> the effective mass varies, as shown in Fig. 109. Starting at a negatively infinite value, the effective mass rapidly rises, until when  $m = s/\omega^2$  or  $\omega = \sqrt{(s/m)}$  resonance occurs and  $m_e$  is zero, i.e. the mechanical impedance then

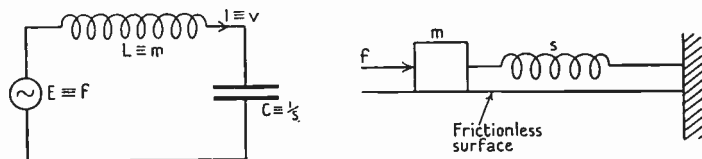


FIG. 108. The diagram on the left is the electrical analogue of the mechanical system on the right.  $s$  is assumed to be massless.

vanishes. This happens at a frequency of  $50 \sim$ . As  $\omega/2\pi$  increases, the effective mass approaches asymptotically the value of the rigid mass.

This elementary example corresponds closely to a hornless coil-driven speaker at low frequencies.  $m$  represents the total mass of the diaphragm, including the accession to inertia, whilst  $s$  is the elastic constraint due to the centring device and surround. In general the vibrating structures with which we are concerned do not behave as rigid masses. By invoking the effective mass concept, the structure becomes virtually a rigid mass of value  $m_e$  at the driving-point. The idea only applies, of course, to the steady state.

As a second illustration of the effective-mass principle, suppose we take the case of a horn type moving-coil speaker in Chap. XX, § 2. The mass is that of the coil and diaphragm, whilst the stiffness is due to the annular surround and throat chamber, the mechanical radiation resistance being associated with the latter. From formula (5), Chap. XX, § 2, the effective mass is

$$m_e = m - \frac{s_1}{\omega^2} - \frac{s_2 r^2}{\omega^2 r^2 + s_2^2},$$

this being shown graphically in Fig. 152. The curve is similar in

nature to the more elementary example of Fig. 109. If  $r = \infty$  the loss disappears and the value of  $m_e = m - \{(s_1 + s_2)/\omega^2\}$ , which gives a curve identical in form with that of Fig. 109. The effective mass is not influenced when the resistance is in series, but profound modifications may occur when it is in parallel with either mass or stiffness. For example, in the above formula, if  $s_1 = 0$  and  $r$  is very small,  $m_e \doteq m$ , and is therefore independent of frequency. Another example

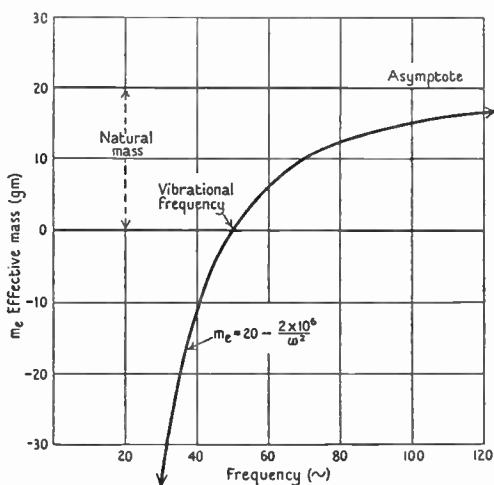


FIG. 109. Curve illustrating effective mass of mechanical system in Fig. 108 at various frequencies.

occurs in Fig. 111, where  $m_e$  of a conical diaphragm is reduced to a low value at higher frequencies owing to transmission loss.

## 5. Measurement of effective mass

In a moving-coil system the effective mass referred to the driving-point, i.e. the coil, is, from Chapter VII,  $m_e = -C^2 L_m / Z_m^2$ , where  $Z_m^2 = R_m^2 + \omega^2 L_m^2$  and  $m_e$  refers to the complete vibrating structure. Thus, if a coil is attached to some specific point on a structure by a very stiff spider, the effective mass can be found by taking measurements of  $R_m$  and  $L_m$  with an A.C. bridge. Since  $r_e = C^2 R_m / Z_m^2$  the mechanical resistance is found in the same way. Knowing  $C^2$ , the values of  $m_e$  and  $r_e$  are calculable. In a moving-coil speaker the coil is fixed solidly to the diaphragm, so that no difficulty is encountered respecting mechanical coupling. The same principle can

be extended to reed-driven cones, since the formulae are valid then (Chap. VII). Here difficulties arise due to the iron, as described in § 3, and the method is not satisfactory. The effective mass of the reed *alone* can be measured up to its resonant frequency and somewhat beyond it, but the accuracy dwindles at higher frequencies owing to the behaviour of the iron.

## 6. Coil-driven circular aluminium disk

A coil 2.5 cm. mean radius wound on a paper tube having a free length of 2.5 cm. was securely fixed coaxially to an aluminium disk [35 b] 10 cm. radius and 0.055 cm. thick. The coil was situated in the radial magnetic field of a circular electromagnet and the disk suspended freely by several thin elastic threads, the axial frequency in the absence of the field being about 3  $\sim$ . Bridge measurements of the inductance and resistance of the coil, free and stationary, were taken over a certain frequency band. Some of the observed and deduced data are given in Table 21, whilst a curve showing the effective mass is plotted in Fig. 110.

TABLE 21

*Showing data for computing the effective mass of an aluminium disk*

Radius of disk, 10 cm. Thickness,  $5.5 \times 10^{-2}$  cm. Mass, 47 gm. Mass of coil, former, adhesive and connecting wires, 7.8 gm. Mean radius of coil, 2.5 cm. D.C. resistance of coil without leads, 0.95 ohm. Accession to inertia at zero frequency, 3.5 gm.  $C^2 = 2 \times 10^4$ . No baffle.

Fre- quency ( $\sim$ )	$L_m$ , motional inductance (henry)	$R_m$ , motional resistance (ohms)	$m_e$ , effective mass (gm.)	Remarks
0	—	—	+58.3	Natural mass (47+7.8) plus ac- cession to inertia (3.5).
60	$-6.5 \times 10^{-4}$	$10^{-2}$	+216	First centre-stationary mode at 69 $\sim$ .
75	$+7.1 \times 10^{-4}$	$3 \times 10^{-2}$	-127	
100	$+4.2 \times 10^{-4}$	$7 \times 10^{-2}$	-113	
120	$+10^{-2}$	23.3	$-3.2 \times 10^{-1}$	First centre-moving mode. One circle of minimum amplitude at 120.6 $\sim$ .
120.6	0	39.5	0	
125	$-7.2 \times 10^{-3}$	$6.3 \times 10^{-1}$	+4.5	
150	$-1.45 \times 10^{-3}$	$4 \times 10^{-2}$	+15.4	
200	$-4.5 \times 10^{-4}$	$6 \times 10^{-2}$	+27.5	

Starting from zero frequency, where limiting motion is assumed,  $m_e$  is the sum of the natural mass (disk plus coil) and  $m_i$  the accession

to inertia. Since no baffle was used throughout the experiments,  $m_i$  in the neighbourhood of zero frequency is half the value with an infinite baffle [3 a]. The first centre-stationary mode occurs in the neighbourhood of  $69 \sim (A)$ , and the first centre-moving mode at  $120.6 \sim (B)$ . Near the centre-stationary mode  $m_e$  attains a positive maximum and then falls to a negative minimum. The amplitude of the motion is a minimum when  $m_e = 0$ , since the effective mechanical resistance and impedance are then maxima.

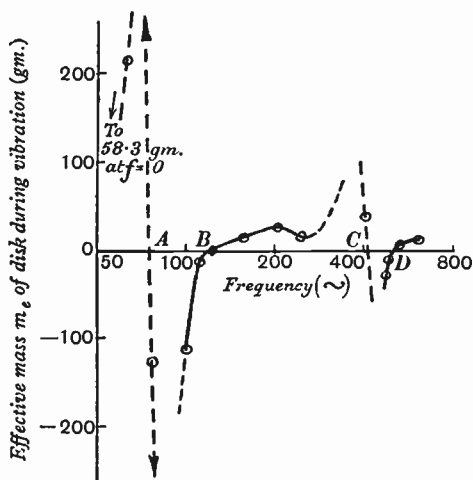


FIG. 110. Curve showing variation with frequency in effective mass of coil-driven free edge aluminium disk 10 cm. radius. *A*, first centre-stationary mode; *B*, first centre-moving mode; *C*, second centre-stationary mode; *D*, second centre-moving mode.

The arithmetical value at the maximum is much in excess of the natural mass of the disk and coil. Rising from the negative maximum the effective mass becomes zero in the neighbourhood of the first centre-moving symmetrical mode at  $120.6 \sim$ . Thereafter it increases, but near  $260 \sim$  there is a minimum value due to some irregularity. The second centre-stationary mode occurs at  $410 \sim (C)$ . The second centre-moving mode occurs at  $484 \sim (D)$ . The third centre-moving mode, which should occur in the neighbourhood of  $1,100 \sim$ , is absent. Considered as a separate vibrator, the portion of the disk within the coil has a mode near that of the outer annulus. Moreover, mutual

interference suppressed both modes. When allowance is made for the coil mass and the portion of the disk within the coil, the frequencies of the modes determined experimentally are in close accord with those found by calculation [38]. From the shape of the curve of Fig. 110 and the known behaviour of a flat disk, it is possible to throw light on the more complicated action of conical diaphragms used for loud speakers by examination of their effective mass curves.

### 7. Loud-speaker diaphragms

The results of measurements on two conical loud-speaker diaphragms, (1) with the edge reinforced by a narrow annulus of presspahn to prevent radial modes; (2) with an annular rubber surround, are portrayed graphically in Fig. 111. Further details are set forth in Table 22 [35 a, b].

TABLE 22

*Data for conical coil-driven loud-speaker diaphragms*

Radius at periphery of paper cone with reinforced edge (curve 1)	12.2 cm.
Radius at periphery of paper cone with rubber surround (curve 2)	12.2 cm.
Radial width of rubber surround	1.8 cm.
Apical angle of both cones	90°
Natural frequency of reinforced edge cone on elastic threads without magnetic field	Less than 3 ~
Natural frequency of cone as a whole on rubber surround without magnetic field	About 30 ~
Baffle	6 ft. square

In case (1), starting from zero frequency, where  $m_e$  is the natural mass plus the accession to inertia, the value gradually increases due to increase in the latter\* up to 200 ~. Thereafter the rise is chiefly concerned with the elastic and inertia forces of the diaphragm structure, the action being similar to that of the aluminium disk in the last section. The maximum at  $B_1$ † is similar to the case of the disk in Fig. 110, where a centre-stationary mode is approached. Beyond  $B_1$  the curve drops rapidly as in the disk case. In the present instance this is due in part to the air-column vibrations (Chap. XVIII, § 15), which increase the motional resistance  $R_m$  and reduce  $L_m$  to some extent. The rise after 1,000 ~ is caused by the presspahn annulus

\* At zero frequency (limiting motion)  $m_i$  with a 6-ft. baffle is half its value with an infinite baffle [3 a]. As the frequency rises the baffling becomes more effective and  $m_i$  increases.

† The dimple at 300 ~ is due to the seam of the cone.

at the edge executing a vibrational mode, the inner circumference being relatively at rest, i.e. a stationary-centre type. Just above 1,500  $\sim m_e$  is negative. If the curve were continued it would cross the axis at about 2,000  $\sim$  where the main centre-moving symmetrical mode occurs. Beyond this the effective mass is quite small.

Curve 2 relates to a diaphragm similar to that of curve 1, but mounted on an annular rubber surround.\* The fundamental mode of the latter as an annular membrane introduces a condition at  $A_2$  of

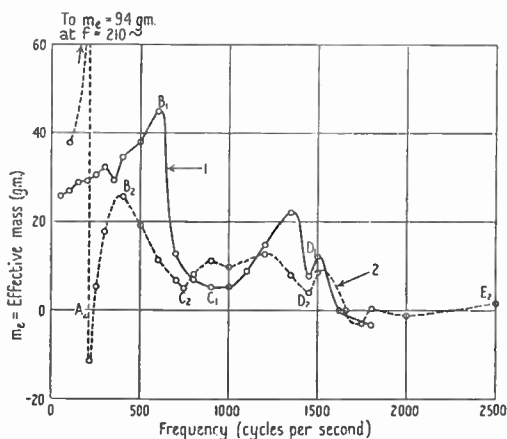


FIG. 111. Curves showing effective mass of coil-driven conical paper diaphragms 12.2 cm. radius, apical angle  $90^\circ$ .

- (1) Edge of diaphragm reinforced by narrow presspahn ring to suppress radial modes.
- (2) Edge of diaphragm bent over and supported by rubber annulus.

the same nature as a centre-stationary mode. The underlying theory is given in Chap. IV, § 12. The remainder of the curve can be explained in the same manner as curve 1. Above 800  $\sim$  there are two undulations due to resonance of the membrane and the bent-over portion at the edge of the diaphragm to which it is attached.

Similar results have been obtained with thin aluminium cones of the type discussed in Chap. XVIII, § 17.

Hitherto our attention has been confined to symmetrical modes of vibration since the changes in effective mass far exceed those at a radial mode. In fact, unless the diaphragm is abnormally asym-

\* At zero frequency, owing to the surround elasticity,  $m_e = -\infty$  (see Fig. 33).

metrical about the polar axis, due to the seam or to bad construction, the variation in  $m_e$  at a radial mode is quite insignificant. From theoretical considerations this must be so, because contiguous identical radial sectors, having equal and opposite motions, do not affect the driving-point impedance. With some diaphragms there is a variation in  $m_e$ , but it is of no importance dynamically. The main item is enhanced radiation resistance due to asymmetry caused by the seam (Fig. 125, curve 1).

In all the preceding cone cases the mass of the coil and its former is included in that of the diaphragm. Below 1,400  $\sim$  the coil can probably be regarded merely as an added mass, but above 1,400  $\sim$  the vibrational characteristics of the diaphragm depend upon the coil mass (Chap. XVIII). To obtain  $m'_e$ , the effective mass due to the diaphragm alone, it is merely necessary to subtract the mass of the coil and its former. This can be done on the diagrams by shifting the horizontal axis upwards by an amount  $m_c$ . The value of  $m'_e$  so obtained is the contribution due solely to the diaphragm when it is driven under specified conditions. It is not the effective mass of the diaphragm as an isolated structure.

### 8. Cones complete to the vertex

It was mentioned in a previous section that satisfactory effective mass curves cannot be obtained with reed-driven cones by measuring  $L_m$  and  $R_m$ . To obviate this difficulty a coil-drive system of the form illustrated in Fig. 112 is used. The air-gap in the magnet should be fairly large, centring being accomplished by elastic threads, so that the natural frequency of the system is very low. To get the effective mass of the cone *per se*, that of the driving mechanism must be subtracted. The latter should be tested by itself to ensure constancy over the frequency range. If some form of centring device is used in preference to the elastic suspension, which is admittedly somewhat delicate, care must be taken to ensure that it has only one vibrational frequency which is well below audibility. It must be remembered that the majority of such devices have more than one mode of vibration (see Chap. IV).

A second method of determining  $m_e$  is to attach the cone to a tunable vibrator, e.g. a rod clamped at both ends and magnetically driven, and, by the method of beats or by observing the amplitude, to find the fundamental frequency of the loaded vibrator [36]. The

cone is then removed and replaced by a mass  $m_e$  to give the same resonant frequency. Several rods may be needed to cover a wide frequency band. When  $m_e$  is negative the cone *raises* the vibrational frequency of the rod. The procedure is therefore to load the latter with an additional mass. Having found the vibrational frequency with the cone, the latter is removed together with an amount  $m_e$ , so that the resonance occurs at the same frequency as before. In place of a rod any other suitable vibrator can be used, e.g. a stretched wire or tape of magnetic material whose tension can be varied [36]. It is important that the tape be driven to make the cone vibrate along its

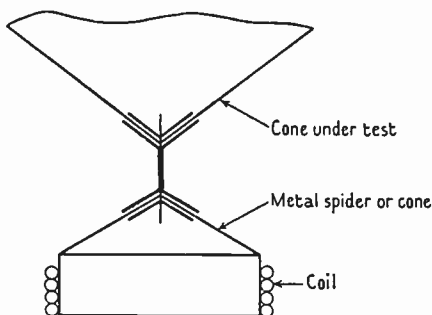


FIG. 112. Illustrating attachment of cone to driving mechanism for finding the effective mass at various frequencies.

axis without wobble or sideways motion. The effective mass of a conical shell is quite different if driven axially and at  $90^\circ$  thereto, since it is relatively supple in the latter case.

### 9. Measurement of accession to inertia ( $m_i$ )

(a) If the effective mass  $m_e$  is measured in air and *in vacuo* by any of the preceding methods, and if the diaphragm is assumed to preserve the same shape in both cases, the difference in the two values, namely,  $m_{ea} - m_{ev} = m_i$ .

(b) At low frequencies when  $R_m$  is negligible and the diaphragm moves as a whole, we have, from (18) Chap. VII,

$$(m_n + m_i) = m = \frac{s}{\omega^2} - \frac{C^2}{\omega^2 L_m}$$

$$C^2 = \omega^2 \left( \frac{s}{\omega^2} - m \right) (L_1 - L_0). \quad (1)$$

or



*In vacuo* under the above conditions

$$C^2 = \omega^2 \left( \frac{s}{\omega^2} - m_n \right) (L_v - L_0). \quad (2)$$

From (1) and (2)

$$m_i = (m - m_n) = \left( m_n - \frac{s}{\omega^2} \right) \left( \frac{L_v - L_1}{L_1 - L_0} \right). \quad (3)$$

If the diaphragm is suspended so that the fundamental frequency due to  $s$ , i.e.  $\omega = \sqrt{(s/m)}$ , is well below audibility, the term  $s/\omega^2$  can be omitted. Formula (3) then becomes [2 b]

$$m_i = m_n \left( \frac{L_v - L_1}{L_1 - L_0} \right). \quad (4)$$

In neither case is a knowledge of  $C^2$  essential. The advantage of the method is that structural changes in the conical diaphragm of a moving-coil speaker are unnecessary. When the resonance frequency, due to the surround, occurs in the audible range, formula (3) must be used.\*

(c) When a vacuum is not available and *the diaphragm moves as a whole*, we have from (1) for measurement in air,

$$C^2 = \omega^2 \left( \frac{s}{\omega^2} - m \right) (L_1 - L_0). \quad (5)$$

If the diaphragm is removed, and the coil† is suspended by fine threads so as to have a very low axial frequency of vibration,

$$C^2 = \omega^2 m_c (L_0 - L_c), \quad (6)$$

since  $s_c/\omega^2$  is negligible. Equating (5) and (6) we obtain

$$m_i = m_c \left( \frac{L_0 - L_c}{L_0 - L_1} \right) - \left( m_n - \frac{s}{\omega^2} \right), \quad (7)$$

since  $m = m_n + m_i$ . When  $s/\omega^2$  for the diaphragm is negligible,

$$m_i = m_c \left( \frac{L_0 - L_c}{L_0 - L_1} \right) - m_n. \quad (8)$$

## 10. Experimental results

Using method (c) a series of experiments was conducted on a diaphragm whose dimensions are shown in Fig. 113.

Measurements of  $L_1$  and  $L_0$  were made using the bridge method of § 2 in conjunction with a powerful oscillator and a sensitive vibra-

\* When an inductance bridge is not available, the method described in reference [34 b] can be adopted.

† The use of a similar coil obviates removal of that from the diaphragm.

tion galvanometer. The coil-stationary condition was adequately simulated by short-circuiting the magnet winding on itself, since the metal was soft iron of low remanence. The coil was, therefore, always in the same mean position.

The value of  $L_1$  is zero at the electromechanical resonance frequency, and below this it is negative, owing to the capacity action associated with the motional back e.m.f.

The experimental data are set forth in Table 24 [2 b]. There is a fair agreement between the calculated and experimental values of  $m_i$  at 200 and 150  $\sim$ . In this respect it should be noted that the calculated results refer to a flat disk in an infinite baffle, whereas those obtained by experiment pertain to a conical diaphragm with a finite baffle. Strictly, therefore, the comparison is not between theory and practice for a rigid disk, but between two dissimilar shapes (cone and disk) to show the existing resemblance. So far as could be discerned stroboscopically, the diaphragm moved as a whole at the test frequencies. The value of  $m_i$  is down at 100  $\sim$ , since the size of the baffle was inadequate to prevent appreciable interference between the back and front of the diaphragm. As the frequency is

reduced below 100  $\sim$ ,  $m_i$  slowly decreases when the baffle is only 6 feet square. Readings were also obtained without the baffle. At 25  $\sim$   $m_i$  was about one-half its value at 200  $\sim$ . This is in accord with the rigid disk theory, where  $m_i$  is halved on removal of the infinite baffle [3 a]. In the latter condition the shape of the diaphragm has a definite effect. For a rigid disk  $m_i = \frac{8}{3}\rho a^3$ , and for an axially

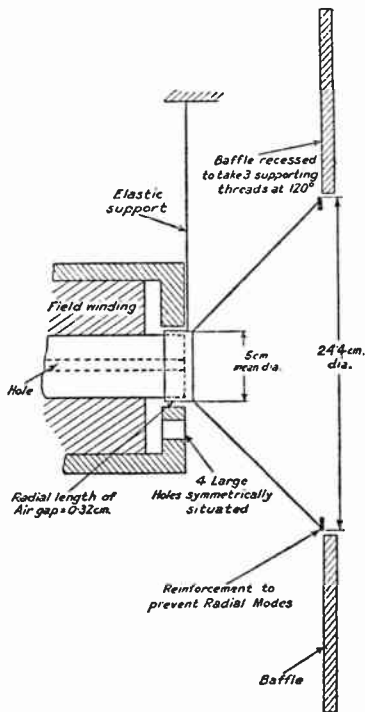


FIG. 113. Illustrating arrangement of diaphragm used for the determination of  $m_i$ , the accession to inertia. The presspahn reinforcement prevents radial modes. Angle of cone 90°.

vibrating sphere  $m_i = \frac{2}{3}\pi\rho a^3$ , so the ratio disk to sphere is  $4/\pi$ . A double cone would doubtless give a value of  $m_i$  approaching that for a sphere of like radius.

TABLE 23

*Illustrating the method of finding  $m_c(L_0 - L_c)$  of expression (6)*

The effect of the bridge leads cancels out. Turns on coil = 40 of 28 s.w.g. about 2.5 cm. mean radius. Effective mass of coil, leads, and suspension,  $m_c = 7.5$  gm.

<i>f.</i> Frequency (cycles per second)	$L_0$ Inductance of coil at rest, including bridge leads (microhenrys)	$L_c$ Inductance of coil in motion without diaphragm, including bridge leads (microhenrys)	$m_c(L_0 - L_c)$ (gram- microhenrys)
100	+324	$-6.624 \times 10^3$	$5.21 \times 10^4$
150	+310	$-2.776 \times 10^3$	$2.31 \times 10^4$
200	+302	$-1.398 \times 10^3$	$1.275 \times 10^4$

TABLE 24

*Data illustrating computation of  $m_i$*

Effective mass of coil, diaphragm, leads, etc. = 25 gm. Baffle 6 feet square.

<i>f.</i> Frequency (cycles per second)	$L_0$ Inductance of coil at rest, including bridge leads (microhenrys)	$L_1$ Inductance of coil in motion with diaphragm, including bridge leads (microhenrys)	$m_i$ Accession to inertia (gm.)	
			Experiment using baffle 6 ft. square	Calculation assuming infinite baffle
100	+324	-1,208	9	12
150	+310	-315	12	12
200	+302	-34	13	12

### 11. Effect of adding a mass to a diaphragm

Experiments were performed to find the mass of a 10-gm. weight added to a diaphragm [2b], computed from values of  $L_1$  and  $L_0$ , using a formula given hereafter [formula (11)]. When attached with adhesive on top of the cone half-way down the slant side, the measured mass at 80 ~ was zero. Stroboscopic examination revealed that the mass pitched, tossed, and rolled like a ship on an angry sea. The diaphragm simulated the sea, and its dynamical state was so perturbed that the portion in the immediate vicinity of the mass 'broke up'. Thus the mass had no electrical counterpart in the

measurement of  $L_1$ . A like result was obtained with the mass attached to the centre of a paper disk glued across the mouth of the cone. When situated at the stiff outer edge or near the coil, the measured value agreed quite well with the actual value. These experiments show how easy it is to make a diaphragm break up locally at a frequency well below that of the main symmetrical mode of vibration (about 2,000  $\sim$ ). Under this condition no reliance can be placed on measurements of mass.

From (5), when  $s$  is negligible, the total mass

$$m = \frac{C^2}{\omega^2(L_0 - L_1)}. \quad (9)$$

When a mass  $m_1$  is added, and  $m$  is the same as above,

$$m_1 + m = \frac{C^2}{\omega^2(L_0 - L_2)}, \quad (10)$$

$L_2$  being the inductance with the coil in motion. Eliminating  $C^2/\omega^2$  from (9) and (10)

$$m_1 = m \left( \frac{L_2 - L_1}{L_0 - L_2} \right). \quad (11)$$

## 12. Measurement of $C^2$

This quantity is defined statically\* as  $(2\pi r n B_p)^2$ , so that it can be found from measurements of  $B_p$  as described in Chapter XIV. The weighing method has the merit of being allied to practical conditions, but the current is direct. With A.C. there are two effects which modify  $C^2$ , (a) hysteresis and eddy-current losses in the magnet, (b) deformation of the radial field due to the coil current. The influence of (a) is to cause a phase change between total coil current and that which corresponds to the operative mechanical force. The latter is  $CI \cos \theta$ , where  $\theta$  is the angle between the two currents. The value of  $\cos \theta$  varies according to the type of magnet and the radial length of the gap, but is usually from 0.9 to 1.0.

$C$  can also be measured at various frequencies by suspending a coil of known mass in the correct position in the air-gap, using a very weak constraint. Then from (6) we have

$$C^2 = - \frac{\omega^2 m_c}{L_{mc}}, \quad (12)$$

since  $R_{mc}$  is negligible with no diaphragm. The results up to about 2,000  $\sim$  are likely to be fairly accurate, and they are measured under

\* Definition 43.

conditions closely allied to practical requirements. Beyond this frequency trouble may be experienced with the iron, as described elsewhere (§ 3).

If the axial amplitude ( $\xi_{\max}$ ) of the coil is measured by optical means, then  $\text{Force} = C \cos \theta I_{\max} = \omega^2 \xi_{\max} m_c$ , so

$$C \cos \theta = \frac{\omega^2 \xi_{\max} m_c}{I_{\max}}. \quad (13)$$

### 13. Measurement of the axial stiffness $s$

When  $C$  is known, calculable axial forces can be applied to the coil by means of direct current. Measurement of the displacement by optical means, e.g. a cathetometer, enables the force-deflexion characteristic to be plotted.  $s$  is the slope thereof. For large deflexions the characteristic will be curved, due to variation in  $C$  as the coil emerges from the magnet and, in some cases, to non-linearity of the constraint. The deflexion is limited, since neither the centring device nor the surround will stretch beyond a certain amount. As an alternative, the deflexional forces can be produced by weights or a stiffness meter can be used [188]. Care must be taken to ensure that the forces are applied directly to the coil, but not to the diaphragm.

The stiffness coefficient can also be found dynamically. If the resonance frequency of the diaphragm on the constraint is found by any suitable method (see Chap. XIX, § 2), then  $s = \omega_0^2 m_e$ , where  $m_e$  is the natural mass plus the accession to inertia. The former is found by weighing and the latter by a calculation; or  $m_e$  can be measured directly as shown in § 5. When the resonance frequency is found without a baffle, and it occurs below 100  $\sim$ ,  $m_i = \frac{8}{3} \rho_0 a^3$  for diaphragms up to about 14 cm. radius. To incorporate the influence of the surround  $a$  can be taken as its mean radius.

## XVII

### RESPONSE CURVES

1. THERE are various ways of regarding response. Suppose a microphone is situated at a certain point in the same enclosure as a loud speaker. If the grid of the power valve is supplied with constant voltage at all frequencies, the output from the microphone amplifier represents the performance of the speaker under *certain* conditions. With a condenser microphone which registers sound pressure, the square of the readings is a measure of the power at the position of the microphone. Owing to reflection within the enclosure, the energy distribution is quite different from that in free air, unless the damping due to absorbent material on the walls is very great. This condition is difficult to obtain at low frequencies. Due to focusing of the radiation, the results vary according to the position of the microphone relative to the axis of the speaker. There are the following variable factors: (1) size of enclosure, (2) mean absorption coefficient of enclosure, (3) relative position of speaker in enclosure, (4) distance of microphone from speaker, (5) relative angular position of the axes of these two. Considering these items in actual usage, where room characteristics, loud-speaker location, and listener's position are very diverse, it seems that acoustical test conditions are seldom likely to be simulated. It is necessary, therefore, to conduct tests under conditions from which the maximum amount of information regarding speaker performance is likely to be obtained. Tests are invariably conducted in a damped enclosure, and the higher the damping the better.

#### 2. Minimum microphone distance

In Chap. V, § 2, it is shown that when a rigid disk vibrates in an infinite baffle, nodal points occur on the axis at high frequencies. As a working rule it was stipulated that to avoid the nodal regions, the distance of the microphone from the speaker should exceed  $\omega a^2/2\pi c$ . Although this formula only applies rigorously to a rigid circular disk in an infinite plane, it can also be used for conical diaphragms and horns, where  $a$  is to be regarded as an equivalent radius.

#### 3. Axial pressure

Axial measurements made with an inductor speaker in a 'dead' room, the diaphragm being set in one wall, gave the curve [141] of Fig. 114.

The free-space infinite baffle condition is simulated if the wall housing the diaphragm is non-absorbent. An absorbent wall introduces free-space conditions (solid angle  $4\pi$ ), where one side of the speaker is screened. Owing to focusing, the axial pressure curve is not a criterion of the performance to be expected in an average room. In fact, apart from transients, if the output is constant over a definite frequency band, the influence of reflection in an ordinary room is to make the distribution much more uniform. Thus by placing the speaker in a suitable position a pleasing result can be obtained, provided the room is not too small. In general, if an axial pressure curve in a

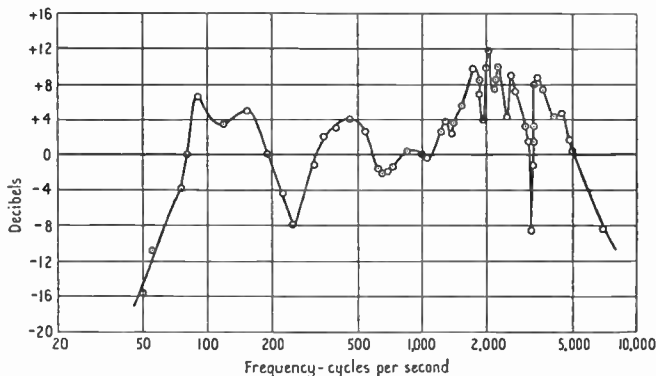


FIG. 114. Response of inductor dynamic speaker when measured on its axis with the microphone at a distance of 60 cm. The current to the speaker was kept at the constant value of 5 mA. (Zero on decibel scale refers to 5.5 dynes per sq. cm.)

'dead' room shows a fairly uniform characteristic, the upper frequencies are usually weak except on the axis, and in an average room the reproduction sounds woolly and inert. Assuming the diaphragm to be simulated by a rigid disk, the axial pressure curve for constant output is shown in Fig. 99. In practice, as shown in § 13, the effective radius of the disk decreases with rise in frequency. This introduces a modification in the axial pressure curve.

To overcome the objection to axial pressure curves several courses can be pursued, two of which will be described. Assuming the radiation to have circular symmetry about the polar axis, measurements of the pressure are taken at a suitable distance from the speaker at various angles  $\phi$  with the axis. The angle  $\phi$  is varied from 0 to  $\pm 90^\circ$ , or, if the symmetry is satisfactory, only from 0 to  $90^\circ$ . If the speaker

is set in a non-absorbent wall, the infinite baffle condition is approximated when the remainder of the enclosure is highly absorbent. By integrating the square of the pressure over a hemispherical surface whose radius is the microphone distance from the speaker, the power output on one side of the diaphragm can be found at any frequency. If the speaker is set in an absorbent wall, the conditions are those of infinite space as described above. This procedure is laborious and necessitates a large number of readings to cover a wide frequency band. The same experiments can be performed if the speaker is set in the ground out-of-doors where the infinite baffle condition is well simulated [45, 135]. Care must be exercised to exclude radiation from the back of the speaker. Any form of absorbent enclosure used for this purpose must not introduce resonance.

In general, to reduce reflection and standing-wave effects at the microphone to a small pressure value compared with the direct radiation, a very large room with much absorbent material is required. This is commensurate with high expenditure which may not always be commercially justifiable. When, in the interests of economy, comparatively small rooms are used, it is difficult to eliminate standing-wave effects at the lowest frequencies. Under this condition the open-air test is advocated.

#### 4. Warble tone [124]

Sometimes the test frequency  $\omega_0/2\pi$  is varied  $\pm\Delta\omega_0/2\pi$  cycles per second ( $\Delta$  being a small fraction) at a definite rate, say ten to fifteen times per second, to reduce the influence of standing waves. This is known as a warble tone. It is not proposed to analyse the procedure mathematically, but some comments will be made below for practical guidance. To ensure freedom from errors at the low frequencies a large testing-room is required, and  $\Delta\omega_0/2\pi$  must be a small fraction of  $\omega_0/2\pi$ , so that the test substantially pertains to conditions at the main frequency [124]. At low frequencies a resonance peak may only last a few cycles, so that with  $\Delta\omega_0/2\pi = 100 \sim$  it could easily be obliterated. There is also the variation in absorption of the room with frequency to be considered. Referring to Fig. 10, Chap. II, one of the critical factors is  $l = S'P_1 - SP_1$ , the difference in length of the image and direct rays. For a partial node to occur at the microphone,  $\Delta\omega_0/\pi = c/l$ , so the proportionate frequency change is

$$\Delta\omega_0/\omega_0 = \pi c/\omega_0 l = \lambda/2l.$$



If  $l$  is constant the proportionate change increases with increase in wave-length, i.e. at low frequencies. As indicated above, this change must be within definite limits to obtain representative results. The maximum permissible value of  $l$  depends upon the room dimensions; the larger the room the greater  $l$ . The largest value is obtained for a given room when the speaker and microphone are centrally situated, the distance between them being the minimum,  $a^2\omega/2\pi c$  (Chap. V, § 2). The optimum position can be located by a little elementary geometry. Good results are obtained if  $l \geq 3\lambda$ , where  $\lambda$  is the lowest test frequency. On the whole the warble tone should be used with discretion. In general a pure tone is preferable for test purposes, but there must be complete assurance that standing-wave phenomena have been reduced to an insignificant order of importance. There are well-known means of discovering whether a test room is adequately damped, and these should always be used in the first place to determine the properties of the room throughout the entire frequency range.

### 5. Orbital method

Another method of test is to rotate the microphone in a circle whose centre is on the speaker axis, but whose plane is at  $45^\circ$  thereto [125 a]. The diameter of the circle should exceed half a wave-length of the lowest test frequency, so that difficulties are not experienced with standing waves. A sluggish thermoammeter is used to measure the output from the amplifier following the condenser microphone. Thus an average of the square of the sound pressure, and therefore of the energy density, is obtained over a large area. Assuming listeners to be seated within the solid angle subtended at the speaker by the orbit, the test gives an approximate indication of the performance to be expected. This method is useful in cases where the floor and wall absorption in the test room is insufficient to simulate free-air conditions closely. The influence of standing waves is averaged out and the tests can be conducted very rapidly compared with that in Chap. XV, § 5, which involves integration over a hemisphere.

### 6. Definition of 'Response'

The average energy density (see definition 5) in a room where a loud speaker is emitting sound at a constant rate is [210]  $e = 4P/cAa_s$ , where  $P$  is the power radiated and  $a_s$  the mean absorption coefficient

(see § 14). This can also be written [215]  $e = \frac{1}{\rho_0 c^2 V} \iiint p^2 dV$ , where  $V$  is the volume of the room. From these two formulae we obtain [125 a]

$$P = \frac{Aa_s}{4V\rho_0 c} \iiint p^2 dV, \quad (1)$$

where  $p$  is the root mean square pressure *measured at every point in the room*. Now

$$\frac{1}{V} \iiint p^2 dV$$

is the mean, or average of the pressure squared *throughout* the room and will be written  $p_{av}^2$ . Thus the formula in (1) becomes

$$P = \frac{Aa_s}{4\rho_0 c} p_{av}^2 = \frac{K_1}{4} p_{av}^2, \quad (2)$$

where  $K_1 = Aa_s/\rho_0 c$ . If the speaker resistance in action is  $R_1 = R_0 + R_m$ , the maximum sound power for a given voltage swing on the grid of the power valve is obtained when the valve resistance is equal to that of the speaker transferred to the anode circuit by the transformer. The power is then, with a perfect speaker of radiation resistance  $R$ ,  $P = E^2/4R$  [Chap. XV, § 1 (b)]. Hence the absolute efficiency is [Chap. XV, § 1 (b)]

$$\eta_{ab} = \frac{K_1 p_{av}^2}{(E^2/R)}. \quad (3)$$

The orbital method gives  $p_{av}^2$ , not for the whole room, but for a representative part of it. The coefficient  $K_1$ , together with the room dimensions, influence the spatial distribution and the level at any prescribed distance from the speaker. If, however, it is agreed to specify the conditions of test in each case, the ratio  $p_{av}^2/(E^2/R)$  is defined as the 'response' of the speaker—under the specified conditions.\* It is customary, as in all acoustical work, to express the 'response' in decibels, so we have [125 a, 130]

$$r_s = 20 \log_{10} \frac{p_{av}}{E/\sqrt{R}}. \quad (4)$$

This is an index of the absolute efficiency throughout the microphone orbit for the given conditions of test. These should be stated on the test schedule as follows: (1) room dimensions, (2) nature of absorbent material on surfaces and mean coefficient of absorption, (3) method

\* This is the definition adopted by the Institute of Radio Engineers based on reference [125 a], and is used when the orbital or other methods of test are employed.

of test, e.g. orbital, axial, etc., (4) size of baffle, if used, or position of speaker in wall or otherwise, (5) resistance of power valve.

## 7. Testing apparatus

A schematic diagram of the apparatus is shown in Fig. 115. The speaker and the condenser microphone, whose complete calibration curve is known, are suitably situated in a damped enclosure or outside in free air, according to test conditions [125 a, 130]. The output voltage of the oscillator, when open-circuited or connected to the attenuator, is adjusted to some suitable value as indicated by the valve voltmeter. Alternatively the adjustment can be made to obtain

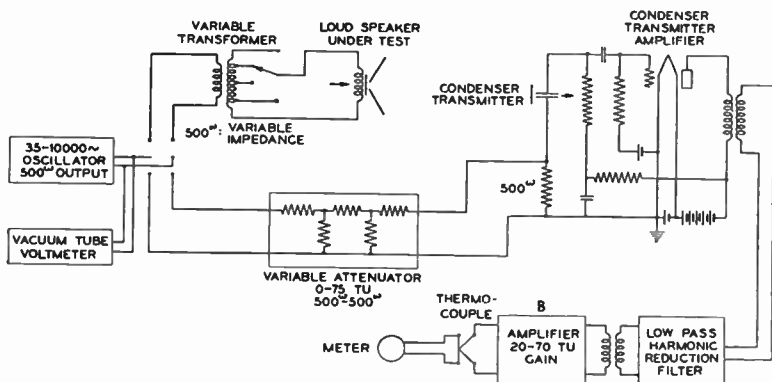


FIG. 115. Schematic circuit of loud-speaker response measuring system.

a suitable current in the speaker. This should be sufficient to cause a sound pressure at the microphone well above the level of any extraneous noise. The oscillator is then connected to the speaker and the control on the amplifier *B* manipulated until a mid-scale reading is obtained on the sluggish thermoammeter, as a result of sound waves from the loud speaker acting on the microphone. The oscillator is now switched from the speaker to the input of the attenuator, and the latter adjusted until the mid-scale reading is again obtained. The attenuator reading in decibels is an index of the relative performance of the speaker at the test frequency, provided the microphone calibration is constant. If this is not so, the variation in level from some selected frequency must be added to or subtracted from the attenuator readings, according to the calibration-curve data. Alternatively,

if the datum-level is found for each reading, as shown hereafter, the same thing is accomplished.

To fix the datum-level, the open circuit voltage of the oscillator is made equal\* to the square root of its output impedance, so that  $E'/\sqrt{R'} = 1$ . Then from the calibration curve of the microphone the output voltage corresponding to a r.m.s. sound pressure of one dyne cm.<sup>-2</sup> (one bar) on the diaphragm is known. Amplifier *B* is set to give its mid-scale reading under this condition. The oscillator is then connected to the attenuator and the latter varied until the mid-scale reading is again attained. This setting of the attenuator is the decibel datum from which the response curves can be plotted.

### 8. Features of the orbital method

It is unnecessary to calibrate the oscillator output or the *B* amplifier. The low pass filter ensures that all harmonics are excluded from the readings, so tests are made on the fundamental frequency alone. The filter can be altered to cover a wider range as the frequency rises without affecting the calibration, provided the *B* amplifier is adjusted to preserve mid-scale or any other constant reading. If the filter is not used, the output wave form must be checked by a cathode ray or other oscillograph, or by other suitable means.

If the speaker under test is not overloaded and its characteristic power input-current curve is linear, the response is independent of variation in oscillator voltage, since any change affects the speaker current and the attenuator equally. It is important, however, to keep the microphone polarizing voltage constant to prevent variation in sensitivity. The voltage should be equal to that used during the calibration test of the instrument.

### 9. Automatic operation

The whole of the foregoing procedure can be done automatically if desired. It is preferable to equalize the microphone and its amplifier to obtain uniform voltage output at all frequencies for constant sound pressure on the diaphragm. If this is not done, the record must be corrected accordingly. When the microphone is kept stationary the frequency range can be swept through by aid of a constant output beat-oscillator, consisting of a weak oscillator of constant high frequency and a strong variable one. The condenser of the latter unit

\* Numerically.

is varied to cover the necessary range. Its vanes are shaped to give a logarithmic frequency scale, or this result may be obtained by a driving cam. If the same motor is used to drive the condenser and the record paper, variations in speed are immaterial. The filter can be altered at intervals by contacts on the condenser driving-gear operating either direct or through relays. The output from the amplifier *B* is taken to a linear rectifier and thence to a linear recording mechanism, which need not be photographic. In a scheme of this nature a record can be taken in about three minutes. Specially prepared record paper 'corrected' for the microphone calibration can

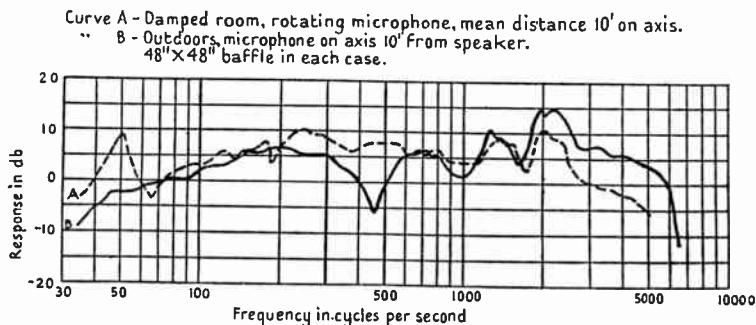


Fig. 116. Comparison of indoor and outdoor response measurements on moving-coil hornless speaker.

be used if desired. Alternatively the record can be corrected by a special geometrical appliance [169].

## 10. Experimental data

As a typical example suppose we examine Fig. 116. The dotted curve refers to the rotating-microphone method used in a room whose reverberation time (see definition 14) at 512  $\sim$  was  $10^{-1}$  sec. [142]. The orbit of the microphone was at  $45^\circ$  to the speaker axis and 8 feet in diameter, thereby entailing a low-frequency limit of 70  $\sim$  for a representative orbital mean value. The average microphone distance was 10 feet. At 50  $\sim$  there is a definite peak, which is attributed to the standing-wave pattern in the room where the distance between maxima is about 12 feet, this being 50 per cent. greater than the orbit. As the frequency rises above 50  $\sim$  there are the usual fluctuations in response, associated with vibrational modes of the system, which are generally most prominent in the 2,000  $\sim$

region. The symmetrical modes prevail here as shown in Chapter XVIII. Compared with the full-line outdoor curve, the absorption of the room above 2,000  $\sim$  appears to have reduced the resonances 5 decibels, which corresponds to a power ratio of 3/1. Actually this is not the case since the apparent decay is attributed to two causes: (a) focusing of the radiation in the neighbourhood of the axis at high frequencies, (b) reduction in room absorption at lower frequencies. In connexion with (a), the wide orbit of the microphone means that it enters the weaker portion of the sound field, so the average value of  $p^2$  is less than that on the axis. Consequently any curve taken by the orbital method is more representative than one taken on the axis with a stationary microphone. Herein lies the efficacy of the method. The full-line outdoor curve refers to axial pressure, and due to cone resonances the curve rises 10 decibels above its level at 800  $\sim$ .

### 11. Interference on axis

The dip in the full-line curve of Fig. 116 at 460  $\sim$  is of considerable interest. It is due to interference of the radiation from the front and rear of the baffle which was 4 feet square [142]. At any axial point the sound pressure is the resultant of these two. When the two sides of the diaphragm are regarded as simple sources of opposite phase, there is a minimum on the axis when  $2kd = 2n\pi$ , where  $2d = d_1$  is the equivalent distance between the sources (Chap. II). At any axial point  $P_1$ , far distant from the diaphragm, the relative phase of the radiation from the two sides depends approximately upon the *radius* of a circular baffle, so this is  $d_1$ . From above the condition for minima is  $d_1 = 2d = 2n\pi/k = n\lambda$  or  $\omega = 2\pi nc/d_1$ , whilst for maxima  $2kd = (2n-1)\pi$  or  $\omega = (2n-1)\pi c/d_1$ . Taking  $n = 1$  and  $d_1 = 2$  feet, the minimum should occur at about 570  $\sim$ , whereas it actually occurs at 460  $\sim$ . Since the baffle is square and sound waves bend round it with a definite radius of curvature, the equivalent distance  $d_1$  is increased to 2.44 feet, i.e. about 20 per cent. The influence of the square baffling and the cornering of the waves is therefore appreciable. The next minimum is 920  $\sim$ , and it will be seen that a dip occurs in this neighbourhood. At higher frequencies the focusing of the radiation on each side of the baffle is pronounced, so the front-to-rear interference substantially vanishes.

The first maximum occurs at 230  $\sim$  although it does not show up appreciably on the curve. Other maxima occur at 690  $\sim$  and at

1,150 ~. Obviously these effects average out in the orbital method of test. In § 5 we saw that the microphone distance should exceed  $a^2\omega/2\pi c$ . The consequence of violating this test canon is illustrated in Fig. 117 [125 a], which shows two response curves for a moving-coil horn speaker of the type in Fig. 82 A. The full-line curve refers to a microphone stationed only 2 inches from the plane of the horn mouth. The crevasses at 750 ~ and at higher frequencies are due

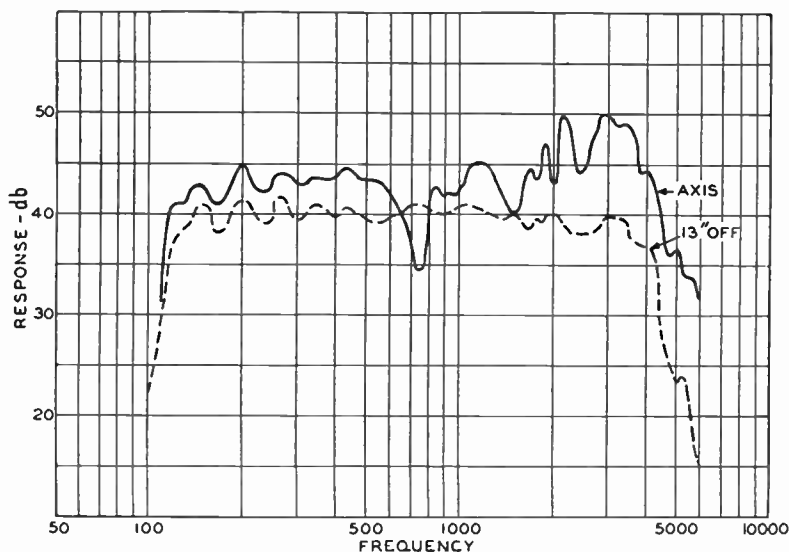


FIG. 117. Response-frequency characteristics of moving-coil speaker with 115 cycle cut-off exponential horn. Measured outdoors 2 inches from plane of horn mouth with centre of condenser microphone diaphragm on horn axis and 13 inches from axis.

to interference of radiation from various parts of the opening. With a rigid disk and baffle system the pressure would vanish instead of being a minimum (Chap. V, § 2).

## 12. Influence of baffle dimensions

(a) *Flat baffle.* The influence of reducing the size of the baffle from 4 ft. to 2 ft. 6 in. square is illustrated in Fig. 118 [142], both curves being taken in free air 35 feet above the ground. The reduction in level below 300 ~\* with the smaller baffle is very marked and bears

\* Power level.

out the analysis in Chapter II. With this baffle, serious interference occurs on the axis. At 400 ~ there is a maximum, whilst a minimum occurs at 800 ~. Below 200 ~ the vertical distance between the curves for the two baffles remains almost constant. This is in accord with the theory in Chapter II. At very low frequencies the curves will approach and ultimately intersect at the origin.

(b) *Box baffle.* As shown in Chapter II the function of a baffle is to screen the two sides of a diaphragm from each other, thereby reducing interference. A large flat baffle not only does this, but it

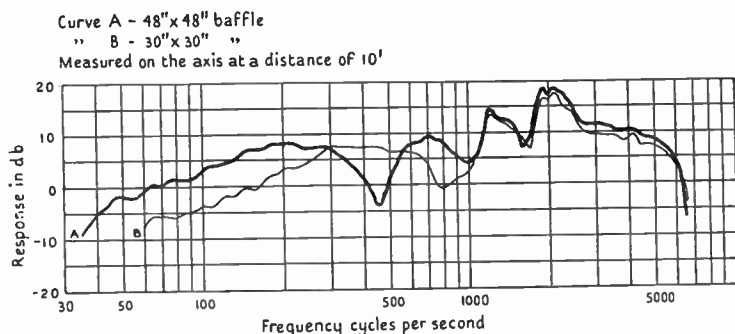


FIG. 118. Outdoor response curves of moving-coil speaker with flat baffles of different sizes

increases the solid angle into which each side discharges (Chap. II). This enhances the acoustic loading. Flat baffles are not very suitable for domestic reproducers, so it is customary to use a cabinet which can be regarded as a box baffle. For equal distances between the two sides of the diaphragm (round the baffle), the box type is inferior to the flat baffle and invariably introduces resonances, particularly if it is located near a wall. Comparison curves of flat and box baffles giving equal distance separation between the sides of the diaphragm are shown in Fig. 119.\* The various points enumerated above are clearly emphasized in these curves. The solid angle at the back of the diaphragm is increased considerably, and that at the front decreased accordingly. These opposite effects do not compensate, owing in part to the box acting as a stumpy horn of constant section. Reflection from the back of the box (mouth of the horn) causes loss at very low frequencies and introduces resonances in the middle

\* [142].



register. By constructing the rear of the box in the form of a short logarithmic horn these defects can be obviated to some extent. In particular, if the box is lined with absorbent material to give an exponential contour, the reproduction is much improved due to damping of the resonances. From the theory of horns in Chapter X it is evident that the loading on the rear of the diaphragm increases above the cut-off frequency of the exponential baffle. If the dimensions are known this frequency is easily found. Assuming it to be 200 ~ the register above this will be reinforced at the rear, so that

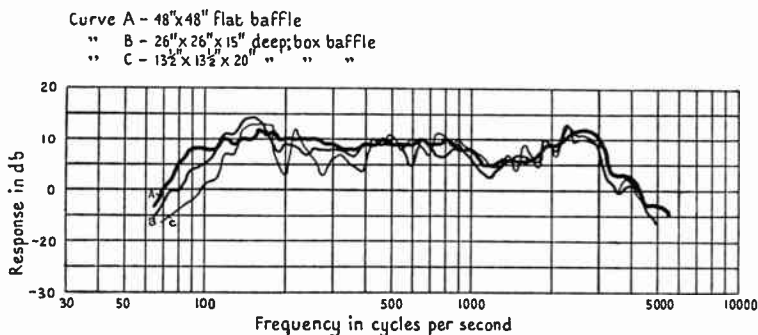


FIG. 119. Response of moving-coil speaker in three different baffles having equal circulation path lengths.

if the upper register at the front is rather powerful when a flat baffle is used, the box baffle will give a better tonal balance. The upper register from the rear will be reduced due to absorption. On the whole, therefore, there is every reason to believe that the use of an absorbent box baffle will yield good reproduction, and this is borne out in practice. A design embodying these principles is shown pictorially in Fig. 120 [180].

### 13. Polar curves

These curves are got with the same apparatus as that required for response tests excepting that the microphone is not rotated. It is placed at various angles with the polar axis of the speaker, at a distance well beyond that where nodal points occur (Chap. V, § 2), usually in a horizontal plane containing this axis. Tests on a horn speaker having a 115 ~ cut-off [125 a] are shown in Fig. 121, the microphone being 12 feet from the mouth of the horn. Owing to

the large opening focusing begins quite early in the frequency range. To obtain a reasonable amount of sound above 4,000  $\sim$ , it is necessary for a listener to be tolerably near the axis of the horn. On the other hand, owing to room reflection, the distribution of sound under ordinary listening conditions is such that levelling up occurs, and the characteristic tends to the form obtained by the orbital method. This is valid for steady sounds. Unless a listener is near the axis

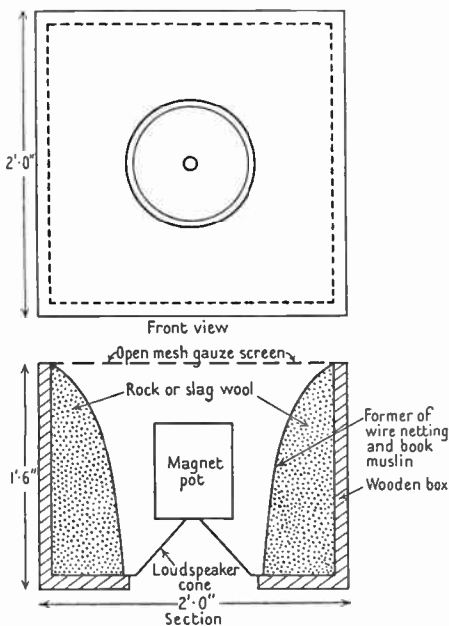


FIG. 120. Illustrating exponential box-baffle with absorbent lining.

transients will be weak, since the steady state is never reached, and the room absorption increases with the frequency which reduces the 'attack'.

Numerous radiation characteristics of a 90° conical diaphragm 15 cm. radius at various frequencies [135] are shown in Fig. 122. The rear of the cone was surrounded by a large box, this being buried in the ground to simulate the infinite baffle condition. Up to 600  $\sim$  the distribution is tolerably uniform over a hemispherical surface. This is to be expected, since the diameter of the cone is then about one-half

the wave-length. Beyond this point focusing sets in and gradually increases up to 3,000  $\sim$ , beyond which frequency it remains fairly constant. The radiation at 1,300  $\sim$  is more acutely focused than that

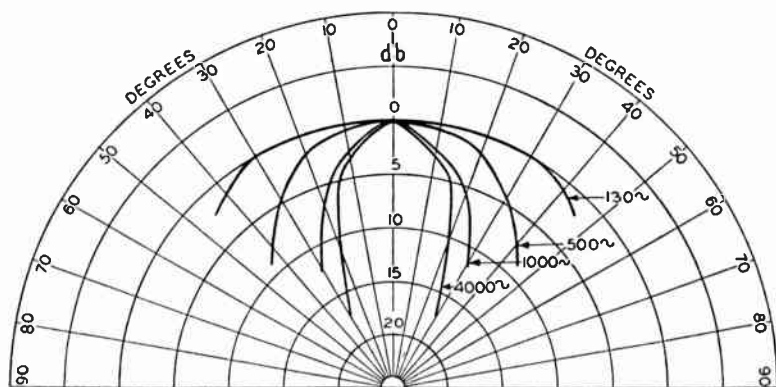


FIG. 121. Polar curves showing response (expressed relative to the axis response) of moving-coil speaker with 115 cycle cut-off exponential horn at various angles from horn axis and 12 feet from the mouth.

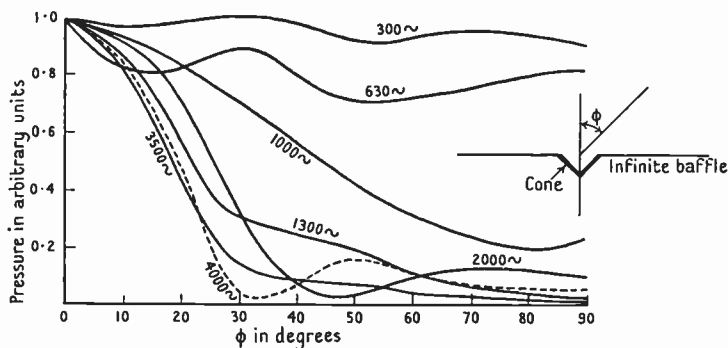


FIG. 122. Radiation characteristics of cone in infinite baffle

at 2,000  $\sim$ , and this can doubtless be explained on the score of one or more nodal circles. From Fig. 44 it will be seen that a nodal circle accentuates the focusing propensities of a disk. The constancy of beam angle above 3,000  $\sim$  is due to three things: (a) conical shape, (b) nodal circles, (c) transmission loss in the diaphragm which reduces the amplitude towards the edge, thereby giving the effect of a smaller radius. Apart from diaphragm loss the general shape of the charac-

teristic is modified at higher frequencies due to the conical shape. The peripheral portions are nearer to any particular spatial point than they would be in the case of a vibrating disk, and this entails a different phase in the two cases. Also the cone acts as a short horn or intensifier to high-frequency radiation from its vertex, whilst at about 800 to 1,000  $\sim$  the air-column resonances occur (Chap. XVIII, § 15).

By aid of Fig. 38 the radius of the equivalent rigid disk can be calculated for the cone, the procedure being as follows: Selecting 2,000  $\sim$  the experimental value of  $G = J_1(z)/z = 0.155$  when  $\phi = 30^\circ$ . From

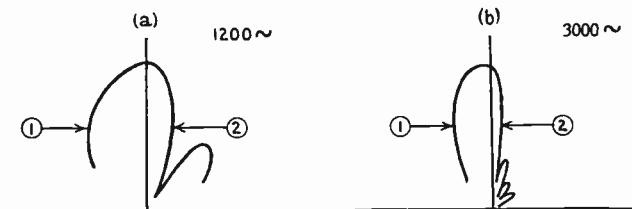


FIG. 123. Polar curves showing distribution from Blatthaller Speaker. (1) diaphragm  $18 \times 25$  cm., (2) diaphragm  $53 \times 53$  cm. (a) is for 1200  $\sim$  and (b) for 3000  $\sim$ .

the curve of Fig. 38 the theoretical value of  $z = ka \sin \phi$  when  $G = 0.155$  is 2.6. Thus  $ka \sin \phi = 2.6$ ; so  $a = 14$  cm. A similar calculation for  $\phi = 20^\circ$  makes  $a = 12.6$  cm. These computations show that the cone does not exactly simulate a rigid disk, but the similarity is adequate for all practical purposes, provided a suitable radius is found. Applying the same procedure at 4,000  $\sim$ ,  $a = 9.4$  cm. at  $30^\circ$  and 9.1 cm. at  $20^\circ$ , showing that the radius of the equivalent rigid disk decreases progressively with rise in frequency due largely to transmission loss. In this way the focusing at higher frequencies is curbed.

The polar diagram for a corrugated duralumin diaphragm comprising a rectangle  $18 \times 25$  cm. is shown in Fig. 123 A, whilst in Fig. 123 B the enhanced focusing, due to increase in size to  $53 \times 53$  cm., is shown clearly [144 b]. In the latter case the main beam is only  $10^\circ$  on either side of the axis, whilst at 1,200  $\sim$  it is  $20^\circ$ , but the side loops are larger than those at 3,000  $\sim$ . These diaphragms are used in the Blatthaller speaker described in Chapter XIII.

#### 14. Room effects in loud-speaker reproduction

The response curves in §§ 10, 11, were taken under conditions entirely different from those under which the loud speaker is used in practice.

In a 'dead' room where reflection is almost absent, except perhaps at the lowest frequencies, the condition of outdoor listening is adequately simulated. An auditor situated 5 or 10 metres from the speaker at  $70^\circ$  to its axis will in general hear little or none of the upper register. Seated on the axis this register will be overpowering if the total output from the speaker (integrated over a solid angle  $4\pi$ ) is the same throughout the audio-frequency range for constant input volts to the power valve. In an average room, owing to reflection, the  $70^\circ$  position would, in some cases, be the more satisfactory of the two, but this depends upon the response of the speaker and the absorption of the room under consideration. Owing to (1) the lack of appreciable absorption in an ordinary room at low frequencies, (2) standing-wave phenomena associated with reflection and room resonance, the notes of the lower register build up to an intensity greater than that of the upper register which suffers more attenuation. Although at certain parts of the room the sound pressure is much in excess of the free-air condition, at others it may be in defect [129]. Experiment shows that in small rooms these phenomena are pronounced. It is possible for a condition to occur whereby low frequencies are not audible comparatively near the speaker, but are violently accentuated at a certain location; for example, near the opposite corner of the room. This may, of course, be due in part to the speaker acting as a double source of sound (Chap. II). In this respect reference should be made to Fig. 12 where the distribution of radiation from a speaker with a flat baffle, in the proximity of a large reflecting wall, is shown for free-air conditions.

As yet it has not been possible to specify tests which, if conducted in 'dead' rooms, will give an accurate idea of loud-speaker performance under average domestic conditions. The best approximation is to take a comprehensive frequency characteristic, including polar diagrams, in a room typical of the average where a speaker is likely to be used. The specification of such a room is one upon which considerable controversy is likely to arise. Rooms are like people; there are no two of them alike! Nevertheless it ought to be possible to define what a standard test room should be, so that from the speaker characteristics obtained therein a fair conception of performance in the home is assured. To realize in practice the reproducing qualities of a speaker taken under such conditions, it is necessary that full scope for sound-mixing by aid of reverberation in the listening-room

be given. But the reverberation should not be sufficient to modify the reproduced sounds to any serious extent. The optimum acoustic conditions in the listening-room must, of necessity, be a compromise between these two requirements.

Experiment indicates that too small a room is unsatisfactory from the viewpoint of proper listening. The smallest room should have a floor-space not less than 150 square feet. It should contain a reasonable amount of sound-absorbing material, but should not approximate to an acoustically 'dead' room [129]. An average absorption of from 20 to 25 per cent. over the whole surface appears to give the best results. Symbolically this can be stated as follows:

$$a_s = \frac{\sum_{n=0}^m A_n a_{sn}}{\sum_{n=0}^m A_n} = \frac{A_1 a_{s1} + A_2 a_{s2} + A_3 a_{s3} + \dots + A_m a_{sm}}{A_1 + A_2 + A_3 + \dots + A_m} = 0.2 \text{ to } 0.25, \quad (5)$$

where  $A_m$ ,  $a_{sm}$  are the area of one portion of the room and its absorption coefficient, respectively. This quotient and the reverberation time should be independent of frequency as far as possible. It is important also that structural features such as walls and ceilings, as well as articles of furniture, should be sensibly free from resonance and 'boom'.

Apropos of these suggestions some simple calculations may be of value. To deal with these it is convenient to introduce a little elementary theory. When a simple source of sound functions steadily in a room of surface area  $A$ , whose average absorption coefficient is  $a_s$ , the mean energy density (see definition 5) of the sound throughout the room can be shown to be [210]

$$e = \frac{4P}{cAa_s}. \quad (6)$$

If the power radiated by the source is  $P$ , that absorbed by the walls is  $Pa_s$ , leaving  $P(1-a_s)$  to be reflected. Taking the collected initial reflections from all the room surfaces, and considering this as the output from a subsidiary generator or source, the average reflected energy density is

$$e_r = \frac{4P(1-a_s)}{cAa_s}. \quad (7)$$

Assuming the primary source to be a simple one, radiating equally

in all directions, the direct sound energy density at a point distant  $r$  from the source is

$$e_d = \frac{P}{4\pi r^2 c}. \quad (8)$$

The ratio

$$\frac{\text{energy density due to reflection}}{\text{energy density due to direct radiation}}$$

is, therefore,

$$\varphi = \frac{e_r}{e_d} = \frac{16\pi r^2(1-a_s)}{Aa_s}, \quad (9)$$

or, in decibels, 
$$10 \log \varphi = 10 \log_{10} \frac{16\pi r^2(1-a_s)}{Aa_s}. \quad (10)$$

If the room dimensions, in feet, are  $18 \times 14 \times 10$ , its total superficial area is 1,144 square feet. As an average distance from the source, for listening purposes, one can select 8 feet. When  $a_s = 0.25$ , as suggested above, the reflected sound is 9.26 db. above the level of the direct sound, and this is a considerable amount. This order of magnitude is to be expected at low frequencies. At the higher frequencies, if the absorption coefficient is 0.5, the difference in level is 4.5 db. which is preferable. It is clear, therefore, that in any ordinary room the reflected energy due to a source radiating uniformly in all directions swamps that coming direct from the source. Now the radiation from speakers is decidedly directional at the upper frequencies, owing to the focusing effect explained in Chapter V. If, therefore, a listener sits on the axis of a hornless moving-coil speaker at a distance of 8 feet, the difference in level between the direct and reflected energy, at the higher frequencies, will be much less than that indicated by formula (10). Assuming that the sound source is either the mouth of a horn or only *one* side of a diaphragm, it is possible to obtain an approximate estimate of the difference in level, provided the polar distribution curve of the speaker in free air, or its equivalent, is known. If  $P$ , the power radiated, is also known, the sound pressure  $p$  can be found at any angular and linear distance from the horn or diaphragm. Thus the direct energy density  $e_d = p^2/\rho_0 c^2$  is known, and we obtain

$$\begin{aligned} 10 \log \varphi &= 10 \log_{10} \frac{4\rho_0 c^2 P(1-a_s)}{p^2 c A a_s} \\ &= 10 \log_{10} \frac{4\rho_0 c P(1-a_s)}{p^2 A a_s}, \end{aligned} \quad (11)$$

where the formula applies to the particular direction and distance for which  $p$  is given.

If the beam plays on a heavy curtain or other highly absorbent material, the ratio at high frequencies found from (11) will be too large.

The majority of speakers for domestic purposes are in effect double sources (Chap. II). The radiation from the back of the diaphragm is reflected from the wall in opposite phase from that at the front, and an already complicated situation becomes somewhat chaotic. In general the major proportion of the upper register issues from the concave side of the diaphragm, so the chief difficulty in regard to reflection pertains to the long waves in the lower register. Working on an elaboration of the principles set forth in Chapter II, it might be possible to derive a rough analytical expression for the difference in level. It is felt, however, that the plurality of conditions impels one to empirical methods of investigation.

Reinforcement arising from reflection means that the amplitude of vibration of a diaphragm to give a definite loudness level is much less than that for 'free-air' or 'dead'-room conditions (Chap. XIX). This is fortunate since, with a good speaker, a level of 70 to 80 db. above the threshold of audibility can be secured without introducing serious alien frequencies due to motion of the moving coil into the leakage field of the magnet (Chap. XIV). A level of this order is usually considered to be adequate for comfortable audition under normal circumstances.

Hitherto our remarks have been concerned solely with the steady state. What applies then does not necessarily hold for transients. Seated on the *axis* of a reproducer in an average room, the lower frequencies in a transient will not be heard to the same extent as in the steady state, so the transient will sound sharper. On the other hand, if conditions for steady-state listening are adjusted to the optimum at an angle of, say,  $60^\circ$  from the axis of a highly directional speaker, transients will be rather flat due to a lack of upper frequencies. At the same time a modification will occur due to the low velocity of propagation in the diaphragm (Appendix). Also, apart from the acoustic conditions of the room, there may be appreciable distortion due to the resonances of the speaker (Chap. XVIII). It follows, therefore, since speech and music depend so much upon the transient state for interpretational and characteristic qualities, that the problem degenerates into more of a Chinese puzzle than ever. In settling the optimum acoustical listening conditions, cognizance must be taken of both the transient and steady states.



## XVIII

### MEASUREMENT OF VIBRATIONAL FREQUENCIES OF CONICAL SHELLS

1. THERE are two salient types of vibration pertaining to conical shells: (a) radial modes, as in a bell, (b) symmetrical modes, as in a disk. These are illustrated in Fig. 124. Radial modes are associated with bending, whilst symmetrical modes depend upon bending and extension. So far as the vibrational modes of cylindrical and spherical

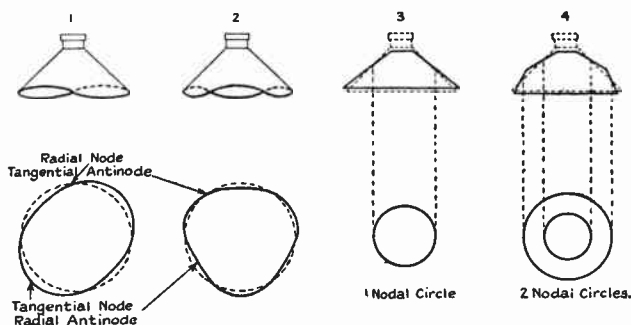


FIG. 124. Showing shape of homogeneous loss-free conical shell when executing certain modes of vibration *in vacuo*. (1) First radial mode; (2) second radial mode; (3) first centre-moving symmetrical mode; (4) second centre-moving symmetrical mode. The sketches are purely diagrammatic.

shells are concerned, one has only to turn to the works of applied mathematicians to find an answer. The symmetrical vibrational modes of conical shells are secrets closely guarded from the mathematician, only to be discovered by the experimental methods of the acoustical engineer. To an extent this is unfortunate, since the apparatus is costly and the time vastly in excess of that required for a mere computation. Although a general empirical formula has not been devised, the information given herein is adequate to predict the main symmetrical vibrational frequency band of conical shells used in the design of hornless moving-coil loud speakers.

### 2. Radial modes

When a free-edge conical shell is driven axially at low frequencies there are a large number of modes of vibration\* of the form illustrated

\* An axial motion is superposed on that of the alternate sectors moving in opposite directions.

in Fig. 124 (1 and 2), and these are associated with bending. The fundamental frequency of a homogeneous seamless conical shell is characterized by 4 radial nodes, the next by 6, then 8, and so on.\* When the diaphragm has a seam a considerable degree of asymmetry is introduced and at times it is possible to obtain 2 radial nodes [114 a, b].

There are various ways of measuring these nodal frequencies, the principal of which are: (a) stroboscopically [114 a, b], (b) A.C. bridge. For merely obtaining the frequency values, without reference to the sound output, (a) is rapid and simple. The diaphragm is illuminated during vibration by an intermittent light source whose frequency is slightly less than, or greater than, that of the driving current. This can conveniently be effected by a number of neon lamps driven independently, or by a slotted circular disk illuminated from behind and rotated by a variable speed motor. Owing to interference concomitant with oppositely vibrating contiguous sectors, there is little sound when the nodal pattern is fairly regular, provided the input current is pure. With a seam irregularities are introduced, and the acoustic output is enhanced. It is quite easy to see the nodal pattern stroboscopically, and no difficulty is experienced in picking out the various modes of vibration. By using a free-edge coil-driven cone of moderate dimensions, it is possible to obtain a peripheral amplitude of 1 cm. The aerial eddy currents at the edge are strong enough to extinguish a lighted match, and the nodal points can be explored with a gas flame passed round the edge. Under such conditions the nodal points and the shape of the diaphragm during vibration are actually visible without intermittent illumination. Further, the aerial eddies enable exploration to be effected by an 'acoustic compass'. A very light single-bladed paper or pith propeller is suspended axially by a delicate thread. The centre is placed above the edge of the vibrating diaphragm and the propeller carried round slowly. At a node the compass sets itself along the basal radius of the cone, whilst at an antinode it is tangential to the cone. During the passage between two nodes the compass turns through 180°.

Although the sound output corresponding to the impressed frequency may be very small, the vibration is usually accompanied by appreciable noise due to bending of the paper. It is quite easy to

\* In a large number of commercial speakers the cones are moulded and seamless, the surround being an integral part of the diaphragm.

get several vibrational modes by aid of an audio-frequency amplifier, a pick-up, and gramophone frequency records of 40 to 100  $\sim$ . The appropriate frequencies can be found by varying the turntable speed.

The behaviour of two conical free-edge paper shells of different thicknesses is exemplified by the data given in Tables 25, 26.

TABLE 25 [114 a]

*Showing radial modes of a free-edge cone driven by a circular coil*

Radius of coil = 2.5 cm.; projected radius of diaphragm = 12.2 cm.;  
apical angle (plane) = 90°; thickness of paper = 0.014 cm.

<i>Drive frequency</i>	<i>Number of radial nodes</i>	<i>Frequency from curve</i>	<i>Number of radial nodes</i>	<i>Frequency ratio to fundamental</i>
36.5	4	37	4	1
43	6	50	6	1.35
52	8			
60	10			
75	8	69	8	1.86
95	10	92	10	2.48
118	12	120	12	3.24
150	14	150	14	4.06
190	16	190	16	5.13
225	18	230	18	6.22

TABLE 26 [114 b]

*Showing frequencies of radial modes of a free-edge cone driven by a circular coil*

$a = 12.2$  cm.;  $t = 2.1 \times 10^{-3}$  cm.;  $n = 1,000$  turns;  $\psi = 90^\circ$ ;  $m_c = 4.7$  gm.

<i>Drive frequency (cycles per second)</i> $t = 2.1 \times 10^{-3}$ cm.	<i>Number of radial nodes (from curve)</i> $t = 2.1 \times 10^{-3}$ cm.	<i>Frequency ratio to fundamental</i>	
		$t = 2.1 \times 10^{-3}$ cm.	$t = 1.4 \times 10^{-3}$ cm.
55	4	1.0	1.0
76	6	1.38	1.35
101	8	1.84	1.86
133	10	2.42	2.48
170	12	3.1	3.24
220	14	4.0	4.06
285	16	5.2	5.13
332	18	6.05	6.22

The conical shells used during the experiments were constructed in the well-known manner with a seam or overlap 0.65 cm. wide. As indicated previously, this mars the symmetry and introduces irregularities in the nodal figures. For example, in Table 25 it will be seen that there are 8 and 10 radial nodes at two different frequencies.

The same phenomenon was obtained for the cone in Table 26, but the results have been omitted. To obtain the frequencies for a substantially symmetrical cone, the experimental results were plotted and a mean curve drawn through them. These mean values are set forth in the last three columns of Tables 25 and 26. From columns 3 and 4 of the latter table the frequency ratios of various modes to the fundamental are seen to be alike for cones which only differ in thickness. In fact the ratio of the basic frequencies  $55/36.5 = 1.51$ , which is the same as that of the thicknesses. This indicates that the radial vibrations are associated chiefly with pure bending, as in the case of a cantilever reed or a disk, where  $\omega/2\pi$  varies directly as the thickness. The sector frequency is half that of the drive.

By increasing the rigidity at the edge of the cone, e.g. turning it over and glueing it to a presspahn ring or a rubber annulus, the edge is so stiff that large forces are required to cause perceptible bending. Consequently the radial modes are substantially suppressed although there is a tendency for perturbations to occur between the edge and the apex.

### 3. Bridge measurements of radial modes

When it is desired to secure data relating to the strength of the resonances, a bridge method is of service [114 b] (Chap. XVI, § 2). It is of great assistance if the nodal frequencies are primarily located by stroboscopic means, since they are very sharp and easily missed in bridge work unless great care is exercised. A representative curve is plotted in Fig. 125, curve 1. To locate the resonances readings had to be taken to 0.05 cycle per second, since such a narrow frequency band is covered—about 6 cycles. Commencing at 50 ~ each peak corresponds to a radial mode. Beyond 135 ~ the magnitude abates rapidly, whilst above 250 ~ these modes are comparatively innocuous. As explained previously, the irregularity of the nodal sequence is due to asymmetry arising from the seam of the cone.

Curve 2, Fig. 125, shows the effect of reinforcing the edge with a narrow ring of presspahn. As explained above, bending is suppressed and the radial modes are well-nigh extinguished. A slight resonance occurs at 250 ~ which on stroboscopic examination was seen to be caused by the seam. The latter tended to remain at rest, whilst the thinner and more pliant portions of the diaphragm on either side moved in opposition.

#### 4. Effect of annular surround

When the edge of the diaphragm is bent over and supported by an annular rubber membrane or surround, radial modes suffer extinction, but a very powerful resonance is introduced due to the membrane acting as an auxiliary diaphragm [114 a, b] (Chap. IV, § 12). This is illustrated in striking fashion by curve 3, Fig. 125, where an enormous increase in output occurs over the range 200 to 300 ~.

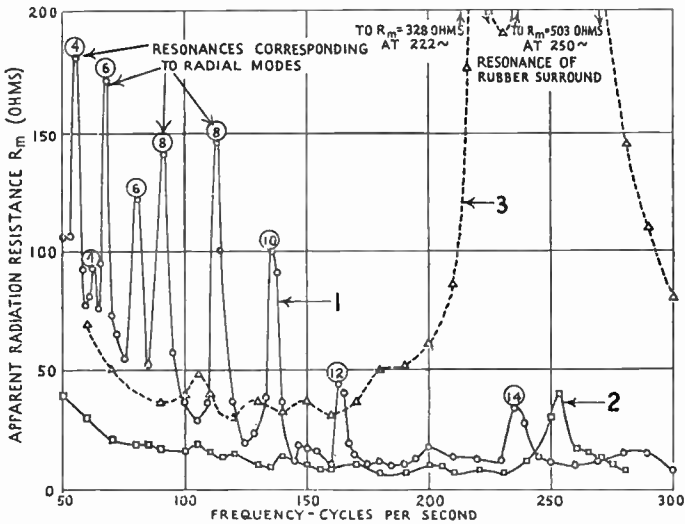


FIG. 125. Apparent radiation resistance  $R_m$  corresponding to conical diaphragm 12.2 cm. radius, apical angle  $90^\circ$  driven by moving coil.

- (1) Edge free showing resonances due to radial modes.
- (2) Edge reinforced with narrow ring of presspahn which suppresses radial modes.
- (3) Edge supported by rubber surround, this acting as an annular membrane.

Below 200 ~ the output exceeds that for a reinforced edge. This particular example illustrates precisely what must not be done in speaker design. The radial tension of the surround is excessive, the vibrational frequency much too high, and the range covered is too narrow. Fig. 126 has been reproduced to demonstrate that with reduction in radial tension a wider proportionate frequency range is covered. The resonance frequency of the surround as an annular membrane is 129.5 ~, whilst the frequency of the diaphragm, as a whole, on the surround is 18.7 ~ (not shown). In Chap. IV, § 7,

formula (10), it is shown that the ratio of these frequencies is  $\pi(m_e/m_{es})^{\frac{1}{2}}$ . Using the above experimental results, we obtain 7/1, and this is in reasonable agreement with the value found from the formula.

In Fig. 126, owing partly to inequality of radial tension around the periphery of the cone, also to the fact that the effective mass curves of the diaphragm and surround intersect in two points near together (Fig. 33), more than one peak is visible, so the resonance

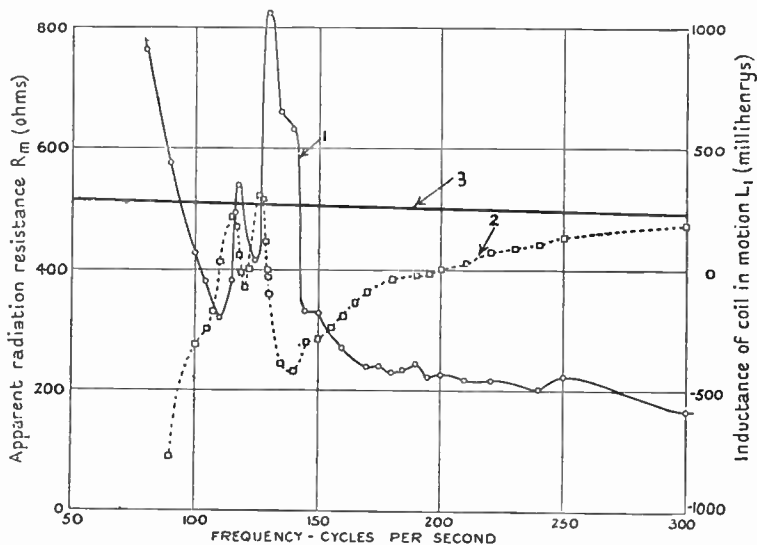


FIG. 126.

- (1) Apparent radiation resistance corresponding to lower register of conical diaphragm 12 cm. radius with rubber surround 2 cm. wide. The resonance of the surround occurs at 129.5 cycles per second. Turns on moving coil = 1200.
- (2)  $L_1$  = inductance of coil in motion. Owing to resonance of the surround there are five frequencies at which  $L_1 = 0$ . The electromechanical resonance of the system apart from the elastic effect of the surround, occurs at about 200 cycles per second.
- (3)  $L_0$  = inductance of coil at rest.

band is broadened. The main peak appears to be very prominent, but from an acoustic aspect it is not so serious as suggested by the diagram. The output ratio at 129.5 ~ to that on the flat portion of the curve above 150 ~ is 4/1, i.e. 6 decibels, which is not very important at 129.5 ~ owing to inherent insensitivity of the ear in this region.

As shown in Chap. IV, § 12, the higher modes of vibration of the rubber annulus *in vacuo* follow the sequence 2, 3, 4, etc. In our case the fundamental frequency is lowered due to accession to inertia, so the higher modes cannot be found accurately by simple arithmetic. The higher modes of the annulus prevent the output-level from falling, as it would with a reinforced edge alone.

### 5. Comparison of the three 'edge' conditions

We are now in a position to compare the three cases: (a) free edge, (b) reinforced edge, (c) supported edge. From an inspection of the curves one can see that the reinforced edge will give reproduction with an attenuated lower register. Obviously this is of little value in commercial apparatus. The free edge appears to have a fairly good lower register. This is to an extent deceptive, since the musical register is not continuous but consists of a series of notes at definite frequency intervals. Some of these notes fall in the valleys of the curve, and on broadcast reproduction the bass register is not so powerful as one might expect. In the reproduction of percussion instruments like the piano the bass is weak, since the radial modes are rendered aperiodic by the damping due to the magnetic field.

The bass register is fully restored in the case of the rubber surround, provided the natural frequency is not too high. A value below 129.5 cycles would doubtless be better, but the reproduction from this diaphragm is very pleasant indeed. With the surround frequency at 250 cycles the bass register appears to be good in certain cases, but is quite lacking in others. Also there is a 'boom' with speech.

The 129.5-cycle resonance is rendered aperiodic by the magnetic field, whilst the 250-cycle resonance is oscillatory. Moreover, the surround resonance should not occur above a certain frequency.

In some practical reproducers where the diaphragm resonates on a surround (other than rubber—e.g. leather) or on a centring device between 50 and 150 cycles, there appears to be a powerful lower register. This, however, is located round the resonance frequency, and is decidedly objectionable.

### 6. Stresses in a conical shell

(a) *Statical*. The simple statical case, where a vertical force  $f$  acts at the minor radius of a conical frustum seated on a smooth horizontal plane, is selected for consideration (Fig. 127). When the plane

apical angle  $\psi \rightarrow 180^\circ$  the cone degenerates into an annulus and the stresses are due to bending and shear.\* When  $\psi = 0$ , the minor radius remaining constant, a cylinder is obtained and the stress is purely compressive—excluding any long-strut buckling effect. Between these two extremes the stresses are entirely different. The force acting at any horizontal section can be resolved vertically and horizontally. The vertical component causes compression, bending, and shear, whilst the horizontal component simulates the fluid pressure

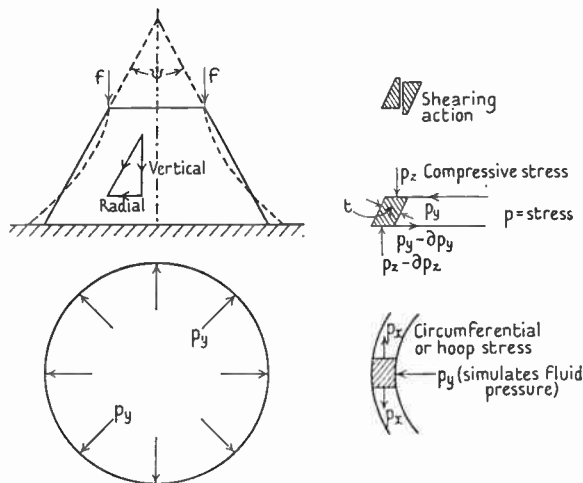


FIG. 127. Illustrating stresses in a statically loaded conical shell.

in a boiler. It causes a circumferential or hoop stress which varies with the distance from the vertex. The variation in this stress introduces bending and shear. The cone, therefore, undergoes a vertical displacement and a circumferential distension, ultimately assuming a curved shape of the type suggested by Fig. 127. Obviously the relative magnitudes of the stresses depend, for a cone of given major radius, upon the apical angle  $\psi$ .

(b) *Dynamical.* From Fig. 127 it will be clear that when a free-edge conical shell is driven, either on a frustum or from the vertex, the principal stresses are still bending and extension, the latter implying positive and negative values. When the vibrations of a shell are mainly associated with one or other of these stresses, it is usually

\* Assuming the annulus to be unsupported except at the edge.



possible to determine the modes of vibration analytically. The analysis, however, becomes very formidable when both types of stress are of primary importance, as in the case of a conical shell of moderate thickness executing symmetrical modes.

Considering the radial modes only, it is evident from Fig. 124 that the deformation of the shell does not involve appreciable extension or contraction of the surface midway between the inside and outside.\* Practical experience shows that it is very easy to press a shell inwards at the periphery. The operation is clearly one associated with bending alone, since any extension of the middle surface would require con-

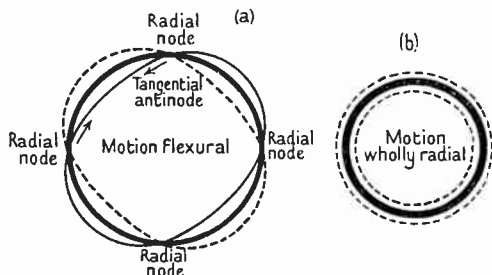


FIG. 128. Diagram illustrating (a) flexural (bending) and (b) radial (extensional) vibrations of a circular ring.

siderable force to produce it. This becomes very evident if we attempt to 'stretch' a piece of paper.

The problem of the symmetrical modes of a conical shell can be approached by aid of two limiting cases, namely, a disk, when  $\psi = 180^\circ$ , and a cylinder, when  $\psi = 0$ . For a disk or a ring the vibrational frequency  $\omega/2\pi \propto t/a^2$ , where  $t$  is the thickness and  $a$  the radius (Fig. 128 A). The action is then entirely one of bending with its accompanying shear. In considering a cylinder,† we take the purely radial vibrations concomitant with extension of the middle surface (Fig. 128 B). The vibrational frequency ( $\omega/2\pi \propto 1/a$ ) is independent of thickness‡, since an increase in  $t$  causes a corresponding gain in stiffness. Now we have seen in (a) that the stresses in a conical shell are bending and extensional or circumferential. Thus a formula for the vibrational frequencies of a shell complete to the vertex will naturally have the form  $\omega/2\pi \propto t^{n_1} a^{-n_2}$ , where  $n_1 < 1$  and  $n_2 > 1$ . Since  $n_1, n_2$  vary with  $t, a, \psi$ , and  $b$  (the minor radius) the formula

\* [118b, 118c].

† A hollow cylinder or ring.

‡ If it is small.

ultimately takes the form

$$\frac{\omega}{2\pi} = K \sqrt{\left(\frac{q}{\rho(1-\sigma^2)}\right)} t^{\phi(a,b,t,\psi)} a^{-\zeta(a,b,t,\psi)},$$

where  $\phi$  and  $\zeta$  are functions of  $a$ ,  $b$ ,  $t$ , and  $\psi$ . In practice the issue is complicated by three essential conditions. Firstly, the radius of the driving coil for any class of speaker is fixed; secondly, there is the mass of this coil; thirdly, there is the former on which the coil is wound and the degree of stiffness it imposes at the minor radius of the cone. If the coil former is several times the thickness of the cone, the extensional deformation at the joint will be reduced appreciably.\* Thus we are concerned not merely with the case of a conical shell, but with a more complicated structure due to the addition of a driving coil. In the experimental work described below, the coil formers were of the same order of thickness as the paper cones, so that considerable alteration in frequency would not be expected from this source. Greater variation arises from the mass of the coil, but its influence can be determined by extrapolation. These disturbing factors modify the indices  $n_1$  and  $n_2$ . Apart from coil mass, etc., the influence of keeping  $b$  constant, instead of letting it increase or decrease proportionately with  $a$ , is to make  $n_2 < 1$ . As the major radius  $a$  is increased the frequency decreases slowly, owing to the great stiffness near the apex.

With the aid of experimental data we now propose to show that both bending and circumferential stresses are of importance in loud-speaker diaphragms and other moderately thick conical shells. It is a well-known mechanical principle, applicable to the vibrations of, say, a cone driven from the vertex or on a frustum, that the dynamic deformation curve is such as to make the potential energy associated with the deformation a minimum [219]. Now the potential energy  $V$  is divisible into two parts associated with bending and extension, respectively. In each case it is proportional to the square of the deflexion or extension, i.e.  $\delta^2$  or  $x^2$ . For bending  $V \propto t^3$ , whilst for extension  $V \propto t$ . Thus the total potential energy of the shell can be expressed in the form  $V = A_1 t^3 \delta^2 + B_1 t x^2$  (bending + extension). The kinetic energy of the shell depends upon  $t$ , since this controls the mass when the other dimensions are fixed. If we write  $T = D_1 t \omega^2$ ,

\* As the extension is small in any case, it is doubtful whether the coil former has any serious influence except as regards bending action.

then, since the two energies must be equal, it follows that

$$\omega = \sqrt{\frac{V}{D_1 t}} = \sqrt{\frac{A_1 t^2 \delta^2 + B_1 x^2}{D_1}}$$

When the cone is extremely thin it will bend readily, but will stoutly resist being stretched circumferentially, especially in the vicinity of the vertex, where the perimeter is small. Thus the term  $B_1 x^2$  will be insignificant compared with  $A_1 t^2 \delta^2$ . This follows from the fact that the absence of appreciable extension implies small potential energy of deformation. Consequently the vibrational frequency is  $\omega = \sqrt{(A_1 t^2 \delta^2 / D_1)}$  or  $\omega \propto t$ . Thus the frequency decreases without limit with the thickness of the shell, the action being almost entirely associated with bending.

Beyond a certain value of  $t$  (increasing) the term  $B_1 t x^2$  becomes of importance, because the resistance of the shell to bending is relatively large and  $\delta^2$  diminishes accordingly. Thus the frequency will rise but slowly as  $t$  increases. If the term  $A_1 t^2 \delta^2$  were negligible compared with  $B_1 t x^2$ , the frequency would be independent of the thickness. In practice, however, this is not the case, since the frequency increases with thickness in the loud-speaker diaphragms tested. For given radii  $a$ ,  $b$  and material,  $\omega \propto t^{n_1}$ , where  $n_1$  lies between 0.2 and 0.5 according to conditions. The index  $n_1$  decreases with increase in thickness. It is evident, therefore, that the bending action in speaker diaphragms cannot be ignored. For a number of shells treated experimentally, the vibrational frequency corresponding to one nodal circle *happens* to be given approximately by

$$\omega = \frac{m}{a} \sqrt{\frac{q}{\rho}},$$

where  $m = \cot \frac{1}{2} \psi$ . This means that the frequency is  $m$  times that of the purely radial mode of a cylindrical ring whose radius is that at the base of the shell. As a case in point take a glass cone where  $a = 12.7$  cm.,  $t = 1.65 \times 10^{-1}$  cm.,  $\psi = 107^\circ$ ,  $m = 0.74$ ,  $\sqrt{(q/\rho)} = 5 \times 10^5$  cm. sec.<sup>-1</sup> The value of the frequency calculated as above is 4,630  $\sim$ , whilst the empirical value is 4,500  $\sim$ . In the case of a 90° aluminium cone  $a = 19$  cm., the values are 4,260 and 4,400  $\sim$ , respectively. In the latter case the frequency of a cylindrical ring, having the same radius as the truncated end of the cone, i.e.  $b = 2.5$  cm., is  $4,260 \times 19/2.5 = 3.24 \times 10^4 \sim$ . Consequently, if the vibration were purely radial, the frequency of the conical shell would

be appreciably in excess of the observed value, owing to the large potential energy in the neighbourhood of the minor radius. Thus we again confirm that bending cannot be ignored [115 a].

To illustrate the transition from disk to cone, we made use of the purely radial vibrations of a cylindrical ring. When the cylinder is of adequate length there are longitudinal vibrations at higher frequencies with corresponding nodal positions. These may be of importance in a large cone of small apical angle. As mentioned later on in connexion with an experiment involving a long paper tube, the extension and contraction on either side of a nodal circle is accompanied by radial contraction and expansion in virtue of Poisson's ratio effect. It is clear, therefore, that the mechanical and acoustical conditions associated with the vibration of conical shells are extremely complex.

### 7. Sub-harmonics [117 a]

In testing diaphragms [112, 118 a], it is sometimes found that radial modes occur at half the frequency of the driving force. This effect can be illustrated by Melde's famous experiment. A light horizontal string is fixed at one end, the other being attached to one prong of a massive tuning-fork. When the fork vibrates along the direction of the string the latter is set into transverse vibration, *its frequency being half that of the fork* [219].

In a mechanical system, having one degree of freedom and a constraint of the form  $s = s_0(1 + \alpha\xi)$ , where  $\xi$  is the displacement, driven by a force  $f = f_0 \cos \omega t$ , it can be shown under certain conditions that the system contains the frequencies  $\omega/4\pi$ ,  $\frac{3}{4}\omega/\pi$ ,  $\frac{5}{4}\omega/\pi$ ... The first of these is a sub-harmonic of half-frequency. In a cone there is more than one degree of freedom, so that it is possible to have frequencies  $\frac{1}{2}$ ,  $\frac{1}{4}$ ... that of the driving force. If the cone has a vibrational mode at  $\omega/4\pi$  it will be revealed when certain conditions are fulfilled (117 a).

To obtain sub-frequencies with a cone, the amplitude of vibration must exceed a certain value. The sub-harmonic of half-frequency is the most powerful, those of lower frequencies being unimportant unless the amplitude is unduly large. Small moulded conical diaphragms are prone to the production of harmonics of half-frequency, when the input is large. The harmonics seem to occur at the symmetrical vibrational modes of the cone. Since the amplitude is then

abnormal, the effect of a non-linear characteristic due to the centring device and surround, or to the diaphragm itself, will be prominent. The sub-harmonics can be suppressed by glueing a piece of felt to some suitable part of the cone [112a].

### 8. Investigation of symmetrical modes by A.C. bridge

By employing an A.C. bridge  $R_m$  can be measured. If a vacuum chamber is available the mechanical loss can be found and thence the electrical resistance due to sound radiation (Chap. VII), provided the resistive loss due to the iron does not differ seriously\* for the free and fixed conditions of the coil. For the present tests a vacuum chamber was not used, so that the resistance values include losses and are therefore 'apparent'. Nevertheless they are a useful guide to the behaviour of the diaphragm. The result of measurements on a large flat cone [114 b]  $\psi = 160^\circ$  of stiff Whatman paper is shown in Fig. 129, curve 1. A small resonance occurs at 350  $\sim$ , this being accompanied by a nodal circle and numerous radial nodes. The main resonance occurs at 664  $\sim$ . It is accompanied by two nodal circles and radial nodes. There are two other resonances at 590 and 620  $\sim$ . The resonance at 950  $\sim$  is accompanied by three nodal circles and radial nodes.

Although the term circular nodes has been used, it merely signifies the form of the figure with a symmetric homogeneous conical shell. The actual dust figures were quite irregular and not always continuous. This is clearly due to asymmetry and heterogeneity of the paper. The amplitude of the diaphragm a short distance from the coil exceeded that of the latter. At certain frequencies an annulus, midway between the coil and the periphery, moved relatively little. Some idea of the relative motion of various parts of the cone, particularly above 500  $\sim$ , can be obtained by using a stethoscope to explore the surface. A better arrangement is a small microphone alone or fitted with a tube or a short horn of small mouth area.

The inductance of the coil in motion is plotted in Fig. 129, curve 2. The variations in this case are an excellent guide to the behaviour

\* See Chap. XVI, § 3.

of the diaphragm. The points of inflexion in the curve occur approximately at the corresponding resonance frequencies. Curve 2 crosses the static inductance curve 3 at the resonance frequency of 664 cycles, which indicates that the dynamic condition is devoid of mass—i.e.  $m_e$  the effective mass of the system is zero. Below 664 cycles per second  $L_1 > L_0$  and  $m_e$  is negative, whilst above 664 cycles per second  $L_0 > L_1$  and  $m_e$  is positive.  $m_e$  is also positive below 240 cycles per

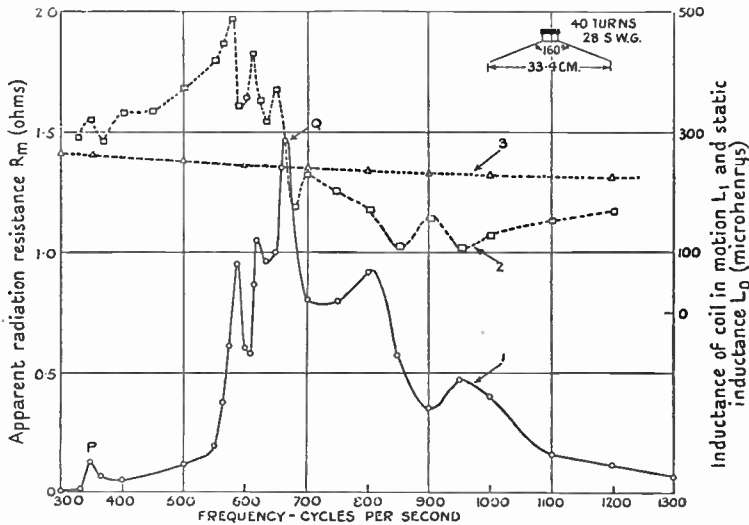


FIG. 129.

- (1) Apparent radiation resistance  $R_m$  for large flat cone ( $a = 16.7$  cm.,  $\psi = 160^\circ$ ), showing the main symmetrical mode at  $Q = 664$  cycles per second.
- (2)  $L_1 =$  inductance of coil in motion. Variations in inductance correspond to changes in the effective mass of the dynamical system. This curve cuts the static inductance curve at  $f = 664$  cycles, showing that the effective mass is zero at the main centre-moving symmetrical mode.
- (3)  $L_0 =$  inductance of coil when fixed (see Table 36 for values).

second, at which frequency the first centre-stationary mode occurs—not shown in diagram.

A list of some of the modes is given in Table 27.

As in other paper cones with seams the radial nodes viewed stroboscopically were irregular, and the same pattern occurred at more than one frequency. The radial modes at low frequencies were accompanied by considerable noise due to bending of the stiff paper. This

TABLE 27

*Showing frequencies of various modes of free-edge coil-driven conical diaphragm*

See top of Fig. 129; thickness of paper  $t = 5 \times 10^{-2}$  cm.;

$n = 40$  turns 28 s.w.g.;  $\psi = 160^\circ$ ;  $m_c = 7.84$  gm.

Total natural mass of diaphragm  $m_n = 48$  gm.

<i>Drive frequency (cycles per second)</i>	<i>Nodal pattern</i>	<i><math>R_m</math> Apparent radiation resistance (ohms)</i>
49.2	Four radii.	1.22
71	Six radii.	0.193
97	Eight radii.	0.142
Intermediate	Not observed.	Not observed.
350	One circle and radial nodes.	0.128
664	Two circles and radial nodes.	1.46
800	Not observed.	0.92
950	Three circles and radial nodes.	0.48

resembled a well-known stage effect used for simulating violent storms. By aid of a microphone the output from the diaphragm under such conditions was recorded with the result depicted in Fig. 130. On the low-frequency wave (49.2  $\sim$ ) a high-frequency ripple of large amplitude is superposed. The frequency of the ripple is identical with the main centre-moving symmetrical mode of the cone (900 to 1,000  $\sim$ ). It is higher than that shown in Fig. 129 since a coil of smaller mass was used in the experiments associated with the oscillographic record. This radial mode was evidently sufficiently vigorous to impulse the diaphragm, causing it to oscillate at its main symmetrical frequency. These experiments show that the main radial modes pertain to the lower frequencies, whilst the symmetrical ones occur higher up the scale. With a disk the radial and symmetrical modes are interlaced, so to speak. As the angle of the cone increases, the frequencies of the cone increase more rapidly than those of the disk. If, however, the material is very thick, this conclusion does not apply. Beyond a certain thickness the frequency of the symmetrical modes increases very slowly due to the influence of hoop stress, whereas the radial modes increase more rapidly since  $\omega \propto t$ .\* Thus in a chime bell the two types of vibration occur at about the same frequency.

Coming now to shells of the type used for hornless loud speakers,

\* This relationship is assumed for thin shells, but it does not appear to agree with experimental results [118 b, 118 c].

the results of tests on a diaphragm under two different edge conditions are shown in Fig. 131 [114 b]. The first resonances in the neigh-

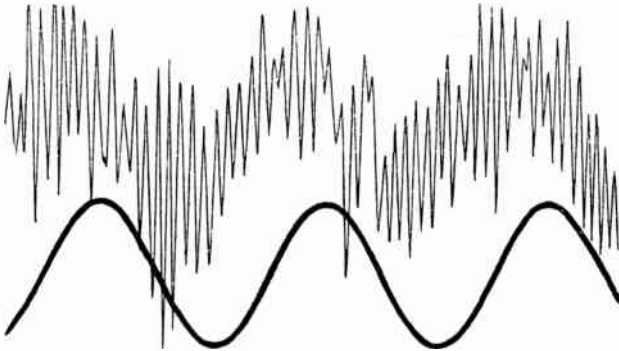


FIG. 130. Record of acoustic output from the diaphragm of Fig. 129 when driven at its first radial mode, namely 49.2 cycles per second by a steady current in the coil (heavy sine wave). Impulsing due to asymmetry of motion causes oscillations of the same frequency as the main centre-moving symmetrical mode to be superposed on the 49.2 cycle radiation.

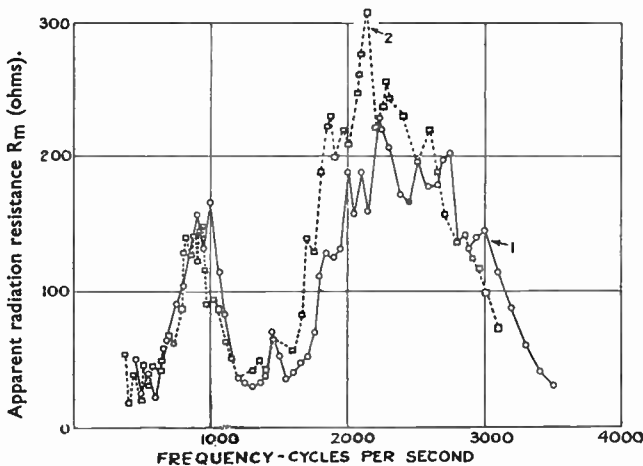


FIG. 131. Apparent radiation resistance corresponding to upper register of conical diaphragm, 12 cm. radius,  $\psi = 90^\circ$ ,  $t = 2.1 \times 10^{-2}$  cm.,  $m_c = 7.8$  gm., with (1) reinforced edge, (2) free edge.

bourhood of 1,000  $\sim$  are due to the air-column vibrations, whilst those at 2,000  $\sim$  are the symmetrical modes of the conical shell. It is clear that with a light paper cone the air-column vibrations



are of importance compared with those of the shell itself. Apart from the peak beyond 2,000  $\sim$  there is little difference between the free-edge and reinforced-edge conditions. The influence of a rubber surround at the mouth is to lower the frequency of the air-column vibrations without materially affecting the output. The large peak which occurs at 2,450  $\sim$  must not be taken too seriously. It is impossible to conduct tests on the same diaphragm with free, reinforced, and supported edge simultaneously. Secular changes occur during the time taken to make the necessary alterations. In each case the curves are characterized by a serrated profile in the resonant region. By taking closer frequency intervals the number of serrations would be increased enormously. The serrations are due to local perturbations arising from small dimples on the surface, asymmetry caused by the seam, and to heterogeneity of the paper.

### 9. Investigation of symmetrical modes by microphone (115 a)

When an annular disk is driven quite symmetrically by a circular coil, the nodal figures corresponding to the centre-moving modes are concentric circles. With an annulus having inner and outer radii of 2.5 and 12.2 cm., respectively, the ratios of the first three modes are roughly 1 : 4 : 9, provided the mass of the driving coil is negligible. In a practical case the latter condition would only be realized approximately, the corresponding ratio being 1 :  $p$  :  $q$ , where  $p < 4$  and  $q < 9$ .

Owing to the different nature of the stresses in a disk and in a conical shell, the nodal ratios of the one bear no resemblance to those of the other. Accurate inferences cannot be made regarding these ratios from experiments on paper cones, owing to four pertinent factors: (i) heterogeneity, (ii) internal transmission loss, (iii) radiation loss, and (iv) low density of paper. By taking a heavy conical cast glass shade, illuminating results can be obtained. Fig. 132 shows three resonances of an ordinary glass lampshade. These were obtained in a large highly-damped room with a special microphone situated on the axis of the shade at a distance of about 180 cm. To avoid the influence of standing waves, the tone supplied to the driving coil was varied  $\pm 50 \sim$  continuously throughout the range of frequencies. The resonances were so sharp that the frequencies could be determined readily by ear, although the output curve was recorded automatically. At each frequency the nodal figures were found, and data relating thereto are given in Table 28.

TABLE 28

*Data for annealed glass cone*

Major radius  $a$  of shell = 12.7 cm.;  $\psi = 107^\circ$ ; radius of driving coil = 2.5 cm.; minor radius  $b = 1.4$  cm.; thickness  $t \doteq 1.65 \times 10^{-1}$  cm. Mass  $m_c$  of driving coil = 4 gm.

<i>Nodal pattern</i>	<i>Radii of nodal circles</i>	<i>Frequency (~)</i>
One circle	0.8a	4,500
Two circles	0.6a, 0.92a	5,700
Three circles	0.44a, 0.78a, 0.95a	7,500

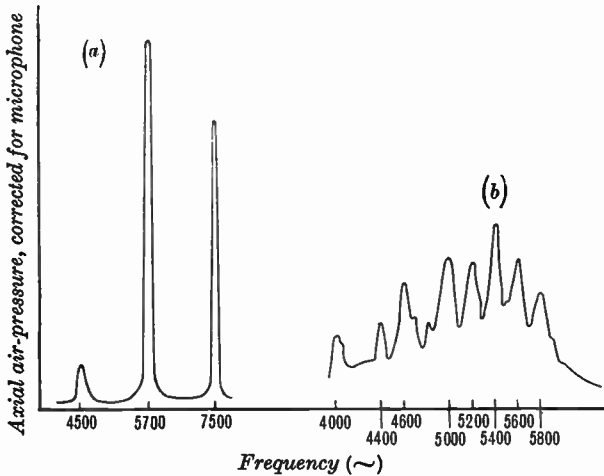


FIG. 132.

- (a) Axial air-pressure curve for free-edge conical glass shell corrected for microphone characteristic.  $a = 12.7$  cm.,  $b = 1.4$  cm., radius of coil 2.5 cm.,  $t \doteq 1.65 \times 10^{-1}$  cm.,  $\psi = 107^\circ$ ,  $m_c = 4$  gm.
- (b) Axial air-pressure curve for free-edge spun conical aluminium shell corrected for microphone characteristic.  $a = 19$  cm.,  $b = 2.5$  cm.,  $t = 4.5 \times 10^{-2}$  cm.,  $\psi = 90^\circ$ ,  $m_c = 6$  gm.

Although nodal circles are specified, neither was the drive sufficiently symmetrical nor was the cone sufficiently homogeneous to obtain perfect circles. Whereas the first mode is by far the most powerful with an annular disk, it is the second which stands out here. There may have been modes above 7,500 ~, but the apparatus did not permit investigation beyond 9,000 ~.

Experiments have also been conducted with aluminium cones, and some of the results are portrayed in Figs. 132 B, 133 A, B. There are

more than three peaks, but as the two thick aluminium cones were spun whilst the thin one had a seam, the homogeneity cannot be expected to be as good as that of *annealed*-cast glass. It should also be observed that here the second peak is by no means the maximum.

As a matter of interest and comparison, curve 1 of Fig. 134 shows the behaviour of a typical paper cone. The preliminary notch on the curve at  $1,700 \sim$  is an indication of the first mode. There are signs

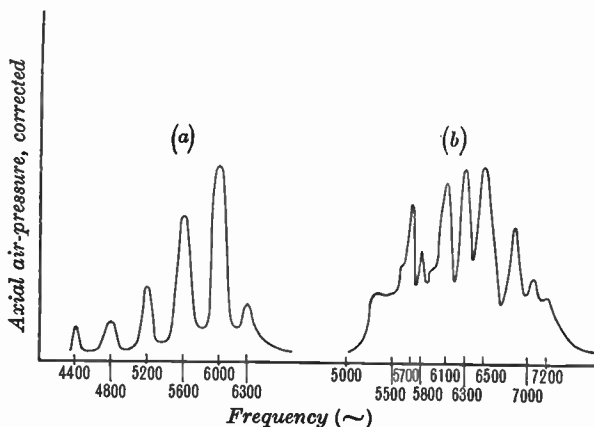


FIG. 133.

- (a) Axial air-pressure curve for free-edge spun conical aluminium shell as in Fig. 132B; but  $t = 8 \times 10^{-2}$  cm.,  $m_c = 6$  gm.  
 (b) Axial air-pressure curve for free-edge conical aluminium shell with seam (seccotined).

$$a = 10.9 \text{ cm.}, b = 2.5 \text{ cm.}, t = 7.5 \times 10^{-3} \text{ cm.}, \psi = 90^\circ, m_c = 1.3 \text{ gm.}$$

of others, whilst the main mode is fairly clearly shown. But the modes of paper and aluminium cones do not stand out in the same conspicuous manner as those of the glass shade. This applies particularly in the case of paper when a light driving coil is used.

The occurrence of the modes in cluster formation, as compared with the segregation that obtains in the case of a disk, is very striking. This is due to the different nature of the two vibrational systems. When the frequencies of the various modes cannot be definitely allocated, we shall refer to the frequency corresponding to the greatest output. At frequencies exceeding that of the main mode the output falls away, due mainly to transmission loss.

In a number of the curves the uncorrected microphone readings have been given, which tend to exaggerate the output from 2,000 to 5,000  $\sim$  owing to pressure doubling (reflection), and resonance due to the cavity at the front of the microphone. This is immaterial since the object of the experiments was to locate vibrational frequencies and to ascertain the general influence of apical angle, coil mass, etc.

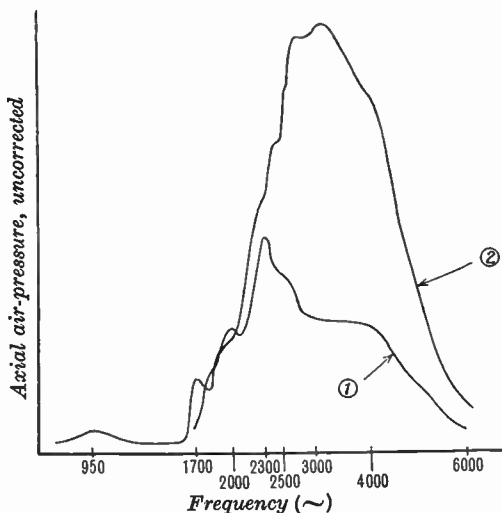


FIG. 134.

Curve 1. Axial air-pressure curve for free-edge conical paper shell uncorrected for microphone characteristic.

$a = 12$  cm.,  $b = 2.5$  cm.,  $t = 2.1 \times 10^{-2}$  cm.,  $\psi = 90^\circ$ ,  $m_c = 7.8$  gm.

Curve 2. As for curve 1, but  $m_c = 2.7$  gm. The reduced coil-mass results in increased and more uniform output above 2,300  $\sim$ .

Where the profile lacks peaks, as shown in Fig. 134, curve 2, the impulse method outlined in a later section is used.

### 10. Influence of thickness of shell on acoustic-output curve

When a curve delineating the acoustic output is taken on the axis of a coil-driven conical shell of given radii and apical angle, the profile depends upon the thickness and mass of the diaphragm. The general effect is clearly exhibited in Figs. 132, 133, and 134, which we shall now analyse. The curve for the thick heavy glass shade consists of three precipitous peaks separated by deep valleys. Owing to the great

mass of the cone the general output-level is small and it is only at resonant points, where the mass is offset by elasticity, that the output is readily audible. The thickest of the three aluminium shells shows the influence of considerable mass, but the valleys are shallower than those of the glass shade. Decrease in thickness is accompanied by a greater general output-level and the perceptible rising of the valleys towards the peaks. Finally, with a paper cone, especially when the mass of the driving coil is small (Fig. 134, curve 2), the valleys and peaks coincide. Nothing is left to indicate the symmetrical modes except a boldly-rounded contour. The reduced coil and shell masses yield a greater amplitude between peaks, whilst the frictional damping and acoustic loading reduce the peaks. Although not fully understood hitherto, the combined influence of these factors has been invaluable in the operation of modern acoustic apparatus. And so empiricism has been justified.

### 11. Influence of coil-mass on acoustic output and frequency of vibration

The mass of the coil affects (i) the mechanical impedance, (ii) the amplitude of vibration, (iii) the profile of the response curve, and (iv) the frequency of vibration.

Referred to the driving point, the mechanical impedance at a frequency  $\omega/2\pi$  is  $r_e + i\omega m_e$ , where  $r_e$  is the mechanical resistance and  $m_e$  the effective mass of the complete structure which may be positive, negative, or zero. Since the coil can be considered as a rigid structure when vibrating axially,  $m_e$  can be written  $m_e = m'_e + m_c$ , where  $m'_e$  refers to the shell and  $m_c$  to the coil. The value of  $m'_e$  is a small proportion of the natural mass in the nodal region, so that the impedance is reduced appreciably when a coil of small mass is used. It follows that for any given driving force the amplitude of vibration, and therefore the output, increases. In fact, to preserve a good balance between the upper and lower registers, the mass of the coil must lie within prescribed limits. The latter are, of course, determined experimentally and depend to an extent upon the taste of the listener. If the mean frequency of the main nodal group is too low, the reproduction is woolly and lacks interpretational qualities. When it is too high we are wafted back to our juvenile days of playing tunes with paper and a comb. For any particular diaphragm there is a certain coil-mass giving maximum output. The mass, however,

varies with frequency owing to inconstancy of the diaphragm impedance (see Chap. VIII, § 9).

The profound influence of coil-mass on the profile of the axial pressure curve, and therefore upon the frequency characteristic, is displayed in Fig. 134. Whereas in curve 1 of Fig. 134, with a 7.8-gm. coil, the notches and peaks are an indication of 'modes', the same cannot be said of curve 2, where the coil-mass is 2.7 gm. The increased amplitude, sound-radiation, and transmission loss concomitant with

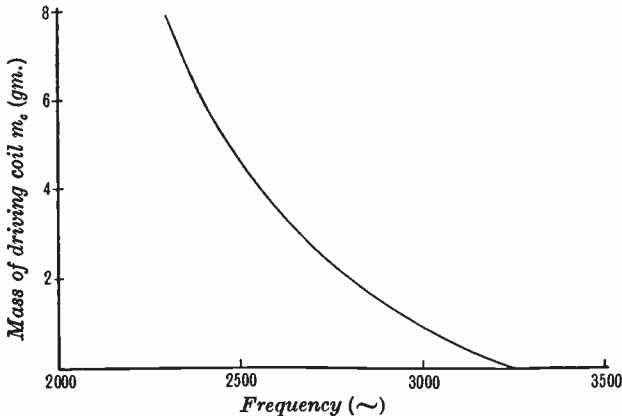


FIG. 135. Curve showing influence of coil-mass on frequency of main symmetrical mode of cone used for Fig. 134.

reduced mass-reactance culminates in a substantially uniform output-level over a certain frequency band. In fact, from the viewpoint of axial pressure, there is a good mechanical band-pass-filter effect.

So far as the influence of mass on the frequency of vibration is concerned, we cannot derive much inspiration from circular disks, since the vibrational conditions are dissimilar. One usually associates added mass with a reduction in frequency, especially when the mass does not contribute to the stiffness of the vibrator. Since the modes of vibration are partly extensional, the influence of mass is less prominent than it would be under a bending régime.

To illustrate this feature a series of experiments was performed on a coil-driven shell, the frequency of the combination being determined for various coil-masses. Variation in mass was effected by the simple expedient of removing turns from the coil until a practical limit was reached. The results are shown graphically in Fig. 135. By

extending the curve until it intersects the horizontal axis, the frequency for a coil of zero mass is obtained. Owing to the stiffness imposed by the cylindrical paper former, this value may be on the high side. The frequency does not alter seriously with reduction in coil-mass until the latter is quite small.

In the ideal case of a lossfree disk driven *in vacuo* where the coil does not contribute any stiffness, the influence of variations in coil-mass can be found from an effective mass-frequency curve by the simple expedient of shifting the frequency axis to the point where  $m = m_c$ ,  $m_c$  being the coil-mass. Owing, however, to variation in acoustic loading and transmission loss with frequency, this artifice cannot be applied accurately to paper cones. This should be evident from Fig. 134, which shows the influence of variation in coil-mass—the shape of the curve being altered completely if a light coil is used.

## 12. Influence of major radius on vibrational frequency

When the radius of the driving coil is fixed, the main vibrational frequency for given conditions obviously decreases with increase in the major radius, i.e. at the mouth or base of the shell. The rate of decrease depends, amongst other things, upon the mass of the coil. Some experimental data bearing upon the frequency variation are given in Table 29.

TABLE 29

*Showing variation in main frequency of cone with major radius*

Material	Thickness $t$ (cm.)	Major radius $a$ (cm.)	Minor radius $b$ (cm.)	Mass of coil $m_c$ (gm.)	Main frequency ~
Paper	$2.1 \times 10^{-2}$	12	2.5	7.8	2,300
"	"	7.5	2.5	7.8	2,900
"	"	5.0	2.5	7.8	3,600

Taking logarithms of  $a$  and  $\omega/2\pi$  it is found on plotting that the frequency is approximately  $7.9 \times 10^3/\sqrt{a}$ . It must be realized, however, that the heavy driving coil, whose mass exceeded that of either of the two smaller cones, caused an appreciable reduction in frequency.

## 13. Influence of shell thickness on main frequency [114 b]

As stated previously, bending is predominant in an extremely thin shell, and, as in the case of a disk, the main vibrational frequency depends in part on the thickness. Thus one might anticipate

a relationship of the form  $\omega = k_2 t^{n_1}$ . Increase in thickness will be accompanied by a steady drop in  $n_1$ , since the circumferential stress becomes of increasing importance. Data concerning this matter are set forth in Table 30, the apical angles of all the cones tested being  $90^\circ$ .

TABLE 30  
Apical angle  $\psi = 90^\circ$ .

Material	Major radius <i>a</i> (cm.)	Minor radius <i>b</i> (cm.)	Mass of coil <i>m<sub>c</sub></i> (gm.)	Thickness <i>t</i> (cm.)	Main frequency ~
Aluminium	19	2.5	6	$4.5 \times 10^{-2}$	5,400
„	19	2.5	6	$8 \times 10^{-2}$	6,000
Paper	12	2.5	1.7	$2.1 \times 10^{-2}$	2,900
„	12	2.5	1.7	$4 \times 10^{-2}$	3,300

#### 14. Influence of apical angle on frequency of vibration

The rise in frequency with reduction in  $\psi$  is quite rapid from  $180^\circ$  to  $100^\circ$ . Beyond this the rise is curbed, whilst below  $90^\circ$   $\omega/2\pi$  falls away very slowly indeed. The general appearance of the air-pressure curves for various angles is shown in Figs. 134, 136, 137, where the resonances are in the neighbourhood of 2,000 ~.

The relative power-output throughout the frequency range is not given by the ordinates of the axial air-pressure curves. This is due to (i) the microphone characteristic not being uniform, (ii) the current through the driving unit not being constant, since constant voltage was applied to the grid of the power valve, (iii) the spatial distribution of sound not being spherical, (iv) variation in interference on the axis according to the number of nodal circles, i.e. the dynamic deformation curve of the shell. This is immaterial since the problem of the moment concerns the *frequencies* of vibration. In curve 2 of Fig. 134, where the frequency is indeterminate, an impulse method is used.

It has already been shown that when  $\psi$  is  $90^\circ$  the main frequency is clearly defined with a heavy coil, but loses definition when a light coil is used, Fig. 134. As the angle decreases, the definition is much improved, as will be seen from Fig. 136, for  $\psi = 60^\circ$ . Two curves are given, one of which (curve 1) applies when there is a re-entrant cone at the minor radius. An auxiliary resonance is introduced at 1,900 ~ and the main peak is shifted to 2,300 ~. In curve 2 there is a series of minor resonances at 7,000 ~. (See Chap. IV, § 8 for re-entrant cone.)



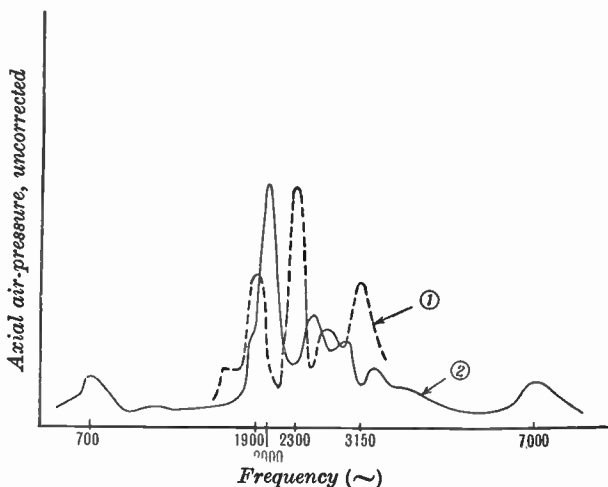


FIG. 136. Axial air-pressure curves, for free-edge conical paper shell with  $\psi$  equal to  $60^\circ$ , other dimensions as for Fig. 134, curve 1. Curve 1, with re-entrant cone 2.5 cm. in radius at apex. Curve 2, without re-entrant cone. The resonance at  $700 \sim$  is due to the air column within the cone.

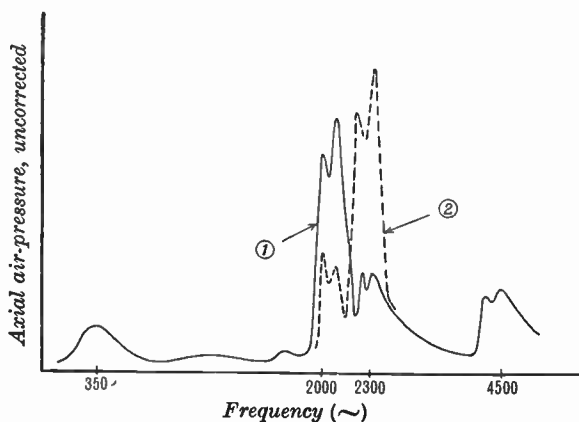


FIG. 137. Axial air-pressure curves for free-edge conical paper shell with  $a = 12$  cm.,  $b = 2.5$  cm.,  $t = 2.1 \times 10^{-2}$  cm.,  $\psi = 30^\circ$ . Curve 1,  $m_c = 4.4$  gm. Curve 2,  $m_c = 2.7$  gm. The resonance at  $350 \sim$  is due to the air column within the cone.

The change caused by alteration in coil-mass is indicated in Fig. 137, where  $\psi = 30^\circ$ . The main frequency is raised and the output enhanced, also the mode before the main peak becomes more prominent.

The acuteness of the main peak is in striking contrast with Fig. 134, where  $\psi = 90^\circ$ . Moreover, a  $90^\circ$  cone is better suited for a loud speaker than one of  $30^\circ$ . It is inferred that, owing to the small angularity of a  $30^\circ$  cone, bending is of less importance relatively, and the corresponding transmission loss is smaller.

When the angle becomes appreciably greater than  $90^\circ$ , the main modes occur at too low a frequency to be of much value for loud-speaker work. It so happens, therefore, that for general reproduction an angle about midway between a disk and a cylinder gives the best results.

The slow change in frequency with reduction in  $\psi$  below  $90^\circ$  arouses curiosity regarding its ultimate value when  $\psi$  approaches zero and the axial length tends to infinity. When a certain angle is reached, the cone becomes long enough for relatively important longitudinal vibrations to occur. It might be thought that the acoustic energy associated with such vibrations is very small. This is undoubtedly true, but the extension and compression of the shell give rise to an important auxiliary effect. By virtue of lateral expansion and contraction (Poisson's ratio effect) the cone vibrates radially and this augments the general output. Tests on a paper cylinder revealed resonance. So far as could be ascertained by ear, a large portion of the sound was generated in this manner (see Fig. 128 B).

## 15. Air-column vibrations

In investigating the vibrational modes of conical shells the frequency of a certain group was found to be dependent solely on the axial length and major radius [116]. The material of the shell and its thickness had a relatively insignificant effect. These vibrations are due to the air column within the cone, which is closed at the minor radius by the magnet. Conditions differ from that of, say, a tuning-fork held at the mouth of a resonator, for in the cone case the resonator is its own source by virtue of its vibration. Experimental data pertaining to air-column vibrations in cones of different materials are set forth in Table 31.

An empirical formula for the main frequency is  $\omega/2\pi = c/2(l+ka)$ , where  $c$  is the velocity of sound in free air,  $l$  the axial length of cone plus part of coil former,  $a$  the major radius, and  $k$  the end-correction coefficient, which varies between 0.6 and 0.8.

The form of the air-pressure curve in the vicinity of the resonance

TABLE 31

*Showing air-column vibrations in conical shells*

<i>Material</i>	<i>Thickness</i> <i>t</i> (cm.)	<i>Major</i> <i>radius</i> <i>a</i> (cm.)	<i>Minor</i> <i>radius</i> <i>b</i> (cm.)	<i>Apical</i> <i>angle</i> <i>degrees</i>	<i>Main</i> <i>air-column</i> <i>frequency</i> (~)
Paper	$2.1 \times 10^{-2}$	12.2	2.5	30°	350
"	"	12.2	2.5	60°	700
"	"	12.2	2.5	90°	900
Aluminium	$8 \times 10^{-2}$	19	2.5	90°	570
Glass	$1.65 \times 10^{-1}$	12.7	2.5	107°	1,100

is of interest, and typical examples are given in Figs. 134, 136, 137. The column resonances occur *above* the main nodal group when  $\psi$  is 135° and the air column is short. For a standard-size paper cone the column resonance is portrayed in Fig. 131 at 900 ~. The output is then quite large, being about 50 per cent. of that at the main nodal frequency which occurs just above 2,000 ~. With heavy cones, e.g. of thick aluminium or glass, the amplitude of vibration is reduced considerably owing to large mass-reactance, and the column vibrations are of little importance in comparison with the symmetrical modes of the shell itself.

### 16. Criterion of suitability of materials for speaker diaphragms

We have seen that the resonance group in paper cones 12 cm. radius or thereabouts covers a frequency band from 2,000 to 4,000 ~, after which the output decays rapidly. Since metal is stiffer than paper, it might be thought that a thin cone thereof would elevate the frequency of the resonance band and give a better upper register. To obtain some knowledge of the main resonance frequency to be expected, it is necessary to consider the mechanical properties of materials. In formulae associated with the natural oscillations of vibrators, Young's elastic modulus  $q$  is encountered, together with Poisson's ratio  $\sigma$  ( $< 1$ ). For example, the frequency of the purely radial vibrations of a circular ring of rectangular section is given by

$$\text{(Fig. 128 B)} \quad \omega = \frac{2}{a} \frac{1}{\sqrt{(1-\sigma^2)}} \sqrt{\frac{q}{\rho}}. \quad (1)$$

The frequencies of the purely flexural modes of the ring are given by

$$\text{(Fig. 128 A)} \quad \omega = \frac{n(n^2-1)}{\sqrt{(n^2+1)}} \frac{t}{\sqrt{3}a^2} \frac{1}{\sqrt{(1-\sigma^2)}} \sqrt{\frac{q}{\rho}}, \quad (2)$$

where  $n = 2, 3, \dots$ . Now Poisson's ratio varies from about 0.2 to 0.4, according to the material, so that as a first approximation  $\sqrt{(1-\sigma^2)}$  can be taken as unity.

As we have already seen, the frequency of a conical shell does not increase directly as the thickness. For a given radius and apical angle it depends upon  $t^{n_1}$ , where  $n_1$  is governed by the thickness and the coil-mass. For average loud-speaker diaphragms  $n_1$  varies from about 0.2 to 0.4. Under this condition the frequency is given by

$$\omega \propto t^{n_1} \sqrt{\frac{q}{\rho}} \tag{3}$$

Now  $t = \rho_1/\rho$ , where  $\rho_1$  is the mass per unit area and  $\rho$  the density. Substituting this value of  $t$  in (3), we find that

$$\omega \propto \rho_1^{n_1} \sqrt{\frac{q}{\rho^{1+2n_1}}} \tag{4}$$

In comparing the frequencies obtainable from shells of different materials, when  $\rho_1$  is fixed, the value of  $n_1$  will doubtless vary if there is a wide difference in thickness, e.g. very thin aluminium and paper, where the density ratio is about 4 : 1. This, however, depends upon the thickness of the aluminium. Where  $n_1$  and the mass per unit area are identical for two shells of different materials, the frequency criterion is  $\sqrt{(q/\rho^{1+2n_1})}$ . On this basis we can compare the frequencies of paper and aluminium shells of equal radius, apical angle, and mass, driven by identical moving coils. Data are given in Table 32.

TABLE 32

$n_1 = 0.2$  in both cases, this being an experimental value based on paper shells.

Material	Thickness (cm.)	Density gm. cm. <sup>-3</sup>	q dynes cm. <sup>-2</sup>	Criterion $\sqrt{\frac{q}{\rho^{1+2n_1}}}$	Frequency ratio	
					Calcula- tion	Experi- ment
Paper	$3 \times 10^{-2}$	0.66	$1.9 \times 10^{10}$	$1.84 \times 10^5$	} 2.3	2.0
Aluminium	$7.5 \times 10^{-3}$	2.7	$7.2 \times 10^{11}$	$4.22 \times 10^5$		

The agreement between theory and practice is quite good when it is realized that  $n_1$  for the aluminium shell should exceed 0.2. This value was obtained with paper some four times the thickness of the aluminium. Formula (4) can obviously be also used to compare the shell masses when the vibrational frequencies are identical.

It is of interest to remark that for a disk, where  $n_1 = 1$ , the criterion is  $\sqrt{(q/\rho^3)}$ . Thus a material with the largest  $\sqrt{(q/\rho^3)}$  gives the disk of smallest mass for a given frequency and radius. The velocity

of sound in a uniform bar of material  $\sqrt{(g/\rho)}$  is only a criterion when both *thickness* and radius are constant. This is not of much practical importance here.

### 17. Sheet-metal cones

Cones have been constructed of aluminium sheet  $2.5 \times 10^{-3}$  cm. and  $7.5 \times 10^{-3}$  cm. thick. In the thinner of the two bending was predominant, and the resonance band much too low [114b, 115a]. Heavy transients caused loud crinkling sounds and 'break-up' of the diaphragm was visible to the naked eye. The thicker cone had a much more powerful upper register, the crinkling being absent. Speech was clear-cut and sharp, but there was no marked shrillness when reproducing sibilants, e.g. the letter 's' did not whistle. A lack of body was evident which suggested a defective response between 200 and 3,500  $\sim$ . A curve relating to this diaphragm is shown in Fig. 133b. The air-column resonances occur about 800 to 900  $\sim$ , but the symmetrical modes with coils of 4.7 and 1.3 gm. lie between 4,000–5,300  $\sim$  and 5,200–7,200  $\sim$ , respectively. Here again the influence of coil-mass in lowering the output and the frequency is evident. These resonance bands are much too high for comfortable audition. The response curve shows that aluminium is not a suitable material for hornless speaker cones. So far as experimental evidence goes, the best results are obtained with paper cones of low density and suitable transmission loss.\* Their resonance bands are wider† and more highly damped than those of aluminium, whilst a fairly uniform level (in decibels) is maintained up to about 4,000  $\sim$ . In order to increase the width of the frequency band, the surface of the cone is sometimes circularly corrugated. Typical examples of plain and corrugated paper cones, having identical dimensions, are shown in Fig. 138, which represent axial-pressure curves corrected for the microphone. Both cones were mounted on annular leather surrounds. The mass of the coil was 3.45 gm., the paper thickness  $1.5 \times 10^{-2}$  cm., the apical angle  $105^\circ$ , and the major radius 10 cm. [126].

### 18. Vibrational frequencies by impulse method

When a structure is impulsed it executes various natural modes of oscillation which ultimately die out due to losses [113b, 114a, c]. If

\* By using bakelized paper 5 mils thick, the upper register can be extended beyond 4,000  $\sim$ . The mass of the cone is approximately the same as that of a cone of untreated paper twice the thickness.

† i.e. the symmetrical vibrational modes cover a wider frequency band.

a diaphragm is situated in a heavily-damped enclosure with a suitable microphone, its acoustic output wave form, when impulsed, can be obtained. This gives useful information relating to the vibrational frequencies which are likely to be of importance in loud-speaker operation. For conducting tests of this nature the circuitual arrangement of Fig. 139 is employed. A relay vibrating about ten to twenty

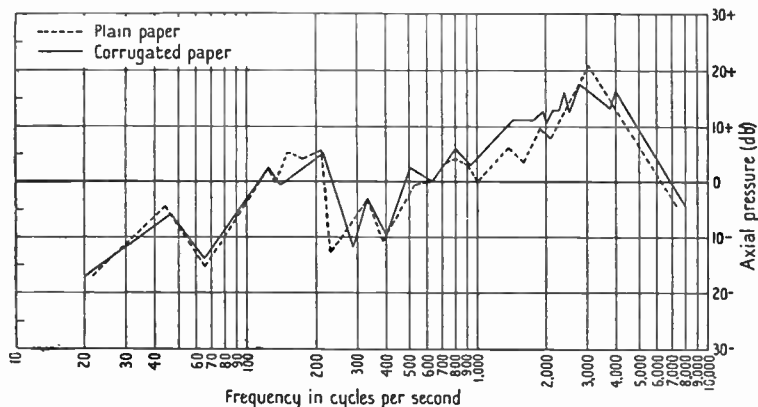


FIG. 138. Axial response curves of plain and corrugated paper cones [126].

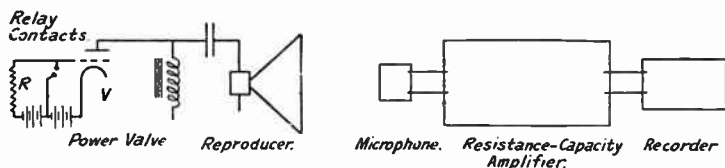


FIG. 139. Apparatus for obtaining acoustic output from a speaker electrically impulsed.

times per second is used to short-circuit a high inductionless resistance  $R$ . In this way the grid bias on the valve  $V$  is altered and the anode current suddenly increases or decreases, the wave form being a series of Morse dots. Thus the loud-speaker current varies in like manner and severe impulsing occurs. The microphone, which should be one of the well-known types with a substantially flat response characteristic, is usually situated on the axis of the speaker, or other apparatus under test,\* and its output is suitably amplified and controlled by an attenuator before being passed on to an oscillograph

\* For example, a microphone could be tested if necessary. For this to be effective the search microphone must be aperiodic.

for delineation of the wave form photographically. Two oscillograph vibrators are used, one for the actual record, the other for the time base. The above method is invaluable in cases where the profile of the axial pressure or motional resistance curves are merely rounded and lack peaks indicative of vibrational modes (see Fig. 134, curve 2). A number of records of different diaphragms are reproduced in Figs. 140, 142, 143, which show oscillations not suppressed by the magnetic field and mechanical losses.

The complex oscillation of Fig. 140 pertains to a hornless speaker. There are two low-frequency components of 33 and 190  $\sim$  superposed on a 2,000  $\sim$  oscillation. The 33  $\sim$  oscillation is that of the diaphragm as a whole, on the surround, whilst the 190  $\sim$  one is the gravest mode of the surround acting as an annular membrane. After removal of the latter the record takes the form of Fig. 141. The low-frequency oscillations have vanished, but the 2,000  $\sim$  oscillation, due to the main symmetrical mode of the shell, remains. A very strong magnetic field would be required to suppress this mode. These records were taken with the microphone on the axis. When it is placed at an angular distance therewith the effect is quite different owing to focusing and to the velocity of sound-propagation in the diaphragm being less than that of sound in air. The set of records in Fig. 142 illustrates the influence of axial and angular distance upon the transient wave form. Increase in axial distance reduces the oscillations, due to the main mode, which follow the first peak. This is doubtless due to a reduction in the standing-wave effect between microphone and speaker, since it is not established until after the peak occurs. The diaphragm, 12.2 cm. radius, 90° apical angle, was mounted on an annular rubber surround whose gravest mode was 129.5  $\sim$  (Fig. 126). The mode cannot be traced on the record and this is a condition to be fulfilled for good reproduction. The resonance of the diaphragm as a whole on the surround, at 18.7  $\sim$ , is completely extinguished. The aperiodic state is shown by the high-frequency oscillation superposed on a decay curve. This represents the diaphragm being forced back to its equilibrium position by the surround, but restrained from oscillation by the magnetic field. It is in great contrast with Fig. 140, where both of the surround oscillations occur.

A record for the aluminium cone [115 c] of Fig. 133 B shows that the oscillation is not a simple damped sine wave since more than one mode is present. The frequency is variable initially but settles down

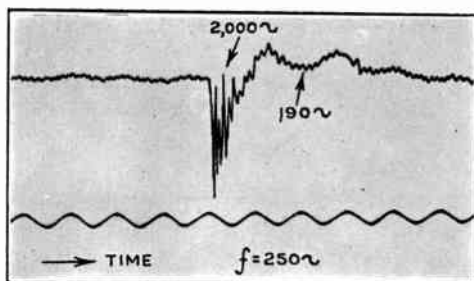


FIG. 140. Impulse record of hornless moving-coil loud speaker with annular rubber surround. The coil of 40 turns was transformer coupled to the valve.  $B_p = 7,000$  lines  $\text{cm.}^{-2}$ , i.e. about 0.6 full strength. Microphone on speaker axis.

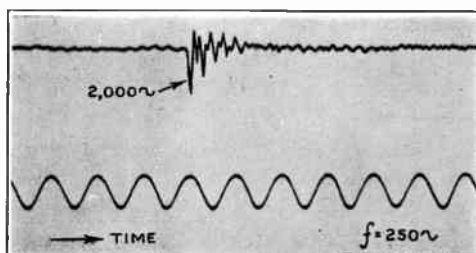


FIG. 141. As in Fig. 140 but with rubber surround removed.

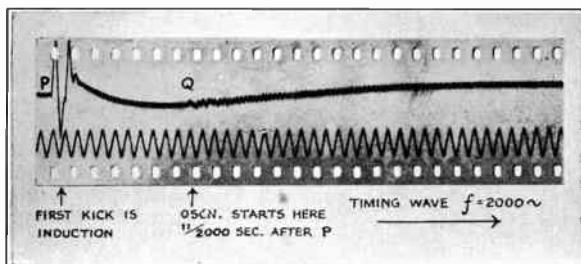
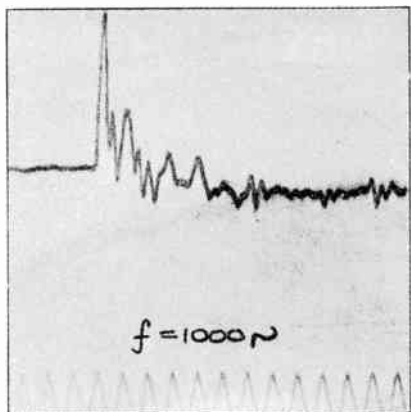
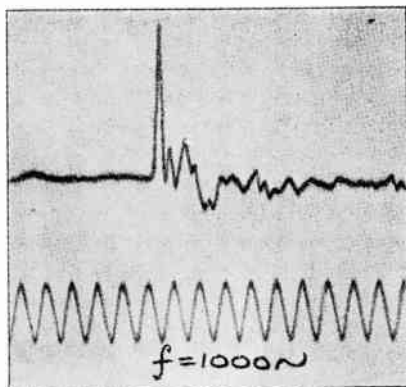


FIG. 143. Impulse record of coil-driven annealed conical glass lamp shade. Microphone on axis at a distance of 187 cm. from the cone.

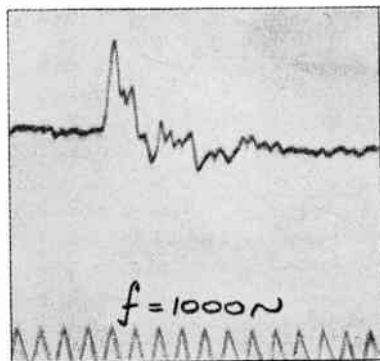




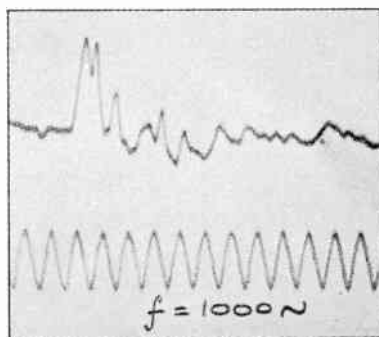
(a) Impulse record of conical diaphragm used for test data of Fig. 126, taken with microphone on axis at 23 cm. from mouth of cone. The symmetrical mode recorded is 2,600 ~.



(b) As at (a) but microphone 70 cm. from mouth of cone.



(c) As at (a) but microphone 25 cm. away from axis.



(d) As at (a) but microphone 28 cm. in front of cone, and 40 cm. away from axis.

FIG. 142

ultimately to the main mode. A record for the thick glass cone of Fig. 132 is shown in Fig. 143 [115 c]. The acoustic output was so small that considerable amplification had to be employed. The preliminary kick at  $P$  is interesting and is due to induction between the driving coil and the microphone\* leads. The start of the acoustic record is  $Q$ , so the distance  $PQ$  represents to the timing wave scale the time taken for sound to travel from the diaphragm to the microphone. The oscillation which commences at  $Q$  is small but persistent, due to low decrement. It never actually dies away before break and a faint trace is visible between  $P$  and  $Q$ . The record is superposed on a low-frequency oscilla-

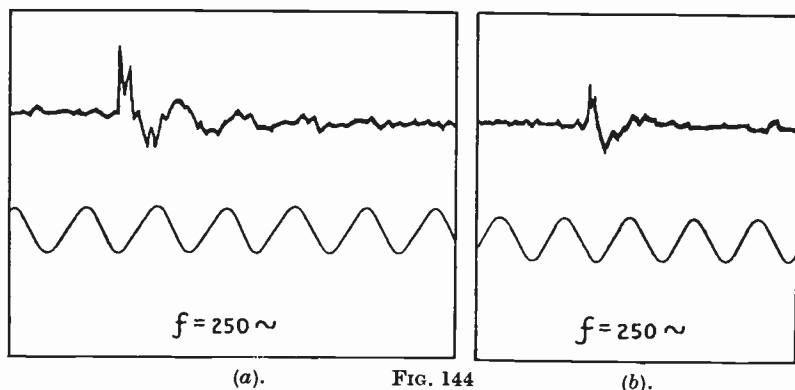


FIG. 144(a). Impulse record of driving mechanism of Fig. 82. (a) without horn. FIG. 144(b). As at Fig. 144(a), but with straight exponential horn 4 ft. 6 in. long. The damping effect of the horn is evident.

tion due to the resistance-capacity and transformer couplings between the valves of the microphone amplifier and the oscillograph. The velocity of sound can be calculated from this record, using the following data: Timing wave = 2,000  $\sim$ ; microphone at 187 cm. on axis; time interval  $11/2,000$  sec., giving  $c = 3.4 \times 10^4$  cm. sec.<sup>-1</sup>

With hornless speakers the damping is relatively small. At low frequencies the magnetic damping is the main factor, whilst at high frequencies transmission loss assists. In horn speakers the damping due to the resistive loading is high, so that one would expect the natural oscillations of the system to be more profoundly damped. That this inference is borne out in practice will be seen from Fig. 144, showing the damping influence of the horn.

\* Absent from foregoing records, because experimental arrangement was different.

These examples demonstrate the utility of the impulse method for studying the natural oscillations of a diaphragm. Owing to irregularity in some of the records it is almost impossible to determine the frequencies of any but the more powerful oscillations. Broadly speaking it is possible to ascertain the main symmetrical mode and to find whether that due to the surround, or the diaphragm on the surround, is rendered aperiodic by the magnetic field. The behaviour of diaphragms under less violent conditions can be studied by suddenly applying or switching off a steady sine wave. Oscillograms obtained

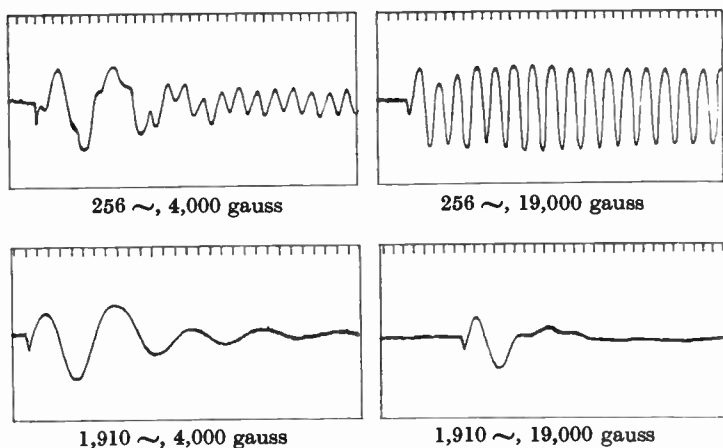


FIG. 145. Acoustical output when a steady sine wave is applied to the Blatthaller speaker. The influence of a strong magnetic field in hastening the 'attack' is shown clearly.

from the Blatthaller speaker (Chap. XIII) under these conditions are shown in Figs. 145, 146.

In taking impulse records care must be exercised to ensure that oscillations or aperiodic effects, due to transformers or choke-condenser combinations, are not superposed upon those of the diaphragm in such a way as to mask the wave form to be recorded. It is hardly necessary to remark that the above procedure can be applied to any vibrating system by attaching a moving coil in a suitable position.

### 19. Damping of low-frequency oscillations in moving-coil speaker [115 b]

The problem before us is to examine the conditions under which the motion of the diaphragm, as a whole, on the annular surround, or

centring device, or both, is oscillatory or aperiodic. An output circuit for high-resistance coils is shown in Fig. 147 A. For simplicity  $L$  and

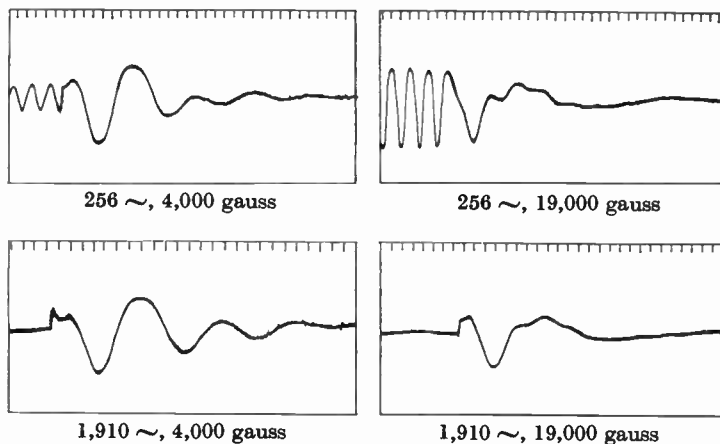


FIG. 146. Acoustical output of Blatthaller speaker when a steady sine wave input is interrupted suddenly. The damping influence of a strong magnetic field in hastening the decay of the oscillation is shown clearly.

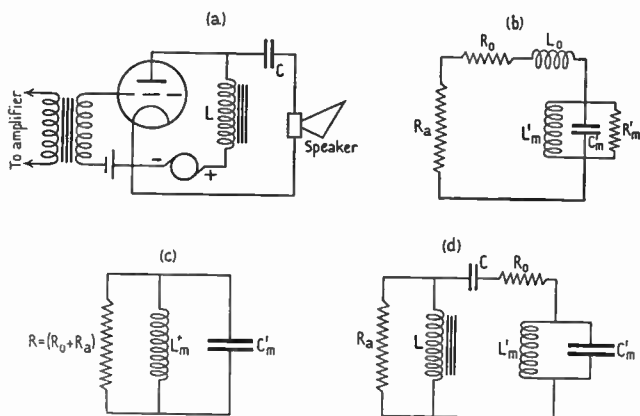


FIG. 147.

(a) Power valve and speaker with choke-condenser output circuit.

(b), (c), (d) Circuits equivalent to (a) under conditions specified in the text.

$C$  are assumed to be very large, e.g. 100 henrys,  $50 \mu\text{F}$  giving a natural frequency of about  $2 \sim$ . If the speaker is represented by its

equivalent circuit\* the diagram of Fig. 147 B is obtained. It is important to realize that this is not the electrical analogue of the mechanical system, for here  $L'_m \equiv$  compliance, whilst  $C'_m \equiv$  mass, which is the reverse of the usual conditions. Below  $100 \sim$  the reactance of  $L_0$  and the damping of  $R'_m$  are negligible, so the circuit ultimately reduces to the form illustrated in Fig. 147 C. The differential equation for this circuit is

$$\left(D^2 + \frac{1}{C'_m R} D + \frac{1}{L'_m C'_m}\right)E = 0, \quad (5)$$

where  $E$  is the p.d. across  $C'_m$ . The well-known condition for aperiodicity is

$$\frac{1}{4C'_m R^2} > \frac{1}{L'_m C'_m}$$

or

$$L'_m > 4C'_m R^2. \quad (6)$$

From Chapter VII we have  $L'_m = C^2/s$  and  $C'_m = m/C^2$ , where

$s =$  axial stiffness due to surround and centring device,

$m =$  equivalent mass *in vacuo* plus accession to inertia =  $m_a + m_i$ .

At low frequencies  $m_a = m_n$ , natural mass, so  $m = m_n + m_i$ . Substituting the values of  $L'_m, C'_m$  in (6), we get, for aperiodicity,

$$C^2 > 2\sqrt{(smR^2)}. \quad (7)$$

When the coil circuit is open  $\omega = \sqrt{(s/m)}$ , which on substitution for  $s$  in (7) yields

$$C^2 > 2\omega m R. \quad (8)$$

Thus aperiodicity is obtained only when the field strength exceeds a certain value. Expression (8) can also be written

$$R < \frac{C^2}{2\omega m}, \quad (9)$$

which means that for a given speaker  $R$  must be less than a certain amount, namely,  $C^2/2\omega m$ . It may happen, however, that this condition cannot be fulfilled. For example, from Fig. 147 C the smallest value of  $R$  occurs when the coil is short-circuited on itself, i.e.  $R_a = 0$ . If  $R_0$  exceeds  $C^2/2\omega m$ , the motion cannot be aperiodic. The latter state is more readily secured by a low than by a high value of  $s$ . This means that the natural frequency of the diaphragm, on open circuit, should be low and the power valve should have a low resistance. Let  $C^2 = 1.2 \times 10^7$ ,  $R_0 = 1,400$  ohms,  $R_a = 2,600$  ohms, frequency of diaphragm  $\dagger 50 \sim$ ,  $m = 24$  gm. Then we get  $2\omega m R = 6 + 10^7$ ,

\* Chap. VII, § 1.

† On the surround and centring device.

which exceeds  $C^2$ , so the motion is oscillatory. Aperiodicity could be obtained by reducing  $s$  to give a diaphragm frequency of  $10 \sim$ . This is quite a typical illustration, and in general the motion is oscillatory when the frequency occurs in the audible range.

When  $\frac{1}{2\pi\sqrt{LC}}$  is within the audible range\* there are two oscillatory circuits, and a variety of conditions is possible. These are as follows: (a) two distinct damped oscillations, (b) a damped oscillation superposed on an aperiodic decay curve, (c) an aperiodic decay curve due to the two circuits. The prevailing condition depends upon the damping of the circuits  $LC$  and  $L'_m C'_m$ . An approximate representation of the arrangement is shown in Fig. 147 D, this being applicable to low frequencies. Since the two circuits are directly coupled, the behaviour of one is modified by the presence of the other [115 b]. In general, the damping is insufficient to cause aperiodicity, and there are two oscillations whose frequencies are different from those of the circuits alone. Consequently the lower register is reproduced with a 'boom'.

## 20. Longitudinal oscillation of coil former

A coil of known mass is wound on a test former several times longer than that commonly used in speaker construction. A number of equally spaced longitudinal cuts is made round the end. The strips so obtained are bent over and glued to a large cylindrical lead block weighing 6 Kg. or more, whose gravest mode is supersonic. A speaker magnet is placed with its axis vertical and the block arranged to accommodate the coil in its customary position in the field. Measurements of motional resistance are made in the usual way. Data for a 40-turn coil are portrayed in Fig. 148 [114 b]. The motional resistance is normal up to  $4,000 \sim$  and it is caused partly by variation in iron loss for the free and stationary conditions (see Chap. XVI, § 3). Beyond this the coil amplitude increases rapidly, and at  $4,600 \sim$  a powerful longitudinal resonance of the coil on its former occurs. As a check, the frequency can be calculated from the coefficients of the system:

Mean radius of cylindrical former  $a = 2.5$  cm.

„ thickness „ „  $t = 2.1 \times 10^{-2}$  cm.

\* Fig. 147 D.

Axial length of cylindrical former  $l = 2$  cm.

Density of paper former  $\rho = 0.66$  gm. cm.<sup>-3</sup>

Mass of coil alone  $m_c = 6.8$  gm.

Young's modulus  $q = 3.4 \times 10^{10}$  dynes cm.<sup>-2</sup>

The above value of  $q$  exceeds that for paper in its normal state. In baking the varnish on the coil, the coil former is also put in the oven,

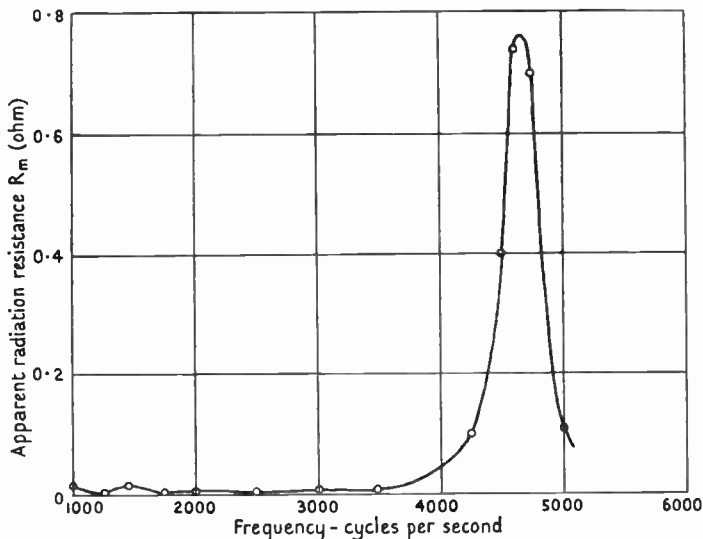


FIG. 148. Apparent radiation resistance of coil of 40 turns 28 s.w.g., whose paper-tube former was securely fixed to a heavy lead block in place of a diaphragm.

and this elevates  $q$  from 50 to 80 per cent. according to the state of the paper. Using the preceding data we find  $A = 0.33$  cm.<sup>2</sup>,  $m_f = 0.45$  gm., so the effective coil mass  $m_c + \frac{1}{3}m_f = 7$  gm. Using formula (19 a), Chap. IV, since  $s = qA/l$ , we find  $\omega/2\pi = 4,500 \sim$ , which is in good agreement with the experimental value. The length of former used here is about three times that for normal speaker construction. In the latter case therefore  $\omega/2\pi = 4,500\sqrt{3} = 7,800 \sim$ . As shown in Chapter IV a frequency of this order is desirable.

## 21. Stiffness of a conical shell

When a mechanical system simulates a simple loaded massless helical spring, the dynamical and statical stiffness coefficients are identical. The former is defined as  $s = \omega^2 m$ , where  $m$  is the mass. Where

flexible disks or conical shells are concerned, the dynamical and statical stiffness coefficients are no longer identical, owing to the totally different physical conditions in the two cases. Since it is impracticable to define the stiffness of a conical shell on the above simple lines, other means must be sought to convey the idea of stiffness. It is proposed to find the thickness of the homogeneous disk of equal radius, whose first centre-moving symmetrical mode occurs at the same frequency as that of the conical shell of like material. This must be regarded as purely illustrative, since the stresses in the two cases are of a totally different nature. The following data apply to a free-edge conical diaphragm:

Thickness of paper =  $5 \times 10^{-2}$  cm.

Radius of cone = 16.7 cm.

Apical angle =  $160^\circ$

First symmetrical mode = 350 ~	}	including coil-mass of 7.8 gm. which lowered frequencies.
Second „ „ = 664 ~		

The frequency of the first symmetrical mode of a paper disk (one nodal circle) *in vacuo*, without the coil, is 22 ~. Since  $\omega \propto t$ , the disk whose first symmetrical mode is 350 ~ has a thickness\*

$$(350/22) \times 5 \times 10^{-2} = 0.8 \text{ cm.},$$

and its mass is about 15 times that of the cone. The equivalent disk is therefore  $350/22 = 16$  times as thick as the cone. If the vibrational frequency of the cone were found *in vacuo* without the coil, this ratio would be appreciably larger. A second example of a diaphragm having a smaller apical angle is given below.

Thickness of paper  $t = 2.1 \times 10^{-2}$  cm.

Radius of cone  $a = 12$  cm.

Apical angle  $\psi = 90^\circ$

Young's modulus  $q = 1.9 \times 10^{10}$  dynes cm.<sup>-2</sup>

First symmetrical mode without coil = 3,200 ~.

The first mode of a paper disk of equal radius *in vacuo* is 11 ~. Thus the thickness of the equivalent disk is

$$(3,200/11) \times 2.1 \times 10^{-2} = 6.1 \text{ cm.}$$

\* For the sake of illustration it is assumed that  $\omega \propto t$  whatever the thickness, but this is not rigorous.



This is 180 times the mass of the cone and nearly 300 times as thick. These calculations demonstrate the enormous increase in stiffness due to conicality.

## XIX

### DESIGN CONSIDERATIONS IN HORNLESS MOVING-COIL SPEAKERS

1. THESE instruments cannot be designed in the same precise way as horn-type speakers (Chap. XX). The design is usually determined largely by trial and error. A critical musical perception is an asset for this purpose. The experimental data in Chapter XVIII, together with the theory in Chapter VIII, will be found to be of service in design work. In many speakers the lower register predominates to the detriment of speech reproduction, which is accompanied by an unpleasant boom. To avoid this the frequency of the diaphragm on its axial constraint should be well below audibility, and the centring device must have small mass. The magnetic field ought to be much more intense than that in the average speaker, and for this purpose permanent magnets are of little use. There are four main resonances, namely, (1) that cited above, (2) the surround vibrating as an annular membrane, (3) the air column within the cone, (4) the symmetrical modes of the cone. In some speakers the surround is a loose ring of cloth, so that (2) will then be absent. When (2) is present the fundamental should occur preferably between 100 and 140  $\sim$ . With a cone 12 cm. radius the air-column resonances occur from 800 to 1,000  $\sim$  and help to fill up the gap between the high and the low frequencies. If a cone 7 cm. radius were chosen, its symmetrical modes would commence at a much higher frequency than with a cone 12 cm. radius. With a driving coil whose mass is 2.5 gm. the output might be unduly powerful above 3,000  $\sim$ , thereby causing the letter 's' to whistle. The frequency range properly covered by a single diaphragm is limited. An average value for a diaphragm 12 cm. radius is from 70 to 4,000  $\sim$ . To extend the range another speaker must be employed. In so doing it is essential to use an output circuit of the type illustrated in Fig. 164, where each speaker is fed with current pertaining to its own frequency range only. This obviates waste. Particular care is required to avoid noticeable resonances in the higher frequency speaker units. A powerful magnetic field is desirable to damp resonances and give adequate output. To get the best results, the mass of the driving coil has to be chosen carefully (see

Chap. XVIII, § 11). Inductive reactance of the coil is an important factor. Unless it is sufficiently small, the working current is reduced appreciably.

There are no published data on the design and performance of high-frequency moving-coil units *per se*. A brief description of a wide-range hornless speaker (80 to 10,000  $\sim$ ) is given in Chap. XX, § 16, and further details will be found in [90 b].

Instead of using a moving coil the diaphragm can be driven by two crystals of Rochelle salt (sodium potassium tartrate) linked up to give an amplified motion. Two plates of crystal are cut in relation to their axes so that one tends to dilate and the other to contract (and vice versa) when an e.m.f. is applied to the crystals via electrodes of metal foil. The plates are cemented together and clamped so that only one corner can move, the motion being perpendicular to the planes of the electrodes. The action is similar to that in bimetallic strips used in recording thermometers and thermal relays. The drive is fixed to the free corner of the crystal unit and is connected to the diaphragm by a lever mechanism to amplify the motion, thereby enabling the mechanical impedances to be matched (see Chap. XIII, § 10). Although this drive is most suitable for high-frequency speakers, units have been constructed for reproducing the lower and middle registers [164 c, 208 a].

The question of baffles above 4,000  $\sim$  is of little moment, but it is convenient to mount the high-frequency units in the same baffle as the main unit. The electrical connexions are preferably such that, when supplied with a sine-wave current, all diaphragms move simultaneously in the same direction. Since the radii of the upper frequency diaphragms is smaller than that of the main unit, focusing of the sound is less pronounced above 4,000  $\sim$  than it would be with a single unit (Chap. V, § 1).

## 2. Coil current at low-frequency resonance [80 d]

This can be obtained using the circuit of Fig. 149 A, when a constant sine-wave voltage of varying frequency is applied to the power valve. The current-frequency curve of Fig. 149 has a crevasse at the resonant point, owing to the enormous increase in electrical motional resistance [113 a]. If the current is also measured at the resonant frequency, with the speaker coil fixed, the motional electrical resistance (includes loss) can be computed.

Let  $E_2, E'_2$  be the voltages on the secondary of the transformer when the coil is free and fixed, respectively, as measured with a Moullin voltmeter, and  $I_2, I'_2$  be the corresponding currents; then

$$R_m = \left( \frac{E_2}{I_2} - \frac{E'_2}{I'_2} \right), \quad (1)$$

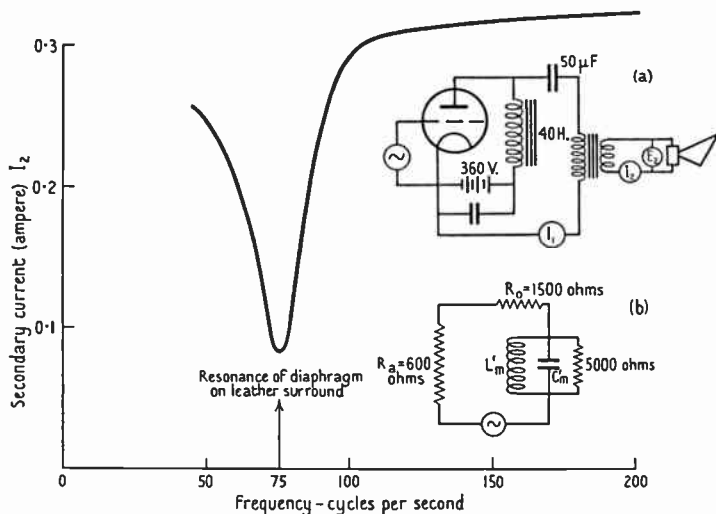


FIG. 149. Showing crevasse in current-frequency curve of hornless moving-coil speaker at resonance frequency of the diaphragm on its leather surround. The signal voltage applied to the grid of the power valve was constant throughout.

approximately, since the reactance is relatively small in both cases. In Fig. 149  $R_m \doteq 50$  ohms, and since the transformer ratio is 10:1, the corresponding anode circuit load is 5,000 ohms. The valve resistance is 600 ohms, whilst the total coil resistance referred to the anode circuit is  $R_1 = 1,500 + 5,000 = 6,500$  ohms. Thus the circuit resistance increases from a nominal value of 2,100 ohms to 7,100 ohms at resonance, thereby causing the current to fall in the ratio  $2,100/7,100 = 0.3/1$ . It follows that the output is only  $\frac{1}{11}$  its value with a constant current, e.g. with a pentode valve of high internal resistance. Thus the resonance can be curbed appreciably by using a power valve of low resistance.

### 3. Increase in amplitude at resonance [80 d]

From Chapter VII the electrical radiation resistance due to a rigid diaphragm resonating on its axial constraint is

$$R_r = \frac{C^2}{r_r}. \quad (2)$$

In the absence of axial constraint the mechanical impedance is almost wholly reactive, since the radiation resistance  $r_r$  is relatively small. Then the electrical radiation resistance

$$R'_r = \frac{C^2 r_r}{\omega^2 m_e^2}. \quad (3)$$

From (2) and (3)

$$\frac{R_r}{R'_r} = \frac{\omega^2 m_e^2}{r_r^2}, \quad (4)$$

this being the power ratio of a resonant to a non-resonant system when the coil current is constant. The amplitude magnification is  $\omega m_e / r_r$ , this being analogous to  $\omega L / R$  for a tuning coil. Using the value of  $r_r$  from (2) in this formula, we obtain the amplitude magnification at resonance, namely,

$$\mu = \frac{\omega m_e R_r}{C^2}. \quad (5)$$

Incorporating the reduced value of current at resonance when a triode is used, (5) becomes

$$\mu = \frac{\omega m_e R_r}{C^2} \frac{I_2}{I'_2}. \quad (6)$$

Using the data\*  $C^2 = 3.6 \times 10^{13}$ ,  $R_r = 5 \times 10^{10}$ ,  $m_e = 20$  gm.,  $I_2 / I'_2 = 0.3$ ,  $\omega / 2\pi = 75 \sim$ , we obtain  $\mu = 4$ . Care must be exercised in practice to keep the amplitude within the linear portion of the force-displacement characteristic of the diaphragm constraint. When this condition is violated the wave form is flattened as shown in Fig. 103, and powerful alien tones may be created. This, in combination with the rectification effect discussed in Chapter XIV, limits the amount of power which can be radiated at low frequencies.

### 4. Power output at resonance [80 d]

The total power (radiation + loss) is  $I_2^2 R_m$ . If  $E$  is the anode voltage change, the primary current at low frequencies is substantially

\* Given in absolute electromagnetic units. To convert  $C^2$  and  $R_r$  to practical units multiply by  $10^{-9}$ .

$E$ /total resistance. The total anode circuit resistance at resonance is\*  $R_a + \text{normal optimum load resistance} + \varphi^2 R_m = 3.5R_a + \varphi^2 R_m$ , where  $2.5R_a$  is the normal load and  $\varphi$  the transformer ratio. Thus  $I_2 = \varphi E / (3.5R_a + \varphi^2 R_m)$  and the power

$$I_2^2 R_m = \frac{E^2 \varphi^2 R_m}{(3.5R_a + \varphi^2 R_m)^2}. \quad (7)$$

By differentiating (7) with respect to  $R_m$ , the condition for maximum power is found to be

$$R_m = \frac{3.5R_a}{\varphi^2}. \quad (8)$$

Using the data in § 2 (8) gives  $R_m = 21$  ohms. Actually  $R_m$  was 50 ohms, so the power at resonance was not a maximum. If the mechanical resistance  $r$ , is constant, then from (2), in the absence of loss,  $R_m$  decreases with reduction in  $C^2$ . Thus in the present case the power at resonance, and therefore the amplitude, would increase if the magnetic field strength was reduced. Although this condition should be avoided, it is quite prevalent in commercial apparatus, doubtless in the interests of economy.

The advantages of an intense magnetic field are:

1. With any given triode the stronger the field the greater the reduction in current at resonance. A corresponding reduction in amplitude and output ensues.

2. The electromagnetic damping is enhanced, thereby reducing the growth and decay periods. This provides a better 'attack', whilst natural oscillations of the diaphragm are more heavily damped.

3. The general output is augmented and the relative power due to resonances reduced.

## 5. Relationship between amplitude and loudness level [80d]

To bring the problem within the purview of simple analysis we shall choose a speaker diaphragm 10 cm. radius operating in a hard wall, the remainder of the enclosure being 'dead'. The results apply to pure tones only. In practice, sounds are complex and masking effects play an important role.

The sound-distribution at distances exceeding 200 cm. is uniform provided the radius of the diaphragm is small compared with the wave-length. If the power radiated from *one* side of the diaphragm is  $P$  ergs sec.<sup>-1</sup>, that passing through one square centimetre on the

\* Away from resonance  $\varphi^2 R_m$  is negligible compared with  $2.5R_a$ .

surface of a hemisphere of radius  $r$  is  $P/2\pi r^2 = P_1$ . Also, from Chap. VI, § 2,  $P_1 = p^2/\rho_0 c$ , and from (72a), Chap. II,

$$P = \frac{\pi \rho_0 a^4 \omega^4 \xi_{\max}^2}{4c}. \quad (9)$$

Equating the two values of  $P_1$  and substituting for  $P$  from (9), we obtain the r.m.s. sound pressure,

$$p = \frac{\rho_0 a^2 \omega^2 \xi_{\max}}{2\sqrt{2}r}. \quad (10)$$

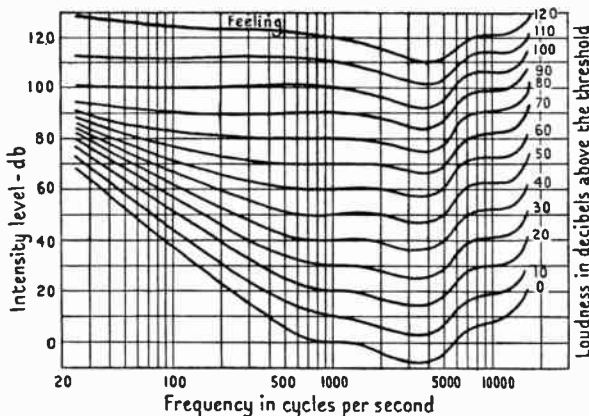


FIG. 150. 'Isobels' or curves of equal loudness level [80d] for pure tones propagated as plane or spherical waves in air.

The datum-level of sound intensity is taken as  $10^{-9}$  ergs  $\text{cm.}^{-2} \text{sec.}^{-1}$ , this corresponding closely to a r.m.s. pressure of  $2 \times 10^{-4}$  dyne  $\text{cm.}^{-2}$  under normal conditions at  $18^\circ \text{C}$ . Using (10) and the formula in definition 15, the level above the datum is

$$\text{db.} = 74 + 20 \log_{10} \frac{\rho_0 a^2 \omega^2 \xi_{\max}}{2\sqrt{2}r}. \quad (11)$$

Taking  $\xi_{\max} = 0.1$  cm.,  $r = 500$  cm.,  $\omega/2\pi = 64$   $\sim$ , db. = +77. Using the curves of Fig. 150, the corresponding loudness-level is 60 db., which is on the low side. If the diaphragm were set in the centre of a wall in an average room, the intensity would be some 10 db. higher due to reflection. This gives 87 above the datum and corresponds to a loudness of 80 db., which is ample for domestic purposes.

## DESIGN OF HORN TYPE MOVING-COIL SPEAKERS

1. THERE are two salient methods of approaching the present problem, both of which will be considered in detail and the results compared [71, 76]. As in the design of various forms of mechanism associated with vibrations, recourse is had to the electrical analogue of the mechanical system. In a resistanceless low-pass filter the attenuation over a wide frequency band is zero, but increases rapidly beyond the cut-off point. The object in speaker design is to simulate this as closely as possible. A very sharp cut-off is not imperative, since difficulty might be experienced in connecting the speakers for different frequency ranges and ensuring a smooth overall response curve. Where only one speaker is used, a sharp cut-off should be avoided, since it affects the reproduction adversely.

## 2. Method 1 [76]

The type of unit to be considered is illustrated in Fig. 82 A and the electrical analogue of the mechanical system is shown schematically in Fig. 151 A. The diaphragm (assumed to behave as a rigid structure) is represented by an inductance  $L_1$ , whilst the surround compliance is represented by a condenser  $C_1$ . The compliance of the air chamber between the diaphragm and the horn throat is represented by  $C_2$ , whilst  $M$  stands for the pneumatic transformer action due to the diaphragm being of greater diameter than the throat, Fig. 151 c. Obviously the ratio of the air velocity at the throat to that in contact with the diaphragm is  $A_a/A_0$ . This, therefore, is the transformer ratio. The resistance  $R_2$  simulates the throat resistance  $\rho_0 c A_0$ . In placing  $R_2$  across the secondary of the transformer we have tacitly assumed that the throat impedance of the horn is wholly resistive. As the cut-off frequency of the horn is approached, the reactance, due to the particle velocity and pressure being out of phase, increases, and if incorporated would be in series with  $R_2$ . It is quite adequate for our purpose, however, if we confine the analysis to frequencies above the horn cut-off, where the phase angle is small. At high frequencies, where the wave-length is comparable with the diaphragm radius, interference and reduction in output ensue, unless the design is specifically arranged to avoid this. Moreover, it is



assumed that arrangements of the type illustrated in Figs. 82 A, 163 are employed in both methods of design, so that the pressure from all parts of the diaphragm arrives at the throat in substantially the same phase. Even so there is a reactive component, but it will be neglected.

It is analytically inconvenient to have the transformer, so it and  $R_2$  are replaced by  $R = (A_d/A_0)^2 R_2$ , as in ordinary electrical problems

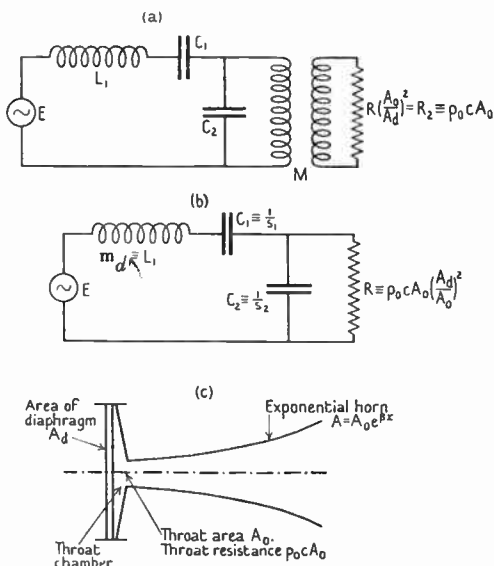


FIG. 151. (a), (b). Electrical analogue of mechanical system illustrated in (c). In the design given in the text it is assumed that the impedance at the back of the diaphragm is negligible. When this is inadmissible it may be necessary to connect a condenser  $C_3$  shunted by a resistance  $R_3$  between  $E$  and  $L_1$ . If the radiation at higher frequencies is appreciable an additional series resistance is required. (See § 12 and Fig. 158.)

[62], Fig. 151 B. We have to select the various circuit coefficients so that the power dissipated in  $R$ , i.e. that radiated as sound, will be fairly constant over a wide frequency band. To secure this condition the inductance  $L_1$  must be small, i.e. the coil and diaphragm must be very light, but commensurate with the duty to be performed. The fundamental frequency of the system is that of the coil and diaphragm on the annular surround. As a guide this can be taken

as the geometric mean of the upper and lower cut-off frequencies, i.e.  $\omega_0 = \sqrt{(\omega'_c \omega_c)}$ . Taking  $\omega'_c/2\pi = 50 \sim$  and  $\omega_c/2\pi = 4,000 \sim$ , the natural frequency *in vacuo* should be of the order  $\sqrt{(2 \times 10^5)} = 446 \sim$ . Assume it to be  $400 \sim$  and the coil and diaphragm mass 1 gm. The stiffness of the surround  $s_1 = \omega_0^2 m_d = 6.4 \times 10^8$  dynes cm.<sup>-1</sup> To secure a good upper register  $C_2$  must be quite small so that it resonates with  $L_1$  at a fairly high frequency. This necessitates a large chamber stiffness which in turn will restrict the diaphragm amplitude and therefore the low-frequency output. Neglecting  $R$  for the time being, the high-frequency cut-off is  $\omega_c = \sqrt{(1/L_1 C_2)} \equiv \sqrt{(s_2/m_d)}$ , since the impedance of  $C_1$  is negligible above  $1,000 \sim$ . In practice it is necessary to make  $R$  relatively low, and this prevents the cut-off being sharp. There is no sudden change in the diaphragm impedance, and the attenuation beyond the cut-off frequency increases very gradually. If  $\omega_c/2\pi = 4,000 \sim$ , then from the above formula  $s_2 = 6.4 \times 10^8$  dynes cm.<sup>-1</sup> It is now necessary to ascertain how much clearance this figure leaves for the diaphragm excursion. From formula (16), Chap. IV,  $s_2 = \gamma A_d^2 p_0/V$ , which in the present instance gives  $V = 2.2 \times 10^{-3} A_d^2$ . Taking the effective diaphragm radius as 3 cm., the chamber volume  $V$  is 1.8 cm.<sup>3</sup> The clearance depends upon the geometrical form of the throat chamber and diaphragm. As a practical guide we shall assume the permissible amplitude  $\xi_{\max}$  to be one-half the depth\* of the chamber if it were cylindrical. In the present case  $\xi_{\max} = 1.8/18\pi = 3.2 \times 10^{-2}$  cm. According to the data in Table 33, § 15, the radiation at  $200 \sim$ , with a throat radius of 0.85 cm. and an amplitude of  $3.2 \times 10^{-2}$  cm., could be as much as 1 watt. Below this frequency the output, with constant diaphragm amplitude, would decay as  $1/\omega^2$ , so at  $60 \sim$  it would be 0.09 watt, assuming, of course, that the cut-off point of the horn resides below this. The requirements of a public-address system would not then be met if it was intended to reproduce very low frequencies. To obtain greater output in this neighbourhood, the volume of the throat chamber must be augmented. Doubling the depth permits double amplitude and quadruple power, so at  $60 \sim$  we should get 0.36 watt. This means half the chamber stiffness and the upper cut-off frequency is halved. The former is now  $s_2 = 1.6 \times 10^8$  dynes cm.<sup>-1</sup> and the latter  $2,000 \sim$ .

We now proceed to predict the performance to be expected from

\* This is probably a conservative allowance.

the two cases treated above, i.e. cut-offs at 2,000 and 4,000  $\sim$ , on the basis of constant driving force throughout the frequency range. To accomplish this object it is necessary to determine the mechanical impedance of the system, as presented to the driving force on the moving coil, in the form  $z_e = r_e + i\omega m_e$ . First of all we deal with the electrical analogue. The electrical impedance can be found either by aid of Kirchhoff's circuital law or by the simple method of admittances. Choosing the latter way, the admittance of  $C_2 R$  is (Fig. 151 B)

$$\frac{1}{Z_2} = \frac{1}{R} + i\omega C_2 = \frac{1 + i\omega C_2 R}{R}.$$

Thus 
$$Z_2 = \frac{R(1 - i\omega C_2 R)}{1 + \omega^2 C_2^2 R^2}. \quad (1)$$

The total circuital impedance is, therefore,

$$Z = \frac{R}{1 + \omega^2 C_2^2 R^2} + i \left( \omega L_1 - \frac{1}{\omega C_1} - \frac{\omega C_2 R^2}{1 + \omega^2 C_2^2 R^2} \right). \quad (2)$$

Transforming (2) to mechanical quantities, we have

$$z_e = \frac{s_2^2 r}{s_2^2 + \omega^2 r^2} + i\omega \left[ \left( m_d - \frac{s_1}{\omega^2} \right) - \frac{s_2 r^2}{s_2^2 + \omega^2 r^2} \right]. \quad (3)$$

Thus the effective mechanical resistance opposing the driving force on the coil is

$$r_e = \frac{s_2^2 r}{s_2^2 + \omega^2 r^2}, \quad (4)$$

and the effective mass is

$$m_e = \left( m_d - \frac{s_1}{\omega^2} \right) - \left( \frac{s_2 r^2}{s_2^2 + \omega^2 r^2} \right). \quad (5)$$

In (5) the portion within the first bracket is the effective mass of the diaphragm and the surround, whilst the second quantity is that of the throat chamber as modified by the horn. The effective motional mechanical resistance  $r_e$  must not be confused with  $r$  the resistance shunting  $s_2$ . The two are different, since one refers to a series and the other to a shunt connexion. The difference is a matter of the phase and magnitude of the velocity. From (4) and (5) it is possible to plot curves showing  $r_e$  and  $m_e$ , provided  $r$  is known. Assuming a throat radius of 0.85 cm., the resistance is  $\rho_0 c A_0 = 95$  dynes cm.<sup>-1</sup> sec.<sup>-1</sup> Allowing for transformer action,  $r = 95(A_d/A_0)^2 = 1.45 \times 10^4$  mechanical ohms. The requisite curves are plotted in Fig. 152. The

power radiated is  $P = (f/z_e)^2 r_e$ , and if  $f$  is constant,

$$P \propto \frac{r_e}{z_e^2} \quad (6)$$

This is portrayed graphically at various frequencies in Fig. 153 to

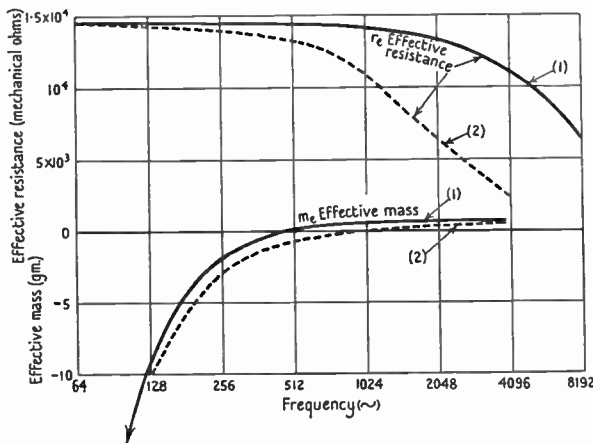


FIG. 152. Effective resistance and effective mass curves for diaphragm of horn type moving-coil speaker.

For (1)  $s_2 = 6.4 \times 10^8$  dyne cm.<sup>-1</sup>; for (2)  $s_2 = 1.6 \times 10^8$  dyne cm.<sup>-1</sup>

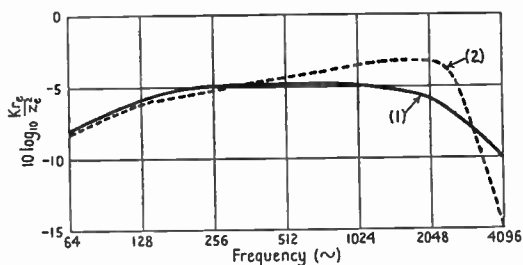


FIG. 153. Curves showing influence of throat chamber stiffness on performance of horn type moving-coil speaker.

For (1),  $s_2 = 6.4 \times 10^8$  dyne cm.<sup>-1</sup>; theoretical cut-off 4,000  $\sim$ ;  
for (2),  $s_2 = 1.6 \times 10^8$  dyne cm.<sup>-1</sup>; theoretical cut-off 2,000  $\sim$ .

a logarithmic scale of ordinates. It is clear that the speaker with the stiffer throat-chamber and higher cut-off frequency has the better upper register of the two (curve 1).

It is now advisable to test the assumption of constant driving force

corresponding to equal input to the power valve at all frequencies. To do this we commence by calculating the electrical impedance of the secondary circuit of the transformer connecting the power valve to the speaker. At the resonance of the diaphragm on its surround (400  $\sim$ ), the mechanical impedance is substantially  $r_e$ . From formula (2), Chap. XIX, the electrical motional resistance,\* assuming absence of loss,  $R_r = C^2/r_e$ . The mean air-gap flux density of the magnet  $B_g$  can be taken as  $2 \times 10^4$ , whilst the length of aluminium ribbon on the coil is 760 cm., giving a value of  $C^2 = (B_g l)^2 = 2.3 \times 10^5$  practical units (abs. units  $\times 10^{-9}$ ). Since  $r_e = 1.45 \times 10^4$ ,  $R_r = 16$  ohms. The coil resistance being 15 ohms gives a sum of 31 ohms, to which must be added the influence of the valve and the secondary of the transformer. Choosing equality of valve and speaker resistances, the total effective secondary value is about 60 ohms. The electrical inductance of the coil is important at high frequencies only. Taking its value as  $8.4 \times 10^{-4}$  henrys † as based on Table 36, the reactance at 4,000  $\sim$  is about 20 ohms. It is easy to show that the motional reactance  $\omega L_m$  is negligible throughout the frequency range. Thus the impedance of the secondary circuit and, therefore, the driving current will be substantially constant at all frequencies, provided the coil resistance does not increase with rise in frequency. From Table 36 we see that the resistance does increase, so that the output will decay to an extent in the upper register. In general this is not serious up to 4,500  $\sim$ .

The efficiency  $\eta = R_r/(R_0 + R_r) = \frac{16}{31} = 0.52$ , which is a high value attributable to the special coil construction (Fig. 82) and the intense magnetic field.

*Horn.* If the cut-off frequency is 60  $\sim$ , from Chapter X,  $\beta/2k = 1$ , so  $\beta = 0.022$ . According to Chap. X, § 6, the radius of the final opening should be about  $\frac{1}{4}\lambda = 140$  cm. Since the horn curve is  $A = A_0 e^{\beta l}$ ,  $l = (4.6/\beta) \log_{10} a/a_0 = 460$  cm. or approximately 15 feet.

### 3. Method 2 [71]

The mechanical construction of the driving mechanism differs from that in the previous method and is illustrated schematically in Fig. 154. The driving coil is connected to the diaphragm by a spider of appropriate stiffness, whilst *in vacuo* the fundamental frequency

\* At resonance  $R_M = R_r$

† The coil considered here is the same diameter as that cited in Table 36, but is one-third the length and has only 50 turns. The air-gap is smaller here, which means increased iron loss and inductance.

of the diaphragm on the annular surround is below audibility. The electrical analogue is given in Fig. 155 A.  $L_1$  represents the mass of the coil and its former with the spider; the compliance of the latter is given by condenser  $C_1$ . The throat-chamber compliance is equivalent to  $C_2$ , whilst  $L_2$  simulates the mass of the diaphragm assumed

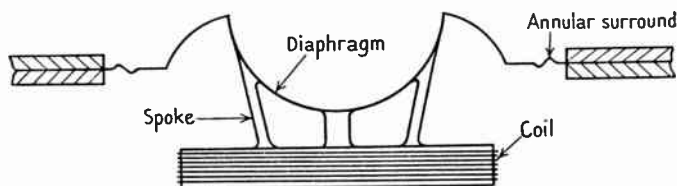


FIG. 154. Illustrating diaphragm and coil construction for horn type speaker (method 2 in text). See caption to Fig. 151 regarding the impedance at the back of the diaphragm.

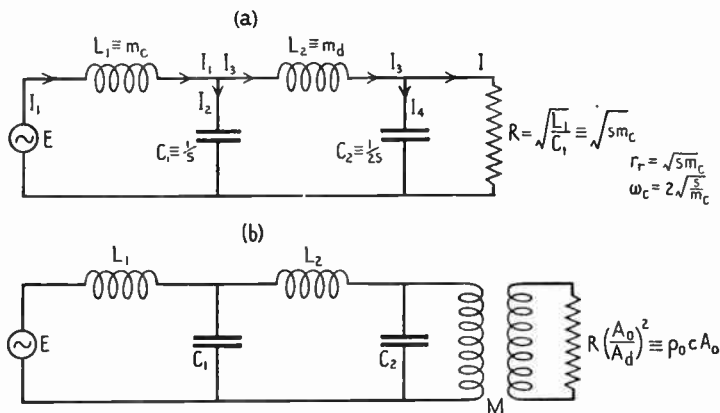


FIG. 155. Electrical analogue of diaphragm air-chamber and horn, in moving-coil speaker (method 2 in text).

to vibrate as a rigid structure. The coupling transformer due to the throat chamber, shown in Fig. 155 B, is omitted, so  $R$  represents the mechanical resistance on the diaphragm due to radiation. The compliance of the annular surround, which would be represented by a condenser in series with  $L_1$ , as in Fig. 151, is so large that its influence can be neglected. The network in Fig. 155 A, which simulates the mechanism of the speaker, is of the  $1\frac{1}{2}$  section type with mid-shunt termination. The surge impedance of an infinite network of this type over a wide frequency range is a resistance of value  $R = \sqrt{(L_1/C_1)}$ .

As the cut-off point is approached, a reactive component appears which causes a reduction in the diaphragm velocity. In the present case, if the above surge impedance is assumed, the attenuation up to 80 per cent. of the upper cut-off point will be substantially uniform, provided  $L_1 = L_2$  and  $C_1 = 2C_2$ . For simplicity we shall assume that the horn functions above its cut-off point, where the phase angle between pressure and particle velocity is small enough for the power factor  $\cos \theta$  to be taken as unity.

First of all we shall examine the circuit of Fig. 155A analytically and derive an expression for the radiated power  $I^2R$  in terms of the circuit coefficients. Using Kirchoff's principle, that the sum of the p.d.s round a closed circuit vanishes, together with the conditions  $L_1 = L_2$ ,  $C_1 = 2C_2$ , we have for the first circuit:

$$i\omega L_1 I_1 - \frac{iI_2}{\omega C_1} = E; \quad (7)$$

for the second circuit:

$$i\omega L_1 I_3 - \frac{2iI_4}{\omega C_1} + \frac{iI_2}{\omega C_1} = 0, \quad (8)$$

the positive sign prefixed to the third term signifying that the p.d. is now taken in the opposite direction from that indicated in the second term of (7); for the third circuit:

$$IR + \frac{2iI_4}{\omega C_1} = 0; \quad (9)$$

and for the currents:

$$I_1 = I_2 + I_3 \quad \text{and} \quad I_3 = I_4 + I. \quad (10)$$

We have to determine the power  $I^2R$  from (7), (8), (9), and (10). The plan adopted is to eliminate each current in turn, starting with  $I_1$ , and ending up with  $I$  in terms of  $E$  and the circuit coefficients. Substituting from (10) for  $I_1$  in (7), we have

$$i\omega L_1(I_2 + I_3) - \frac{iI_2}{\omega C_1} = E; \quad (11)$$

so 
$$iI_2 \left( \omega L_1 - \frac{1}{\omega C_1} \right) + i\omega L_1 I_3 = E,$$

or 
$$\frac{iI_2}{\omega C_1} (y^2 - 1) + i\omega L_1 I_3 = E, \quad (12)$$

where  $y^2 = \omega^2 L_1 C_1$ . Substituting in (12) for  $iI_2/\omega C_1$  from (8),

$$\frac{2iI_4(y^2 - 1)}{\omega C_1} - i\omega L_1(y^2 - 2)I_3 = E. \quad (13)$$

From (9),  $\frac{2iI_4}{\omega C_1} = -IR$ , and from (9), (10),  $I_3 = I\left(1 + \frac{i\omega C_1 R}{2}\right)$ .

Inserting these values in (13) we find, on separation of the real and imaginary parts, together with the substitution  $y = \omega L_1/R$ , that

$$IR\left\{\left(\frac{1}{2}y^4 - 2y^2 + 1\right) - iy(y^2 - 2)\right\} = E. \quad (14)$$

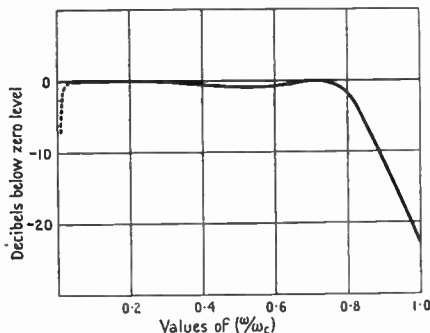


FIG. 156. Curve illustrating performance of horn speaker designed according to method 2 (see text). The abscissae are fractions of the upper cut-off frequency  $\omega_c/2\pi$ .

Thus the power supplied to the horn is

$$I^2 R = \frac{E^2}{R} \frac{1}{\left\{\left(\frac{1}{2}y^4 - 2y^2 + 1\right)^2 + y^2(y^2 - 2)^2\right\}}$$

or

$$P = \frac{E^2}{R} \frac{1}{\left(1 + y^4 - y^6 + \frac{1}{4}y^8\right)}. \quad (15)$$

Now  $y^2 = \omega^2 L_1 C_1$  and the upper frequency cut-off of the network is given approximately by  $\omega_c^2 = 4/L_1 C_1$ , so  $y^2 = 4(\omega/\omega_c)^2$ . Writing  $\omega/\omega_c = \varphi$  in (15) and transforming to mechanical quantities, we obtain the power [71]

$$P = \frac{10^{-7} f^2}{r_r} \left[ \frac{1}{1 + 16\varphi^4 - 64\varphi^6 + 64\varphi^8} \right]. \quad (16)$$

The quantity in brackets specifies the performance, provided the driving force and throat resistance are constant. Since this pertains in the analysis, the output is represented by the bracketed quantity, which is plotted on a decibel basis in Fig. 156. The output-level is practically unaltered up to 80 per cent. of the upper cut-off frequency.



#### 4. Details of design

To make comparison with the design considered in method 1, the salient dimensions are unaltered. The output is to be maintained constant up to 4,000  $\sim$ , which entails a theoretical cut-off at 5,000  $\sim$ . We have  $\omega_c = 2\sqrt{(s/m_c)}$ . Since  $m_c = 0.5$  gm., we get  $s = 1.25 \times 10^8$  dynes cm.<sup>-1</sup> If there are six spokes to the spider, the stiffness of each is approximately  $2.1 \times 10^7$  dynes cm.<sup>-1</sup> For flat spokes (on the assumption of a free end cantilever) the deflexion  $x = fl^3/3qI$ , so the stiffness  $s = f/x = 3qI/l^3$ . For a rectangular section  $I = bt^3/12$ , so the thickness  $t = l\sqrt[3]{(4s/qb)}$ . Assuming  $l = 0.7$  cm.,  $b = 0.15$  cm.,  $q$  for aluminium,  $7.2 \times 10^{11}$  dynes cm.<sup>-2</sup>, the thickness is  $t = 0.064$  cm. From formula (16), Chap. IV, the stiffness of the throat chamber, when closed at the horn, is (writing  $2s$  for  $s$ )  $2s = \gamma A_d^2 p_0/V$ . Using the preceding value of  $s$  and taking the effective radius of the diaphragm as 3 cm. (as in method 1), the chamber volume  $V = 4.5$  cm.<sup>3</sup> The height of a cylindrical chamber is  $4.5/9\pi = 0.16$  cm. and the maximum permissible amplitude 0.08 cm. The terminal resistance of the network, this being the mechanical resistance at the diaphragm, is from Fig. 155 A\*  $r_r = \sqrt{(m_d s)} = 8,000$  dynes cm.<sup>-1</sup> sec.<sup>-1</sup> This is about one-half the value in the previous design, so that for given output the amplitude will be nearly  $\sqrt{2}$  times greater. Now  $r_r = \rho_0 c A_0 (A_d/A_0)^2$ , so the throat area  $A_0 = \rho_0 c A_d / r_r = 4.25$  cm.<sup>2</sup>, corresponding to a radius  $a_0 = 1.16$  cm., which exceeds that in the other design by 36 per cent.

#### 5. Comparison with method 1

For comparison with the first method we have agreed to use diaphragms of identical mass and radius. The construction, however, must be modified to incorporate the spider. The total coil mass, including former and spider, is 0.5 gm., 0.11 gm. of this being due to the latter. Adding 0.09 gm. for fixing the coil of the spider, 0.3 gm. is left for the conductor whose length is reduced in the ratio 3:5 compared with method 1. Thus  $C^2$  is now  $2.3 \times 10^5 \times \frac{3}{25} = 8.3 \times 10^4$  in practical units.

From Chapter VII, the electrical terminal resistance  $R_m = r_r C^2/z_e^2$ . Since the input impedance  $z_e = r_r$  the formula becomes

$$R_m = \frac{C^2}{r_r} = \frac{8.3 \times 10^4}{8,000} \doteq 10 \text{ ohms.}$$

$$* m_d = m_e.$$

The coil resistance in the first method is 15 ohms, so it is now  $\frac{2}{3} \times 15 = 9$  ohms. Consequently the acoustic efficiency  $\eta = \frac{10}{19} = 0.53$  which to all intents and purposes is identical with the value found previously by method 1. In both of these designs it is of importance to notice that the back e.m.f. induced due to motion of the coil in the magnetic field is very small compared with that in a hornless speaker. This is due to the smaller amplitude in the horn speaker required to radiate a given power (see Table 33). Thus the motional capacity is small enough to be disregarded in comparison with the motional resistance. Owing to the greater chamber volume the present design is capable of greater output at very low frequencies than that of method 1. The power delivered to the horn is  $P = \omega^2 \xi_{\max}^2 r_r / 2$ . Now the maximum permissible amplitudes vary directly as the chamber volumes, since the diaphragms are of equal radius. Thus the power ratio of the designs is

$$\frac{P_2}{P_1} = \left( \frac{V_2}{V_1} \right)^2 \frac{r_{r2}}{r_{r1}} = \left( \frac{4.5}{1.8} \right)^2 \frac{8 \times 10^3}{1.45 \times 10^4} \doteq 3.4,$$

or 5.3 db. at the lowest frequencies. In method 2 the permissible amplitude is (from above) 0.08 cm., which with  $r_r = 8,000$  gives the ultimate power as  $P \doteq 2.5 \times 10^{-6} \omega^2$ . At 100  $\sim$  this means a maximum output of 1 watt and at 60  $\sim$  one of 0.36 watt, which is ample for a single speaker covering a wide frequency band. For picture-theatre work it is customary to specify a maximum output at the lower cut-off frequency. Under this condition the above design procedure would have to be more or less reversed. It could, of course, be used as a basis and the essential modifications made to ensure adequate low-frequency output.

## 6. Horn

The only essential difference between the data in the two cases is that  $a_0$  is now 1.16 cm., which gives a length of 14 feet as compared with 15 feet found previously.

## 7. High frequencies

The two designs show a different behaviour at the upper frequencies, provided the diaphragm is rigid in each case. The input impedance in 1 is partly resistive, and partly reactive due to the coil mass. At higher frequencies the latter component curbs the diaphragm velocity and reduces the output as shown in Fig. 153. In practice, however,

resonances come to the rescue and the output is maintained up to 4,500  $\sim$ , as shown in Fig. 100. The origin of these resonances is most likely in the diaphragm. Its spherical shape does not give such high rigidity as that of a cone, and nodal circles are likely to occur near the axis. We ought to mention, however, that the reactance component due to the air can be represented by an inductance in series with  $R$  in Fig. 151 B. This gives a parallel oscillatory circuit, but it may be too heavily damped for resonance to have an appreciable effect on the speaker performance. The input impedance in method 2 is wholly resistive up to a higher frequency than in method 1. Thus the output is maintained fairly uniform up to a higher frequency, but the cut-off is sharper. In practice resonances doubtless contribute their quota and off-set the influence of frictional loss at the horn throat.

### 8. Factors controlling the efficiency\*

Since  $\omega_c = 2\sqrt{s/m_c}$  and  $r_r = \sqrt{sm_c}$ , we have  $r_r = \frac{1}{2}(\omega_c m_c)$ . Now  $R_m = C^2/r_r = 2C^2/\omega_c m_c$ , where  $m_c$  includes the coil, conductor insulation, former, and spider. Let  $m_c = \varphi m'_c$ , where  $m'_c$  is the mass of the conductor alone. We have  $m'_c = \rho_2 lA$ , so

$$R_m = \frac{2C^2}{\omega_c \varphi \rho_2 lA}. \quad (17)$$

Also the conductor resistance

$$R_c = \frac{\rho_1 l}{A}, \quad (18)$$

where  $\rho_1$  can include the influence of iron loss in the magnet. Using the value  $C^2 = (B_g l)^2$ , with the aid of (17) and (18), the efficiency [71] is

$$\eta = \frac{1}{1 + (R_c/R_m)} = \frac{1}{1 + 1/x}, \quad (19)$$

where

$$x = \frac{R_c}{R_m} = \frac{B_g^2}{\varphi \omega_c \rho_1 \rho_2}.$$

For a given upper cut-off frequency the efficiency increases with  $x$ , as shown in Fig. 96. As might be expected, the flux density should be as large as possible for high efficiency. The product of specific resistance and density ( $\rho_1 \rho_2$ ) is to be as small as practicable. Here aluminium scores over copper, since  $\rho_1 \rho_2$  for the former is half its value for the latter. When  $B_g$  and  $\rho_1 \rho_2$  are fixed, the efficiency increases with

\* §§ 8, 9, 10 refer to method 2.

rise in the upper cut-off frequency. Now  $\omega_c = 2\sqrt{(s/m_c)}$ , so that if the stiffness is constant,  $m$  decreases with rise in  $\omega_c$ . There is, however, a limit, since  $m$  is the diaphragm mass of fixed diameter. Its thickness cannot be reduced a great deal, since the resonance frequency would be quite low, thereby modifying the performance. Also with a diaphragm of inadequate rigidity, the speaker might be prone to rattling with large low-frequency input.  $\varphi$  is an important factor and its value should be as near unity as possible. This can only be accomplished by adopting a special form of coil design, e.g. strip wound on edge, as shown in Fig. 82B. There is, of course, the problem of attaching the coil to the spider, and this is where the second design is at a disadvantage compared with the first, since the *inactive* mass of material is a goodly proportion of the coil mass.

### 9. Relationship between power and throat area [71]

From formula (16), Chap. IV, and Fig. 155 A, the chamber stiffness is

$$2s = \frac{\gamma A_d^2 p_0}{V} = \omega_c r_r, \quad (20)$$

since  $\omega_c = 2\sqrt{(s/m_c)}$  and  $r_r = \sqrt{(sm_c)}$ .

The mechanical resistance at the diaphragm is

$$r_r = \frac{\rho_0 c A_d^2}{A_0}, \quad (21)$$

from which it follows that

$$V = \frac{\gamma A_0 p_0}{\rho_0 c \omega_c} = \frac{3 \cdot 3 \times 10^4 A_0}{\omega_c}. \quad (22)$$

Thus for a given throat area and upper cut-off frequency the volume of the air chamber is constant. The permissible displacement, being one-half of the height of the equivalent cylindrical chamber, is  $V/2A_d = \xi_{\max}$ . But  $P = \frac{1}{2}\omega^2 \xi_{\max}^2 r_r$ , so that from above

$$P = 600A_0 \left(\frac{\omega}{\omega_c}\right)^2 \text{ watts.} \quad (23)$$

For a given throat area, the output increases with decrease in the cut-off frequency, since this permits a larger chamber volume and greater amplitude. Alternatively, if  $\omega_c$  is fixed, a large throat area is required to deliver considerable power. There is, however, a limit beyond which trouble with the diaphragm arises due to increase in diameter and thickness.

### 10. Upper limit of throat area ( $A_0$ ) [71]

From § 8\*  $r_c = \frac{1}{2}(\omega_c m_d) = \rho_0 c A_d^2 / A_0$  from (21), so

$$A_0 = \frac{2\rho_0 c A_d^2}{m_d \omega_c} = \frac{84 A_d^2}{m_d \omega_c}. \quad (24)$$

For any given shape of diaphragm  $m_d = \varpi_1 \rho_2 A_d t$ , where  $\varpi_1$  is a constant. Thus

$$A_0 = \frac{\varpi_2 A_d}{t \omega_c}, \quad (25)$$

where  $\varpi_2 = 84/\varpi_1 \rho_2$ . When the fundamental frequency of the diaphragm is fixed,  $A_d$  can be found in terms of  $\omega_c$  for any specific shape. Thus the largest permissible throat area can be determined. To secure rigidity the diaphragm must be either conical, spherical, or some such form as shown in Fig. 82 A. The relationship between  $A_d$  and  $t$  is then not of the simple form which pertains to a disk, and may have to be found experimentally. This will be realized by reference to Chapter XVIII, where it is shown that the influence of circumferential or hoop stress is of prime importance when the thickness exceeds a certain amount.

### 11. Experimental data on horns

Some data obtained with exponential horns and modifications thereof are shown graphically† in Fig. 157 [68]. These horns were driven by an electrical unit actuated by a power valve to whose grid a constant input voltage was supplied. It is seen that the power from a horn 16 in. long begins to fall rapidly below 360 ~. To extend the range down to 120 ~ a horn 4.5 times as long is required. Even so, the power with such a horn at 120 ~ is slightly less than it is with a shorter one at 360 ~. The length of the horn increases more rapidly than the cut-off frequency decreases, e.g.  $4.5 > 360/120$ . This bears out the theory in Chapter X that the radius of the opening must increase with the wave-length. The rate of expansion being fixed, it follows that the horn-length increases with the wave-length. There is little necessity to comment on the shapes of the curves above 500 ~, except to mention that they are typical of the results obtained from moving-coil horn-type speakers. There is a fairly sharp cut-off about 5,000 ~ in all cases, but in all probability it is mainly due to

\*  $m_d = m_c$  by hypothesis, where  $m_d$  is the mass of the diaphragm alone.

† A vertical scale is not given since it is absent in the original. It is not clear whether the output was measured on the axis or integrated over a hemisphere.

interference in the throat chamber, when  $\lambda$  is comparable with the diameter of the diaphragm

When a cylindrical section 12 in. long is inserted half-way along a horn 7 feet long, the transmitted wave is suddenly unable to expand. Part of its energy is diverted backwards, i.e. it is reflected with consequent loss in output [68]. The result is to raise the cut-off frequency from 100 to 140  $\sim$  and to cause a reduction in output up to approximately 450  $\sim$ . It is only fair to remark, however, that the aural effect would be almost negligible. The influence of a 12-in.

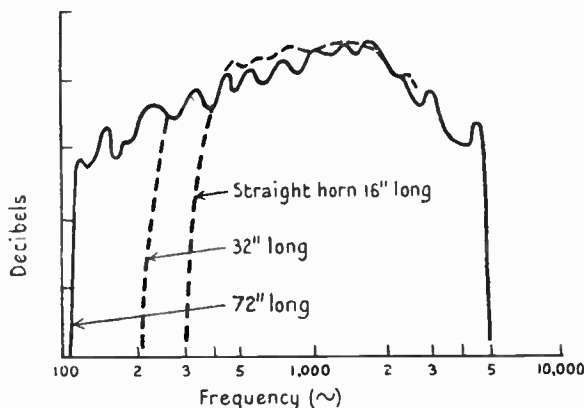


FIG. 157. Curves illustrating performance of straight exponential horns of different lengths.

parallel section at the throat is to reduce the output from 450 to 200  $\sim$ , and to lower the cut-off frequency by 10  $\sim$ .

## 12. Directional baffle speaker, i.e. large diaphragm with horn

The arrangement is shown diagrammatically in Fig. 158 A. The diaphragm radius is of the order 7 cm., the assembly being akin to the ordinary moving-coil speaker excepting that a wide horn is used to increase the efficiency [11, 15]. It also increases the directional properties. The sound from the rear of the diaphragm is suppressed by an absorbent cabinet. The absorption at low frequencies is small compared with that at high frequencies, where the absorption coefficient is substantially unity. In investigating the design, the first step is to determine the electrical analogue of the mechanical system. It is not easy to assess the effective mass of the coil and diaphragm,

owing to the various vibrational modes which occur throughout the acoustic register. From Fig. 111, for a cone with an annular surround, the effective mass is seen to be very variable, particularly in the neighbourhood of resonances. If the effective-mass curve of the diaphragm, under the conditions indicated in Fig. 158 A, is known, the

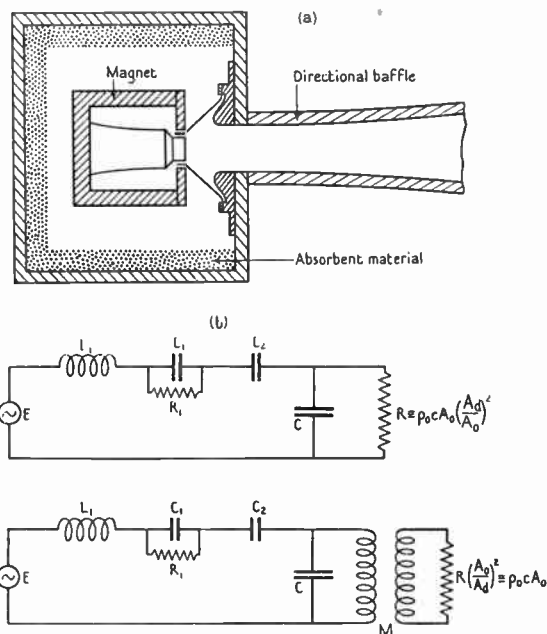


FIG. 158.

(a) Schematic arrangement of directional baffle speaker. In some cases the sides of the box are perforated.

(b) Electrical analogue of the mechanical system in (a). The effect of radiation from the back of the cone can be included in  $R_1$ , but it is preferable to use a separate series-resistance  $R_2$  (not shown) between  $C_1$ ,  $R_1$ , and  $C_2$ .

The separation of the diaphragm and the front of the air chamber is 0.32 cm.

value of the inductance in the analogous electrical circuit of Fig. 158 B is calculable. This, however, is not permissible in the present case, since we start *ab initio*. All we can do, therefore, is to substitute some form of diaphragm amenable to calculation in order to establish the design. Moreover, we select a rigid disk on the assumption that the magnet does not interfere seriously with the sound radiation from the rear.

The mass is the sum of coil, diaphragm, and accession to inertia, i.e.  $m_e = m_c + m_n + m_i$ . If we confine our attention to the frequency register above the horn cut-off, where the particle velocity and pressure are substantially in phase,  $m_i$  on the horn side of the diaphragm is negligible. On the cabinet side the low-frequency condition differs from that of radiation into one-half of infinite space, and the accession to inertia is thereby modified. Its value depends upon the form and size of the box, together with the absorption coefficient. As a first approximation we shall take  $m_i$  to be the value calculated from formula (14), Chap. III. Thus  $m_e$  is found, so the analogous electrical quantity  $L_1$  can be determined. The elastic effect of the air in the box can be ascertained by aid of formula (16), Chap. IV. Since  $\gamma p_0 = \rho_0 c^2$ , the analogous capacity  $C_1 \equiv V_1/A_d^2 \rho_0 c^2 = 1/s_1$ , where  $V_1$  is the volume of the box and  $A_d$  the effective area of the diaphragm ( $\pi a^2$ ). Owing to absorption of sound within the box, this condenser is to be shunted by a resistance  $R_1$  which decreases as the absorption increases. When the latter is zero  $R_1$  is obviously infinite.

There is also the resistance  $R_2$  due to radiation from the back of the diaphragm. This can be treated as a series resistance between  $C_1$  and  $C_2$  in Figs. 158 B, C (not shown). As a first approximation the mechanical resistance can be calculated from the formula in Chap. VIII, § 1, viz.  $r_r = \rho_0 c A G_1$ . It varies with frequency\* in a manner similar to that of the dotted curve  $G_1$  of Fig. 17.

The elastic effect of the annular surround is represented by a series condenser  $C_2$ , since the box and surround constraints are additive, both opposing axial motion of the diaphragm. Allowance can be made for sound radiation and increased mass due to the surround by supposing the diameter of the diaphragm to be augmented by an appropriate amount. This completes the diagram for the rear portion.

In front of the diaphragm there is the stiffness of the throat chamber and the resistance imposed by the horn. These are in parallel since the horn acts as a leak on the chamber. From above,

$$C \equiv \frac{V}{A_d^2 \rho_0 c^2} = \frac{1}{s},$$

where  $V$  is the volume between the diaphragm of effective area  $A_d$  and the throat entrance. Above the horn cut-off frequency the

\*  $L_1$ ,  $R_1$ , and  $R_2$  vary with frequency.



throat resistance is approximately  $r_0 = \rho_0 c A_0$ . The resistance across  $C$  exceeds this owing to the transformer action of the chamber. If  $A_d$  refers to the diaphragm, we have  $r_r = r_0 (A_d/A_0)^2$ , and the electrical value  $R$  follows immediately. The value of  $A_d$  depends upon the load required on the diaphragm, and also the interference at higher frequencies where the wave-length approaches the diaphragm diameter. The complete electrical analogue of the mechanical system, as shown in Fig. 158, has now been determined.

In designing the speaker [15], the magnitudes of the various components in Fig. 158 B must be chosen to give a relatively uniform response over as wide a frequency band as possible. Some design data may be of assistance in this direction. A reasonable throat diameter\* for a cone 7 cm. radius is about 11 cm. If the cut-off frequency is 50  $\sim$ , the flaring index  $\beta = 2k = 200\pi/(3.4 \times 10^4)$ , which amounts to  $1.84 \times 10^{-2}$  (Chap. X). The radius at the horn-opening must be about  $\frac{1}{4}\lambda$  to  $\frac{1}{6}\lambda$ , i.e. the final radius is of the order 130 cm. Since the area at any axial distance is  $A = A_0 e^{\beta l}$ , we have

$$l = \frac{4.6}{\beta} \log_{10} \frac{a}{a_0} = 346 \text{ cm.}$$

or 11.5 feet.

The resistance at the throat  $r_0 = \rho_0 c A_0 = 4 \times 10^3$  mechanical ohms, so at the diaphragm  $r_r = 4 \times 10^3 (7/5.5)^4 = 1.05 \times 10^4$  mechanical ohms. At the back of the diaphragm  $r_r$  steadily rises from a low value at 50  $\sim$  to 6,500 mechanical ohms at 1,500  $\sim$  above which it is substantially constant apart from cone resonances. This resistance reduces the diaphragm amplitude and, therefore, the output on the horn side.

Chamber stiffness

$$\frac{1}{C} \equiv s = \frac{\rho_0 c^2 A_d^2}{V} = 9.3 \times 10^7 \text{ dynes cm.}^{-1}$$

The value of  $C_2$  is best calculated from the natural frequency of the diaphragm on the surround in absence of the horn, box, and electromagnetic damping. Taking the natural frequency as 30  $\sim$ , the coefficient of restitution or stiffness is

$$\begin{aligned} s_2 &= \omega^2 m_e \\ &= 2.9 \times 10^5 \text{ dynes cm.}^{-1}, \end{aligned}$$

\* In practice the throat is square, 4 in.  $\times$  4 in., whilst the conical diaphragm is 3 in. radius.

where  $m_e = 8$  gm. So far as the box is concerned  $R_1$  can be omitted for simplicity, since the stiffness

$$\frac{1}{C_1} \equiv s_1 = \frac{\rho_0 c^2 A_d^2}{V_1} = 2.6 \times 10^5 \text{ dynes cm.}^{-1}$$

is relatively so small. Thus we are concerned with (1) mass of diaphragm, (2) stiffness of surround, (3) stiffness of air chamber, (4) resistive load on diaphragm. The low-frequency cut-off of the mechanism is substantially that of  $m_e$  and  $s_2$ , i.e.  $30 \sim$ . The actual cut-off acoustically is settled by the horn. Apart from diaphragm

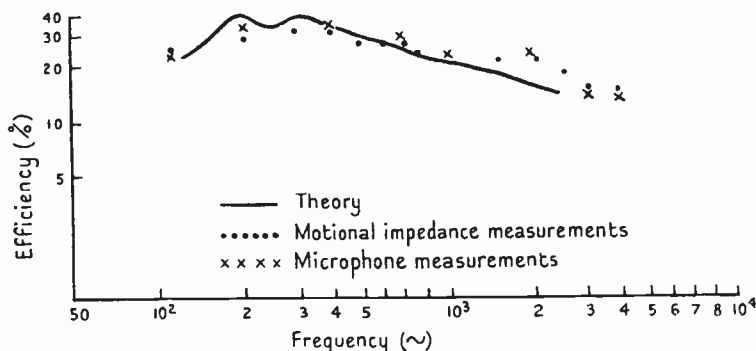


FIG. 159. Efficiency curve of directional baffle speaker. The radiation from the back of the cone is included in all cases. Owing to focusing of the radiation at higher frequencies (see Fig. 160), the response curve taken on, or at a small angular distance from, the axis is fairly constant up to  $5,500 \sim$ . The lower register can be extended down to  $60 \sim$  by using a baffle 10 ft. long and 6 ft.  $\times$  6 ft. at the mouth.

resonances, which augment the upper register and tend to preserve uniformity of output, the upper cut-off is due to  $m_e$  and to  $s$ . Thus  $\omega_c = \sqrt{s/m_e}$ , so the frequency is  $600 \sim$ . Actually the cut-off is obliterated by the shunting effect of  $R$ , but the output in the upper register slowly decays. The efficiency found by measurement of motional resistance in air ( $R_m$ ), and by microphone measurements on a certain speaker in the open air (Chap. XV), is shown in Fig. 159 [15]. The output declines above  $300 \sim$ . It would decay more rapidly above  $2,000 \sim$  if the diaphragm behaved as a rigid structure. As in other types of speaker, resonances are required to boost the output at higher frequencies. The power above  $5,000 \sim$  is attenuated due mainly to mass reactance. Owing to the large horn-opening (58 in.  $\times$  43 in.)

there is a strong directional effect over the whole frequency band, as shown by the polar diagrams of Fig. 160. The focusing in a central plane orthogonal to the long axis of the baffle mouth is more uniform over the frequency range from 400 ~ upwards than that in the central plane containing this axis. This is due to the sound pressure steadily falling away towards the edge with increase in frequency [11]. The effect is equivalent to a reduction in the linear dimensions of the radiator, so the focusing increases less rapidly than that for a rigid diaphragm. The axial pressure at a distance of 20 feet from the speaker is substantially constant from 100 to 5,000 ~. Instruments

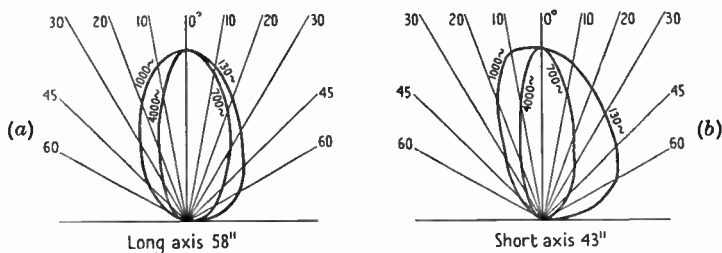


FIG. 160. Polar radiation characteristics of directional baffle speaker (a) in plane containing long axis of baffle mouth, (b) in plane containing short axis of baffle mouth.

of this type are used in cinemas where large acoustic power is required. An output of from 1 to 2 watts can be obtained.

### 13. Speakers for picture theatres [7, 11]

(a) There are three salient types of speaker used in this class of work, all of which operate on the moving-coil principle. They are (1) horn type, (2) directional baffle, (3) flat baffle type.\* Class (2) is in reality a special form of (3) in which the baffle is replaced by a stumpy exponential horn to increase the resistive load on the diaphragm. The latter is usually about 7 cm. radius as compared with 2.5 cm. for class (1). The salient characteristics are as follows:

(b) *Efficiency.* On the average the efficiency of the horn type is of the same order as that of the directional baffle speaker. The latter is from 6 to 9 decibels higher than a single cone in a flat baffle.

(c) *Radiation distribution characteristics.* Each type exhibits focus-

\* This type is introduced for comparison. It is now used chiefly to give large output at low frequencies. See § 16. Under this condition the possibility of sub-harmonics, Chap. XVIII, § 7, must not be overlooked.

ing at higher frequencies. For (1) and (2) an angle of  $20^\circ$  on each side of the axis of symmetry is covered at  $4,000 \sim$ . The width of the beam increases with fall in frequency. This gives satisfactory results in small theatres, but in large ones, two or more speakers must be suitably situated\* and directed specifically to cover a greater angle. The distribution from a single cone unit in a flat baffle is less focused than that in types (1) and (2).

(d) *Response characteristics.* Typical curves taken on the axes of types (1) and (2) are shown in Fig. 161. Although axial curves are

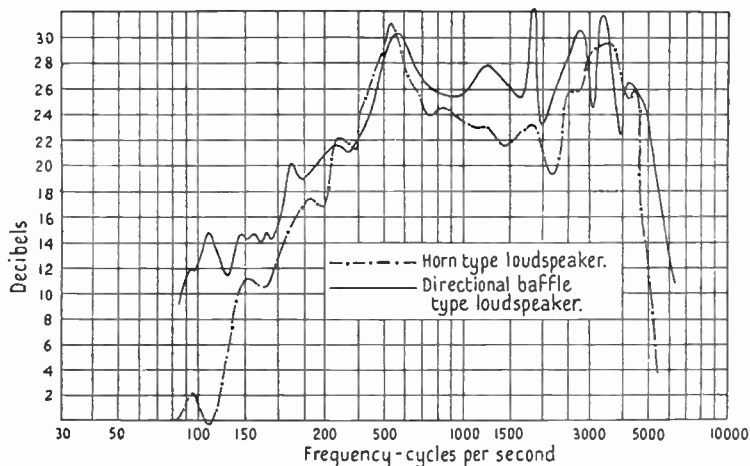


FIG. 161. Relative frequency response characteristics of two speakers [11].

an imperfect index of performance, these two are comparable, since the horn opening was of the same order of size as that of the directional baffle, namely, 5 ft.  $\times$  3 ft. The latter type covers a somewhat wider range and is better at low frequencies. Type (3) gives a curve which is somewhat similar to that of the directional baffle type excepting that its level is several decibels lower. In certain cases the upper and lower frequencies may be *relatively* more powerful for a flat than a directional baffle, but as this depends upon design, no hard and fast rules can be recommended.

(e) *Input power capacity.* The input is limited either by the permissible temperature rise of the coil or the restriction of axial ampli-

\* The speakers are usually located at the centre of the screen to obtain the correct acoustic illusion.

tude. To obtain a reasonable response up to 4,500  $\sim$ , all classes of speaker must have coils of small mass, and the temperature problem is much the same in each case. On the average a maximum *input* of from 4 to 6 watts can be handled, but in certain cases this can be exceeded. As regards axial amplitude, this is limited chiefly by clearance in the throat chamber in types (1) and (2), but no difficulty arises for average purposes. For the above input to type (3), difficulty may arise at low frequencies owing to excessive amplitude.

#### 14. Sound power required in theatres

Picture theatres are usually designed to have suitable acoustical properties, and damping material is added where it is required, so that the sound power is properly distributed throughout the audience. From measurements on a large number of theatres of different sizes, it is possible to establish data from which the maximum sound power to be delivered by the speakers can be calculated. A curve of this nature is plotted in Fig. 162 [7]. Over a large range it is substantially linear. Since the power is greatest at low frequencies, this curve can be interpreted to mean that for a theatre of  $4 \times 10^5$  cubic feet with a seating capacity of 2,000 persons, the speakers must be capable of delivering just over 2 watts at, say, 80  $\sim$ .<sup>\*</sup> If the efficiency of the speakers is 25 per cent., the undistorted output of the amplifier must be at least 8 watts. Speakers of types (1) and (2) can take an input of about 6 watts, so that two would be required. Suitable orientation would give a good distribution characteristic.

In the flat baffle type the resistive loading is small, a large amplitude being required to radiate 2 watts. From Table 33, for a diaphragm 10 cm. radius, the amplitude at 80  $\sim$  is found to be 0.7 cm., which approximates to the axial length of the air-gap. An amplitude of this magnitude would introduce distortion due to two causes, (a) inadequate stretch of the annular surround and centring device, (b) variation in the value of the force factor, due to the coil moving out of the gap into the weaker leakage field (Chap. XIV). If the axial amplitude is limited to 0.15 cm., the power radiated at 80  $\sim$  from a diaphragm 12.5 cm. radius cannot exceed 0.23 watt. For the above theatre nine speakers would be required. It ought to be noted that this result is independent of efficiency. If the speakers are designed to cope with greater amplitudes, say 0.2 cm., the requisite number

\* In some cases the power is taken as 2 watts per 1,000 persons.

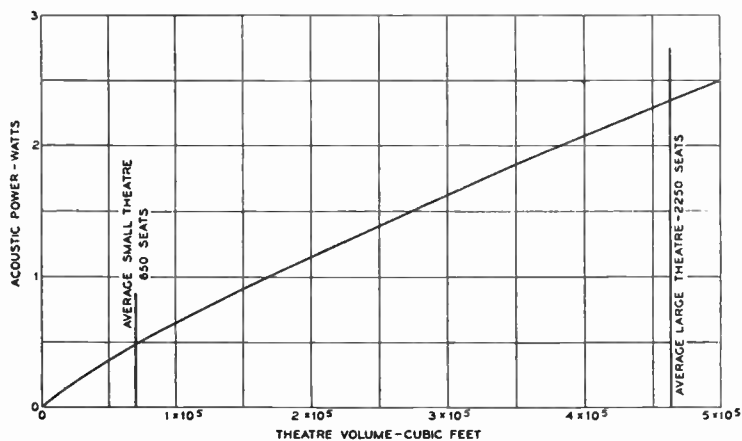


FIG. 162. Acoustic power required in theatres of various sizes.

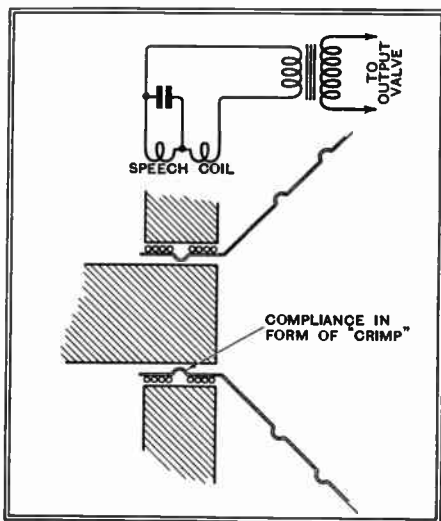


FIG. 162 A. Diagrams illustrating wide range type of hornless moving-coil speaker. The coil is split, and the two portions joined together by a compliant link.

is reduced to five. Assuming the efficiency to be 6 per cent., the maximum input to each speaker, for a radiation of 0.23 watt, is

nearly 4 watts, and this is permissible. For an amplitude of 0.2 cm. the input is about 7 watts, which can be handled in a good design. The amplifier must be capable of delivering an undistorted output 34 watts, which is over four times that for types (1) and (2). On a cost basis it is necessary to contrast two speakers of types (1) or (2) and an amplifier to deliver 8 to 10 watts, with seven speakers of type (3) plus an amplifier to deliver 34 watts. Obviously the first proposition is the more economical of the two.

If the low-frequency limit were raised to  $100 \sim$  the number of speakers of type (3) could not be decreased, whilst lowering the limit to  $60 \sim$  would entail a larger number to deliver the maximum power at that frequency.

The low-frequency power can be obtained with smaller amplitudes if the size of the diaphragm is augmented. This reduces the number of speakers to give low-frequency power, but additional units are required for the upper frequencies. So far as type (1) is concerned, if large low-frequency power is to be radiated, several driving units can be coupled to a large horn, the external connexions being such that all units move in phase. To preserve an adequate response down to  $50 \sim$  necessitates a very large horn, and preferably a special low-frequency driving unit. This is not only costly but the horn occupies a large space. In general the choice of speaker lies between the horn and the directional baffle types. On the whole there is little in it. The flat baffle speaker is too inefficient for this class of work. It is useful, however, where a restricted range of very low frequencies is required, e.g.  $40$  to  $300 \sim$ , since large diaphragms can be used. The range above  $300 \sim$  can be supplied by one or more horn units.

In common with other branches of applied science the design and installation of apparatus for sound reproduction is decided not only on technical points, but by experience and general economical considerations. These latter can only be learned by direct contact with the real thing.

### 15. Amplitude to radiate 1 watt at various frequencies

The amplitude of a driving mechanism to radiate a definite power depends upon the frequency and the acoustic loading on the diaphragm, i.e. upon the type of speaker.

(a) *Flat baffle type.* The maximum available power from this type of speaker at low frequencies is shown, in Chapter II, to be equal to

that from one side of a rigid disk in an infinite baffle, the other conditions being identical. At high frequencies the radiation is focused, and that from the rear can be excluded. Consequently our computations will be based upon the power from *one* side of a rigid disk in an infinite baffle. Using formula (6), Chap. VIII and putting  $\xi_{\max} = \sqrt{2}\xi_0$ , we obtain

$$P = \frac{1}{2}\rho_0 c A \omega^2 \xi_{\max}^2 G_1, \quad (26)$$

where  $A = \pi a^2$ .

If  $P = 10^7$  ergs per sec. and  $\rho_0 c = 42$ , (26) transposes to

$$\xi_{\max} = \frac{386}{a\omega\sqrt{G_1}}. \quad (27)$$

At low frequencies, when  $ka \leq 0.5$ ,  $G_1 = \frac{1}{2}k^2 a^2$ . Thus  $\xi_{\max} \propto 1/\omega^2$  and the amplitude is very large indeed, as shown in Table 33 for a disk 10 cm. radius.

(b) *Horn type.* The following hypotheses will be used to simplify the calculations: (i) the speaker operates sensibly above the horn cut-off frequency, the pressure and particle velocity being in phase, (ii) the pressure from all parts of the diaphragm reaches the horn throat in the same phase, (iii) the diaphragm moves as a rigid structure. The impedance of the throat is, by (i), wholly resistive, its value being  $\rho_0 c A_0$ , where  $A_0$  is the throat area. The load on the diaphragm is  $\rho_0 c A_0 (A_d/A_0)^2$ , so the power

$$P = \frac{\rho_0 c A_d^2 \omega^2 \xi_{\max}^2}{2A_0}, \quad (28)$$

where  $A_d$  = area of diaphragm. Inserting  $P = 10^7$ ,  $\rho_0 c = 42$  in (28) we obtain

$$\xi_{\max} = \frac{386a_0}{a_d^2 \omega}, \quad (29)$$

where  $a_0$ ,  $a_d$  are the respective radii.

Taking  $a_0 = 0.85$  cm.,  $a_d = 3.0$  cm. a series of values of  $\xi_{\max}$  is given in Table 33, so that they can be compared directly with those for the rigid disk 10 cm. radius in an infinite baffle. To facilitate this the ratio of the amplitudes is given in column 4. At 50 ~ the amplitude of the disk is 15.9 times that of the diaphragm of the horn speaker. Neither of these cases would occur in practice, since  $\xi_0$  exceeds the permissible displacement of the surround. Consequently larger diaphragms or a plurality of units is required. From 1,000 ~ onwards the ratio is constant, which signifies that the mean resistance of the rigid disk matches that of the medium. Thus it is  $\rho_0 c A$ , and



the amplitude in both cases varies inversely as the frequency. Analytically, from (26) and (27) the ratio

$$\frac{\text{disk}}{\text{horn}} \text{ is } \varphi = \frac{\xi_d}{\xi_h} = \frac{a_d^2}{aa_0\sqrt{G_1}}. \quad (30)$$

For given radii  $\varphi$  depends upon

$$\frac{1}{\sqrt{G_1}} = \sqrt{\frac{1}{1 - \{J_1(2ka)/ka\}}}.$$

At frequencies where  $ka > 1.9$ ,  $G_1$  is substantially unity (Chap. VIII), so (30) reduces to  $\xi_d/\xi_h = a_d^2/aa_0$ . If the diaphragm and throat radii are identical  $a_d = a_0$ , and the above becomes  $a_0/a$ . Thus the influence of reduction in throat area is to lower the amplitude for the horn in the ratio  $a_d^2/a_0^2$ , i.e. the square of the transformation ratio, as might be expected. When  $a = a_0 = a_d$  the amplitude is identical in both cases.

The diaphragm amplitude in a directional baffle type of speaker is computed in the same manner as that for the horn. In either case, if operation occurs near the cut-off frequency, the requisite amplitude, for an output of 1 watt, exceeds that obtained from the preceding formulae.

TABLE 33

*Showing amplitude of rigid disk ( $a = 10$  cm.) and diaphragm ( $a_d = 3$  cm.) of horn speaker to radiate 1 watt at various frequencies from one side.*

Frequency ~	Diaphragm Amplitude (cm.)		Ratio $\xi_d/\xi_h$
	Horn $\xi_h$	Disk $\xi_d$	
30	$10^{-1} \times 1.9$	5.06	26.6
50	$10^{-1} \times 1.16$	1.84	15.9
100	$10^{-2} \times 5.8$	$4.56 \times 10^{-1}$	7.86
200	$10^{-2} \times 2.9$	$1.15 \times 10^{-1}$	3.96
500	$10^{-2} \times 1.16$	$1.97 \times 10^{-2}$	1.7
800	$10^{-2} \times 7.25$	$10^{-2}$	1.38
1,000	$10^{-2} \times 5.8$	$6.14 \times 10^{-3}$	1.06
2,000	$10^{-2} \times 2.9$	$3.07 \times 10^{-3}$	1.06
4,000	$10^{-2} \times 1.45$	$1.54 \times 10^{-3}$	1.06
8,000	$10^{-2} \times 7.25$	$7.7 \times 10^{-4}$	1.06

## 16. Reproduction of frequencies above 5,000 ~

The range of important audible frequencies lies within the limits 40 to 15,000 ~. No single speaker has yet been designed to cover this range. As a general rule the output from the average hornless speaker decays rapidly above 4,000 ~. By modifying the construction and

introducing the basic principle of the mechanical filter, the range in a single speaker may be extended up to 10,000  $\sim$ . A design embodying this principle is shown diagrammatically in Fig. 162 A [90 b]. The coil is divided into two portions separated by a compliance in the form of a circular corrugation. The diaphragm is also broken up into sections separated by compliances of like nature. The electrical analogue of the mechanical system comprises inductances in series and condensers in shunt, as in a low-pass filter (Fig. 155). The electrical impedance of the complete coil is maintained fairly uniform by connecting a condenser across one-half of it to by-pass the current above 1,000  $\sim$ . The compliant link in the coil is such that beyond this frequency there is little motion of the shunted half. Thus the effective mass of the coil is reduced at higher frequencies and the sound output is maintained substantially constant\* over a much wider frequency range than in speakers of ordinary design.

With horn speakers large low-frequency output can only be obtained by having relatively large diaphragms and throat-chamber clearances, which reduce the high-frequency output. To cover a wide frequency range more than one speaker can be used. In a certain public-address system two horn-type speakers and two or more hornless speakers with a large baffle are used to cover the range 40 to 10,000  $\sim$  or more [18 a]. The latter speakers reproduce frequencies from 40 to 300  $\sim$ , the first horn speaker (12-ft. horn) reproduces the range 300 to 3,000  $\sim$ , and the second horn speaker, described below, extends the range to 10,000  $\sim$  or even higher, according to requirements. The speakers are connected to the power valves by a filter arrangement whereby each unit is supplied with current corresponding to its own range only. The input is such that equality of output from the hornless and first horn speakers occurs at 300  $\sim$ , and for the two horn speakers at 3,000  $\sim$ . A combination of this type is used for noiseless wide frequency range films and for hill and dale gramophone records. In the latter a power range approaching that of a full orchestra (60 to 70 db.) can be obtained, whilst the playing-time of a record 12 in. diameter is fifteen minutes.

In designing a speaker to cover the audible range above 3,000  $\sim$ , use is made of Fig. 151 B, whereby the diaphragm mass, its natural frequency on the annular surround, and also the throat chamber stiffness can be settled. The diaphragm area must be kept within

\* See Chap. XVIII, § 11, for influence of coil mass.

bounds to avoid interference within the air chamber, due to the wave-length being comparable with the diameter. The fundamental frequency of the diaphragm on the surround must exceed 4,000  $\sim$ , whilst that of the mass and the stiffness due to the air chamber and surround combined should fall below the upper frequency limit.

A sectional diagram, showing the construction of a speaker [6] designed on these lines, is given in Fig. 163. The diaphragm, of duralumin  $5 \times 10^{-3}$  cm. thick, is a hollow spherical cap 1.25 cm. radius whose curvature provides the requisite rigidity. The self-supporting coil is of aluminium ribbon (see Fig. 82) wound edgewise, being

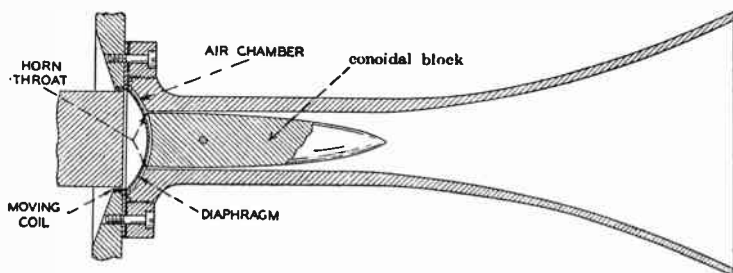


FIG. 163. Sectional diagram showing the diaphragm, air chamber, and horn construction of speaker for reproducing frequencies above 3,000  $\sim$ . In the design data given in the text it is assumed that the influence of the air chamber between the diaphragm and the centre pole can be neglected. When this is not so, an additional condenser  $C_3$  shunted by a resistance  $R_3$  must be included between  $E$  and  $L_1$  (see  $C_1 R_1$  in Fig. 158, also § 12).

attached to the diaphragm at the annular surround. The total mass of the diaphragm structure is only 0.16 gm., which, with the surround stiffness of  $2.8 \times 10^8$  dynes cm.<sup>-1</sup>, yields a natural frequency of 6,600  $\sim$  (equivalent to resonance of  $L_1$  and  $C_1$  of Fig. 151 B). The separation between the air-chamber and the diaphragm is  $2.5 \times 10^{-2}$  cm. entailing a stiffness of  $3.5 \times 10^8$  dynes cm.<sup>-1</sup> This separation is sufficient to permit an adequate amplitude at the lowest frequency to be reproduced. If the power and the radiation resistance are constant, so also is the diaphragm velocity. Thus  $\xi_{\max} = K/\omega$ , so the amplitude varies inversely with the frequency. Referring to Fig. 151 B, if  $R$  is very large the resonance frequency of the diaphragm with the surround and air-chamber stiffness ( $L$  with  $C_1 + C_2$  in series) is

$$\frac{\omega}{2\pi} = \frac{1}{2\pi} \sqrt{\left( \frac{(2.8 + 3.5)10^8}{0.16} \right)} = 10^4 \sim.$$

The horn throat is annular, its area being 0.19 cm.<sup>2</sup> Its diameter just exceeds half that of the diaphragm, so the air pressure from the remotest parts of the chamber reaches the throat in the same phase. The wave-length at  $10^4 \sim$  is 3.4 cm., and since the greatest distance from any point on the diaphragm (2.5 cm. diameter) is only about 0.6 cm., i.e. nearly three half-wave-lengths, interference is not serious.

An exponential horn about 12 cm. long, having a flaring index  $\beta$  (Chap. X) to give a 2,000  $\sim$  cut-off, is used. The resistive termina-

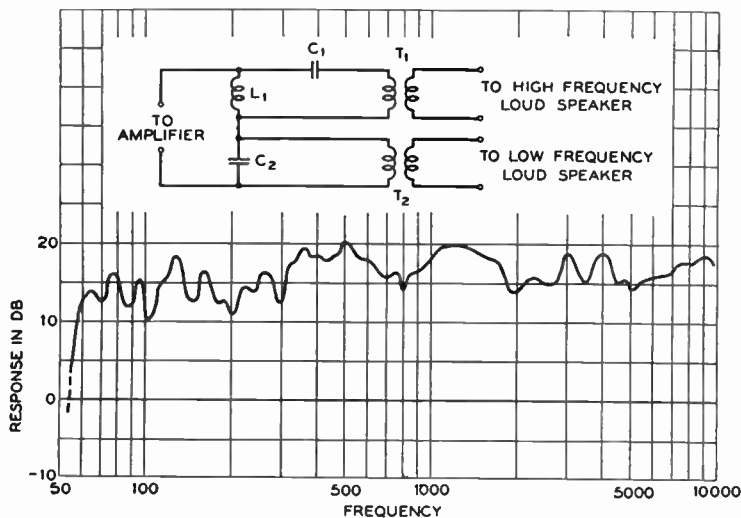


FIG. 164. Combined response-frequency curve of two speakers; (a) speaker with 60 cycle cut-off exponential horn, (b) high frequency horn speaker, in circuit shown.

tion  $\rho_0 c \frac{A_d^2}{A_0} = \frac{42 \times 4.91^2}{0.19} = 5,300$  mechanical ohms. Within the horn

there is a conoidal block designed to give the requisite gradation in area according to the law  $A = A_0 e^{\beta x}$  (Chap. X). As explained above, the opening is annular instead of being circular, thereby avoiding interference. To extend the range beyond  $10^4 \sim$ , more than one annular gap could be used with a type of block to correspond. The magnetic field strength is 18,000 lines cm.<sup>-2</sup>, thereby providing high damping.

A complete response curve of high- and low-frequency loud-speaker units is shown in Fig. 164. The low-frequency unit was used with

a 60  $\sim$  cut-off horn, the high-frequency speaker being suspended in the horn opening. The electrical coupling network was such that frequency ranges of 60 to 3,000  $\sim$  and 3,000  $\sim$  upwards were covered by the two units, respectively. By restricting the frequencies to their respective speakers, the power is used most economically, whilst the large low-frequency currents which would cause damage to the high-frequency unit, owing to excessive amplitude, are relegated to their proper channel. The arrangement of Fig. 164 is such that  $L_1$  bypasses the low frequencies, whilst  $C_1$  obstructs them;  $C_2$  bypasses the high frequencies. The arrangement permits two transformers to be used. Thus  $T_2$  can have a primary inductance adequate for low frequencies, whilst for  $T_1$  it can be reduced considerably. This is of importance, since the leakage inductance is also reduced, and the high-frequency reactance does not curb the high-frequency currents appreciably.

The interpretational qualities in speech and music reside in the upper frequencies [211], and it is not possible to obtain naturalness unless the range extends to  $1.2 \times 10^4 \sim$ . This applies particularly to severe transients such as hand-clapping, footsteps, jingling of coins or keys, rustling of paper, etc. There is no difficulty in calculating the natural frequency of a coin, assumed to be a homogeneous free-edge circular disk. For example, the fundamental mode of a half-penny (2.54 cm. diameter) is about 12,000  $\sim$ . Consequently it is quite easy to understand why the higher frequencies are indispensable if coin-jingling is to be reproduced. The overtones of orchestral instruments of various kinds extend well up to  $10^4 \sim$ . Even the flute, usually cited as an emblem of acoustical purity, requires quite an extensive range. One of the reasons why the reproduced version of the human voice sounds unnatural from the average loud speaker is due to the absence of frequencies above 5,000  $\sim$ . To any musician with a faculty for discrimination, a musical range which does not extend beyond 4,000 to 5,000  $\sim$  is definitely lacking in brilliance and naturalness. Absence of the upper register is aggravated to an extent by accentuation of the lower register by speaker resonances, and, in the average room, by low absorption. When the upper register is inserted, it must be carefully adjusted in loudness to match the lower register. The tolerance is not very great and it is easy to cause harshness.

Since the horn aperture in the high-frequency unit is quite small

(about 2.5 cm. radius), the radiation is distributed more uniformly than that from a single speaker with a large opening [125 b]. This is a great advantage, because it avoids concentration of the sound field and enables the number of speakers required for a definite area to be reduced. On the basis of a rigid disk the focusing would only be appreciable above 8,000  $\sim$ , and this entails quite a wide beam angle over a fair frequency range.

In a recent development of the high-frequency horn speaker four Rochelle crystal units are used as a diaphragm. These units are constructed as described in Chap. XIX, § 1, the four free corners being at the centre of the diaphragm. The response characteristic rises rapidly above 1,200  $\sim$ . By including a choke in the primary circuit of the output transformer the current and, therefore, the voltage across the secondary terminals can be reduced with rise in frequency. The crystal is connected across the secondary winding and the applied voltage is such that the output from 2,000 or 3,000  $\sim$  upwards is fairly uniform. The upper frequency cut-off point depends upon the design [164 c].

The nearer the reproducer reaches perfection, the more it reveals imperfections in the input.\* Since gramophone reproduction is all scratch noise above 5,000  $\sim$ , the use of an auxiliary speaker would be injurious and obviously impossible. In broadcast programmes, induction, valve, and other noises, which are imperceptible in a system inadequate to reproduce above 4,500  $\sim$ , would assume undue proportions if the range were extended to 12,000  $\sim$ . Consequently, to realize the full benefits obtainable by extending the upper register, the noise-level of the input in the studio and in the transmitting and receiving apparatus—not to mention the ether—must be very low indeed. In other words, a radical improvement of this nature at the receiver must be accompanied by a reduction in noise-level in the remainder of the system. Such an arrangement would clearly be of use only in local station work. But the listener need not be perturbed. So long as an insatiable appetite—not entirely of his own creation—exists for turning knobs to bring in a plethora of foreign stations, accompanied by the mutterings and mumblings of an overwrought ether, the designer has no choice but to cut off everything above 5,000  $\sim$ .

\* This paragraph was applicable when the manuscript was prepared in 1933.

## APPENDIX

### 1. Young's modulus ( $q$ ) and the velocity of sound in paper $\sqrt{(q/\rho)}$

Any formula for vibrational frequencies includes  $\sqrt{(q/\rho)}$ , the velocity of longitudinal (sound) waves in a uniform bar of material. It is

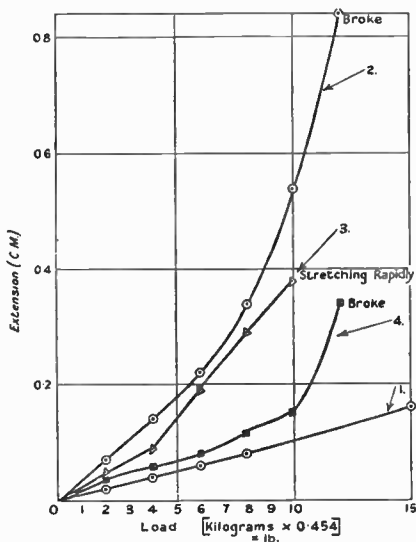


FIG. 165. Load-extension curves for paper strips, width 2.54 cm., length 50 cm., thickness (1) =  $4 \times 10^{-2}$  cm., (2) =  $1.5 \times 10^{-2}$  cm., (3) =  $2.1 \times 10^{-2}$  cm., (4) =  $2.3 \times 10^{-2}$  cm.

usually found in company with  $1/\sqrt{(1-\sigma^2)}$ , where  $\sigma$  is Poisson's ratio expressed  $<1$ . As shown in Chap. XVIII, § 16,  $1/\sqrt{(1-\sigma^2)}$  is frequently assumed to be unity. Under this condition we are left with  $\sqrt{(q/\rho)}$ , which is sufficiently accurate for our requirements. This ratio can be measured in several ways, two of which will now be discussed: (1)  $q$  can be found as in stress-strain tests by observing the extension corresponding to given loads [184], the density being obtained from mass-volume measurements, (2)  $\sqrt{(q/\rho)}$  can be measured directly by a vibrational method, using a rectangular strip of paper [191].

The curves of Fig. 165 show load-extension readings for various grades of paper [184]. These were selected from a large number of

test data. In certain instances the load-extension relationship was linear, within prescribed limits. Curve 1 illustrates a typical case where linearity occurs. By testing more than one sample of paper  $q$  was found to vary. The load-extension curve was not always linear, whilst in certain cases the paper stretched abnormally, as shown in curve 2. On the other hand a different batch of paper sheets showed uniformity and gave linear characteristics. The tests are summarized in Table 34.

TABLE 34

*Showing  $q$  and  $\sqrt{(q/\rho)}$  for paper*

<i>Type of paper</i>	<i>Thickness (cm.)</i>	<i>Mass per unit area (gm. cm.<sup>-2</sup>)</i>	<i>Density <math>\rho</math> (gm. cm.<sup>-3</sup>)</i>	<i><math>q</math> (dynes cm.<sup>-2</sup>)</i>	<i><math>\sqrt{(q/\rho)}</math> (cm. sec.<sup>-1</sup>)</i>
A	$1.5 \times 10^{-3}$	$1.0 \times 10^{-2}$	$6.7 \times 10^{-1}$	$2.0 \times 10^{10}$	$1.73 \times 10^5$
B	$2.1 \times 10^{-3}$	$1.4 \times 10^{-2}$	$6.6 \times 10^{-1}$	$1.9 \times 10^{10}$	$1.7 \times 10^5$
C	$4.0 \times 10^{-3}$	$2.5 \times 10^{-2}$	$6.0 \times 10^{-1}$	$1.9 \times 10^{10}$	$1.78 \times 10^5$
D	$2.3 \times 10^{-3}$	$1.8 \times 10^{-2}$	$7.8 \times 10^{-1}$	$4.6 \times 10^{10}$	$2.4 \times 10^5$

The test specimen did not always return to its original length after removal of the load. Accurate observation, however, reveals that this phenomenon occurs, to an extent, even in the best steel; in fact there is no material which is truly elastic. It is only to be expected that paper will be inferior to steel in this respect. Owing to variation in  $q$  and in  $\rho$ , a paper cone will not behave as an isotropic homogeneous shell, so that irregularities in its nodal figures are to be expected. Constancy of  $\sqrt{(q/\rho)}$  is not an acid test of homogeneity, since both  $q$  and  $\rho$  may vary in equal proportion in the same direction. If a faulty piece of paper were used in a speaker delivering large output, there would be alien frequencies owing to curvature of the stress-strain characteristic.

When paper is baked in an oven for several hours at, say,  $110^\circ\text{C}$ ., the value of  $q$  is elevated appreciably [96 b]. For example, the normal  $q$  for one grade of paper is  $1.9 \times 10^{10}$  dynes cm.<sup>-2</sup>, whilst after baking it rose to  $3.4 \times 10^{10}$  dynes cm.<sup>-2</sup>. As a corollary it is seen that  $q$  varies with the sample and the humidity or moisture content. Consequently the data given herein must only be regarded as average values indicative of the order of magnitude to be expected. In making accurate calculations pertaining to a definite class of paper, it is preferable to measure  $\sqrt{(q/\rho)}$  at the time of the experiment rather than extract it from physical tables.



In the vibrational method [191] a rectangular strip of paper is securely clamped to the free end of an electromagnetically-operated vibrating reed. The resonance frequency of the paper strip is obtained by varying the frequency of the supply current driving the reed until maximum amplitude occurs. Then  $\sqrt{(q/\rho)} = 0.98l^2\omega/t$ . The results obtained in this way are in close agreement with those found by direct static measurement. Although in loud-speaker apparatus high accuracy in the measurement of  $\sqrt{(q/\rho)}$  is immaterial, it is interesting to compare the two methods. Owing to variation in thickness and to surface irregularities it is not possible to get the true value of  $t$ . An error of 5 per cent. in the value of  $t$  entails the same error in  $\sqrt{(q/\rho)}$  by the vibrational method.

Statically we have

$$\sqrt{\frac{q}{\rho}} = \sqrt{\frac{\text{stress}}{\rho \text{ strain}}} = \sqrt{\left(\frac{fl}{btx} \frac{t}{\rho_1}\right)} = \sqrt{\frac{fl}{\rho_1 bx}},$$

where  $b$  is the breadth of the paper,  $l$  the length,  $\rho_1$  the mass per unit area, and  $x$  the extension. If the mass of the whole test-piece is measured, the mean  $\rho_1$  is found, so that the accuracy depends chiefly on the measurement of extension, which presents no serious difficulties. It appears, therefore, that the only variant in the static case is  $1/\sqrt{\rho_1}$ , so that on the whole one method is about as accurate as the other.

In Chap. XVIII, § 6, it is shown that during vibration conical shells used in speaker construction are subjected to both bending and extensional stresses. The latter is a hoop or circumferential type. Thus a mean value of  $\sqrt{(q/\rho)}$  found by the two methods outlined above may possibly be nearer the mark than either alone.\* In a vibrational method the stress varies from zero at the neutral axis to a maximum at the upper and lower surfaces, being positive on one side of the axis and negative on the other. In the extensional method it is wholly positive. Any departure from the elastic state is revealed by the latter method, but not by the former, where it is completely camouflaged. Hence, for safety, the extensional method is to be preferred.

## 2. Radial velocity of propagation in conical diaphragm

In a conical shell the energy is propagated from the vertex, not only as a result of bending, but of circumferential distension and contrac-

\* It is shown in Chap. XVIII, § 16, that  $\sqrt{(q/\rho)}$  is not the criterion by which the suitability of a material for vibrational purposes is to be judged.

tion. This compound effect is different from purely longitudinal waves in a uniform bar of the material, the velocity being greater in the latter instance. As in a disk the velocity is greater in the neighbourhood of the most rigid portion, i.e. the vertex. To obtain data relating to the velocity in a paper cone, measurements were made during the course of some experiments on dust figures. The apical angle of the cone ( $148^\circ$ ) and the surface roughness were adequate to prevent the lycopodium powder sliding off the nodal lines. A series of rings was formed lying between a circle 10 cm. radius and the periphery 22 cm. radius. The distance between the rings represents half a wave-length. It was not quite constant, but a mean value has been taken. The data so obtained are set forth in Table 35.

TABLE 35

*Showing radial velocity in conical diaphragm [96 a, 183]  
 $5 \times 10^{-2}$  cm. thick*

<i>Frequency</i> ~	<i>Wave-length</i> $\lambda$ (cm.)	<i>Radial velocity</i> $v_r = \lambda f$ (cm. sec. <sup>-1</sup> )
1,600*	4.4	$7.0 \times 10^3$
2,000	3.8	$7.6 \times 10^3$
2,900	3.0	$8.7 \times 10^3$

Near the apex the velocity exceeds the values in the table. The radial velocity in the outer part of the diaphragm is roughly  $\frac{1}{2}$  that of sound in air and about  $\frac{1}{25}$  that of sound in a straight bar of the material. It increases with rise in frequency approximately in accordance with the relationship  $v_r \propto \omega^{\frac{1}{2}}$ , which also holds near the outer edge of a homogeneous circular disk [38, 96 a]. This increase is reminiscent of a telephone cable where the higher frequencies travel more quickly, but are more highly attenuated than the lower frequencies.

Since sound travels more rapidly through the air than it does in the cone, radiation from the vertex at 1,600 ~ reaches a distant point on the axis about 5 cycles sooner than that from the periphery. This, of course, only concerns the transient state, since phase is immaterial for steady motion.

By aid of data in Chap. XVIII, Fig. 132 A, the velocity of propagation in a glass cone can be computed. Taking the case of two nodal

\* Accompanied at this frequency by radial nodes.

circles  $v_r = 5.7 \times 10^4$  cm. sec.<sup>-1</sup> at 5,700 ~ which exceeds the velocity of sound in air. It is, however, only  $\frac{1}{5}$  that of longitudinal waves in a glass rod. In the above case the vibrational frequency was reduced somewhat due to the mass of the coil. Otherwise  $v_r$  would have been greater than  $5.7 \times 10^4$  cm. sec.<sup>-1</sup>, but at a higher frequency.

## 3.

TABLE 36 [96 b]

Showing static inductance  $L_0$ , static resistance  $R_0$ , and effective permeability  $\mu_e$  with 40-turn and 1,000-turn coils in magnet FIG. 87.

Air-gap = 0.32 cm.; coil temp. = 20° C.; inductance of 40-turn coil in air =  $1.32 \times 10^{-4}$  henry; 1,000-turn coil =  $8.3 \times 10^{-2}$  henry; D.C. resistance of 40-turn coil = 0.95 ohm (no leads); 1,000-turn coil = 1,257 ohms.

Mean radius of coil = 2.5 cm.

Axial length of coil = 0.95 cm.

Frequency (cycles per second)	$L_0$ Inductance of coil with field winding short- circuited (henry)		$R_0$ Resistance (ohms)	Added resistance due to iron (ohms)	$\mu_e$ Effective permeability of electromagnet	
	40 turns	1,000 turns			40 turns	1,000 turns
	50	$3.22 \times 10^{-4}$	$2.21 \times 10^{-1}$	1,388	131	2.44
100	$3.0 \times 10^{-4}$	$2.1 \times 10^{-1}$	1,395	138	2.28	2.53
150	$2.86 \times 10^{-4}$	$1.98 \times 10^{-1}$	1,403	146	2.16	2.38
200	$2.78 \times 10^{-4}$	$1.91 \times 10^{-1}$	1,412	155	2.1	2.3
500	$2.48 \times 10^{-4}$	$1.65 \times 10^{-1}$	1,460	203	1.88	1.99
1,000	$2.22 \times 10^{-4}$	$1.49 \times 10^{-1}$	1,570	313	1.68	1.8
2,000	$2.06 \times 10^{-4}$	$1.34 \times 10^{-1}$	1,800	543	1.56	1.61
3,000	$1.94 \times 10^{-4}$	$1.25 \times 10^{-1}$	2,200	943	1.47	1.51
4,000	$1.8 \times 10^{-4}$	$1.19 \times 10^{-1}$	2,750	1,493	1.36	1.43
5,000	$1.7 \times 10^{-4}$	$1.12 \times 10^{-1}$	3,500	2,243	1.29	1.35

The inductances of the coils out of the magnet are almost exactly proportional to the squares of the number of turns. Since the magnetizing force on the iron is greater with 1,000 than with 40 turns, the inductance per turn of the former exceeds that of the latter. The air-core ratio is 628 : 1—it should be 625 : 1 for the inductance to vary absolutely as  $n^2$ —whilst in the magnet it varies from 687 : 1 at 50 cycles to 659 : 1 at 5,000 cycles. The variation in effective permeability is obviously identical. The ratio of the resistances due to iron loss, however, is greater than that for the inductances, since the former depends upon  $B_1^2$ ,  $x > 1$ , whilst the latter depends upon  $B_1$ , the flux in the pole piece due to A.C. in the coil.

The results in Table 36 were obtained when the flux density in the pole tips was very low. When  $B$  is  $10^4$  lines cm.<sup>-2</sup>, the coil being

cemented to the centre pole, there is an alteration of 1 per cent. in  $R_0$ . If the poles were saturated the change in  $R_0$  might be greater than this.

4.

TABLE 37

<i>Frequency</i> ~	<i>Pulsatance</i> $\omega$	$k = \omega/c$
50	314.2	$9.26 \times 10^{-3}$
100	628.4	$1.85 \times 10^{-2}$
200	1,257	$3.7 \times 10^{-2}$
300	1,885	$5.55 \times 10^{-2}$
400	2,514	$7.4 \times 10^{-2}$
500	3,142	$9.26 \times 10^{-2}$
600	3,770	$1.11 \times 10^{-1}$
700	4,399	$1.3 \times 10^{-1}$
800	5,028	$1.48 \times 10^{-1}$
900	5,655	$1.67 \times 10^{-1}$
1,000	6,284	$1.85 \times 10^{-1}$

$$c = 3.43 \times 10^4 \text{ cm. sec.}^{-1}$$

## REFERENCES

### ABBREVIATIONS

1. *A.E.G.M.* *A. E. G. Mitteilungen.*
2. *A.P.* *Annalen der Physik.*
3. *B.T.J.* *Bell System Technical Journal.*
4. *C.J.R.* *Canadian Journal of Research.*
5. *E.N.T.* *Elektrische Nachrichten-Technik.*
6. *E.T.Z.* *Elektrotechnische Zeitschrift.*
7. *E.u.M.* *Elektrotechnik u. Maschinenbau.*
8. *G.E.R.A.* *General Electric Review, America.*
9. *J.A.I.E.E.* *Journal American Institute Electrical Engineers.*
10. *J.A.S.A.* *Journal Acoustical Society, America.*
11. *J.F.I.* *Journal Franklin Institute, America.*
12. *J.I.E.E.* *Journal Institution Electrical Engineers, London.*
13. *J.I.E.E.J.* *Journal Institution Electrical Engineers, Japan.*
14. *J.S.I.* *Journal Scientific Instruments, London.*
15. *J.S.M.P.E.* *Journal Society Motion Picture Engineers, America.*
16. *P.I.R.E.* *Proceedings Institute Radio Engineers, America.*
17. *P.M.* *Philosophical Magazine, London.*
18. *P.R.* *Physical Review, America.*
19. *P.P.S.L.* *Proceedings Physical Society, London.*
20. *P.R.S.L.* *Proceedings Royal Society, London.*
21. *P.Z.* *Physikalische Zeitschrift.*
22. *S.Z.* *Siemens Zeitschrift.*
23. *W.E.* *Wireless Engineer and Experimental Wireless, London.*
24. *W.V.S.K.* *Wissenschaftliche Veröffentlichungen aus dem Siemens-Konzern.*
25. *W.W.R.R.* *Wireless World and Radio Review, London.*
26. *Z.f.H.* *Zeitschrift für Hochfrequenztechnik.*
27. *Z.T.P.* *Zeitschrift für technische Physik.*

### (A) SCIENTIFIC PAPERS

#### *Accession to Inertia*

1. Lamb, H. *P.R.S.L.* A. 98, 205, 1920.
2. McLachlan, N. W. and Sowter, G. A. V. *P.M.* (a) 11, 1, 1931; (b) 11, 1137, 1931; (c) 12, 771, 1931.
3. McLachlan, N. W. (a) *J.I.E.E.* 69, 612, 1931; (b) *P.M.* 14, 1012, 1932; (c) *P.M.* 15, 443, 1933.
4. — (a) *P.P.S.L.* 44, 546, 1932; (b) *J.A.S.A.* 5, 167, 1933.
5. Strutt, M. J. O. *W.E.* 9, 143, 1932.

#### *Cinema and Public Address Speakers*

6. Bostwick, L. G. *J.A.S.A.* 2, 242, 1930.
7. — and Blattner, D. G. *J.S.M.P.E.* 14, 161, 1930.
8. Graf, H. *Z.T.P.* 10, 334, 1929.
9. Hanna, C. R. *J.A.I.E.E.* 47, 607, 1928.
10. Kellogg, E. W. *J.A.S.A.* 3, 94, 1931.

11. Malter, L. *J.S.M.P.E.* 14, 611, 1930.
12. Neumann, H. *Z.T.P.* 11, 548, 1929.
13. — (a) *W.V.S.K.* 9, 226, 1930; (b) *S.Z.* 10, 562, 1930.
14. — and Trendelenberg, F. *Z.f.H.* 37, 149, 1931.
15. Olson, H. F. *J.A.S.A.* 2, 485, 1931.
16. Trendelenberg, F. *S.Z.* 7, 141, 1927.
17. — *E.T.Z.* 48, 1685, 1927.
18. Wentz, E. C. and Thuras, A. L. *B.T.J.* 7, 140, 1928.
- 18a. Watkins, S. S. A. Data given to author regarding new Western Electric Co. installations.
19. Wigge, H. *A.E.G.M.* H. 1, 34, 1931.
20. — *S.Z.* 11, 163, 1931.
21. Zwicker, C. *E.u.M.* 48, 936, 1930.

*Condenser or Electrostatic Speakers*

22. Edelman, P. E. *P.I.R.E.* 19, 256, 1931.
23. Greaves, V. F., Kranz, F. W. and Crozier, W. D. *P.I.R.E.* 17, 1142, 1929.
24. Green, G. *P.M.* 2, 497, 1926.
25. — *P.M.* 7, 115, 1929.
26. Hähnle, W. *W.V.S.K.* 11, 1, 1932.
27. Hanna, C. R. *J.A.S.A.* 2, 150, 1931.
28. Kyle, C. U.S. Patent, 1,644,387.
29. — U.S. Patent, 1,746,540.
30. McLachlan, N. W. (a) British Pat. 206,601 (1922); (b) *J.A.S.A.* 5, 167, 1933.
31. Vogt, H. *E.T.Z.* 52, 1402, 1931.
32. — *Z.T.P.* 12, 632, 1931.
33. — Technical data sent to author, 31/12/1932.

*Effective Mass*

34. McLachlan, N. W. and Sowter, G. A. V. *P.M.* (a) 11, 1, 1931; (b) 12, 771, 1931.
35. McLachlan, N. W. (a) *W.W.R.R.* 29, 166, 1931; (b) *P.P.S.L.* 44, 88, 1932.
36. Strutt, M. J. O. *W.E.* 9, 143, 1932.
37. — *A.P.* 10, 244, 1931.
38. Warren, A. G. *P.M.* 9, 881, 1930.

*Efficiency*

39. Bostwick, L. G. *J.A.S.A.* 2, 242, 1930.
40. — and Blattner, D. G. *J.S.M.P.E.* 14, 161, 1930.
41. Cook, E. D. *G.E.R.A.* 33, 505, 1930.
42. Graf, H. *Z.T.P.* 10, 334, 1929.
43. Hanna, C. R. *J.A.I.E.E.* 47, 607, 1928.
44. McLachlan, N. W. and Sowter, G. A. V. *P.M.* 12, 771, 1931.
45. Malter, L. *J.S.M.P.E.* 14, 611, 1930.
46. Neumann, H. *Z.T.P.* 11, 548, 1929.
47. — *W.V.S.K.* 9, 226, 1930.
48. Oliver, D.A. *W.E.* 7, 653, 1930.
49. Olson, H. F. *J.A.S.A.* 2, 485, 1931.
50. Wentz, E. C. and Thuras, A. L. *B.T.J.* 7, 140, 1928.

*Finite Pressure Amplitude of Sound*

51. Earnshaw, S. *Phil. Trans. Roy. Soc.* **150**, 133, 1860.
52. Fay, R. D. *J.A.S.A.* **3**, 222, 1931.
53. Payman, W., Robinson, H., and Shepherd, W. C. F. Safety of Mines Research Board Nos. 18, 19, 1926.
54. Rayleigh, Lord. *P.R.S.L. A.* **84**, 247, 1910.
55. Taylor, G. I. *P.R.S.L. A.* **84**, 371, 1910.

*Horns*

56. Ballantine, S. *J.F.I.* **203**, 85, 1927.
- 56a. Goldsmith, A. N. and Minton, J. P. *P.I.R.E.* **12**, 423, 1924.
57. Hall, W. M. *J.A.S.A.* **3**, 552, 1932.
58. Hanna, C. R. and Slepian, J. *J.A.I.E.E.* **43**, 250, 1924.
59. Hoersch, V. A. *P.R.* **25**, 218, 1925.
60. — *P.R.* **25**, 225, 1925.
61. Kellogg, E. W. *G.E.R.A.* **27**, 556, 1924.
62. Maxfield, J. P. and Harrison, H. C. *J.A.I.E.E.* **45**, 243, 1926.
63. Stenzel, H. *A.E.G.M. H.* **5**, 310, 1931.
64. — *Z.T.P.* **12**, 621, 1931.
65. Stewart, G. W. *P.R.* **16**, 313, 1920.
66. — *P.R.* **25**, 230, 1925.
67. Webster, A. G. *Proc. Nat. Acad. Sc. Washington*, **5**, 275, 1919.
68. Williams, S. *J.F.I.* **202**, 413, 1926.

*Horn Type Moving-Coil Speakers*

69. Bostwick, L. G. *J.A.S.A.* **2**, 242, 1930.
70. — and Blattner, D. G. *J.S.M.P.E.* **14**, 161, 1930.
71. Hanna, C. R. *J.A.I.E.E.* **47**, 607, 1928.
72. — *J.A.S.A.* **2**, 150, 1931.
73. Malter, L. *J.S.M.P.E.* **14**, 611, 1930.
74. Olson, H. F. (a) *J.A.S.A.* **2**, 485, 1931; (b) *J.S.M.P.E.* May 1932.
75. Stenzel, H. *A.E.G.M. H.* **5**, 310, 1931.
76. Wentz, E. C. and Thurax, A. L. *B.T.J.* **7**, 140, 1928.

*Hornless Moving-Coil Speakers (Theory)*

77. Cosens, C. R. *W.E.* **6**, 353, 1929.
78. Hähnle, W. *W.V.S.K.* **10**, 73, 1931.
- 78a. — *W.V.S.K.* **11**, 1, 1932.
79. McLachlan, N. W. (a) *W.W.R.R.* **20**, 372, 1927; (b) *P.M.* **7**, 1011, 1929;
80. — *W.E.* (a) **9**, 151, 1932; (b) **9**, 573, 1932; (c) *P.M.* **10**, 204, 1933; (d) *W.E.* **10**, 375, 1933.
81. Riegger, H. *W.V.S.K.* **3**, 67, 1924.
82. Schweikert, G. *Z.f. Fernm.* **9**, 1, 1928.

*Hornless Moving-Coil Speakers (Practice)*

83. Bedford, A. V. *J.A.S.A.* **2**, 251, 1930.
84. Benecke, H. F. O. *A.E.G.M. H.* **9**, 588, 1929.
85. Fischer, F. A. and Lichte, H. *A.E.G.M. H.* **1**, 25, 1929.
86. Kellogg, E. W. and Rice, C. W. *J.A.I.E.E.* **44**, 982, 1925.
87. Lodge, O. J. British Patent 9712 of 1898.

88. McLachlan, N. W. *W.W.R.R.* (a) 17, 604, 1925; (b) 20, 440, 1927.  
 89. — British Patents, 270,412 and 271,021 (1926).  
 90. — *W.E.* 3, 152, 1926.  
 90a. Midgley, H. British Patents, 332,272; 14509/32; 14395/33.  
 90b. Olson, H. F. *P.I.R.E.* 22, 33, 1934.

*Impedance Measurements*

91. Bligh, N. R. and Clarke, H. M. *W.E.* 5, 491, 1928.  
 92. Clarke, H. M. *W.E.* 6, 380, 1929.  
 93. Cook, E. D. *G.E.R.A.* 33, 505, 1930.  
 94. Kurokawa, K. and Hirota, T. *J.I.E.E.J.* 458, 1049, 1926.  
 95. — *J.I.E.E.J.* 469, 865, 1927.  
 96. McLachlan, N. W. and Sowter, G. A. V. *P.M.* (a) 11, 1, 1931; (b) 12, 771, 1931.  
 97. Nakai, S. *J.I.E.E.J.* 474, 26, 1928.  
 98. Oliver, D. A. *W.W.R.R.* 29, 579, 1931.

*Magnets and Flux Measurements*

99. Jasse, E. *E.u.M.* 50, 617, 1932.  
 100. McLachlan, N. W. *W.W.R.R.* (a) 27, 600, 1930; (b) 28, 492 and 521, 1931.  
 101. — *P.M.* 13, 115, 1932.  
 102. Neumann, H. *Z.T.P.* 11, 548, 1929.  
 103. — *W.V.S.K.* 9, 226, 1930.  
 104. Webb, C. E. *W.E.* 9, 67, 1932.

*Nodal Lines*

105. Benecke, H. F. O. *Z.T.P.* 13, 481, 1932.  
 106. McLachlan, N. W. *W.W.R.R.* (a) 25, 33 and 62, 1929; (b) 28, 479 and 514, 1931.  
 107. — (a) *W.E.* 8, 540, 1931. (b) *P.P.S.L.* 44, 408, 1932.  
 108. — and Sowter, G. A. V. *P.M.* (a) 11, 1, 1931; (b) 12, 771, 1931.  
 109. Strutt, M. J. O. *W.E.* 8, 238, 1931.  
 110. Vogt, H. *E.T.Z.* 52, 1402, 1931.  
 111. Warren, A. G. *W.E.* 8, 313, 1931.

*Oscillations of Disks, Conical Shells, Speakers, Impulse Records, Transients*

112. Benecke, H. F. O. *W.E.* 10, 257, 1933.  
 112a. British Thomson-Houston Co. (England). Technical data sent to author 7/1/1933; also on 30/11/1933.  
 113. McLachlan, N. W. *W.W.R.R.* (a) 23, 154 and 729, 1928; (b) 24, 346 and 385, 1929; (c) 28, 479 and 514, 1931; (d) 29, 169 and 193, 1931.  
 114. — and Sowter, G. A. V. *P.M.* (a) 11, 1, 1931; (b) 12, 771, 1931; (c) 13, 115, 1932.  
 115. McLachlan, N. W. (a) *P.P.S.L.* 44, 408, 1932; *W.E.* (b) 9, 559, 1932; (c) 9, 626, 1932.  
 116. — *Nature*, 129, 202, 1932.  
 117. Neumann, H. *Z.T.P.* 12, 627, 1931.  
 117a. Pedersen, P. O. *W.E.* 10, 313, 1933; see reference given therein.  
 118. Spenke, E. *W.V.S.K.* 10, 128, 1931.  
 118a. Strafford, F. R. W. *W.E.* 10, 141, 1933.



- 118b. Strutt, M. J. O. *A.P.* 17, 729, 1933.  
 118c. Urk, A. T. van, and Hut, G. B. *A.P.* 17, 915, 1933.  
 119. Warren, A. G. *P.M.* 9, 881, 1930.

*Power Radiated from Vibrators (Theory)*

120. Backhaus, H. *A.P.* 5, 1, 1930.  
 120a. Fischer, F. A. *E.N.T.* 10, 19, 1933.  
 121. McLachlan, N. W. (a) *A.P.* 15, 440, 1932; (b) *P.M.* 15, 443, 1933.  
 122. Stenzel, H. *A.P.* 11, 947, 1930.  
 122a. Strutt, M. J. O. *P.M.* 7, 537, 1929.

*Response Curves, Acoustic and Sound Field Measurements*

123. Backhaus, H. *A.P.* 5, 1, 1930.  
 124. Barrow, W. L. *J.A.S.A.* 3, 562, 1932.  
 125. Bostwick, L. G. (a) *B.T.J.* 8, 135, 1929; (b) *J.A.S.A.* 2, 242, 1930.  
 126. B. T.-H. Co. (England). Technical data sent to author, 7/1/1933.  
 127. Garton, C. G. and Lucas, G. S. *W.E.* 6, 62, 1929.  
 128. Gerlach, E. *Z.T.P.* 8, 515, 1927.  
 129. Howe, A. B. and Kirke, H. L. Letter to author, 12/12/1932.  
 130. Institute Radio Engineers. Standardization Report, 1931.  
 131. Kellogg, E. W. and Rice, C. W. *J.A.I.E.E.* 44, 982, 1925.  
 132. — *J.A.S.A.* 2, 157, 1930.  
 133. — *J.A.S.A.* 4, 56, 1932.  
 134. McLachlan, N. W. *P.P.S.L.* 44, 408, 1932.  
 135. Malter, L. and Wolff, I. *J.A.S.A.* 2, 201, 1930.  
 136. Meyer, E. *Z.T.P.* 7, 612, 1926.  
 137. — *E.N.T.* (a) 3, 290, 1926; (b) 4, 203, 1927.  
 138. — and Grützmacher, M. *E.N.T.* 4, 88, 1927.  
 139. — *Z.T.P.* 10, 306, 1929.  
 140. Oliver, D. A. *W.E.* (a) 7, 653, 1930; (b) 10, 420, 1933.  
 141. — *W.W.R.R.* 29, 579, 1931.  
 142. Olney, B. *P.I.R.E.* 19, 1113, 1931.  
 143. Olson, H. F. *J.A.S.A.* 2, 485, 1931.  
 144. Trendelenberg, F. (a) *W.V.S.K.* 4, 200, 1925; (b) *E.T.Z.* 48, 1685, 1927.  
 145. Vogt, H. *E.T.Z.* 52, 1402, 1931.  
 146. — *Z.T.P.* 12, 632, 1931.  
 147. — Technical data sent to author, 31/12/1932.  
 148. Wolff, I. and Ringel, A. *P.I.R.E.* 15, 363, 1927.  
 149. Wolff, I. *P.I.R.E.* 16, 1729, 1928.

*Spatial Sound Distribution from Vibrators*

150. Backhaus, H. and Trendelenberg, F. *Z.T.P.* 7, 130, 1926.  
 151. — *A.P.* 5, 1, 1930.  
 152. Fischer, F. A. *E.N.T.* 10, 19, 1933.  
 153. Lindsay, R. B. *P.R.* 32, 515, 1928.  
 154. McLachlan, N. W. *W.W.R.R.* (a) 20, 345 and 440, 1927; (b) 21, 357, 1927.  
 155. — (a) *P.R.S.L.* A. 122, 604, 1929; (b) *P.P.S.L.* 44, 540, 1932.  
 156. — *P.M.* (a) 14, 747, 1932; (b) 14, 1012, 1932; (c) *A.P.* 15, 422, 1932.  
 157. Malter, L. and Wolff, I. *J.A.S.A.* 2, 201, 1930.

- 157a. Oliver, D. A. *W.E.* 10, 420, 1933.  
 158. Ruedy, R. *C.J.R.* 5, 149, 1931.  
 159. Stenzel, H. *E.N.T.* (a) 4, 239, 1927; (b) 6, 165, 1929; (c) 7, 90, 1930.  
 160. — *Z.T.P.* 10, 569, 1929.  
 161. — *A.P.* 11, 947, 1930.  
 162. Strutt, M. J. O. *A.P.* 11, 129, 1931.

*Miscellaneous*

163. Aigner, F. *Z.T.P.* 13, 218, 1932. Power output from final stage.  
 163a. Amsel, O. *Z.T.P.* 14, 202, 1933. Measurement of driving forces.  
 164. Ballantine, S. (a) *P.I.R.E.* 17, 929, 1929. Reciprocity in electromagnetic systems; (b) *J.F.I.* 1927. Theory of horns; (c) *P.I.R.E.* Oct. 1933. Piezo-Electric L. S.  
 165. Barrow, W. L. *A.P.* 11, 147, 1931. The Warble Tone.  
 166. Benecke, H. F. O. *A.E.G.M. H.* 8, 506, 1928. L. S. Survey.  
 166a. — *A.E.G.M. H.* 8, 459, 1931. L. S. Survey.  
 167. Binder, W. *P.Z.* 23, 85, 1932. L. F. amplitude measurement on cone.  
 168. Brenzinger, M. and Dessauer, F. *P.Z.* 29, 654, 1929. Direct control of air by electric oscillations.  
 169. Brittain, F. H. *J.S.I.* 9, 169, 1932. Template for correcting response curves.  
 169a. Flanders, P. B. *B.T.J.* 11, 402, 1932. Measurement of acoustic impedance.  
 170. Fleischmann, L. *Naturw.* 16, 795, 1928. Tone production by points at high a.c. potentials.  
 170a. Fletcher, H. and Munson, W. A. *J.A.S.A.* 5, 82, 1933. Loudness, its definition, measurement, and calculation.  
 171. Forstmann, A. *H.T. u. Elektroakustik*, 39, 11, 1932. Mechanical and electrical equivalents.  
 172. Gerdien, H. *Telef. Zeit.* 43, 28, 1926. Distortionless reproduction.  
 173. Gerlach, E. *Filmtechnik*, 6, 947, 1930. L. S. development.  
 174. — *Nachrichtentechnik*, 1, 165, 1931. Some L. S. problems.  
 175. Geuter. *A.E.G.M. H.* 8, 467, 1931. Mass production of L. S.  
 176. Hähnle, W. *W.V.S.K.* 11, 1, 1932. Electrical and mechanical equivalents.  
 177. Hanna, C. R. (a) *P.I.R.E.* 13, 437, 1925. Design of reed drive mechanism. (b) *J.F.I.* 1927. Theory of horns.  
 178. Harbottle, H. R. *J.I.E.E.* 71, 605, 1932. Telephone Measurements.  
 179. Hickendraht, H. and Lehmann, W. *Helvetica Physica Acta*, 4, 359, 1931. Piezoacoustical investigations.  
 180. Howe, A. B. British Patent 378,286. Exponential box baffle.  
 181. Irons, E. J. *P.M.* 7, 873, 1929. Conical and other resonators.  
 182. — *P.M.* 9, 346, 1930. Conical and other resonators.  
 183. McLachlan, N. W. *W.W.R.R.* 26, 586, 1930. Radial velocity in conical diaphragm.  
 183a. — *World Radio*, July 28 to Dec. 8, 1933. Twenty articles on L. S. Performance and Design.  
 184. — *P.M.* 13, 115, 1932. Young's Modulus and  $\sqrt{(q/\rho)}$  for paper.  
 185. — *W.E.* (a) 9, 329, 1932; (b) 10, 204, 1933. Electromechanical rectification.  
 186. Meyer, E. *E.N.T.* 4, 509, 1927. Non-linear distortion.

187. Neumann, H. *S.Z.* 10, 562, 1930. Large Blatthaller speaker.
188. Oliver, D.A. *J.S.I.* 7, 318, 1930. Stiffness meter.
189. ——— *Nature*, 128, 268, 1931. L.S. curves and loudness.
190. ——— *W.W.R.R.* 29, 579, 1931. Inductor dynamic speaker.
191. ——— *P.M.* 14, 318, 1932.  $\sqrt{(g/\rho)}$  for paper.
192. Paddle, L. H. Technical data sent to author, 14/2/1933. Reducing distortion due to non-uniform magnetic field in moving-coil speaker.
193. Riegger, H. *Z.T.P.* 5, 577, 1924. Distortionless reproduction.
194. Ruedy, R. *C.J.R.* 5, 297, 1931. Longitudinal and radial oscillation of rods.
195. Schilgen, F. and Starkloff, C. *E.T.Z.* 52, 1589, 1931. L. S. installation for public address purposes.
196. Schottky, W. *P.Z.* 25, 672, 1924. General principles.
197. ——— *Z.T.P.* 5, 574, 1924. General principles.
198. ——— *E.N.T.* 2, 157, 1925. L. S. theory (Blatthaller).
199. Sivian, L. J., Dunn, H. K., and White, S. D. *J.A.S.A.* 2, 330, 1931. Spectra of musical instruments.
- 199a. Sivian, L. J. and White, S. D. *J.A.S.A.* 4, 288, 1933. Minimum audible sound fields.
200. Snow, W. B. *J.A.S.A.* 3, 155, 1931. Frequency range of musical instruments.
201. Strutt, M. J. O. *W.E.* 8, 238, 1931. Measurement of diaphragm amplitude.
202. Trendelenberg, F. *W.V.S.K.* 4, 200, 1925. General survey of L. S.
203. ——— *S.Z.* 7, 141, 1927. Blatthaller speaker.
204. ——— *E.T.Z.* 48, 1685, 1927. Blatthaller speaker.
205. ——— *Z.f.H.* 32, 131, 1928. Electroacoustical investigations.
206. Warren, A. G. *P.P.S.L.* 40, 296, 1928. Sound pressure and particle velocity at an orifice.
- 206a. ——— *W.E.* 8, 313, 1931. Amplitude measuring apparatus.
207. Wigge, H. *Z.f.H.* 37, 16, 1931. Distortionless supply from output transformer.
208. Willms, F. *E.N.T.* 9, 68, 1932. Sound transmission with wide frequency range.
- 208a. *W.W.R.R.* 34, 5, 1934. Piezo-Electric L. S.

## (B) BOOKS

209. Beattie, R. T. *Hearing in Man and Animals.*
210. Crandall, I. *Vibrating Systems and Sound.*
211. Fletcher, H. *Speech and Hearing.*
212. Geiger, H. and Scheel, K. *Handbuch der Physik 8, Akustik.*
213. Gray, A., Mathews, G. B., and MacRobert, T. M. *Treatise on Bessel Functions.*
- 213a. Hughes, L. E. C. *Engineering Acoustics.*
- 213b. Jahnke and Emde. *Funktionentafeln.*
214. Kennelly, A. E. *Electrical Vibration Instruments.*
215. Lamb, H. *Dynamical Theory of Sound.*
216. ——— *Hydrodynamics.*
217. MacRobert, T. M. *Spherical Harmonics.*
218. McLachlan, N. W. *Wireless Loud Speakers.*
- 218a. ——— *Bessel Functions for Engineers.* 2d. ed., 1955.

219. Rayleigh, Lord. *Theory of Sound 1 and 2.*
220. Stewart, G. W. and Lindsay, R. B. *Acoustics.*
221. Watson, G. N. *Theory of Bessel Functions.*
- 221a. West, W. *Acoustical Engineering.*
222. Whittaker, E. T. and Watson, G. N. *Modern Analysis.*
- 222a. Wilson, P. and Webb, G. *Modern Gramophones and Electrical Reproducers.*
223. Wood, A. B. *Sound.*

## ADDITIONAL REFERENCES

224. Sato, K. *Japanese Journal of Physics*, 5, 103, 1929. Sound field of a conical horn.
225. Barnes, E. J. *W.E.* 7, 248, 1930; 7, 301, 1930. Measurement of loud speaker performance.
226. Cohen, B. S. and Paul, R. W. *W.E.* 7, 421, 1930. Hornless moving-coil loud speaker with Balsa wood diaphragm.
227. Stenzel, H. *Handbuch der Experimentalphysik*, 17/2, 254, 1933. Lautsprecher.
228. Goldman, S. *J.A.S.A.* 5, 181, 1934. Measurement of directional characteristics of horns.
229. McLachlan, N. W. *Theory and application of Mathieu Functions*, 1947.
230. McLachlan, N. W. *Ordinary Nonlinear Differential Equations in Engineering and Physical Sciences*, 2nd, ed., 1956. See list of references therein.

## INDEX

- absorption coefficient, 2, 44, 288, 301.  
 accession to inertia, 4, 54.  
 — of conical diaphragm, 282.  
 — frequency correction factor, 60, 61.  
 — of flexible disk, 58.  
 — of rigid disk, 57.  
 — measurement of, 279.  
 — reduction of vibrational frequency due to, 89.  
 — of various vibrators, 61.  
 acoustical admittance, 4.  
 — image, 43.  
 — impedance, 3.  
 — mho, 4.  
 — ohm, 3.  
 — reactance, 3, 181, 182.  
 — resistance, 3, 181, 182.  
 — transformer-ratio, 349.  
 air-chamber, horn speaker, 350, 355, 365.  
 — hornless speaker, 73.  
 — stiffness, 73.  
 amplitude, finite sound pressure, 198.  
 — and loudness, relationship, 347.  
 — to radiate 1 watt, 372.  
 analogue, electrical, 350, 355, 364.  
 annular membrane or surround, 70, 81.  
 — stiffness, 85.  
 — vibrational modes, 81.  
 antinode, 2.  
 audibility, threshold of, 2.  
  
 baffle, definition, 3.  
 — box, 297.  
 — disk without baffle, 36.  
 — effect on sound distribution, 38.  
 — flat, 36.  
 — increase in power due to, 35, 41.  
 — infinite, 3, 8, 30.  
 — influence on accession to inertia, 57, 62, 281.  
 — spherical vibrators without, 122.  
 bakelite cones, 332.  
 balanced armature mechanism, 218.  
 bar, definition, 1.  
 bending, potential energy of, 313.  
 Bessel functions, 21, 39, 53, 64, 79-87, 96, 101-9, 116-20, 173-75, 184  
 — zeros or, 80.  
 Blatthaller speaker, 222.  
 boundary conditions, circular membrane, 79.  
 — annular membrane, 81.  
 boundary conditions, theory of horns, 203.  
 bridge measurements, 266.  
  
 $C^2$ , measurement of, 283.  
 cantilever reed mechanism, 213.  
 centring devices, 69.  
 cinema speakers, 368.  
 circuit, equivalent electrical, 135, 142, 337.  
 — output or power, 135, 142, 337.  
 clearance in throat chamber, 351, 358, 364.  
 coercive force of magnet, 237.  
 coil-driven circular membrane, 221.  
 — free-edge disk, 274.  
 compliance, 5.  
 condensation of medium, 9.  
 condenser speakers, description, 226, 229.  
 — circular membrane, 169.  
 — motional capacity, 164, 165.  
 — performance of, 166, 171.  
 — rectangular membrane, 87, 169.  
 — theory of, 158.  
 cone, re-entrant, 73.  
 conical diaphragm, air-column vibrations, 329.  
 — bridge measurements, 307, 316.  
 — criterion of constructional material, 330.  
 — damping of oscillations, 336.  
 — edge condition, 310.  
 — effective mass, 276.  
 — impulse records, 332.  
 — influence of apical angle, 327.  
 — influence of coil mass, 324.  
 — influence of thickness, 323, 326.  
 — nodal lines on, 304.  
 — oscillation of coil-former, 339.  
 — radial modes, 304.  
 — stiffness, 340.  
 — stresses in, 310.  
 — symmetrical modes, 304, 316-29.  
 criterion of magnet, 241.  
 cubical elasticity, coefficient of, 10.  
 current in moving coil, 137, 266, 345.  
  
 decibel, definition, 7.  
 diffraction of sound waves, 1.  
 dilatation of medium, 10.  
 disk, flexible, 63.  
 — effective mass, 63.  
 — power radiated by, 118-21.

- disk, sound distribution from, 104, 106.  
 — vibrational modes, 63.  
 — rigid, 8, 30, 49, 94, 143.  
 — — power radiated by, 145.  
 — — pressure at any point on, 49.  
 — — sound distribution from, 94.  
 — — total pressure on, 143.  
 distortion, moving-coil speaker, 263.  
 — reed speaker, 214.  
 divergent waves, in horn, 180.  
 — — spherical, 21.  
 double sound source, 32.  
 — — power from, 34.  
 driving mechanisms, 213.  
 — — balanced armature, 218.  
 — — Blatthaller, 222.  
 — — cantilever reed, 213.  
 — — condenser speakers, 226, 228.  
 — — directional-baffle speaker, 221.  
 — — horn speaker, 224.  
 — — hornless moving coil, 219.  
 — — inductor dynamic, 217.  
 — — lever mechanism, 225.  
 — — moving-coil membrane, 221.  
 — — Riffel, 223.  
 dynamic deformation curve, definition, 5.  
 — — of circular membrane, 80.  
 effective mass, definition, 4.  
 — — of annular membrane, 82.  
 — — of conical diaphragm, 276.  
 — — of dielectric in condenser speaker, 167.  
 — — of flat reed, 63.  
 — — of flexible disk, 63.  
 — — of free-edge disk, 274.  
 — — of mass and helical spring, 271.  
 — — of rigid disk, 146, 147.  
 — — measurement of, 273.  
 efficiency, absolute, 253, 255.  
 — acoustical, 253.  
 — mechanical, 255.  
 — measurement of, 255, 259.  
 — of directional-baffle speaker, 367.  
 — of hornless speaker, 256, 257.  
 — of horn speaker, 258.  
 electrical analogue of mechanical system, 350, 355, 364.  
 electrical and mechanical equivalents, 6.  
 electrical equivalent diagram, 337.  
 electrical impedance, measurement of, 266.  
 electromechanical conversion factor, 5.  
 — rectification, 159, 239, 245.  
 — resonance, 134, 150.  
 electrostatic force, 158-61.  
 endurance test, 264.  
 energy, kinetic, 89.  
 equivalent mass, definition, 5.  
 — — of membrane, 89, 90.  
 — — of disk, 90.  
 extension, potential energy of, 313.  
 extensional vibrational modes, 312.  
 fluid pressure on vibrators, 49.  
 — — on membrane, 59.  
 — — on rigid disk, 49.  
 flux, magnetic, 230.  
 — measurement of, 231.  
 — sound, 3.  
 frequency range, hornless speaker, 343, 374.  
 — — horn speaker, 374.  
 — — of reproduction, 374.  
 functions, Bessel, 21, 39, 53, 64, 79-87, 96, 101-9, 184.  
 — hypergeometric, 50, 56, 57.  
 — Struve, 57, 143, 189.  
 Gauss's theorem, 57.  
 harmonics, in speaker output, 264.  
 — zonal spherical, 20.  
 hemisphere, vibrating radially, 48, 61, 123.  
 — — axially, 48, 60, 61, 128.  
 — — sound distribution from, 111.  
 high-frequency speakers, 374.  
 horns, acoustical impedance, 181, 182.  
 — Bessel type, 184.  
 — characteristic curves, 187.  
 — conical, 180.  
 — damping of oscillations in, 335.  
 — design of, 354, 359, 366.  
 — experimental data, 362.  
 — exponential, 182.  
 — finite sound amplitude in, 199.  
 — power delivered to, 185.  
 — reflection at mouth, 188, 194.  
 — simulating impedance, 190.  
 — speaker design, 349.  
 — theory of, 177.  
 — throat chamber, 350, 351, 376.  
 — throat impedance, 181, 183.  
 — throat pressure, 203.  
 — velocity of sound in, 182, 183, 196.  
 hysteresis quadrant, 237.  
 image, acoustical, 43.  
 impedance, acoustical, 3.  
 — electrical, 6, 132.  
 — mechanical, 4.

- impedance, motional, 5.  
 — of long tube, 32.  
 — of moving coil, 134.  
 — measurement of, 266.  
 — per unit area, 4.  
 — of spherical vibrator, 47.
- impulse records, conical diaphragm, 334.  
 — — glass cone, 335.  
 — — horn speaker, 335.
- inductor dynamic speaker, 217.
- inertia, accession to, 4.  
 — measurement of, 279.  
 — component of surface pressure, 10, 13-18, 179.
- infinitesimal pressure amplitude, 13-18, 178.
- inherent mechanical loss, measurement of, 139.
- intensity level, definition, 2.
- interference, definition, 1.  
 — spatial, 94, 221.
- iron loss due to magnet, 220, 270, 271, 384.
- isobels, curves of equal loudness level, 348.
- kinetic energy, flexible disk, 89.  
 — — membrane, 89.
- Legendre polynomials, 20, 32.
- lever mechanism for speakers, 225.
- linearity test, 262.
- loudness, definition, 2.  
 — curves of equal, 348.
- low-frequency resonance, 70, 345.  
 — — in condenser speaker, 174.  
 — — in moving-coil speaker, 70.
- magnets, electro- and permanent, 230.  
 — axial flux distribution, 234, 239.  
 — design of, 237.  
 — electromechanical rectification, 239, 245.  
 — flux measurements, 231.  
 — leakage, 232, 234.  
 — optimum working point, 237.  
 — output criterion, 241.  
 — of minimum volume, 238.
- masking of sound, definition, 3.
- mass, effective, 4.  
 — equivalent, 5.
- matching resistance of medium, 3.
- Mathieu equation, 245, 250.
- mechanical, efficiency, 255.  
 — equivalent, 6.  
 — impedance, 4.  
 — reactance, 4.
- mechanical resistance, 4.
- membrane, annular, 81.  
 — — effective mass, 82.  
 — — in hornless speaker, 70.  
 — — sound distribution from, 104.  
 — — vibrational modes, 81.  
 — — circular, 78, 79, 85, 87.  
 — — axial sound pressure, 103.  
 — — effective mass, 87.  
 — — power radiated by, 117.  
 — — spatial sound distribution from, 103.  
 — — vibrational frequencies, 79.  
 — rectangular strip, 87.
- microphone, minimum distance from speaker, 285.
- modulation products, 160, 252.
- motional capacity of speaker, 133, 164, 165.  
 — impedance of speaker, 132, 164.  
 — inductance of speaker, 132, 164.  
 — resistance of speaker, 132, 164.
- moving-coil principle, description, 219.  
 — — theory, 131.
- moving coil, current in, 344.  
 — — optimum mass, 153.  
 — — reactance, 132.  
 — — resistance, 132.  
 — — speaker, design, 343, 349.  
 — — — L.F. resonances, 70.  
 — — — H.F. resonances, 316-36.  
 — — — damping of oscillations, 336.  
 — — — impulse records, 334.  
 — — — relationship between amplitude and loudness, 347.
- multi-diaphragm speaker, 127.
- naturalness in reproduction, 378.
- neon lamp stroboscope, 305.
- nodal circles, on cones, 304, 316-22.  
 — — on disks, 64.  
 — — on membranes, 80.
- nodal radii on cones, 304-7.
- non-linear characteristic of speaker, 158, 214, 239, 263.
- orbital method of response measurement, 288.
- oscillations of conical diaphragms, 334.  
 — of horn speaker, 335.  
 — of surround, 71, 81, 277.
- partial nodes, 2.
- particle velocity, 11, 14, 16, 202.
- permeability of magnet, 384.
- plane sound waves, 10.
- point sound source, 25.

- polar curves of sound distribution, 98, 105, 296.
- polarizing voltage on speaker, 159.
- potential energy of deformation, 313.
- power radiated by simple source, 26.
- by double source, 34.
- by flexible disk, 118-21.
- by hemisphere, 125-30.
- by rigid disk, 30, 145.
- by sphere, 123.
- measurement of sound, 258, 260.
- electrical input, 253.
- pressure, on vibrating surface, 49.
- acoustic, 50, 52.
- inertia, 57.
- infinitesimal sound, 10, 13-18, 178, 179.
- finite sound, 198.
- at horn throat, 203.
- at any point in fluid, 16.
- propagation of sound, theory, 9.
- radial modes of vibration, 304.
- nodes, 305.
- velocity in diaphragm, 382.
- reactance, acoustical, 3, 181, 182.
- of moving coil, 134, 150.
- mechanical, 4.
- rectangular membrane speaker, 169, 226.
- plate, sound distribution from, 100.
- rectification, electromechanical, 159, 239, 245.
- reflection, coefficient of, 2.
- reproduction above 5,000  $\sim$ , 374.
- resistance, acoustical, 3, 181, 182.
- mechanical, 4.
- motional, 5.
- of moving coil, 134.
- of medium, 3.
- resonance of diaphragm on surround, 70, 308, 345.
- of surround, 70, 81, 308.
- response, definition, 289.
- orbital method, 288.
- automatic record, 291.
- experimental data, 292.
- polar curves, 296.
- reverberation, definition, 2.
- time, 2.
- Riffel speaker, 223.
- rigid disk, analysis of coil-driven, 143.
- axial pressure, 151.
- constant power from, 257.
- power from, 145, 152.
- amplitude to radiate 1 watt, 372.
- pressure on, 49, 143.
- rigid disk, reed driven, 153.
- Rochelle salt speakers, 344, 379.
- room effects in reproduction, 299.
- sensation level, 2.
- simulating impedance, 4.
- solid angle definition, xii.
- influence of, 30.
- sound distribution from vibrators, 94.
- from group of radiators, 112.
- sound energy density, 1, 301.
- flux, 1.
- finite amplitude of, 198.
- power for cinemas, 370.
- pressure, 3.
- propagation, 9.
- waves, 3-dimensional, 13.
- source, simple, 25.
- double, 32.
- strength of, 25, 33.
- speakers for cinemas, 368.
- spherical harmonics, equation of, 20.
- zonal, 20.
- vibrators, 47, 106.
- waves, 13.
- static pressure, 1.
- stiffness, definition, 5.
- measurement of, 284.
- meter, 284.
- strength test of speaker, 265.
- stresses in conical shell, 310.
- stroboscope, in studying nodal figures, 305.
- Struve's function, 57, 143, 189.
- sub-harmonics, 315.
- surround, of conical diaphragm, 70, 81, 277, 308.
- theory of sound propagation, 9.
- thickness of paper, effect on diaphragm behaviour, 323, 326.
- throat chamber of horn speaker, 350, 351, 376.
- pressure in, 203.
- stiffness of, 351, 353, 358, 365.
- throat of horn, resistance of, 181, 183.
- impedance of, 181, 183.
- threshold of audibility, 2.
- transient, definition, 6.
- theory, 204.
- transmission loss in diaphragm, 90.
- valve circuits for speakers, 135, 142, 158, 167, 170, 227.
- velocity of sound, in air, 1.
- in diaphragm, 382.



- velocity of sound, in paper, 380.  
velocity, particle, 3, 11, 14, 16, 202,  
203.  
— potential, 16, 21, 57, 106, 122, 178.  
vibrational frequencies of conical dia-  
phragms, 304.  
— — of annular membrane, 81.  
— — of circular membrane, 79.
- vibrational frequencies of flexible disk,  
63.  
— — of flexible reed, 66.  
volume of throat chamber, 351, 358,  
361.  
warble tone, 287.  
Young's modulus for paper, 380.

# **MICROWAVE TRANSMISSION DATA**

**by Theodore Moreno**

Radio engineers, microwave systems designers, applied physicists, power and communications engineers will find this book both an excellent introduction to general transmission-line theory and a detailed study of microwave transmission lines and associated components. Originally produced as a classified government publication, it was completely rewritten and enlarged (4 entirely new chapters) under the auspices of the Sperry Corporation for declassified publication following the war.

Ordinary transmission-line theory, attenuation, power carrying capacity, parameters of coaxial lines, breakdown in a coaxial line, higher modes; flexible cables, coaxial line structures and transformers; field distribution and power-carrying capacity of wave guides, wave guides without metal walls; attenuation in wave guides through conductor losses, dielectric losses, or both; obstacles, discontinuities and junctions; resonant structures; coupling between coaxial lines and wave guides, tunable wave guide impedance transformers; wave guides partially and completely filled with dielectric material; cavity resonators, calculation of resonator parameters, effects of temperature and humidity; and many other important topics are carefully analyzed. Of particular importance, even the most theoretical discussions are related to practical questions of design — there is nothing which is not of immediate value or reference use to the engineer.

Complete, revised and enlarged edition. 324 circuit diagrams, figures, etc. Tables of dielectric, flexible cable, etc., data. Index. ix + 248pp.  
5-3/8 x 8. \$459 Paperbound \$1.50

# THE ELECTROMAGNETIC FIELD

by Max Mason and Warren Weaver

This classic work has been widely adopted as a standard text by universities throughout the country, and is used considerably by graduate engineers. Clearly written and readable, it presents a consistent and systematic treatment of the field of electromagnetics.

In the first of four chapters, the authors discuss Coulomb's law and its implications; in Chapter 2, they treat the general theory of electrostatics for conductors and dielectrics. Chapter 3 covers magnetostatics; and Chapter 4 deals with the Maxwell field equations. There is a mathematical appendix giving a continuous exposition of vector analysis, and a table that converts any quantity into absolute electrostatic, absolute electromagnetic, or practical units. Vector methods, expansion methods and rational units are used throughout.

**PARTIAL CONTENTS:** I. **Coulomb's Law & Some Analytic Consequences.** Discrete charges. Complexes of charge. Ponderable bodies. II. **The Electrostatic Problem for Conductors & Dielectrics.** Distribution problem: Conductors. Special & general methods of solution. Dielectrics. III. **Magnetostatics.** The fundamental law. Complexes of charge. Ponderable bodies. Magnetism. Steady currents: Ohm's law. IV. **The Maxwell Field Equations.**

Introduction. 147 problems. Formula & subject indexes. Mathematical appendix. Table for change of units. 61 diagrams. xiii + 390pp. 5 3/8 x 8.

S185 Paperbound \$2.00

# Catalogue of Dover

## SCIENCE BOOKS

### DIFFERENTIAL EQUATIONS (ORDINARY AND PARTIAL DIFFERENTIAL)

**INTRODUCTION TO THE DIFFERENTIAL EQUATIONS OF PHYSICS, L. Hopf.** Especially valuable to engineer with no math beyond elementary calculus. Emphasizes intuitive rather than formal aspects of concepts. Partial contents: Law of causality, energy theorem, damped oscillations, coupling by friction, cylindrical and spherical coordinates, heat source, etc. 48 figures. 160pp. 5½ x 8. S120 Paperbound \$1.25

**INTRODUCTION TO BESSEL FUNCTIONS, F. Bowman.** Rigorous, provides all necessary material during development, includes practical applications. Bessel functions of zero order, of any real order, definite integrals, asymptotic expansion, circular membranes, Bessel's solution to Kepler's problem, much more. "Clear . . . useful not only to students of physics and engineering, but to mathematical students in general," Nature. 226 problems: Short tables of Bessel functions. 27 figures. x + 135pp. 5½ x 8. S462 Paperbound \$1.35

**DIFFERENTIAL EQUATIONS, F. R. Moulton.** Detailed, rigorous exposition of all non-elementary processes of solving ordinary differential equations. Chapters on practical problems; more advanced than problems usually given as illustrations. Includes analytic differential equations; variations of a parameter; integrals of differential equations; analytic implicit functions; problems of elliptic motion; sine-amplitude functions; deviation of formal bodies; Cauchy-Lipshitz process; linear differential equations with periodic coefficients; much more. Historical notes. 10 figures. 222 problems. xv + 395pp. 5½ x 8. S451 Paperbound \$2.00

**PARTIAL DIFFERENTIAL EQUATIONS OF MATHEMATICAL PHYSICS, A. G. Webster.** Valuable sections on elasticity, compression theory, potential theory, theory of sound, heat conduction, wave propagation, vibration theory. Contents include: deduction of differential equations, vibrations, normal functions, Fourier's series. Cauchy's method, boundary problems, method of Riemann-Volterra, spherical, cylindrical, ellipsoidal harmonics, applications, etc. 97 figures. vii + 440pp. 5½ x 8. S263 Paperbound \$2.00

**ORDINARY DIFFERENTIAL EQUATIONS, E. L. Ince.** A most compendious analysis in real and complex domains. Existence and nature of solutions, continuous transformation groups, solutions in an infinite form, definite integrals, algebraic theory. Sturmian theory, boundary problems, existence theorems, 1st order, higher order, etc. "Deserves highest praise, a notable addition to mathematical literature," Bulletin, Amer. Math. Soc. Historical appendix. 18 figures. viii + 558pp. 5½ x 8. S349 Paperbound \$2.55

**ASYMPTOTIC EXPANSIONS, A. Erdélyi.** Only modern work available in English; unabridged reproduction of monograph prepared for Office of Naval Research. Discusses various procedures for asymptotic evaluation of integrals containing a large parameter; solutions of ordinary linear differential equations. vi + 108pp. 5½ x 8. S318 Paperbound \$1.35

**LECTURES ON CAUCHY'S PROBLEM, J. Hadamard.** Based on lectures given at Columbia, Rome, discusses work of Riemann, Kirchoff, Volterra, and author's own research on hyperbolic case in linear partial differential equations. Extends spherical cylindrical waves to apply to all (normal) hyperbolic equations. Partial contents: Cauchy's problem, fundamental formula, equations with odd number, with even number of independent variables; method of descent. 32 figures. lii + 316pp. 5½ x 8. S105 Paperbound \$1.75

## NUMBER THEORY

**INTRODUCTION TO THE THEORY OF NUMBERS**, L. E. Dickson. Thorough, comprehensive, with adequate coverage of classical literature. Not beyond beginners. Chapters on divisibility, congruences, quadratic residues and reciprocity, Diophantine equations, etc. Full treatment of binary quadratic forms without usual restriction to integral coefficients. Covers infinitude of primes, Fermat's theorem, Legendre's symbol, automorphs, Recent theorems of Thue, Siegel, much more. Much material not readily available elsewhere. 239 problems. 1 figure. viii + 183pp. 5 $\frac{3}{4}$  x 8. S342 Paperbound \$1.65

**ELEMENTS OF NUMBER THEORY**, I. M. Vinogradov. Detailed 1st course for persons without advanced mathematics; 95% of this book can be understood by readers who have gone no farther than high school algebra. Partial contents: divisibility theory, important number theoretical functions, congruences, primitive roots and indices, etc. Solutions to problems, exercises. Tables of primes, indices, etc. Covers almost every essential formula in elementary number theory! "Welcome addition . . . reads smoothly," Bull. of the Amer. Math. Soc. 233 problems. 104 exercises. viii + 227pp. 5 $\frac{3}{4}$  x 8. S259 Paperbound \$1.60

## PROBABILITY THEORY AND INFORMATION THEORY

**SELECTED PAPERS ON NOISE AND STOCHASTIC PROCESSES**, edited by Prof. Nelson Wax, U. of Illinois. 6 basic papers for those whose work involves noise characteristics. Chandrasekhar, Uhlenbeck and Ornstein, Uhlenbeck and Ming, Rice, Doob. Included is Kac's Chauvenet-Prize winning "Random Walk." Extensive bibliography lists 200 articles, through 1953. 21 figures. 337pp. 6 $\frac{3}{4}$  x 9 $\frac{3}{4}$ . S262 Paperbound \$2.35

**A PHILOSOPHICAL ESSAY ON PROBABILITIES**, Marquis de Laplace. This famous essay explains without recourse to mathematics the principle of probability, and the application of probability to games of chance, natural philosophy, astronomy, many other fields. Translated from 6th French edition by F. W. Truscott, F. L. Emory. Intro. by E. T. Bell. 204pp. 5 $\frac{3}{4}$  x 8. S166 Paperbound \$1.25

**MATHEMATICAL FOUNDATIONS OF INFORMATION THEORY**, A. I. Khinchin. For mathematicians, statisticians, physicists, cyberneticists, communications engineers, a complete, exact introduction to relatively new field. Entropy as a measure of a finite scheme, applications to coding theory, study of sources, channels and codes, detailed proofs of both Shannon theorems for any ergodic source and any stationary channel with finite memory, much more. "Presents for the first time rigorous proofs of certain fundamental theorems . . . quite complete . . . amazing expository ability," American Math. Monthly. vii + 120pp. 5 $\frac{3}{4}$  x 8. S434 Paperbound \$1.35

## VECTOR AND TENSOR ANALYSIS AND MATRIX THEORY

**VECTOR AND TENSOR ANALYSIS**, G. E. May. One of clearest introductions to increasingly important subject. Start with simple definitions, finish with sure mastery of oriented Cartesian vectors, Christoffel symbols, solenoidal tensors. Complete breakdown of plane, solid, analytical, differential geometry. Separate chapters on application. All fundamental formulae listed, demonstrated. 195 problems. 66 figures. viii + 193pp. 5 $\frac{3}{4}$  x 8. S109 Paperbound \$1.75

**APPLICATIONS OF TENSOR ANALYSIS**, A. J. McConnell. Excellent text for applying tensor methods to such familiar subjects as dynamics, electricity, elasticity, hydrodynamics. Explains fundamental ideas and notation of tensor theory, geometrical treatment of tensor algebra, theory of differentiation of tensors, and a wealth of practical material. "The variety of fields treated and the presence of extremely numerous examples make this volume worth much more than its low price," Alluminio. Formerly titled "Applications of the Absolute Differential Calculus." 43 illustrations. 685 problems. xii + 381pp. S373 Paperbound \$1.85

**VECTOR AND TENSOR ANALYSIS**, A. P. Wills. Covers entire field, from dyads to non-Euclidean manifolds (especially detailed), absolute differentiation, the Riemann-Christoffel and Ricci-Einstein tensors, calculation of Gaussian curvature of a surface. Illustrations from electrical engineering, relativity theory, astro-physics, quantum mechanics. Presupposes only working knowledge of calculus. Intended for physicists, engineers, mathematicians. 44 diagrams. 114 problems. xxxii + 285pp. 5 $\frac{3}{4}$  x 8. S454 Paperbound \$1.75

## DOVER SCIENCE BOOKS

### PHYSICS, ENGINEERING

#### MECHANICS, DYNAMICS, THERMODYNAMICS, ELASTICITY

**MATHEMATICAL ANALYSIS OF ELECTRICAL AND OPTICAL WAVE-MOTION**, H. Bateman. By one of century's most distinguished mathematical physicists, a practical introduction to developments of Maxwell's electromagnetic theory which directly concern the solution of partial differential equation of wave motion. Methods of solving wave-equation, polar-cylindrical coordinates, diffraction, transformation of coordinates, homogeneous solutions, electromagnetic fields with moving singularities, etc. 168pp. 5 $\frac{3}{8}$  x 8. S14 Paperbound \$1.60

**THERMODYNAMICS**, Enrico Fermi. Unabridged reproduction of 1937 edition. Remarkable for clarity, organization; requires no knowledge of advanced math beyond calculus, only familiarity with fundamentals of thermometry, calorimetry. Partial Contents: Thermodynamic systems, 1st and 2nd laws, potentials; Entropy, phase rule; Reversible electric cells; Gaseous reactions: Van't Hoff reaction box, principle of LeChatelier; Thermodynamics of dilute solutions: osmotic, vapor pressures; boiling, freezing point; Entropy constant. 25 problems. 24 illustrations. x + 160pp. 5 $\frac{3}{8}$  x 8. S361 Paperbound \$1.75

**FOUNDATIONS OF POTENTIAL THEORY**, O. D. Kellogg. Based on courses given at Harvard, suitable for both advanced and beginning mathematicians, Proofs rigorous, much material here not generally available elsewhere. Partial contents: gravity, fields of force, divergence theorem, properties of Newtonian potentials at points of free space, potentials as solutions of Laplace's equation, harmonic functions, electrostatics, electric images, logarithmic potential, etc. ix + 384pp. 5 $\frac{3}{8}$  x 8. S144 Paperbound \$1.98

**DIALOGUES CONCERNING TWO NEW SCIENCES**, Galileo Galilei. Classic of experimental science, mechanics, engineering, as enjoyable as it is important. Characterized by author as "superior to everything else of mine." Offers a lively exposition of dynamics, elasticity, sound, ballistics, strength of materials, scientific method. Translated by H. Grew, A. de Salvio. 126 diagrams. xxi + 288pp. 5 $\frac{3}{8}$  x 8. S99 Paperbound \$1.65

**THEORETICAL MECHANICS; AN INTRODUCTION TO MATHEMATICAL PHYSICS**, J. S. Ames, F. D. Murnaghan. A mathematically rigorous development for advanced students, with constant practical applications. Used in hundreds of advanced courses. Unusually thorough coverage of gyroscopic baryscopic material, detailed analyses of Coriolis acceleration, applications of Lagrange's equations, motion of double pendulum, Hamilton-Jacobi partial differential equations, group velocity, dispersion, etc. Special relativity included. 159 problems. 44 figures. ix + 462pp. 5 $\frac{3}{8}$  x 8. S461 Paperbound \$2.00

**STATICS AND THE DYNAMICS OF A PARTICLE**, W. D. MacMillan. This is Part One of "Theoretical Mechanics." For over 3 decades a self-contained, extremely comprehensive advanced undergraduate text in mathematical physics, physics, astronomy, deeper foundations of engineering. Early sections require only a knowledge of geometry; later, a working knowledge of calculus. Hundreds of basic problems including projectiles to moon, harmonic motion, ballistics, transmission of power, stress and strain, elasticity, astronomical problems. 340 practice problems, many fully worked out examples. 200 figures. xvii + 430pp. 5 $\frac{3}{8}$  x 8. S467 Paperbound \$2.00

**THE THEORY OF THE POTENTIAL**, W. D. MacMillan. This is Part Two of "Theoretical Mechanics." Comprehensive, well-balanced presentation, serving both as introduction and reference with regard to specific problems, for physicists and mathematicians. Assumes no prior knowledge of integral relations, all math is developed as needed. Includes: Attraction of Finite Bodies; Newtonian Potential Function; Vector Fields, Green and Gauss Theorems; Two-layer Surfaces; Spherical Harmonics; etc. "The great number of particular cases . . . should make the book valuable to geo-physicists and others actively engaged in practical applications of the potential theory," Review of Scientific Instruments. xii + 469pp. 5 $\frac{3}{8}$  x 8. S486 Paperbound \$2.25

**DYNAMICS OF A SYSTEM OF RIGID BODIES (Advanced Section)**, E. J. Routh. Revised 6th edition of a classic reference aid. Partial contents: moving axes, relative motion, oscillations about equilibrium, motion. Motion of a body under no forces, any forces. Nature of motion given by linear equations and conditions of stability. Free, forced vibrations, constants of integration, calculus of finite differences, variations, precession and nutation, motion of the moon, motion of string, chain, membranes. 64 figures. 498pp. 5 $\frac{3}{8}$  x 8. S229 Paperbound \$2.35

**THE DYNAMICS OF PARTICLES AND OF RIGID, ELASTIC, AND FLUID BODIES: BEING LECTURES ON MATHEMATICAL PHYSICS**, A. G. Webster. Reissuing of classic fills need for comprehensive work on dynamics. Covers wide range in unusually great depth, applying ordinary, partial differential equations. Partial contents: laws of motion, methods applicable to systems of all sorts; oscillation, resonance, cyclic systems; dynamics of rigid bodies; potential theory; stress and strain; gyrostatics; wave, vortex motion; kinematics of a point; Lagrange's equations; Hamilton's principle; vectors; deformable bodies; much more not easily found together in one volume. Unabridged reprinting of 2nd edition. 20 pages on differential equations, higher analysis. 203 illustrations. xi + 588pp. 5 $\frac{3}{8}$  x 8. S522 Paperbound \$2.35

## CATALOGUE OF

**PRINCIPLES OF MECHANICS**, Heinrich Hertz. A classic of great interest in logic of science. Last work by great 19th century physicist, created new system of mechanics based upon space, time, mass; returns to axiomatic analysis, understanding of formal, structural aspects of science, taking into account logic, observation, a priori elements. Of great historical importance to Poincaré, Carnap, Einstein, Milne. 20 page introduction by R. S. Cohen, Westeyan U., analyzes implications of Hertz's thought and logic of science. 13 page introduction by Helmholtz. xiii + 274pp. 5½ x 8. S316 Clothbound \$3.50  
S317 Paperbound \$1.75

**MATHEMATICAL FOUNDATIONS OF STATISTICAL MECHANICS**, A. I. Khinchin. A thoroughly up-to-date introduction, offering a precise and mathematically rigorous formulation of the problems of statistical mechanics. Provides analytical tools to replace many commonly used cumbersome concepts and devices. Partial contents: Geometry, kinematics of phase space; ergodic problem; theory of probability; central limit theorem; ideal monatomic gas; foundation of thermodynamics; dispersion, distribution of sum functions; etc. "Excellent introduction . . . clear, concise, rigorous," Quarterly of Applied Mathematics. viii + 179pp. 5½ x 8. S146 Clothbound \$2.95  
S147 Paperbound \$1.35

**MECHANICS OF THE GYROSCOPE, THE DYNAMICS OF ROTATION**, R. F. Deimel, Prof. of Mechanical Engineering, Stevens Inst. of Tech. Elementary, general treatment of dynamics of rotation, with special application of gyroscopic phenomena. No knowledge of vectors needed. Velocity of a moving curve, acceleration to a point, general equations of motion, gyroscopic horizon, free gyro, motion of discs, the damped gyro, 103 similar topics. Exercises. 75 figures. 208pp. 5½ x 8. S66 Paperbound \$1.65

**MECHANICS VIA THE CALCULUS**, P. W. Norris, W. S. Legge. Wide coverage, from linear motion to vector analysis; equations determining motion, linear methods, compounding of simple harmonic motions, Newton's laws of motion, Hooke's law, the simple pendulum, motion of a particle in 1 plane, centers of gravity, virtual work, friction, kinetic energy of rotating bodies, equilibrium of strings, hydrostatics, shearing stresses, elasticity, etc. Many worked-out examples. 550 problems. 3rd revised edition. xii + 367pp. S207 Clothbound \$3.95

**A TREATISE ON THE MATHEMATICAL THEORY OF ELASTICITY**, A. E. H. Love. An indispensable reference work for engineers, mathematicians, physicists, the most complete, authoritative treatment of classical elasticity in one volume. Proceeds from elementary notions of extension to types of strain, cubical dilatation, general theory of strains. Covers relation between mathematical theory of elasticity and technical mechanics; equilibrium of isotropic elastic solids and anisotropic solid bodies; nature of force transmission, Volterra's theory of dislocations; theory of elastic spheres in relation to tidal, rotational, gravitational effects on earth; general theory of bending; deformation of curved plates; buckling effects; much more. "The standard treatise on elasticity," American Math. Monthly. 4th revised edition. 76 figures. xviii + 643pp. 6½ x 9¼. S174 Paperbound \$2.95

## NUCLEAR PHYSICS, QUANTUM THEORY, RELATIVITY

**MESON PHYSICS**, R. E. Marshak. Presents basic theory, and results of experiments with emphasis on theoretical significance. Phenomena involving mesons as virtual transitions avoided, eliminating some of least satisfactory predictions of meson theory. Includes production study of  $\pi$  mesons at nonrelativistic nucleon energies contrasts between  $\pi$  and  $u$  mesons, phenomena associated with nuclear interaction of  $\pi$  mesons, etc. Presents early evidence for new classes of particles, indicates theoretical difficulties created by discovery of heavy mesons and hyperons. viii + 378pp. 5½ x 8. S500 Paperbound \$1.95

**THE FUNDAMENTAL PRINCIPLES OF QUANTUM MECHANICS, WITH ELEMENTARY APPLICATIONS**, E. C. Kemble. Inductive presentation, for graduate student, specialists in other branches of physics. Apparatus necessary beyond differential equations and advanced calculus developed as needed. Though general exposition of principles, hundreds of individual problems fully treated. "Excellent book . . . of great value to every student . . . rigorous and detailed mathematical discussion . . . has succeeded in keeping his presentation clear and understandable," Dr. Linus Pauling, J. of American Chemical Society. Appendices: calculus of variations, math. notes, etc. 611pp. 5½ x 8½. T472 Paperbound \$2.95

**WAVE PROPAGATION IN PERIODIC STRUCTURES**, L. Brillouin. General method, application to different problems: pure physics—scattering of X-rays in crystals, thermal vibration in crystal lattices, electronic motion in metals; problems in electrical engineering. Partial contents: elastic waves along 1-dimensional lattices of point masses. Propagation of waves along 1-dimensional lattices. Energy flow. 2, 3 dimensional lattices. Mathieu's equation. Matrices and propagation of waves along an electric line. Continuous electric lines. 131 illustrations. xii + 253pp. 5½ x 8. S34 Paperbound \$1.85

## DOVER SCIENCE BOOKS

**THEORY OF ELECTRONS AND ITS APPLICATION TO THE PHENOMENA OF LIGHT AND RADIANT HEAT**, H. Lorentz. Lectures delivered at Columbia Univ., by Nobel laureate. Unabridged, form historical coverage of theory of free electrons, motion, absorption of heat, Zeeman effect, optical phenomena in moving bodies, etc. 109 pages notes explain more advanced sections. 9 figures. 352pp. 5 $\frac{3}{8}$  x 8. S173 Paperbound \$1.85

**SELECTED PAPERS ON QUANTUM ELECTRODYNAMICS**, edited by J. Schwinger. Facsimiles of papers which established quantum electrodynamics; beginning to present position as part of larger theory. First book publication in any language of collected papers of Bethe, Bloch, Dirac, Dyson, Fermi, Feynman, Heisenberg, Kusch, Lamb, Oppenheimer, Pauli, Schwinger, Tomonaga, Weisskopf, Wigner, etc. 34 papers: 29 in English, 1 in French, 3 in German, 1 in Italian. Historical commentary by editor. xvii + 423pp. 6 $\frac{1}{8}$  x 9 $\frac{1}{4}$ . S444 Paperbound \$2.45

**FOUNDATIONS OF NUCLEAR PHYSICS**, edited by R. T. Beyer. 13 of the most important papers on nuclear physics reproduced in facsimile in the original languages; the papers most often cited in footnotes, bibliographies. Anderson, Curie, Joliot, Chadwick, Fermi, Lawrence, Cockroft, Hahn, Yukawa. Unparalleled bibliography: 122 double columned pages, over 4,000 articles, books, classified. 57 figures. 288pp. 6 $\frac{1}{8}$  x 9 $\frac{1}{4}$ . S19 Paperbound \$1.75

**THE THEORY OF GROUPS AND QUANTUM MECHANICS**, H. Weyl. Schroedinger's wave equation, de Broglie's waves of a particle, Jordan-Hoelder theorem, Lie's continuous groups of transformations, Pauli exclusion principle, quantization of Mawell-Dirac field equations, etc. Unitary geometry, quantum theory, groups, application of groups to quantum mechanics, symmetry permutation group, algebra of symmetric transformations, etc. 2nd revised edition. xxii + 422pp. 5 $\frac{3}{8}$  x 8. S268 Clothbound \$4.50  
S269 Paperbound \$1.95

**PHYSICAL PRINCIPLES OF THE QUANTUM THEORY**, Werner Heisenberg. Nobel laureate discusses quantum theory; his own work, Compton, Schroedinger, Wilson, Einstein, many others. For physicists, chemists, not specialists in quantum theory. Only elementary formulae considered in text; mathematical appendix for specialists. Profound without sacrificing clarity. Translated by C. Eckart, F. Hoyt. 18 figures. 192pp. 5 $\frac{3}{8}$  x 8. S113 Paperbound \$1.25

**INVESTIGATIONS ON THE THEORY OF THE BROWNIAN MOVEMENT**, Albert Einstein. Reprints from rare European journals, translated into English. 5 basic papers, including Elementary Theory of the Brownian Movement, written at request of Lorentz to provide a simple explanation. Translated by A. D. Cowper. Annotated, edited by R. Fürth. 33pp. of notes elucidate, give history of previous investigations. 62 footnotes. 124pp. 5 $\frac{3}{8}$  x 8. S304 Paperbound \$1.25

**THE PRINCIPLE OF RELATIVITY**, E. Einstein, H. Lorentz, M. Minkowski, H. Weyl. The 11 basic papers that founded the general and special theories of relativity, translated into English. 2 papers by Lorentz on the Michelson experiment, electromagnetic phenomena. Minkowski's "Space and Time," and Weyl's "Gravitation and Electricity." 7 epoch-making papers by Einstein: "Electromagnetics of Moving Bodies," "Influence of Gravitation in Propagation of Light," "Cosmological Considerations," "General Theory," 3 others. 7 diagrams. Special notes by A. Sommerfeld. 224pp. 5 $\frac{3}{8}$  x 8. S93 Paperbound \$1.75

## STATISTICS

**ELEMENTARY STATISTICS, WITH APPLICATIONS IN MEDICINE AND THE BIOLOGICAL SCIENCES**, F. E. Croxton. Based primarily on biological sciences, but can be used by anyone desiring introduction to statistics. Assumes no prior acquaintance, requires only modest knowledge of math. All basic formulas carefully explained, illustrated; all necessary reference tables included. From basic terms and concepts, proceeds to frequency distribution, linear, non-linear, multiple correlation, etc. Contains concrete examples from medicine, biology. 101 charts. 57 tables. 14 appendices. iv + 376pp. 5 $\frac{3}{8}$  x 8. S506 Paperbound \$1.95

**ANALYSIS AND DESIGN OF EXPERIMENTS**, H. B. Mann. Offers method for grasping analysis of variance, variance design quickly. Partial contents: Chi-square distribution, analysis of variance distribution, matrices, quadratic forms, likelihood ratio tests, test of linear hypotheses, power of analysis, Galois fields, non-orthogonal data, interblock estimates, etc. 15pp. of useful tables. x + 195pp. 5 x 7 $\frac{3}{8}$ . S180 Paperbound \$1.45

**FREQUENCY CURVES AND CORRELATION**, W. P. Elderton. 4th revised edition of standard work on classical statistics. Practical, one of few books constantly referred to for clear presentation of basic material. Partial contents: Frequency Distributions; Pearsons Frequency Curves; Theoretical Distributions; Standard Errors; Correlation Ratio—Contingency; Corrections for Moments, Beta, Gamma Functions; etc. Key to terms, symbols. 25 examples. 40 tables. 16 figures. xi + 272pp. 5 $\frac{1}{2}$  x 8 $\frac{1}{2}$ . Clothbound \$1.49



## HYDRODYNAMICS, ETC.

**HYDRODYNAMICS**, Horace Lamb. Standard reference work on dynamics of liquids and gases. Fundamental theorems, equations, methods, solutions, background for classical hydrodynamics. Chapters: Equations of Motion, Integration of Equations in Special Cases, Vortex Motion, Tidal Waves, Rotating Masses of Liquids, etc. Excellently planned, arranged, Clear, lucid presentation. 6th enlarged, revised edition. Over 900 footnotes, mostly bibliographical. 119 figures. xv + 738pp. 6 $\frac{1}{2}$  x 9 $\frac{1}{4}$ . S256 Paperbound \$2.95

**HYDRODYNAMICS, A STUDY OF LOGIC, FACT, AND SIMILITUDE**, Garrett Birkhoff. A stimulating application of pure mathematics to an applied problem. Emphasis is on correlation of theory and deduction with experiment. Examines recently discovered paradoxes, theory of modelling and dimensional analysis, paradox and error in flows and free boundary theory. Classical theory of virtual mass derived from homogenous spaces; group theory applied to fluid mechanics. 20 figures, 3 plates. xiii + 186pp. 5 $\frac{3}{8}$  x 8. S22 Paperbound \$1.85

**HYDRODYNAMICS**, H. Dryden, F. Murhaghan, H. Bateman. Published by National Research Council, 1932. Complete coverage of classical hydrodynamics, encyclopedic in quality. Partial contents: physics of fluids, motion, turbulent flow, compressible fluids, motion in 1, 2, 3 dimensions; laminar motion, resistance of motion through viscous fluid, eddy viscosity, discharge of gases, flow past obstacles, etc. Over 2900-item bibliography. 23 figures. 634pp. 5 $\frac{3}{8}$  x 8. S303 Paperbound \$2.75

## ACOUSTICS AND OPTICS

**PRINCIPLES OF PHYSICAL OPTICS**, Ernst Mach. Classical examination of propagation of light, color, polarization, etc. Historical, philosophical treatment unequalled for breadth and readability. Contents: Rectilinear propagation, reflection, refraction, dioptrics, composition of light, periodicity, theory of interference, polarization, mathematical representation of properties, etc. 279 illustrations. 10 portraits. 324pp. 5 $\frac{3}{8}$  x 8. S170 Paperbound \$1.75

**THE THEORY OF SOUND**, Lord Rayleigh. Written by Nobel laureate, classical methods here will cover most vibrating systems likely to be encountered in practice. Complete coverage of experimental, mathematical aspects. Partial contents: Harmonic motions, lateral vibrations of bars, curved plates or shells, applications of Laplace's functions to acoustical problems, fluid friction, etc. First low-priced edition of this great reference-study work. Historical introduction by R. B. Lindsay. 1040pp. 97 figures. 5 $\frac{3}{8}$  x 8. S292, S293, Two volume set, paperbound \$4.00

**THEORY OF VIBRATIONS**, N. W. McLachlan. Based on exceptionally successful graduate course, Brown University. Discusses linear systems having 1 degree of freedom, forced vibrations of simple linear systems, vibration of flexible strings, transverse vibrations of bars and tubes, of circular plate, sound waves of finite amplitude, etc. 99 diagrams. 160pp. 5 $\frac{3}{8}$  x 8. S190 Paperbound \$1.35

**APPLIED OPTICS AND OPTICAL DESIGN**, A. E. Conrady. Thorough systematic presentation of physical and mathematical aspects, limited mostly to "real optics." Stresses practical problem of maximum aberration permissible without affecting performance. Ordinary ray tracing methods; complete theory ray tracing methods, primary aberrations; enough higher aberration to design telescopes, low powered microscopes, photographic equipment. Covers fundamental equations, extra-axial image points, transverse chromatic aberration, angular magnification, similar topics. Tables of functions of N. Over 150 diagrams. x + 518pp. 5 $\frac{3}{8}$  x 8 $\frac{1}{2}$ . S366 Paperbound \$2.98

**RAYLEIGH'S PRINCIPLE AND ITS APPLICATIONS TO ENGINEERING**, G. Temple, W. Bickley. Rayleigh's principle developed to provide upper, lower estimates of true value of fundamental period of vibrating system, or condition of stability of elastic system. Examples, rigorous proofs. Partial contents: Energy method of discussing vibrations, stability. Perturbation theory, whirling of uniform shafts. Proof, accuracy, successive approximations, applications of Rayleigh's theory. Numerical, graphical methods. Ritz's method. 22 figures. ix + 156pp. 5 $\frac{3}{8}$  x 8. S307 Paperbound \$1.50

**OPTICKS**, Sir Isaac Newton. In its discussion of light, reflection, color, refraction, theories of wave and corpuscular theories of light, this work is packed with scores of insights and discoveries. In its precise and practical discussions of construction of optical apparatus, contemporary understanding of phenomena, it is truly fascinating to modern scientists. Foreword by Albert Einstein. Preface by I. B. Cohen, Harvard. 7 pages of portraits, facsimile pages, letters, etc. cxvi + 414pp. 5 $\frac{3}{8}$  x 8. S205 Paperbound \$2.00

## DOVER SCIENCE BOOKS

**ON THE SENSATIONS OF SOUND, Hermann Helmholtz.** Using acoustical physics, physiology, experiment, history of music, covers entire gamut of musical tone: relation of music science to acoustics, physical vs. physiological acoustics, vibration, resonance, tonality, progression of parts, etc. 33 appendixes on various aspects of sound, physics, acoustics, music, etc. Translated by A. J. Ellis. New introduction by H. Margenau, Yale. 68 figures. 43 musical passages analyzed. Over 100 tables. xix + 576pp. 6½ x 9¼.  
\$114 Clothbound \$4.95

## ELECTROMAGNETICS, ENGINEERING, TECHNOLOGY

**INTRODUCTION TO RELAXATION METHODS, F. S. Shaw.** Describes almost all manipulative resources of value in solution of differential equations. Treatment is mathematical rather than physical. Extends general computational process to include almost all branches of applied math and physics. Approximate numerical methods are demonstrated, although high accuracy is obtainable without undue expenditure of time. 48pp. of tables for computing irregular star first and second derivatives, irregular star coefficients for second order equations, for fourth order equations. "Useful. . . . exposition is clear, simple . . . no previous acquaintance with numerical methods is assumed." Science Progress. 253 diagrams. 72 tables. 400pp. 5¾ x 8.  
\$244 Paperbound \$2.45

**THE ELECTROMAGNETIC FIELD, M. Mason, W. Weaver.** Used constantly by graduate engineers. Vector methods exclusively; detailed treatment of electrostatics, expansion methods, with tables converting any quantity into absolute electromagnetic, absolute electrostatic, practical units. Discrete charges, ponderable bodies. Maxwell field equations, etc. 416pp. 5¾ x 8.  
\$185 Paperbound \$2.00

**ELASTICITY, PLASTICITY AND STRUCTURE OF MATTER, R. Houwink.** Standard treatise on rheological aspects of different technically important solids: crystals, resins, textiles, rubber, clay, etc. Investigates general laws for deformations; determines divergences. Covers general physical and mathematical aspects of plasticity, elasticity, viscosity. Detailed examination of deformations, internal structure of matter in relation to elastic, plastic behaviour, formation of solid matter from a fluid, etc. Treats glass, asphalt, balata, proteins, baker's dough, others. 2nd revised, enlarged edition. Extensive revised bibliography in over 500 footnotes. 214 figures. xvii + 368pp. 6 x 9¼.  
\$385 Paperbound \$2.45

**DESIGN AND USE OF INSTRUMENTS AND ACCURATE MECHANISM, T. N. Whitehead.** For the instrument designer, engineer; how to combine necessary mathematical abstractions with independent observations of actual facts. Partial contents: instruments and their parts, theory of errors, systematic errors, probability, short period errors, erratic errors, design precision, kinematic, semikinematic design, stiffness, planning of an instrument, human factor, etc. 85 photos, diagrams. xii + 288pp. 5¾ x 8.  
\$270 Paperbound \$1.95

**APPLIED HYDRO- AND AEROMECHANICS, L. Prandtl, O. G. Tietjens.** Presents, for most part, methods valuable to engineers. Flow in pipes, boundary layers, airfoil theory, entry conditions, turbulent flow, boundary layer determining drag from pressure and velocity, etc. "Will be welcomed by all students of aerodynamics." Nature. Unabridged, unaltered. An Engineering Society Monograph, 1934. Index. 226 figures. 28 photographic plates illustrating flow patterns. xvi + 311pp. 5¾ x 8.  
\$375 Paperbound \$1.85

**FUNDAMENTALS OF HYDRO- AND AEROMECHANICS, L. Prandtl, O. G. Tietjens.** Standard work, based on Prandtl's lectures at Goettingen. Wherever possible hydrodynamics theory is referred to practical considerations in hydraulics, unifying theory and experience. Presentation extremely clear. Though primarily physical, proofs are rigorous and use vector analysis to a great extent. An Engineering Society Monograph, 1934. "Still recommended as an excellent introduction to this area," Physikalishe Blätter. 186 figures. xvi + 270pp. 5¾ x 8.  
\$374 Paperbound \$1.85

**GASEOUS CONDUCTORS: THEORY AND ENGINEERING APPLICATIONS, J. D. Cobine.** Indispensable text, reference, to gaseous conduction phenomena, with engineering viewpoint prevailing throughout. Studies kinetic theory of gases, ionization, emission phenomena; gas breakdown, spark characteristics, glow, discharges; engineering applications in circuit interrupters, rectifiers, etc. Detailed treatment of high pressure arcs (Suitts); low pressure arcs (Langmuir, Tonks). Much more. "Well organized, clear, straightforward." Tonks, Review of Scientific Instruments. 83 practice problems. Over 600 figures. 58 tables. xx + 606pp. 5¾ x 8.  
\$442 Paperbound \$2.75

**PHOTOELASTICITY: PRINCIPLES AND METHODS, H. T. Jessop, F. C. Harris.** For engineer, specific methods of stress analysis. Latest time-saving methods of checking calculations in 2-dimensional design problems, new techniques for stresses in 3 dimensions, lucid description of optical systems used in practical photoelasticity. Useful suggestions, hints based on on-the-job experience included. Partial contents: strain, stress-strain relations, circular disc under thrust along diameter, rectangular block with square hole under vertical thrust, simply supported rectangular beam under central concentrated load, etc. Theory held to minimum, no advanced mathematical training needed. 164 illustrations. viii + 184pp. 6¼ x 9¼.  
\$137 Clothbound \$3.75

**MICROWAVE TRANSMISSION DESIGN DATA, T. Moreno.** Originally classified, now rewritten, enlarged (14 new chapters) under auspices of Sperry Corp. Of immediate value or reference use to radio engineers, systems designers, applied physicists, etc. Ordinary transmission line theory; attenuation; parameters of coaxial lines; flexible cables; tuneable wave guide impedance transformers; effects of temperature, humidity; much more. "Packed with information . . . theoretical discussions are directly related to practical questions," U. of Royal Naval Scientific Service. Tables of dielectrics, flexible cable, etc. ix + 248pp. 5½ x 8.  
S549 Paperbound \$1.50

**THE THEORY OF THE PROPERTIES OF METALS AND ALLOYS, H. F. Mott, H. Jones.** Quantum methods develop mathematical models showing interrelationship of fundamental chemical phenomena with crystal structure, electrical, optical properties, etc. Examines electron motion in applied field, cohesion, heat capacity, refraction, noble metals, transition and di-valent metals, etc. "Exposition is as clear . . . mathematical treatment as simple and reliable as we have become used to expect of . . . Prof. Mott," Nature. 138 figures. xiii + 320pp. 5¾ x 8.  
S456 Paperbound \$1.85

**THE MEASUREMENT OF POWER SPECTRA FROM THE POINT OF VIEW OF COMMUNICATIONS ENGINEERING, R. B. Blackman, J. W. Tukey.** Pathfinding work reprinted from "Bell System Technical Journal." Various ways of getting practically useful answers in power spectra measurement, using results from both transmission and statistical estimation theory. Treats: Autocovariance, Functions and Power Spectra, Distortion, Heterodyne Filtering, Smoothing, Decimation Procedures, Transversal Filtering, much more. Appendix reviews fundamental Fourier techniques. Index of notation. Glossary of terms. 24 figures, 12 tables. 192pp. 5¾ x 8½.  
S507 Paperbound \$1.85

**TREATISE ON ELECTRICITY AND MAGNETISM, James Clerk Maxwell.** For more than 80 years a seemingly inexhaustible source of leads for physicists, mathematicians, engineers. Total of 1082pp. on such topics as Measurement of Quantities, Electrostatics, Elementary Mathematical Theory of Electricity, Electrical Work and Energy in a System of Conductors, General Theorems, Theory of Electrical Images, Electrolysis, Conduction, Polarization, Dielectrics, Resistance, much more. "The greatest mathematical physicist since Newton," Sir James Jeans. 3rd edition. 107 figures, 21 plates. 1082pp. 5¾ x 8.  
S186 Clothbound \$4.95

## CHEMISTRY AND PHYSICAL CHEMISTRY

**THE PHASE RULE AND ITS APPLICATIONS, Alexander Findlay.** Covers chemical phenomena of 1 to 4 multiple component systems, the "standard work on the subject" (Nature). Completely revised, brought up to date by A. N. Campbell, N. O. Smith. New material on binary, tertiary liquid equilibria, solid solutions in ternary systems, quinary systems of salts, water, etc. Completely revised to triangular coordinates in ternary systems, clarified graphic representation, solid models, etc. 9th revised edition. 236 figures. 505 footnotes, mostly bibliographic. xii + 449pp. 5¾ x 8.  
S92 Paperbound \$2.45

**DYNAMICAL THEORY OF GASES, James Jeans.** Divided into mathematical, physical chapters for convenience of those not expert in mathematics. Discusses mathematical theory of gas in steady state, thermodynamics, Boltzmann, Maxwell, kinetic theory, quantum theory, exponentials, etc. "One of the classics of scientific writing . . . as lucid and comprehensive an exposition of the kinetic theory as has ever been written," J. of Institute of Engineers. 4th enlarged edition, with new material on quantum theory, quantum dynamics, etc. 28 figures. 444pp. 6¼ x 9¼.  
S136 Paperbound \$2.45

**POLAR MOLECULES, Pieter Debye.** Nobel laureate offers complete guide to fundamental electrostatic field relations, polarizability, molecular structure. Partial contents: electric intensity, displacement, force, polarization by orientation, molar polarization, molar refraction, halogen-hydrides, polar liquids, ionic saturation, dielectric constant, etc. Special chapter considers quantum theory. "Clear and concise . . . coordination of experimental results with theory will be readily appreciated," Electronics Industries. 172pp. 5¾ x 8.  
S63 Clothbound \$3.50  
S64 Paperbound \$1.50

**ATOMIC SPECTRA AND ATOMIC STRUCTURE, G. Herzberg.** Excellent general survey for chemists, physicists specializing in other fields. Partial contents: simplest line spectra, elements of atomic theory; multiple structure of line spectra, electron spin; building-up principle, periodic system of elements; finer details of atomic spectra; hyperfine structure of spectral lines; some experimental results and applications. 80 figures. 20 tables. xiii + 257pp. 5¾ x 8.  
S115 Paperbound \$1.95

**TREATISE ON THERMODYNAMICS, Max Planck.** Classic based on his original papers. Brilliant concepts of Nobel laureate make no assumptions regarding nature of heat, rejects earlier approaches of Helmholtz, Maxwell, to offer uniform point of view for entire field. Seminal work by founder of quantum theory, deducing new physical, chemical laws. A standard text, an excellent introduction to field for students with knowledge of elementary chemistry, physics, calculus. 3rd English edition. xvi + 297pp. 5¾ x 8.  
S219 Paperbound \$1.75

## DOVER SCIENCE BOOKS

**KINETIC THEORY OF LIQUIDS, J. Frenkel.** Regards kinetic theory of liquids as generalization, extension of theory of solid bodies, covers all types of arrangements of solids; thermal displacements of atoms; interstitial atoms, ions; orientational, rotational motion of molecules; transition between states of matter. Mathematical theory developed close to physical subject matter. "Discussed in a simple yet deeply penetrating fashion . . . will serve as seeds for a great many basic and applied developments in chemistry," *J. of the Amer. Chemical Soc.* 216 bibliographical footnotes. 55 figures. xi + 485pp. 5 $\frac{3}{8}$  x 8.

\$94 Clothbound \$3.95  
\$95 Paperbound \$2.45

## ASTRONOMY

**OUT OF THE SKY, H. H. Nininger.** Non-technical, comprehensive introduction to "meteoritics"—science concerned with arrival of matter from outer space. By one of world's experts on meteorites, this book defines meteors and meteorites; studies fireball clusters and processes, meteorite composition, size, distribution, showers, explosions, origins, much more. viii + 336pp. 5 $\frac{3}{8}$  x 8.

T519 Paperbound \$1.85

**AN INTRODUCTION TO THE STUDY OF STELLAR STRUCTURE, S. Chandrasekhar.** Outstanding treatise on stellar dynamics by one of greatest astro-physicists. Examines relationship between loss of energy, mass, and radius of stars in steady state. Discusses thermodynamic laws from Caratheodory's axiomatic standpoint; adiabatic, polytropic laws; work of Ritter, Emden, Kelvin, etc.; Stroemgren envelopes as starter for theory of gaseous stars; Gibbs statistical mechanics (quantum); degenerate stellar configuration, theory of white dwarfs; etc. "Highest level of scientific merit," *Bulletin. Amer. Math. Soc.* 33 figures. 509pp. 5 $\frac{3}{8}$  x 8.

S413 Paperbound \$2.75

**LES MÉTHODES NOUVELLES DE LA MÉCANIQUE CÉLESTE, H. Poincaré.** Complete French text of one of Poincaré's most important works. Revolutionized celestial mechanics: first use of integral invariants, first major application of linear differential equations, study of periodic orbits, lunar motion and Jupiter's satellites, three body problem, and many other important topics. "Started a new era . . . so extremely modern that even today few have mastered his weapons," *E. T. Bell.* 3 volumes. Total 1282pp. 6 $\frac{1}{4}$  x 9 $\frac{1}{4}$ .

Vol. 1 S401 Paperbound \$2.75

Vol. 2 S402 Paperbound \$2.75

Vol. 3 S403 Paperbound \$2.75

The set \$7.50

**THE REALM OF THE NEBULAE, E. Hubble.** One of the great astronomers of our time presents his concept of "island universes," and describes its effect on astronomy. Covers velocity-distance relation; classification, nature, distances, general field of nebulae; cosmological theories; nebulae in the neighborhood of the Milky way; etc. 39 photos, including velocity-distance relations shown by spectrum comparison. "One of the most progressive lines of astronomical research," *The Times, London.* New Introduction by A. Sandage. 55 illustrations. xxiv + 201pp. 5 $\frac{3}{8}$  x 8.

S455 Paperbound \$1.50

**HOW TO MAKE A TELESCOPE, Jean Texereau.** Design, build an f/6 or f/8 Newtonian type reflecting telescope, with altazimuth Couder mounting, suitable for planetary, lunar, and stellar observation. Covers every operation step-by-step, every piece of equipment. Discusses basic principles of geometric and physical optics (unnecessary to construction), comparative merits of reflectors, refractors. A thorough discussion of eyepieces, finders, grinding, installation, testing, etc. 241 figures, 38 photos, show almost every operation and tool. Potential errors are anticipated. Foreword by A. Couder. Sources of supply. xiii + 191pp. 6 $\frac{1}{4}$  x 10.

T464 Clothbound \$3.50

## BIOLOGICAL SCIENCES

**THE BIOLOGY OF THE AMPHIBIA, G. K. Noble,** Late Curator of Herpetology at Am. Mus. of Nat. Hist. Probably most used text on amphibia, most comprehensive, clear, detailed. 19 chapters, 85 page supplement: development; heredity; life history; speciation; adaptation; sex, integument, respiratory, circulatory, digestive, muscular, nervous systems; instinct, intelligence, habits, economic value classification, environment relationships, etc. "Nothing comparable to it!" *C. H. Pope,* curator of Amphibia, Chicago Mus. of Nat. Hist. 1047 item bibliography. 174 illustrations. 600pp. 5 $\frac{3}{8}$  x 8.

S206 Paperbound \$2.98

**THE ORIGIN OF LIFE, A. I. Oparin.** A classic of biology. This is the first modern statement of theory of gradual evolution of life from nitrocarbon compounds. A brand-new evaluation of Oparin's theory in light of later research, by Dr. S. Margulis, University of Nebraska. xxv + 270pp. 5 $\frac{3}{8}$  x 8.

S213 Paperbound \$1.75

**THE BIOLOGY OF THE LABORATORY MOUSE**, edited by G. D. Snell. Prepared in 1941 by staff of Roscoe B. Jackson Memorial Laboratory, still the standard treatise on the mouse, assembling enormous amount of material for which otherwise you spend hours of research. Embryology, reproduction, histology, spontaneous neoplasms, gene and chromosomes mutations, genetics of spontaneous tumor formations, of tumor transplantation, endocrine secretion and tumor formation, milk influence and tumor formation, inbred, hybrid animals, parasites, infectious diseases, care and recording. "A wealth of information of vital concern. . . recommended to all who could use a book on such a subject." Nature. Classified bibliography of 1122 items. 172 figures, including 128 photos. ix + 497pp. 6¼ x 9¼. S248 Clothbound \$6.00

**THE TRAVELS OF WILLIAM BARTRAM**, edited by Mark Van Doran. Famous source-book of American anthropology, natural history, geography, is record kept by Bartram in 1770's on travels through wilderness of Florida, Georgia, Carolinas. Containing accurate, beautiful descriptions of Indians, settlers, fauna, flora, it is one of finest pieces of Americana ever written. 13 original illustrations. 448pp. 5½ x 8. T13 Paperbound \$2.00

**BEHAVIOUR AND SOCIAL LIFE OF THE HONEYBEE**, Ronald Ribbands. Outstanding scientific study; a compendium of practically everything known of social life of honeybee. Stresses behaviour of individual bees in field, hive. Extends von Frisch's experiments on communication among bees. Covers perception of temperature, gravity, distance, vibration; sound production; glands; structural differences; wax production; temperature regulation; recognition, communication; drifting, mating behaviour, other highly interesting topics. "This valuable work is sure of a cordial reception by laymen, beekeepers and scientists," Prof. Karl von Frisch, Brit. J. of Animal Behaviour. Bibliography of 690 references. 127 diagrams, graphs, sections of bee anatomy, fine photographs. 352pp. S410 Clothbound \$4.50

**ELEMENTS OF MATHEMATICAL BIOLOGY**, A. J. Lotka. Pioneer classic, 1st major attempt to apply modern mathematical techniques on large scale to phenomena of biology, biochemistry, psychology, ecology, similar life sciences. Partial contents: Statistical meaning of irreversibility; Evolution as redistribution; Equations of kinetics of evolving systems; Chemical, inter-species equilibrium; parameters of state; Energy transformers of nature, etc. Can be read with profit by even those having no advanced math; unsurpassed as study-reference. Formerly titled "Elements of Physical Biology." 72 figures. xxx + 460pp. 5½ x 8. S346 Paperbound \$2.45

**TREES OF THE EASTERN AND CENTRAL UNITED STATES AND CANADA**, W. M. Harlow. Serious middle-level text covering more than 140 native trees, important escapes, with information on general appearance, growth habit, leaf forms, flowers, fruit, bark, commercial use, distribution, habitat, woodlore, etc. Keys within text enable you to locate various species easily, to know which have edible fruit, much more useful, interesting information. "Well illustrated to make identification very easy," Standard Cat. for Public Libraries. Over 600 photographs, figures. xiii + 288pp. 5½ x 6½. T395 Paperbound \$1.35

**FRUIT KEY AND TWIG KEY TO TREES AND SHRUBS** (Fruit key to Northeastern Trees, Twig key to Deciduous Woody Plants of Eastern North America), W. M. Harlow. Only guides with photographs of every twig, fruit described. Especially valuable to novice. Fruit key (both deciduous trees, evergreens) has introduction on seeding, organs involved, types, habits. Twig key introduction treats growth, morphology. In keys proper, identification is almost automatic. Exceptional work, widely used in university courses, especially useful for identification in winter, or from fruit or seed only. Over 350 photos, up to 3 times natural size. Index of common, scientific names, in each key. xvii + 125pp. 5½ x 8½. T511 Paperbound \$1.25

**INSECT LIFE AND INSECT NATURAL HISTORY**, S. W. Frost. Unusual for emphasizing habits, social life, ecological relations of insects rather than more academic aspects of classification, morphology. Prof. Frost's enthusiasm and knowledge are everywhere evident as he discusses insect associations, specialized habits like leaf-rolling, leaf mining, case-making, the gall insects, boring insects, etc. Examines matters not usually covered in general works: insects as human food; insect music, musicians; insect response to radio waves; use of insects in art, literature. "Distinctly different, possesses an individuality all its own," Journal of Forestry. Over 700 illustrations. Extensive bibliography. x + 524pp. 5½ x 8. T519 Paperbound \$2.49

**A WAY OF LIFE, AND OTHER SELECTED WRITINGS**, Sir William Osler. Physician, humanist, Osler discusses brilliantly Thomas Browne, Gui Patin, Robert Burton, Michael Servetus, William Beaumont, Laennec. Includes such favorite writing as title essay, "The Old Humanities and the New Science," "Books and Men," "The Student Life," 6 more of his best discussions of philosophy, literature, religion. "The sweep of his mind and interests embraced every phase of human activity," G. L. Keynes. 5 photographs. Introduction by G. L. Keynes, M.D., F.R.C.S. xx + 278pp. 5½ x 8. T488 Paperbound \$1.50

**THE GENETICAL THEORY OF NATURAL SELECTION**, R. A. Fisher. 2nd revised edition of vital reviewing of Darwin's Selection Theory in terms of particulate inheritance, by one of greatest authorities on experimental, theoretical genetics. Theory stated in mathematical form. Special features of particulate inheritance are examined: evolution of dominance, maintenance of specific variability, mimicry, sexual selection, etc. 5 chapters on man's special circumstances as a social animal. 16 photographs. x + 310pp. 5½ x 8. S466 Paperbound \$1.85

## DOVER SCIENCE BOOKS

**THE AUTOBIOGRAPHY OF CHARLES DARWIN, AND SELECTED LETTERS**, edited by Francis Darwin. Darwin's own record of early life; historic voyage aboard "Beagle;" furor surrounding evolution, his replies; reminiscences of his son. Letters to Henslow, Lyell, Hooker, Huxley, Wallace, Kingsley, etc., and thoughts on religion, vivisection. We see how he revolutionized geology with concepts of ocean subsidence; how his great books on variation of plants and animals, primitive man, expression of emotion among primates, plant fertilization, carnivorous plants, protective coloration, etc., came into being. 365pp. 5 3/8 x 8.

T479 Paperbound \$1.65

**ANIMALS IN MOTION**, Eadweard Muybridge. Largest, most comprehensive selection of Muybridge's famous action photos of animals, from his "Animal Locomotion." 3919 high-speed shots of 34 different animals, birds, in 123 types of action; horses, mules, oxen, pigs, goats, camels, elephants, dogs, cats, guinea pigs, sloths, lions, tigers, jaguars, raccoons, baboons, deer, elk, gnus, kangaroos, many others, walking, running, flying, leaping. Horse alone in over 40 ways. Photos taken against ruled backgrounds; most actions taken from 3 angles at once: 90°, 60°, rear. Most plates original size. Of considerable interest to scientists as biology classic, records of actual facts of natural history, physiology. "Really marvelous series of plates," Nature. "Monumental work," Waldemar Kaempffert. Edited by L. S. Brown, 74 page introduction on mechanics of motion. 340pp. of plates. 3919 photographs. 416pp. Deluxe binding, paper. (Weight: 4 1/2 lbs.) 7 3/4 x 10 1/2.

T203 Clothbound \$10.00

**THE HUMAN FIGURE IN MOTION**, Eadweard Muybridge. New edition of great classic in history of science and photography, largest selection ever made from original Muybridge photos of human action: 4789 photographs, illustrating 163 types of motion: walking, running, lifting, etc. in time-exposure sequence photos at speeds up to 1/6000th of a second. Men, women, children, mostly undraped, showing bone, muscle positions against ruled backgrounds, mostly taken at 3 angles at once. Not only was this a great work of photography, acclaimed by contemporary critics as work of genius, but it was also a great 19th century landmark in biological research. Historical introduction by Prof. Robert Taft, U. of Kansas. Plates original size, full of detail. Over 500 action strips. 407pp. 7 3/4 x 10 1/2. Deluxe edition.

T204 Clothbound \$10.00

**AN INTRODUCTION TO THE STUDY OF EXPERIMENTAL MEDICINE**, Claude Bernard. 90-year old classic of medical science, only major work of Bernard available in English, records his efforts to transform physiology into exact science. Principles of scientific research illustrated by specified case histories from his work; roles of chance, error, preliminary false conclusion, in leading eventually to scientific truth; use of hypothesis. Much of modern application of mathematics to biology rests on foundation set down here. "The presentation is polished . . . reading is easy," Revue des questions scientifiques. New foreword by Prof. I. B. Cohen, Harvard U. xxv + 266pp. 5 3/8 x 8.

T400 Paperbound \$1.50

**STUDIES ON THE STRUCTURE AND DEVELOPMENT OF VERTEBRATES**, E. S. Goodrich. Definitive study by greatest modern comparative anatomist. Exhaustive morphological, phylogenetic expositions of skeleton, fins, limbs, skeletal visceral arches, labial cartilages, visceral clefts, gills, vascular, respiratory, excretory, peripheral nervous systems, etc., from fish to higher mammals. "For many a day this will certainly be the standard textbook on Vertebrate Morphology in the English language," Journal of Anatomy. 754 illustrations. 69 page biographical study by C. C. Hardy. Bibliography of 1186 references. Two volumes, total 906pp. 5 3/8 x 8.

Two vol. set \$449, 450 Paperbound \$5.00

## EARTH SCIENCES

**THE EVOLUTION OF IGNEOUS ROCKS**, N. L. Bowen. Invaluable serious introduction applies techniques of physics, chemistry to explain igneous rock diversity in terms of chemical composition, fractional crystallization. Discusses liquid immiscibility in silicate magmas, crystal sorting, liquid lines of descent, fractional resorption of complex minerals, petrogen, etc. Of prime importance to geologists, mining engineers; physicists, chemists working with high temperature, pressures. "Most important," Times, London. 263 bibliographic notes. 82 figures. xviii + 334pp. 5 3/8 x 8.

S311 Paperbound \$1.85

**GEOGRAPHICAL ESSAYS**, M. Davis. Modern geography, geomorphology rest on fundamental work of this scientist. 26 famous essays present most important theories, field researches. Partial contents: Geographical Cycle; Plains of Marine, Subaerial Denudation; The Penplain; Rivers, Valleys of Pennsylvania; Outline of Cape Cod; Sculpture of Mountains by Glaciers; etc. "Long the leader and guide," Economic Geography. "Part of the very texture of geography . . . models of clear thought," Geographic Review. 130 figures. vi + 777pp. 5 3/8 x 8.

S383 Paperbound \$2.95

**URANIUM PROSPECTING**, H. L. Barnes. For immediate practical use, professional geologist considers uranium ores, geological occurrences, field conditions, all aspects of highly profitable occupation. "Helpful information . . . easy-to-use, easy-to-find style," Geotimes. x + 117pp. 5 3/8 x 8.

T309 Paperbound \$1.00

## CATALOGUE OF

**DE RE METALLICA**, Georgius Agricola. 400 year old classic translated, annotated by former President Herbert Hoover. 1st scientific study of mineralogy, mining, for over 200 years after its appearance in 1556 the standard treatise. 12 books, exhaustively annotated, discuss history of mining, selection of sites, types of deposits, making pits, shafts, ventilating, pumps, crushing machinery; assaying, smelting, refining metals; also salt alum, nitre, glass making. Definitive edition, with all 289 16th century woodcuts of original. Biographical, historical introductions. Bibliography, survey of ancient authors. Indexes. A fascinating book for anyone interested in art, history of science, geology, etc. Deluxe Edition. 289 illustrations. 672pp. 6¾ x 10. Library cloth. S6 Clothbound \$10.00

**INTERNAL CONSTITUTION OF THE EARTH**, edited by Beno Gutenberg. Prepared for National Research Council, this is a complete, thorough coverage of earth origins, continent formation, nature and behaviour of earth's core, petrology of crust, cooling forces in core, seismic and earthquake material, gravity, elastic constants, strain characteristics, similar topics. "One is filled with admiration . . . a high standard . . . there is no reader who will not learn something from this book." London, Edinburgh, Dublin, Philosophic Magazine. Largest Bibliography in print: 1127 classified items. Table of constants. 43 diagrams. 439pp. 6¼ x 9¼. S414 Paperbound \$2.45

**THE BIRTH AND DEVELOPMENT OF THE GEOLOGICAL SCIENCES**, F. D. Adams. Most thorough history of earth sciences ever written. Geological thought from earliest times to end of 19th century, covering over 300 early thinkers and systems; fossils and their explanation, vulcanists vs. neptunists, figured stones and paleontology, generation of stones, dozens of similar topics. 91 illustrations, including Medieval, Renaissance woodcuts, etc. 632 footnotes, mostly bibliographical. 511pp. 5¾ x 8. T5 Paperbound \$2.00

**HYDROLOGY**, edited by O. E. Meinzer, prepared for the National Research Council. Detailed, complete reference library on precipitation, evaporation, snow, snow surveying, glaciers, lakes, infiltration, soil moisture, ground water, runoff, drought, physical changes produced by water hydrology of limestone terranes, etc. Practical in application, especially valuable for engineers. 24 experts have created "the most up-to-date, most complete treatment of the subject," Am. Assoc. of Petroleum Geologists. 165 illustrations. xi + 712pp. 6¼ x 9¼. S191 Paperbound \$2.95

## LANGUAGE AND TRAVEL AIDS FOR SCIENTISTS

### SAY IT language phrase books

"**SAY IT**" in the foreign language of your choice! We have sold over ½ million copies of these popular, useful language books. They will not make you an expert linguist overnight, but they do cover most practical matters of everyday life abroad.

Over 1000 useful phrases, expressions, additional variants, substitutions.

Modern! Useful! Hundreds of phrases not available in other texts: "Nylon," "air-conditioned," etc.

The ONLY inexpensive phrase book completely indexed. Everything is available at a flip of your finger, ready to use.

Prepared by native linguists, travel experts.

Based on years of travel experience abroad.

May be used by itself, or to supplement any other text or course. Provides a living element. Used by many colleges, institutions: Hunter College; Barnard College; Army Ordinance School, Aberdeen; etc.

Available, 1 book per language:

Danish (T818) 75¢  
Dutch (T817) 75¢  
English (for German-speaking people) (T801) 60¢  
English (for Italian-speaking people) (T816) 60¢  
English (for Spanish-speaking people) (T802) 60¢  
Esperanto (T820) 75¢  
French (T803) 60¢  
German (T804) 60¢  
Modern Greek (T813) 75¢  
Hebrew (T805) 60¢

Italian (T806) 60¢  
Japanese (T807) 75¢  
Norwegian (T814) 75¢  
Russian (T810) 75¢  
Spanish (T811) 60¢  
Turkish (T821) 75¢  
Yiddish (T815) 75¢  
Swedish (T812) 75¢  
Polish (T808) 75¢  
Portuguese (T809) 75¢

## DOVER SCIENCE BOOKS

**MONEY CONVERTER AND TIPPING GUIDE FOR EUROPEAN TRAVEL**, C. Vomacka. Purse-size hand-book crammed with information on currency regulations, tipping for every European country, including Israel, Turkey, Czechoslovakia, Rumania, Egypt, Russia, Poland. Telephone, postal rates; duty-free imports, passports, visas, health certificates; foreign clothing sizes; weather tables. What, when to tip. 5th year of publication. 128pp. 3½ x 5¼. T260 Paperbound 60¢

**NEW RUSSIAN-ENGLISH AND ENGLISH-RUSSIAN DICTIONARY**, M. A. O'Brien. Unusually comprehensive guide to reading, speaking, writing Russian, for both advanced, beginning students. Over 70,000 entries in new orthography, full information on accentuation, grammatical classifications. Shades of meaning, idiomatic uses, colloquialisms, tables of irregular verbs for both languages. Individual entries indicate stems, transitivity, perfective, imperfective aspects, conjugation, sound changes, accent, etc. Includes pronunciation instruction. Used at Harvard, Yale, Cornell, etc. 738pp. 5¾ x 8. T208 Paperbound \$ 2.00

**PHRASE AND SENTENCE DICTIONARY OF SPOKEN RUSSIAN**, English-Russian, Russian-English. Based on phrases, complete sentences, not isolated words—recognized as one of best methods of learning idiomatic speech. Over 11,500 entries, indexed by single words, over 32,000 English, Russian sentences, phrases, in immediately useable form. Shows accent changes in conjugation, declension; irregular forms listed both alphabetically, under main form of word. 15,000 word introduction covers Russian sounds, writing, grammar, syntax. 15 page appendix of geographical names, money, important signs, given names, foods, special Soviet terms, etc. Originally published as U.S. Gov't Manual TM 30-944. iv + 573pp. 5¾ x 8. T496 Paperbound \$2.75

**PHRASE AND SENTENCE DICTIONARY OF SPOKEN SPANISH**, Spanish-English, English-Spanish. Compiled from spoken Spanish, based on phrases, complete sentences rather than isolated words—not an ordinary dictionary. Over 16,000 entries indexed under single words, both Castilian, Latin-American. Language in immediately useable form. 25 page introduction provides rapid survey of sounds, grammar, syntax, full consideration of irregular verbs. Especially apt in modern treatment of phrases, structure. 17 page glossary gives translations of geographical names, money values, numbers, national holidays, important street signs, useful expressions of high frequency, plus unique 7 page glossary of Spanish, Spanish-American foods. Originally published as U.S. Gov't Manual TM 30-900. iv + 513pp. 5¾ x 8¾. T495 Paperbound \$1.75

## SAY IT CORRECTLY language record sets

The best inexpensive pronunciation aids on the market. Spoken by native linguists associated with major American universities, each record contains:

14 minutes of speech—12 minutes of normal, relatively slow speech, 2 minutes of normal conversational speed.

120 basic phrases, sentences, covering nearly every aspect of everyday life, travel—introducing yourself, travel in autos, buses, taxis, etc., walking, sightseeing, hotels, restaurants, money, shopping, etc.

32 page booklet containing everything on record plus English translations easy-to-follow phonetic guide.

Clear, high-fidelity recordings.

Unique bracketing systems, selection of basic sentences enabling you to expand use of SAY IT CORRECTLY records with a dictionary, to fit thousands of additional situations.

Use this record to supplement any course or text. All sounds in each language illustrated perfectly—imitate speaker in pause which follows each foreign phrase in slow section, and be amazed at increased ease, accuracy of pronunciation. Available, one language per record for

French	Spanish	German
Italian	Dutch	Modern Greek
Japanese	Russian	Portuguese
Polish	Swedish	Hebrew
English (for German-speaking people)		English (for Spanish-speaking people)

7" (33 1/3 rpm) record, album, booklet. \$1.00 each.

**SPEAK MY LANGUAGE: SPANISH FOR YOUNG BEGINNERS**, M. Ahlman, Z. Gilbert. Records provide one of the best, most entertaining methods of introducing a foreign language to children. Within framework of train trip from Portugal to Spain, an English-speaking child is introduced to Spanish by native companion. (Adapted from successful radio program of N.Y. State Educational Department.) A dozen different categories of expressions, including greeting, numbers, time, weather, food, clothes, family members, etc. Drill is combined with poetry and contextual use. Authentic background music. Accompanying book enables a reader to follow records, includes vocabulary of over 350 recorded expressions. Two 10" 33 1/3 records, total of 40 minutes. Book. 40 illustrations. 69pp. 5¼ x 10½. T890 The set \$4.95



## LISTEN &amp; LEARN language record sets

LISTEN & LEARN is the only extensive language record course designed especially to meet your travel and everyday needs. Separate sets for each language, each containing three 33 1/3 rpm long-playing records—1 1/2 hours of recorded speech by eminent native speakers who are professors at Columbia, New York U., Queens College.

Check the following features found only in LISTEN & LEARN:

Dual language recording. 812 selected phrases, sentences, over 3200 words, spoken first in English, then foreign equivalent. Pause after each foreign phrase allows time to repeat expression.

128-page manual (196 page for Russian)—everything on records, plus simple transcription. Indexed for convenience. Only set on the market completely indexed.

Practical. No time wasted on material you can find in any grammar. No dead words. Covers central core material with phrase approach. Ideal for person with limited time. Living, modern expressions, not found in other courses. Hygienic products, modern equipment, shopping, "air-conditioned," etc. Everything is immediately useable.

High-fidelity recording, equal in clarity to any costing up to \$6 per record.

"Excellent . . . impress me as being among the very best on the market," Prof. Mario Pei, Dept. of Romance Languages, Columbia U. "Inexpensive and well done . . . ideal present," Chicago Sunday Tribune. "More genuinely helpful than anything of its kind," Sidney Clark, well-known author of "All the Best" travel books.

**UNCONDITIONAL GUARANTEE.** Try LISTEN & LEARN, then return it within 10 days for full refund, if you are not satisfied. It is guaranteed after you actually use it.

6 modern languages—FRENCH, SPANISH, GERMAN, ITALIAN, RUSSIAN, or JAPANESE\*—one language to each set of 3 records (33 1/3 rpm). 128 page manual. Album.

Spanish	the set \$4.95	German	the set \$4.95	Japanese*	the set \$5.95
French	the set \$4.95	Italian	the set \$4.95	Russian	the set \$5.95

\* Available Oct. 1959.

## TRÜBNER COLLOQUIAL SERIES

These unusual books are members of the famous Trübner series of colloquial manuals. They have been written to provide adults with a sound colloquial knowledge of a foreign language, and are suited for either class use or self-study. Each book is a complete course in itself, with progressive, easy to follow lessons. Phonetics, grammar, and syntax are covered, while hundreds of phrases and idioms, reading texts, exercises, and vocabulary are included. These books are unusual in being neither skimpy nor overdetailed in grammatical matters, and in presenting up-to-date, colloquial, and practical phrase material. Bilingual presentation is stressed, to make thorough self-study easier for the reader.

**COLLOQUIAL HINDUSTANI**, A. H. Harley, formerly Nizam's Reader in Urdu, U. of London. 30 pages on phonetics and scripts (devanagari & Arabic-Persian) are followed by 29 lessons, including material on English and Arabic-Persian influences. Key to all exercises. Vocabulary. 5 x 7½. 147pp. Clothbound \$1.75

**COLLOQUIAL ARABIC**, DeLacy O'Leary. Foremost Islamic scholar covers language of Egypt, Syria, Palestine, & Northern Arabia. Extremely clear coverage of complex Arabic verbs & noun plurals; also cultural aspects of language. Vocabulary. xviii + 192pp. 5 x 7½. Clothbound \$1.75

**COLLOQUIAL GERMAN**, P. F. Oöring. Intensive thorough coverage of grammar in easily-followed form. Excellent for brush-up, with hundreds of colloquial phrases. 34 pages of bilingual texts. 224pp. 5 x 7½. Clothbound \$1.75

**COLLOQUIAL SPANISH**, W. R. Patterson. Castilian grammar and colloquial language, loaded with bilingual phrases and colloquialisms. Excellent for review or self-study. 164pp. 5 x 7½. Clothbound \$1.75

**COLLOQUIAL FRENCH**, W. R. Patterson. 16th revised edition of this extremely popular manual. Grammar explained with model clarity, and hundreds of useful expressions and phrases; exercises, reading texts, etc. Appendixes of new and useful words and phrases. 223pp. 5 x 7½. Clothbound \$1.75

## DOVER SCIENCE BOOKS

**COLLOQUIAL PERSIAN**, L. P. Elwell-Sutton. Best introduction to modern Persian, with 90 page grammatical section followed by conversations, 35 page vocabulary. 139pp. Clothbound \$1.75

**COLLOQUIAL CZECH**, J. Schwarz, former headmaster of Lingua Institute, Prague. Full easily followed coverage of grammar, hundreds of immediately useable phrases, texts. Perhaps the best Czech grammar in print. "An absolutely successful textbook," JOURNAL OF CZECHOSLOVAK FORCES IN GREAT BRITAIN. 252pp. 5 x 7½. Clothbound \$2.50

**COLLOQUIAL RUMANIAN**, G. Nandris, Professor of University of London. Extremely thorough coverage of phonetics, grammar, syntax; also included 70 page reader, and 70 page vocabulary. Probably the best grammar for this increasingly important language. 340pp. 5 x 7½. Clothbound \$2.50

**COLLOQUIAL ITALIAN**, A. L. Hayward. Excellent self-study course in grammar, vocabulary, idioms, and reading. Easy progressive lessons will give a good working knowledge of Italian in the shortest possible time. 5 x 7½. Clothbound \$1.75

## MISCELLANEOUS

**TREASURY OF THE WORLD'S COINS**, Fred Reinfeld. Finest general introduction to numismatics; non-technical, thorough, always fascinating. Coins of Greece, Rome, modern countries of every continent, primitive societies, such oddities as 200-lb stone money of Yap, nail coinage of New England; all mirror man's economy, customs, religion, politics, philosophy, art. Entertaining, absorbing study; novel view of history. Over 750 illustrations. Table of value of coins illustrated. List of U.S. coin clubs. 224pp. 6½ x 9¼. T433 Paperbound \$1.75

**ILLUSIONS AND DELUSIONS OF THE SUPERNATURAL AND THE OCCULT**, D. H. Rawcliffe. Rationally examines hundreds of persistent delusions including witchcraft, trances, mental healing, peyotl, poltergeists, stigmata, lycanthropy, live burial, auras, Indian rope trick, spiritualism, dowsing, telepathy, ghosts, ESP, etc. Explains, exposes mental, physical deceptions involved, making this not only an exposé of supernatural phenomena, but a valuable exposition of characteristic types of abnormal psychology. Originally "The Psychology of the Occult." Introduction by Julian Huxley. 14 illustrations. 551pp. 5¾ x 8. T503 Paperbound \$2.00

**HOAXES**, C. D. MacDougall. Shows how art, science, history, journalism can be perverted for private purposes. Hours of delightful entertainment, a work of scholarly value, often shocking. Examines nonsense news, Cardiff giant, Shakespeare forgeries, Loch Ness monster, biblical frauds, political schemes, literary hoaxers like Chatterton, Ossian, disambrotonist school of painting, lady in black at Valentino's tomb, over 250 others. Will probably reveal truth about few things you've believed, will help you spot more easily the editorial "gander" or planted publicity release. "A stupendous collection . . . and shrewd analysis," New Yorker. New revised edition. 54 photographs. 320pp. 5¾ x 8. T465 Paperbound \$1.75

**YOGA: A SCIENTIFIC EVALUATION**, Kovoov T. Behanan. Book that for first time gave Western readers a sane, scientific explanation, analysis of yoga. Author draws on laboratory experiments, personal records of year as disciple of yoga, to investigate yoga psychology, physiology, "supernatural" phenomena, ability to plumb deepest human powers. In this study under auspices of Yale University Institute of Human Relations, strictest principles of physiological, psychological inquiry are followed. Foreword by W. A. Miles, Yale University. 17 photographs. xx + 270pp. 5¾ x 8. T505 Paperbound \$1.65

Write for free catalogs!

Indicate your field of interest. Dover publishes books on physics, earth sciences, mathematics, engineering, chemistry, astronomy, anthropology, biology, psychology, philosophy, religion, history, literature, mathematical recreations, languages, crafts, art, graphic arts, etc.

Science B

HILL  
REFERENCE  
LIBRARY  
C. PAUL

Write to Dept. catr  
Dover Publications, Inc.  
180 Varick St., N. Y. 14, N. Y.

15